



**Brisbane River Catchment Flood Study:
Comprehensive Hydrologic
Assessment**

15 May 2015
Revision: 4
Reference: 238021

Monte Carlo Simulation Report

Prepared for the State of Queensland (acting through): Department of State Development, Infrastructure and Planning/Department of Natural Resources and Mines

Document control record

Document prepared by:

Aurecon Australasia Pty Ltd

ABN 54 005 139 873

Level 14, 32 Turbot Street
Brisbane QLD 4000

Locked Bag 331
Brisbane QLD 4001

Australia

T +61 7 3173 8000

F +61 7 3173 8001

E brisbane@aurecongroup.com

W aurecongroup.com

A person using Aurecon documents or data accepts the risk of:

- Using the documents or data in electronic form without requesting and checking them for accuracy against the original hard copy version.
- Using the documents or data for any purpose not agreed to in writing by Aurecon.

Document control					aurecon	
Report title		Monte Carlo Simulation Report				
Document ID		238021-0000-REP-WW-0002	Project number		238021	
File path		238021-0000-REP-WW-0002_Monte Carlo Simulation Report.docx				
Client		Prepared for the State of Queensland (acting through): Department of State Development, Infrastructure and Planning/Department of Natural Resources and Mines			Client contact	Pushpa Onta
Rev	Date	Revision details/status	Prepared by	Author	Verifier	Approver
A	29 January 2014	Draft for Client Review	C Smyth	F Diermanse J Beckers D. Carroll H. Schuurmans	A Bailey	R Ayre
B	1 April 2014	Draft For Client Review	C Smyth	F Diermanse J Beckers D. Carroll H. Schuurmans	A Bailey	R Ayre
C	21 July 2014	Draft For Client Review	C Smyth	F Diermanse J Beckers D. Carroll H. Schuurmans	A Bailey	R Ayre
0	10 October 2014	Final Issue	C Smyth	F Diermanse J Beckers D. Carroll H. Schuurmans	A Bailey	R Ayre
1	03 November 2014	Final Issue	C Smyth	F Diermanse J Beckers D. Carroll H. Schuurmans	A Bailey	R Ayre

2	15 December 2014	Final Issue	C Smyth	F Diermanse J Beckers D. Carroll H. Schuurmans	A Bailey	R Ayre
3	12 March 2015	Final	C Smyth	F Diermanse J Beckers D. Carroll H. Schuurmans	A Bailey	R Ayre
4	15 May 2015	Final	C Smyth	F Diermanse J Beckers D. Carroll H. Schuurmans	A Bailey	R Ayre

Current Revision

4

Approval

Author signature		Approver signature	
Name	Rob Ayre	Name	Craig Berry
Title	Technical Director	Title	Water Services Leader, Brisbane

Copyright notice (electronic)

“The State of Queensland [Department of Natural Resources and Mines] supports and encourages the dissemination and exchange of information provided in this publication and has endorsed the use of the Australian Governments’ Open Access and Licensing Framework.

Save for the content on this website supplied by third parties, the Department logo, the Queensland Coat of Arms, any material protected by a trademark, XXXX [ie third party copyright material] and where otherwise noted, The Department has applied the Creative Commons Attribution 4.0 International licence. The details of the relevant licence conditions are available on the Creative Commons website (accessible using the links provided) as is the [full legal code for the CC BY 4.0 International licence](#).

The parties assert the right to be attributed as authors of the original material in the following manner:

© State of Queensland [Department of Natural Resources and Mines] 2015

As far as practicable, third party material has been clearly identified. The Department has made all reasonable efforts to ensure that this material has been reproduced on this website with the full consent of the copyright owners. Their permission may be required to use the material.”

Brisbane River Catchment Flood Study: Comprehensive Hydrologic Assessment

Date 15 May 2015
Reference 238021
Revision 4

Aurecon Australasia Pty Ltd

ABN 54 005 139 873

Level 14, 32 Turbot Street
Brisbane QLD 4000

Locked Bag 331
Brisbane QLD 4001
Australia

T +61 7 3173 8000

F +61 7 3173 8001

E brisbane@aurecongroup.com

W aurecongroup.com



Important things you should know about this final report

Report subject to change

This report is subject to change as the assessments undertaken have been based solely upon hydrological modelling and are subject to continuous improvement. Aspects of these assessments that are affected by hydraulics will need to be verified during the hydraulic modelling phase. Therefore the estimates presented in this report should be regarded as interim and possibly subject to change as further iteration occurs in conjunction with the hydraulic modelling phase of the Brisbane River Catchment Flood Study.

Exclusive use

This report and hydrologic model data has been prepared by Aurecon at the request of the State of Queensland acting through the Department of State Development, Infrastructure and Planning (“Client”).

The basis of Aurecon’s engagement by the Client is that Aurecon’s liability, whether under the law of contract, tort, statute, equity or otherwise, is limited as set out in the Conditions of Contract schedules: DSDIP-2077-13 and agreed variations to the scope of the contract (terms of the engagement).

Third parties


It is not possible to make a proper assessment of this report without a clear understanding of the terms of engagement under which the report has been prepared, including the scope of the instructions and directions given to and the assumptions made by the consultant who has prepared the report.

The report is scoped in accordance with instructions given by or on behalf of the Client. The report may not address issues which would need to be addressed by a third party if that party’s particular circumstances, requirements and experience with such reports were known; and the report may make assumptions about matters of which a third party is not aware.

Aurecon therefore does not assume responsibility for the use of, or reliance on, the report by any third party and the use of, or reliance on, the report by any third party is at the risk of that party.

Limits on scope and information

Where the report is based on information provided to Aurecon by other parties including state agencies, local governments authorised to act on behalf of the client, and the Independent Panel of Experts appointed by the client, the report is provided strictly on the basis that such information that has been provided is accurate, complete and adequate. Aurecon takes no responsibility and disclaims all liability whatsoever for any loss or damage that the Client or any other party may suffer resulting from any conclusions based on information provided to Aurecon, except to the extent that Aurecon expressly indicates in the report or related and supporting documentation, including the hydrologic



models, analytical tools and associated datasets and metadata, that it has accepted or verified the information to its satisfaction.

Legal documents

The report may contain various remarks about and observations on legal documents and arrangements such as contracts, supply arrangements, leases, licences, permits and authorities. A consulting engineer can make remarks and observations about the technical aspects and implications of those documents and general remarks and observations of a non-legal nature about the contents of those documents. However, as a Consulting Engineer, Aurecon is not qualified, cannot express and should not be taken as in any way expressing any opinion or conclusion about the legal status, validity, enforceability, effect, completeness or effectiveness of those arrangements or documents or whether what is provided for is effectively provided for. They are matters for legal advice.

Aurecon team

The Aurecon Team consists of Aurecon as lead consultant, supported by Deltares, Royal HaskoningDHV, and Don Carroll Project Management and Hydrobiology.



Executive summary

Brisbane River catchment flood study

The State of Queensland, Australia, initiated a comprehensive hydrologic assessment as part of the Brisbane River Catchment Flood Study (BRCFS) in response to the devastating floods in January 2011 and subsequent recommendations of the Queensland Floods Commission of Inquiry. In accordance with this recommendation, the State of Queensland is managing the conduct of this study in a number of separate phases. Aurecon Team, consisting of Aurecon, Deltares, Don Carroll project management and Royal HaskongDHV, was commissioned to undertake the second phase of the study: a Comprehensive Hydrologic Assessment (CHA). The main objective of the CHA is to produce a set of competing methods for estimating design floods in the Brisbane River catchment, followed by an extensive reconciliation process to identify the most reliable design flood estimates of a range of flood flows for annual exceedance probabilities across the entire Brisbane River system. The CHA needs to consider two scenarios, referred to as 'no-dam' and 'with-dam'. The dams referred to are the major water storages that exist within the catchment; these are Somerset Dam and Wivenhoe Dam, both of which have flood mitigation capacity. Other reservoirs considered are the Cressbrook Creek, Lake Manchester, Moogerah and Perseverance dams.

The results of the comprehensive hydrologic assessment will serve as input for a hydraulic assessment, which is also part of the Brisbane River Catchment Flood Study. The main purpose of the hydraulic assessment is to derive flood levels, whereas the hydrologic assessment serves to derive flood flows (peak discharges and volumes).

Objective of this report

This report describes one of the methods considered for estimating design floods in the Brisbane River catchment: a Monte Carlo Simulation technique. The report describes, in detail, the methodology and data sources. Monte Carlo Simulation results are discussed in a follow-up report in which results of three design flood estimation techniques are reconciled.

Monte Carlo simulation

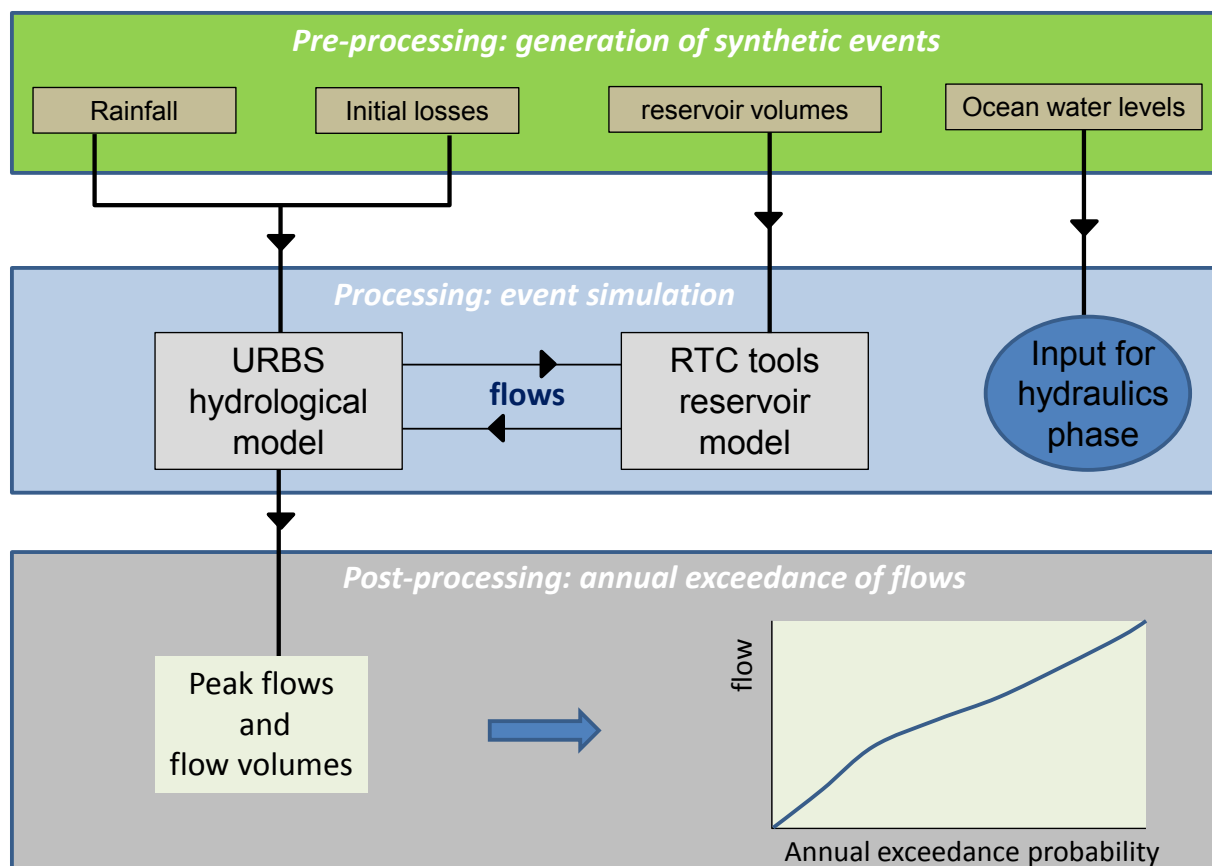
In the Monte Carlo Simulations approach, a large number of synthetic events is simulated with the combination of a hydrological model and a reservoir simulation model. Flood flow exceedance probabilities at key locations are derived from the model simulation results. The method has the advantage over more "traditional" approaches in flood risk analysis in that it explicitly considers all relevant physical processes that contribute to flood events. A practical disadvantage is that it is generally more complex to implement. The main challenge in the MCS approach is to generate realistic and representative synthetic flood events. This means the synthetic events should correctly account for probabilities of occurrence of factors contributing to flood flows such as rainfall (depth,

duration, spatial and temporal patterns), antecedent moisture conditions, initial reservoir volumes and ocean water levels. Furthermore, the likelihood of combined occurrences (correlations) of these factors needs to be taken into account. And, finally, the relevant physical processes in the catchment during flood events need to be correctly simulated.

Components of the computational framework

The Monte Carlo Framework consists of three major components:

1. Pre-processing: a combination of advanced statistical techniques to generate a large set of realistic and representative synthetic flood events. These events are characterised by rainfall, antecedent moisture conditions, initial reservoir volumes and ocean water levels
2. Processing: simulation of the synthetic events with a combination of a hydrological model (URBS) and a reservoir simulation model (RTC tools) to obtain peak discharges and flow volumes at each location of interest
3. Post-processing: Statistical techniques to combine the results of I and II to derive annual exceedance probabilities for a range of flood flows across the entire Brisbane River system



Schematic view of the Monte Carlo Simulation framework



Sources of data, models and statistics

As described in the previous section, the Monte Carlo simulation framework contains a large number of components, consisting of models, statistics and data. Some models have been developed within the context of the current study; others were taken from other sources, often with minor adaptations. The most prominent source was Australian Rainfall and Runoff (ARR): the national guideline document for the estimation of design flood characteristics in Australia. ARR is published by Engineers Australia.

Rainfall statistics: IFD curves

The relation between rainfall depth (or intensity), rainfall duration and frequency is described by IFD-curves, ie Intensity-Frequency-Duration curves. These curves have been obtained from different sources, such as ARR and GTSMR (Generalised Tropical Storm Method – Revision, Bureau of Meteorology). The different sources were used for different ranges of duration and frequency. The report of Aurecon (2014a) describes how these IFD curves have been combined into a single IFD table. The same sources were used to translate point rainfall statistics to catchment rainfall statistics by means of areal reduction factors. The IFD curves describe “burst” statistics, which means they refer to time intervals with fixed durations that generally do not correspond to the beginning and ending of rainfall events.

Rainfall patterns

The IFD curves in combination with areal reduction factors describe statistics of the area-averaged rainfall depth in a catchment. Besides rainfall depth, the spatial and temporal pattern of rainfall also influences peak flows and flow volumes. Realistic synthetic spatio-temporal rainfall patterns, provided by the STEPS model of the Bureau of Meteorology, are used in the Monte Carlo simulation framework.

Monte Carlo sampling techniques


The choice of sampling method is crucial for the BRCFS-hydrology phase. There are several candidate methods, each with their own advantages and disadvantages. The following three methods have been considered and tested:

1. The Cooperative Research Centre – Catchment Hydrology (CRC-CH) method (Rahman et al, 2001; 2002)
2. The Total Probability Theorem (TPT) method (ARR, 2013a)
3. The Complete Storm Simulation (CSS) Method, a method that was developed within the context of the current study

The TPT method was chosen as the preferred method for the current study through the Pilot Study investigation, because this method provided the best match between the rainfall IFD curves on one hand and the available synthetic spatio-temporal rainfall patterns on the other hand. The other two methods (CSS and CRC-CH) are nevertheless considered very promising for future applications of Monte Carlo applications, especially if more synthetic spatio-temporal rainfall patterns become available.

Initial losses

Initial losses refer to the proportion of the rainfall that is absorbed by the soil at the beginning of the event. They are a measure of the antecedent moisture conditions of the soil. Information on initial losses in the Brisbane River Catchment is available from the URBS model calibration as carried out by Seqwater (2013a). Analyses were carried out for seven sub-catchments, in which initial losses were assumed uniform over the entire sub-catchment. In the current study, statistical distribution functions



were derived from the resulting initial losses of Seqwater (2013a). Furthermore, the likelihood of combined occurrences high (low) initial losses in the various subcatchments were quantified and implemented in the Monte Carlo framework.

Ocean water levels

Statistics of peak ocean water levels in Moreton Bay were adopted from GHD (2014). Furthermore, the (weak) correlation between rainfall depth and peak ocean water levels was taken into account by adopting a recently developed correlation model from ARR (Zheng et al, 2013a,b). Realistic time series for ocean water levels are generated through a combination of a “mean” time series of astronomical tide, in combination with a standardised storm surge hydrograph. The latter was based on recorded time series for the Sunshine coast as derived by (Aurecon, 2013b).

Ocean water levels do not affect flows in the hydrological model and therefore will not be of influence on design flood flows as computed in the current studies. The ocean water levels serve as input for the hydraulics phase of the Brisbane River catchment flood study.

Reservoir volumes

A 123-year reservoir model simulation was carried out by the Queensland Department of Science, Information Technology, Innovation and the Arts (DSITIA). The output consisted of a 123-year series of reservoir volumes for six dams in the area: Cressbrook Creek, Lake Manchester, Moogerah, Perseverance, Somerset and Wivenhoe. The resulting series were used in the current study to derive relevant statistics of initial reservoir volumes. Furthermore, the likelihood of combined occurrences of high (low) initial volumes in the various reservoirs were quantified and implemented in the Monte Carlo framework.

Hydrological model


The Brisbane River catchment hydrological model was developed by Seqwater and implemented in the URBS hydrological model suite (Carroll, 2012a). The model was calibrated by Seqwater (2013a) and subsequently recalibrated by Aurecon (2014b). In the model, the Brisbane River catchment is divided into seven distinct sub-catchment models based on review of topography and drainage patterns, major dam locations, key locations of interest for real time flood operations, and consideration of the best use of available data including water level gauges. Dams and reservoirs are modelled within URBS as well, with the exception of Wivenhoe Dam and Somerset Dam.

Reservoir simulation model

Wivenhoe Dam and Somerset Dam are modelled in RTC tools, an open source, modular toolbox dedicated to real-time control (RTC) of hydraulic structures like weirs, pumps, hydro turbines, water intakes, etc. The Dam Operations Module is based upon the Loss of Communications (LOC) emergency flood operation procedure described in the Flood Manual (Seqwater, 2013b).

Framework implementation in Delft-FEWS

The Monte Carlo Simulation model for the BRCFS was implemented in the Delft-FEWS framework. Delft-FEWS is a component-based modelling framework that incorporates a wide range of general data handling utilities and open interfaces to many hydrological and hydraulic models that are commonly used around the world, including the URBS hydrological model and RTC tools for reservoir modelling. Delft-FEWS can be used for data storage and retrieval tasks, simple forecasting systems and in highly complex operational forecasting systems. The advantage of using FEWS for all communication between components is that intermediate results (time series data) can be inspected for checking and debugging. Moreover, the modular setup of FEWS enables to replace components



without much effort. A further advantage is that institutes like Seqwater and the Bureau of Meteorology are familiar with Delft-FEWS. This means the framework can easily be transferred to these and others institutes, which provides great opportunities to develop similar tools for other catchments.

Output

The output of the Monte Carlo Simulations framework consists of design peak flows and associated annual exceedance probabilities. Furthermore, the framework produces hydrographs that correspond to these design flood flows. These results are produced for 23 locations of interest in the Brisbane River catchment, but this number can be increased if desired. The computation results of the framework are discussed in a separate report on the reconciliation of results of the comprehensive hydrologic assessment. In that report, MCS design flood flows are compared to design flows of two other methods: statistical flood frequency analysis and the design event approach. Based on the comparison, a choice is made on the reconciled design flood flows that form the primary output of the comprehensive hydrologic assessment.

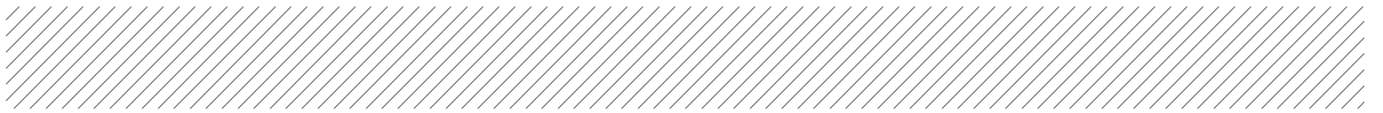
Conclusions

The proposed Monte Carlo Simulation approach provides what is required for the BRCFS-hydrology phase: a joint probability approach for the derivation of design flows and volumes, taking into account spatial and temporal variation of rainfall over the Brisbane River catchment. The method has the advantage over more “traditional” approaches in flood risk analysis in that it explicitly considers all relevant physical processes that contribute to flood events. A practical disadvantage is that it is generally more complex to implement. Computation times for a single output location near the catchment outlet are in the order of five hours on a 64 bit machine, Windows 7, Solid State Drive (SSD) with 16Gb and 4 cores (duplicated, so actually 8 cores). For upstream locations with smaller catchment areas the runtime is in the order of two to three hours.



Contents

1	Introduction	1
1.1	Project overview	1
1.2	Objective of this document	2
1.3	Scope	2
1.4	Outline	3
1.5	Choice of sampling method	3
2	Proposed computational scheme of the MCS framework	4
2.1	Flood processes in the Brisbane river catchment	4
2.2	Hydrological model and dam operations model	6
2.3	Monte Carlo Simulation workflow	7
2.4	Separate simulations for each location of interest	9
3	Rainfall sampling methods	10
3.1	Introduction	10
3.2	Brief description of methods	10
3.3	Required input statistics	13
3.4	Rainfall duration	13
3.5	Advantages and disadvantages of the sampling methods	14
3.6	Consequences for other random variables	16
4	Derivation of catchment rainfall depth	18
4.1	Introduction	18
4.2	Events versus bursts IFD tables	19
4.3	Areal IFD curves	32
4.4	Conclusions	38
5	Spatio-temporal rainfall patterns	39
5.1	Introduction	39
5.2	BoM synthetic rainfall patterns	40
5.3	Basic statistics for burst rainfall of the synthetic events	41
5.4	Incorporation in the MCS framework	45
5.5	Observed versus synthetic rainfall patterns	54
5.6	Selection of patterns for low AEP-events	61
6	Sampling of other random variables	62
6.1	Introductions	62
6.2	Initial losses	62



6.3	Ocean water levels	72
6.4	Reservoir volumes	80
6.5	Base flow	96
7	Hydrological model and dam operations model	98
7.1	Introduction	98
7.2	URBS hydrological model	98
7.3	RTC tools dam operations model	100
8	Computation of frequency curves	106
8.1	Introduction	106
8.2	Monte Carlo estimates of flood frequencies	106
8.3	Stratified sampling and importance sampling	107
8.4	Additional post-processing for the TPT method	109
9	Implementation of the MCS framework in Delft-FEWS	110
9.1	Introduction	110
9.2	Pre-processing: generation of (storm) events	110
9.3	Processing: hydrological modelling and reservoir modelling	111
9.4	Post processing: derivation and plotting of frequency curves	113
9.5	Computational performance	115
9.6	Overall assessment	115
10	Conclusions	116
10.1	Proposed framework	116
11	References	118
12	Glossary	121
12.1	Hydrologic terms	121
12.2	Study related terms	123

Appendices

Appendix A

'No-dams' design peak discharges

Appendix B

'With-dams' frequency tables and figures for peak discharges

Appendix C

'No-dams' design flow volumes

Appendix D

'With-dams' design flow volumes

Appendix E

Comparison of 'with-dams' and 'no-dams' results

Appendix F

Peak discharge versus AEP of the rainfall depth

Appendix G

Frequency curves per burst duration

Appendix H

Case study for the TPT and CRC –CH methods

Figures

Figure 2-1 Brisbane river catchment, showing the seven sub-catchments of the URBS hydrological model	4
Figure 2-2 Computational workflow for the 'no dams' scenario	6
Figure 2-3 Computational workflow for the 'with dams' scenario	7
Figure 2-4 Schematic view of the proposed Monte Carlo Simulation framework. It also shows the chapters in which each component is described.	8
Figure 3-1 Annual exceedance probability and corresponding peak discharges as estimated from 10 different MC runs with crude Monte Carlo and 10 different MC runs with Monte Carlo with importance sampling: 20,000 samples	12
Figure 3-2 Fitted GPD distribution function to the average rainfall depths over the full Brisbane catchment of 44 calibration events obtained from Seqwater	13
Figure 3-3 Probability distribution of event duration for three test-stations in the upper Brisbane	14
Figure 3-4 Schematic view of the TPT, CRC-CH and CSS methods	17
Figure 4-1 Frequency distributions of event durations from rainfall data at Emu Creek, for various durations (from 6 to 48 hours) of the dry period before and after the event in the definition of a rainfall event	20
Figure 4-2 Fit of the exponential distribution function through empirical frequencies of observed event durations at Emu Creek	21
Figure 4-3 Double-log plot of event depth (mm) versus duration (hrs), example from Emu Creek data. Two regression lines are shown: for all events (orange) and for the most extreme events only (green)	22
Figure 4-4 BoM IFD data (symbols) fitted to equation (2) (dashed lines) for three different AEP's	24
Figure 4-5 Event-depth as a function of ARI for several durations, according to the BoM IFD tables for Emu Creek. Exponential fits are shown as thin black lines	25
Figure 4-6 Event-IFD curves (symbols) compared to transformed burst-IFD tables. Both graphs are based on Emu Creek rainfall data	25
Figure 4-7 Empirical event IFD curves for Emu Creek and transformed burst-tables using the mapping equation (9) and average coefficients	28
Figure 4-8 Empirical burst-IFD table for Emu Creek (dashed lines) compared to BoM data (symbols)	28
Figure 4-9 Empirical burst-IFD table for Kirkleagh (dashed lines) compared to BoM data (symbols)	29
Figure 4-10 Event IFD Curves for Emu Creek, derived using the CRC-CH method (6 duration classes)	30
Figure 4-11 ARF from ARR (ARR, 2013c)	33
Figure 4-12 Comparison of catchment IFD curves as derived from BoM point rainfall IFDs and ARR Areal Reduction factors (full lines) and from catchment average rainfall time series (symbols)	34
Figure 4-13 Example of crossing IFD curves	35

Figure 4-14 Comparison of catchment IFD curves as derived from BoM point rainfall IFDs and ARR Areal Reduction factors (full lines) and from catchment average rainfall time series (symbols), location Brisbane	36
Figure 4-15 Comparison of catchment IFD curves as derived from BoM point rainfall IFDs and ARR Areal Reduction factors (full lines) and from catchment average rainfall time series (symbols), location Loamside	36
Figure 4-16 Comparison of catchment IFD curves as derived from BoM point rainfall IFDs and ARR Areal Reduction factors (full lines) and from catchment average rainfall time series (symbols), location Moggill	37
Figure 4-17 Comparison of catchment IFD curves as derived from BoM point rainfall IFDs and ARR Areal Reduction factors (full lines) and from catchment average rainfall time series (symbols), location Mount Crosby	37
Figure 4-18 Comparison of catchment IFD curves as derived from BoM point rainfall IFDs and ARR Areal Reduction factors (full lines) and from catchment average rainfall time series (symbols), location Savages Crossing	38
Figure 5-1 Example of spatial variation of rainfall, observed during ex-tropical Cyclone Marcia, February 2015; Figure Courtesy of Michel Raymond, Seqwater	39
Figure 5-2 Flow cart for production of space-time rainfall patterns (copied from SKM 2013).	40
Figure 5-3 Boxplots of maximum 24 hours burst per catchment [mm] based on 60 patterns per event. The boxes are formed by first and third quartile – the median is plotted as a black dot – the whiskers are at maximum 1.5 time the interquartile range. Outside this range points are plotted as individual outliers	43
Figure 5-4 Boxplots of the relative contribution (%) of each catchment within the total max 24 hour burst	43
Figure 5-5 Boxplots of maximum 48 hours burst per catchment [mm] based on 60 patterns per event. The boxes are formed by first and third quartile – the median is plotted as a black dot – the whiskers are at maximum 1.5 time the interquartile range. Outside this range points are plotted as individual outliers	44
Figure 5-6 Boxplots of the relative contribution (%) of each catchment within the total max 48 hour burst	44
Figure 5-7 Comparison of sampled combinations of depth and duration in the CRC-CH method for events with rainfall AEP>1/2,000 (blue dots) and combinations of depth and duration of the 660 BoM synthetic rainfall patterns (red dots)	46
Figure 5-8 IFD curves for AEP = 1/2 and AEP = 1/2000 versus combinations of depth and duration of bursts in the 660 BoM synthetic rainfall patterns (red dots)	47
Figure 5-9 Simulated peak discharges versus AEP of the rainfall event at location Tinton, for burst durations of 24 hours. The circles indicate events with “within bursts”. The colour of the circle indicates the magnitude of the within burst in terms of AEP ratios. For example, a red colour indicates the existence of a within burst rainfall depth with an AEP that is a factor 2-3 smaller than the AEP of the 24 hour rainfall depth	49
Figure 5-10 Number of valid rainfall patterns per duration and AEP after application of the within burst filter criterion; Location Moggill	50
Figure 5-11 Number of valid rainfall patterns per duration and AEP after application of the within burst filter criterion; Location Peachester	50
Figure 5-12 Relative differences in calculated rainfall depth between CSS method and IFD tables as functions of duration for the total Brisbane catchment (full Brisbane) as well as for all the sub-catchments. The different colours represent different ARI's	52
Figure 5-13 Relative differences in calculated rainfall depth between CSS method and IFD tables as functions of ARI for the total Brisbane catchment (full Brisbane) as well as for all the sub-catchments. The different colours represent different durations	53

Figure 5-14 Empirical distributions of contributions of individual sub-catchments to the total catchment rainfall	55
Figure 5-15 Histograms of contributions of individual sub-catchments to the total catchment rainfall	55
Figure 5-16 Average contribution of individual sub-catchments to the total catchment rainfall	56
Figure 5-17 Empirical distributions of contributions of individual sub-catchments to the total catchment rainfall. Probability weights were applied for the BoM synthetic (simulated) events	57
Figure 5-18 Histograms of contributions of individual sub-catchments to the total catchment rainfall. Probability weights were applied for the BoM synthetic (simulated) events	57
Figure 5-19 Average contribution of individual sub-catchments to the total catchment rainfall. Probability weights were applied for the BoM synthetic (simulated) events	58
Figure 5-20 Empirical distributions of contributions of individual sub-catchments: comparison between 68 pre-1955 events and 57 post-1955 events	59
Figure 5-21 Empirical distributions of contributions of individual sub-catchments to the total catchment rainfall. Rainfall data was based on post 1955 events only	59
Figure 5-22 Histograms of contributions of individual sub-catchments to the total catchment rainfall. Rainfall data was based on post 1955 events only	60
Figure 5-23 Average contribution of individual sub-catchments to the total catchment rainfall. Rainfall data was based on post 1955 events only	60
Figure 5-24 Value of P_s as a function of the annual exceedance probability of the rainfall	61
Figure 6-1 Comparison of the standardised initial loss distribution and the fitted standardised beta distribution	64
Figure 6-2 Empirical standardised distributions for Initial losses of the 7 sub-catchments, in combination with the standardised initial loss distribution of ARR [2013]. Initial Loss data were adopted from Seqwater [2013a]	65
Figure 6-3 Derived median initial losses of the seven sub-catchments, based on 38 calibrated events of Seqwater (2013a)	66
Figure 6-4 Beta-distribution fitted on the (normalised) observed initial losses of the Stanley River sub-catchment	67
Figure 6-5 Correlations per sub-catchment between rainfall depth/intensity and initial losses	68
Figure 6-6 Correlation plots of simulated and observed initial losses for four sub-catchments (Upper, Stanley, Lockyer and Bremer). The axes show empirical probabilities	70
Figure 6-7 Bivariate samples of the Gaussian copula ($\rho=0.8$) and the student-t copula ($\rho=0.8$, $\nu=5$)	72
Figure 6-8 Bivariate samples of the Gaussian copula ($\rho=0.8$) and the student-t copula ($\rho=0.8$, $\nu=2$)	72
Figure 6-9 Frequency distribution for ocean water levels at Luggage point; numbers based on (GHD, 2014)	73
Figure 6-10 Standard Fréchet distribution	74
Figure 6-11 N=10,000 samples from the bivariate logistic model for four different values of the dependence parameter α . The axes show marginal exceedance probabilities of the sampled x and y-values	75
Figure 6-12 Recorded time series histories (normalised) for storm surges on the Sunshine Coast. Figure copied from (Aurecon, 2013b)	77
Figure 6-13 Example of a generated series of surge, astronomical tide and resulting ocean water level	78
Figure 6-14 Examples of a generated series of surge, astronomical tide and resulting ocean water level. In each subplot, the resulting peak ocean water level is the same. Differences between subplots are caused by differences in the peak of the surge and differences in “timing”	78
Figure 6-15 Eight time series of ocean water levels of Figure 6-14. The time series were shifted horizontally to make sure the peaks occurred at the same time	79
Figure 6-16 Histogram of difference in timing between peak flows at Brisbane City and peak ocean water levels at the Brisbane River outlet, for simulated 72 hour bursts. Positive values refer to peak flows occurring later than peak ocean water levels	80

Figure 6-17 Dams and reservoirs in the Brisbane river catchment	81
Figure 6-18 Annual mean volume of Wivenhoe Dam	82
Figure 6-19 Annual mean volume of Moogerah Dam	82
Figure 6-20 Monthly mean rainfall over Wivenhoe Dam catchment	83
Figure 6-21 Histogram of occurrence of maximum 1, 2, 3 and 4 day rainfall	84
Figure 6-22 Box plot for monthly mean reservoir volumes of Wivenhoe Dam	84
Figure 6-23 Box plot for monthly mean reservoir volumes of Somerset Dam	85
Figure 6-24 Q-Q plots showing estimated probabilities of non-exceedance of derived reservoir volumes for 123 bursts. P-values at the vertical axes were derived directly from the series of 123 bursts, p-values at the horizontal axes were derived from the statistics of the entire series of 123 years. Plots are shown for the highest 1,2,3 and 4-day rainfall bursts	86
Figure 6-25 Scatter plots of rainfall depth and reservoir volume for Wivenhoe dam	87
Figure 6-26 Empirical probabilities of rainfall depth and reservoir volume for Wivenhoe dam	88
Figure 6-27 Scatter plots of empirical probabilities of reservoir volumes at the beginning of the 123 selected highest 4-day rainfall bursts: Wivenhoe dam (horizontal axis) plotted against the other five other dams	89
Figure 6-28 Scatter plots of empirical probabilities of reservoir volumes of all daily observations in the simulated series of 123 years: Wivenhoe dam (horizontal axis) plotted against the other five other dams. The red circles correspond to the highest 123 4-day rainfall bursts	91
Figure 6-29 Histogram of Wivenhoe reservoir volumes at the beginning of the highest 1-day, 2-day, 3-day and 4-day rainfall bursts. The red dashed line is the full supply level	92
Figure 6-30 Histogram of Moogerah dam reservoir volumes at the beginning of the highest 1-day, 2-day, 3-day and 4-day rainfall bursts. The red dashed line is the full supply level	93
Figure 6-31 Derived empirical distribution function of reservoir volumes at the start of 1-day, 2-day, 3-day and 4-day rainfall bursts	93
Figure 6-32 Observed (red) and simulated (blue) pairs of reservoir volumes at the beginning of high rainfall bursts; Wivenhoe dam versus the other five dams	95
Figure 6-33 Observed (red) and simulated (blue) pairs of reservoir volumes at the beginning of high rainfall bursts; Combinations of Cressbrook, Perserverance, Moogerah, Manchester and Somerset dams	96
Figure 7-1 Schematic view of Wivenhoe Dam	102
Figure 7-2 Schematic view of Somerset Dam	103
Figure 7-3 Somerset Dam loss of communications procedure	104
Figure 9-1 Schematic representation of the first step of the method	111
Figure 9-2 Schematic representation of the second step of the method	112
Figure 9-3 Screenshot of hydrographs generated by the FEWS-MCS framework	113
Figure 9-4 Example of a frequency curve	113
Figure 9-5 Schematic representation of the third step of the method	114

Tables

Table 3-1 Summary of advantages and disadvantages CRC-CH and TPT	15
Table 4-1 Case study stations and length of the observational records	26
Table 4-2 Mapping parameters for burst to event IFD table for the three test stations	27
Table 4-3 IFD mapping parameters for different event definitions (dry period duration)	31
Table 4-4 Selected IFD mapping parameters	31
Table 5-1 Overview of space-time rainfall patterns in Excel spreadsheets	41
Table 5-2 The 12 'sub-catchments' listed in the spreadsheet	41
Table 5-3 Maximum burst durations considered	48

Table 5-4 Number of valid rainfall patterns per duration for AEP=1/2000, after application of the within burst filter criterion. Numbers lower than 20 are highlighted with a grey colour	51
Table 6-1 Standardised initial loss distribution, estimated from Figure 5-21 of ARR, 2013. The standardised values represent a fraction of the median initial loss	63
Table 6-2 Parameters of the beta-distribution that provide the optimal fit of the standardised distribution of Table 6-1	64
Table 6-3 Derived median initial losses of the seven sub-catchments, based on 38 calibrated events of Seqwater (2013a]	66
Table 6-4 Selected parameters of the beta-distribution that provide the optimal fit for the standardised distribution functions of initial losses	66
Table 6-5 Derived correlations between the seven sub-catchments	67
Table 6-6 Derived correlations per sub-catchment between rainfall depth/intensity and initial losses	68
Table 6-7 Derived Spearman rank correlations between rainfall totals of the 123 highest 1,2,3 and 4-day rainfall events and the rainfall of the preceding periods (10, 30 and 90 days) for the catchments of six dams	69
Table 6-8 Frequency distribution for ocean water levels, adopted from GHD (2014)	73
Table 6-9 Probability of exceedance of ocean water levels with shown AEP, during a period of three days	76
Table 6-10 Conditional exceedance probability, $F(Y>y X=x)$, in case the dependence parameter α is equal to 0.85. The value of x is the rainfall depth with an AEP as shown in the second header row, the value of y is the ocean water level with an AEP as shown in the first column	76
Table 6-11 Full supply levels of the six reservoirs as assumed in the simulations	80
Table 6-12 Correlations between rainfall and reservoir volumes for selected bursts (1, 2, 3 and 4-day rainfall extremes)	88
Table 6-13 Rank correlations between volumes of the six reservoirs: $\rho = \sin(\pi\tau/2)$, where τ is Kendall's rank correlation	89
Table 6-14 Selected γ -values for the six reservoirs	95
Table 6-15 Adopted baseflow volume factors	96
Table 7-1 The seven sub-catchments used to model of the Brisbane river catchment	99
Table 7-2 Maximum number of sluice gates that are allowed being open	105



1 Introduction

1.1 Project overview

The Queensland Floods Commission of Inquiry Final Report, which was issued in March 2012, contains a recommendation (Recommendation 2.2) that requires a flood study be conducted of the Brisbane River catchment. In accordance with this recommendation, the State of Queensland is managing the conduct of this study in a number of separate phases, namely:

- Phase 1: Data Collection, Collation, Review and Storage of Existing Data (complete)
- Phase 2: Comprehensive Hydrologic Assessment (current)
- Phase 3: Comprehensive Hydraulic Assessment
- Phase 4: Brisbane River Floodplain Management Study and Brisbane River Floodplain Management Plan

The Aurecon Team, consisting of a combination of Aurecon, Deltares, Don Carroll project management and Royal HaskoningDHV, was commissioned to undertake the Comprehensive Hydrologic Assessment (CHA). This assessment needs to be comprehensive with a requirement for various methodologies to be utilised and for them to corroborate each other. The study needs to include a Monte Carlo framework that can account for the variability of nominated input parameters, including rainfall, both spatially and temporally, antecedent conditions and reservoir levels.

The main objective of the CHA is to develop and apply a state of the art method that produces consistent and robust hydrologic models and analytical techniques that will enable the CHA to provide best estimates of a range of flood flows for annual exceedance probabilities across the entire Brisbane River system. The method needs to be able to account for two scenarios: the conditions referred to as 'no-dam' or pre-dams, and the conditions 'with-dam' or post-dams. The dams referred to are the major water storages that exist within the catchment; these are Somerset Dam and Wivenhoe Dam, both of which have flood mitigation capacity. Other reservoirs considered are the Cressbrook Creek, Lake Manchester, Moogerah and Perseverance dams.

The hydrologic assessment methodology also needs to be iterative, both within itself and in conjunction with the subsequent hydraulic study, so as to ensure consistency with the hydraulic modelling and its determination of flood levels in the Lower Brisbane River and its tributaries. The combined output from the hydrologic assessment and the hydraulic modelling assessment will be used to underpin the Brisbane River Floodplain Management Study (BRFMS) and the Brisbane River Floodplain Management Plan (BRFMP).



1.2 Objective of this document

The current document describes the enhanced Monte Carlo Simulation (MCS) framework and methodology.

1.3 Scope

The client's request for proposals (DSDIP, 2013), describes a number of requirements for the MCS framework, which can be summarised as follows:

- The proposed MCS framework should ensure that the hydrologic modelling captures all the significant flood generating and modifying influences appropriately and that all dominant correlations are well reflected in design flows. The critical elements of the flood formation and flood modification processes are:
 - The magnitude of design rainfall depths/intensities over the catchment and their variation with average exceedance probability (AEP), rainfall duration and location within the catchment
 - The large degree of spatial and temporal variability of storm rainfalls over the catchment and its impacts on (a) the peak magnitudes and hydrograph shapes of design inflow floods for different AEPs, (b) the flood operation of Somerset and Wivenhoe Dams, and (c) the relative magnitudes of flood contributions from different sub-catchments and their interactions to produce critical flood levels at sites of interest
 - The extent to which storm event rainfalls are correlated with pre-event rainfalls over different time periods: (a) pre-event rainfall over periods of days to weeks which determines the initial wetness state of the catchment (initial losses) and initial inundation conditions of floodplains; and (b) pre-event rainfall over a season or multi-year period which determines the initial volume in the dams at the onset of the flood event
 - The extent to which storm event rainfalls over the catchment are correlated with the forcing factors that produce high storm tides and thus determine the downstream boundary conditions for hydraulic modelling of floods in the lower Brisbane River system
 - Modelling of any significant features in the Lower Brisbane River floodplain which have the potential to modify flood hydrographs significantly
- The framework should consider the following two principal approaches for the stochastic simulation of rainfall that are currently being applied in Australia: the TPT approach and the CRC-CH approach (explained in Section 3). The relative advantages and limitations of the two approaches need to be evaluated and a methodology has to be proposed that incorporates the best elements of both approaches, together with any enhancements necessary to overcome perceived limitations. Alternative approaches, besides TPT and CRC-CH may also be proposed and considered, if advantages of the alternative approach can be demonstrated
- Correlations between storm inputs, initial conditions in the catchment, reservoir volumes and ocean level anomalies need to be taken into account

This document describes the setup of the MCS framework and the analyses that were carried out since project commencement.



1.4 Outline

Section 2 provides an overview of the components of the proposed MCS framework. Section 3 discusses the sampling methods for rainfall with special emphasis on joint probability methods: CRC-CH, TPT and a suggested third approach, CSS. Section 4 describes the derivation of catchment average rainfall depths, based on IFD curves. Section 5 describes the 'redistribution' of catchment rainfall, using synthetic spatio-temporal patterns as generated by the BoM. Section 6 describes the statistics and correlations of the other random variables of the MCS framework (besides rainfall). Section 7 describes the hydrological model and the reservoir simulation model. Section 8 describes the derivation of exceedance frequencies of flood levels. Section 9 describes the proposed implementation of the framework in the Delft-FEWS software environment, as well as discussing expected computation times. Section 10 draws the main conclusions.

The appendix describes a pilot study for the joint probability approach with comparisons between the performances of the TPT and CRC-CH methods.

1.5 Choice of sampling method

Eventually, the TPT method was chosen as the preferred method *for the current study*, because this method provided the best match between the rainfall IFD curves on one hand and the available synthetic spatio-temporal rainfall patterns on the other hand (see Section 5 for a detailed explanation). The other two methods (CSS and CRC-CH) are nevertheless considered very promising for future applications of Monte Carlo applications, especially if more synthetic spatio-temporal rainfall patterns become available. To document the knowledge on CSS and CRC-CH methods that was developed during the current studies, the report therefore also contains analyses that are specific to these two methods, even though in the end they haven't been used to compute design flows for the Brisbane River catchment flood studies.

The steps in the TPT approach (ARR, 2013) can be summarized as follows:

1. Choose a range of durations around the critical storm duration. For each duration carry out the following steps (2-4):
2. Divide the range of relevant values of the AEP of the rainfall depth into N_b bins of equal size in terms of their standardized normal variate
3. For each bin, take N_s samples of the remaining random variables (initial losses and rainfall patterns) and run the hydrological model to evaluate the conditional exceedance probability of peak discharge and water levels, given the rainfall depth
4. Derive the exceedance probabilities of a range of discharges or water levels through application of the total probability theorem.

The TPT and CRC-CH methods differ in their sampling schemes. The TPT method uses an efficient stratified sampling scheme, which is not incorporated in the CRC-CH approach because the latter uses variable event durations.

2 Proposed computational scheme of the MCS framework

2.1 Flood processes in the Brisbane river catchment

The Brisbane River catchment has a total catchment area of 13,750 km² to the Port Office Gauge which is located in the heart of Brisbane City. The catchment is bounded by the Great Dividing Range to the west and a number of smaller coastal ranges including the Brisbane, Jimna, D’Aguilar and Conondale Ranges to the north and east. Most of the Brisbane River catchment lies to the west of the coastal mountain ranges. The catchment is complex in nature, combining urban and rural land, flood mitigation dams, tidal influences and numerous tributaries with the potential for individual or joint flooding.

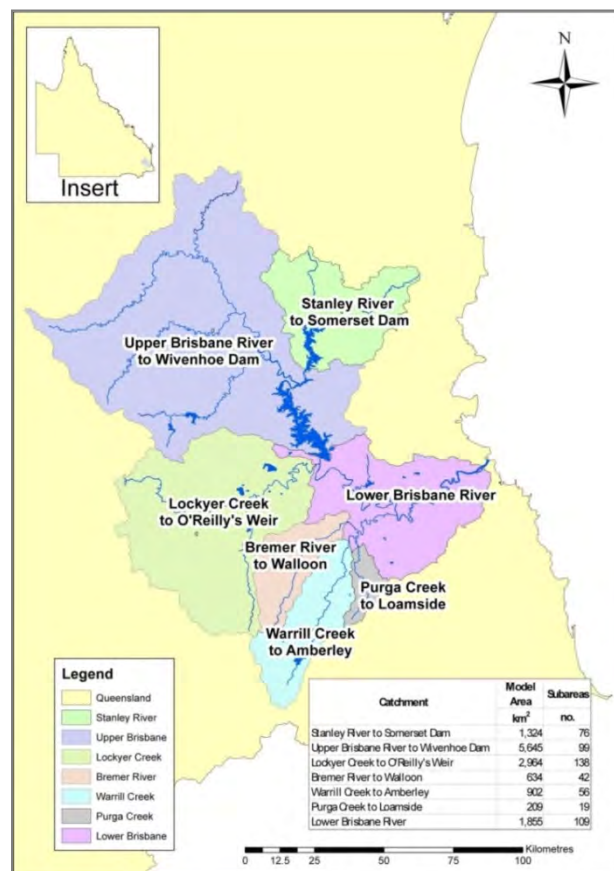



Figure 2-1 Brisbane river catchment, showing the seven sub-catchments of the URBS hydrological model



The Brisbane River has a total length of 309 km. The river system consists of the Brisbane River and six major tributaries. Cooyar Creek, Emu Creek and Cressbrook Creek are all major tributaries of the Upper Brisbane River. The Stanley River catchment is the only major tributary that flows from the Conondale and D'Aguilar Ranges. Lockyer Creek flows from the escarpment of the Great Dividing Range and joins the Brisbane River just downstream of Wivenhoe Dam. The remaining tributary is the Bremer River which rises in the Little Liverpool Range and joins the Brisbane River at Ipswich.

The Brisbane River is tidal to just below Mt Crosby Weir, which is located some 90 km from the mouth of the river. The Bremer River is also tidal in its lower reaches and it is affected by backwater when the Brisbane River is in flood. The Bremer River passes through rural and agricultural land as well as through numerous townships and two major cities. As such, flooding in the river has the potential to affect large numbers of residents and cause damage to businesses and industries.

The Brisbane River itself has two major dams located in its upper reaches, both of which were built to supplement Brisbane's water supply and to provide flood mitigation. Wivenhoe Dam was built in 1984 and has a catchment area of approximately 7,020 km². Somerset Dam on Lake Somerset is located upstream of Lake Wivenhoe on the Stanley River near Kilcoy, and has a catchment area of 1,340 km². Therefore, approximately only half the overall catchment is regulated. There are also numerous smaller dams located within the catchment on the tributaries of the Brisbane River.

The largest recorded gauge heights in the city of Brisbane, since European settlement in 1824, were in 1841 and 1893, with a depth of approximately 6.5 m above the highest tide level (Van den Honert and McAneney, 2011). Both events occurred in the pre-dam situation. The largest flood of the 20th century was in January 1974, when a gauge height of 5.45 m+AHD was recorded at the Brisbane City gauge. During the recent floods of 2011, the peak level at the same gauge reached 4.46 m+AHD. The peak level of the 2011 flood was attenuated due to the mitigating effects of the Wivenhoe dam, which was constructed in response to the 1974 event.

The floods of 1893 and 1974 were both caused by excessive rainfall from decaying tropical cyclones. The 2011 floods were caused by the interaction of a low-pressure system situated off the mid and south Queensland coasts, and monsoonal troughs (Van den Honert and McAneney, 2011). In general, extreme events in the Brisbane catchment are caused by cyclones, East Coast lows and tropical storms. Extreme rainfall events in the Brisbane river catchment occur more frequently during La Niña years and are characterised by several hundreds of millimetres of rainfall over a period of three to five days falling in most parts of the catchment.

The main factors that influence flood levels in the Brisbane river catchment are:

1. **Rainfall depth.** Rainfall is the driving force of flood events and (extremely) high rainfall depths most likely result in (extremely) high flood levels
2. **Event duration.** High flood levels in the Lower Brisbane River are typically associated with periods of three to five days with several hundreds of millimetres falling over most of the catchment. For smaller tributaries, high flood levels can be the results of high rainfall depths occurring in short duration events. The flash flood in the Lockyer catchment in January 2011, causing several fatalities, is an example of such an event
3. **Spatial-temporal distribution of rainfall.** This distribution is relevant because it determines eg the percentage of rainfall falling upstream of the major dams, the co-occurrence of flood peaks from the tributaries and runoff percentages
4. **Antecedent soil moisture conditions (initial losses).** The antecedent soil moisture conditions strongly affect initial rainfall losses and, hence, runoff percentages. For example the 2013 rainfall event occurred after a relatively dry spell and resulted in runoff percentages upstream of the Wivenhoe dam of only about 30%, while runoff percentages during the 2011 event, which occurred after a very wet spell, were in the order of 65%

5. **Reservoir volumes.** The reservoir volumes at the start of a rainfall event largely determines the volume that can be safely stored for the purpose of flood peak attenuation
6. **Ocean water levels:** High ocean water levels can increase flood levels in the Lower Brisbane River and lower Bremer River. Note that ocean water levels do not affect flows in the hydrological model and therefore will not be of influence on design flood flows as computed in the current studies. The ocean water levels “only” serve as input for the hydraulics phase of the Brisbane River catchment flood study

These factors are all incorporated into the MCS framework. This means that the relevant statistical properties of these factors, including mutual correlations, need to be quantified. Furthermore, the influence of these factors on the flood levels needs to be determined. This is done with a combination of a hydrological model and dam operations model, both briefly described in Section 2.2. Section 2.3 provides a brief overview of the MCS framework, which combines the statistics and hydrological modelling. Details of the framework are provided in subsequent sections of the report.

2.2 Hydrological model and dam operations model

The Brisbane River hydrological model was developed by Seqwater and implemented in the URBS hydrological model suite (Carroll, 2012a). The model was calibrated by Seqwater (2013a) and subsequently recalibrated by Aurecon (2014b). In the model, the Brisbane River catchment is divided into seven distinct sub-catchment models (see Figure 2-1) based on review of topography and drainage patterns, major dam locations, key locations of interest for real time flood operations, and consideration of the best use of available data including water level gauges. Dams and reservoirs are modelled within URBS as well, with the exception of Wivenhoe Dam and Somerset Dam. The latter two are modelled in RTC tools, an open source, modular toolbox dedicated to real-time control (RTC) of hydraulic structures like weirs, pumps, hydro turbines, water intakes, etc. Figure 2-2 and Figure 2-3 show the computational workflow for the ‘no dams’ and ‘with dams’ scenarios. More details on the hydrological and dam operation models are provided in Section 7.

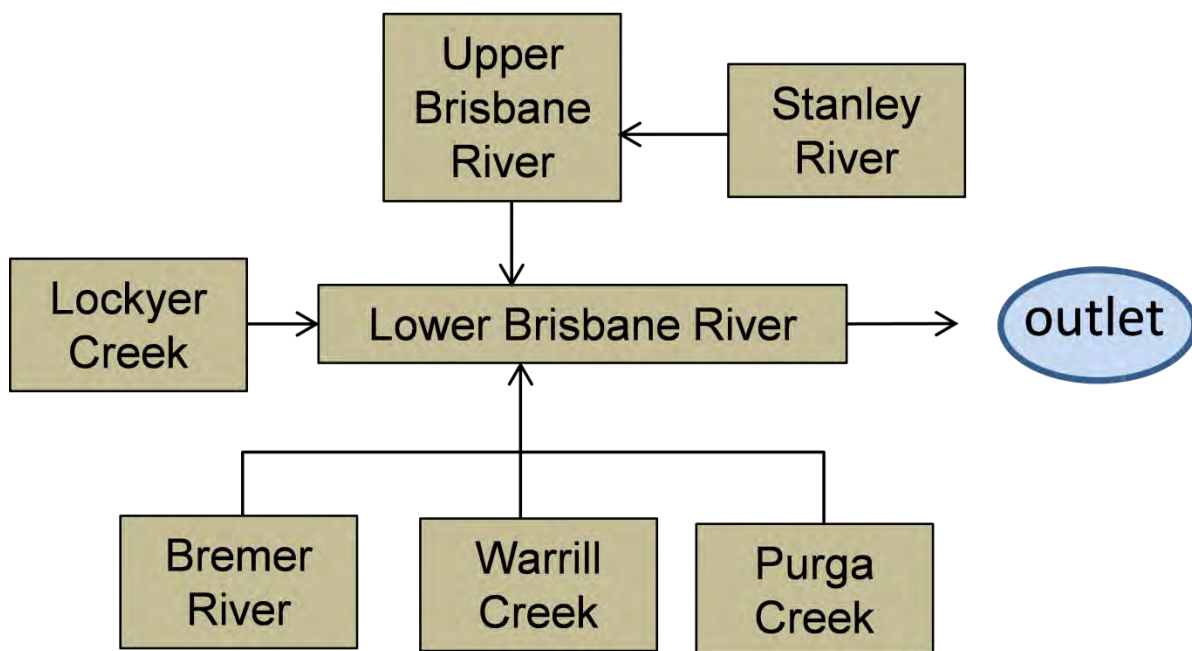


Figure 2-2 Computational workflow for the ‘no dams’ scenario

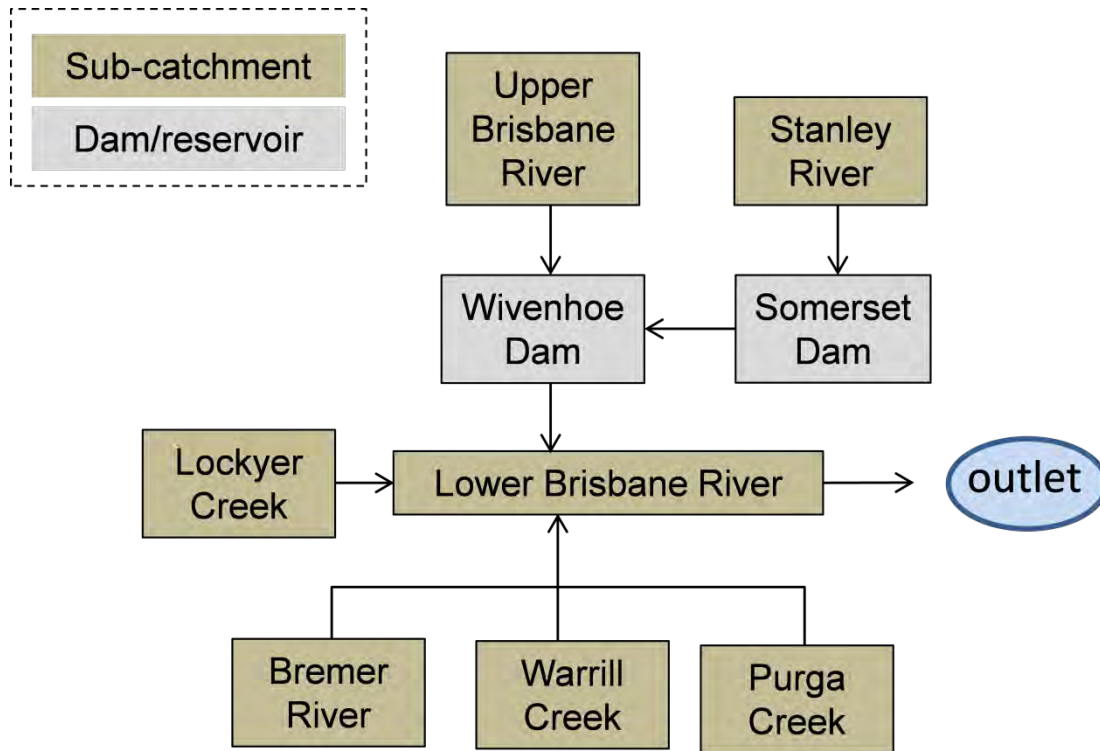


Figure 2-3 Computational workflow for the 'with dams' scenario

2.3 Monte Carlo Simulation workflow

Figure 2-4 shows the computational scheme of the proposed setup of the MCS framework and the chapters in which each component is described. The procedure in this Figure is carried out separately for each river location/gauge of interest. The scheme can be applied for a TPT or CRC-CH based sampling method (see Section 3 and Appendix A for an explanation of these methods), but also for potential alternative sampling strategies.

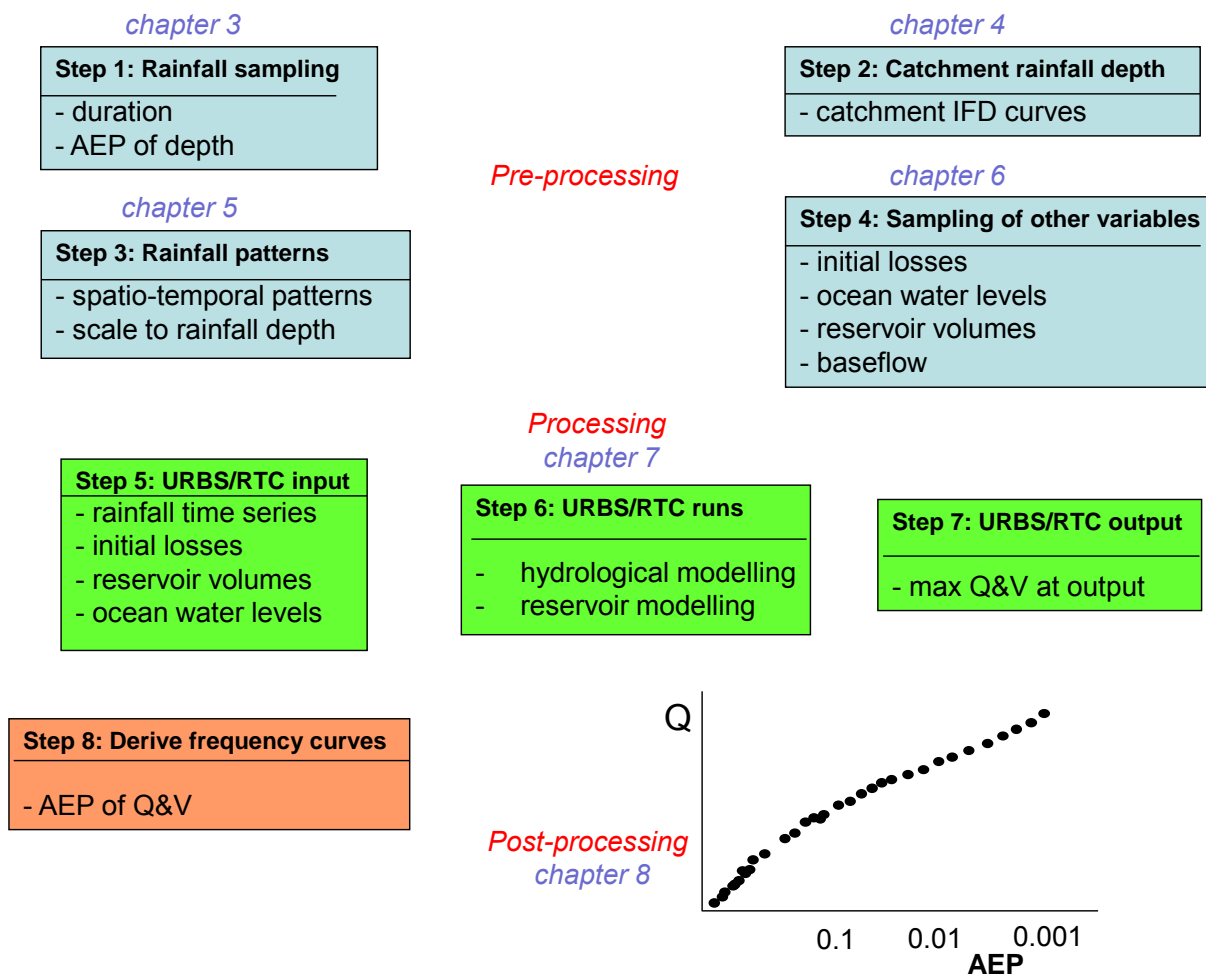


Figure 2-4 Schematic view of the proposed Monte Carlo Simulation framework. It also shows the chapters in which each component is described.

The three stages of Figure 2-4 and the steps of the computation can be summarised as follows.

- I. *Pre-processing (steps 1-4)*: Generate N synthetic events, characterized by rainfall depth, rainfall duration, spatial and temporal distribution of rainfall, initial losses, reservoir volumes and ocean water levels. In the sampling process, mutual correlations between these variables are taken into account
 1. For each event, select (TPT-method, see chapter 3) or sample (CRC-CH method, CSS method, see chapter 3) the rainfall duration and the AEP of the rainfall depth
 2. For each event, derive the catchment-average rainfall depth, based on the duration and AEP of step 1. Here, the catchment refers to the upstream catchment of the river gauge/location under consideration. Two alternative methods are available for this purpose:
 - a. Use the available IFD curves from the Bureau of Meteorology (Green et al, 2012) and CRC-FORGE correction factors for more extreme events to derive point rainfall intensities for each of the sub-area of the URBS model. Subsequently apply an Areal Reduction Factor (ARF) to the rainfall intensities (ARR, 2013c) and derive the catchment average rainfall depth
 - b. Derive the catchment average rainfall depth directly from catchment-averaged IFD curves. These curves have been derived from series of observed catchment averaged rainfall depths

- Option a is implemented in the framework, option b was used as a verification
3. For events with rainfall AEP > 1/2000, sample one of the synthetic rainfall patterns as generated by the BoM stochastic space-time simulation model and reported in SKM (2013) and Jacobs (2014) and scale the rainfall intensities of these patterns in such a way that the catchment average total rainfall depth of each event is in accordance with step 2. For events with rainfall AEP < 1/2000, GTSMR based patterns (BoM, 2003) are used to model the spatio-temporal rainfall distribution
 4. For each event, sample initial losses, reservoir volumes, ocean water levels and baseflow. In the sampling process, mutual/spatial correlations and correlations with rainfall intensities are taken into account where relevant. Continuing losses are assumed a function of the AEP of the rainfall. This function is derived in the reconciliation process, where MCS results are compared with results of other methods
- II. *Processing (steps 5-7):* Simulate the N synthetic events with the URBS hydrological model and RTC dam operations module and derive the (N) peak discharges and flow volumes at the catchment outlet
5. Prepare input files for the URBS/RTC models, based on the sampled values of steps 1-4
 6. Simulate the N synthetic events with the URBS hydrological model and RTC dam operations model
 7. Derive the N peak discharges and flow volumes at the catchment outlet
- III. *Post-processing (step 8)*
8. Apply MCS post-processing to peak discharges and flow volumes for a set of pre-defined Average Return Intervals (ARI) or Annual Exceedance Probabilities (AEP)

The computation scheme of Figure 2-4 provides what is required for the BRCFS-hydrology phase: a joint probability approach for the derivation of design flows and volumes, taking into account spatial and temporal variation of rainfall over the Brisbane River catchment. The above description of the MCS framework is very general. Details will be given in the subsequent sections of this report.

2.4 Separate simulations for each location of interest

In total 23 different locations within the catchment have been identified for assessment in the Brisbane River catchment study. During the early stages of the project it has been suggested by the IPE that a single simulation might be sufficient to generate representative rainfall for the downstream and upstream locations simultaneously. This would indeed be the case if the spatial and temporal patterns accurately describe the probability distributions of all sub-areas in the catchment. However, the authors believe that this is not the case. As explained in Section 2.3, the synthetic rainfall patterns generated by the BoM stochastic space-time simulation model will be scaled in such a way that they correspond to the areal rainfall statistics. Since each location of interest has its own drainage area and therefore its own areal rainfall statistics, the rescaling needs to be done separately for each output location of interest.

Nevertheless, it can be expected that for some clusters of output locations a single run will provide similar results as the proposed approach in which separate runs are carried out for each location individually. This might be the case for the cluster of locations along the Lower Brisbane River (Savages crossing, Mount Crosby weir, Moggill, Centenary Bridge and Brisbane). For the moment, this option is not implemented in the framework, but this could be facilitated if desired.



3 Rainfall sampling methods

3.1 Introduction

The choice of sampling method is crucial for the BRCFS-hydrology phase. There are several candidate methods, each with their own advantages and disadvantages. Currently, there are two published MCS methods for estimating design floods in Australia: the Cooperative Research Centre – Catchment Hydrology (CRC-CH) method (Rahman et al, 2001; 2002) and the Total Probability Theorem (TPT) method (see eg ARR, 2013a). The TPT and CRC-CH methods differ in their sampling schemes, but also in the type of rainfall statistics that is used. CRC-CH method uses storm event statistics, whilst the TPT method is based upon storm burst statistics. These differences will be discussed in the current section. Furthermore, an alternative sampling method, the Complete Storm Simulation (CSS) Method, is introduced.

3.2 Brief description of methods


The steps taken in the CRC-CH methodology (Rahman et al, 2001; 2002) can be summarized as follows:

1. Sample the storm event duration
2. Sample the rainfall depth, conditioned on duration, from IFD curves
3. Sample a rainfall temporal pattern
4. Sample the initial loss
5. Run the rainfall runoff-routing model to derive the peak discharge or peak water level at the catchment outlet

More details on the method can be found in Appendix A.

The steps in the TPT approach (ARR, 2013) can be summarized as follows:

1. Choose a range of durations around the critical storm duration. For each duration carry out the following steps (2-4):
2. Divide the range of relevant values of the AEP of the rainfall depth into N_b bins of equal size in terms of their standardized normal variate
3. For each bin, take N_s samples of the remaining random variables (initial losses and rainfall patterns) and run the hydrological model to evaluate the conditional exceedance probability of peak discharge and water levels, given the rainfall depth
4. Derive the exceedance probabilities of a range of discharges or water levels through application of the total probability theorem



The TPT and CRC-CH methods differ in their sampling schemes. The TPT method uses an efficient stratified sampling scheme, which is not incorporated in the CRC-CH approach because the latter uses variable event durations. The CRC-CH method is therefore considered unsuitable for extreme floods (Mirfenderesk et al, 2013). This is for instance demonstrated in the paper of Rahman et al (2002b), which showed a significant variability of estimated peak discharges for high Average Return Intervals (ARI). This could be resolved by increasing the number of samples. However, that would lead to millions of hydrological model runs to reduce the variability to a desired level for low values of the AEP, making the method untenable.

For this reason, an alternative approach was trialled to replace crude Monte Carlo sampling scheme as commonly applied in the CRC-CH method by “importance sampling”. Importance sampling (Engelund & Rackwitz, 1993; Koopman et al, 2009) is a Monte Carlo sampling technique in which the percentage of extreme events can be increased by adapting the sampling distribution functions. The applicability of the method was tested for a hypothetical catchment, similar to the example used by Rahman et al (2002). Details are presented in the appendix of this document, results are briefly summarised here.

Both the crude Monte Carlo and importance sampling approaches were applied using $N=20,000$ simulated storm events, representing a series of 4,000 years (5 storms per year on average). The procedure was repeated 10 times to assess the variability in the Monte Carlo estimates, and the results are shown in Figure 3-1. Two disadvantages of the crude Monte Carlo sampling method are clearly demonstrated in this graph:

- The variation in estimated design discharges increases with decreasing value of the annual exceedance probability
- For annual exceedance probabilities that are smaller than the reciprocal of the number of simulated years (4,000 in this case) there are no estimates available

If importance sampling is applied, the variance in estimated peak discharges decreases dramatically and estimates are available for a much wider range of AEPs. This clearly demonstrates that the CRC-CH can also be applied for extremely low AEPs without the need for millions of model simulations. This creates opportunities for using the CRC-CH method in applications where probabilities of extremes are relevant, such as dam design studies.

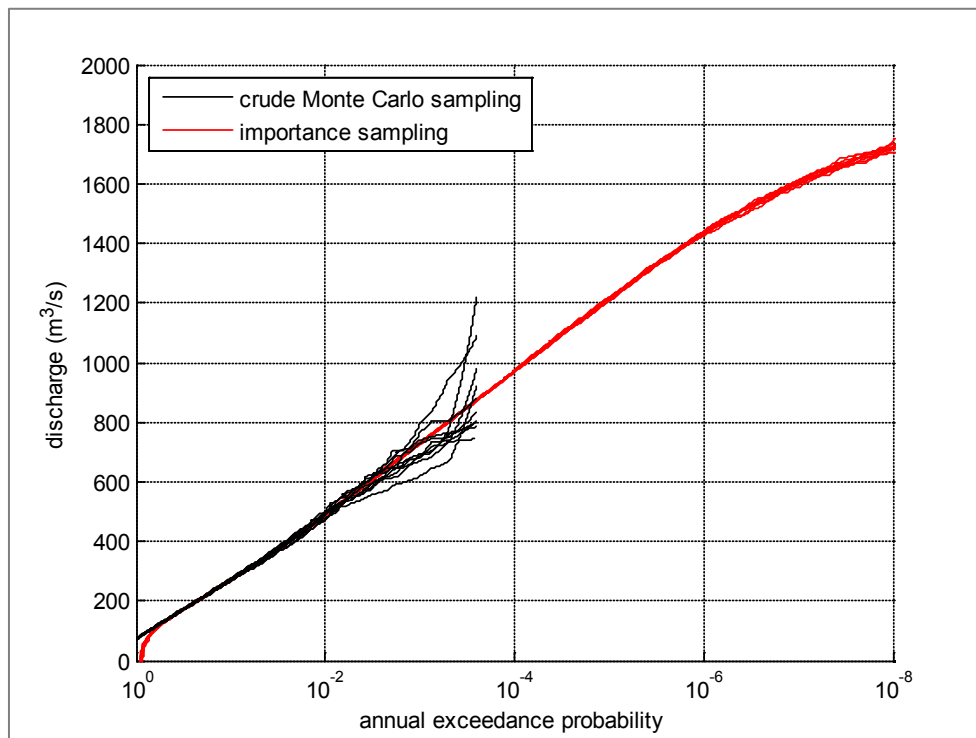


Figure 3-1 Annual exceedance probability and corresponding peak discharges as estimated from 10 different MC runs with crude Monte Carlo and 10 different MC runs with Monte Carlo with importance sampling: 20,000 samples

During the initial stages of the BRCFS it was proposed to explore a third method, which was referred to as Complete Storm Simulation (CSS) Method. The essence of this third method is as follows:

1. Derive distribution functions for the area-average rainfall depths from historical records in each of the sub-catchments of the Brisbane River (Figure 3-2)
2. Sample the catchment total rainfall depth from the fitted distribution for the catchment under consideration
3. Select a synthetic space-time rainfall field from the BoM model and scale this event in such a way that the rainfall depth is in accordance with step 2

Like the CRC-CH, the CSS approach is based on event statistics. However, no use is made of IFD tables. The duration of rainfall is determined by the synthetic rainfall patterns from the BoM (see Section 5). It is assumed that the synthetic rainfall patterns represent the distribution of storm durations for a given rainfall depth. This assumption is a weak point of the CSS approach, which needs to be addressed.

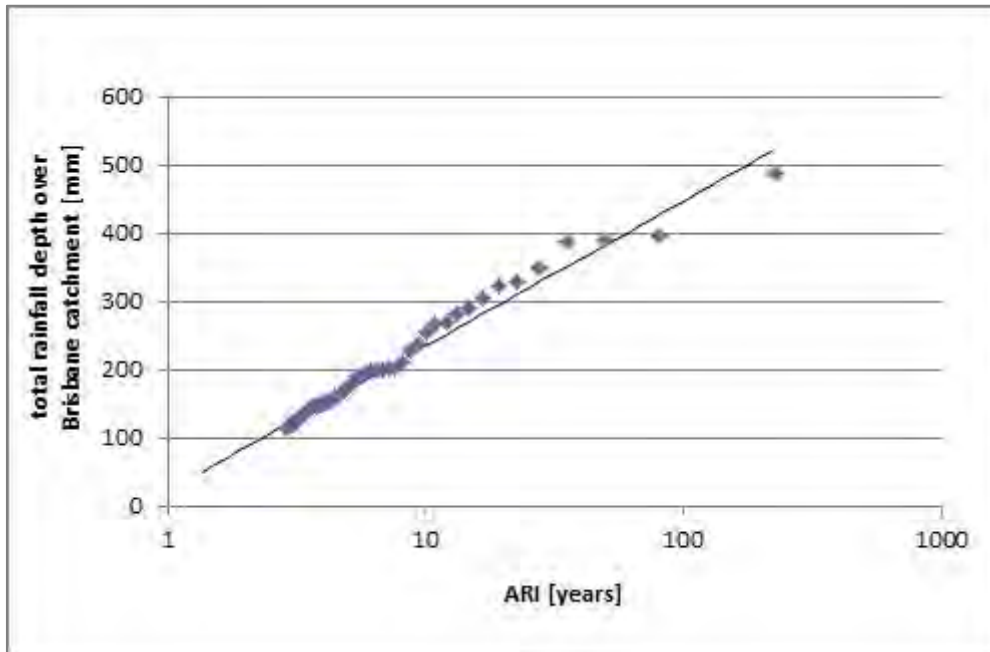


Figure 3-2 Fitted GPD distribution function to the average rainfall depths over the full Brisbane catchment of 44 calibration events obtained from Seqwater

3.3 Required input statistics

The TPT, CRC-CH and CSS differ in the type of rainfall statistics that are used. The TPT method is based on storm burst statistics, the CRC-CH and CSS are applied to storm event statistics (even though CRC-CH could also be applied to bursts statistics). This is reflected in a number of other differences between the methods:

- The CRC-CH method takes the storm duration as a random variable; the TPT method considers a fixed set of potentially critical durations and selects the maximum peak discharge over the considered durations. The duration is not a random variable in the TPT approach but rather a yardstick to measure rainfall depth. The CSS method does not consider the duration explicitly as a random variable, the duration of rainfall is determined by the synthetic space-time rainfall fields from the BoM
- The CRC-CH and CSS methods use a parameter, λ , which represents the number of events per year. The TPT method uses rainfall statistics that is already defined in terms of exceedance probabilities per year
- As a consequence of the difference in rainfall statistics (burst- versus event-based), the distributions of other random variables differ between TPT method on the one hand and CRC-CH and CSS methods on the other. However, the probability distributions of initial losses, initial reservoir storage levels and temporal patterns should be consistent with the rainfall statistics (see Section 3.6)

3.4 Rainfall duration

The probability distribution of event durations is required in the CRC-CH approach and can be derived from observed durations of historical events. For this purpose, an exponential function is fitted to the observed durations. This was done for three test-locations in the upper Brisbane River Catchment: Ravensbourne, Emu Creek and Kirkleagh. The results are shown in Figure 3-3. Trend lines have been fitted to the various stations results to highlight the difference in behaviour. It appears that the duration

distributions of Ravensbourne and Emu Creek are similar, whereas the rainfall events recorded at the Kirkleagh station tend to last longer. This is likely due to its location closer to the coast.

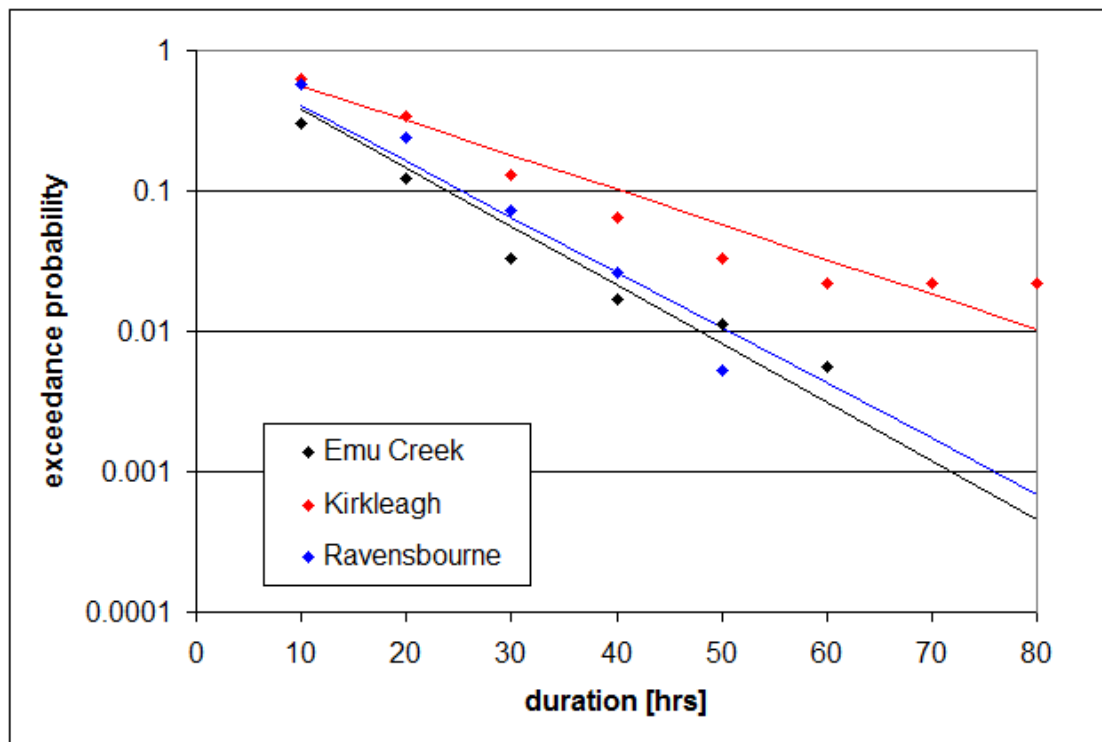


Figure 3-3 Probability distribution of event duration for three test-stations in the upper Brisbane

The duration statistics depend on the definition of an event. Using a definition with a long dry period before and after the event leads to aggregation of short events to fewer long events. Thus, a long dry period shifts the distribution to longer durations. This will be further elaborated in Section 4.2.2.

3.5 Advantages and disadvantages of the sampling methods

3.5.1 CRC-CH versus TPT method

The CRC-CH method is referred to as conceptually superior to TPT by Mirfenderesk et al [2013]. The CRC-CH methodology considers whole storm events and is therefore more suitable for volume-sensitive applications, compared to the TPT method (Carroll, 2012b, Aurecon, 2013a). Although it is suggested that the CRC-CH method is not suitable for extreme floods (Mirfenderesk et al, 2013) because of sampling requirements, it was demonstrated in section 3.2 that this can be solved through application of importance sampling. The latter implies that the CRC-CH is an attractive alternative for the TPT, particularly for applications where runoff volumes are important as is the case for the Brisbane River Catchment Flood Study.

The TPT method has some practical advantages over the CRC-CH method. First of all, the methodology builds on the existing Design Event Analysis (DEA) and will therefore be more readily taken up by the industry's practitioners (Mirfenderesk et al, 2013). Related to this issue is the fact that the available IFD curves from the Bureau of Meteorology can be applied directly in the TPT method to quantify the natural variability in rainfall intensities, since these IFD curves were derived using storm bursts. For the event-based CRC-CH method, these curves need to be transformed to IFD curves

based on events, which means an empirical relationship is required that will introduce additional uncertainties and, potentially, errors. A better alternative for the CRC-CH approach would be to derive IFD curves for events directly from rainfall data, but this would be a costly and time-consuming process. Furthermore, their derivation inherently requires a degree of subjectivity in terms of the definition of an “event”, and such a definition may have significant influence on the resulting design discharges. For instance, in the original paper on the CRC-CH method (Rahman et al, 2002) an event is defined as “a period of ‘significant rainfall’ that is separated from previous and subsequent events by a ‘dry period’ of e.g. 6 hours”. For example, this would mean that two subsequent days with high rainfall in the afternoon hours would be considered as separate events, while for the Brisbane River catchment the combined rainfall in these two days may actually be critical. For bursts, this dilemma plays no role, as the definition of bursts and associated statistics are well-defined.

A disadvantage of the TPT approach is that the concept of a single critical duration may introduce a probability bias, for example if in reality several durations contribute to the exceedance probability. For larger catchments that consist of multiple sub-catchments, each having their own runoff characteristics, it is very well possible that several rainfall durations contribute to the probability of an extreme discharge.

A summary of the two methods is provided in Table 3-1.

Table 3-1 Summary of advantages and disadvantages CRC-CH and TPT

Feature	CRC-CH	TPT
Flood Volumes	✓	x
Extreme Events	x	✓
DEA		✓
IFD (BoM)	x	✓
Event Definition	x	
Probability Bias		x

3.5.2 CSS methodology

The main potential advantage of the CSS method is that statistical extrapolation is applied on total rainfall depth instead of rainfall intensities. This seems to fit better with a relatively large area like the Brisbane River catchment, where total volumes are more relevant than short intensities. Furthermore, the CSS method has the advantage that it appears to be rather straightforward in application.

The CSS approach does not make use of IFD tables. It assumes that synthetic storms are available that characterizes the depth duration relationship, in this case we propose using the synthetic BoM storm patterns. According to the BoM (Alan Seed, personal communication) these patterns may not be representative; the patterns are plausible realisations of rainfall events, but they cannot be considered to represent a correct distribution of event durations. This may introduce a bias in the CSS approach if certain durations are under- or overrepresented in the set of storm patterns.

The CSS approach has not been applied before, which means the application within the BRCFS is somewhat experimental. In order to verify the critical assumption of the method that the BoM storm patterns represent a correct distribution of storm durations, event-based IFD tables were derived from the time series generated by the CSS method. This allows for validation of the method that is needed to obtain the same level confidence as for the other two methods. This validation is carried out in Section 5.4.4.

3.5.3 Conclusion

The TPT approach is most likely to be accepted by 'the industry', because it is built on the DEA approach and uses the well-established BoM burst IFD tables. The CRC-CH methodology on the other hand has the potential of better inclusion of long duration events and volumes, which is critical for the Brisbane River catchment. The practical applicability of the CRC-CH method depends on the existence of a reliable transformation procedure of burst statistics into event statistics, which is explored in Section 4. The CSS method is similar to the CRC-CH method, but focuses on total catchment event depth. All three methods fit within the proposed Delft-FEWS framework of Section 2.

3.6 Consequences for other random variables

The choice for burst- or event-based rainfall statistics has a number of consequences for the probability distributions of other random variables in the Monte Carlo sampling. This concerns the variables that are correlated with the rainfall. For independent variables (eg surge level¹) the probability distribution does not depend on the choice of rainfall statistics.

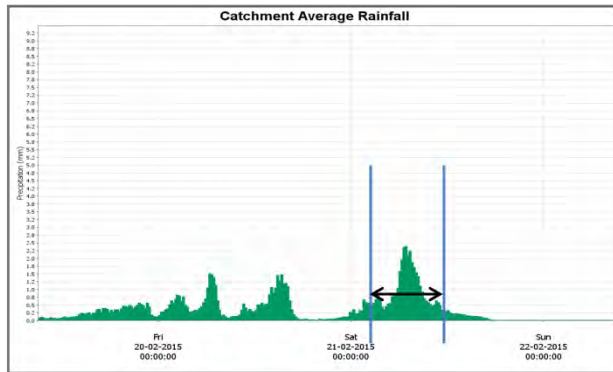
Two of these correlated random variables are the initial losses and initial reservoir storage levels. Their values depend on the starting point of the hydrological model simulation. If the hydrologic simulation is undertaken only for a burst rainfall period, then the initial loss will be lower and the reservoir levels higher, due to pre-burst rainfall. In contrast, if the simulation is done for complete storm events, there is no pre-burst rainfall because all rainfall is included in the pluviograph. Consequently, the initial losses will be higher and the reservoir levels at the start of the simulation are more likely to be lower.

In the proposed MCS method of Figure 2-4, use is made of spatio-temporal patterns of synthetically generated rainfall events. These events are selected and rescaled in such a way that the sampled burst depth of the catchment under consideration is replicated. These events will also provide a pre-burst rainfall which will automatically lead to a decrease of initial losses at the moment the actual burst starts. In the TPT method, which uses bursts, a correction is therefore applied on the initial losses that takes this pre-burst rainfall into account. The correction is based on the amount of pre-burst rainfall in the selected synthetic rainfall pattern. This means all pre-burst rainfall of the synthetic pattern is subtracted from the initial loss, taking into account that initial losses cannot be less than zero.

For reservoir levels, similar corrections are required. However, statistics of initial water levels are derived from simulations with rainfall bursts, which means the correction for initial reservoir volumes is needed for the event based methods like CSS and CRC-CH. The proposed correction is to add the volume equivalent of the net rainfall to the initial reservoir volumes.

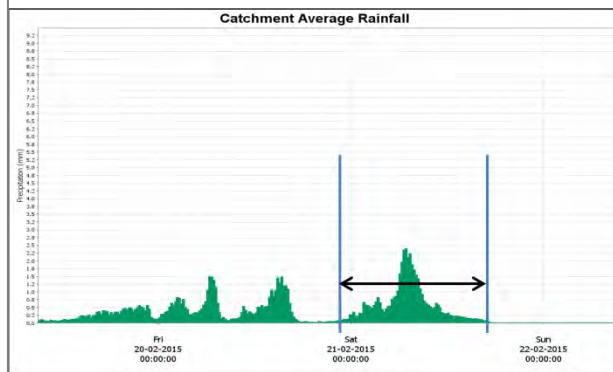
The spatial and temporal storm patterns that are used to distribute the average rainfall over space and time should be consistent with the choice for a burst- or event-based sampling. The typical rainfall pattern for a complete storm event differs (more variable) from that of a short period of intense rainfall within that storm (more uniform). Carroll & Rahman (2005) quantify this variability through parameterization of temporal patterns using the multiplicative cascade model. In our approach this is automatically taken care of by the synthetic rainfall patterns. In the event based CRC-CH approach, a synthetic rainfall pattern will be selected for which the total depth and duration are in accordance with the depth and duration as sampled from the probability distributions. For the burst-based TPT approach, a synthetic rainfall pattern will be selected which contains a burst period for which the total depth and duration are in accordance with the sampled depth and duration. These differences in selection procedures of storm patterns will automatically result in patterns that are consistent with the considered approach (burst versus event).

¹ "Independent" in this case refers to the fact that ocean water levels are not influenced by rainfall. Note, however, that in a *statistical sense* these two variables are dependent.



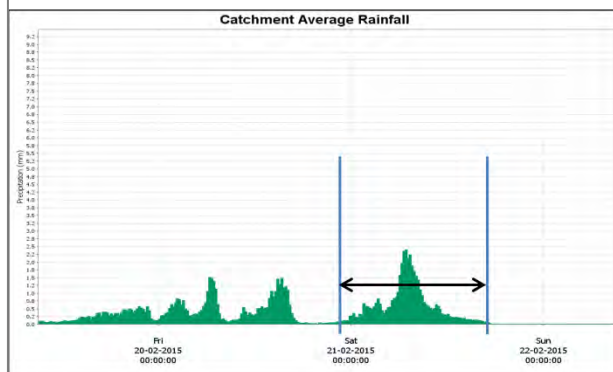
TPT method

- Burst duration is fixed
- Pre-burst & post-burst rainfall excluded
- Stochastic event selection based on burst duration and burst rainfall depth



CRC-CH method

- Duration is variable and defined as event instead of a burst
- Stochastic event selection based on event duration and event rainfall depth



CSS method

- Duration is variable and defined as event instead of a burst
- Stochastic event selection based on event rainfall depth only

Figure 3-4 Schematic view of the TPT, CRC-CH and CSS methods



4 Derivation of catchment rainfall depth

4.1 Introduction

This section discusses the rainfall statistics which is arguably the most important input variable to the hydrological model. Rainfall statistics are generally described by an Intensity-Frequency-Duration (IFD) table. The rainfall in the IFD curve is the rainfall depth (mm) over a given time interval [Chow, Maidment and May, 1988]. Alternatively, the total rainfall depth (in mm) is given, which is equal to the rainfall intensity multiplied by the duration. In the current report rainfall *depth* is generally used instead of *intensity*. It was nevertheless decided to maintain the term “IFD” to refer to rainfall statistics as this is the terminology that the reader is most likely familiar to.

There are two fundamentally different ways of deriving rainfall statistics: The first approach is to define a ‘window’ of fixed duration and to measure the average rainfall over this window. The annual maxima (AM) or peaks over threshold (POT) in this series form the basis for the IFD *burst*-tables that were derived by the Bureau of Meteorology (BoM) and CRC-FORGE. The second approach is to identify rainfall *events* and to construct a bivariate probability distribution of event duration and average rainfall for these events. In the first case, the duration is a yardstick that is used to measure rainfall depth. In the latter case, the duration is a property of the event that has a probability distribution of its own.

The BoM IFD tables were created by analysing rainfall records from a single gauging station and applying a time interval of some duration as a yardstick to measure total rainfall depth over that duration. Hence, the durations in these IFD tables are not related to the duration of actual rainfall events. A duration in the BoM IFD table can be an excerpt from a much longer rainfall event. The BoM does not provide event-based IFD tables.

To establish event-based IFD tables from raw rainfall time series data is extremely laborious. The CRC-FORGE project has taken many BoM staff years to complete the burst IFD tables. Moreover, these burst-IFD tables are now considered a standard reference and it is highly desirable to be able to use these tables as a basis for the BRCFS. On the other hand, as stated in the previous chapter, there are some advantages in using events statistics in the joint probability approach, which is why these statistics are preferred in the CRC-CH and CSS methods. In order for these methods to become ‘standard practice’, event statistics should become available without having to redo the laborious work of the BoM. The solution may be found by establishing a link between the required event-IFD tables and the BoM burst-IFD tables.

To relate event-IFD tables to burst-IFD tables, general expressions for the IFD relations are first derived. The coefficients of these relations can be fitted to observational data or to the BoM IFD tables. Next, a transformation procedure is derived to generate event-IFD tables from burst-IFD tables.

In Section 4.2 and Section 4.2.6, differences between burst statistics and event statistics are discussed and a mapping relationship between burst- and event-IFD tables is proposed. Section 4.3 describes the transformation from point IFD tables to catchment IFD tables.

4.2 Events versus bursts IFD tables

4.2.1 Burst-IFD tables

The BoM IFD tables are sometimes referred to as ‘burst’-IFD rainfall tables. These tables describe the probability that the rainfall depth over a given duration exceeds a given value in any one year. The duration is a yardstick that is used to measure the rainfall depth. It has no probability distribution. A set of IFD tables for Australia were derived by the BoM in 1987 and included in Volume 2 of ARR (1987). A Log-Pearson Type III distribution was fitted to the annual maximum series of the available rainfall data at the time using the method of moments.

A revision of the IFD tables was carried out in 2012-2013. Notable differences to the 1987 study are the use of a Generalised Extreme Value (GEV) distribution and different fitting procedures: for the short duration rainfall, a Bayesian Generalised Least Squares Regression (BGLSR) was used (Johnson et al, 2012a) and for the longer durations the L-moments fitting procedure (Hosking and Wallis, 1997). A spatial smoothing method was applied to obtain a spatially coherent signal as well as remove the inherent noise in the point data from rain gauges (The, 2012). The interaction between topography and rainfall was taken into account and an adjustment for inconsistencies across durations and AEP was applied.

The updated IFD tables for locations in Australia are made available through the BoM website www.bom.gov.au. The burst-IFD information for various probability ranges will be obtained from different sources (see Aurecon, 2014a):

- For T=1 to 100 (AEP = 63% to 1%): the IFD curves from the BoM are used
- For T=100 to 2000 (AEP = 1% to 0.05%): the results from CRC-FORGE are used. These are defined in terms of growth factors (ratios to the 1% AEP). The CRC-FORGE tables are valid up to five-day duration. For longer durations, the table are extrapolated
- For T>2000 (AEP < 0.05%): the IFD of the PMP are used as the reference. For this, the AEP of the PMP is estimated using the procedure described by Laurenson and Kuczera (1999). The result for shorter durations are extrapolated to get the PMP for durations longer than five days. Between 0.05% and AEP of PMP the intensities are interpolated using the ARR (1999) method. Beyond the AEP of the PMP, the intensities are extrapolated on log-log scale

4.2.2 Event-IFD tables

In contrast to the burst-IFD tables, the event-based IFD tables are derived by first defining and identifying rainfall events. Next, a bivariate probability distribution of duration and rainfall depth can be constructed. This distribution gives the probability in any given year of the occurrence an event of a specified duration during which a specified rainfall depth is exceeded. It thus includes the probability of an event exceeding a specified duration. Taking the probability distribution of durations out of the bivariate event rainfall distribution leads to an event-IFD table that looks similar to the burst-IFD table, although the two tables are fundamentally different because of their differing assumptions.

The conditional probability of rainfall depth (R) on duration (D) can be described as:

$$P(R | D) = \frac{P(R, D)}{P(D)} \quad (1)$$

Where duration $P(D)$ is assumed to be exponentially distributed.

An event can be defined, for example, by defining the event as the rain period between two relatively dry spells for example as adopted by Rahman et al, 2002. The rain periods are easily found, especially for extreme events. The preceding and post event dry spells are the critical part of the event definition. Specifically, the maximum rainfall during the dry spell and the minimum duration need to be specified. The choice for a definition will influence the number of events and their statistics. Rahman et al. (2002) define an event by pre- and post-event dry spells of six hours duration each. The average rainfall over the six-hour dry period must be smaller than 0.25 mm/hr and no single hour during the dry spell should have more than 1.2 mm of rainfall. However, other definitions are possible.

Figure 4-1 shows the frequency distribution of event durations at Emu Creek, for several lengths of the dry period before and after the rainfall event. The graph shows that using a longer dry period in the event definition leads to fewer short duration events and more long duration events, as a result of aggregation of several short rainfall events to fewer long events. The choice of event duration distribution clearly depends on the rather subjective definition of the beginning and ending of an event. Furthermore, duration statistics also depend on the number of events considered in a year, since usually only the “larger” events are relevant.

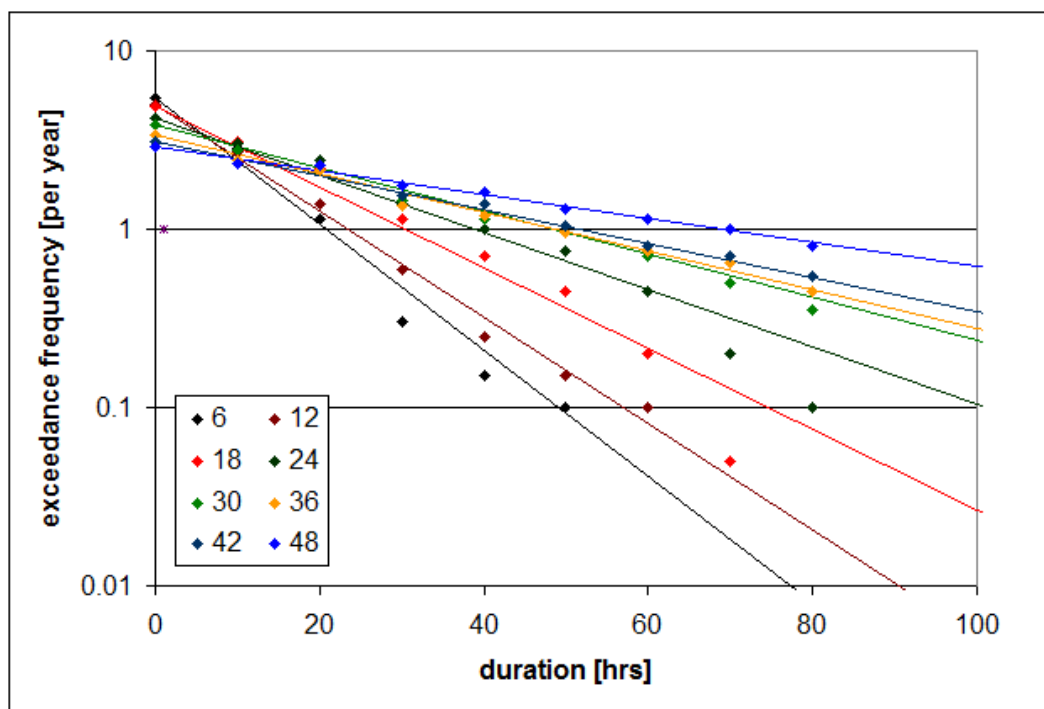


Figure 4-1 Frequency distributions of event durations from rainfall data at Emu Creek, for various durations (from 6 to 48 hours) of the dry period before and after the event in the definition of a rainfall event

Rahman et al (2002) used an exponential distribution to the empirical duration exceedance frequencies of selected events, and this approach was adopted in the current studies. Figure 4-2 indicates that durations of storm events at Emu Creek indeed obey an exponential distribution with an average duration of about 22 hours. In this case, events were selected that exceed a threshold rainfall depth that was chosen such that 5 events per year were selected.

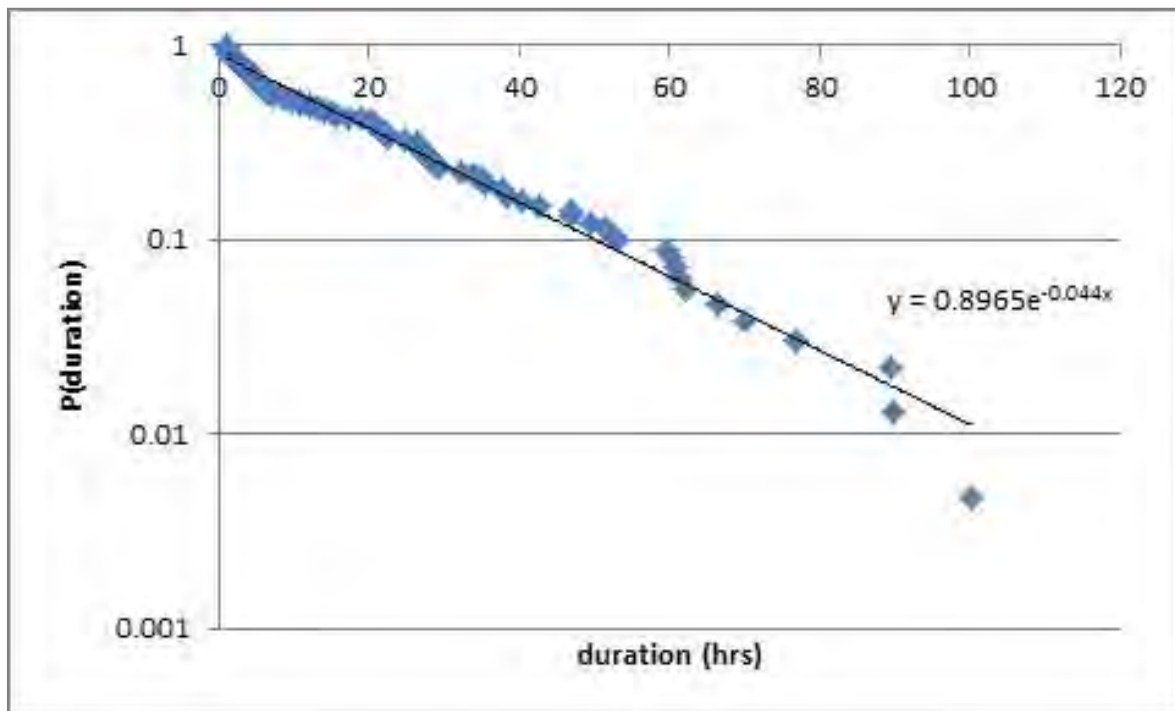


Figure 4-2 Fit of the exponential distribution function through empirical frequencies of observed event durations at Emu Creek

Once the rainfall events have been identified, the procedure (based on Rahman et al 2002) to derive event-IFD tables is as follows:

- For each event, determine the total duration, rainfall depth and mean rainfall depth
- Classify the events in duration classes. For the analyses presented in the next sections, six classes were used (2-4, 4-6, 6-10, 10-16, 16-24 and >24 hours)
- Define a 'representative duration' per class, typically the median duration of all events in that class
- Rescale the depth of all events in a class to the representative duration, using an empirical log-log relationship between depth and duration within the class
- Compute the statistics of the intensities per class as the probability of exceedance of a rainfall depth, given an event occurring that falls in that duration class

The IFD table derived in this way defines the probabilities of rainfall depths for a rainfall event, conditional on the duration. To derive event-IFD tables for all sub-areas in the Brisbane catchment using this procedure would require processing of hundreds of time series from BoM rainfall gauging stations and applying the same smoothing and adjusting of IFD coefficients as was done in the CRC-FORGE or the BoM IFD revision project. This is beyond the scope of the BRCFS. Instead, a region-wide mapping of burst-IFD tables to event-IFD tables is attempted (see Section 4.2.3).

4.2.3 General description of IFD relations

The recently developed IFD tables for locations in Australia are made available through the BoM website www.bom.gov.au. They can also be derived from a sixth order polynomial and a set of coefficients A-G that differs per location:

$$\ln(\text{depth}) = A + B \ln(\text{dur}) + C \ln(\text{dur})^2 + D \ln(\text{dur})^3 + E \ln(\text{dur})^4 + F \ln(\text{dur})^5 + G \ln(\text{dur})^6 \quad (2)$$

Where depth is expressed in mm and duration (dur) is expressed in hours. This empirical relation can be simplified to a first order relation, thus neglecting the second and higher order terms as:

$$\ln(\text{depth}) = A + B \ln(\text{dur}) \quad (3)$$

Figure 4-3 is a log-log plot of event-depth and duration and a regression line from which the coefficients A and B can be derived. In this case, A is equal to 1.67 and B is 0.50. The regression can be limited to the most extreme events only, which is shown by the second regression line (A=2.83, B=0.46) in Figure 4-3. However, the selection of the most extreme events (highest ARI) is done using equations (4) and (5), which requires the coefficient B. The process thus becomes iterative.

Next, the relationship is generalized to include a dependency on annual exceedance probability (AEP), or in this case Annual Recurrence Interval (ARI), which is the inverse of the exceedance frequency F. To do so, it is first assumed that the coefficient B in equation (3) is independent of ARI.

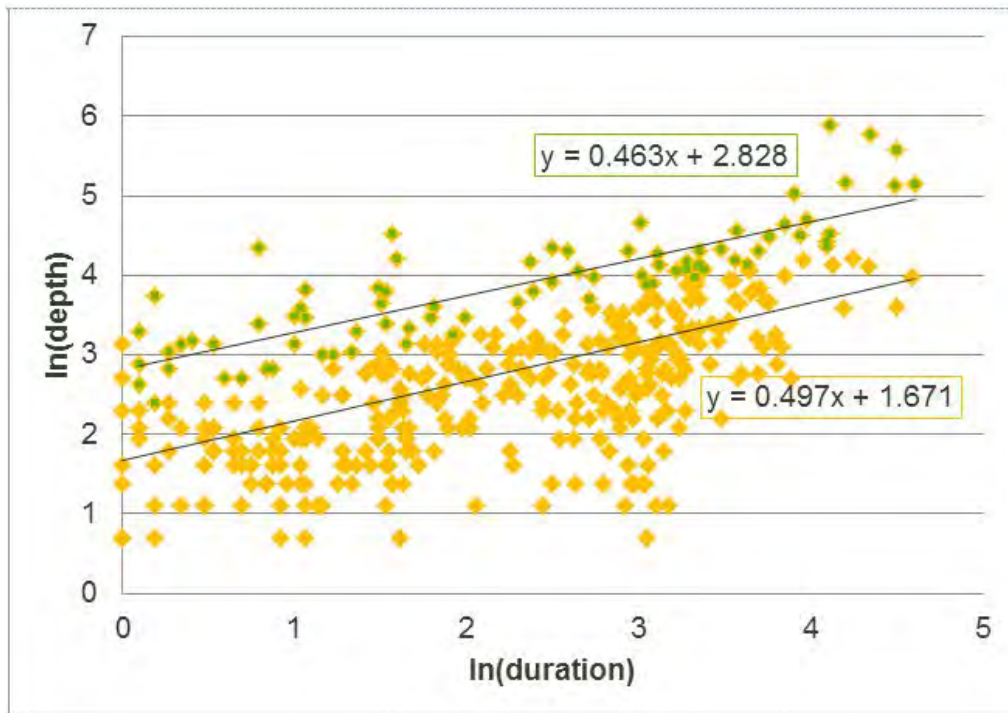


Figure 4-3 Double-log plot of event depth (mm) versus duration (hrs), example from Emu Creek data. Two regression lines are shown: for all events (orange) and for the most extreme events only (green)

Next, the extremity of each event-depth is determined as the deviation from the regression equation (3):

$$A = \ln(\text{depth}) - B \ln(\text{dur}) \quad (4)$$

Or:

$$a = \exp(A) = \frac{\text{depth}}{\text{dur}^B} \quad (5)$$

The a -values for all events are fitted to an exponential distribution:

$$a = \alpha + \beta \ln(\text{ARI}) \quad (6)$$

Which assumes an exponential distribution of event depths for a given duration:

$$\text{depth} = \text{dur}^B (\alpha + \beta \ln(\text{ARI})) = \alpha' + \beta' \ln(\text{ARI}) \quad (7)$$

Combining equations (3), (5) and (6), we arrive at the following general expression for an IFD curve:

$$\ln(\text{depth}) = B \ln(\text{dur}) + \ln(\alpha + \beta \ln(\text{ARI})) \quad (8)$$

This expression is fitted to both the burst- and event-depths and durations from the observational time series at gauging stations in the study area. The three coefficients in equation (8): B , α and β are fitted in a series of regression analyses. This approach is similar to that adopted by Carroll (2008) where equation (8) is expressed in terms of intensity rather than depth.

4.2.4 Mapping of burst-IFD tables to event IFD tables

4.2.4.1 Approach

Once the coefficients of the general IFD expression (8) have been determined, event- and burst-IFD tables can be related to each other. This is done using the following mapping equation (based on Mirfenderesk et al, 2013):

$$\frac{\text{depth}_{\text{event}}}{\text{depth}_{\text{burst}}} = p \text{dur}^q (\text{ARI})^r \quad (9)$$

Inserting equation (8) into equation (9), we can derive that $q=B_{\text{event}}-B_{\text{burst}}$ and, by setting $\text{ARI}=1$, that $p=\alpha_{\text{event}} / \alpha_{\text{burst}}$. To find r , we derive:

$$r = \ln \left(\frac{\alpha_{\text{burst}} \left(\frac{\alpha_{\text{event}} + \beta_{\text{event}} \ln(\text{ARI})}{\alpha_{\text{burst}} + \beta_{\text{burst}} \ln(\text{ARI})} \right)}{\alpha_{\text{event}}} \right) \ln(\text{ARI})^{-1} \quad (10)$$

Which implies that r depends on ARI , whereas equation (9) assumes that r is a constant. For practical reasons, the simplified equation (9) is used. The dependency on ARI is weak and for large ARI (of around 1000, so that $\ln(\text{ARI})=7$), we find that:

$$r \approx \frac{1}{7} \ln \left(\frac{\alpha_{\text{burst}} \left(\frac{\alpha_{\text{event}} + 7\beta_{\text{event}}}{\alpha_{\text{burst}} + 7\beta_{\text{burst}}} \right)}{\alpha_{\text{event}}} \right) \quad (11)$$

The coefficients p , q and r are determined from regression of equation (9) in log-space. Once the coefficients are known, equation (11) provides a general transformation from burst- to event-IFD tables.

4.2.4.2 Validation of assumptions

The crucial assumptions and approximations made in the derivation of the general IFD equation (8) and the burst-to-event mapping equation (9) are:

1. Neglect of the higher order terms in the BoM burst depths (equation (2))
2. Exponential distribution of event-depth for a given duration (equation (7))
3. Assuming a constant parameter r in the mapping equation (9)

The effect of these approximations on the rainfall depth for several durations or ARI's has been investigated in three case studies, based on observational data from three test-stations.

Assumption 1

The neglect of higher order terms in equation (2) was verified by fitting the BoM table data for Emu Creek to equation (2). The results for AEP 1%, 10% and 50% are shown in Figure 4-4. The deviations of the depth values for the durations and AEPs shown in the graph are 3% on average and 6% at most. It is therefore considered acceptable to neglect the higher order terms of equation (2).

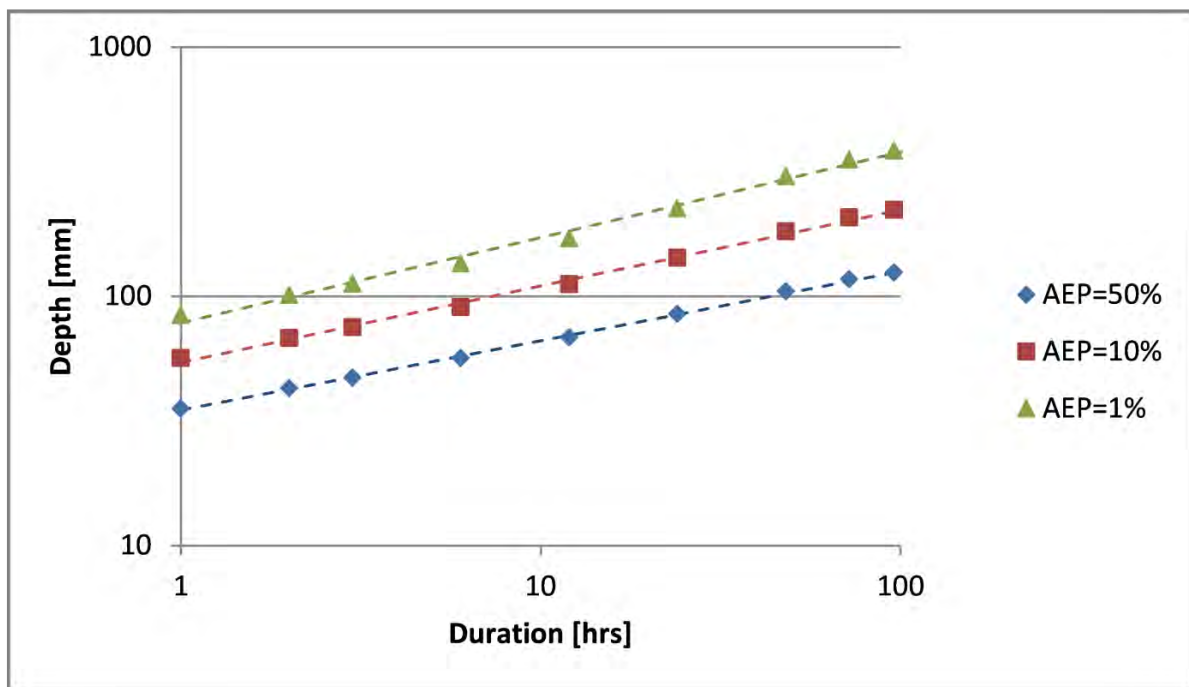


Figure 4-4 BoM IFD data (symbols) fitted to equation (2) (dashed lines) for three different AEP's

Assumption 2

Equation (7) is validated on BoM IFD data for Emu Creek in Figure 4-5. Although the longer duration graphs are slightly curved, the exponential approximation is reasonable except for the longest duration curve. The average deviation of the fitted rainfall depth from the BoM IFD data is 5% and 11% at most. The exponential distribution is therefore considered to be acceptable.

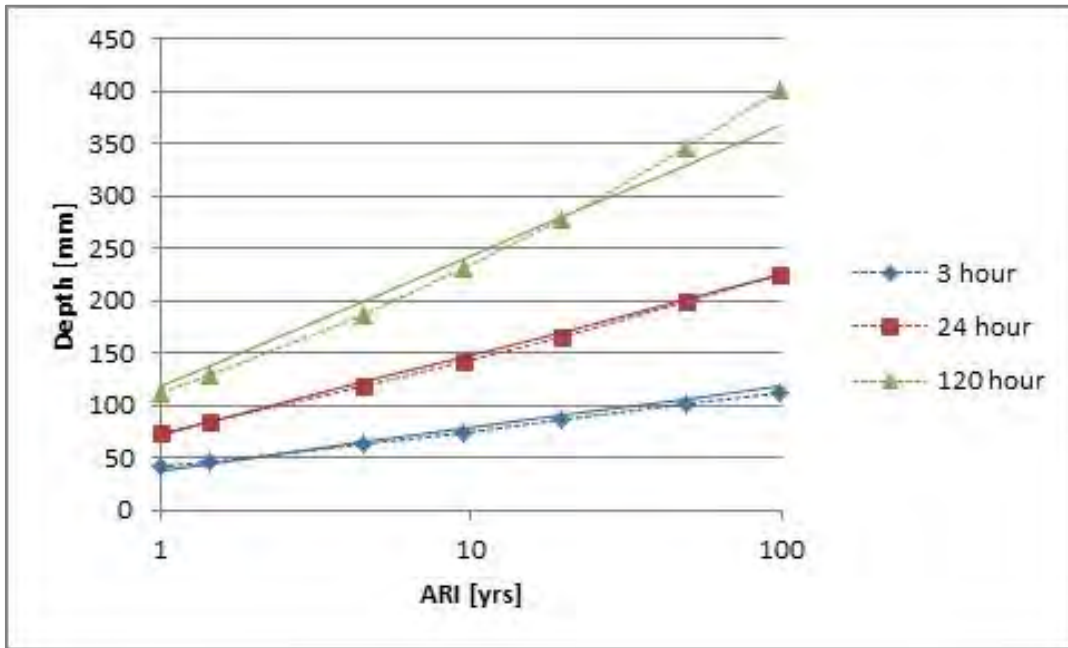


Figure 4-5 Event-depth as a function of ARI for several durations, according to the BoM IFD tables for Emu Creek. Exponential fits are shown as thin black lines

Assumption 3

The third assumption is that the parameter r in the mapping function (equation (9)) is constant. In Figure 4-6, the empirical event graphs are compared to empirical burst graphs that are transformed using equation (9). The differences are not visible in the figure. They are less than 1%. This can be explained by the generally very weak dependency of the mapping on ARI. The parameter r is a very small number (typically 0.01) and has little effect. Even disregarding the ARI dependency of the mapping equation altogether (by setting $r=0$) leads to deviations in rainfall depth of 5% at most.

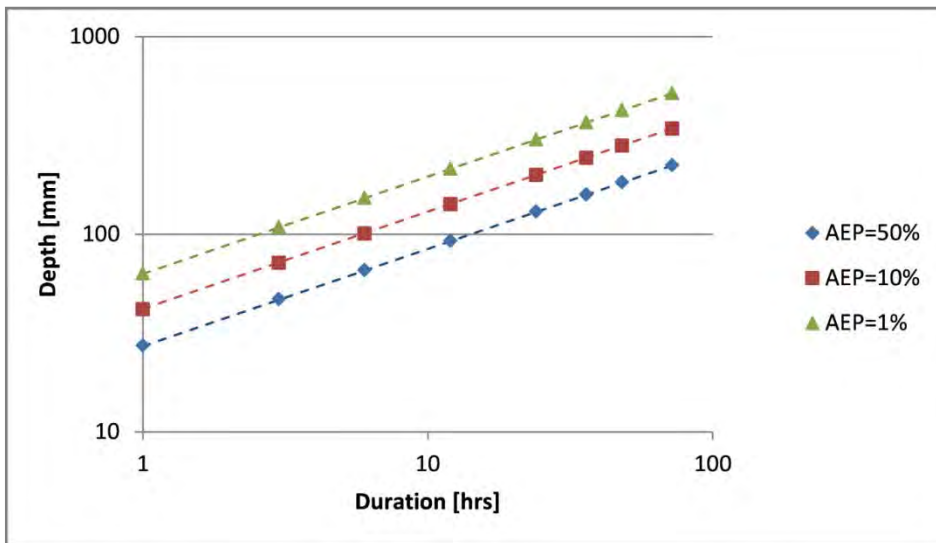


Figure 4-6 Event-IFD curves (symbols) compared to transformed burst-IFD tables. Both graphs are based on Emu Creek rainfall data

4.2.5 Procedure for generating event IFDs

4.2.5.1 Generating event data from rainfall records

Empirical event and burst IFD curves were derived for three gauging stations in the Brisbane River Catchment (see Table 4-1).

Table 4-1 Case study stations and length of the observational records

Station	Id	Latitude	Longitude	Series
Emu Creek	143010	-26.9771	152.28566	1993-2013
Kirkleagh	040318	-27.0258	152.5642	1965-1981
Ravensbourne	040270	-27.3628	152.1594	1959-1990

The raw gauging data are defined on fixed intervals (Ravensbourne and Kirkleagh) or variable intervals (Emu Creek). In the latter case, the gauging data are first transformed into a regular 6-minute fixed interval time series. The first step in the procedure to generate burst or event IFD tables is to identify a list of rainfall events from the time series of rainfall gauging data. A rainfall event is defined as a period of more than 0.25 mm/hour average rainfall and/or hourly intervals of more than 1.25 mm of rainfall depth. The start and end of each event are defined by dry periods of minimum duration dur_{dry} . During these dry periods the average rainfall must be less than 0.25 mm/hour and no hourly rainfall during this period should exceed 1.25 mm.

4.2.5.2 Generating burst-IFD tables

Empirical burst-IFD tables were derived from the list of rainfall events as follows:

1. Separate analyses are done for durations of 1, 2, 3, 6, 12, 24, 48 and 72 hours
2. For each duration, a moving time interval is used to determine, for each event, the maximum rainfall depth over that duration. If the duration of the event is shorter than the length of the interval, the event depth is used as the depth for that duration
3. The annual recurrence interval (ARI) of each rainfall depth is calculated by dividing the total length of the observational period by the rank of the observed rainfall depth in the series of depths. This is done separately for each duration
4. The coefficient B is determined by a linear regression on the log of the duration and event depth of all events (equation (3))
5. A value of a is determined for each burst using equation (5)
6. The coefficients α and β are determined from a linear regression of a versus $\ln(\text{ARI})$, following equation (9). The regression is done using only events having an a -value higher than a threshold of 20. This is equivalent to setting the number of events per year

Once the coefficients B , α and β are known, the IFD burst-table can be constructed for any depth, duration and ARI.

4.2.5.3 Generating event-IFD tables

The empirical event-IFD tables were derived from the list of rainfall events as follows:

1. The annual recurrence interval (ARI) of each event depth is calculated as the total length of the observation period divided by the rank of the observed depth in the full series of event depths
2. The coefficient B is determined by a linear regression on the log of the duration and event depth of all events (equation (3))

3. A value of a is calculated for each event using equation (5)
4. The coefficients α and β are determined from a linear regression of a versus $\ln(\text{ARI})$, following equation (9). Only events having an a -value higher than a threshold of 20 are used in the regression

Once the coefficients B , α and β are known, the IFD event-table can be constructed for any depth, duration and ARI.

4.2.6 Results

The event- and burst- IFD statistics were derived for all three stations following the procedures described in the previous sections. These statistics are fundamentally different in nature (per-event frequencies instead of per-year, classification of durations instead of a fixed duration), but they can be compared by accounting for the number of events per year and adjustment of the values for various event durations within a class to a representative duration per class, as described by Rahman et al. (2002). The adjusted event-based IFD frequencies are by definition lower than those in the burst-IFD tables, because the latter include shorter duration events for a fixed duration.

4.2.6.1 Mapping of burst and event IFD tables

The results for the mapping parameters p , q and r are given in Table 4-2. The parameters for each station are in the same order. The average values over all three station are $p=0.56$ and $q=0.29$. The value of coefficient r is negligible, ie close to zero.

Table 4-2 Mapping parameters for burst to event IFD table for the three test stations

Station	Id	P	q	r
Emu Creek	143010	0.63	0.25	0.011
Kirkleagh	040318	0.56	0.30	-0.001
Ravensbourne	040270	0.50	0.31	-0.013
Average	-	0.56	0.29	-0.001

When using the per-station coefficients from Table 4-2, the mapping of event and burst-IFD tables is almost perfect. However, for the BRCFS, a general transformation for all locations in the area is required. To verify if such a general transformation exists, the averaged coefficients are used to transform the burst IFD tables for each station into event IFD tables. This mapping is considerably less perfect (see Figure 4-7). The average deviation of the depths shown in this graph for Emu Creek is 8%. The largest deviations occur for the shortest durations. They are in the order of 20%. For the BRCFS, however, the longer durations (> 24 hours) and recurrence periods (> 10 years) are most important. The deviations for this part of the IFD table are around 3 or 4%.

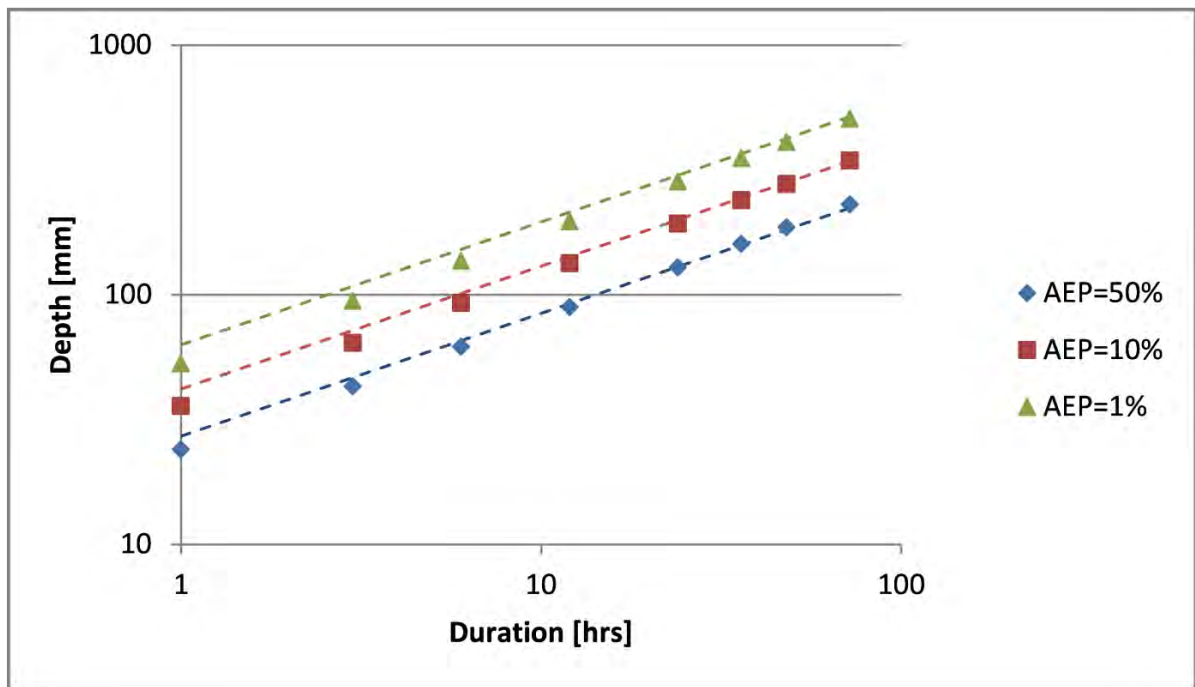


Figure 4-7 Empirical event IFD curves for Emu Creek and transformed burst-tables using the mapping equation (9) and average coefficients

The burst-IFD statistics from the three test stations were compared to the burst IFD tables from the BoM website (<http://www.bom.gov.au/water/designRainfalls/revised-ifd/>) at nearby locations.

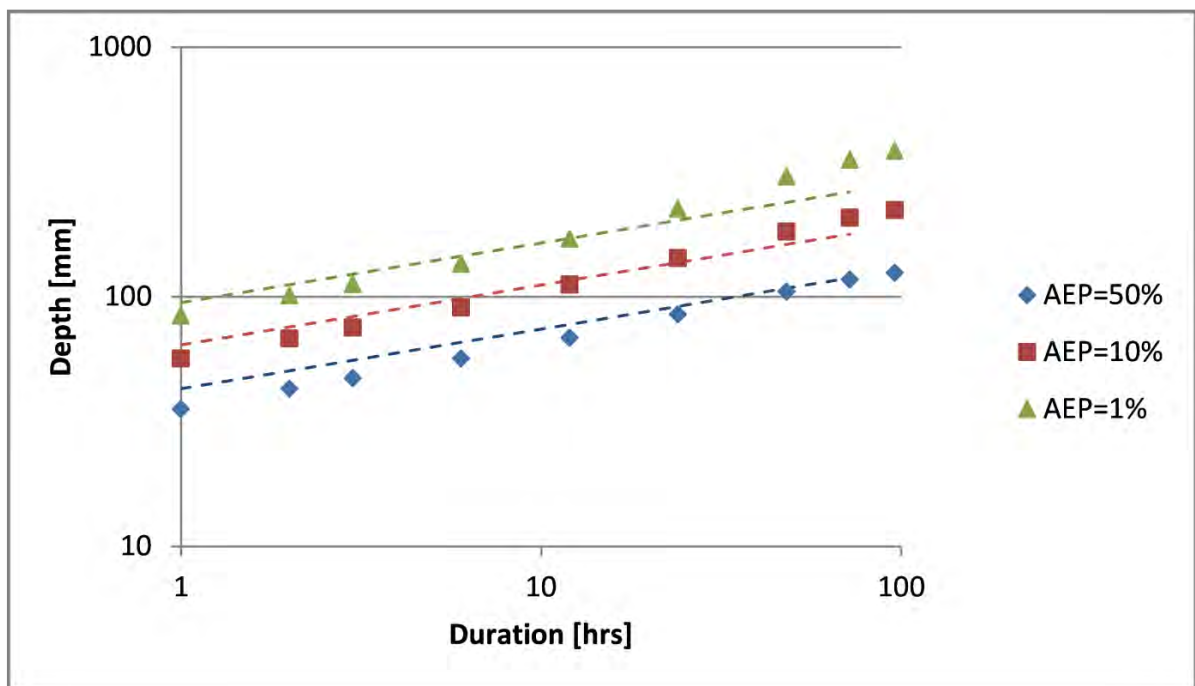


Figure 4-8 Empirical burst-IFD table for Emu Creek (dashed lines) compared to BoM data (symbols)

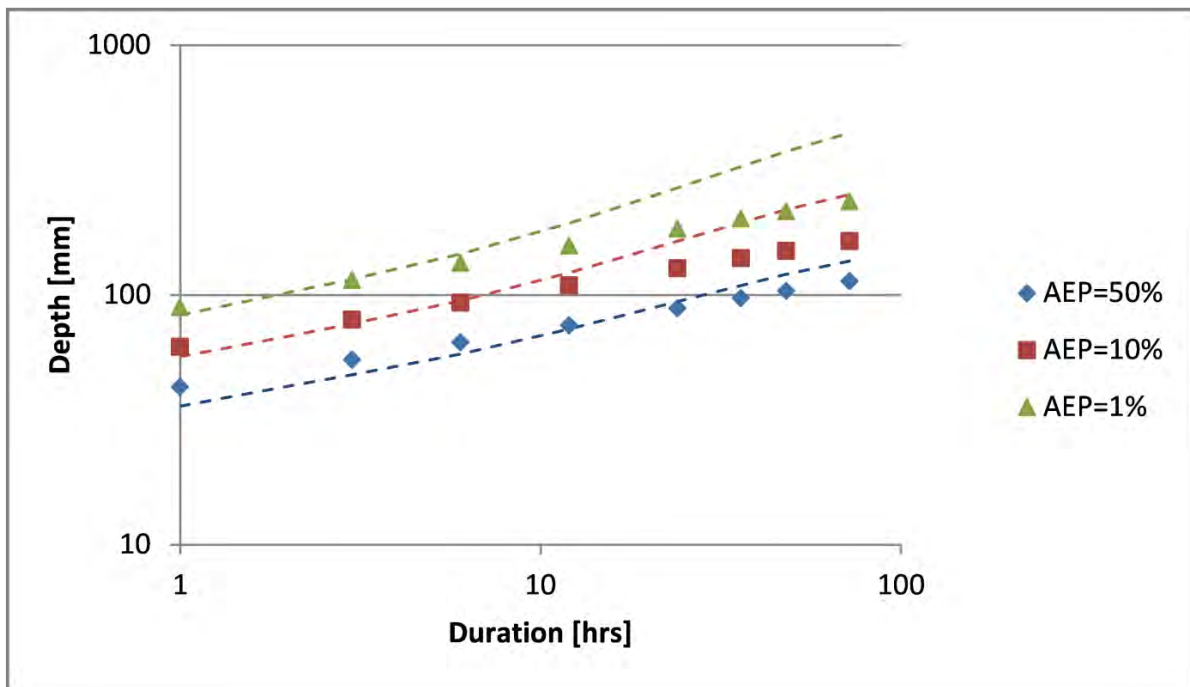


Figure 4-9 Empirical burst-IFD table for Kirkleagh (dashed lines) compared to BoM data (symbols)

The results (see Figure 4-8 for Emu Creek and Figure 4-9 for Kirkleagh) show some deviations. These can be attributed to several causes:

1. The spatial averaging (regional frequency analysis) that is done by the BoM to obtain consistent IFD tables across the country
2. Statistical uncertainty due to the relatively short period of observations for the three test stations
3. The neglect of higher order terms in equation (2) and the differences in the fitting procedure for ARI dependency

The neglect of higher order terms was found to be small previously (see Figure 4-7), so the third cause will only account for a small part of the deviations. Since similar deviations are found for all three test stations, the first cause is probably most relevant. The BoM has included a large set of stations in the frequency analysis, some of which have much longer observational records (also before 1959). It is likely that these data from neighbouring stations gave rise to different overall IFD relationships.

The observational periods at the three test stations are relatively short. The BoM IFD tables are based on a regional analysis, including data from more distant gauging stations, some of which have over 100 years of measurements. This regional analysis produces spatially consistent IFD tables on a national level, however potentially at the cost of deviations from local (point) measurements which include local orographic effects.

The average difference in rainfall depth between the IFD at the three test stations and the BoM IFD tables for durations between 1 and 72 hours and recurrence periods between 1 and 100 years was found to be around 5%. The largest differences of more than 30% were found for durations of more than 48 hours and recurrence periods of 20 years or longer. In conclusion, the deviations of the point burst IFD curves at the three test stations are at least equal to the uncertainty associated with the mapping of burst IFD tables to event IFD tables.

4.2.6.2 Comparison with the CRC-CH method

The empirical event IFD tables that are derived using the CRC-CH method typically display a curvature (Figure 5 in Rahman [2002]) for longer durations and recurrence periods. The event-IFD curves from CRC-CH tend to constant rainfall intensity for long duration-extreme events. This behaviour is not captured by the IFD graphs produced by the method described here, because the general IFD relation (9) does not allow for such a curvature. According to Figure 5 in Rahman [2002], the neglect of a curvature of the event-IFD graphs can lead to a serious underestimation of the most extreme rainfall intensities. For event durations of 100 hours and ARI=100, the difference in rainfall depth can be as large as a factor of 10.

An analysis of the rainfall data from the test stations following the CRC-CH approach was done to investigate the curvature effect. Indeed the results showed an upward curvature of the IFD tables (see Figure 4-10). However, the curvature is found for shorter recurrence periods (ARI=1, 2, 5) instead of for the longer ARI's as reported by Rahman et al (2002). Moreover, the results proved to be rather sensitive to the settings of the procedure, such as the number of duration classes or bins. The uncertainty of the curvature of the IFD curves is considerable.

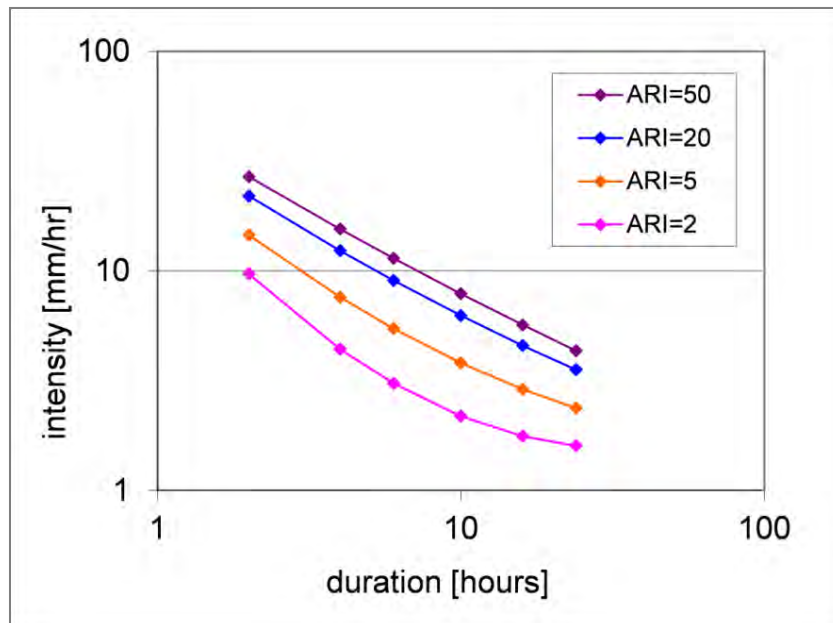


Figure 4-10 Event IFD Curves for Emu Creek, derived using the CRC-CH method (6 duration classes)

Moreover, there are some inconsistencies in the curvature phenomenon. In the CRC-CH method, the curvature is described by a second order polynomial. This polynomial will continue to curve upward for longer durations even until the intensity starts to increase with increasing duration, which is not realistic. In Rahman [2002] and in Figure 4-10, this unrealistic effect occurs beyond the range of the graph.

The curvature is not observed in the BoM burst IFD tables. Although the burst- and event-statistics need not follow the same pattern, they are expected to show similar behaviour for the longest durations and long recurrence periods, because the probability in this regime is determined by the most extreme and long-lasting rain storms. If the event IFD shows a curvature in this regime, it is also expected in the burst-IFD.

To conclude: although the neglect of a curvature of the event-IFD graphs could lead to an underestimation of the event rainfall intensities, preference is given to the more robust equation (9) without any such curvature. The main reasons for this are:

- The uncertainty of the extend of the curvature
- The unrealistic effect that the curvature produces for long durations
- The fact that a curvature is not observed in the BoM burst-IFD tables

4.2.6.3 Sensitivity analysis

In the procedure for deriving empirical IFD tables (both event and burst), the first step is to generate a list of events. For this, a definition of an event is needed. For the results described so far, an event was defined by two dry periods of 24 hours preceding and following the event. A sensitivity analysis was done to investigate the effect of applying a different duration of these dry periods in the event definition. Table 4-3 shows the average mapping parameters over the three test stations for various dry period durations.

Table 4-3 IFD mapping parameters for different event definitions (dry period duration)

Dry period duration	p	Q	R
3 hrs	0.63	0.47	-0.003
6 hrs	0.57	0.46	0.004
12 hrs	0.58	0.37	-0.008
24 hrs	0.57	0.29	-0.001
48 hrs	0.53	0.27	0.004
72 hrs	0.52	0.25	0.003

These results show that the mapping parameters in equation (9) are fairly constant, except for the shortest dry period durations. Parameters p and q have values between 0.5-0.6 and 0.25-0.45 respectively. The parameter r is always a small number, indicating a very weak dependency on recurrence period. The largest variations of the parameters in Table 4-3 (except for the values for a dry period of 3 or 6 hours) lead to changes in the event-depths for various durations and recurrence periods of around 15%. This suggests that the mapping of burst- to event IFD tables is fairly robust. Table 4-4 shows the selected values of p , q and r as implemented in the MCS framework.

Table 4-4 Selected IFD mapping parameters

parameter	value
p	0.63
q	0.29
r	0.00

4.3 Areal IFD curves

4.3.1 Introduction

The Monte Carlo sampling scheme requires IFD curves for the average rainfall over an upstream catchment of a location of interest where the frequency analysis of the runoff peak flows and heights and runoff volumes will be carried out. This section describes how these areal IFD curves are derived. Two different methods are described. The first is the proposed method for the MCS framework, the second is used as comparison/validation.

4.3.2 Method 1: point rainfall and areal reduction factors

The IFD for a sub-area for rainfall bursts is given by the IFD of the BoM grid point that is nearest to the centroid of the sub-area. Through application of the mapping relation as described in the previous sections, event IFDs can be derived for each of these subareas as well. The sub-areas are relatively small (up to 100 km²) and the IFD tables generally vary only gradually, except in steep areas where orographic effects dominate.

The IFD of a sub-catchment is given by the area-weighted sum over all sub-area IFDs that fall within sub-catchment, multiplied by an Areal Reduction Factor (ARF):

$$R_{catchment} = ARF \frac{\sum_i A_i R_i}{\sum_i A_i} \quad (12)$$

Where R_i is the rainfall depth of subarea i and A_i is the surface area of subarea i . Equation (12) is applied to each combination of frequency and duration to derive spatial IFD curves.

The areal reduction factor (ARF) is applied to take into account that the (sub-)catchments under consideration are much larger than the sub-areas. Point IFD relationships that are used for the sub-areas are therefore not directly applicable to an entire sub-catchment. The area-averaged IFD should take into account the statistical effect that point rainfall has higher peak intensities than area-averaged rainfall. The ARF is applied to take this effect into account. It is relevant to note that the ARF depends on the size of the (sub-)catchment under consideration and on the rainfall duration. Figure 4-11 shows the ARF from ARR (2013c) that is used in the Monte Carlo framework. Formally, this ARF is valid for areas between 1 and 10,000 km² and durations up to 100 hours. With 13,500 km² and consideration of durations up to 168 hours, the full Brisbane River catchment is slightly beyond the valid range, however it is assumed that extrapolation of the ARF using this figure is still valid.

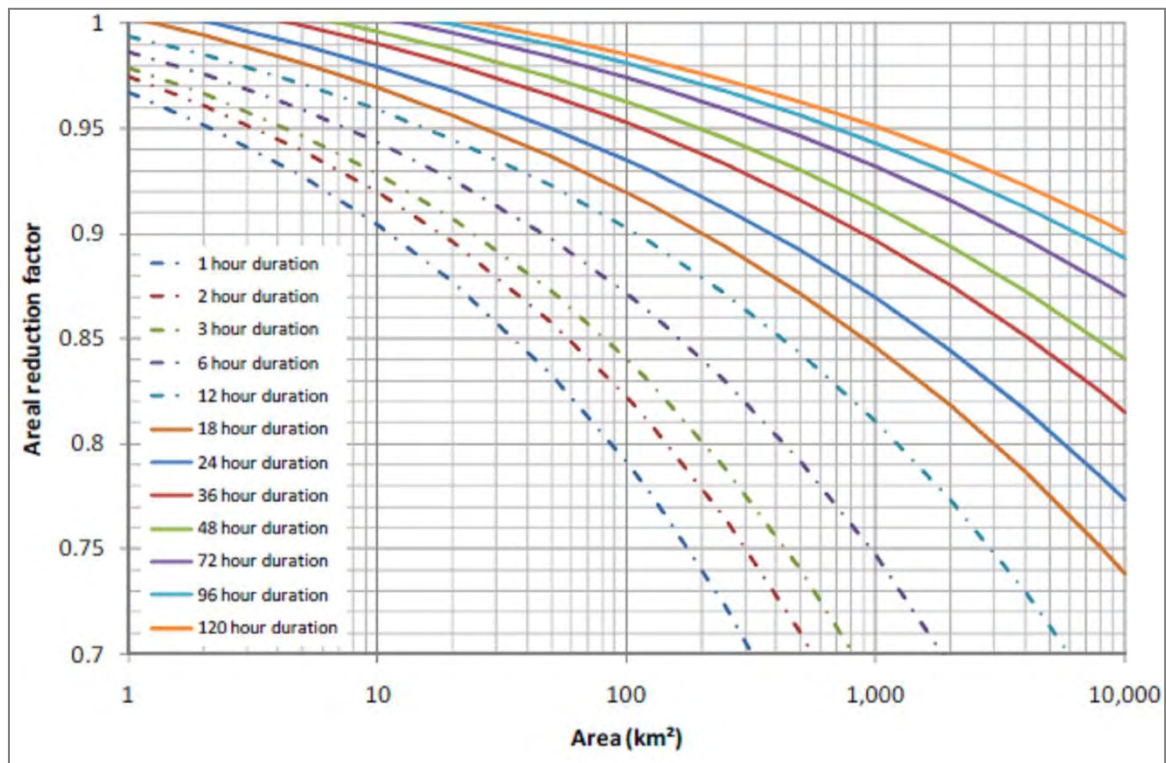


Figure 4-11 ARF from ARR (ARR, 2013c)

4.3.3 Method 2: Catchment IFD curves

An alternative approach is investigated in which catchment averaged IFD curves are used to translate the duration and AEP of rainfall depth into catchment average rainfall depth. The IFD-curves have been provided to the project team by WMAWater (2014). The catchment averaged IFD curves have been derived through application of the following procedure:

1. Selection of rainfall data of stations in or near the (sub-)catchment under consideration
2. Derivation of a series of catchment average rainfall depth through spatial interpolation
3. Selection of rainfall extremes (annual maxima or peaks-over-threshold series) for different burst durations
4. Fitting of extreme value distribution functions (GEV) to derive IFD curves

WMAWater has provided a set of GEV distribution function parameters that describe catchment IFD curves (WMAWater, 2014). These distribution functions were derived for the upstream catchments of 23 river locations in the Brisbane River catchment and for 10 durations (1-10 days). Catchment rainfall data was derived on daily resolution. A conversion factor was applied to translate daily rainfall depth to estimated 24-hour rainfall depths.

4.3.4 Comparison

Figure 4-12 shows a comparison between the catchment IFD curves from both approaches for the upstream catchment of location 'Somerset', which is essentially the catchment of the Stanley River. It shows that differences for this location are large for the rare to extreme range of AEP events. The 2013 ARR IFD curves from the BoM were used in this comparison.

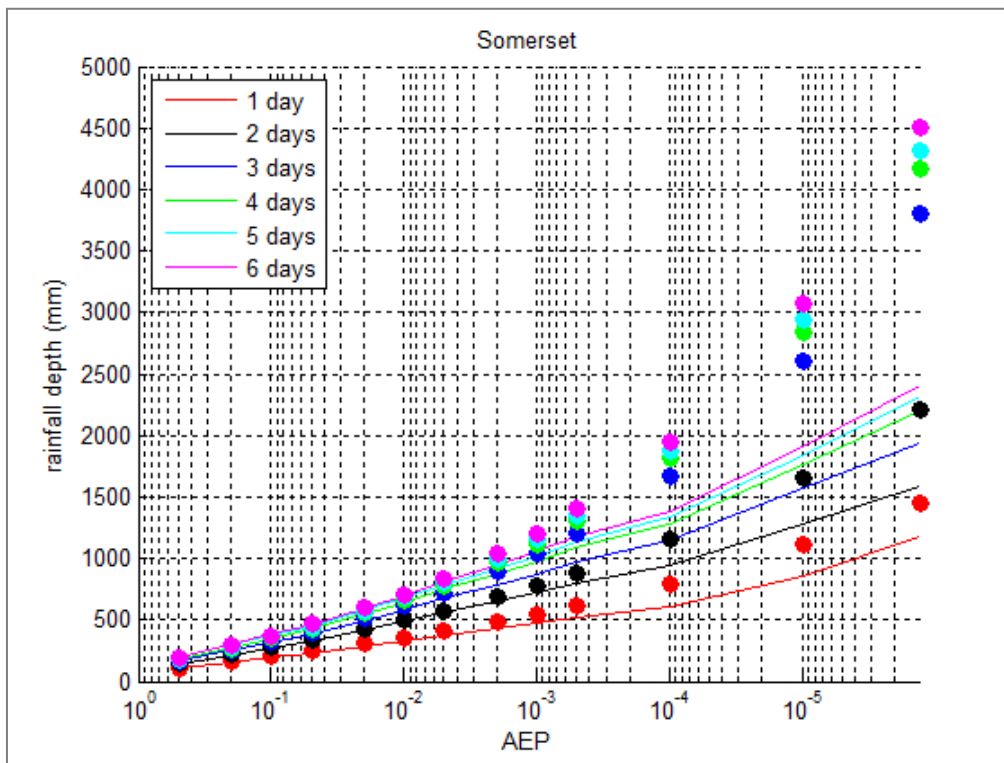


Figure 4-12 Comparison of catchment IFD curves as derived from BoM point rainfall IFDs and ARR Areal Reduction factors (full lines) and from catchment average rainfall time series (symbols)

Another noticeable aspect of the IFD curves as derived from the catchment average rainfall time series is that the GEV distributions for different durations sometimes cross for low values of AEP; see the example of Figure 4-13. This means, for example, that the 5-day rainfall depth for 1/1,000 AEP is higher than the 6-day rainfall depth for 1/1,000 AEP, which is impossible. This may be caused by the use of conversion factors to convert daily restricted rainfall to unrestricted rainfall (Peter Stensmyr, WMAWater, personal communication). These are duration-dependent, and therefore may cause the maximum five-day rainfall to be larger than the maximum six-day rainfall. It is therefore concluded, also after consultation of WMAWater, that the IFD curves as derived from on catchment average rainfall time series are valid up to the range of 100 years ARI (AEP between 1/2 and 1/100).

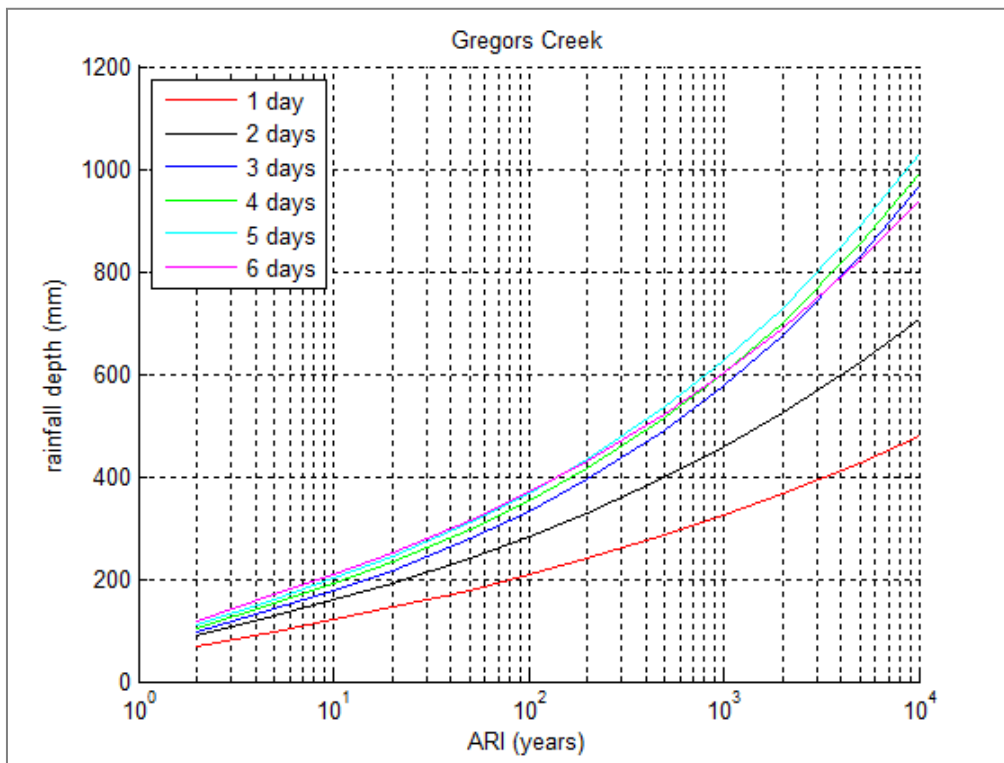


Figure 4-13 Example of crossing IFD curves

The Figures on the following pages make a comparison between the catchment IFD curves from both approaches for the range of AEP's of 1/2 to 1/100 for various locations. It shows the two approaches produce IFD curves that are in the same order of magnitude, but at the same time that differences are not negligible. For locations in the Lower Brisbane catchment, which is the main focus of the MCS analysis, differences appear to be small for durations of 2 days and more. For these locations (Mount Crosby weir, Savages Crossing, Moggill, Brisbane) the choice of catchment IFD curve is therefore expected to have little influence on the derived return values as computed with the MCS framework.

As stated before, the catchment IFD curves of WMAWater are expected to be valid for the range of AEP's from 1/2 to 1/100. For the Monte Carlo simulations in the BRCFS, IFD curves for lower AEP are also required. The IFD curves from WMAWater would therefore need to be "embedded" in the conventional IFD curves that were derived from point rainfall and ARF's. In doing so, another issue that needs to be dealt with is the fact that the IFD curves from WMAWater are not available for durations <24 hours. This means that also for durations <24 hours, IFD curves need to be adopted from the BoM IFD curves. These are all complicating steps that, in the end, are expected to have little effect on derived return values. For this reason it was decided not to implement the catchment IFD curves of WMAWater in the MCS framework.

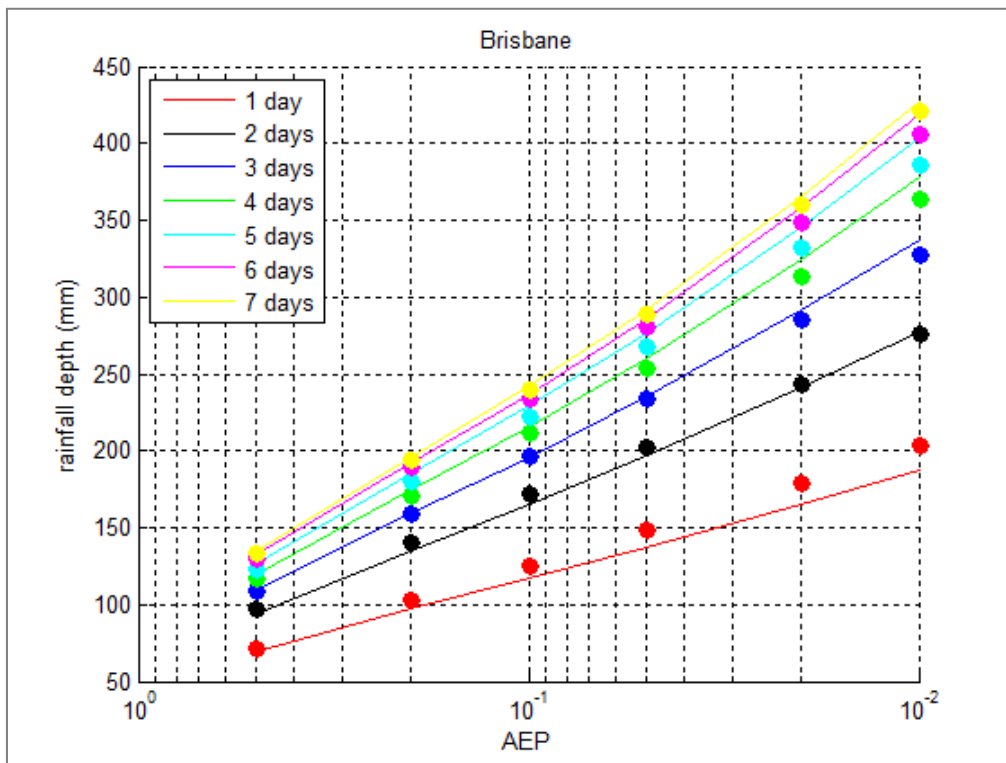
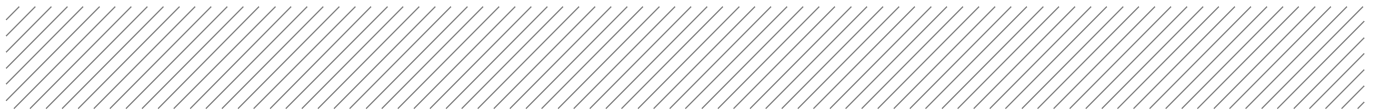


Figure 4-14 Comparison of catchment IFD curves as derived from BoM point rainfall IFDs and ARR Areal Reduction factors (full lines) and from catchment average rainfall time series (symbols), location Brisbane

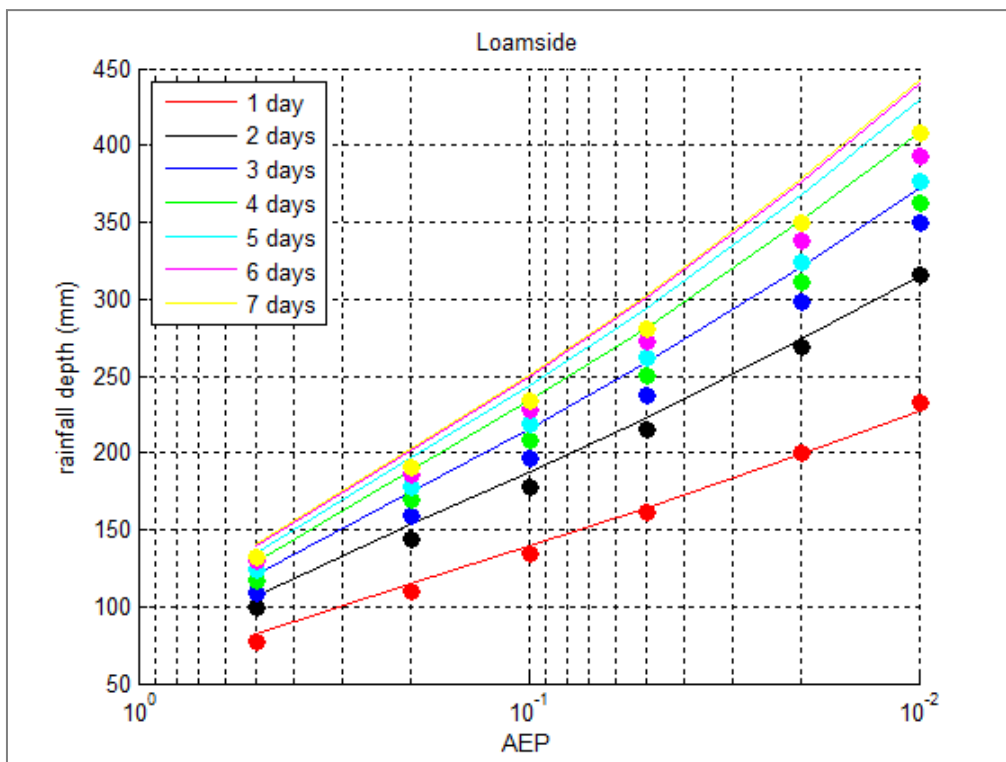


Figure 4-15 Comparison of catchment IFD curves as derived from BoM point rainfall IFDs and ARR Areal Reduction factors (full lines) and from catchment average rainfall time series (symbols), location Loamside

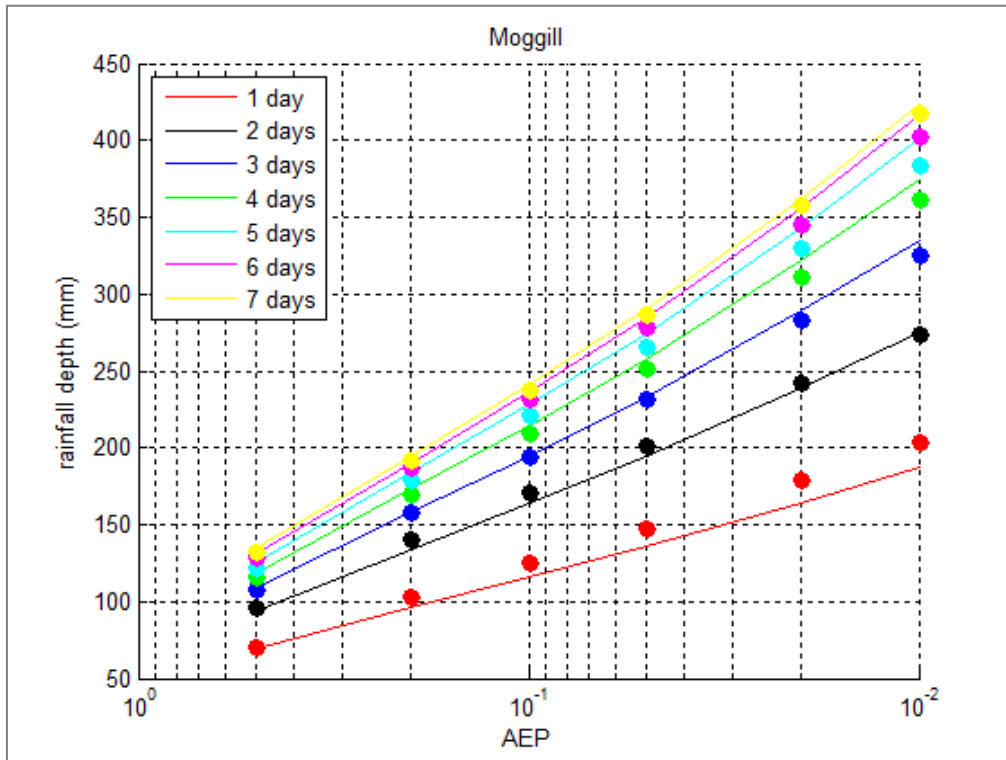
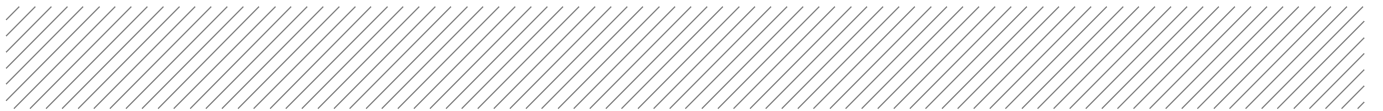


Figure 4-16 Comparison of catchment IFD curves as derived from BoM point rainfall IFDs and ARR Areal Reduction factors (full lines) and from catchment average rainfall time series (symbols), location Moggill

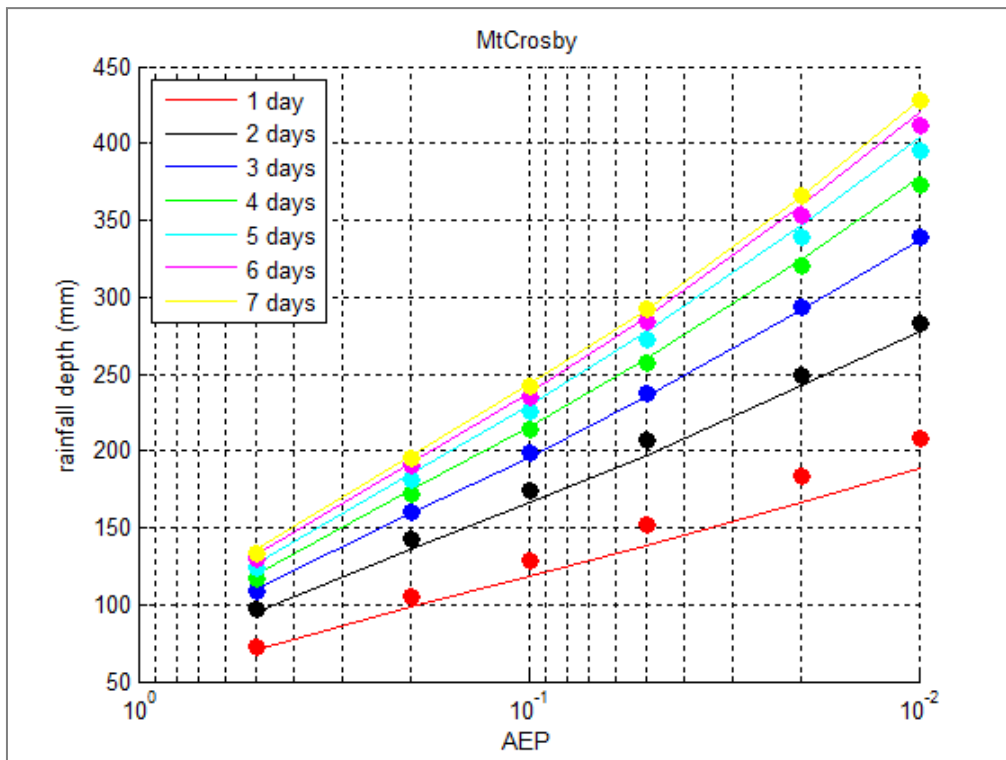


Figure 4-17 Comparison of catchment IFD curves as derived from BoM point rainfall IFDs and ARR Areal Reduction factors (full lines) and from catchment average rainfall time series (symbols), location Mount Crosby

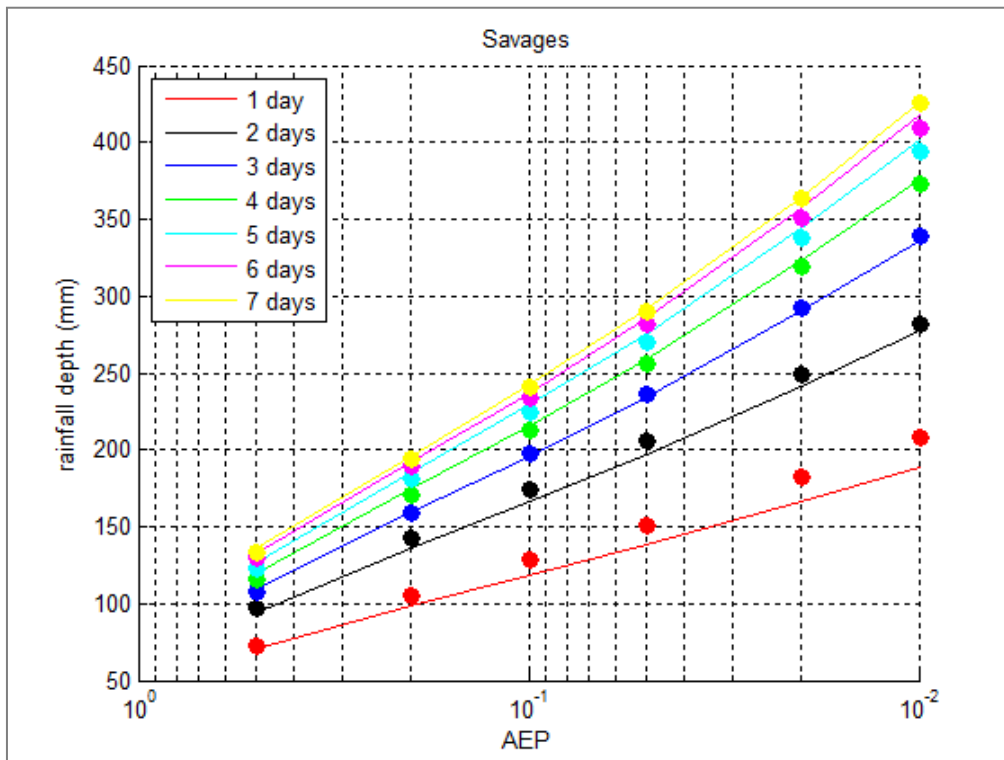


Figure 4-18 Comparison of catchment IFD curves as derived from BoM point rainfall IFDs and ARR Areal Reduction factors (full lines) and from catchment average rainfall time series (symbols), location Savages Crossing

4.4 Conclusions

The mapping equation (9) for point rainfall is a reasonable method to generate event tables from BoM burst tables. The mapping parameters (coefficients p , q and r in equation (9)) are fairly similar for the three test stations Emu Creek, Ravensbourne and Kirkleagh in the upper Brisbane catchment. Thus, the mapping is thought to be sufficiently general for the area around the test stations.

For larger areas, this remains to be seen. A previous mapping study for the area around the Gold Coast, similar transformation functions and coefficients were found (Carroll, personal communication), which gives some confidence in the general nature of the event-to-burst mapping. The differences between empirical event-IFD tables and transformed burst-IFD tables is in the order of 15%. A curvature of the event-IFD tables, as found by Rahman (2002), would give rise to larger deviations. However, the nature of the curvature itself is rather uncertain and we concluded that there are good reasons not to include this in the mapping of event to burst IFD tables.

5 Spatio-temporal rainfall patterns

5.1 Introduction

The previous section described methods to derive the catchment rainfall depth. These methods provide spatially uniform rainfall fields in the sense that the AEP of the rainfall depth is constant all over the catchment. The next step in the Monte Carlo Simulation is to generate spatio-temporal rainfall patterns that are more realistic, ie more in consistent with actual storm events (see, for example, Figure 5-1). For this purpose, an innovative method for stochastic generation of space-time rainfall fields developed by the Bureau of Meteorology was incorporated in the MCS framework.

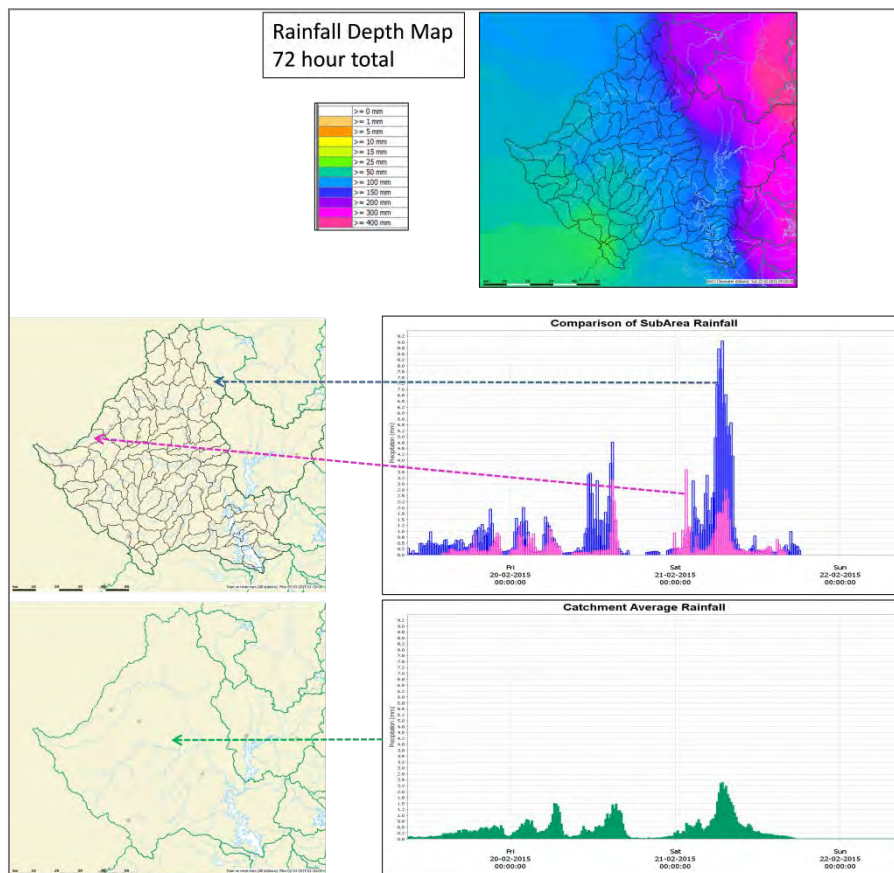


Figure 5-1 Example of spatial variation of rainfall, observed during ex-tropical Cyclone Marcia, February 2015; Figure Courtesy of Michel Raymond, Seqwater

5.2 BoM synthetic rainfall patterns

Data of stochastically generated space-time rainfall patterns for the Brisbane River catchment was provided to the BRCFS project by Seqwater. The method of generating the synthetic events is described in SKM [2013]:

These synthetic flood events were produced using a world-leading technique for stochastic generation of space-time rainfall fields, which were generated from radar data. A multiplicative-random cascade approach was used to generate 90 replicates of stochastic space-time rainfall patterns across the Brisbane River catchment. The position of the catchment was moved around within the generated spatial domain of the stochastic space-time data to six different possible positions and different segments of time were selected from 10 of the longer replicates. This resulted in 600 space time patterns that were adopted for the stochastic simulation. The generated space time patterns were verified against spatial patterns observed in historical rainfall events that have occurred in the Brisbane River catchment between 1954 and 2012.

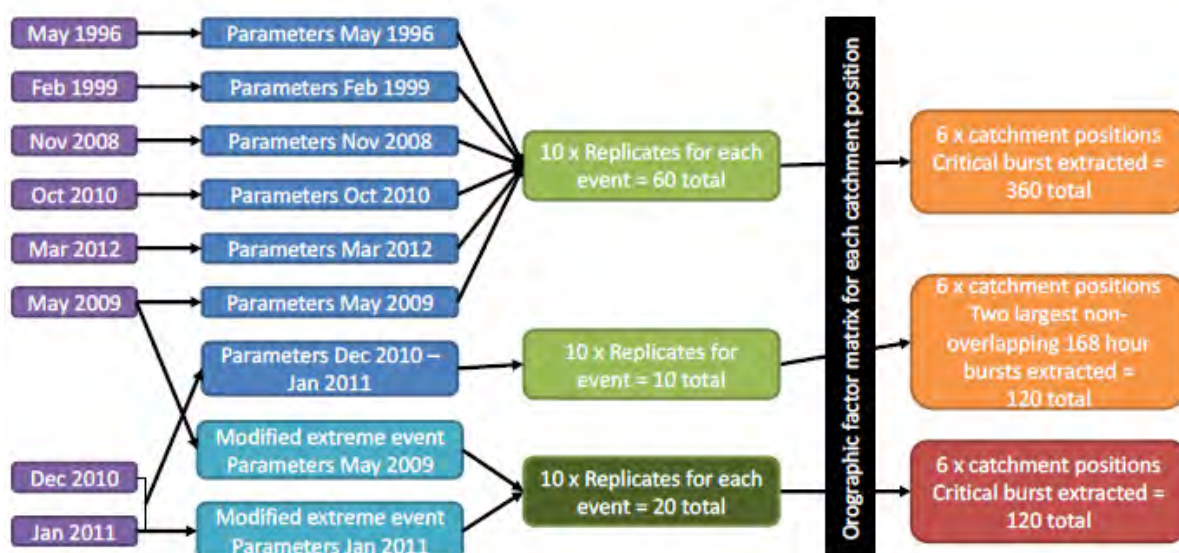


Figure 5-2 Flow cart for production of space-time rainfall patterns (copied from SKM 2013).

Data in SKM [2013] is provided for nine events. In 2014, additional storm pattern were derived based on the 2013 event (Jacobs, 2014), as part of the Brisbane River Catchment Flood Study.

Per event there are nine 'replicates'. The replicates for each single event cover the same period, however the length of the period (number of days) is different for each event. Based on the nine 'replicates' of the nine events, the Brisbane River catchment is placed at six locations (see Figure 6-1 of SKM, 2013) in the 256 km by 256 km square (the model domain of the BoM simulation model).

Table 5-1 gives an overview of the ten events on which the 660 synthetic rainfall patterns are based, the applicable minimum and maximum duration (hours), minimum and maximum ARI and the number of spatial patterns. For each event, a list is provided with the maximum burst rainfall depth in mm for different time frames (eg 24 hours; 36 hours; 48 hours; 72 hours; 120 hours; 168 hours) as well as the burst offset. Furthermore, for each storm pattern a detailed spreadsheet was provided, listing:

- A time series of rainfall for each of the 534 subareas
- Averaged rainfall in 12 sub-catchments (Table 5-2)

This data was used in the current studies to extract space-time patterns for each chosen duration.

Table 5-1 Overview of space-time rainfall patterns in Excel spreadsheets

Event	Min-max applicable duration (h)	Min-max applicable ARI (years)	Number of patterns
1996	24-72	1-1000000	60
1999	24-72	1-1000000	60
2008	24-112	1-1000000	60
2009 normal	24-72	1-1000000	60
2009 slow	24-167	1-1000000	60
2010	24-24	1-1000000	60
2010-2011	24-168	1-1000000	120
2011	24-35	1-1000000	6
	24-168	1-1000000	54
2012	24-167	1-1000000	60
2013	24-142	1-1000000	60

Table 5-2 The 12 'sub-catchments' listed in the spreadsheet

Somerset Dam	Lower Lockyer
Upstream of Linville	All Lockyer
Linville to Gregors Creek	Bremer, Warrill and Purga
Gregors Creek to Wivenhoe	Lower Brisbane Only
All Upstream of Wivenhoe Dam	Moggill
Upper Lockyer	Outlet

5.3 Basic statistics for burst rainfall of the synthetic events

The spatial average rainfall was calculated for nine sub-catchments based on the data of the 534 subareas. Based on these data the maximum 24 hour burst amount is calculated for each of these nine sub-catchments. This is done for all the events and for all patterns.

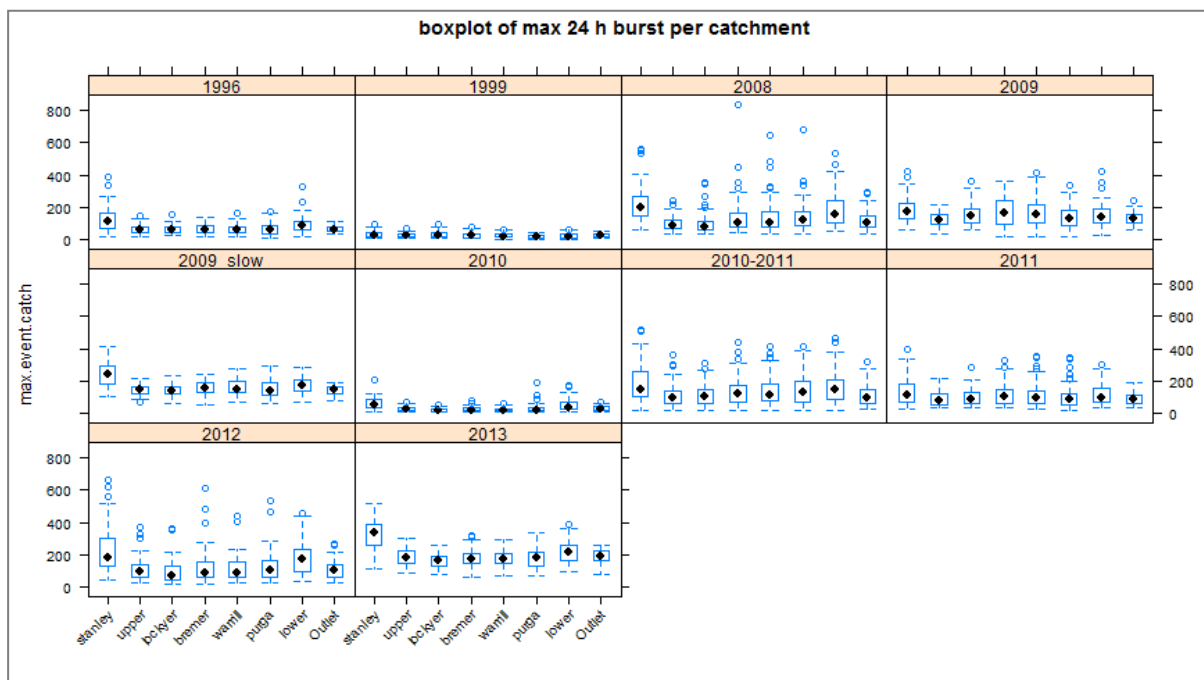


Figure 5-3 shows in a boxplot the variation of the maximum 24 hours burst rainfall per catchment – based on 60 patterns per historic event. It should be noted that the time of occurrence of the burst can differ between the sub-catchments. The boxplots clearly show that rainfall amounts of the patterns are strongly related to the original event – eg the patterns that are based on the 2010 event have lower maximum 24 hours amounts than the patterns based on the 2012 event. Also noticeable is that within one event, the maximum 24 hours burst within one catchment can vary significantly between the 60 patterns.

The relative contribution of each of the eight catchments to the total amount of 24 hour burst rainfall is calculated in percentages. Figure 5-4 shows the results. The same procedure was carried out for the 48 hours burst. In that case there are fewer events because not all events have hourly data for 48 hours or longer (see also the maximum applicable duration in Table 5-1), in that case just the total amount was taken. The results are plotted in Figure 5-5 and Figure 5-6.

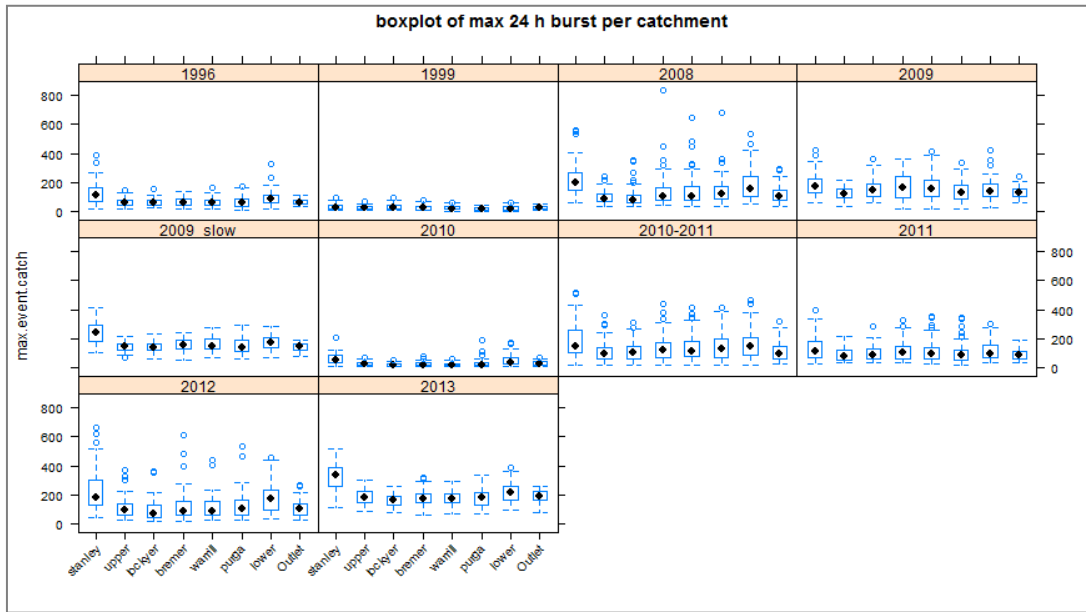
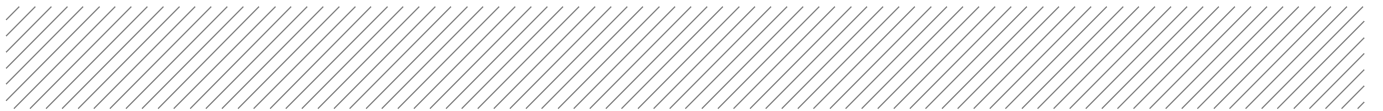


Figure 5-3 Boxplots of maximum 24 hours burst per catchment [mm] based on 60 patterns per event². The boxes are formed by first and third quartile – the median is plotted as a black dot – the whiskers are at maximum 1.5 time the interquartile range. Outside this range points are plotted as individual outliers

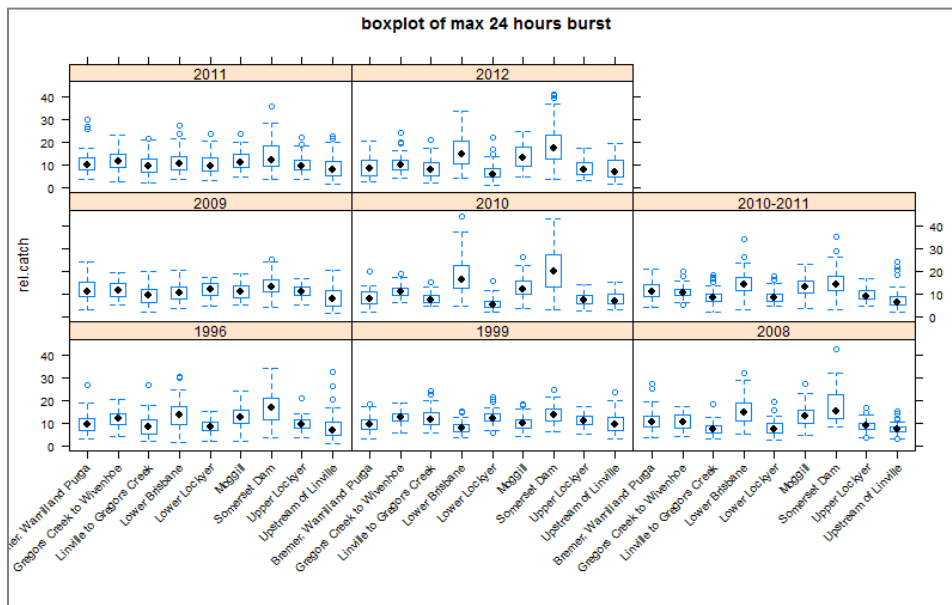


Figure 5-4 Boxplots of the relative contribution (%) of each catchment within the total max 24 hour burst³

² Notice: per catchment the time frame of 24 hours can differ

³ Notice: per catchment the time frame of 24 hours can differ

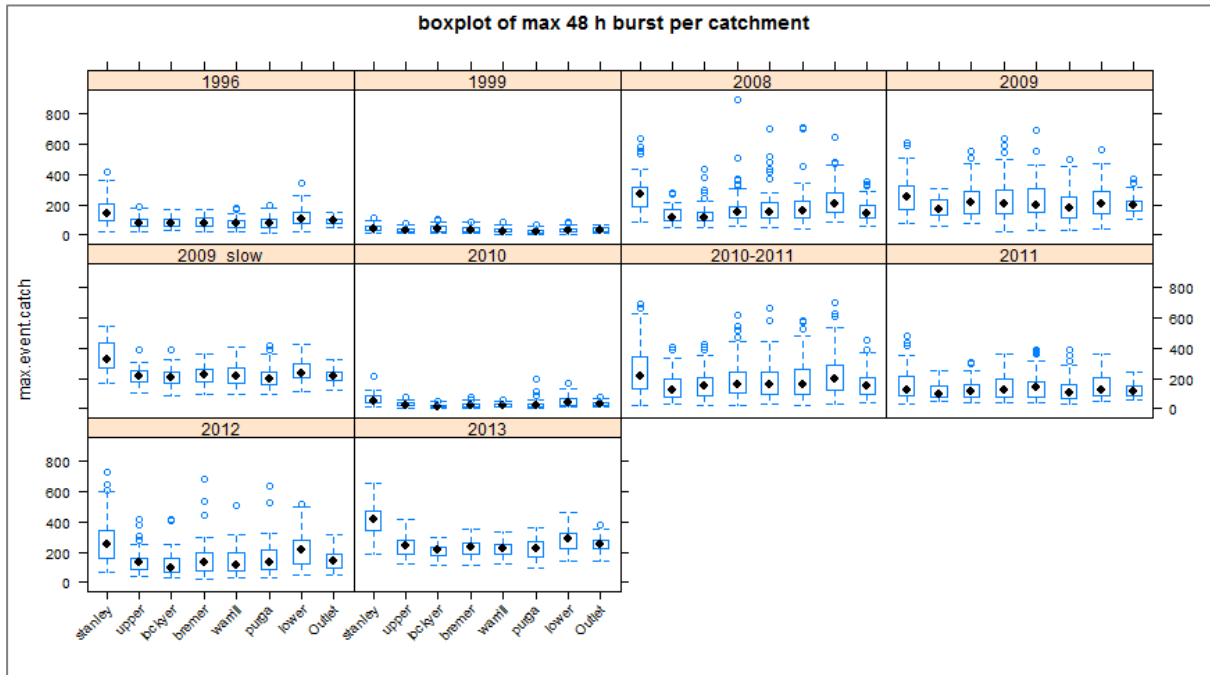
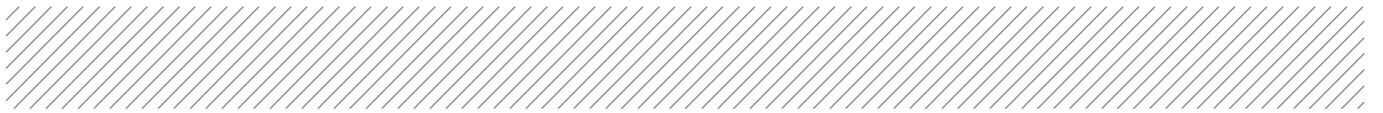


Figure 5-5 Boxplots of maximum 48 hours burst per catchment [mm] based on 60 patterns per event. The boxes are formed by first and third quartile – the median is plotted as a black dot – the whiskers are at maximum 1.5 time the interquartile range. Outside this range points are plotted as individual outliers

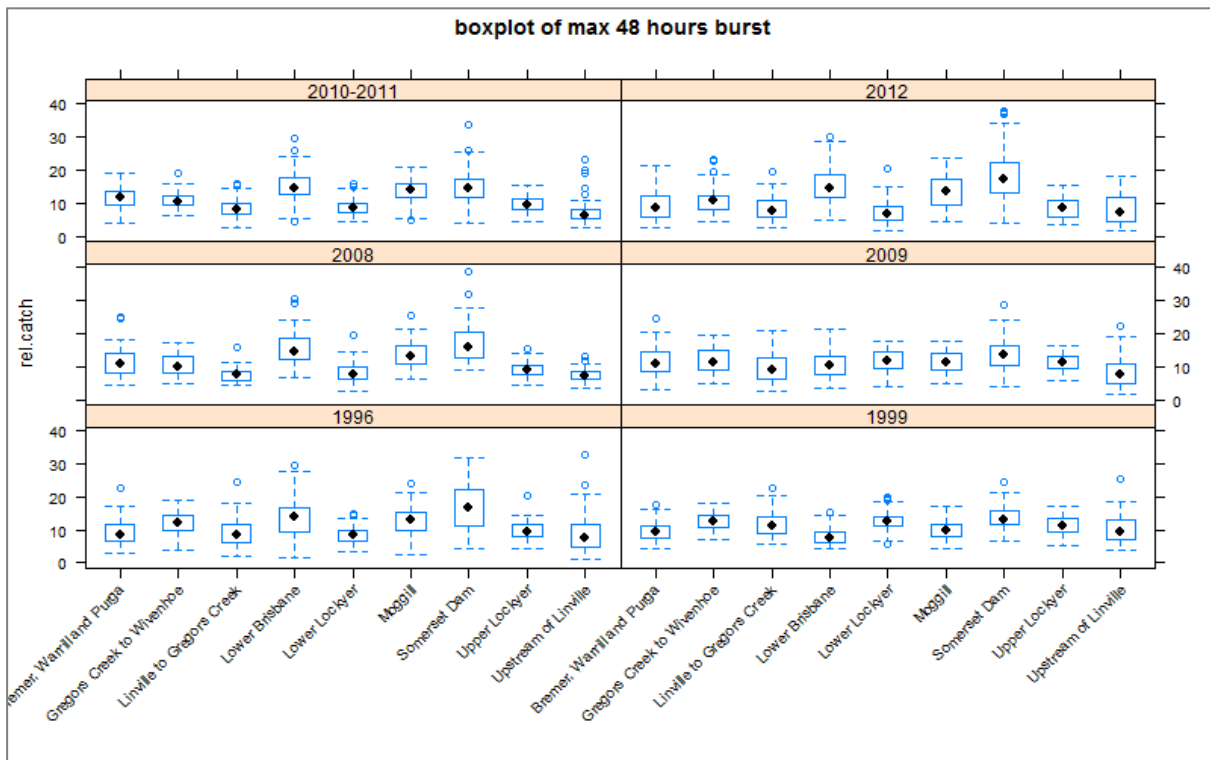


Figure 5-6 Boxplots of the relative contribution (%) of each catchment within the total max 48 hour burst

5.4 Incorporation in the MCS framework

5.4.1 Scaling factor for rainfall depth

Section 2 described the proposed setup of the MCS framework. Sampling of the synthetic storms and subsequent scaling is done in step 3 (see Figure 2-4). In steps 1 and 2, the rainfall duration and (catchment-average) rainfall depth were sampled. The most straightforward sampling method for the synthetic rainfall patterns is to give each pattern (660 in total) an equal probability of being sampled, ie 1 in 660. However, this will lead to samples of storm patterns for which the duration and depth of the rainfall are not in accordance with the sampled rainfall depth and duration in step 1 and 2 of the MCS procedure. This means a filter criterion is required to make a selection of the rainfall patterns for which depth and duration match within acceptable limits with the sampled depth and duration in step 1 and 2.

With respect to rainfall depth, the crucial criterion in the selection process is the scaling factor that needs to be applied. The scaling factor is related to the rainfall depth of the catchment and storm duration under consideration. The synthetic rainfall pattern that is selected in step 3 needs to be scaled in such a way that the catchment rainfall depth is in accordance with the derived value of step 2 for the duration under consideration. Define the following quantities:

R_1 = catchment average rainfall depth as derived in step 2 of Figure 2-4

R_2 = catchment average rainfall depth from the sampled synthetic rainfall pattern

C = scaling factor: $C = R_1/R_2$

The rainfall intensities of the sampled synthetic rainfall pattern are multiplied with the scaling factor, C , to ensure that the catchment rainfall depth is in accordance with the derived value of step 2. To prevent that unrealistic storm patterns are created in the up-scaling process, the scaling factor should be limited to a certain range. According to Alan Seed of the BoM (personal communication) the scaling factor should not be outside the range [0.5, 2]. The allowed scaling factor of 2 in rainfall depth is therefore the first filter criterion that is applied in the selection process of the synthetic rainfall patterns.

Subsequently, a filter criterion for duration is required. Note that in case of the CSS and CRC-CH method, the duration and depth refer to the full event, whereas for the TPT method, duration and depth refer to a burst that occurs somewhere within an event. The selection methods for the synthetic patterns are further discussed separately for the three MCS sampling techniques (CRC-CH, TPT and CSS) in the following sections.

5.4.2 CRC-CH method

Ideally, there are multiple synthetic events to choose from, so we take variability of spatial and temporal patterns into account for each combined “class” of duration and depth. For the CRC-CH method, this is not the case unfortunately. This can be seen in Figure 5-7, which shows a comparison between sampled combinations of depth and duration and combinations of depth and duration of the 660 BoM synthetic rainfall patterns (blue dots). Only events with rainfall AEP > 1/2,000 were considered because for more extreme events, GTSMR based spatio-temporal patterns are used instead of the BoM synthetic rainfall patterns (see Section 5.6). Figure 5-7 shows that, especially for short duration, high rainfall depth events there are essentially no synthetic events to choose from.

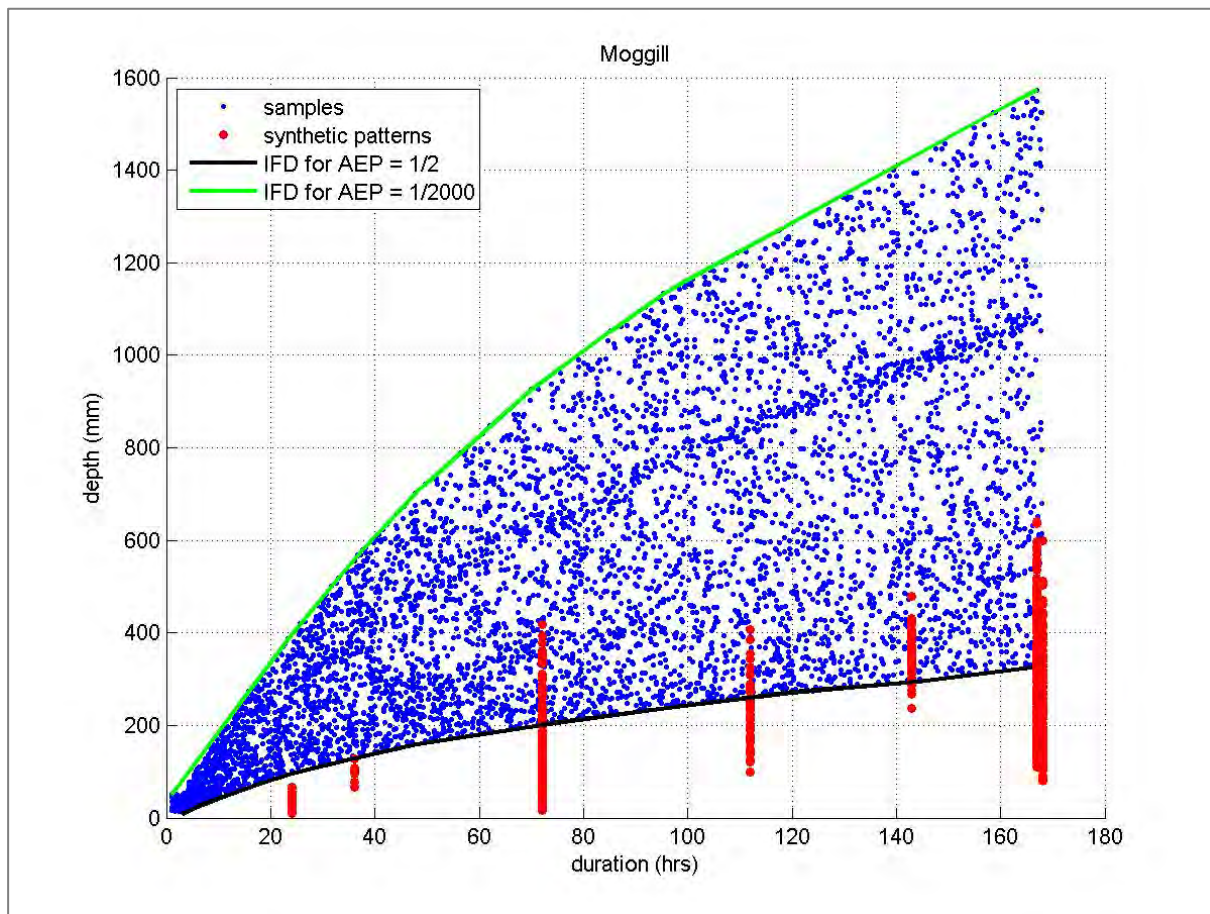


Figure 5-7 Comparison of sampled combinations of depth and duration in the CRC-CH method for events with rainfall AEP>1/2,000 (blue dots) and combinations of depth and duration of the 660 BoM synthetic rainfall patterns (red dots)

This is especially a problem for the smaller upstream catchments, where short duration events are expected to be critical for flood levels. To conclude: for the CRC approach as currently implemented in the MCS framework to be successful, additional synthetic rainfall patterns are required, especially ones with high rainfall depth in a relatively short duration. Since these patterns could not be provided within the remaining timeframe of the project, it was decided not to choose the CRC-CH method to produce the final output of the current project: flood frequency curves and food hydrographs for 23 locations.

5.4.3 TPT method

The TPT does not suffer from the above described problem because it uses rainfall bursts instead of rainfall events. Each synthetic event has only one event duration, but consists of multiple bursts for multiple burst durations. As a consequence, the TPT method generally has more synthetic patterns to choose from that sufficiently match the sample depth and duration. Figure 5-8 shows burst rainfall depths for 9 durations as derived from the data on the synthetic rainfall events (red dots). Each vertical line corresponds to a single duration and consist of 660 burst rainfall depths, ie one duration for each synthetic pattern. The two curves shown in this figure are the IFD curves that correspond to AEPs of 1/2 and 1/2,000. This curves represent the upper and lower bounds of the sampled rainfall depth (at least for events with AEP> 1/2,000, as stated earlier for more extreme events other patterns are used). A comparison between the red dots and the two curves reveals that for each duration there are plenty synthetic events to choose from, taking into account that a scaling factor of 2 is allowed.

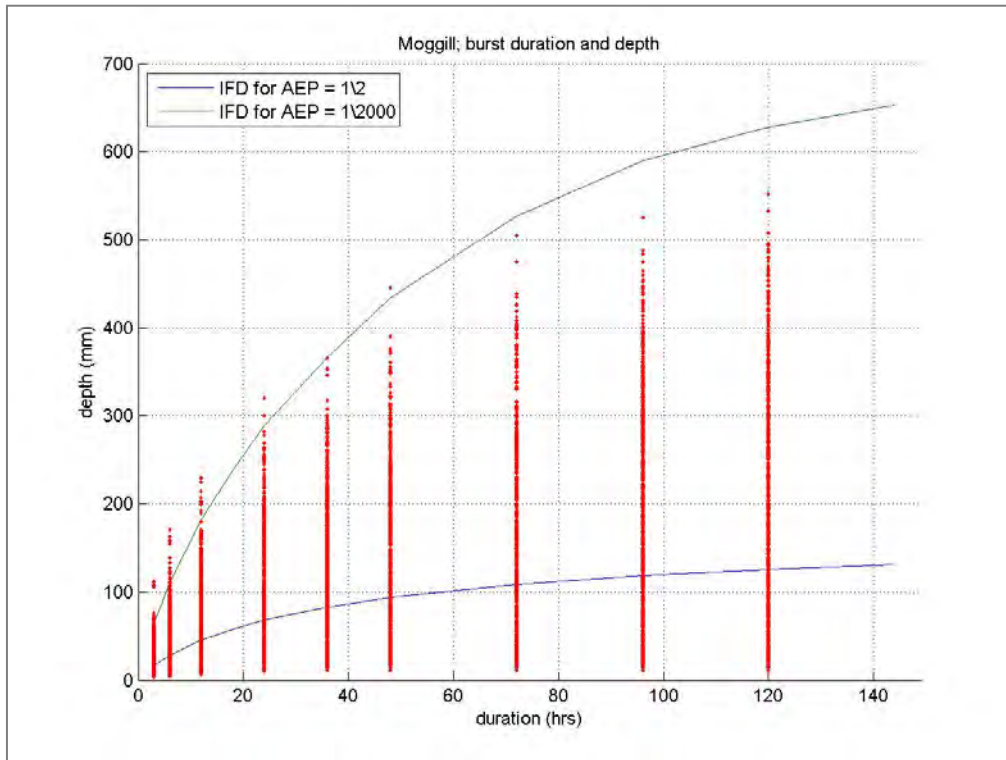


Figure 5-8 IFD curves for AEP = 1/2 and AEP = 1/2000 versus combinations of depth and duration of bursts in the 660 BoM synthetic rainfall patterns (red dots)

There is an additional requirement in the selection process for the synthetic rainfall patterns in the TPT approach: the burst rainfall patterns should not include sub-bursts of higher recurrence intervals, because this would interfere with the assumption that is made in the TPT approach of a critical duration for a sub-catchment of interest. This can be explained as follows: Consider a catchment that is sensitive to rainfall duration of 24 hours. In the TPT approach, several durations are considered and the duration that generates the highest peak discharge is selected as being the critical one. Suppose that, when considering the 48-hour duration, a temporal rainfall pattern is selected that includes a 24-hour burst in which most of the rain falls. This rainfall pattern would generate a high peak flow, because the catchment is sensitive to the 24-hour burst. This would lead to the false conclusion that the 48-hour duration is most critical and that the probability of high peak flow is derived from the probability of 48-hour rainfall depth. This problem can be avoided by excluding rainfall patterns that include sub-bursts with lower annual exceedance probabilities. In practice this can mean that quite a substantial number of rainfall patterns are filtered out. In order to prevent that too many storm patterns are filtered out this way, the within-burst filter criterion is relaxed to some extent. After extensive analysis of the influence of within-burst patterns on peak discharges, the following set of filter criteria was implemented:

If bursts with duration D are considered (in the TPT method), the following sub-bursts are not allowed:

1. Sub-bursts with durations between $D/3$ and D are not allowed to have a lower AEP than the burst with duration D
2. Sub-bursts with durations between $D/5$ and $D/3$ are not allowed to have an AEP that is more than twice as low as the burst with duration D
3. Sub-bursts with durations less than $D/5$ are not allowed to have an AEP that is more than three times as low as the burst with duration D

Storm patterns that violate any of these three criteria are filtered out. The motivation to be less stringent for bursts with durations $<D/3$ is that for catchments for which duration D is critical, durations $<D/3$ are generally not as critical as long as the AEP of the within burst is not too extreme. For the same reason an even more lenient filter criterion can be applied for durations $<D/5$.

The above set of criteria was found to result in the optimal within-burst filter. A more stringent set of criteria reduces the number of valid synthetic storms to sample from, which has the undesired effect of a reduction in variability of spatio-temporal rainfall patterns. A less stringent set of criteria lead to the undesired effect that within bursts are increasing the peak discharge. This is demonstrated in Figure 5-9, which is the result of simulations in which a less stringent filter criterion was applied. The Figure shows simulated peak discharges versus the AEP of the rainfall event at location Tinton, for burst durations of 24 hours. The circles indicate events with “within bursts”. The colour of the circle indicates the magnitude of the within burst in terms of AEP ratios. For example, a red colour indicates the existence of a within burst rainfall depth with an AEP that is a factor 2-3 smaller than the AEP of the 24 hour rainfall depth. This Figure clearly shows that the events with within-bursts dominate the upper range of peak discharges. The presence of within burst criteria in this example will lead to an increase of the peak discharge for given AEPs, which is undesired. A stricter set of filter criteria is therefore required, such as the one described above.

Note that the selected set of filter criteria can only work if a sensible upper limit is set on the bursts durations to be considered in the TPT method. This upper limit needs to take the size of the catchment into account, as short durations (<24 hours) are generally critical for small catchments (<1000 km²), whereas the critical duration tends to increase with increasing catchment size. Table 5-3 shows the proposed durations to be considered. Note that these proposed durations will be reconsidered during the reconciliation phase.

Table 5-3 Maximum burst durations considered

Catchment area (km ²)	Maximum burst duration (hrs)	
	No dams	With dams
<1000	24	-
<5000	48	-
<10,000	72	120
>10,000	96	120

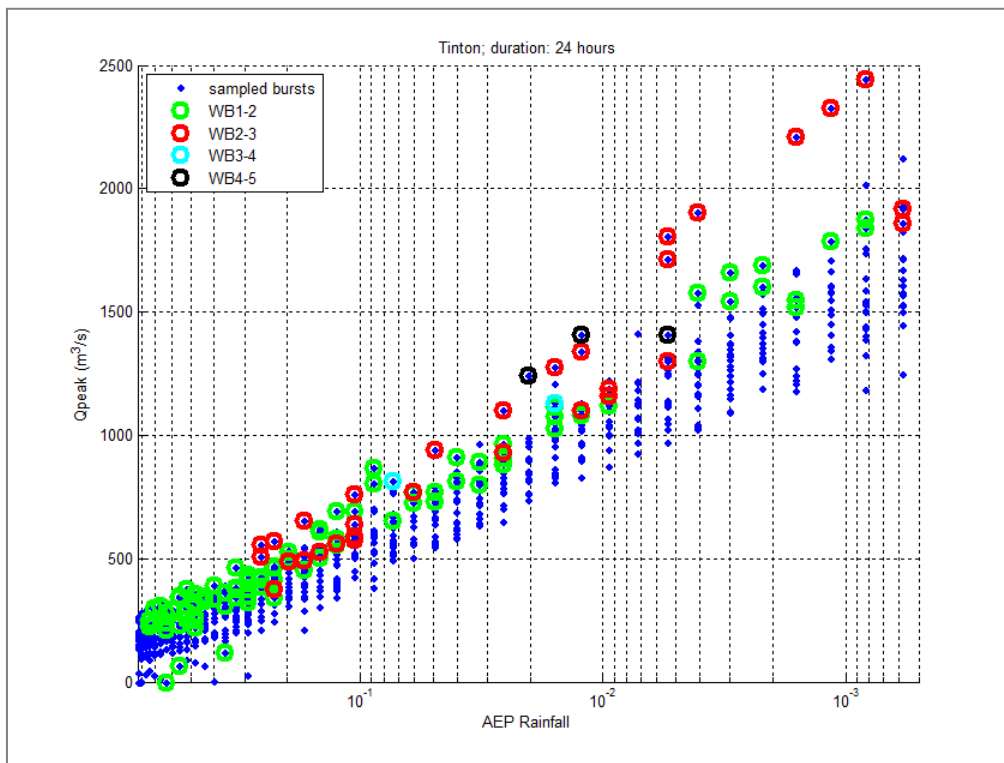


Figure 5-9 Simulated peak discharges versus AEP of the rainfall event at location Tinton, for burst durations of 24 hours. The circles indicate events with “within bursts”. The colour of the circle indicates the magnitude of the within burst in terms of AEP ratios. For example, a red colour indicates the existence of a within burst rainfall depth with an AEP that is a factor 2-3 smaller than the AEP of the 24 hour rainfall depth

Due to the introduction of the filter criteria for rainfall depth (scaling factor ≤ 2) and within-bursts), the number of rainfall patterns to sample from is significantly lower than the total number of 660 patterns. The number of available patterns depend on the considered burst duration and the AEP of the rainfall. Figure 5-10 shows the number of valid patterns for location Moggill (catchment size 12,500 km²) as a function of rainfall AEP for different durations. Figure 5-11 shows a similar plot for location Peachester (103 km²), the location with the smallest catchment of the 23 locations of interest. These Figures show that in general, the number of available valid rainfall patterns decreases with decreasing rainfall AEP and increasing duration. Note that the decrease in valid patterns for increasing durations only holds for durations of less than 24 hours. Above this threshold, the number of valid patterns seems to “stabilize”. The reason why there are more valid patterns for short durations is that for these durations less within-burst periods need to be considered in the filter process. The reason why there are less valid patterns for low AEP is that the scaling criterion becomes more relevant for these extreme events.

For location Moggill there are at least 30 valid patterns for each combination of AEP and duration. For location Peachester, the number of valid patterns for combinations of low AEP and durations > 24 hours is very limited. A further inspection of the number of valid patterns in the low AEP range (Table 5-4) reveals that in particular the three locations in the Stanley River catchment (Peachester, Somerset and Woodford) have low numbers of valid storm patterns for combinations of low AEP and long rainfall durations. All other locations have at least 20 valid patterns available for each combination of duration and AEP. As stated before, it is not allowed to be more lenient on the within-burst filter criterion for these three locations as this would incorrectly influence the derive frequency curves. This means we have to accept that for these three locations the number of valid patterns is limited for combinations of low AEP and long rainfall durations. Fortunately, longer durations are not critical for these relatively

small catchments and are therefore not taken into account in the TPT analysis (see Table 5-3). Furthermore, the added value of using realistic spatio-temporal patterns over spatially uniform patterns is relative low for smaller catchments.

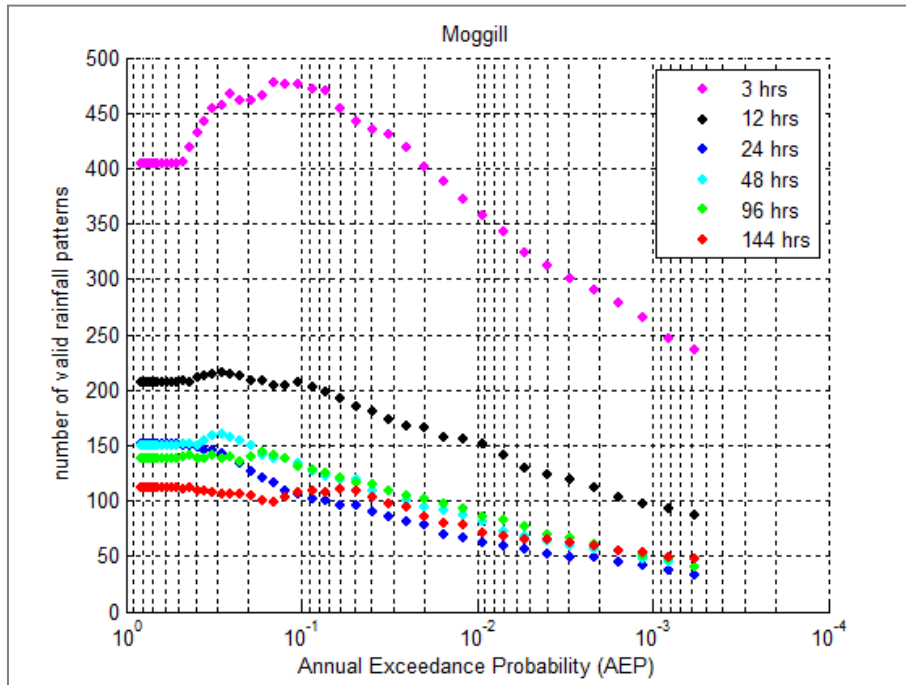


Figure 5-10 Number of valid rainfall patterns per duration and AEP after application of the within burst filter criterion; Location Moggill

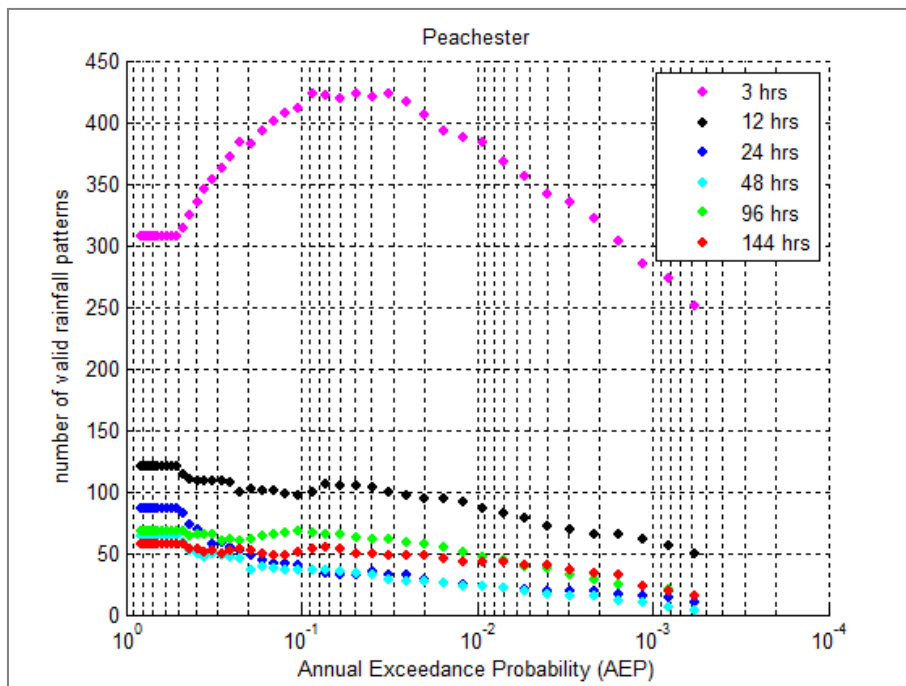


Figure 5-11 Number of valid rainfall patterns per duration and AEP after application of the within burst filter criterion; Location Peachester

Table 5-4 Number of valid rainfall patterns per duration for AEP=1/2000, after application of the within burst filter criterion. Numbers lower than 20 are highlighted with a grey colour

location	Area (km ²)	duration (hrs)										
		3	6	12	18	24	36	48	72	96	120	144
Amberley	902	131	163	107	57	49	36	30	32	43	39	49
Brisbane	13198	238	121	83	40	36	36	42	40	44	43	44
Cent. Bridge	12877	239	132	88	41	36	37	43	38	41	44	48
Fulham Vale	4553	135	159	119	77	56	49	46	58	69	60	51
Gatton	1527	123	171	136	71	55	55	47	33	44	43	31
Glen. Grove	2149	131	172	137	66	51	55	48	30	40	38	34
Greg. Creek	3849	117	150	119	73	58	50	43	56	67	59	51
Helidon	351	120	153	137	77	59	43	39	29	35	34	37
Ipswich	1850	144	170	110	62	49	42	29	31	41	43	49
Kalbar Weir	458	171	162	104	40	45	34	27	30	37	36	46
Linville	1996	92	140	121	70	56	48	37	63	65	55	50
Loamside	209	111	128	81	46	38	21	22	24	27	28	38
Middle Ck	6665	181	167	106	54	44	33	31	40	53	48	53
Moggill	12578	237	141	89	43	34	36	42	40	42	46	49
Mt. Crosby	10507	210	160	100	47	37	38	37	41	47	46	48
Peachester	103	252	118	51	20	11	8	4	15	16	12	17
Rifle Range	2521	119	174	139	66	55	52	49	27	44	37	37
Savages Xing	10126	204	163	100	51	39	37	40	41	51	48	48
Somerset	1324	218	166	72	28	15	11	12	19	18	15	27
Tinton	423	147	167	130	70	50	40	37	36	48	38	45
Walloon	634	144	169	125	65	47	48	32	27	35	38	40
Wivenhoe	6980	184	171	106	55	41	32	33	38	53	46	52
Woodford	245	269	124	68	29	17	10	10	17	20	13	21

The analyses in this section lead to the conclusion that the application of the synthetic patterns can be incorporated well within the TPT sampling method.

5.4.4 CSS method

Like the CRC-CH, the CSS approach is based on rainfall *event* statistics. However, in the CSS, no use is made of IFD tables. The rainfall depth is determined by fitting a distribution function to historical rainfall records. The duration of the rainfall event is determined by the 660 synthetic rainfall patterns from the BoM STEPS model. It is assumed that the BoM synthetic rainfall patterns represent the spatial and temporal distribution of storm durations for a given rainfall depth. This is potentially a weak point of the CSS approach and needs to be verified.

The CSS method was tested on the total Brisbane River catchment as well as on a number of sub-catchments. The following steps are taken:

1. Determine the distribution function for the area-averaged rainfall depths in the total Brisbane catchment based on historical records (see Figure 3-2)

Repeat the steps 2-5 N times (eg $N=10,000$):

2. Randomly select a number between 0 and 1, representing the rainfall depth exceedance probability. Sample the catchment total rainfall depth based on the fitted distribution function (step 1)
3. Search for stochastically generated space-time rainfall patterns for the Brisbane River catchment (the 660 events provided to the BRCFS project by Seqwater) that matches the rainfall depth found in step 2. Hereby a scaling factor is used that is set at a maximum of 2. Randomly select one rainfall pattern in case of several matches
4. Rescale the rainfall amounts of selected synthetic space-time rainfall pattern to match the sampled depth
5. Determine the maximum rainfall depth for the different durations for the total (sub-)catchment under consideration
6. Derive an IFD table for all considered durations and ARIs (AEPs) based on the N sample results of 2-5

The resulting rainfall IFD curves from the CSS method were compared with the IFD tables of BoM. Figure 5-12 shows the relative difference in rainfall depth (CSS minus BoM IFD divided by BoM IFD) as a function of duration for several (sub-)catchments. The lines represent the different ARIs. Figure 5-13 shows the same results with reverted axes. For the different sub-catchments, the performance of the CSS method varies. Overall, the differences with BoM IFD tables are large for 2 years ARI and for short durations. The variation of the performance increases with increasing ARI. Overall differences in rainfall statistics between the CSS method and the BoM IFD tables are significant and can even be higher than 50%.

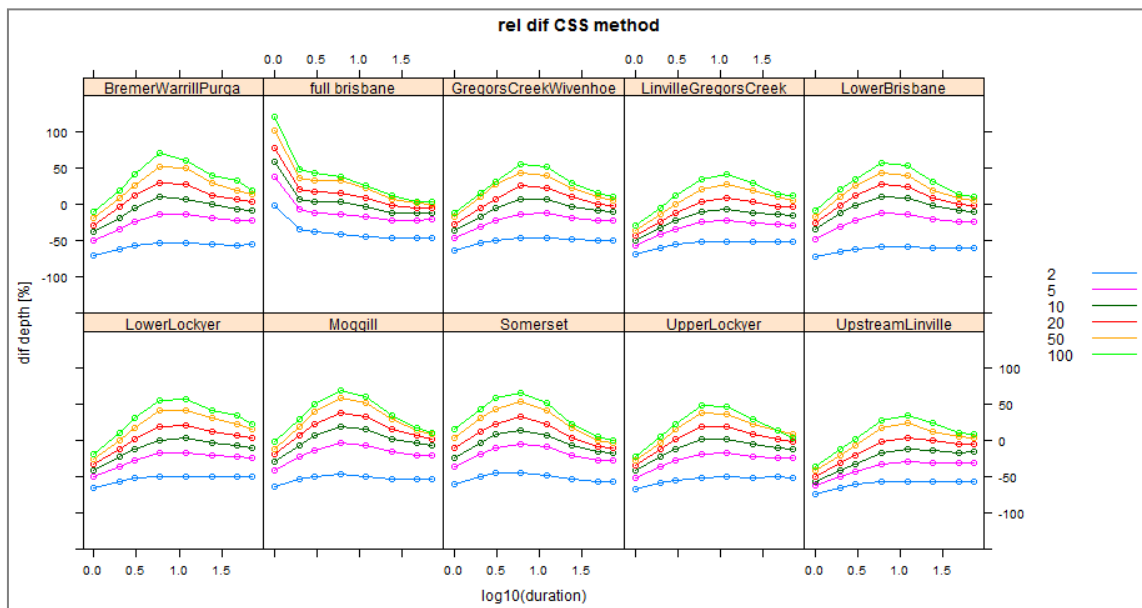


Figure 5-12 Relative differences in calculated rainfall depth between CSS method and IFD tables as functions of duration for the total Brisbane catchment (full Brisbane) as well as for all the sub-catchments. The different colours represent different ARI's

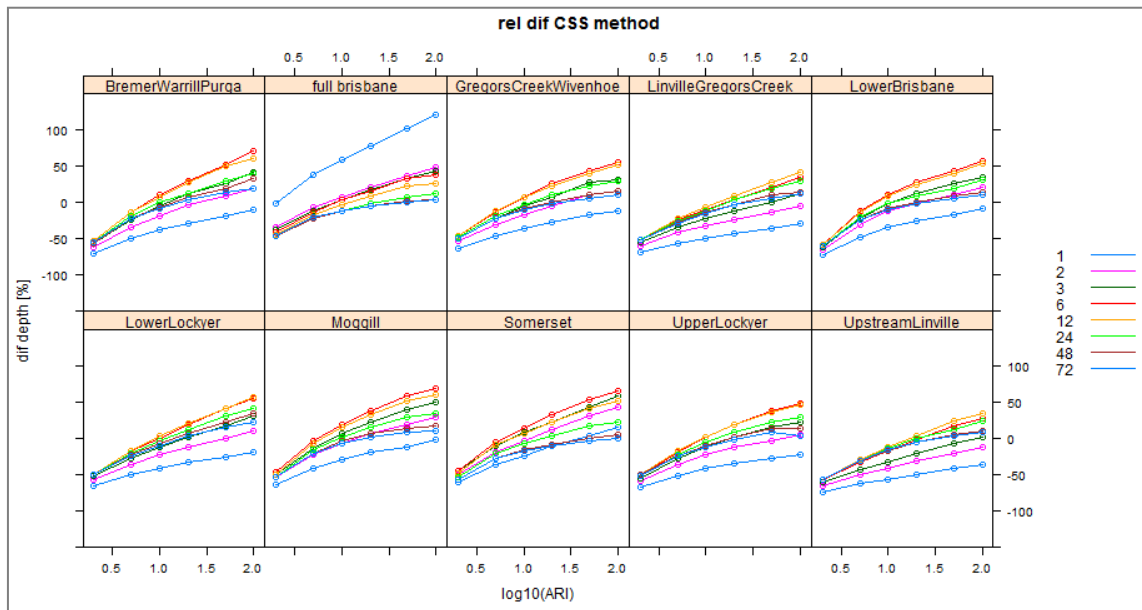


Figure 5-13 Relative differences in calculated rainfall depth between CSS method and IFD tables as functions of ARI for the total Brisbane catchment (full Brisbane) as well as for all the sub catchments. The different colours represent different durations


The main conclusion is that differences in rainfall statistics between the CSS method and the BoM IFD tables are significant and can even be higher than 50%. This difference is considered too large to be neglected, and implies that the CSS method *in the current form with the current data* is rejected as a method for the BRCFS. Possibly, the deviations from the IFD tables can be reduced by a correction function, which, however, would need to be a bivariate duration-depth function. Construction of this correction function is considered beyond the scope of the BRCFS project. Moreover, we feel that the need for such a correction function reduces the merit of the method.

For the Brisbane river catchment, as well as the sub catchments the CSS method shows a systematic underestimation of the rainfall amount for events with durations of less than 24 hours. Apparently, the synthetic rainfall patterns do not represent a correct distribution of short event durations. This is not all too surprising, since the synthetic rainfall patterns were selected for large storm events over the total Brisbane catchment. It is likely that short and intense convective rainfall events are underrepresented.

Another issue of the CSS method is the depth distribution function (step 1). This distribution function is based on 48 events which are not necessarily representative of a correct peak over threshold selection of events. This is likely to be another cause of inconsistencies with the BoM IFD tables.

5.4.5 Conclusion

The use of realistic synthetic spatio-temporal rainfall patterns is a potential major advantage over the more traditional design event approach, which uses a spatially uniform rainfall distribution (uniform with respect to rainfall AEP) and a single standardised temporal pattern. A consistent method for incorporating the available 660 synthetic rainfall patterns in the MCS framework is therefore of crucial importance. It was found that this is possible if the TPT as the sampling method for rainfall depth and duration. This method provided the best match between the rainfall IFD curves on one hand and the available synthetic spatio-temporal rainfall patterns on the other hand. For this reason, the TPT method is chosen as the preferred sampling method *for the current study*. The other two methods



(CSS and CRC-CH) are nevertheless considered very promising for future applications of Monte Carlo applications, especially if more synthetic spatio-temporal rainfall patterns become available.

5.5 Observed versus synthetic rainfall patterns

One of the crucial issues in the BRCFS is whether sampled synthetic events in the MCS framework are in accordance with observed rainfall patterns. For this purpose we compared the spatial distribution of the BoM synthetic events with the rainfall data from the 125 observed events with highest catchment total rainfall depth. The data of the 125 event were provided by WMAWater (WMAWater, 2014), see Section 4.3.3.

To compare the spatial statistics of synthetic and observed events, the catchment was divided in five sub-catchments: Upper Brisbane, Lower Brisbane, Stanley, Lockyer and Bremer (including Warrill and Purga). Furthermore, a sixth sub-catchments was considered: “Upstream Wivenhoe”, ie the combination of Upper Brisbane and Stanley. For each event, synthetic or observed, the percentage of the total rainfall in the Brisbane catchment fell in each individual sub-catchment was derived.

For the 125 observed events this resulted in 125 percentages for each sub-catchment. The set of 125 percentages were translated to histograms and empirical distributions for each sub-catchment. The histograms and distributions show the variation in rainfall percentages of each sub-catchment. A similar exercise was done for the 660 BoM synthetic events. Figure 5-14 to Figure 5-16 compares the results. The Figures show that overall the statistics of BoM synthetic events and observed events match reasonably well.

The most noticeable differences are:

- For the percentage contribution of the Lower Brisbane, the data shows less variation than the synthetic events. According to the data, in almost all events the percentage of the total rainfall that falls in the Lower Brisbane is between 10% and 20%, whereas the synthetic events show more cases with higher or lower percentages
- For the percentage contribution of the Upper Brisbane, the data also shows less variation than the synthetic events. Differences are especially present in the ‘lower tail’. In other words: the number of events in which less than 35% of the total rainfall falls in the Upper Brisbane occur more frequently in the set of synthetic events
- For the Stanley River there also seems to be a mismatch in the lower tail (events with 8-15% rainfall in the Stanley sub-catchment)

In spite of these differences, the results are encouraging. Note that:

- A perfect match can never be expected between statistics of data of different sources
- The lower variation in percentages in the observed events for the Upper and Lower Brisbane may partially be explained by the fact that for the observed events from before 1955 there were a significantly lower number of rainfall stations present in the Brisbane River catchment

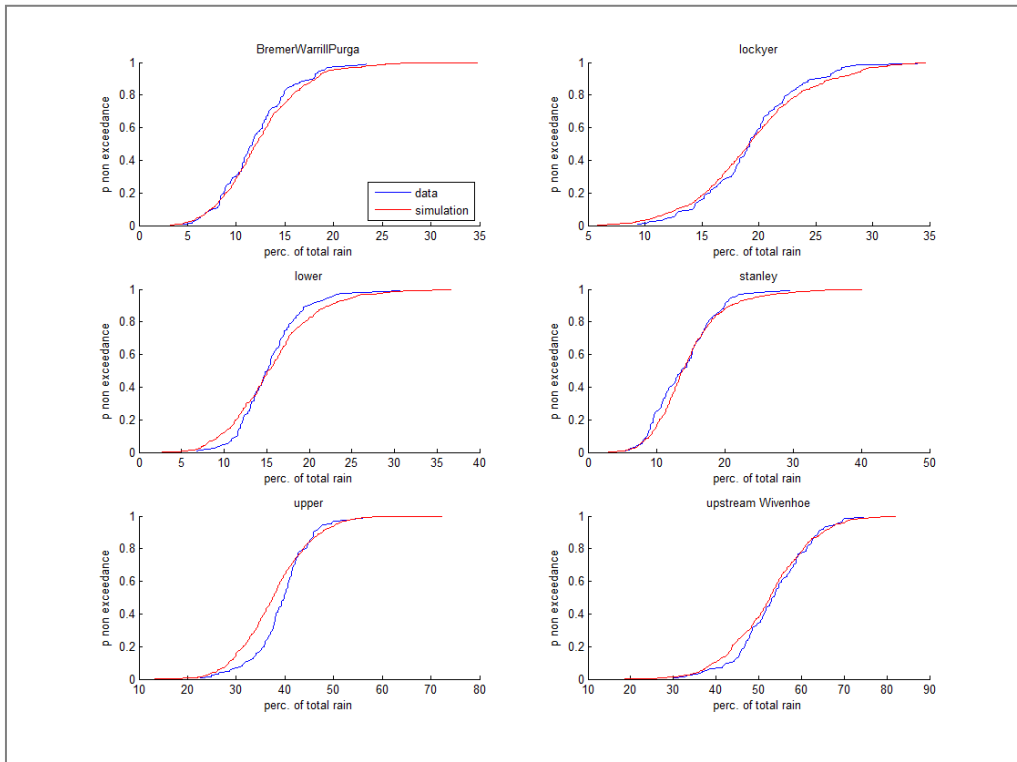
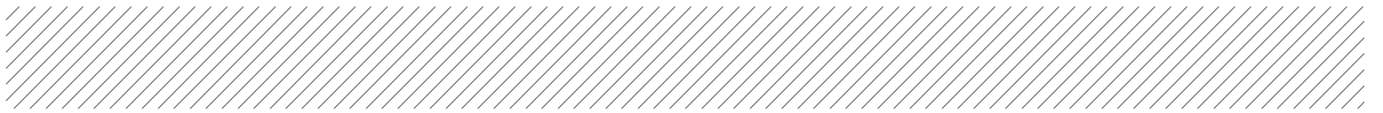


Figure 5-14 Empirical distributions of contributions of individual sub-catchments to the total catchment rainfall

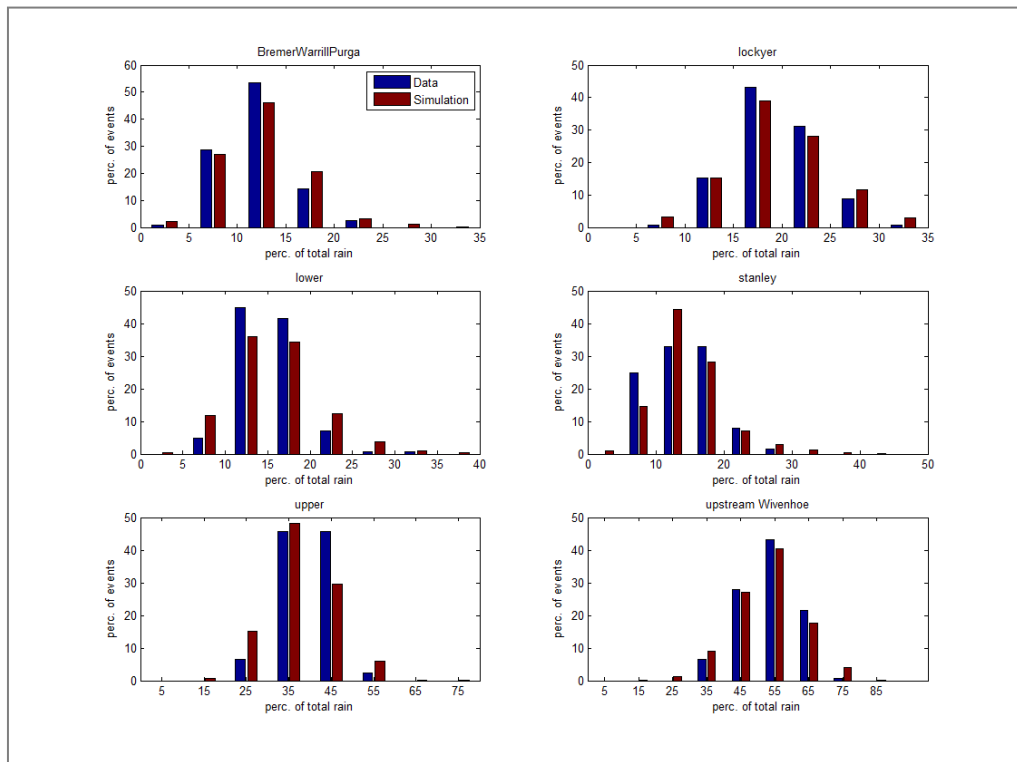


Figure 5-15 Histograms of contributions of individual sub-catchments to the total catchment rainfall

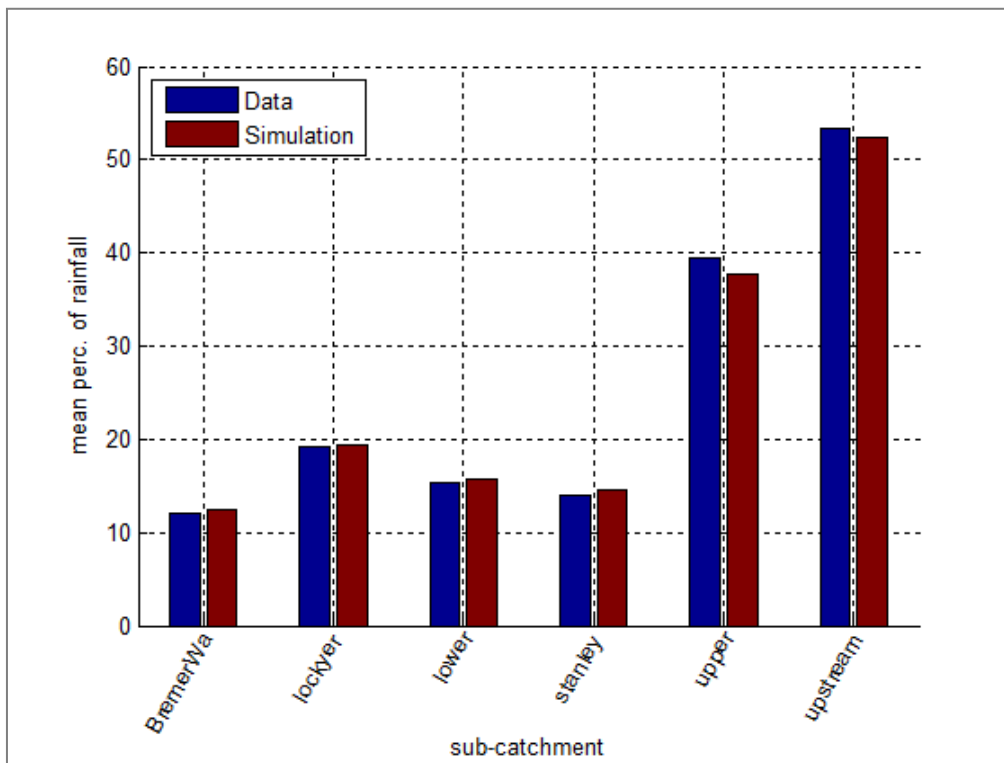


Figure 5-16 Average contribution of individual sub-catchments to the total catchment rainfall

A better match between statistics of BoM synthetic events and observed events can be obtained by awarding (probability) weights to the synthetic events. These weights can be adopted in the MCS framework. For example, it was observed that the percentage of synthetic events in which less than 35% of the total rainfall falls in the Upper Brisbane sub-catchment is 'too high'. If we award lower probability weights to synthetic events with low percentages of rainfall in the Upper Brisbane catchment, differences as observed in and Figure 5-15 should be reduced. Similar weight reductions can be applied to synthetic events that cause the observed differences in the Lower Brisbane sub-catchment. Of course this needs to be done carefully in such a way that "all" criteria are met, noting that a perfect match cannot be expected (also taking uncertainties in observed data into account). Figure 5-17 to Figure 5-19 show the results after introduction of the probability weights. It shows a better match between statistics of observed and simulated events in comparison with Figure 5-14 to Figure 5-16.

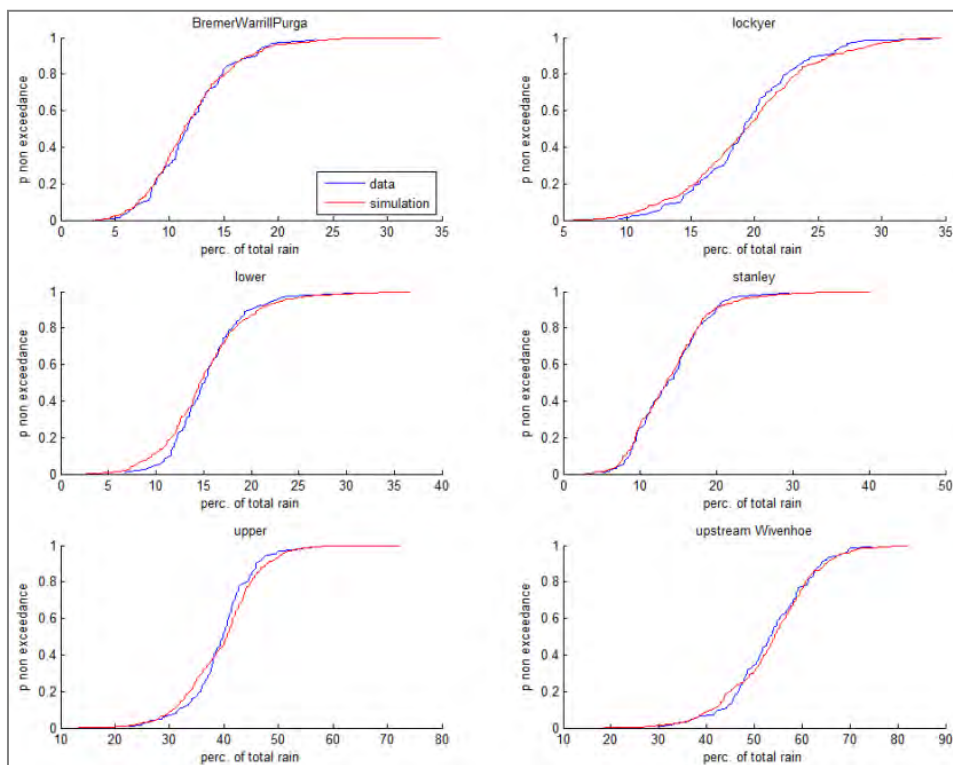


Figure 5-17 Empirical distributions of contributions of individual sub-catchments to the total catchment rainfall. Probability weights were applied for the BoM synthetic (simulated) events

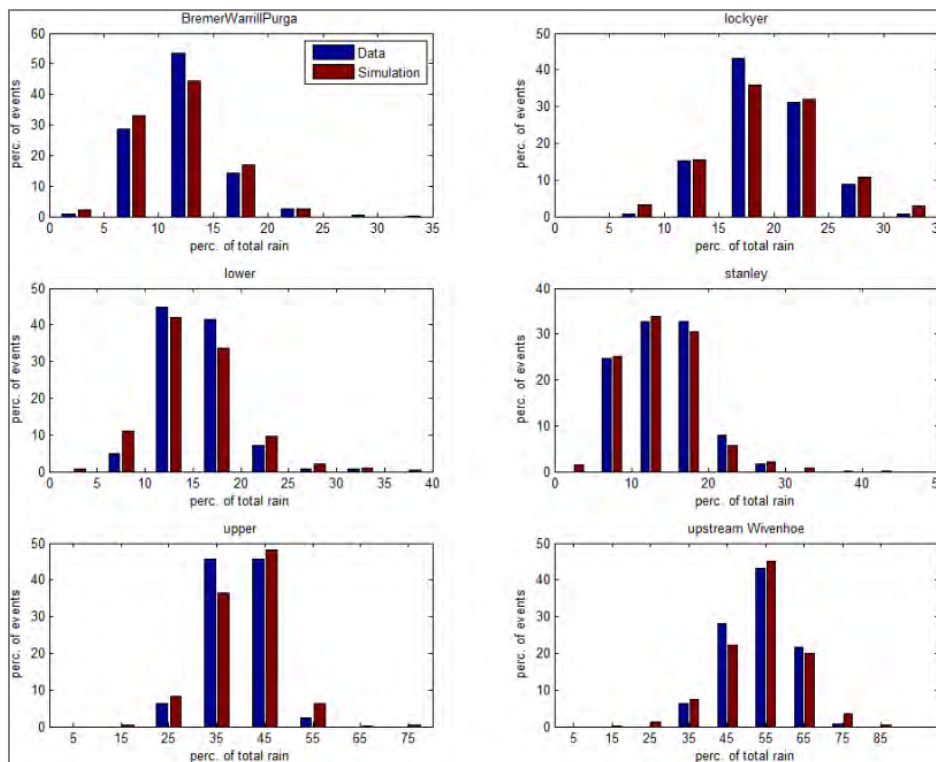


Figure 5-18 Histograms of contributions of individual sub-catchments to the total catchment rainfall. Probability weights were applied for the BoM synthetic (simulated) events

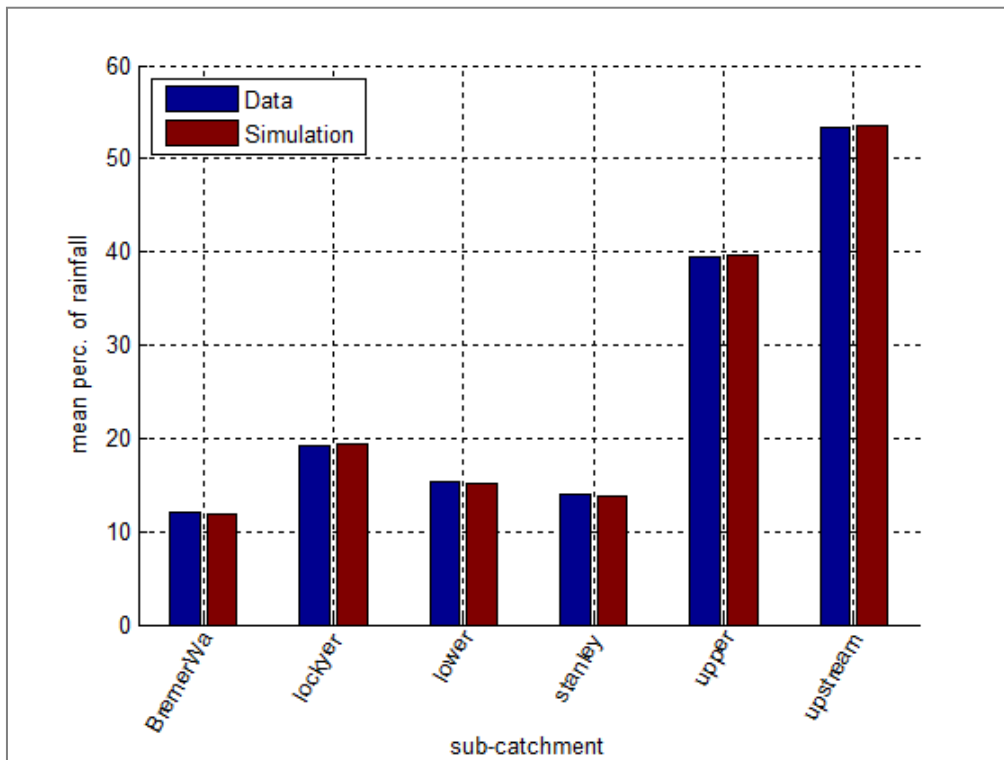


Figure 5-19 Average contribution of individual sub-catchments to the total catchment rainfall. Probability weights were applied for the BoM synthetic (simulated) events

As pointed out previously, there is some degree of uncertainty to what extent the observed percentages of contributions from sub-catchments are affected by variations in the density of the rainfall station network. The low variation in percentages for the Upper and Lower Brisbane may partially be explained by the fact that for the observed events in the period before 1955 there were a significantly lower number of rain gauges present in the Brisbane River catchment. Spatial differences in rainfall may therefore not (or to a lesser extent) have been observed by the available rain gauges.

To investigate this hypothesis, a comparison is made between spatial rainfall statistics of pre- and post-1955 events. Figure 5-20 shows the comparison of empirical distributions of relative sub-catchment contributions between pre-1955 and post 1955 events (both based on the data set of 'top' 125 events of WMAWater, 2014). It shows the curves for the pre-1955 events (blue lines) are generally steeper than for the post-1955 events (red lines), indicating a lower variability of spatial distribution between events. This supports the hypothesis that the lower variation in percentages in the observed events for the Upper and Lower Brisbane (compared to synthetic events) is most likely (partially) caused by the fact that for the observed events from before 1955 there were a significantly lower number of rainfall stations present in the Brisbane River catchment.

A comparison between statistics of 660 BoM synthetic events and post-1955 events (Figure 5-21 to Figure 5-23) shows there is a better match between synthetic events and data than if we compare with the observed data over the complete period of observations (Figure 5-14 to Figure 5-16). Of course, the match is not perfect, which may also be partially due to limited number of observed events. Nevertheless, in our view these Figures indicate that it may be justified *not* to introduce probability weights for the BoM events in the MCS framework to obtain a better fit between observed and synthetic data. This has the advantage that each synthetic event is equally likely to be sampled, which increases the variability of sampled events.

To conclude: the analyses in the current section justify the use of the synthetic rainfall patterns in the sense that they can be expected to generate representative spatial rainfall patterns.

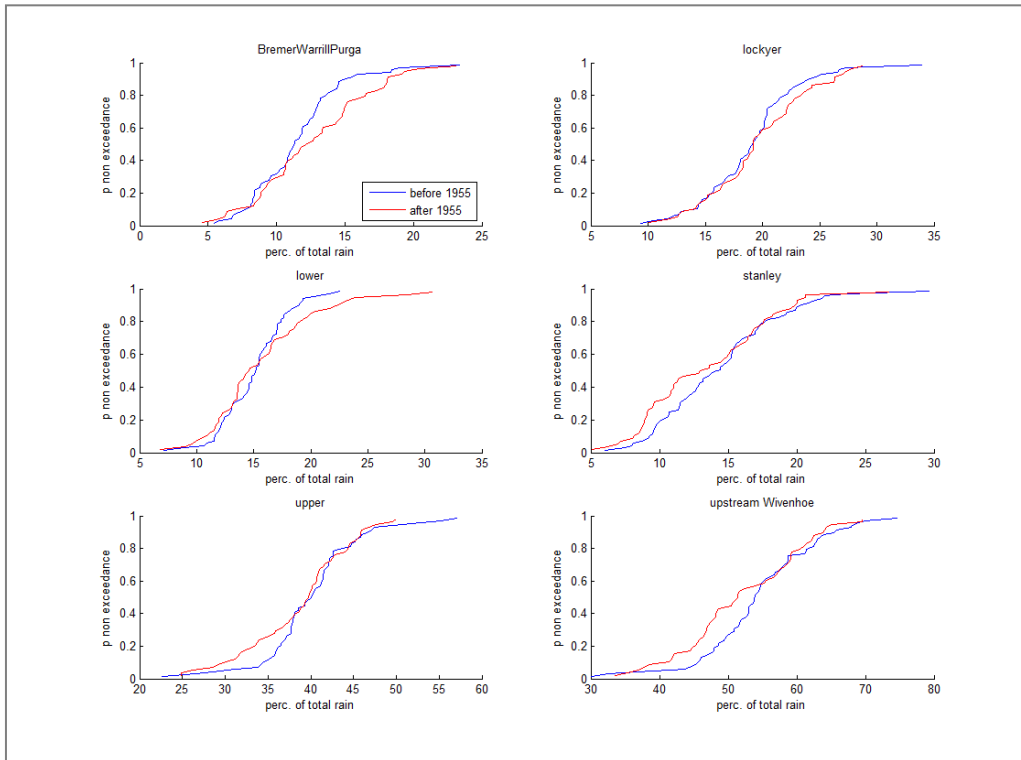


Figure 5-20 Empirical distributions of contributions of individual sub-catchments: comparison between 68 pre-1955 events and 57 post-1955 events

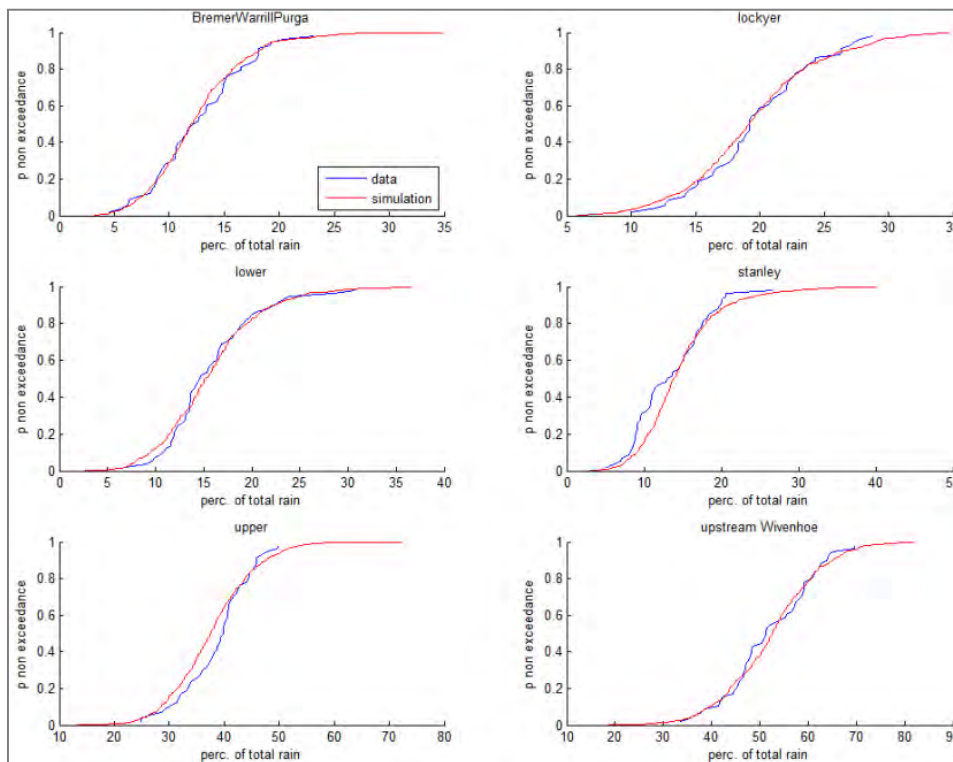


Figure 5-21 Empirical distributions of contributions of individual sub-catchments to the total catchment rainfall. Rainfall data was based on post 1955 events only

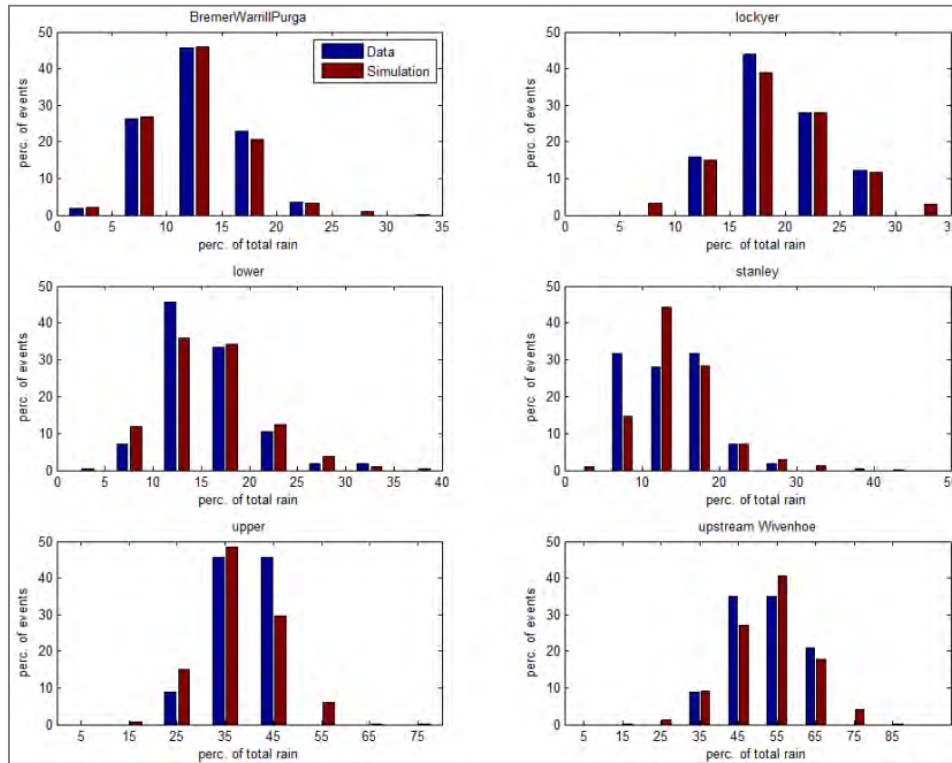
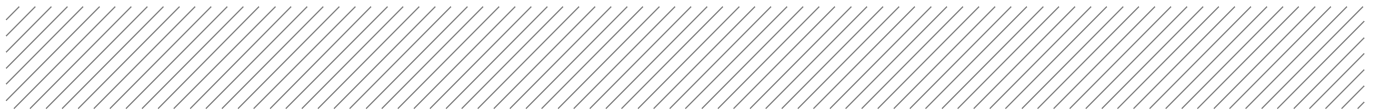


Figure 5-22 Histograms of contributions of individual sub-catchments to the total catchment rainfall. Rainfall data was based on post 1955 events only

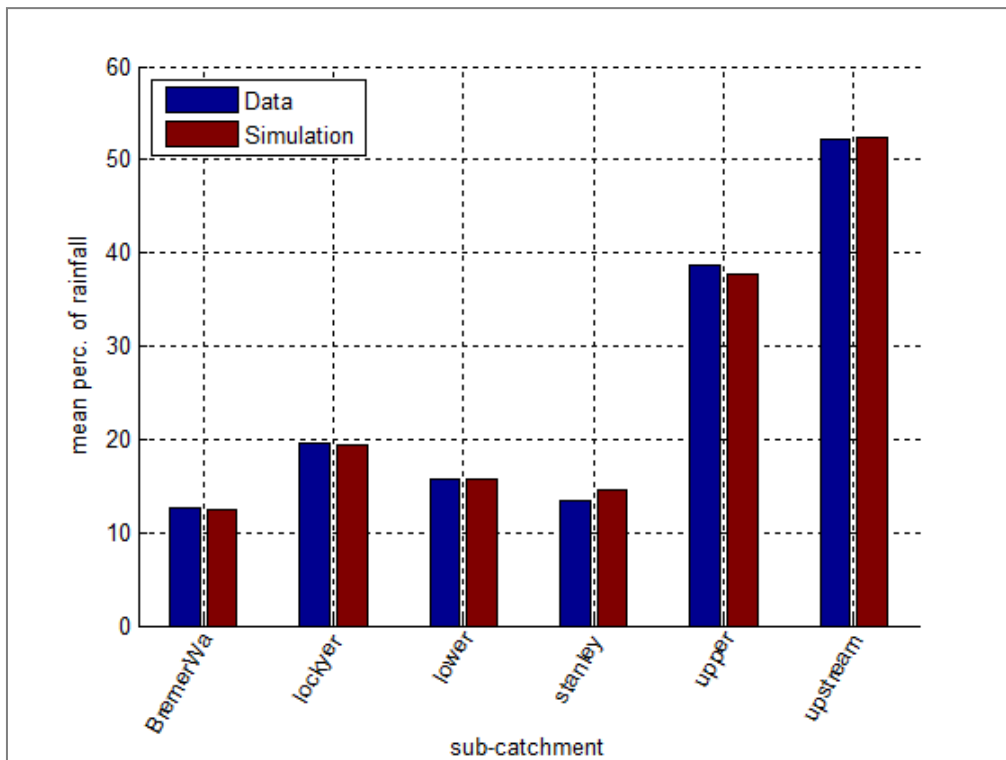


Figure 5-23 Average contribution of individual sub-catchments to the total catchment rainfall. Rainfall data was based on post 1955 events only

5.6 Selection of patterns for low AEP-events

For extreme events, ie events with low rainfall AEP, the selected synthetic rainfall patterns generally need to be scaled up with high scaling factors. This is especially the case for rainfall events with $AEP < 1/2,000$ per year, for which the IFD curve is derived with the GTSMR method (BoM, 2003). Scaling factors higher than 2 may be required and this is undesirable. It was therefore decided to adopt a different approach for events with $AEP < 1/2,000$ per year. For this range, GTSMR-based rainfall patterns are used (BoM, 2003). This means a single spatial distribution is applied, which corresponds to the IFD rainfall depth of a 72-hour, 50-year ARI event. For the temporal distribution, 10 temporal patterns are adopted from the GTSMR approach for a range of durations (24, 36, 48, 72, 96 and 120 hours). For a single duration, each of the 10 available temporal patterns has an equal probability of being sampled.

The change in approach in sampling spatio-temporal rainfall patterns is likely to result in “discontinuities” in the relation between rainfall AEP and peak discharge at $AEP = 1/2,000$. To prevent this from happening, a gradual changeover is introduced by using a mixture of the two type of patterns for rainfall AEPs between $1/2,000$ and $1/20,000$. For this purpose a variable P_s is introduced that represents the probability of sampling a pattern from the set of 660 BoM synthetic patterns. This automatically means that the probability of sampling a GTSMR pattern is equal to $1 - P_s$. The value of P_s is a function of the rainfall AEP:

$$P_s = \begin{cases} 1 & ; AEP > 1/2000 \\ {}^{10}\log(1/2000) - {}^{10}\log(AEP) & ; AEP \in [1/20000, 1/2000] \\ 0 & ; AEP < 1/20000 \end{cases} \quad (13)$$

Figure 5-24 shows P_s as a function of AEP. It shows the probability, P_s , of sampling a pattern from the set of 660 BoM synthetic patterns gradually decreases from 1 to 0 between $AEP = 1/2,000$ and $AEP = 1/20,000$.

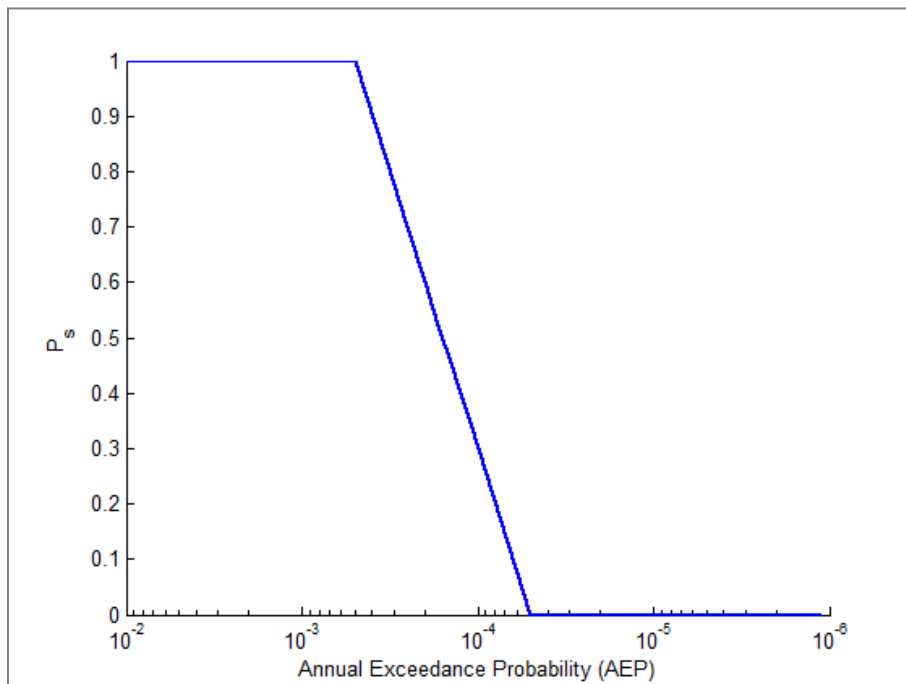


Figure 5-24 Value of P_s as a function of the annual exceedance probability of the rainfall

6 Sampling of other random variables

6.1 Introductions

Section 3 to Section 5 described the procedures to sample rainfall depth, rainfall duration and spatio-temporal rainfall patterns. The current section discusses the sampling procedures of the remaining variables of the Monte Carlo framework:

- Initial losses
- Ocean water levels
- Reservoir volumes

6.2 Initial losses

6.2.1 Marginal distributions

Ilahee et al [2001] proposed a 4-parameter beta-distribution to describe probability distribution of initial losses. The 4-parameter beta-distribution distribution has since become the standard in rainfall based design studies in Australia. The density function of the 2-parameter beta-distribution function is as follows:

$$f(x) = \frac{x^{\alpha-1}(1-x)^{\beta-1}}{B(\alpha, \beta)}; \quad B(\alpha, \beta) = \int_0^1 x^{\alpha-1}(1-x)^{\beta-1} dx; \quad 0 \leq x \leq 1 \quad (14)$$

This density function is defined on the interval [0,1]. The 2-parameter beta-distribution becomes a 4-parameter beta-distribution if the limits, 0 and 1, are replaced by additional function parameters x_L (lower bound) and x_U (upper bound):

$$f(x) = \frac{x^{\alpha-1}(1-x)^{\beta-1}}{(x_L - x_U)B(\alpha, \beta)}; \quad x_L \leq x \leq x_U \quad (15)$$

Recently, an alternative approach was proposed by ARR (2013b). This approach uses a non-parametric standardised initial loss distribution. In this approach, the quantiles of the initial loss distribution are normalised by the median initial loss, ie the initial loss with probability of (non-) exceedance of 50%. It is observed by ARR (2013b) that the normalised distribution function is very similar for most catchments. If the standardised distribution function is indeed applicable to the entire Brisbane River catchment the distribution functions for individual sub-catchments is characterised by a single value: the median initial loss. Table 6-1 shows the standardised initial loss distribution as

derived from ARR (2013b)⁴. It is worth mentioning that the ARR2013b draft report has been updated in 2014, including an update of the standardised distributions. Changes were minor, however, and the distribution function from ARR2013b was suitable for the current study, as demonstrated in this section. It was therefore decided to stick with the standardised distribution function of ARR2013b.

The use of the standardised distribution has the advantage that it uses only a single parameter, which prevents adverse effects from “overfitting”. However, this advantage only holds if the initial losses indeed are distributed according to the standardised distribution. If the latter is not the case, the 4-parameter distribution has the advantage that it is much more flexible and, hence, better able to describe the true probability distribution. This is demonstrated by the fact that the beta-distribution provides a very good fit of the standardised initial loss distribution of ARR [2013] if the parameters of the beta-distribution are taken equal to the values listed in Table 6-2. The fit is shown in Figure 6-1. This implies that if the standardised initial loss distribution function of ARR (2013) is the preferred option, the beta-distribution can still be used to describe this distribution function in the computational framework, which is convenient for implementation. In that case, the beta-distribution with parameters as displayed in Table 6-2 is applied to obtain standardised samples of initial losses. These standardised values are subsequently multiplied by the median loss of the sub-catchment under consideration to obtain “actual” values of initial losses.

Table 6-1 Standardised initial loss distribution, estimated from Figure 5-21 of ARR, 2013. The standardised values represent a fraction of the median initial loss

Probability of exceedance	Standardised initial loss[-]
1	0.25
0.9	0.45
0.8	0.6
0.7	0.7
0.6	0.85
0.5	1
0.4	1.2
0.3	1.5
0.2	1.8
0.1	2.3
0	3.7

⁴ These values were derived from a graph in AR&R (2013b), as no table was provided.

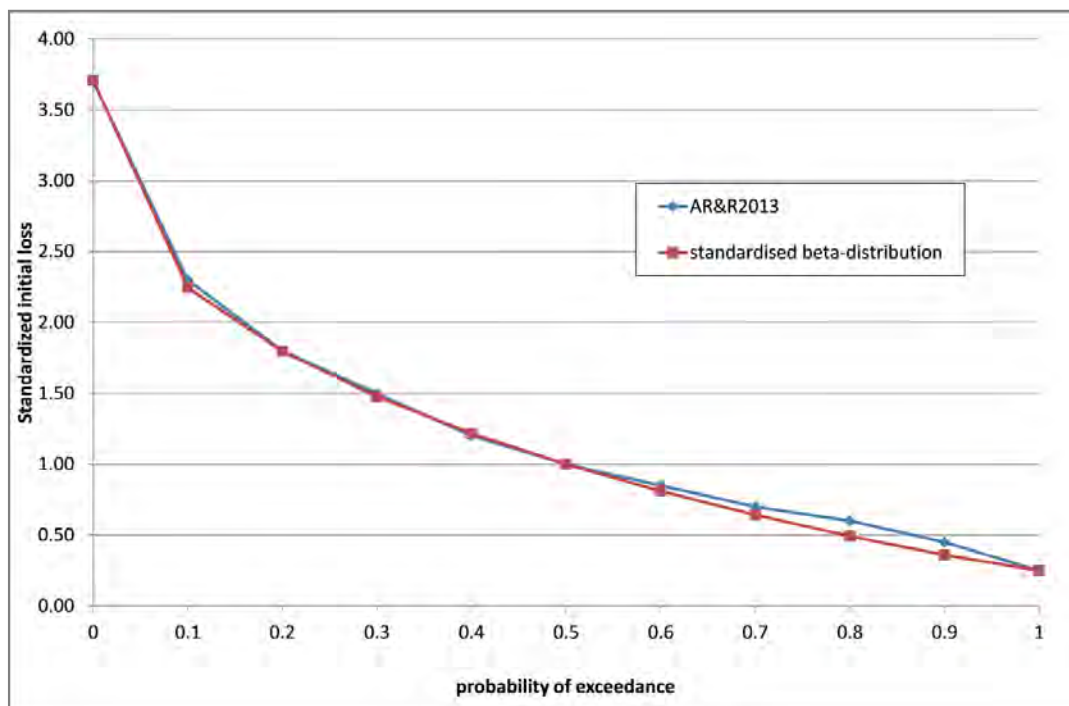


Figure 6-1 Comparison of the standardised initial loss distribution and the fitted standardised beta distribution

Table 6-2 Parameters of the beta-distribution that provide the optimal fit of the standardised distribution of Table 6-1

parameter	value
α	0.91
β	2.54
X_L	0.25
X_U	3.71

Information on initial losses in the Brisbane River Catchment is available from Seqwater (2013a). In their study, initial loss parameters for 48 events were based on model calibrations. Analyses were carried out for the seven sub-catchments (see Figure 2-1), in which initial losses were assumed uniform over the entire sub-catchment. It was recognised by Seqwater (2013a) that: *“decreased scale (increased number of sub-catchments) could provide an opportunity for applying locally specific loss and routing parameters. However increased division and number of models would add greater complexity (hence potential for errors) also decreases the potential to make best use of available gauge data with consideration of rating uncertainties. The final adopted basin sub-division was considered an optimal trade-off between the factors above.”*

Figure 6-2 shows the derived empirical standardised distributions for initial losses of the seven sub-catchments of the Brisbane River catchment, in combination with the standardised initial loss distribution of ARR (2013b) (thick red line). Loss data were adopted from Seqwater (2013a). It shows that the standardised distributions of all sub-catchments except Stanley are well in accordance with the standardised distribution from ARR (2013b). The main difference is the fact the standardised distribution of ARR (2013b) has a lower limit of about 0.2, which means the initial loss is always higher than zero. The empirical distributions of the sub-catchments, on the other hand, indicate that initial losses of zero may occur. Events with zero initial losses are highly relevant for flood frequency analysis as they result in the highest runoff rates. Therefore, a modified version of the standardised

distribution function is proposed (dotted red line). This line can be approximated well by a beta-distribution with parameters listed in Table 6-4.

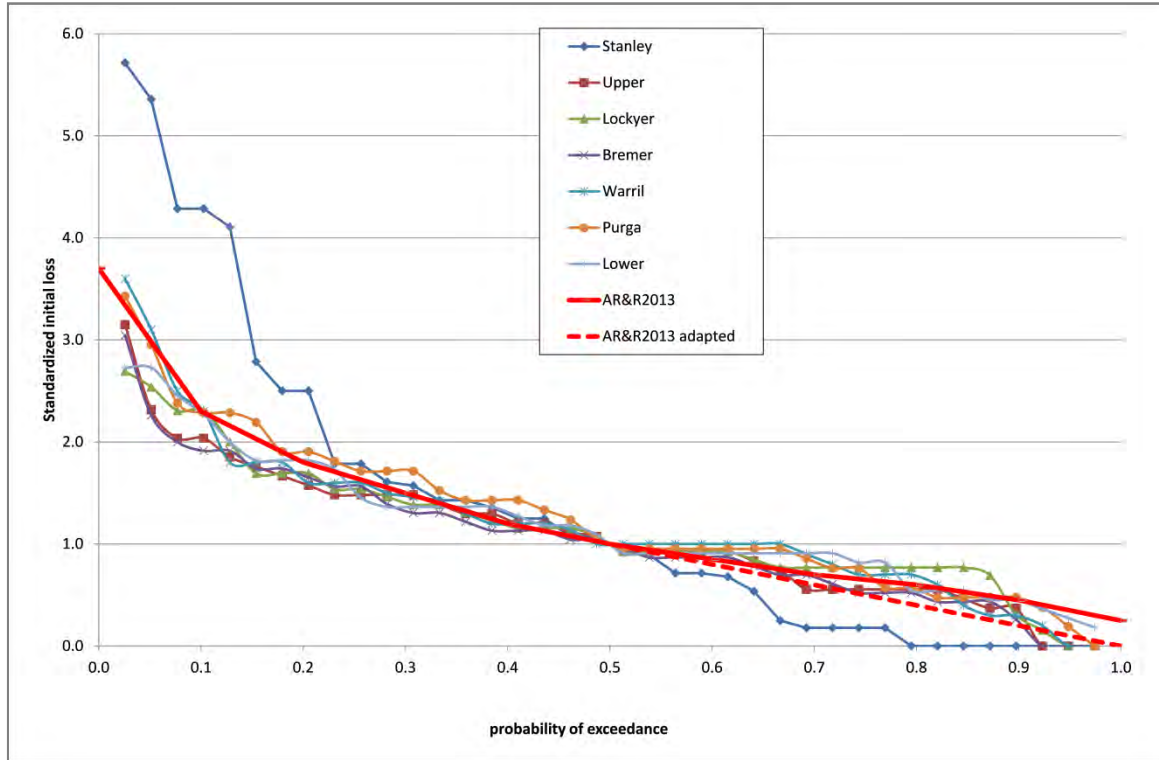


Figure 6-2 Empirical standardised distributions for Initial losses of the 7 sub-catchments, in combination with the standardised initial loss distribution of ARR [2013]. Initial Loss data were adopted from Seqwater [2013a]

The initial loss distribution of the Stanley River catchment deviates from the other sub-catchments because the median initial loss for this sub-catchment is significantly lower than for other sub-catchments (see Figure 6-3). This is caused by the fact that the headwaters of the Stanley River more frequently receive intense rainfall due to the close proximity to the coast and orographic influences of surrounding mountain ranges (Seqwater, 2013a). A separate beta-distribution function was therefore derived for the Stanley River sub-catchment (see Figure 6-4 and Table 6-4).

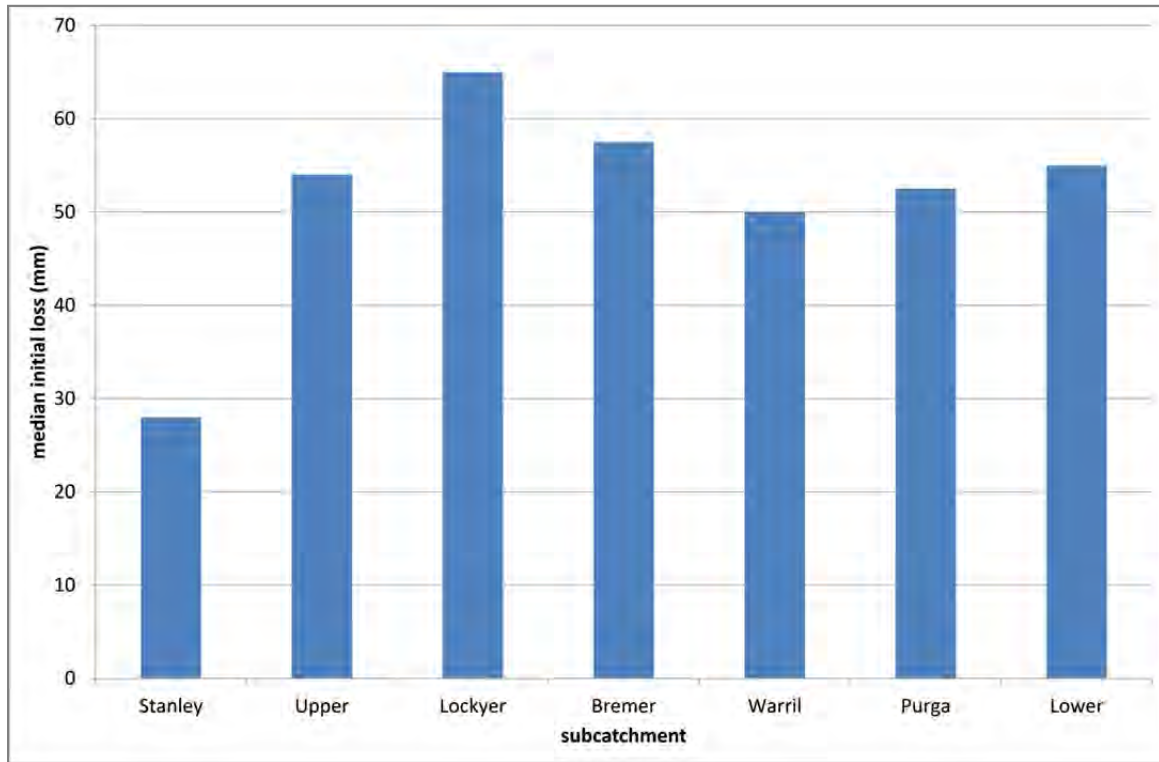


Figure 6-3 Derived median initial losses of the seven sub-catchments, based on 38 calibrated events of Seqwater (2013a)

Table 6-3 Derived median initial losses of the seven sub-catchments, based on 38 calibrated events of Seqwater (2013a]

Stanley	Upper	Lockyer	Bremer	Warri	Purga	Lower
28	54	65	57.5	50	52.5	55

Table 6-4 Selected parameters of the beta-distribution that provide the optimal fit for the standardised distribution functions of initial losses

Parameter	Stanley River sub-catchment	Other sub-catchments
α	0.54	1.15
β	1.62	2.51
X_L	0.00	0.00
X_u	6.00	3.61

The proposed procedure for generating samples of initial losses is as follows:

1. Sample a normalised initial loss from the 4-parameter beta-distribution with parameters listed in Table 6-4
2. Multiply the normalised samples of step 1 with the median loss as shown in Table 6-3

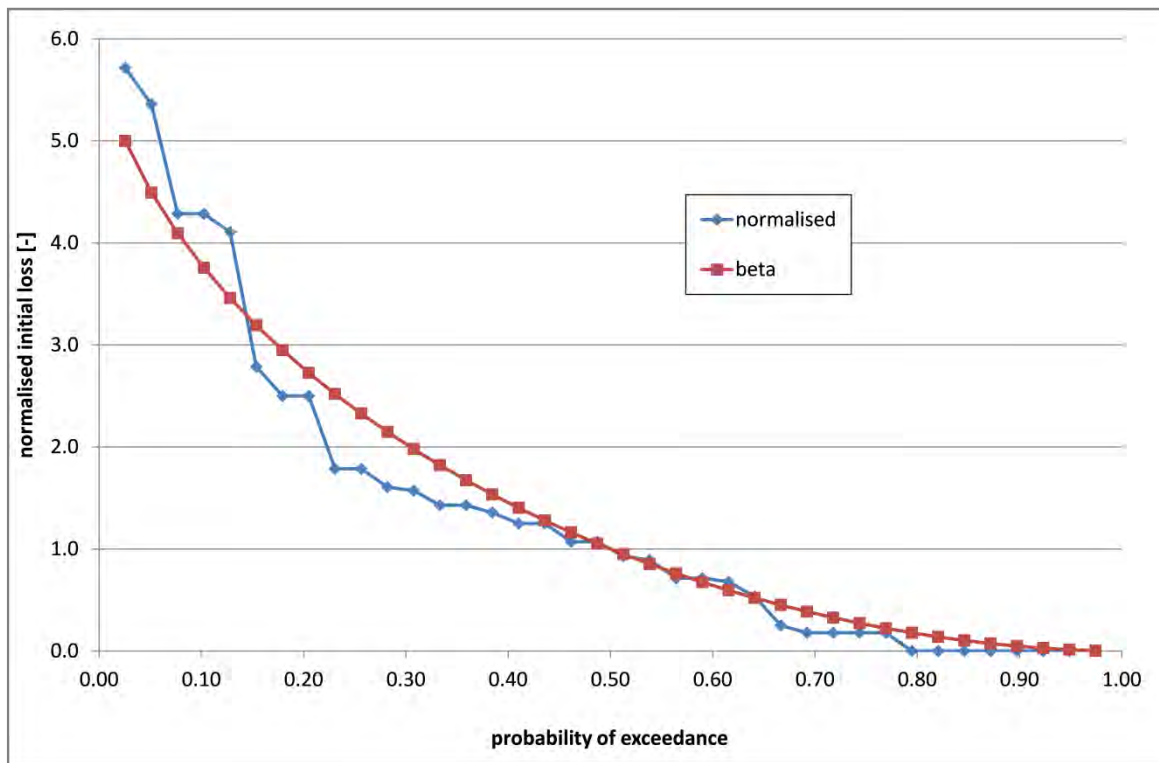


Figure 6-4 Beta-distribution fitted on the (normalised) observed initial losses of the Stanley River sub-catchment

Note: the distribution functions of initial losses as described above have been derived for events, as selected by Seqwater [2013a]. The distribution function of initial losses needs to be consistent with the sampling scheme as applied for rainfall intensities. If the sampling scheme considers bursts instead of events, the distribution functions for initial losses require correction factors. The reason is that initial losses for storm bursts are usually lower than initial losses for storm events. Storm events by definition start after a period of at least a couple of hours of insignificant rain, whereas storm bursts typically occur in the middle of a storm event. Storm bursts therefore start with wetter initial conditions than storm events. As discussed in Section 3.6, this is taken into account in the MCS framework by subtracting pre-burst rainfall of the sampled synthetic rainfall pattern from the initial loss, taking into account that initial losses cannot be lower than zero.

6.2.2 Mutual correlations between initial losses

Initial losses data for the Brisbane River are available from Seqwater (2013a). In their study, initial loss parameters for 48 events were based on model calibrations. Analyses were carried out for the seven sub-catchments (see Figure 2-1), in which initial losses were assumed uniform over the entire sub-catchment. The resulting 48 values for 7 sub-catchments, were used to derive mutual correlations between the seven sub-catchments (Table 6-5).

Table 6-5 Derived correlations between the seven sub-catchments

Area	Stanley	Upper	Lockyer	Bremer	Warril	Purga	Lower
Stanley	1.00	0.42	0.51	0.56	0.49	0.47	0.62
Upper	0.42	1.00	0.81	0.64	0.71	0.64	0.52
Lockyer	0.51	0.81	1.00	0.81	0.71	0.56	0.60
Bremer	0.56	0.64	0.81	1.00	0.87	0.60	0.68

Area	Stanley	Upper	Lockyer	Bremer	Warril	Purga	Lower
Warrill	0.49	0.71	0.71	0.87	1.00	0.64	0.65
Purga	0.47	0.64	0.56	0.60	0.64	1.00	0.89
Lower	0.62	0.52	0.60	0.68	0.65	0.89	1.00

The numbers in Table 6-5 are based on rank correlations and computed as follows: $\rho = \sin(\pi\tau/2)$, where τ is Kendall's rank correlation. The motivation for this choice of correlation measure is that it is consistent with the applied correlation model as described in Section 6.2.3.

Figure 6-5 and Table 6-6 show the correlation between sub-catchment initial losses and corresponding event rainfall intensities. These correlations were based on 35 calibration events adopted from Seqwater (2013a). Figure 6-5 and Table 6-6 display a wide range of correlation coefficients, between almost zero and 0.5.

Table 6-6 Derived correlations per sub-catchment between rainfall depth/intensity and initial losses

	Stanley	Upper	Lockyer	Bremer	Warril	Purga	Lower
depth (mm)	0.03	0.17	0.51	0.35	0.43	0.46	0.22
intensity(mm/hr)	0.02	0.24	0.51	0.37	0.41	0.31	0.21

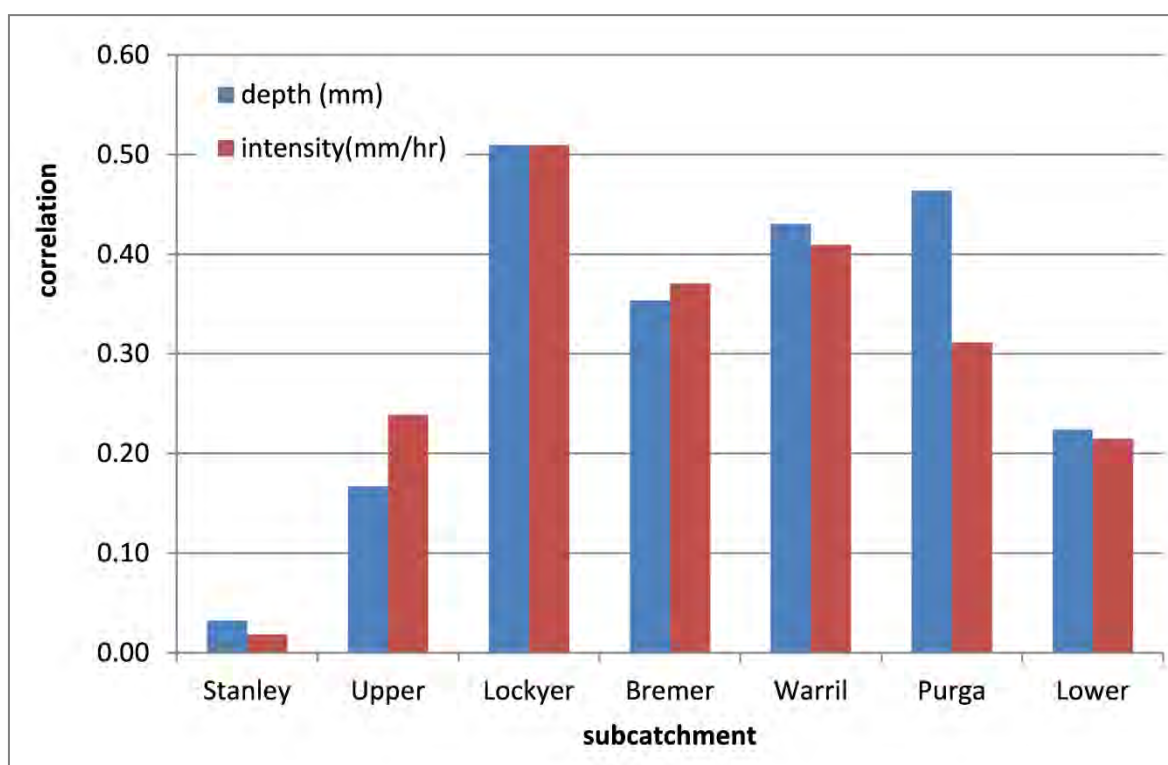


Figure 6-5 Correlations per sub-catchment between rainfall depth/intensity and initial losses

The correlations are all larger than zero. This is somewhat surprising, as the initial loss is an indication of 'dryness' of the catchment. This means that extreme rainfall events apparently generally coincide with relatively dry antecedent soil moisture conditions. This may be an artefact of the calibration of the rainfall-runoff model.

The application of a positive correlation between rainfall depth and initial losses will lead to a reduction in flood levels for low AEP values. To prevent that this contributes to an incorrect underestimation of flood levels, an additional analysis was carried out on a 123-year series of daily rainfall, provided by the Queensland Department of Science, Information Technology, Innovation and the Arts (DSITIA). The series consists of catchment average rainfall depths for six reservoirs in the area. For each catchment, the series of 123 highest k-day rainfall events (k=1, 2, 3 and 4 days) were selected and for each event the (rank) correlation with the rainfall depth of the 10, 30 and 90 days preceding the events was established. Table 6-7 shows the derived correlations are all positive, with one exception. This is in contradiction with the conclusions above that extreme rainfall events seem to generally coincide with relatively dry antecedent soil moisture conditions. Table 6-7 also shows that correlations are weak in general (0.37 or lower), which is in line with the analysis of Hinze Dam Alliance (2012) for the Hinze Dam along the nearby Nerang river. But at the same time, these correlations indicate that the assumption of a positive correlation between initial losses and rainfall totals may be incorrect and may contribute to an underestimation of design flood levels. It is therefore proposed to assume there is no correlation between event rainfall and initial losses.

Table 6-7 Derived Spearman rank correlations between rainfall totals of the 123 highest 1,2,3 and 4-day rainfall events and the rainfall of the preceding periods (10, 30 and 90 days) for the catchments of six dams

Pre-burst period	10 days				30 days				100 days			
Burst duration (days)	1	2	3	4	1	2	3	4	1	2	3	4
Cressbrook	0.30	0.18	0.17	0.12	0.24	0.20	0.11	0.09	0.18	0.13	0.04	0.08
Manchester	0.20	0.13	0.08	0.08	0.05	0.09	0.03	0.02	0.01	0.06	-0.03	0.02
Moogerah	0.15	0.11	0.06	0.07	0.18	0.17	0.07	0.07	0.06	0.01	0.01	0.05
Perseverance	0.29	0.19	0.11	0.09	0.27	0.25	0.11	0.08	0.17	0.09	0.08	0.09
Somerset	0.37	0.26	0.28	0.27	0.34	0.29	0.20	0.19	0.19	0.12	0.11	0.11
Wivenhoe	0.20	0.11	0.22	0.25	0.09	0.07	0.10	0.07	0.16	0.07	0.08	0.06

6.2.3 Sampling procedure

In the Monte Carlo simulations, the correlations of initial losses in the sub-catchments are incorporated using a Gaussian Copula approach (see eg Diermanse and Geerse, 2012; Kaiser and Dickman, 1962). This method requires the n-by-n correlation matrix, ρ , as input, where n is the number of mutually correlated variables. As proven by Fang et al (2002), ρ should be taken equal to $\sin(\pi\tau/2)$, where τ is Kendall's rank correlation matrix. Note that correlation matrix ρ for rainfall and initial losses is available from the analyses of Section 6.2.2. The procedure to generate correlated samples is as follows:

1. Derive a lower triangular matrix L for which: $LL' = \rho$, through Cholesky decomposition of correlation matrix ρ (see, eg Strang, 1982). Note: L' is the transpose of matrix L
2. Sample values u_1, \dots, u_n from the standard normal distribution function; store the results in an 1xn vector u
3. Compute: $u^* = uL'$
4. Compute: $p = \Phi(u^*)$, where Φ is the standard normal distribution function

The resulting vector \mathbf{p} is a sample of n correlated standard uniformly distributed random variables. The p -values represent probabilities of non-exceedance of the individual random variables. The p -values can subsequently be translated to “real-world” variables such as rainfall intensities and initial losses with the (inverse) probability distribution functions of the individual random variables:

$$x_i = F_i^{-1}(p_i) \quad (16)$$

Where x_i is the resulting sample of the i^{th} random variable, F_i is the corresponding probability distribution function and p_i is the probability of non-exceedance of variable i , as sampled with the Gaussian copula. Figure 6-6 shows an example of mutually correlated initial losses that were sampled according to this procedure for four sub-catchments (Stanley, Upper Brisbane, Lockyer and Bremer). For each sub-catchment, 1000 values for the initial losses were sampled and the associated empirical probabilities (blue dots) are compared with the observed empirical probabilities (red dots). It can be seen from Figure 6-6 that, for example, the generated sampled losses for Upper Brisbane and Lockyer sub-catchments are stronger correlated than the sampled losses for Lockyer and Stanley sub-catchments, which is in accordance with Table 6-5 and with the observed losses. The fact that this procedure provides simultaneous samples of mutually correlated variables makes it a powerful tool for Monte Carlo analysis, because this means the samples provide realistic spatial patterns of initial losses.

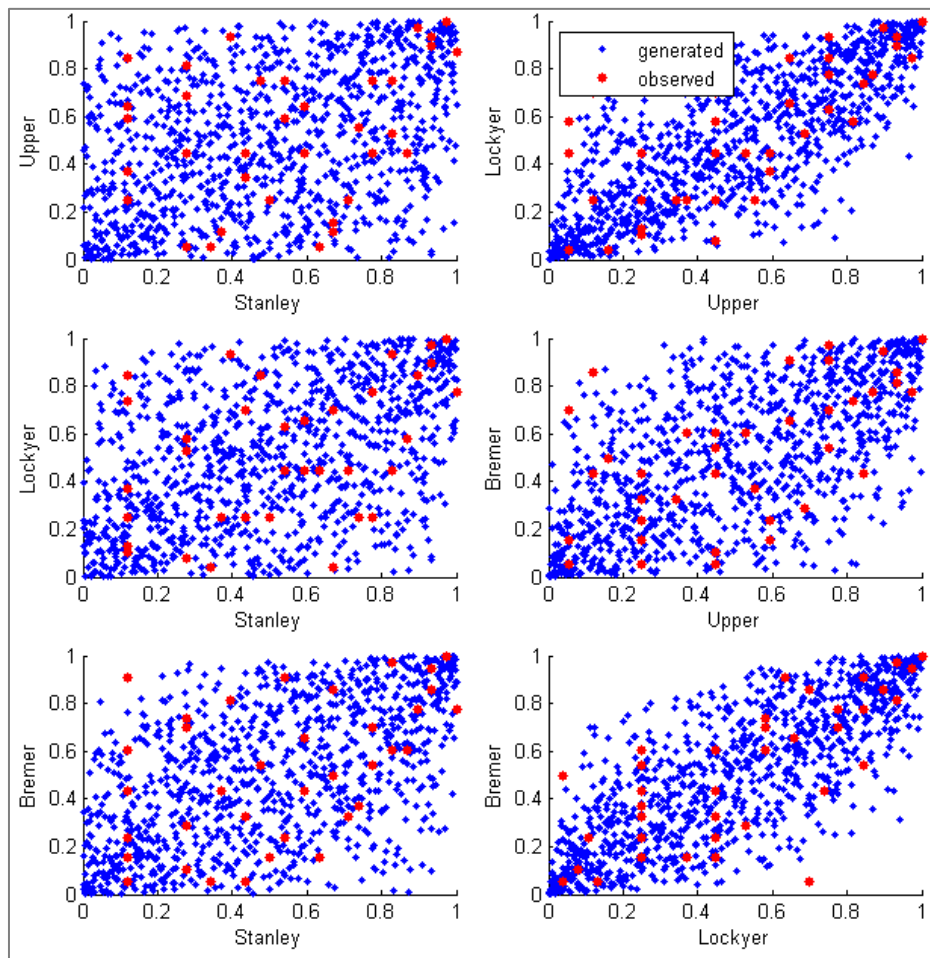


Figure 6-6 Correlation plots of simulated and observed initial losses for four sub-catchments (Upper, Stanley, Lockyer and Bremer). The axes show empirical probabilities

The Gaussian Copula is asymptotically independent, which means there is no increased statistical dependence in the tail ends of the distributions. The model is therefore unable to represent situations where the dependency between the random variables increases for more extreme values, which could potentially have a significant effect on the derived the flood risk. This might also be the case for the initial losses of the sub-catchments of the Brisbane River catchment, as extremely wet antecedent soil conditions in the sub-catchments are likely to coincide. In that case, other correlation models that model asymptotic dependence are required, such as the student-t copula (Fang et al, 2002), the threshold-excess logistic model (Zheng et al, 2013) or the Gumbel-Hougaard Copula (Diermanse and Geerse, 2012). However, the available data set on initial losses is too small to provide evidence for asymptotic dependence, which is why the Gaussian copula is considered to be suitable for now. A sensitivity analysis could be carried out to assess the potential influence of asymptotic dependence in initial losses on the derived flood levels in the Brisbane River catchment. For this purpose, additional Monte Carlo simulations could be carried out with the student-t copula. The student-t copula requires the correlation matrix, ρ , as input, similar to the Gaussian copula. Furthermore, the student-t copula has an additional parameter, ν , which controls the tail dependence. The procedure for the student-t copula is as follows:

1. Compute correlated standard normal variables \mathbf{u}^* , following the procedure of the Gaussian copula
2. Sample a value, s , from the χ_{ν}^2 (chi-square) distribution with ν degrees of freedom
3. Compute $w = \nu/s$; w is a sample of the inverse gamma-distribution with parameters $(\nu/2, \nu/2)$
4. Compute $\mathbf{y} = (\sqrt{w})\mathbf{u}^*$; \mathbf{y} is a vector of correlated samples from the student-t distribution with ν degrees of freedom
5. Compute $\mathbf{p} = t_{\nu}(\mathbf{y})$, where t_{ν} is the student-t distribution with ν degrees of freedom

The resulting p-values are mutually correlated samples from the standard uniform distribution function. The p-values can be translated to “real-world” variables through application of equation (16). Parameter ν should be greater than or equal to 2. The tail dependence is strongest when $\nu=2$ and decreases with increasing value of ν . In the limit $\nu \rightarrow \infty$, the student-t copula is equal to the Gaussian copula. Figure 6-7 compares bivariate samples of the Gaussian copula ($\rho=0.8$) and the student-t copula ($\rho=0.8, \nu=5$). The patterns are very similar, except in the tails (p-values near zero and one). This is more clearly visible in Figure 6-8, where the samples are plotted against a logarithmic axis. For the relatively low probabilities shown in Figure 6-8, the red dots (student-t) are clearly stronger correlated than the blue dots (Gaussian). Since both copulas are symmetric, the same holds for high p-values (not shown in Figure 6-8).

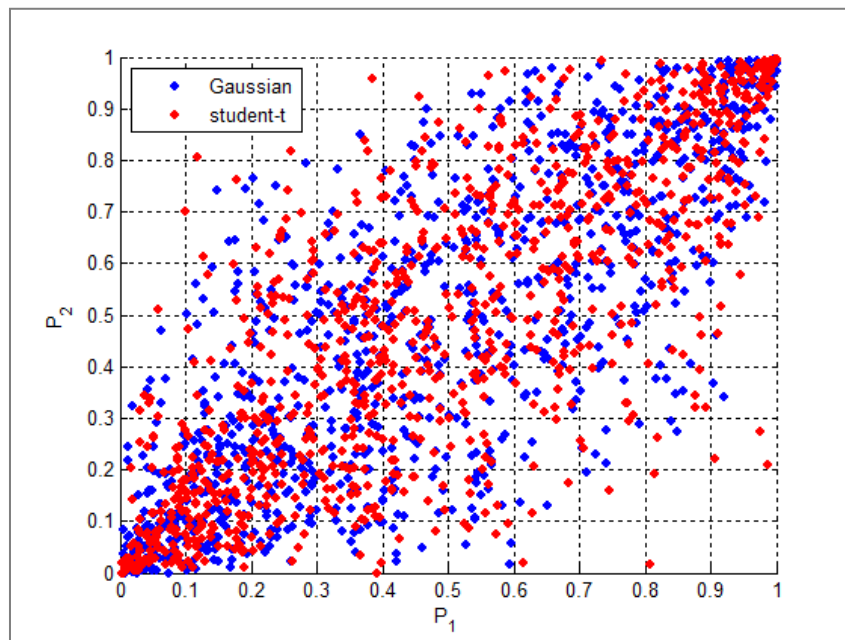
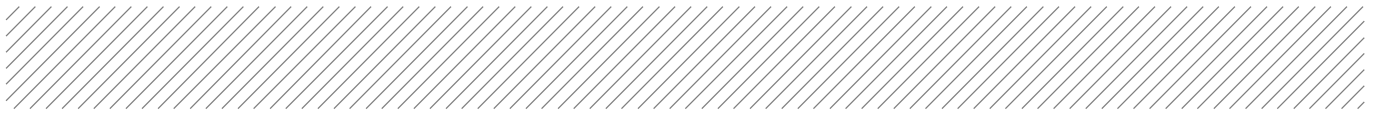


Figure 6-7 Bivariate samples of the Gaussian copula ($\rho=0.8$) and the student-t copula ($\rho=0.8, \rho=5$)

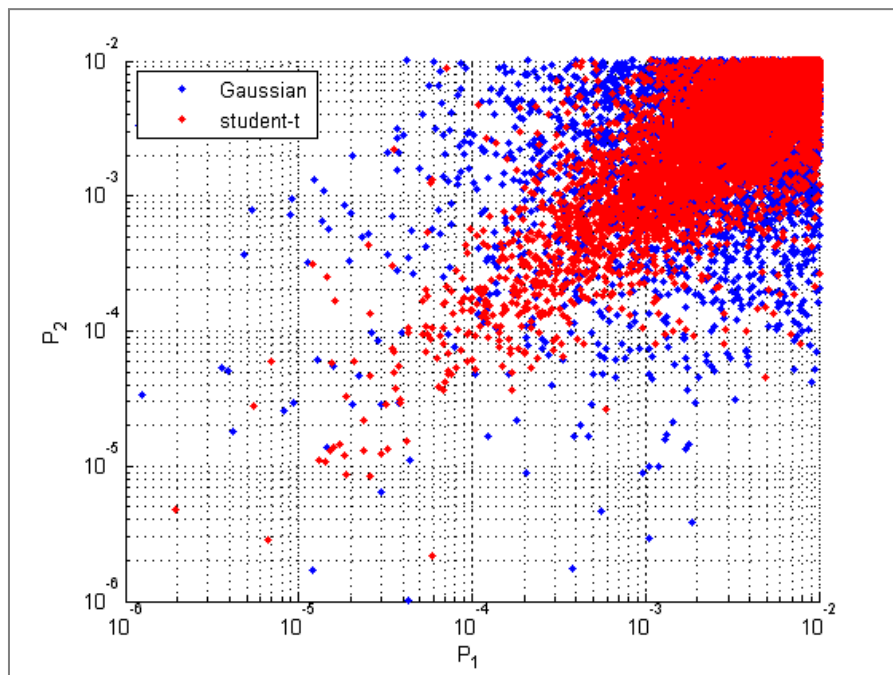


Figure 6-8 Bivariate samples of the Gaussian copula ($\rho=0.8$) and the student-t copula ($\rho=0.8, \nu=2$)

6.3 Ocean water levels

6.3.1 Marginal distribution of ocean water level

Frequency distributions for ocean water levels at location Luggage point in Moreton Bay were adopted from Table 6-1 of (GHD, 2014). The relation between peak ocean water levels and AEP is shown in Table 6-8 and Figure 6-9.

Table 6-8 Frequency distribution for ocean water levels, adopted from GHD (2014)

AEP	Water level (mAHD)
1/5	1.59
1/20	1.68
1/50	1.78
1/100	1.86
1/500	2.30
1/2000	2.76
1/10000	3.25

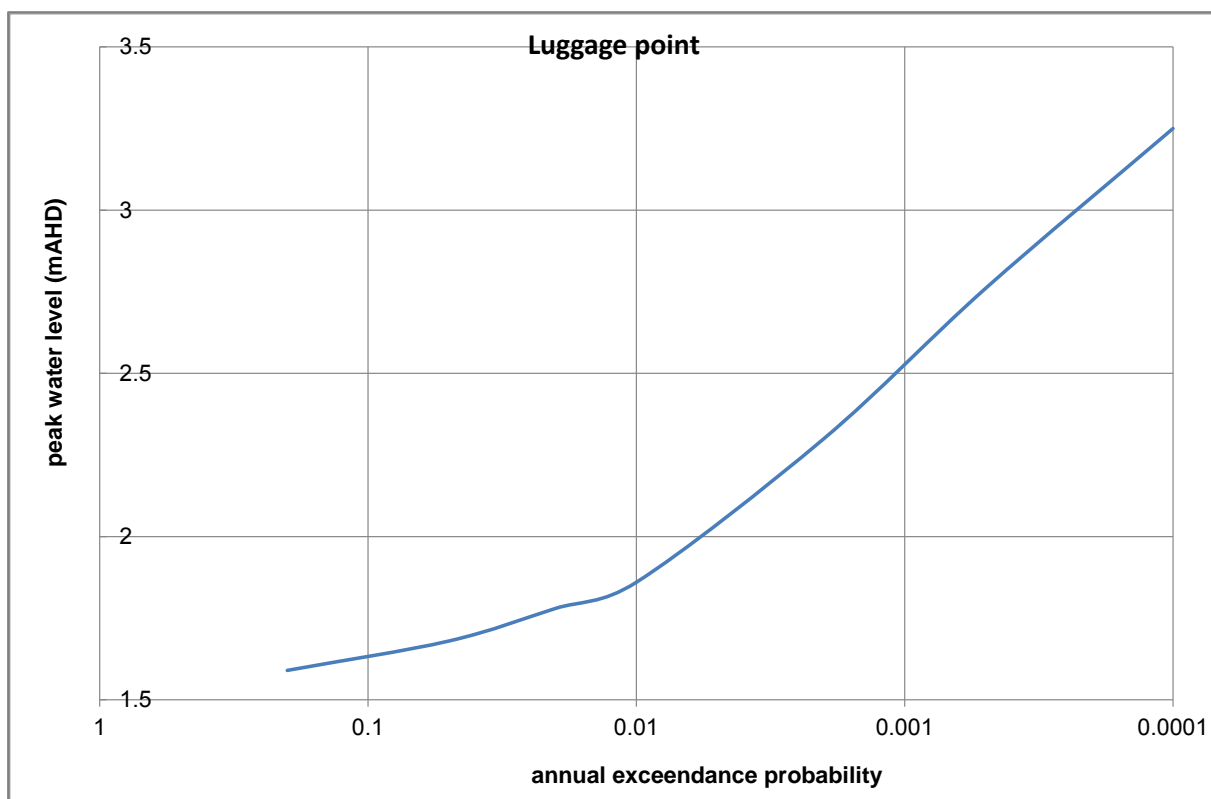


Figure 6-9 Frequency distribution for ocean water levels at Luggage point; numbers based on (GHD, 2014)

6.3.2 Correlation with rainfall depth

The events that cause extreme rainfall depths in the Brisbane River catchment (Cyclones, East coast lows and tropical storms) may also generate a significant storm surge. Increased sea water levels may further increase flood levels in the downstream part of the Brisbane and Bremer Rivers. The timing of peak flows and peak sea water levels is also relevant in this respect; the storm surge may well be over before the peak discharges reach the downstream end of the Brisbane River.

For the correlation between rainfall and storm surge, the approach of Zheng et al. (2013a,b) is followed, who derived correlations for the entire Australian coast line. They use the threshold-excess logistic model of Tawn (1988) to describe the statistical dependence. This model has the following bivariate distribution function:

$$P[X \leq x \cap Y \leq y] = G_{XY}(x, y) = \exp\left[-\left(x^{-1/\alpha} + y^{-1/\alpha}\right)^\alpha\right] ; x \geq x_0, y \geq y_0 \quad (17)$$

Where X and Y are random variables, x and y are potential realisations of X and Y, G is the bivariate distribution function of X and Y, and x_0 and y_0 are thresholds above which function G is valid. In the application of Zheng et al. (2013a,b), X and Y represent transformed values of rainfall and ocean water level, respectively. This means the probabilities as derived from Equation (17) need to be transformed back to actual values of rainfall and ocean water level in order to assess flood levels in river stretches that are influenced by both. The interested reader is referred to Zheng et al. (2013a) for the description of this procedure.

In the application of Zheng et al. (2013a,b), the combined probabilities are assessed by numerical integration. Our objective is to apply their model in a Monte Carlo framework, which means we require [a] the marginal probability distribution function for variable X and [b] the distribution function of variable Y, conditional on X. The distribution function of X can be derived directly from function G:

$$F_X(x) = \lim_{y \rightarrow \infty} G_{XY}(x, y) = \exp\left[-\left(x^{-1/\alpha}\right)^\alpha\right] = \exp\left[-\left(x^{-1}\right)\right] ; x \geq x_0 \quad (18)$$

This distribution is known as the standard Fréchet distribution. Variable Y has the same distribution function. The density function is as follows (see Figure 6-10):

$$f_X(x) = \frac{\exp\left[-\left(x^{-1}\right)\right]}{x^2} ; x \geq x_0 \quad (19)$$

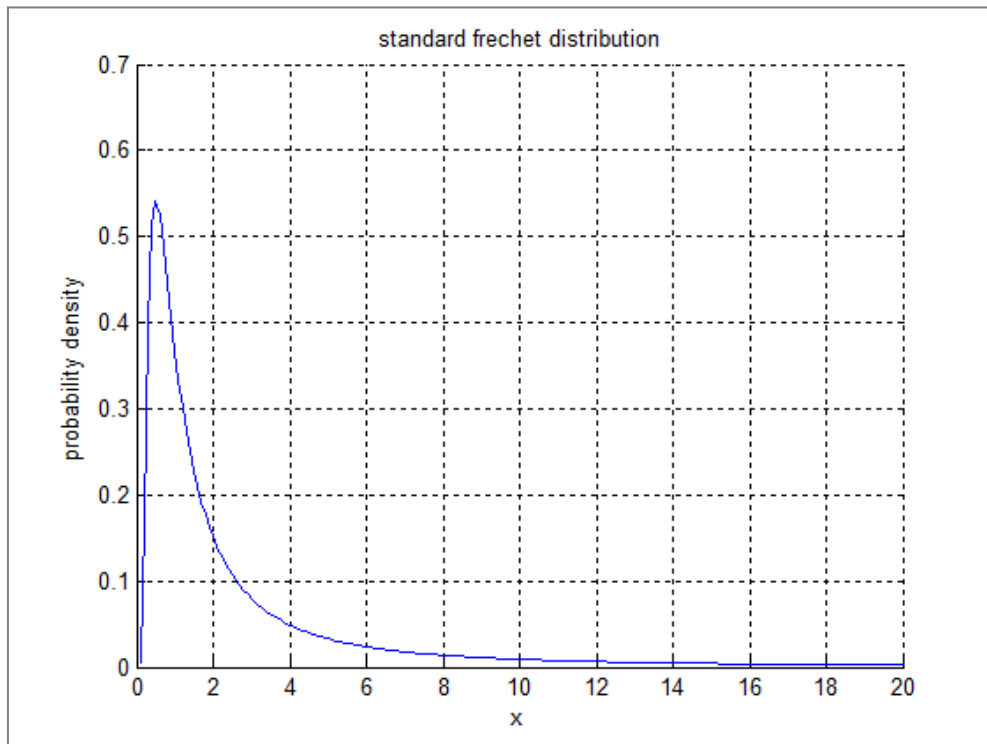


Figure 6-10 Standard Fréchet distribution

The inverse of this distribution function (required for the sampling procedure) is as follows:

$$F^{-1}(p) = \frac{-1}{\ln(p)} \quad (20)$$

where p is the probability of non-exceedance. The conditional distribution function of Y , given $X=x$, is as follows:

$$F_{Y|X}(y|x) = \frac{\frac{\partial G_{XY}(x,y)}{\partial x}}{f_X(x)} = \frac{G(x,y) \left[\alpha (x^{-1/\alpha} + y^{-1/\alpha})^{\alpha-1} \right] \left[\frac{x^{-1/\alpha-1}}{\alpha} \right] x^2}{\exp[-(x^{-1})]} ; x \geq x_0, y \geq y_0 \quad (21)$$

There is no closed form for the inverse of this conditional distribution function, so it has to be computed numerically in the sampling procedure.

If $\alpha=1$, Y and X are independent, whereas if $\alpha=0$, Y and X are fully dependent. This shows the value of α determines the statistical dependence between X and Y : low values of α (close to 0) indicate strong dependence, high values of α (close to 1) indicate weak dependence. Figure 6-11 shows sampled pairs of x,y -values for four different values of α .

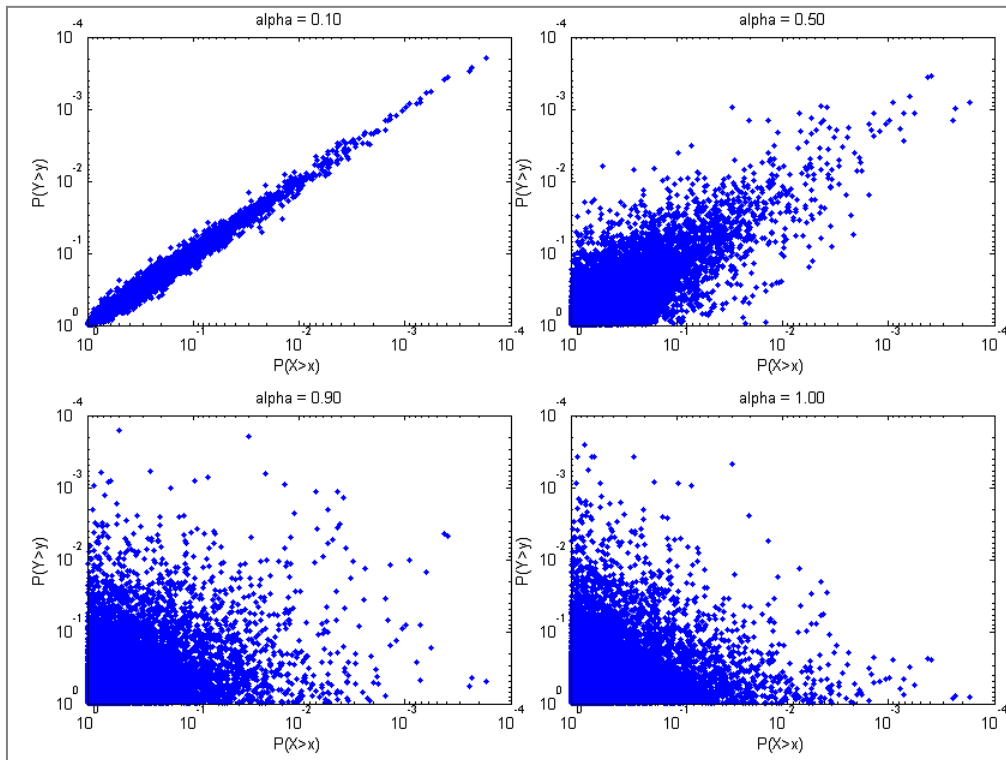


Figure 6-11 $N=10,000$ samples from the bivariate logistic model for four different values of the dependence parameter α . The axes show marginal exceedance probabilities of the sampled x and y -values

According to Zheng et al. (2013a), $\alpha = 0.95$ for rainfall events of less than 12 hours along the Queensland east coast, $\alpha = 0.9$ for rainfall events between 12 and 48 hours and $\alpha = 0.85$ for rainfall events of over 48 hours. These values are adopted in our approach. It may appear from Figure 6-11 that these values result in negligible correlation. However, the statistical dependence increases for

extremes, ie low probabilities of exceedance. This can be observed, for example in the upper right plot of Figure 6-11 (subplot for $\alpha = 0.5$). The rainfall events to be considered in the MCS procedure all have low exceedance probabilities associated with them. Consider, for example, a rainfall event with duration of three days and an AEP of 0.5, which is a relatively moderate event in the MCS procedure. This is an event for which the three-day total rainfall depth is exceeded in a year with a probability of 0.5. The probability that this rainfall depth is exceeded in a specific three-day period is *approximately* equal to $AEP/122$ (ignoring, for the moment, seasonal influences), where 122 is the number of three-day periods in a year. For an AEP of 0.5, this means an approximate probability of exceedance of 0.004 per three-day period.

This shows the statistical dependence for the events to be considered in the MCS procedure is more relevant than initially indicated by Figure 6-11. This is further demonstrated in Table 6-9 and Table 6-10. Table 6-9 shows the exceedance probabilities of ocean water levels with AEP's equal to 0.1, 0.01, 0.001 and 0.0001 during a period of three days. Table 6-10 shows the exceedance probabilities of the same events, but in this case conditional on the occurrence of an extreme rainfall event, assuming $\alpha = 0.85$. For example, the value 0.1 in the last row and column of Table 6-10 can be interpreted as follows: If $\alpha = 0.85$, and a rainfall event with AEP equal to 0.0001 occurs, the probability that an ocean water level with $AEP \leq 0.0001$ occurs (during the three-day period) is equal to 0.10, ie 10%. In case the ocean water level and rainfall would have been independent ($\alpha = 1$), this probability would have been equal to 8.2×10^{-7} (see Table 6-9). This shows that for extreme events, the conditional probabilities increase with several orders of magnitude.

Table 6-9 Probability of exceedance of ocean water levels with shown AEP, during a period of three days

AEP Ocean water level			
0.1	0.01	0.001	0.0001
8.6E-04	8.2E-05	8.2E-06	8.2E-07

Table 6-10 Conditional exceedance probability, $F(Y > y | X = x)$, in case the dependence parameter α is equal to 0.85. The value of x is the rainfall depth with an AEP as shown in the second header row, the value of y is the ocean water level with an AEP as shown in the first column

	AEP rain			
AEP Ocean	0.1	0.01	0.001	0.0001
0.1	0.10	0.35	0.56	0.71
0.01	0.01	0.10	0.34	0.56
0.001	0.00	0.01	0.10	0.34
0.0001	0.00	0.00	0.01	0.10

In the computations of Table 6-10, seasonal influences have been ignored. Zheng et al, (2013b) state that: *“Southern Queensland is more likely to have jointly occurring extreme events in the cold season (April–September). The strong dependence in the cold season in this region may be partially driven by east coast low pressure systems, which often occur in the cold season of southern Queensland.”* So, in the warm season (October to March), which is the season for rainfall extremes in the Brisbane River catchment, the earlier mentioned α -values may slightly overestimate the joint occurrence of extremes of rainfall and ocean water level.

6.3.3 Time series

The procedure as described in the previous section provides peak ocean water levels that are correlated to the rainfall depth and duration. For the URBS model simulations not only the peak ocean water level is required but also a time series of ocean water levels for each simulated event. Such a time series is composed with the following procedure:

1. Sample a peak ocean water level (h_p) and event duration as described in Sections 6.3.1 and 6.3.2
2. Sample the peak of the surge, S_p , from the uniform distribution with intervals $[h_p - a, h_p - b]$, where a and b are constants equal to 1.3 m+AHD and 0.8 m+AHD
3. Assume a trapezoidal storm surge hydrograph with peak surge level equal to S_p (see below on the details on the assumed shape of the storm surge hydrograph)
4. Combine the surge series with an astronomical tide series, taken from a monthly series of “average” tidal conditions. Choose the relative starting points of the surge and astronomical tide series in such a way that tide + surge results in a peak water level that is equal to h_p

The assumed shape of the storm surge hydrograph was adopted from Figure 6-12, which shows recorded time series (normalised) for the Sunshine coast as derived by (Aurecon, 2013b). A schematised version of the 50% line (black line in Figure 6-12) was derived. The resulting dimensionless hydrograph is as follows:

- In 48 hours the surge increases linearly from 0 to 0.5
- In 24 hours the surge increases linearly from 0.5 to 1
- In 30 hours the surge decreases linearly from 1 to 0.5
- In 66 hours the surge decreases linearly from 0.5 to 0

This means the total duration of the surge hydrograph is equal to 168 hours, or 7 days.

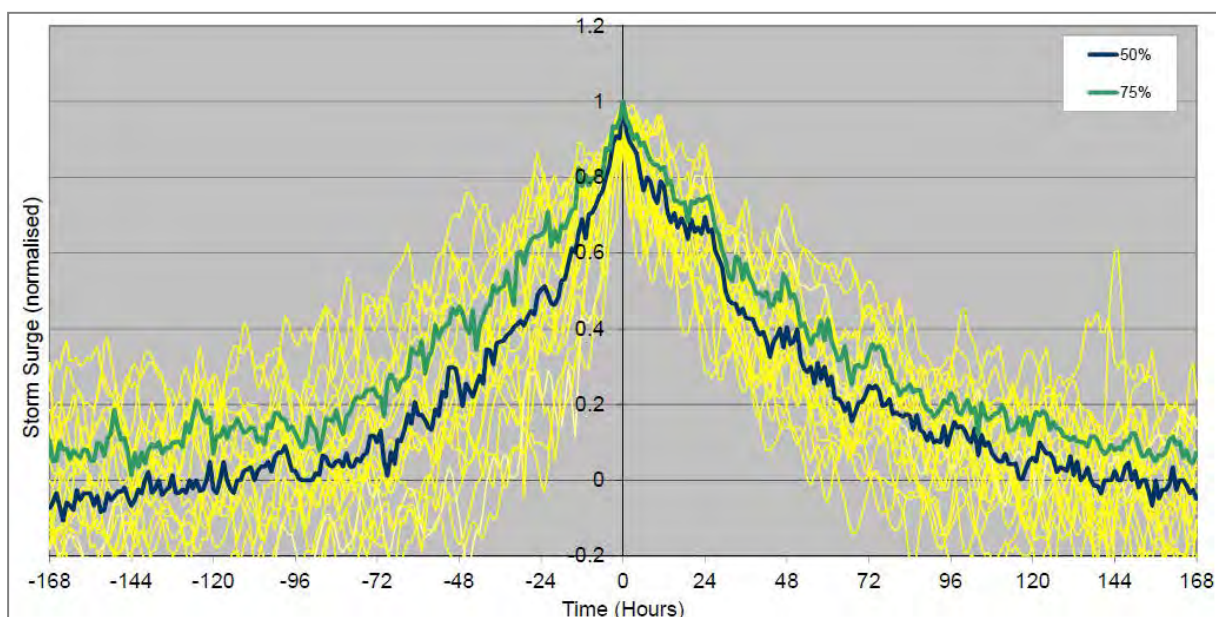


Figure 6-12 Recorded time series histories (normalised) for storm surges on the Sunshine Coast. Figure copied from (Aurecon, 2013b)

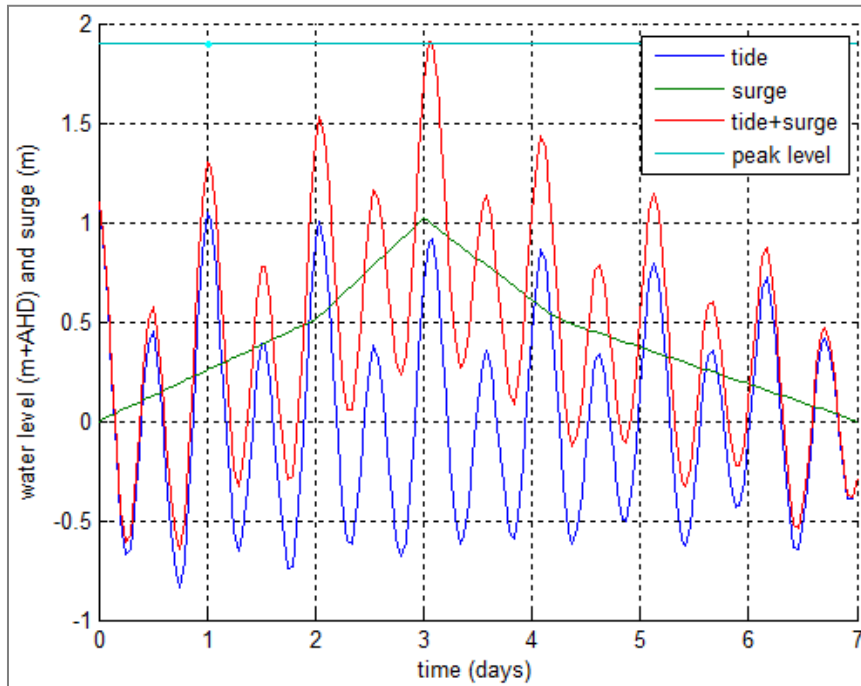


Figure 6-13 Example of a generated series of surge, astronomical tide and resulting ocean water level

Figure 6-13 shows an example of a generated time series for ocean water level (red line) in combination with the generated surge and astronomical tide levels. Figure 6-14 shows examples of multiple generated time series of ocean water levels. In each subplot, the resulting peak ocean water level is the same. Differences between subplots are caused by differences in the peak of the surge and differences in “timing”.

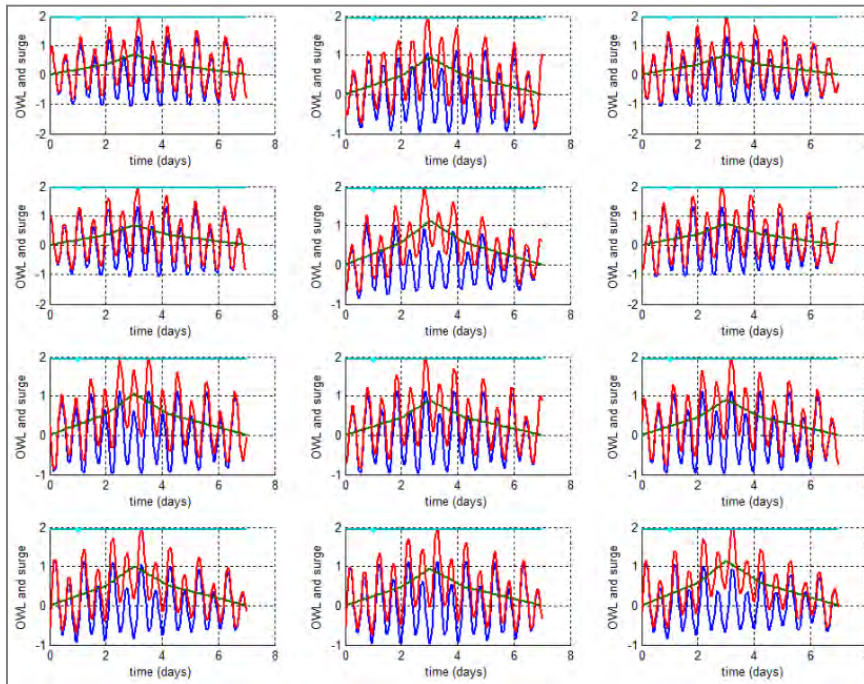


Figure 6-14 Examples of a generated series of surge, astronomical tide and resulting ocean water level. In each subplot, the resulting peak ocean water level is the same. Differences between subplots are caused by differences in the peak of the surge and differences in “timing”

Figure 6-15 shows the resulting time series of ocean water levels (red graphs of Figure 6-14) in a single plot. The time series were shifted horizontally to make sure the peaks occurred at the same time. The figure shows considerable variability, demonstrating that the aspect of timing between the peak of the surge and the peak of the astronomical tide is relevant. In our view this is realistic and shows the benefit of taking this “random” feature into account in the MCS framework.

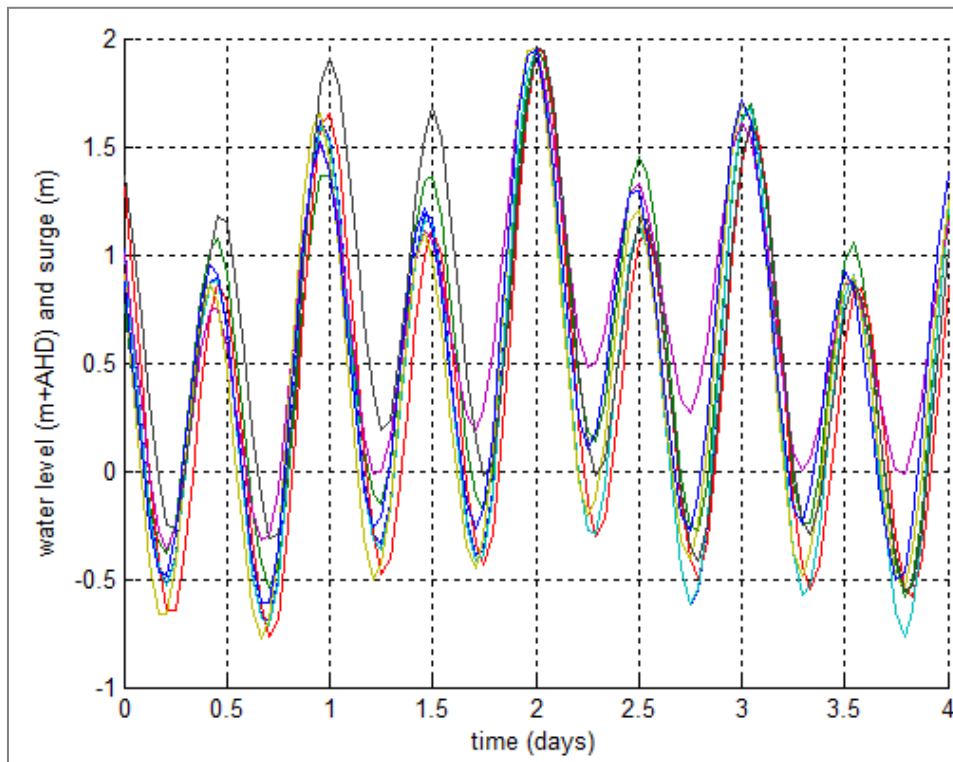


Figure 6-15 Eight time series of ocean water levels of Figure 6-14. The time series were shifted horizontally to make sure the peaks occurred at the same time

6.3.4 Timing

The last issue that needs to be addressed is the timing of the peak storm surge and peak river discharge. In the URBS-model simulations, the input consists of time series of rainfall and ocean water level. The sampling procedure described in the previous sections provides ocean levels and rainfall intensities, but not their relative timing. If the peak of the surge occurs two days before the start of the rainfall event, the surge will have no effect on flood levels, whereas if it occurs near the end of the rainfall event the effect may be substantial. Zheng et al (2013a) state that the dependency parameter (α), of the logistic regression model of equation (17) is based on zero-lag between rainfall and surge, so it makes sense to adapt this zero-lag in the simulation model as well. However, it is not clear from their paper what this means if, for instance, three-day rainfall events are considered. According to Westra (personal communication), the definition of ‘zero-lag’ in Zheng et al (2013) is that the storm surge will occur sometime within the period of the critical rainfall. So, for three-day rainfall events, zero-lag means that the storm surge is assumed to occur sometime in that three-day period. It is therefore proposed to adopt this assumption in the Monte Carlo simulations, and sample a time lag between storm surge peak and rainfall peak uniformly over an n -day period centred around zero, where n depends on the catchment of interest.

Figure 6-16 shows a histogram of difference in timing between peak flows at Brisbane City and peak ocean water levels at the Brisbane River outlet, for simulated 72 hour bursts, for 'no dams' conditions. Positive values refer to peak flows occurring later than peak ocean water levels. It shows that the simulated peak flow at Brisbane City generally occurs later than the simulated peak ocean water level, which is in accordance with what is expected to occur in reality.

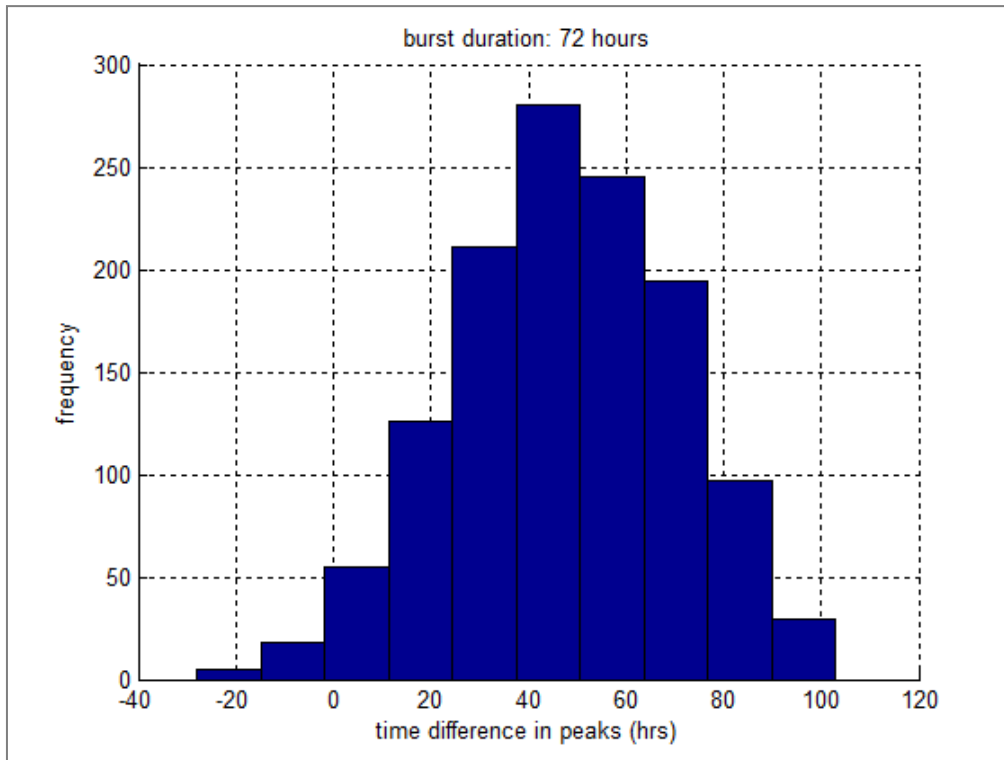


Figure 6-16 Histogram of difference in timing between peak flows at Brisbane City and peak ocean water levels at the Brisbane River outlet, for simulated 72 hour bursts. Positive values refer to peak flows occurring later than peak ocean water levels

6.4 Reservoir volumes

6.4.1 Analysis of reservoir time series

In order to gain insight in the influence of reservoir operation rules on flow series, a 123-year reservoir model simulation was carried out by the Queensland Department of Science, Information Technology, Innovation and the Arts (DSITIA). The input of the simulation consisted of observed rainfall intensities and evaporation rates over the last 123 years. The output consisted of a 123-year series of reservoir volumes for six dams in the area: Cressbrook, Manchester, Moogerah, Perseverance, Somerset and Wivenhoe (see Table 6-11 and Figure 6-17). The resulting series were provided to the BRCFS study by DSITIA and were subsequently used to analyse relevant statistics of reservoir volumes in the area.

Table 6-11 Full supply levels of the six reservoirs as assumed in the simulations

Reservoir	Full Supply Level (m AHD)	Full Supply Volume (ML)
Perseverance	446.075	30,141
Cressbrook	280	81,842
Somerset	99	379,850

Reservoir	Full Supply Level (m AHD)	Full Supply Volume (ML)
Wivenhoe	67	1,165,200
Manchester	50.9	26,000
Moogerah	154.91	83,765



Figure 6-17 Dams and reservoirs in the Brisbane river catchment

Figure 6-18 shows annual averaged volumes for Wivenhoe dam. It shows these volumes are usually between 800,000 ML and 1,200,000 ML. In the early 20th century and early 21st century there were two drought periods during which the simulated reservoir volumes dropped far below 800,000 ML. Similar graphs have been derived for the other five reservoirs in the catchment. As an example Figure 6-19 shows the annual mean volumes of Moogerah dam. In this Figure, the relatively dry periods of the early 20th century and early 21st century are also visible. The annual mean volumes of Moogerah dam clearly have more variation in comparison with Wivenhoe dam, mostly due to its smaller size.

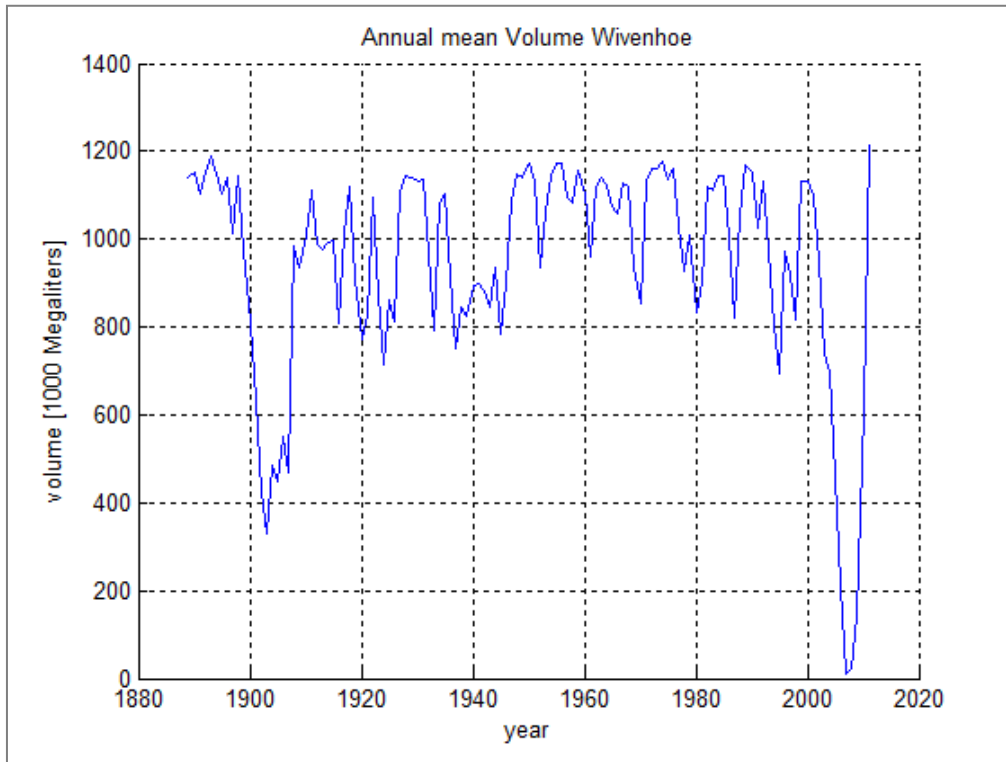
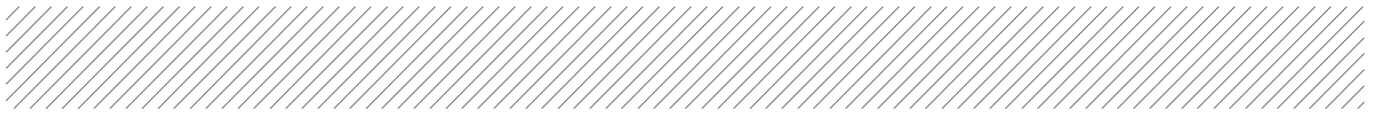


Figure 6-18 Annual mean volume of Wivenhoe Dam

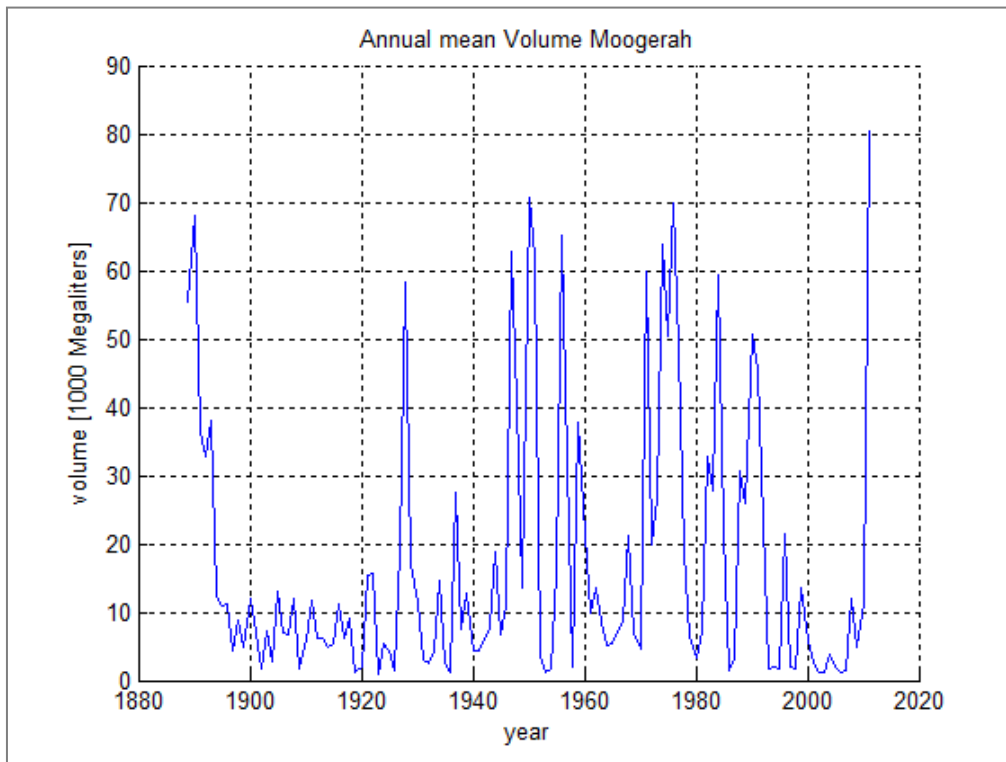


Figure 6-19 Annual mean volume of Moogerah Dam

Figure 6-20 shows monthly mean rainfall depths over the catchment of Wivenhoe dam (ie the Stanley River sub-catchment and Upper Brisbane River sub-catchment). It shows a clear distinction between a wet season (November to March) and a dry season (April to October). The seasonal pattern is also reflected in Figure 6-21, which shows the histograms of occurrences of maximum k -day rainfall events ($k=1, 2, 3, 4$). The majority of these events are observed in the period January to March.

The seasonal pattern in rainfall obviously causes a seasonal pattern in reservoir volumes as well. However, seasonal fluctuations of reservoir volumes in Wivenhoe dam are not significant, as shown in the box plots of Figure 6-22. Monthly median volumes vary from 990,000 ML (November) to 1,039,000 ML (July). For smaller reservoirs, the seasonal differences are more pronounced, as can be seen for example in Figure 6-23 (Somerset Dam).

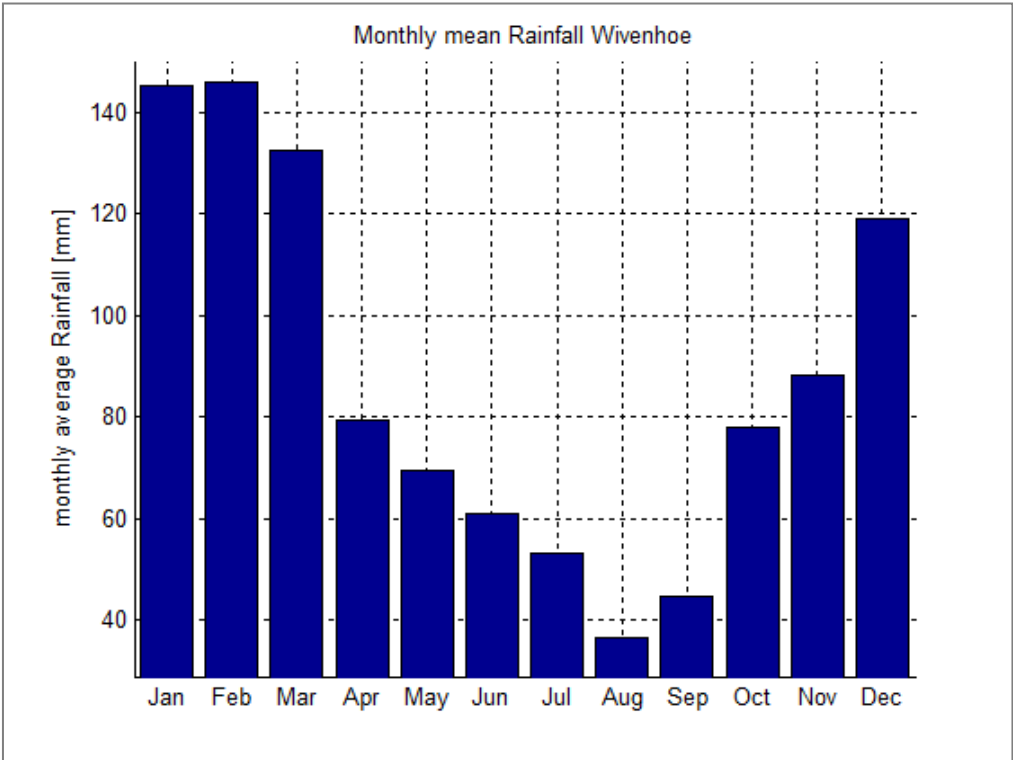


Figure 6-20 Monthly mean rainfall over Wivenhoe Dam catchment

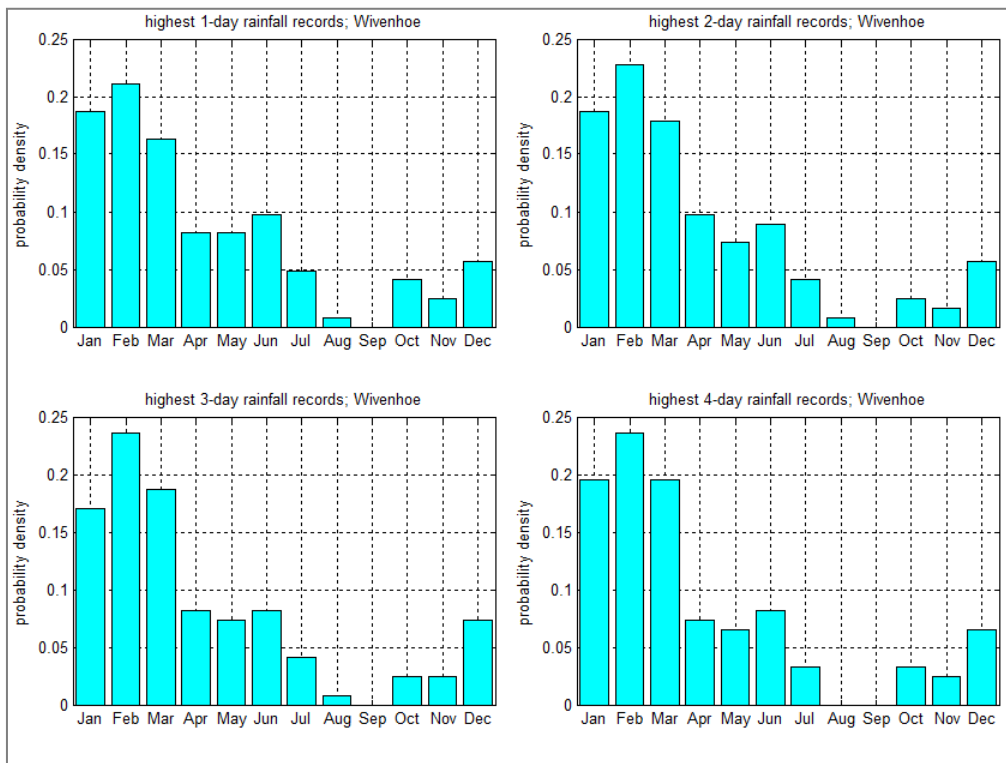
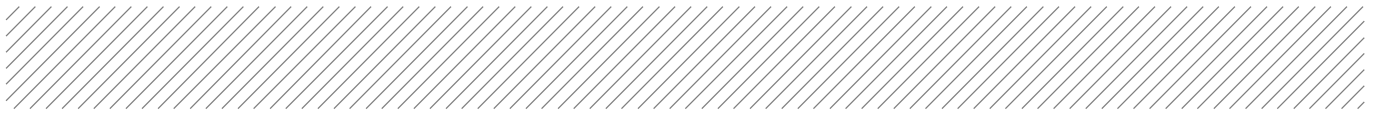


Figure 6-21 Histogram of occurrence of maximum 1, 2, 3 and 4 day rainfall

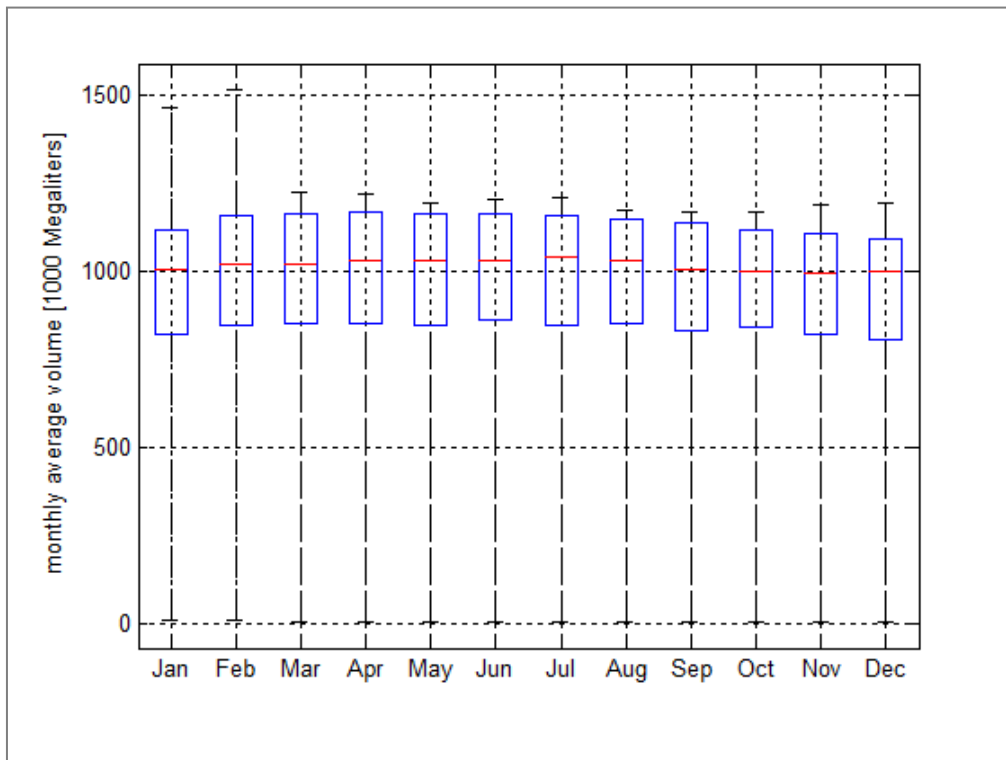


Figure 6-22 Box plot for monthly mean reservoir volumes of Wivenhoe Dam

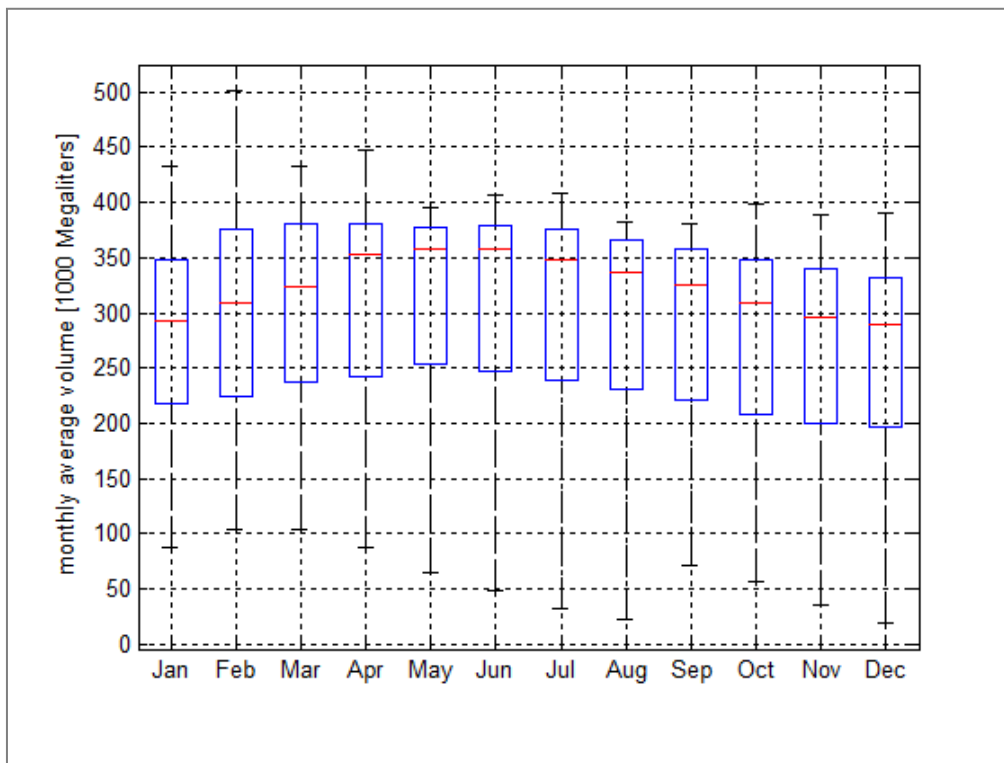


Figure 6-23 Box plot for monthly mean reservoir volumes of Somerset Dam

6.4.2 Analyses of correlations

The following issues were addressed:

1. Are reservoir volumes at the start of a high rainfall burst generally different from 'average conditions' (ie should we derive marginal distribution functions from the complete series of reservoir volumes or from the partial series of reservoir volumes at the start of big rainfall bursts)?
2. Is there significant correlation between the cumulative rainfall depth of a burst and the reservoir volume at the start of a burst?
3. Is there mutual correlation between the reservoir volumes at the start of a burst?

Question 1: *Are reservoir volumes at the start of an extreme rainfall burst generally different from 'average conditions'?*

To address this question, reservoir volumes of the 123 highest rainfall bursts in the simulation period were derived. Subsequently, empirical probabilities were derived for these 123 volumes in two ways. The first estimate is based on the rank in the complete series, consisting of 44,740 daily values. The second estimate is based on the rank in the series of 123 reservoir volumes. In both cases, exceedance probabilities were estimated to be equal to $r/(N+1)$, where r is the rank number and N is the length of the series (44,740 in the first estimate and 123 in the second estimate).

Both probability estimates for Wivenhoe dam are plotted against each other in Figure 6-24. This is done for the reservoir volumes associated with the highest 123 rainfall bursts for 1, 2, 3 and 4 day periods. The values shown are estimated probabilities of *non-exceedance*. It shows that the first probability estimate, based on the complete series, is generally higher than the second probability estimate, based on the series of 123 peak bursts. The Figures for the other five reservoirs (not shown here) reveal a similar type of behaviour. This clearly indicates that the reservoir volume at the beginning of an extreme rainfall burst is generally higher than the reservoir volume on an arbitrary

moment in time. This means the probability distribution of reservoir volumes, to be used in the MCS framework, should be based on observed values at the beginning of high rainfall bursts and not on the complete series of reservoir volumes.

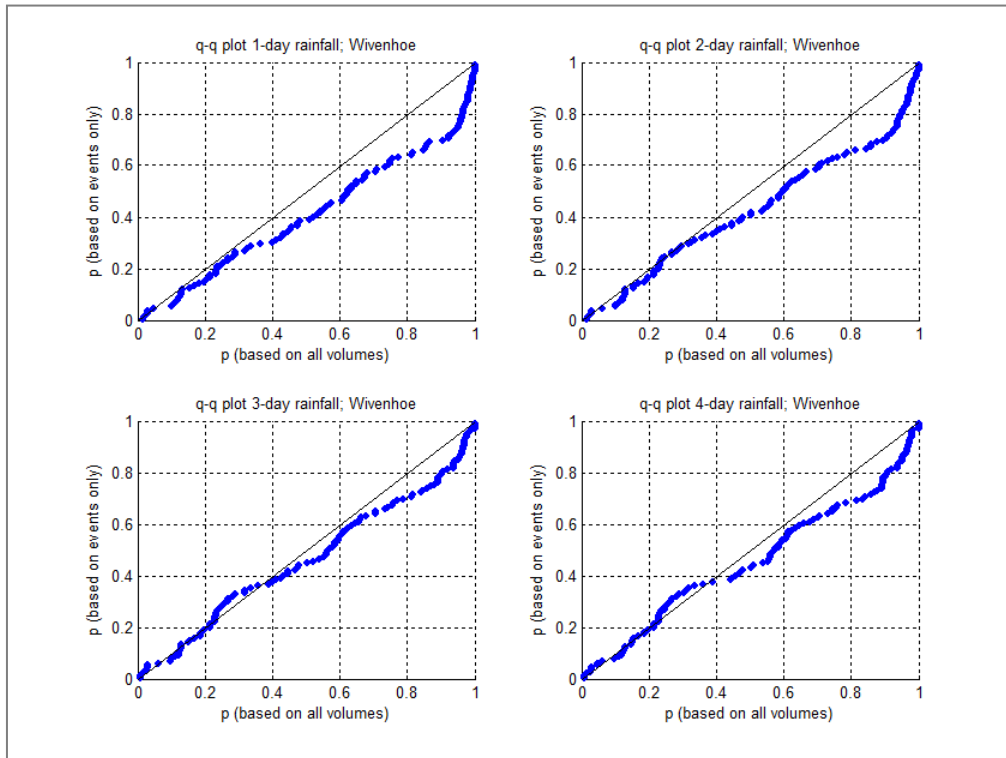


Figure 6-24 Q-Q plots showing estimated probabilities of non-exceedance of derived reservoir volumes for 123 bursts. P-values at the vertical axes were derived directly from the series of 123 bursts, p-values at the horizontal axes were derived from the statistics of the entire series of 123 years. Plots are shown for the highest 1,2,3 and 4-day rainfall bursts

Question 2: *Is there significant correlation between the cumulative rainfall depth of a rainfall burst and the reservoir volume at the start of the burst?*

To address this issue, observed rainfall totals were plotted against reservoir volumes. This was done for 1, 2, 3 and 4-day rainfall extremes. Figure 6-25 shows the results for Wivenhoe dam. The plots seem to indicate that there is a correlation: the highest rainfall totals do not occur in combination with the lowest reservoir volumes. This pattern is also observed for the other dams. However, the relation is weaker than it may appear from Figure 6-25. This is demonstrated in Figure 6-26, where the same data is shown in terms of empirical probabilities of non-exceedance. This means for example that the highest observed reservoir volume is estimated to have an empirical probability of non-exceedance of $1-1/(n+1)$ where n is the size of the data (123 in this case)⁵. The second highest observed volume is estimated to have an empirical probability of non-exceedance of $1-2/(n+1)$, etc. As can be seen in Figure 6-26, the correlation, which is essentially a rank correlation, is much weaker than appeared from Figure 6-25.

⁵ Note that this probability is *conditional*, ie it is the probability, given the fact that the rainfall is among the 123 highest cumulative rainfall volumes in the series of 123 years

To explain the difference, one of the observed combinations of rainfall depth and reservoir volume has been circled in red in both figures. The 4-day cumulative rainfall of this example burst is equal to 411 mm, which is ranked 4th overall 123 rainfall observation and hence has an estimated probability of non-exceedance of $1-4/(n+1) = 0.97$. The corresponding reservoir volume is equal to 807,000 MI, which is ranked 98th in the series of 123 reservoir volumes, and therefore has an estimated probability of non-exceedance equal to $1-98/(n+1) = 0.21$. So, in terms of absolute values, the relatively high rainfall depth of 411 coincides with a reservoir volume that appears to be average in from Figure 6-25. However, in terms of ranking, this reservoir volume is significantly lower than the median value. This is why the correlation in absolute values appears to be stronger than for estimated empirical probabilities and/or ranking numbers.

In general, rank correlation is more informative than Pearson's correlation coefficient (which is derived from absolute values) as explained for example by Genest and Favre (2007). This is why the use of the rank correlation is preferred in the current studies. Table 6-12 shows that both types of correlation coefficients are low for rainfall bursts and reservoir volumes.

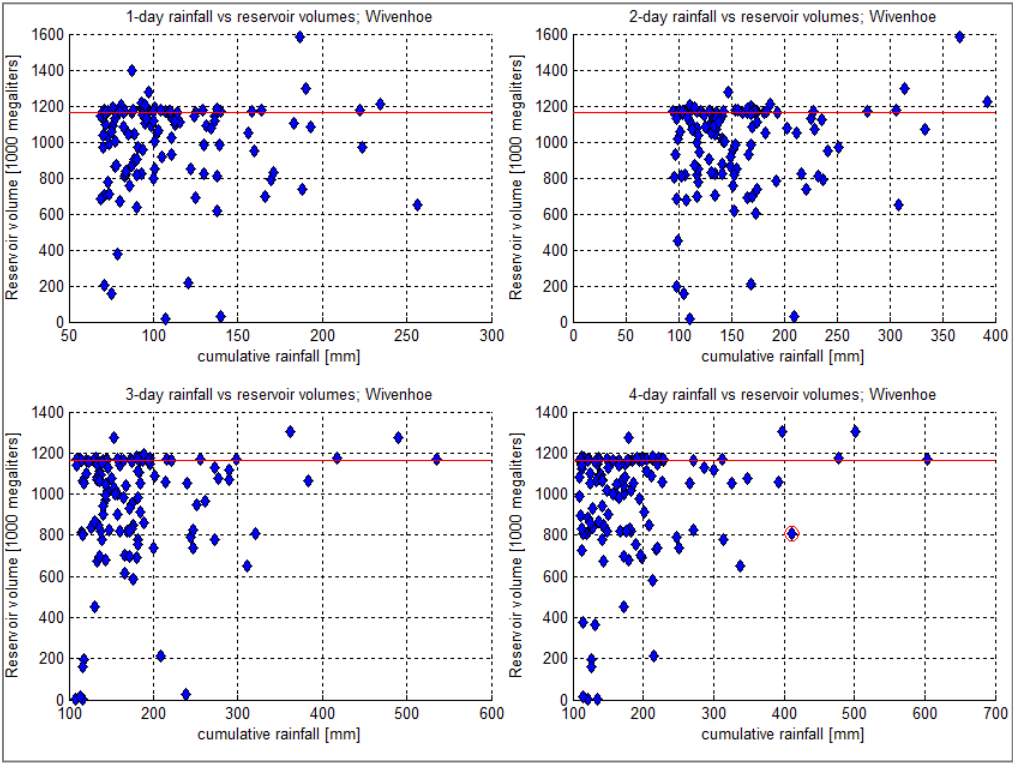


Figure 6-25 Scatter plots of rainfall depth and reservoir volume for Wivenhoe dam

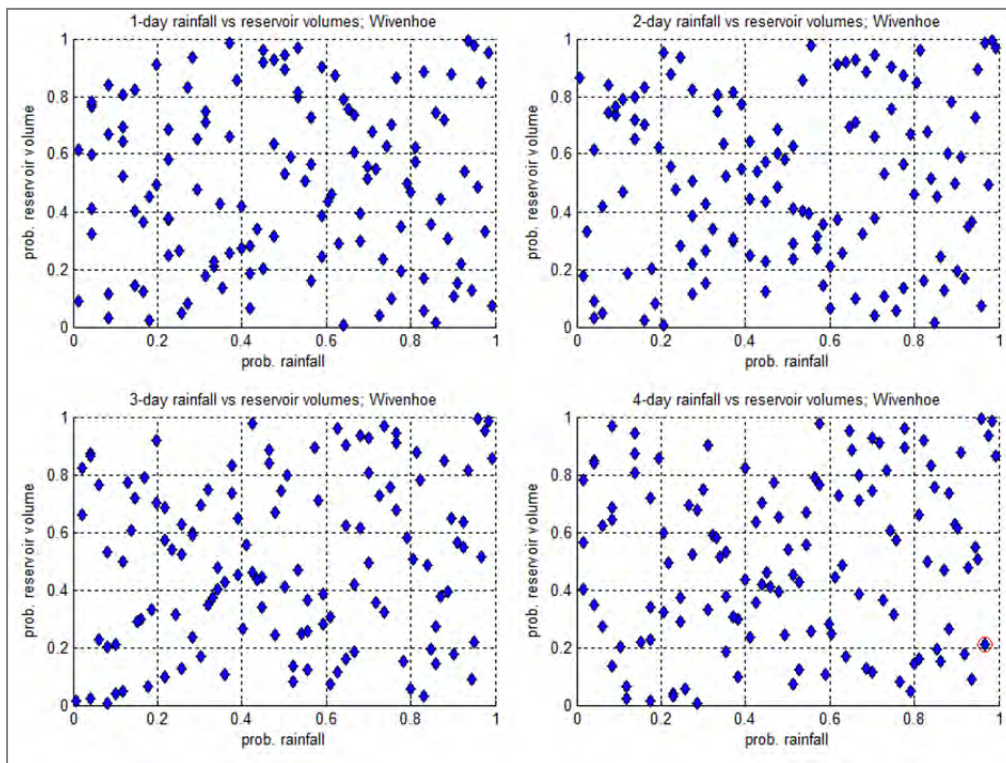


Figure 6-26 Empirical probabilities of rainfall depth and reservoir volume for Wivenhoe dam

Table 6-12 Correlations between rainfall and reservoir volumes for selected bursts (1, 2, 3 and 4-day rainfall extremes)

Dam	Rank-based correlation				Pearson's correlation			
	1 day	2 days	3 days	4 days	1 day	2 days	3 days	4 days
Cressbrook	0.14	0.05	0.02	0.14	0.17	0.07	0.06	0.16
Manchester	0.04	0.09	0.13	0.13	0.06	0.09	0.13	0.16
Moogerah	0.14	-0.11	-0.15	-0.19	0.15	0.02	-0.03	-0.17
Perseverance	0.29	0.08	0.03	0.03	0.23	0.08	0.05	0.04
Somerset	0.12	0.12	0.13	0.17	0.17	0.15	0.16	0.19
Wivenhoe	0.00	0.05	0.16	0.12	0.01	0.13	0.18	0.18

Question 3: *Is there mutual correlation between the reservoir volumes at the start of a burst?*

To address this issue, the 123 bursts with highest rainfall totals in the catchment of Wivenhoe dam were analysed. Reservoir volumes at the beginning of these bursts were gathered for all six reservoirs. Figure 6-27 shows scatter plots of Wivenhoe reservoir volumes versus volumes of the other five dams. These figures show there is clearly correlation present and this needs to be taken into account in the MCS framework. Table 6-13 shows the rank correlations between reservoir volumes, based on observed volumes at the beginning of the 123 highest 4-day rainfall bursts. It shows that mutual correlation between reservoir volumes are far more significant than correlations between rainfall depth and reservoir volumes (compare Table 6-13 with Table 6-12).

Table 6-13 Rank correlations between volumes of the six reservoirs: $\rho = \sin(\pi\tau/2)$, where τ is Kendall's rank correlation

Dam	Cressbrook	Manchester	Moogerah	Perseverance	Somerset	Wivenhoe
Cressbrook	1.00	0.67	0.58	0.99	0.60	0.85
Manchester	0.67	1.00	0.57	0.65	0.77	0.78
Moogerah	0.58	0.57	1.00	0.56	0.47	0.56
Perseverance	0.99	0.65	0.56	1.00	0.60	0.85
Somerset	0.60	0.77	0.47	0.60	1.00	0.86
Wivenhoe	0.85	0.78	0.56	0.85	0.86	1.00

Figure 6-27 reveals some interesting patterns:

- High volumes at Wivenhoe dam do not occur simultaneously with low volumes at Somerset dam. However, high volumes at Somerset dam can occur simultaneously with low volumes at Wivenhoe dam
- Similar observations can be made for Wivenhoe dam and Manchester dam
- For Perseverance dam and Cressbrook dam, the relation with Wivenhoe volumes are opposite: High volumes at Wivenhoe dam can occur simultaneously with low volumes at Perseverance/Cressbrook dams. However, high volumes at Perseverance/Cressbrook dams do not occur simultaneously with low volumes at Wivenhoe dam

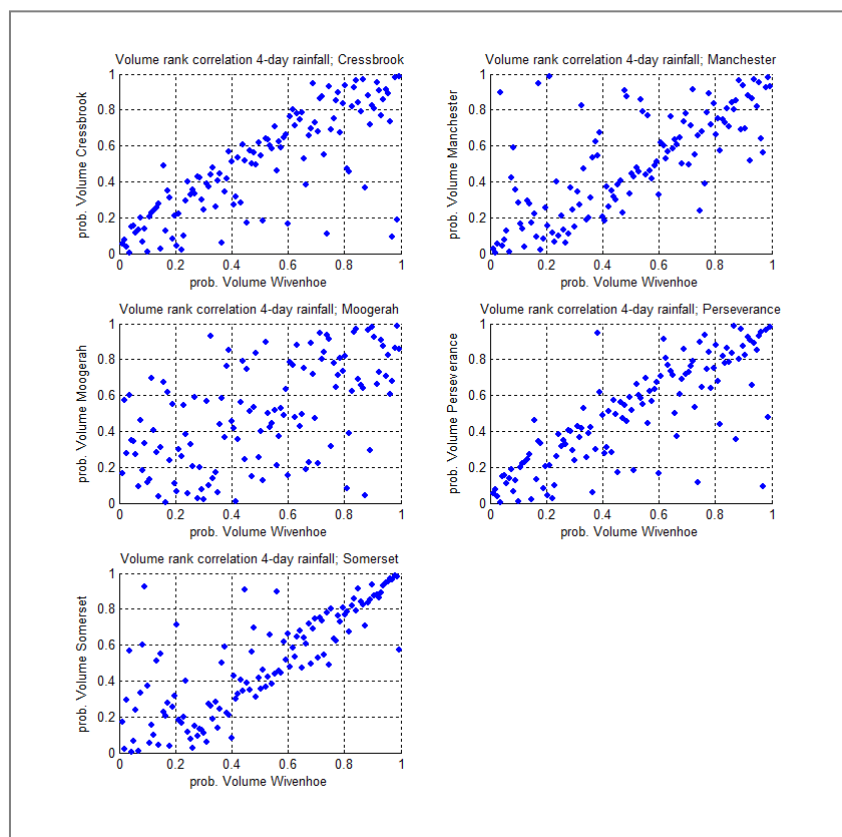


Figure 6-27 Scatter plots of empirical probabilities of reservoir volumes at the beginning of the 123 selected highest 4-day rainfall bursts: Wivenhoe dam (horizontal axis) plotted against the other five other dams




Figure 6-28 shows that the same patterns are observed in the full data set of daily reservoir volumes. The following paragraphs provide a hypothesis for this behaviour.

Somerset Dam has a greater chance of receiving inflows due to its proximity to the coast and so is more likely to fill than Wivenhoe Dam. Somerset Dam is also about one third the capacity of Wivenhoe Dam. Prior to the establishment of the Seqwater grid, as far as the operation of Somerset Dam and Wivenhoe Dam was concerned, the aim for water supply was to empty Somerset Dam into Wivenhoe Dam as quickly as possible to draw the combined storage down to around below 75% which the optimum storage level from a loss perspective. This provides greater opportunity to catch follow up rainfall in Somerset Dam.

This is still done, but there is now an added complication of the existing arrangement due to the inclusion of manufactured water (desalination and recycled potable water). At various thresholds of the combined storages (60% for the desalination and 40% for the recycled water), the natural supply can now be augmented by the use of manufactured water. This water is only pumped into Wivenhoe Dam. The Seqwater grid operates to satisfy two main objective functions:

- Above the threshold levels, the dams are operated to satisfy demands most efficiently
- Below the threshold it is operated to minimise the cost of operation whilst still meeting reduced demands (water restrictions are applied)

Perseverance and Cressbrook dams normally act independently from the Somerset/Wivenhoe system as they supply Toowoomba and not the wider Brisbane region. There is now an emergency pipeline that connects Wivenhoe Dam to Cressbrook/Perseverance dams for use during drought events on the Darling Downs (Toowoomba). This means this supply can also be augmented by the manufactured water. The observed correlations appear reasonable as under drought conditions the Toowoomba supplies would be depleted and would be augmented from supplies from Wivenhoe Dam/manufactured water supplies, meaning Perseverance/Cressbrook Dams are likely to be low, whilst Wivenhoe Dam may medium to high. If Wivenhoe Dam is drawn down then it is likely Perseverance/Cressbrook will also be low.

Conclusions

To conclude, the sampling scheme for reservoir volume should take the following aspects into account:

1. Marginal probability distribution functions of reservoir volumes should be based on observed volumes at the start of big rainfall bursts, ie not on the complete series of reservoir volumes of 123 years
2. Given the occurrence of a high rainfall burst, there is a weak correlation between reservoir volumes on one hand and total rainfall depth on the other hand
3. There is a significant correlation between volumes of different reservoirs at the beginning of high rainfall bursts

The next section will describe the proposed simulation procedure for reservoirs in the Monte Carlo framework.

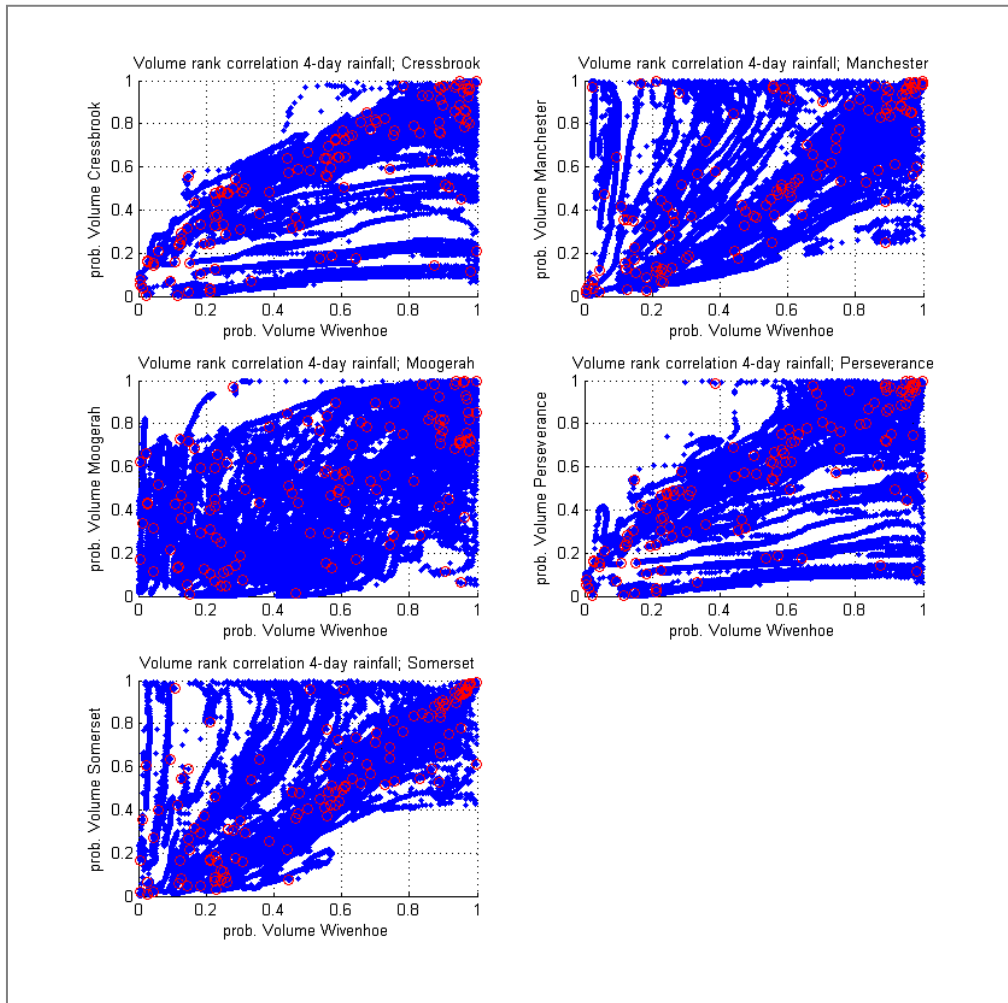


Figure 6-28 Scatter plots of empirical probabilities of reservoir volumes of all daily observations in the simulated series of 123 years: Wivenhoe dam (horizontal axis) plotted against the other five other dams. The red circles correspond to the highest 123 4-day rainfall bursts

6.4.3 Simulation procedure

Marginal distribution functions

The first requirement of the sampling procedure is a marginal probability distribution function of reservoir volumes for each of the six reservoirs. Figure 6-29 and Figure 6-30 show histograms of observed reservoir volumes at the beginning of the highest 1-day, 2-day, 3-day and 4-day rainfall bursts for Wivenhoe and Moogerah dam. The red dashed lines in the figures represent full supply levels. For an individual reservoir, the histograms of the n -day bursts are similar for $n = 1, 2, 3, 4$ days. This is also confirmed by the corresponding empirical distribution functions as shown in Figure 6-31. Note that between the histograms of the six reservoirs there are significant mutual differences.

The histograms are far from “smooth”, which means the well-known distribution functions cannot be expected to properly replicate the observed data. We therefore propose to use the empirical distribution that follows directly from the observed volumes. This means the probability of non-exceedance of a reservoir volume, v , is estimated as follows:

$$F_V(v) = \sum_{i=1}^n I_{[v_i < v]} \quad (22)$$

Where F_V is the empirical distribution function, V is the random variable representing reservoir volume, v is a potential realisation of V , v_i , $i=1..n$ are the n observed reservoir volumes on which the histograms are based and $I_{[\dots]}$ is the indicator function ($I=1$ if $v_i < v$, $I=0$ otherwise).

Figure 6-31 shows the empirical distribution functions of the reservoir volumes at the start of k -day rainfall bursts, for $k=1, 2, 3$ and 4 . As mentioned before, the empirical distribution function is relatively insensitive to the value of k . A single empirical distribution function (derived for $k=4$) is therefore adopted in the MCS framework and applied to the whole range of burst durations.

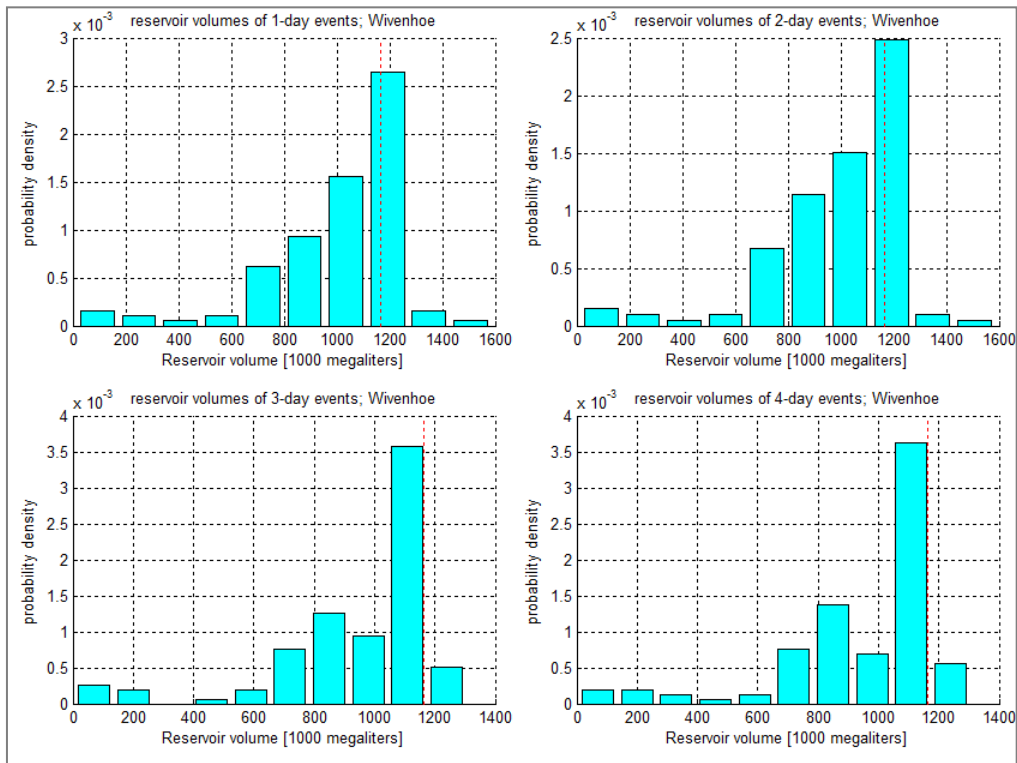


Figure 6-29 Histogram of Wivenhoe reservoir volumes at the beginning of the highest 1-day, 2-day, 3-day and 4-day rainfall bursts. The red dashed line is the full supply level

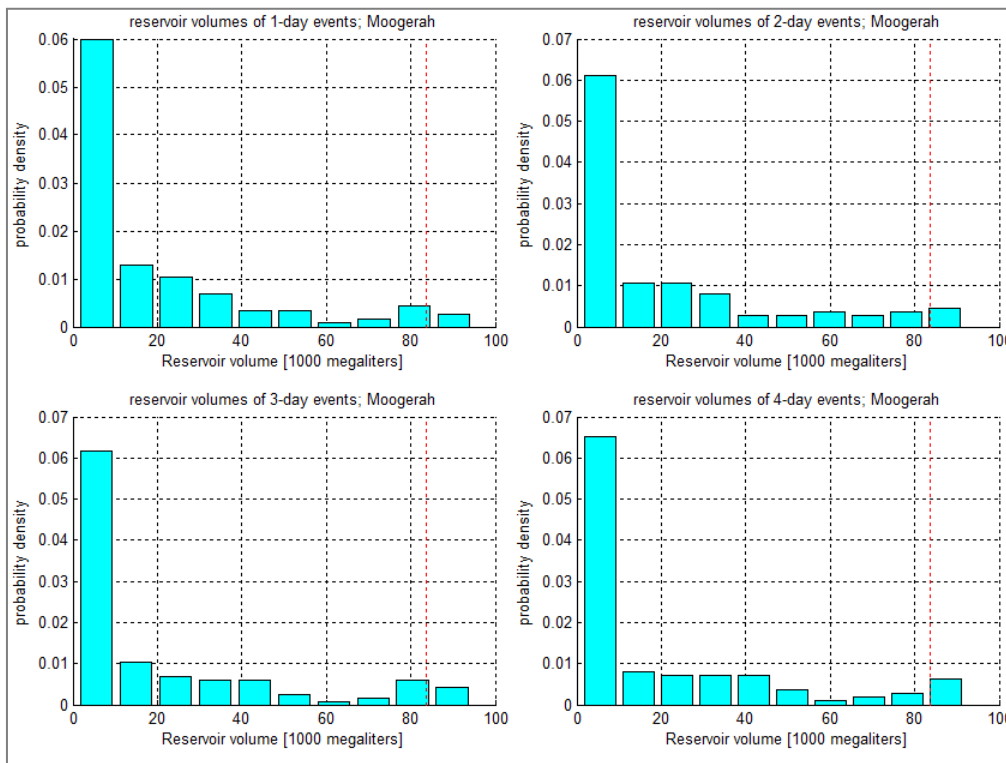


Figure 6-30 Histogram of Moogerah dam reservoir volumes at the beginning of the highest 1-day, 2-day, 3-day and 4-day rainfall bursts. The red dashed line is the full supply level

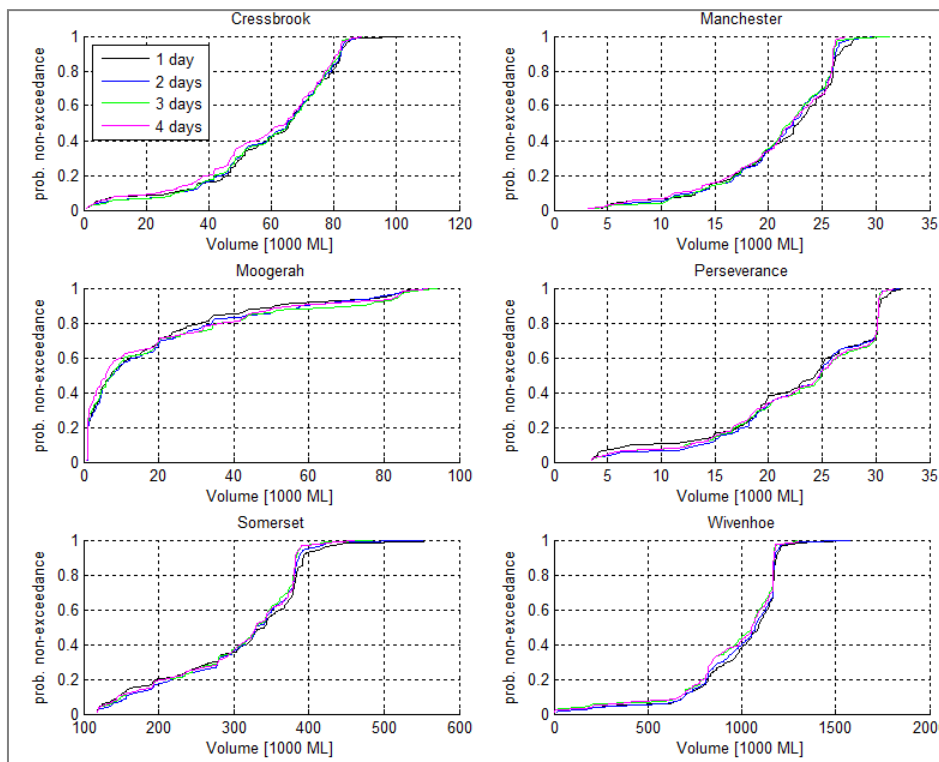


Figure 6-31 Derived empirical distribution function of reservoir volumes at the start of 1-day, 2-day, 3-day and 4-day rainfall bursts

Correlations

The correlation between rainfall and reservoir volumes is covered to a large extent in the sampling procedure by the fact that marginal distributions are based on observed reservoir volumes at the beginning of high rainfall bursts. The ‘remaining’ correlation is weak, ie the correlation between the total rainfall depth of a high rainfall burst and the reservoir volume at the beginning of such a burst.

The remaining challenge of the multivariate sampling scheme is therefore to simulate the mutual dependence between reservoir volumes as described in Section 6.4.2. The correlation matrix as shown in Table 6-13 can be used as starting point. The earlier described correlation models (Gaussian and student-t copula) are not applicable in this case. These copulas are symmetric around the line $y=x$, provided that correlations are positive and this property holds for most copulas. As observed in Section 6.4.2, the correlation structure between Wivenhoe dam on one hand and Somerset, Manchester, Cressbrook and Perseverance dams are clearly asymmetric around the line $y=x$. A copula that is able to represent this asymmetric behaviour is the skewed student-t copula (Azzalini and Capitanio, 2003; Sahu et al. 2003; Smith et al., 2012). This copula function has the following parameters:

- An n -by- n correlation matrix ρ (similar to the Gaussian and student-t copula), where n is the number of reservoirs
- A scalar parameter ν which controls the tail dependence (similar to the student-t copula)
- A 1-by- n vector γ which controls the asymmetric behaviour

Once these parameters are given, the procedure to implement the skewed student-t copula in the Monte Carlo framework is as follows:

1. Derive a lower triangular matrix L for which: $LL' = \rho$, through Cholesky decomposition of correlation matrix
2. Sample values u_1, \dots, u_n from the standard normal distribution function; store the results in an $1 \times n$ vector u
3. Compute: $u^* = uL'$
4. Sample a value, s , from the χ_ν^2 (chi-square) distribution with ν degrees of freedom
5. Compute $w = \nu/s$; w is a sample of the inverse gamma-distribution with parameters $(\nu/2, \nu/2)$.
6. Compute $y = \gamma w + (\sqrt{w})u^*$; y is a vector of correlated samples from the skewed student-t distribution with ν degrees of freedom.
7. Compute $p = t_{\nu}(y)$, where t_{ν} is the skewed student-t distribution with ν degrees of freedom

The correlation matrix, ρ , and degrees of freedom, ν , have been derived from the data, using the available fit procedures for the student-t copula in Matlab. Correlation matrix ρ is shown in Table 6-13, ν is equal to 6. The values of factor γ were taken according to the values shown in Table 6-14. The motivation for the choices of these γ -values is as follows:

- For Wivenhoe dam, a γ -value of zero was chosen because this dam is considered the “reference” for the other five reservoirs
- For Moogerah dam, a γ -value of zero was chosen, because the paired observations of Wivenhoe dam and Moogerah dam did not show an asymmetric pattern
- For Cressbrook and Perseverance dams a negative γ -value was chosen, because this leads to the observed asymmetric pattern in which high volumes at Wivenhoe dam can occur simultaneously with low volumes at Perseverance/Cressbrook dams, while high volumes at Perseverance/Cressbrook dams cannot occur simultaneously with low volumes at Wivenhoe dam

- For Somerset and Manchester dams a positive γ -value was chosen, because this leads to the observed asymmetric pattern in which high volumes at Wivenhoe dam will not occur simultaneously with low volumes at Somerset/Manchester dams, while high volumes at Somerset/Manchester dams can occur simultaneously with low volumes at Wivenhoe dam
- For Cressbrook, Perseverance, Somerset and Manchester dams, $|\gamma|$ was taken equal to 0.5, as this provided a good fit of the data

Table 6-14 Selected γ -values for the six reservoirs

dam:	Cressbrook	Manchester	Moogerah	Perseverance	Somerset	Wivenhoe
γ :	-0.5	0.5	0	-0.5	0.5	0

Figure 6-32 shows simulated reservoir volumes with the skewed-t copula in combination with observed volumes. It shows paired observations of Wivenhoe volumes (horizontal axes) and volumes of the other five dams (vertical axes). It can be seen from this Figure that the observed asymmetric patterns are very well reproduced by the simulation model.

Note that the γ -values in the simulation model were chosen in such a way that the model was able to reproduce the correlation structure between Wivenhoe dam on the one hand and the other dams/reservoirs on the other hand. In other words, the mutual correlations between the other five reservoir were not considered in the fit procedure. The motivation for this “strategy” is that Wivenhoe dam is the most relevant reservoir for flood risks in the Brisbane River catchment, which means a correct representation of correlations with Wivenhoe dam have the highest priority. To verify potential negative side-effect of the chosen parameters, the observed and simulated mutual correlations between volumes of Moogerah, Cressbrook, Perseverance, Somerset and Manchester dams are shown in Figure 6-33. It can be seen that the simulations and observations are in accordance with each other.

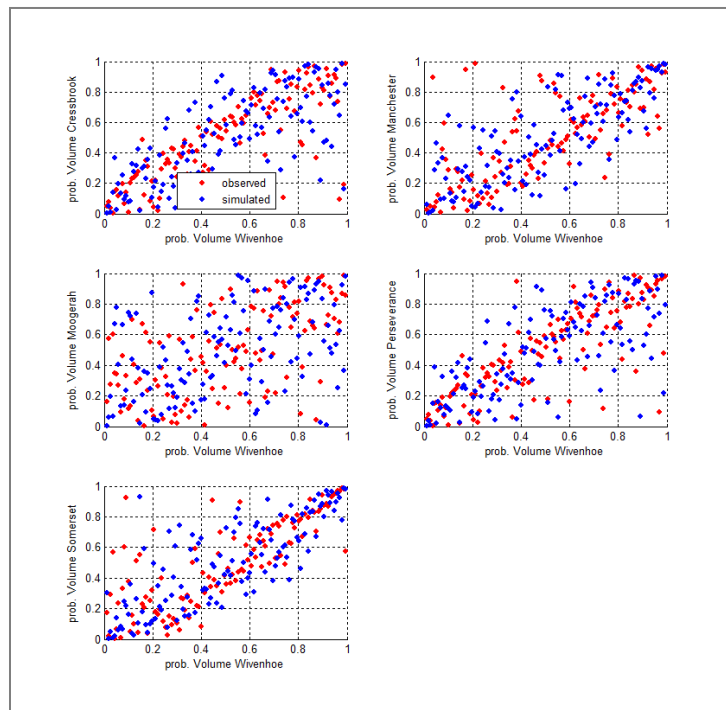


Figure 6-32 Observed (red) and simulated (blue) pairs of reservoir volumes at the beginning of high rainfall bursts; Wivenhoe dam versus the other five dams

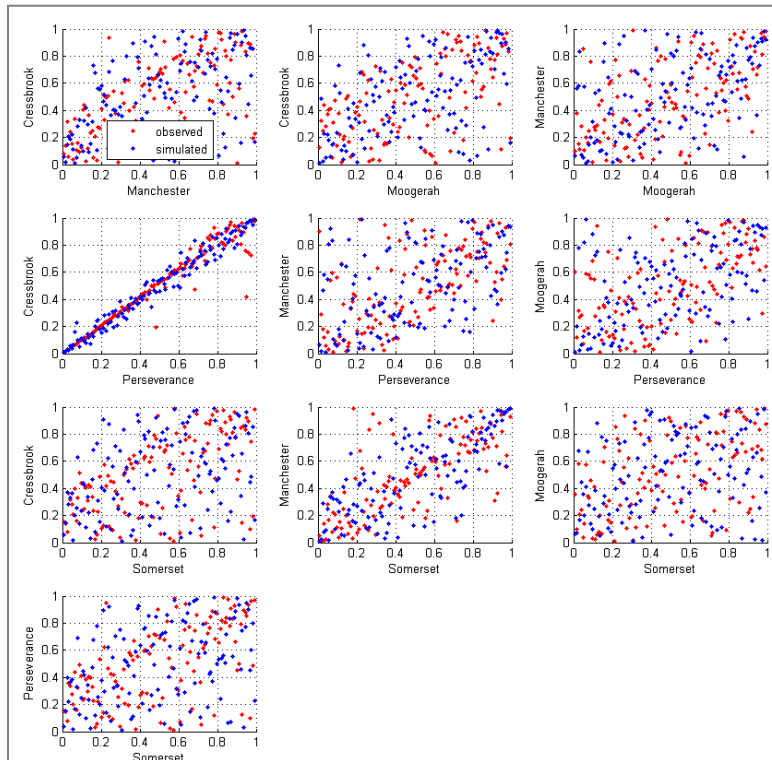


Figure 6-33 Observed (red) and simulated (blue) pairs of reservoir volumes at the beginning of high rainfall bursts; Combinations of Cressbrook, Perserverance, Moogerah, Manchester and Somerset dams


6.5 Base flow

In accordance with the URBS model review presented in (Aurecon, 2014b), a Baseflow Volume Factor is applied according to the magnitude of the design rainfall event. The adopted Baseflow Volume Factors in Figure 6-15 have been sourced from AR&R Revision Project 7.

Table 6-15 Adopted baseflow volume factors

ARI (years)	ARI factor for Baseflow Volume Factor
2	1.6
5	1.2
10	1.0
20	0.8
50	0.7
100	0.6
>100	extrapolated

The base flow volume factor is applied to design events to limit the base flow contribution, especially for the rare to extreme flood magnitude range.



During the calibration phase baseflow parameters were calibrated for each location under investigation. Base flow was considered in the Upper Brisbane River, Stanley River, Bremer River, Warrill Creek and Purga Creek sub-catchments as per the Seqwater (2013) approach. Seqwater noted that there was insufficient reliable information to derive base flow parameters in Lockyer Creek or the Lower Brisbane River. These parameters are based on the URBS baseflow model:

$$BF(i) = BR \cdot BF(i-1) + BC \cdot QR^B M \quad (23)$$

The BR and BC are daily time step parameters and URBS makes internal adjustments to account for the model time step. The BM exponent determines whether linear or non-linear baseflow routing is to be adopted. For the Brisbane River catchment, BM was assumed to be equal to 1, ie a linear model.

It can be shown that BFVF (the ratio of baseflow to quick runoff) = $BC/(1 - BR)$, when BM = 1.

The URBS' RAINURBS module was modified to include the BFVF parameter for the 10 year event as provided in Table 1 of the ARR project 7 report. For the Brisbane catchment this parameter was set to 0.15. Adjustment was made to this value based on the design ARI under investigation using the factors in Table 5 as provided in the ARR project 7 report. A power curve was fitted to these adjustment factors to extrapolate these factors for ARI's greater than 100 years.



7 Hydrological model and dam operations model

7.1 Introduction

Section 3 to 6 were dedicated to the statistical models and data that are used in the Monte Carlo Simulation framework to generate synthetic flood events, characterised by rainfall, antecedent moisture conditions, initial reservoir volumes and ocean water levels. The next step in the MCS framework is to simulate the synthetic events to obtain peak discharges and flow volumes at each location of interest. This step is conducted with a combination of a hydrological model (URBS) and a reservoir simulation model (RTC tools). The workflow of the URBS and RTC model was presented in Section 2 (see Figure 2-3). The following sections provide more details on these models.

7.2 URBS hydrological model

The real time flood operations of Wivenhoe and Somerset Dams require decision support from a suite of calibrated catchment flood hydrology models to estimate flood hydrographs from catchment rainfall inputs. New data obtained during recent flood events (January 2011 and January 2013) has identified a need to develop and calibrate updated flood hydrology models for the Brisbane River Basin. Seqwater (2013a) has conducted a calibration of the existing URBS hydrology model for the Brisbane River catchment. Seqwater recognised that the calibration should not be considered final. Therefore, the URBS model of the Brisbane River catchment was recalibrated as part of the Brisbane River catchment flood study (Aurecon, 2014b). The latter version of the report was adopted in the Monte Carlo Simulation framework.

The Brisbane River hydrological model is based on the URBS hydrological model (Carroll, 2012a). URBS is a rainfall-runoff-routing networked model of sub-catchments based on centroidal inflows. Each storage component is conceptually represented as a non-linear storage. The URBS model setup can readily represent a cascade catchment structure. Key routing variables used by URBS are; stream length, catchment area, fraction urbanised (various degrees) and fraction forested area and, optionally, channel roughness and storage and slope. Backwater effects can be modelled in URBS with multivariate rating relationships.

The Brisbane River catchment was divided into seven distinct sub-catchment models based on review of topography and drainage patterns, major dam locations, key locations of interest for real time flood operations, and consideration of the best use of available data including water level gauges. The seven sub-catchments are further subdivided into sub-areas (534 in total, see Table 7-1). The primary reason for introducing the sub-areas is to be able to properly model spatial variability of rainfall in the catchment.

Table 7-1 The seven sub-catchments used to model of the Brisbane river catchment

no	Description	Size (km ²)	Number of subareas
1	Stanley River to Somerset Dam	1,324	76
2	Upper Brisbane River to Wivenhoe Dam	5,645	99
3	Lockyer Creek to OReillys Weir	2,964	138
4	Bremer River to Walloon	634	42
5	Warrill Creek to Amberley	902	56
6	Purga Creek to Loamside	209	19
7	Lower Brisbane River to the river mouth	1,855	104

In the MCS framework, event rainfall is characterised by hourly rainfall time series for each of the 534 sub-areas that are used as input to the URBS hydrological model. The URBS model provides several methods to compute runoff from total rainfall. For the Brisbane River catchment model, the initial loss-continuing loss model is applied. This means the net rainfall, ie the portion of the rainfall that becomes available for runoff is derived by first subtracting the initial loss from the event rainfall and subsequently subtracting continuing losses from the “remaining” rainfall.

The Brisbane River URBS model adopted the ‘Split’ model to simulate runoff routing. Runoff routing is ‘split’ between sub-catchment routing and stream routing. For sub-catchment routing the following non-linear storage discharge relationship is assumed:

$$S_{catch} = \left\{ \frac{\beta \sqrt{A} (1+F)^2}{(1+U)^2} \right\} Q^m \quad (24)$$

where

S_{catch} = catchment storage [m³/h/s]

β = catchment lag parameter

A = area of sub-area [km²]

U = fraction urbanisation of sub-area

F = fraction forested area of sub-area

m = catchment non-linearity parameter (typically between 0.6 and 0.8)

Channel routing is based on the non-linear Muskingum model as is given as:

$$S_{chnl} = \alpha f \frac{n_m L}{\sqrt{S_c}} (xQ_u + (1-x)Q_d)^n \quad (25)$$

where

S_{catch} = catchment storage [m³/h/s]

α = channel lag parameter

F = reach length factor

L = length of reach [km]

S_c = channel slope [m/m]

Q_u = inflow at upstream end of reach (includes catchment inflow)

- Q_d = outflow at downstream end of the channel reach [m^3/s]
 x = Muskingum translation parameter
 n = Muskingum non-linearity parameter (exponent)
 n_m = Manning's n or channel roughness

Parameters IL (initial loss), CL (continuing loss), α (channel lag parameter) and β (catchment lag parameter) were derived *per* event, based on model calibrations by Seqwater (2013a). Channel slope (S_c) and Manning n_m were not included as variables. Backwater effects of ocean water levels are approximated within URBS using multivariate or dependent rating relationships, but these only affect water levels, not flows.

Dams and reservoirs can be modelled as well in URBS as level pool storages with fixed crest spillway relationships. This module is applied to all dams and reservoirs in the Brisbane River Catchment, with the exception of Wivenhoe Dam and Somerset Dam.

7.3 RTC tools dam operations model


7.3.1 Introduction

Wivenhoe Dam and Somerset dam are simulated with the real-time control software RTC tools. RTC-Tools is an open source, modular toolbox dedicated to real-time control (RTC) of hydraulic structures like weirs, pumps, hydro turbines, water intakes, etc. It can be used in standalone mode or in combination with hydraulic models for general modelling studies as decision support component in operational forecasting and decision-support systems, for example for drought management and water allocation, flood mitigation or the dispatch of hydropower assets. RTC tools is used as a real-time forecasting model for the operational management of the Wivenhoe and Somerset reservoirs by Seqwater.

Somerset Dam and Wivenhoe Dam are operated in accordance with procedures outlined in the *Manual of Operation Procedures for Flood Mitigation at Wivenhoe Dam and Somerset Dam* Revision 11 (Seqwater, 2013b). The capacity of the urban water supply compartment that relates to Wivenhoe Dam's Full Supply Level (FSL) is 1,165,000 ML. The Dam can also store up to a maximum of 1,967,000 ML as temporary flood storage up to EL 80.0 m. Flood releases are made through the main gated spillway, (which contains five radial gates), and also an auxiliary spillway that consists of a three bay fuse plug embankment. The radial gates should be fully open prior to the initiation of the first fuse plug embankment.

For Somerset Dam, the capacity of the urban water supply compartment related to its FSL is 380,000 ML, with 721,000 ML volume available for use for temporary flood storage up to EL 109.7 m. Somerset Dam is equipped with four regulator cone dispersion valves, eight sluice gates and eight sector gates. During flood operations the eight sector gates are fully opened to allow free overflow over the spillway prior to the onset of the flood. The regulator valves are generally not used for flood releases as elevated tailwater levels tend to impair the performance of the valves. Therefore the eight sluice gates and the spillway flows are the main flood release mechanisms for Somerset Dam during a flood event.

The Dam Operations Module as implemented in RTC tools is based upon the Loss of Communications (LOC) emergency flood operation procedure described in the Flood Manual (Seqwater, 2013b). The reason to implement the LOC scenario instead of the regular dam operation strategy is the fact that the latter is relatively complex to implement especially in a Monte Carlo Simulation framework. Bearing in mind that the project has a tight time schedule and that the purpose



of this study is for floodplain management (ie not operational management), the implementation of the LOC was preferred.

The Loss of Communications (LOC) emergency flood operation procedure was successfully implemented in the RTC tools model. The model performance of the RTC tools dam operations model was compared to Seqwater's GoldSim model. Model results were compared for 24 synthetic events, ranging from moderate to extreme flood events. The comparison showed that predicted Wivenhoe Dam outflow hydrographs of RTC tools closely matched the predicted hydrographs of the GoldSim model. As a follow-up activity, the drain-down process incorporated into the LOC was modified to reflect the normal operation procedure and mimic the seven day drainage requirement.

The LOC scenario on average results in slightly 'conservative' estimates of peak discharges and flow volumes in the Lower Brisbane River. For floods within the range of 2,000 m³/s to 16,000 m³/s, the peak flow in the mid-Brisbane River and Lower Brisbane River according to the LOC scenario are on average in the order of 5 to 10% higher than the peak discharges that result from the Dam operations using the Flood Manual procedures (2013 flood Manual). This means the derived frequency curves for the 'With Dam' scenario are conservative as well. For this reason, it has been considered to apply a bias adjustment on the derived frequency curves for the 'with dams' scenario. This bias adjustment would be based on the comparison of GoldSim model simulations for both the LOC strategy and full operation strategy. However, it was concluded that the GoldSim model, suitable for many other tasks, contains assumptions that make it unsuitable for reliably estimating bias adjustment. As a consequence, it was decided not to apply a bias adjustment.

7.3.2 Wivenhoe dam

The target release of Wivenhoe Dam is based on Wivenhoe Dam headwater levels only. Headwater levels are determined by inflow and release rates. Inflow into and outflow from the Wivenhoe Dam reservoir will result in level changes of Wivenhoe Dam. The Level-Volume relation for Wivenhoe Dam is taken from the Wivenhoe Technical Data, as described in Appendix E of the Manual of Operational Procedures for Flood Mitigation at Wivenhoe Dam and Somerset Dam (Seqwater, 2013b) Wivenhoe Dam has two relevant inflows:

1. The unregulated inflow from the Upper Brisbane River, as simulated with the URBS hydrological model
2. The releases from Somerset Dam, as determined from the RTC model of Somerset Dam

As release rates influence the lake level and the lake level influences target outflow rates, the control actions are determined at each time step, based on the situation in the previous time step and taking into account any constraints that may apply. The current implementation of rating curves (level versus total outflow) for the main gated spillway Wivenhoe Dam flow, as well as for the situation of fuse plug breaches is based on the available tables in the Flood Manual (Table 7.3.1 and Appendix F of Seqwater, 2013b). For practical purposes, the individual (radial) gates of Wivenhoe Dam are not modelled in the RTC model. However, constraints related to the successive gate operations (opening and closing) are taken into account in the form of lookup tables.

The discharge increment value (per control time step) is used as a rate of change constraint for the combination of Wivenhoe Dam radial gates. For lake levels below EL74.0 m AHD, a limit of 6 increments per hour, or 3 m/hour, (1 increment = 0.5 m) is taken as the constraint in case the water level is rising and a limit of 3 increments per hour, or 1.5 m/hour, is taken as the constraint in case the water level is falling. For lake levels above EL74.0 m AHD, a limit of 20 increments per hour (10 m/hour) was implemented.

Crest overtopping can also occur, which is modelled as a sharp crested weir for the main Dam (dimensions: 2000 m effective weir length, crest level EL80.1 m AHD, weir coefficient 1.7) and a broad crested weir for the saddle Dams (dimensions: 580 m combined effective weir length, crest level 80.0 m AHD, weir coefficient 1.4). It is assumed that Wivenhoe Dam will not fail if it is overtopped and therefore dam failure will not be modelled. In reality, as stated earlier, overtopping is considered a major threat to the security of Wivenhoe Dam. Wivenhoe Dam is overtopped by an event with a 1 in 100,000 AEP, when the Lake Level reaches EL 80.0 m. However, the process of dam breaching and subsequent flooding downstream is out of the scope of the BRCFS project and therefore the Dam is assumed not breach under any circumstance.

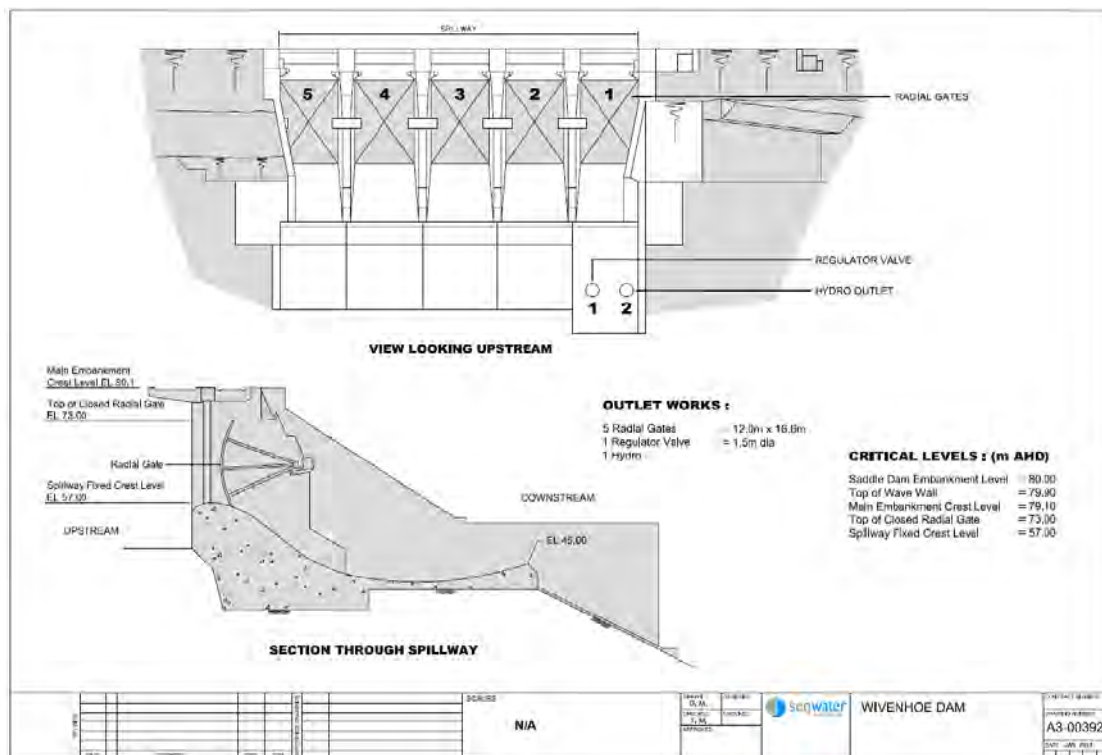


Figure 7-1 Schematic view of Wivenhoe Dam

7.3.3 Somerset Dam

The decision to determine which control action to take at Somerset Dam is dependent on the headwater levels of both Wivenhoe Dam and Somerset Dam. Headwater levels are determined by inflow and release rates. The Level-Volume relation for Somerset Dam is taken from the Somerset Technical Data, as described in Appendix B of the Manual of Operational Procedures for Flood Mitigation at Wivenhoe Dam and Somerset Dam (Seqwater, 2013b). Somerset Dam has one relevant inflow: the Stanley River as simulated with the URBS hydrologic model. The target outflow from Somerset Dam is directly routed to Wivenhoe Dam reservoir without any delay. That is the travel time between the two reservoirs is assumed to be instantaneous.

A lookup table is implemented in RTC tools to describe the relation between outflow releases on one hand and the Somerset HW level and the state of the sluice gates on the other hand. The equations for flow through a fully opened sluice gate is shown below:

$$Q_{\text{Sluice}} = 40.022 \cdot (h - 73.15)^{0.4963}$$

Besides releases through the sluice gates, Somerset Dam can also make releases through the radial gates over an ogee crest spillway. The ogee spillway crest level is EL100.45 m AHD. The following equation was used as the basis to construct the lookup table for each individual spillway crest gate:

$$Q_{crest} = 12.137 * [h - 100.45]^{1.6653}$$

At EL107.45 m AHD, flood waters commence to flow over the *Dam* crest and flow occurs through the 'breeze way'. To account for this discharge, the Dam crest is assumed to operate as a broad crested weir with a spillway width of 135.33 m, a spillway level of EL107.45 m AHD and a weir coefficient of 1.7.

$$Q_{overflow} = 1.7 * 135.33 * (h - 107.455)^{1.5}$$

As with Wivenhoe Dam, Somerset Dam is assumed not to fail if it is overtopped and so therefore failure is not modelled.

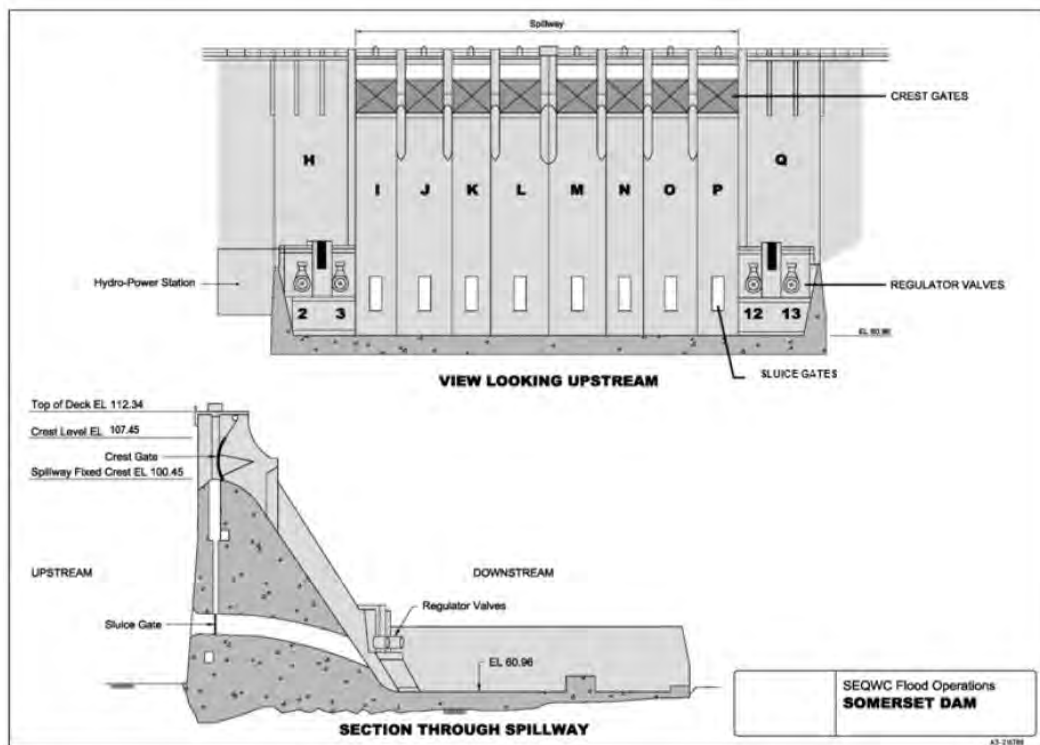


Figure 7-2 Schematic view of Somerset Dam

Only sluice gates are used to adjust the release from Somerset Dam. For this purpose, the 'interaction diagram' of Figure 7-3 is used. The interaction diagram uses the Somerset Dam Headwater level and Wivenhoe Dam Headwater level as the basis for decision making in regard to storing or releasing flood water from Somerset Dam using the Somerset Dam sluice gates. The diagram is divided into four zones, describing for classes of combinations of Wivenhoe and Somerset headwater levels. In RTC tools, a fifth zone is added after consultation with Seqwater (Michel Raymond, pers. Communication). This additional zone is a buffer zone around the operating target line. When the combination of Wivenhoe Dam and Somerset Dam water levels are in Zone 5 (the buffer zone), no Somerset control action is taken on the sluice gates. This zone is introduced (also in the GoldSim model of Seqwater) to prevent unnecessary oscillating behaviour of headwater levels and gate openings.

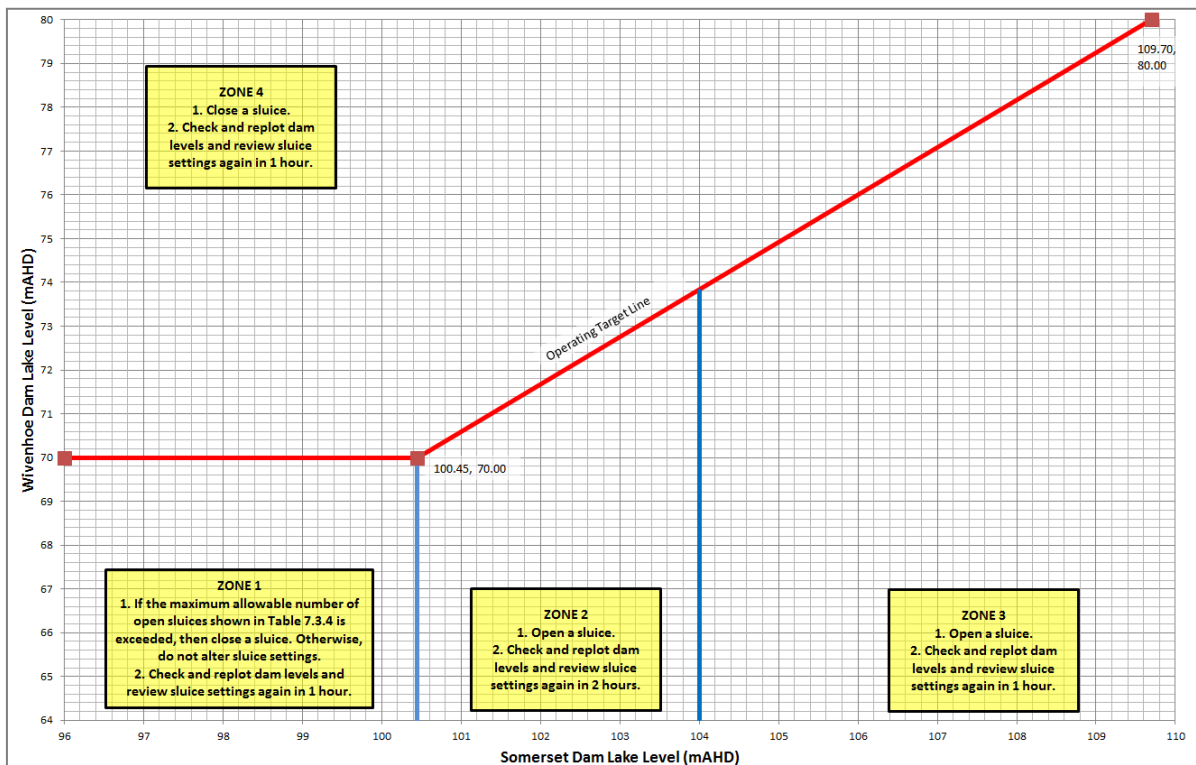


Figure 7-3 Somerset Dam loss of communications procedure

The five zones and control actions are implemented as follows:

Zone 1: *Level Somerset Dam < 100.45 and Level Wivenhoe Dam < 70.0*

As long as the Wivenhoe Dam level is below 70.0 mAHD and the level at Somerset Dam < 100.45 m AHD, RTC Tools will apply no control action to open/close a sluice gate of Somerset Dam, taking into account the constraint of maximum number of sluice gates allowed being open (Table 7-2). When too many sluice gates are open, a sluice gate will be closed. The next control action is in 1 hour.

Zone 2: *100.45 <= Level Somerset Dam < 104 and Level Wivenhoe Dam < Operating Target Line*

RTC Tools will apply a control action to open a sluice gate of Somerset Dam, taking into account the constraint of maximum number of sluice gates allowed to be open. The next control action is in 2 hours.

Zone 3: *Level Somerset Dam >= 104 and Level Wivenhoe Dam < Operating Target Line*

RTC Tools will apply a control action to open a sluice gate of Somerset Dam, taking into account the constraint of maximum number of sluice gates allowed to be open. The next control action is in 1 hour.

Zone 4: *Any Level Somerset Dam /Level Wivenhoe Dam combination where Level Wivenhoe Dam >= Operating Target Line*

RTC Tools will apply a control action to close a sluice gate of Somerset Dam. The next control action is in 1 hour.

Zone 5: *Any Level Somerset Dam/Level Wivenhoe Dam combination where (Level Wivenhoe Dam <= Operating Target Line + 3 cm) AND (Level Wivenhoe Dam >= Operating Target Line – 3 cm)*

RTC Tools will apply no control action to close a sluice gate of Somerset Dam. The next check to see whether a control action is needed is in 15 minutes.

Table 7-2 Maximum number of sluice gates that are allowed being open

Somerset Dam Lake Level (EL metres)	Maximum Allowable Number of Open Sluice Gates
Less than or equal to EL 99.00	0
Between EL 99.00 and EL 99.05	1
Between EL 99.05 and EL 99.15	2
Between EL 99.15 and EL 99.30	3
Between EL 99.30 and EL 99.50	4
Between EL 99.50 and EL 99.75	5
Between EL 99.75 and EL 100.00	6
Between EL 100.00 and EL 100.45	7
Greater than EL 100.45	8

On the basis of all equations and constraints, a rating table was constructed for the releases through the sluice gates, flow over the spillway (with the radial gates fully opened), and flow over the Dam crest. The regulator valves are not modelled and are assumed to be closed during a flood event.

8 Computation of frequency curves

8.1 Introduction

Sections 3 to 6 were dedicated to the statistical models and data that are used in the Monte Carlo Simulation framework to generate synthetic flood events, characterised by rainfall, antecedent moisture conditions, initial reservoir volumes and ocean water levels. Section 7 described the integrated URBS hydrological model and RTC dam operations simulation model, that is used to compute peak discharges and flow volumes at key locations in the catchment. The final step in the Monte Carlo Simulation procedure consists of the derivation of flood flows and associated Annual Exceedance Probabilities (AEPs), based on the simulations of the generated synthetic events. The computation procedure for the frequency curves is described in the following sections.

8.2 Monte Carlo estimates of flood frequencies

This section describes the computation of the (annual) probability that at a location L the discharge level q is exceeded. Similar equations are used for the computations of flow volumes. Define vector \mathbf{X} as the set of all random variables involved in the Monte Carlo Simulation and define \mathbf{x} as a sample ("realisation") of \mathbf{X} . Each \mathbf{x} results in a peak discharge at location L , as computed with the URBS/RTC model. The resulting peak discharge Q can thus be written as a function of \mathbf{x} : $Q=Q(\mathbf{x})$. To compute the exceedance probability of a discharge level q , we need to quantify the combined probability of all realisations, \mathbf{x} , for which $Q(\mathbf{x})>q$. This means the following integral needs to be computed:

$$P[Q > q] = \int_{Q(\mathbf{x}) > q} f_{\mathbf{X}}(\mathbf{x}) d\mathbf{x} = \int_{\mathbf{x}} f_{\mathbf{X}}(\mathbf{x}) I_{[Q(\mathbf{x}) > q]} d\mathbf{x} \quad (26)$$

Where $f_{\mathbf{X}}$ is the joint probability density function (pdf) of \mathbf{x} and I is the indicator function ($I=1$ if $Q>q$, $I=0$ otherwise). Equation (26) is generally too complex to compute analytically. For this reason, joined probability methods like Monte Carlo Simulations are carried out to approximate this integral. The essence of the (crude) Monte Carlo Simulation method is to repeatedly sample \mathbf{x} from density function $f_{\mathbf{X}}$ and to subsequently verify for each sample (through model simulations) if level q is exceeded. The fraction of samples for which q is exceeded is an estimate of the exceedance probability of q and, hence, an estimate for the integral of equation (26). This estimate can be formulated as follows:

$$\hat{P}(Q > q) = \frac{1}{N} \sum_{i=1}^N I_{[q_i > q]} \quad (27)$$

Where N is the number of samples of \mathbf{x} (ie the number of simulated events) and q_i is the derived peak discharge at location L in the i^{th} simulated event.

8.3 Stratified sampling and importance sampling

8.3.1 Introduction

With the crude Monte Carlo Simulation method as described in the previous section, a practical problem arises if estimates are required for discharge levels with small exceedance probabilities. In those cases, crude Monte Carlo sampling requires a large number of simulations to provide an accurate estimate. This is especially unpractical if model simulations are time-consuming. In that case, the number of model simulations may need to be limited. This will be at the expense of the accuracy of the probability estimate. Fortunately, the efficiency of Monte Carlo simulation can be enhanced through application of advanced sampling techniques like Latin hypercube sampling, directional sampling, stratified sampling or importance sampling. The TPT method (see chapter 3) uses stratified sampling, whereas the proposed CRC-CH and CSS methods (also, see chapter 3) of the current study use importance sampling. Both sampling methods are explained in the subsequent sections.

8.3.2 Importance sampling in the CRC-CH and CSS methods

Application of importance sampling means an alternative sampling function, h_x , is used instead of the actual density function, f_x , to generate samples of \mathbf{x} . For this purpose, equation (26) is rewritten as follows:

$$\int_{\mathbf{x}} f_{\mathbf{x}}(\mathbf{x}) I_{[Q(\mathbf{x}) > q]} d\mathbf{x} = \int_{\mathbf{x}} h_{\mathbf{x}}(\mathbf{x}) \left\{ \frac{f_{\mathbf{x}}(\mathbf{x})}{h_{\mathbf{x}}(\mathbf{x})} I_{[Q(\mathbf{x}) > q]} \right\} d\mathbf{x} \quad (28)$$

Since samples are now taken from function h_x , equation (28) can be approximated by:

$$\hat{P}(Q > q) = \frac{1}{N} \sum_{i=1}^N I_{[q_i > q]} \frac{f_x(\mathbf{x}_i)}{h_x(\mathbf{x}_i)} \quad (29)$$

In which \mathbf{x}_i is the i^{th} sample of \mathbf{x} . Note that this is similar to the manner in which the integral of equation (26) is approximated by equation (27). Importance sampling function h_x needs to be chosen in such a way that the probability of sampling an event in which q is exceeded, is significantly higher than if function f_x is used as the sampling function. In this study, this is done by increasing the probabilities of sampling low AEP's of the rainfall depth and long duration events in step 1 of the procedure outlined in Figure 2-4. In the appendix of this report it is demonstrated that this results in a significant increase in computational efficiency and, simultaneously, a significant increase in the accuracy of probability estimates.

Equation (29) provides exceedance probabilities of discharge levels *per event*. In order to derive annual exceedance probabilities, the exceedance probability of equation (29) needs to be multiplied by the number of sampled events per year, λ :

$$\hat{P}(Q > q) = \frac{\lambda}{N} \sum_{i=1}^N I_{[q_i > q]} \frac{f_x(\mathbf{x}_i)}{h_x(\mathbf{x}_i)} \quad (30)$$

8.3.3 Stratified sampling in the TPT method

The TPT method (see eg ARR, 2013a) derives frequency curves of discharge levels separately for a set of potentially critical rainfall durations. The current section describes the computation of the frequency curve *for a single duration*.

The stratified sampling approach is applied to rainfall intensities. This means the range of potential realisations of the rainfall depth is divided into N_b bins (intervals). For each bin, the rainfall depth is set equal to a representative value within the bin, and subsequently the probability of exceedance of q , given this rainfall depth, is computed. The Total Probability Theorem (TPT) is used to combine the derived probabilities of all bins into a single exceedance probability.

$$P[Q > q] = \sum_i^{N_b} P[Q > q | R \in R_i] P[R \in R_i] \quad (31)$$

Where R is the rainfall depth, N_b is the number of intervals (bins) in which the rainfall depth is divided, and R_i is the range of rainfall depths of the i^{th} bin. The conditional probability of occurrence of interval R_i can be obtained directly from IFD curves. The conditional exceedance probability of q , given R_i is estimated through Monte Carlo simulation of the “remaining” random variables, such as initial losses and reservoir volumes, and subsequent URBS model simulations. This is done separately for each bin:

$$\hat{P}[Q > q | R \in R_i] = \frac{1}{N_i} \sum_j^{N_i} I_{[q_{ij} > q]} \quad (32)$$

In which N_i is the number of generated samples to estimate the exceedance probability for the i^{th} bin and q_{ij} is the peak discharge of the j^{th} simulated event for the i^{th} bin. Substitution of eq. (32) in eq. (31) gives:

$$\hat{P}[Q > q] = \sum_i^{N_b} P[R \in R_i] \sum_j^{N_i} \frac{1}{N_i} I_{[q_{ij} > q]} \quad (33)$$

8.3.4 Correction factors for post-processing

The stratified sampling approach of the TPT method and the proposed importance sampling approach for the CRC-CH and CSS methods can both be written in the following form:


$$\hat{P}[Q > q] = \sum_{k=1}^N c_k I_{[q_k > q]} \quad (34)$$

In this equation, N is the total number of samples (simulated events) and c_k is a “correction factor”, accounting for the fact that both methods deviate from the crude Monte Carlo Simulation approach. The value of c_k is as follows:

$$c_k = \frac{\lambda f_X(\mathbf{x}_k)}{N h_X(\mathbf{x}_k)} \quad ; \text{CRC-CH, CSS methods} \quad (35)$$

$$c_k = \frac{P[R \in R_i]}{N_i} \quad ; \text{TPT method}$$

Where λ is the number of sampled events per year ($\lambda=1$ in the TPT method by definition). Index i in the formula for the TPT method is an index for the bin to which simulation k belongs. This means I_{r_i} is the interval of rainfall intensities of the i^{th} bin and N_i refers to the total number of samples in bin i .




In the Monte Carlo framework, both methods are implemented. In the sampling procedure of step 1 of Figure 2-4, the value of c_k is computed for each sample, according to equation (35). In the post-processing (step 8 of Figure 2-4), the computed c_k – values are used according to equation (34) to compute exceedance probabilities of peak discharges and similar for peak water levels and flow volumes.

8.4 Additional post-processing for the TPT method

For the TPT-method, the probability that is computed with eq. (35) is a probability *given* a burst duration. The procedure is repeated several times for a number of potentially critical burst durations. The result of this procedure is a set of probabilities of exceedance of discharge q for each duration. The overall probability is then taken to be:

$$\hat{P}(Q > q) = \max_D \hat{P}(Q > q | D) \quad (36)$$



9 Implementation of the MCS framework in Delft-FEWS

9.1 Introduction

The Monte Carlo simulations framework was implemented within the Delft-FEWS framework. Delft-FEWS is a component-based modeling framework that incorporates a wide range of general data handling utilities and open interfaces to many hydrological and hydraulic models that are commonly used around the world, including the URBS hydrological model and RTC tools for reservoir modeling. Delft-FEWS can be used for data storage and retrieval tasks, simple forecasting systems and in highly complex operational forecasting systems. The advantage of using FEWS for all communication between components is that intermediate results (time series data) can be inspected for checking and debugging. Moreover, the modular setup of FEWS enables to replace components without much effort.

External models (hydrological, hydraulic or otherwise) are connected to Delft-FEWS via a General Adapter (GA). The GA handles the exchange of information between the central FEWS data storage and the external model. The exchange of information is done by input and output files, however reading and writing of various formats is done highly efficiently by FEWS.

The MCS framework consists of three stages:

- Pre-processing: generation of (storm) events (steps 1 to 4 of Figure 2-4)
- Processing: hydrological modelling (steps 5 to 7 of Figure 2-4)
- Post-processing: derivation and plotting of frequency curves (step 8 of Figure 2-4)

After each stage, the intermediate results can be inspected through standard Delft-FEWS visualisation and analysis tools. All three stages are controlled by Delft-FEWS: the input for the modules is prepared by FEWS, the processes are started by Delft-FEWS and the output is imported back into the FEWS data store. The steps are discussed in more detail in the following sections.

9.2 Pre-processing: generation of (storm) events

Rainfall events for flood risk assessment can be generated by several methods. Evaluation of these methods is part of the BRCFS project. Therefore, the sampling is done by a program that is written in a flexible and developer-friendly environment. The Python scripting language (www.python.org) was chosen, because it is reasonably fast, easy to read and free of cost or license.

For the BRCFS, the Monte Carlo sampling is done by a Python script called Treasury. Treasury is called by Delft-FEWS through a General Adapter (GA). The script takes as input the required number of samples, the IFD tables for the area of interest and several other parameters and probability distributions. Some parameters are correlated, which will be taken into account in the sampling. The

script produces a set of rainfall time series (pluviographs), which are stored as an ensemble in a NetCDF file. If importance sampling or stratified sampling is applied to increase sampling efficiency, each sample is accompanied by a correction factor, which is used in the post-processing phase where the formulas of Section 8 are applied to compute frequency curves. The sampled initial and continuing losses are subtracted from the pluviographs, in order to reduce the amount of information that is transferred via FEWS to URBS.

The NetCDF file that contains the rainfall time series and sampling correction factors is imported into Delft-FEWS and stored in the local data store. The data can be inspected using standard Delft-FEWS visualisation tools (graphs and tables). Figure 9-1 is a schematic drawing of the components of this first step of the method.

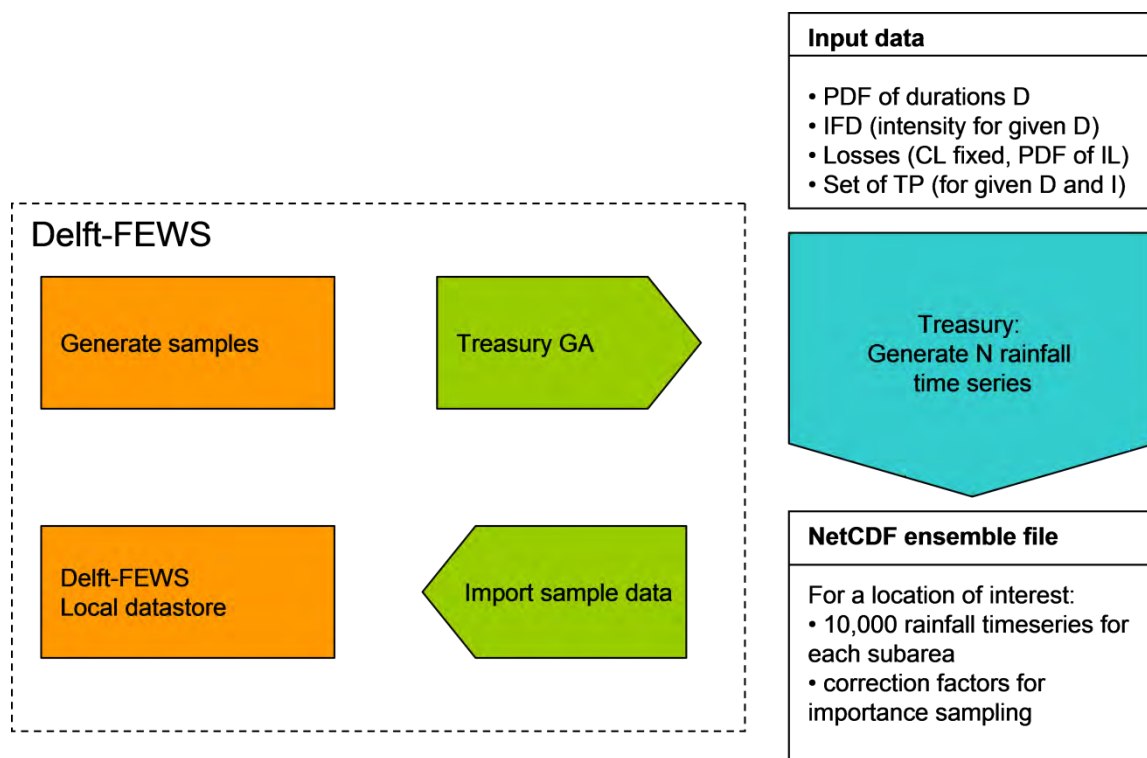


Figure 9-1 Schematic representation of the first step of the method

9.3 Processing: hydrological modelling and reservoir modelling

The next step is the rainfall runoff, routing and reservoir modelling by URBS and RTC models. Four of the six reservoirs as described in Section 6.4 are incorporated in the part of the URBS hydrological model. Wivenhoe and Somerset are both modelled separately in RTC Tools. For the full Brisbane River catchment including Wivenhoe and Somerset dams, a total of seven URBS sub-catchment models and two RTC reservoir models (note: only relevant for the “with dams” simulations) are connected. The output of the upstream models serves as input for the downstream reservoir or sub-catchment model. The models should therefore be run in a specific order. This is taken care of by the FEWS workflows. Before a sub-catchment run is started, the input rainfall time series and discharges from upstream sub-catchments are exported from the Delft-FEWS database and put in a temporary working directory. The output discharge time series from a sub-catchment run is imported back into the FEWS database, from where it can be used as input for the next run if needed. The intermediate

results from each sub-catchment can be inspected using standard FEWS visualisation tools (database viewer and workflow navigator). If necessary, a FEWS display filter can be developed, which is more convenient for frequent inspections. Figure 9-2 is a schematic drawing of the components of this second step of the method. For clarity, only one URBS and one RTC model are shown. In reality, the full Brisbane River catchment consists of a chain of seven URBS and two RTC models.

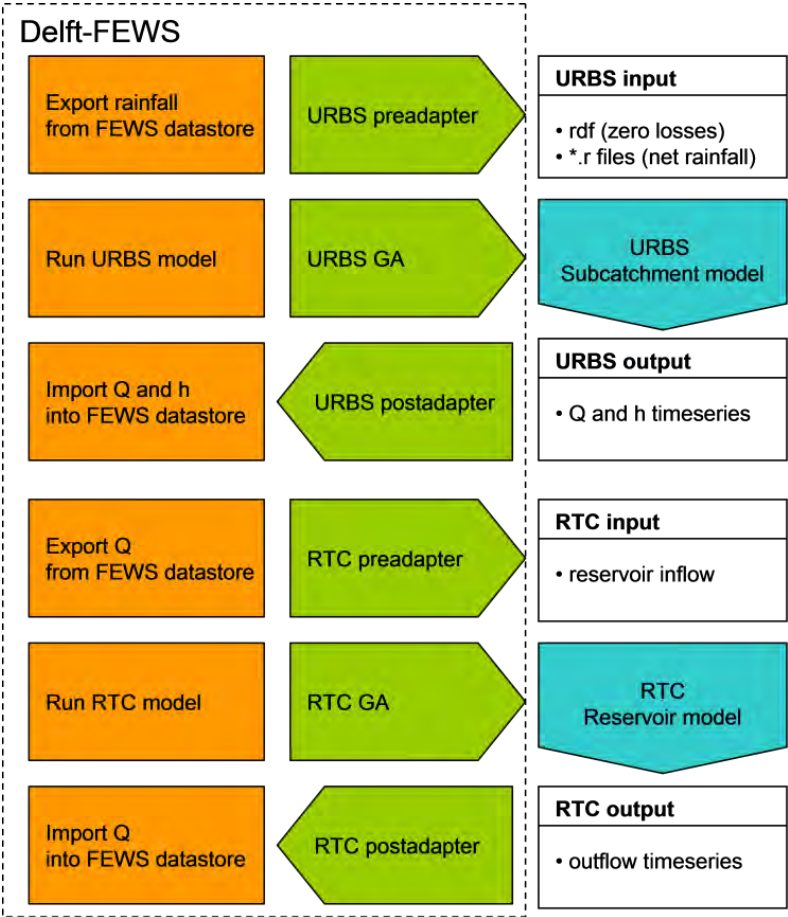


Figure 9-2 Schematic representation of the second step of the method

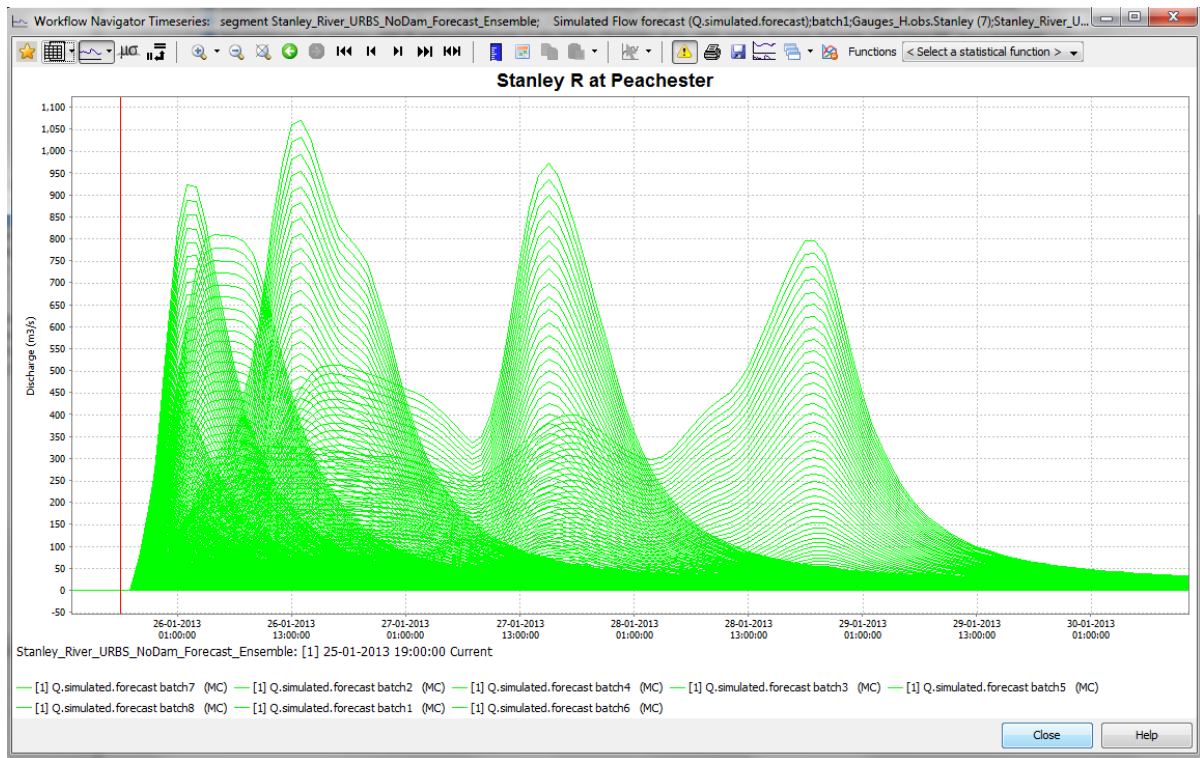


Figure 9-3 Screenshot of hydrographs generated by the FEWS-MCS framework

9.4 Post processing: derivation and plotting of frequency curves

The final step of the probabilistic method is the construction of the frequency curves, where the peak discharges and water levels of the sample runs are plotted against their estimated AEP or ARI. To do so, the maximum Q, V or h per sample are computed and stored in a list. Taking the maximum from a time series is done by a standard FEWS Transformation. Subsequently, the AEP is estimated from the rank of the maximum, the total number of samples and the correction factor for using advanced sampling schemes. This is done by an external Python script. The script also generates a graph in which peak discharges (or flow volumes) are plotted against the AEP on a half-log scale. An example is shown in Figure 9-4.

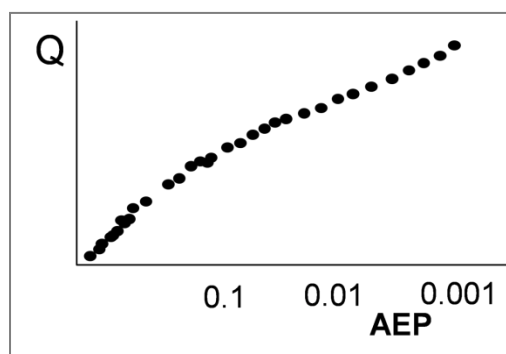


Figure 9-4 Example of a frequency curve

The graph can be shown on the screen by a pop-up PNG display and the underlying data are stored in a CSV file. This file can be imported back into the FEWS data store, so that the original MC samples and the end result are archived together. The PNG plot cannot be stored in the FEWS database, but the graph can easily be re-generated at any time from the generated data in the data store.

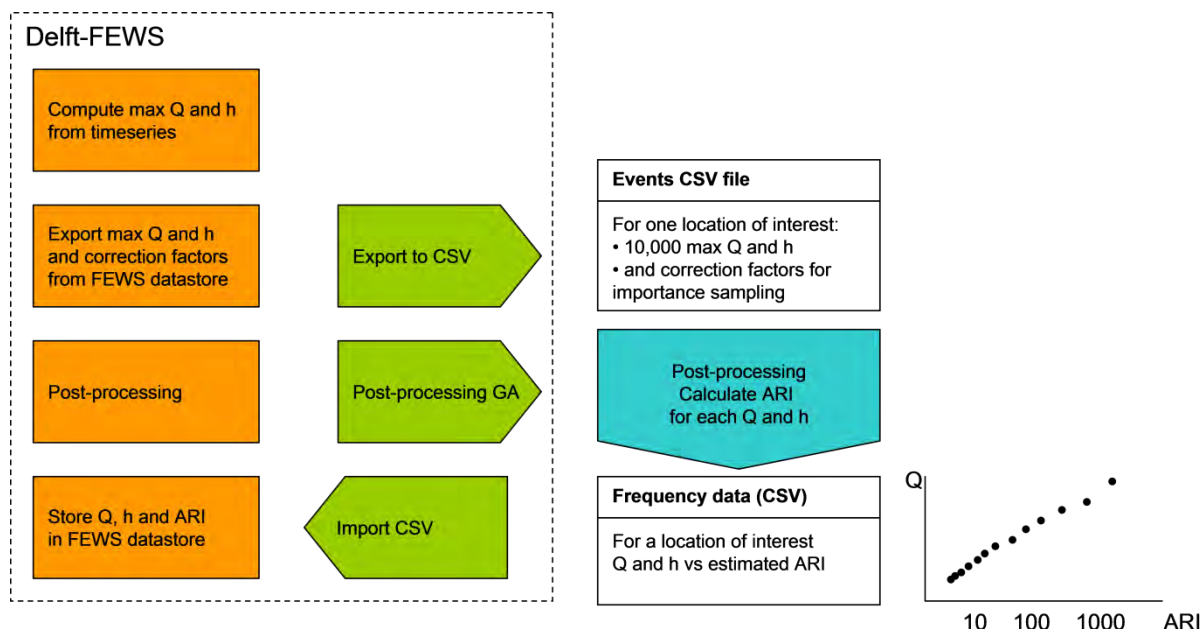


Figure 9-5 Schematic representation of the third step of the method

Subsequently, design flows and design water levels will be derived from the frequency curves. This is dealt with in the same post-processing Python script.

For each location of interest the process for estimating the frequency curve for the peak flow and flood volumes is as follows:

- Conduct simulations for 8 standard durations (12 hours to 120 hours)
- For each rainfall duration, 60 AEPs are considered (ranging from 1 in 2 AEP to the AEP of the PMP) and 21 simulations are performed per AEP
- In other words, this equates to 1260 MCS events per duration, or 10,080 events in total per location
- For each rainfall duration, two output files are created:
 - A CSV-File containing all realisations of the random variables (rainfall depth, reservoir volume, initial loss, peak ocean water level) and the main URBS model output (peak flow, flood volume for different durations)
 - The second file is a netcdf file that contains the hydrographs which are 240 hours in length Both the CSV-file and the NETCDF-file have 1260 rows of data, with one row per event. Since a python script is used and python starts indexing at zero, the ID of the events are the numbers ranging from 0, to 1259



9.5 Computational performance

A Monte Carlo simulation run for the entire Brisbane river catchment with 10,000 samples takes approximately 5-6 hours on 64 bit machine, Windows 7, Solid State Drive (SSD) with 16Gb and 4 cores (duplicated, so actually 8 cores). For 23 output locations this means approximately five days of simulation time is required. Note that upstream locations have smaller catchment areas and will require less computation time.

9.6 Overall assessment

The modular design, based on the Delft-FEWS framework, described in this section allows for flexibility and options for checking of intermediate results and debugging, which is a great advantage for the BRCFS project and subsequent project for which a similar MCS framework is required. Variations in the methodology can be evaluated by replacing a single module, without having to change the overall setup. Although computationally less efficient, these advantages give the modular Delft-FEWS approach the edge over a fully dedicated implementation.




10 Conclusions

10.1 Proposed framework

This report describes the proposed Monte Carlo Simulation (MCS) framework for the comprehensive hydrologic assessment of the Brisbane River Catchment Study. The framework quantifies statistics, correlations and physical interactions of the most relevant flood forcing factors in the Brisbane river catchment: rainfall depth, event duration, spatial-temporal distribution of rainfall, antecedent soil moisture conditions (initial losses), reservoir volumes and ocean water levels. The MCS framework generates a long series of realistic synthetic events for rainfall, ocean water level, initial reservoir levels and antecedent moisture condition. The events are then simulated with the URBS hydrological model in combination with the RTC model for dam operations. Computed peak discharges and flow volumes at the (23) locations of interest are derived from the URBS model output. Frequency curves are subsequently derived with a statistical post-processing procedure. The Monte Carlo simulation framework has been implemented in the Delft-FEWS system

The following conclusions are drawn:

- The proposed computation scheme of Figure 2-4 provides what is required for the BRCFS-hydrology phase: a joint probability approach for the derivation of design flows and volumes, taking into account spatial and temporal variation of rainfall over the Brisbane River catchment
- The method has the advantage over more “traditional” approaches in flood risk analysis in that it explicitly considers all relevant physical processes that contribute to flood events. A practical disadvantage is that it is generally more complex to implement
- The following statistical dependencies (correlations) between random variables were identified as relevant and have been incorporated in the Monte Carlo simulations:
 - Spatial and temporal correlation of rainfall. This dependence is taken into account in the BoM synthetic rainfall patterns, which are incorporated in the Monte Carlo Framework
 - Mutual correlations between antecedent moisture conditions (initial losses) of the various sub-catchments. These correlations are taken into account in the Monte Carlo simulations using a Gaussian copula model
 - Correlation between rainfall and ocean water levels. This is modelled with a threshold-excess logistic model
 - Correlation between rainfall and reservoir volumes. Reservoir volumes at the beginning of high rainfall events are on average significantly higher than reservoir volumes at any given day. For this reason, marginal distribution functions of reservoir volumes are based on observed reservoir volumes at the beginning of high rainfall events. The ‘remaining’ correlation is weak, ie the correlation between the total rainfall depth of a high rainfall event and the reservoir volume at the beginning of such an event. The latter is therefore not included in the MCS framework




– Mutual correlations of reservoir volumes at the beginning of a high rainfall event. These are simulated with the skewed student-t copula model

- For the rainfall sampling scheme, three methods were tested: TPT, CRC-CH and CSS. Eventually, the TPT method was chosen as the preferred method *for the current study*, because this method provided the best match between the rainfall IFD curves on one hand and the available synthetic spatio-temporal rainfall patterns on the other hand. The other two methods (CSS and CRC-CH) are nevertheless considered very promising for future applications of Monte Carlo applications, especially if more synthetic spatio-temporal rainfall patterns become available
- Computation times for a single output location near the catchment outlet are in the order of five hours on a 64 bit machine, Windows 7, Solid State Drive (SSD) with 16Gb and 4 cores (duplicated, so actually 8 cores). For upstream locations with smaller catchment areas the runtime is in the order of two to three hours



11 References

- ARR, 1987, 1998: Australian Rainfall and Runoff – A guide to flood estimation. Institution of Engineers Australia
- ARR, 1998: Australian Rainfall and Runoff – A guide to flood estimation, revised edition 1998, Institution of Engineers Australia
- ARR, 2013a: Australian Rainfall and Runoff – Monte Carlo simulation techniques, Australian rainfall and runoff discussion paper, May 2013
- ARR, 2013b: Australian Rainfall and Runoff – Loss models for catchment simulation – rural catchments, stage 2 report, March 2013
- ARR, 2013c: Australian Rainfall and Runoff – Spatial patterns of design rainfall. Project 2, April 2013
- Aurecon, 2013a: Moogerah Dam AFC Safety Design Hydrology Report, February 2013, Reference:230008
- Aurecon, 2013b: Sunshine Coast Storm Tide Study, December 2013
- Aurecon, 2014a: Brisbane River catchment flood study: design event methodology, Aurecon, October 2014
- Aurecon, 2014b: Brisbane River catchment flood study: hydrologic model calibration report, Aurecon, October 2014
- Azzalini, A. and Capitanio, A. (2003) Distributions generated by perturbation of symmetry with emphasis on a multivariate skew t-distribution, Journal of the Royal Statistical Society Series B, 65(2), 367–389
- BoM, 2003: Guidebook to the Estimation of Probable Maximum Precipitation: GENERALISED TROPICAL STORM METHOD, Bureau of Meteorology, November 2003
- Carroll, D and Rahman, A. (2004). Investigation of subtropical rainfall characteristics for use in the Joint Probability Approach to design flood estimation. In Proc. Second Asia Pacific Association of Hydrology and Water Resources (APHW) Conference, Singapore, 5-8 July 2004. 2, 27-34
- Carroll, D. (2008), Enhanced rainfall event generation for Monte Carlo Simulation technique of design flood estimation. Proc. Of Water Down Under 2008
- Carroll D.G., 2012a, URBS (Unified River Basin Simulator) V 5.00 Dec 2012
- Carroll D.G. 2012b URBS Monte Carlo Modelling Training Notes
- Chow, V.T., D.R. Maidment and L.W. Mays (1988), Applied Hydrology, Tata McGraw-Hill Education, 1988
- Deltares & Aurecon, 2014: Brisbane River catchment flood study: Dam Operations Module Implementation Report, October 2014



Diermanse, F.L.M. and Geerse, C.P.M., 2012: Correlation models in flood risk analysis, Reliability Engineering and System Safety (RESS), pp 64-72

DSDIP, 2013: INVITATION TO OFFER NO. DSDIP-2077-13; For the provision of a comprehensive hydrologic assessment as part of the Brisbane River Catchment Flood Study. State of Queensland; Department of State Development, Infrastructure and Planning, May 2013

Engelund S. and Rackwitz, R. (1993), A benchmark study on importance sampling techniques in structural reliability, Structural Safety, 12 (1993) 255-276

Fang, H., Fang, K. and Kotz, S. (2002), The Meta-elliptical Distributions with Given Marginals, Journal of Multivariate Analysis 82, 1–16

Genest, C. and Favre, A., 2007: Everything You Always Wanted to Know about Copula Modelling but Were Afraid to Ask Journal of hydraulic engineering, 2007/347

GHD, 2014: Brisbane City Council - City Design Coastal Plan Implementation Study Draft Report September 2014

Green, J.H., Johnson, F.M., Xuereb, K., The, C. and Moore, G. (2012). Revised Intensity-Frequency-Duration (IFD) Design Rainfall Estimates for Australia – An Overview. Engineers Australia Hydrology and Water Resources Symposium. Sydney

Hoang, T.M.T. Joint Probability Approach to design flood estimation. Unpublished PhD thesis, Department of Civil Engineering, Monash University

Hosking, J.R.M. and Wallis, J.R., (1997). Regional Frequency Analysis: An Approach Based on L-Moments. Cambridge University Press, Cambridge, UK.224 pp

Ilahee, M., Rahman, A. and Boughton, W. C., 2001: Probability-distributed initial losses for flood estimation in Queensland, Proceedings of the International Congress on Modelling and Simulation

Jacobs, 2014: Additional Stochastic Space-Time Rainfall Replicates for Brisbane River Catchment, June 2014

Johnson, F., Xuereb, K., Jeremiah, E., and Green, J. (2012a). Regionalisation of Rainfall Statistics for the IFD Revision Project. Presented at Hydrology and Water Resources Symposium, Sydney, NSW, November 2012

Kaiser, H.F. and Dickman, K. (1962), Sample and population score matrices and sample correlation matrices from an arbitrary population correlation matrix, Psychometrika 27 (2), 179

Koopman, S. J., Shephard, N. and Creal, D. (2009), Testing the assumptions behind importance sampling, Journal of Econometrics 149 (2009) 2_11

Laurenson, E. M., & Kuczera, G. A. (1999).Annual exceedance probability of probable maximum precipitation. Australian Journal of Water Resources, 3(2), 167-176


Mirfenderesk, H, D. Carrolll E. Chong, M. Rahman1, M Kabir, R. Van Doorn, S. Vis, 2013: Comparison between Design Event and Joint Probability Hydrological Modelling

Rahman A, Weinmann E, Hoang T, Laurenson E & Nathan R (2001) Monte Carlo Simulation of Flood Frequency Curves from Rainfall, Technical Report 4, CRC-CH

Rahman A., Weinmann, P.E., Hoang T.M.T. and Laurenson E.M. (2002) Monte Carlo Simulation of Flood Frequency Curves from Rainfall. Journal of Hydrology 256,196-210

Sahu, S. K., Dey, D. K. and Branco, M. D. (2003) A New Class of Multivariate Skew Distributions with Applications to Bayesian Regression Models, The Canadian Journal of Statistics, 31(2), 129–150

Seqwater, 2013a:Brisbane River Flood Hydrology Models, draft report, August 2013



Seqwater, 2013b, Manual of Operation Procedures for Flood Mitigation at Wivenhoe Dam and Somerset Dam, Revision 11, November 2013

SKM, 2013: Brisbane River Catchment Dams and Operational alternatives study, October 2013

Hinze dam alliance, 2012: Hinze dam stage 3 update, appendix 4A, Flood hydrology report, February 2012
Smith, M. S., Gan, Q. and Kohn, R. J. (2012) Modelling dependence using skew t copulas: Bayesian inference and applications, *Journal of Applied Econometrics*, 27(3), 500–522

Tawn, J. A. (1988). Bivariate Extreme Value Theory: Models and Estimation, *Biometrika*, 75(3), 397-415

The, C. Johnson, F., Hutchinson, M. and Green, J. (2012). Gridding of Design Rainfall Parameters for the IFD Revision Project for Australia. *Engineers Australia HWRS*, pp 1425-1432

Van den Honert, R. and McAneney, J., 2011: The 2011 Brisbane Floods: Causes, Impacts and Implications, *Water* 2011, 3, 1149-1173, ISSN 2073-4441

Westra, S., 2011: Investigation into the joint dependence between extreme rainfall and storm surge in the coastal zone” Proc. Of 34th IAHR World Congress – Balance and Uncertainty, p543

WMAWater, 2014: Brisbane River Spatial Rainfall, WMAWater memorandum, Peter Stensmyr, Mark Babister, March 2014

Zheng, F., Westra, S., Sisson, S., and Leonard, M., 2013a: Flood risk estimation in Australia’s coastal zone: modelling the dependence between extreme rainfall and storm surge, draft paper for the Hydrology and Water Resources Symposium in Perth

Zheng, F., S. Westra, and S. A. Sisson, 2013b, Quantifying the dependence between extreme rainfall and storm surge in the coastal zone, *Journal of Hydrology*, 505, 172-187

12 Glossary

12.1 Hydrologic terms

AEP: Annual Exceedance Probability – is a measure of the likelihood (expressed as a probability) of a flood event reaching or exceeding a particular magnitude in any one year. A 1% (AEP) flood has a 1% (or 1 in 100) chance of occurring or being exceeded at a location in any year

AHD: Australian Height Datum (m), the standard reference level in Australia

AR&R: Australian Rainfall and Runoff (AR&R) is a national guideline document for the estimation of design flood characteristics in Australia. It is published by Engineers Australia. The current 2003 edition is now being revised. The revision process includes 21 research projects, which have been designed to fill knowledge gaps that have arisen since the 1987 edition

CHA: Comprehensive Hydrologic Assessment

CL: Continuing Loss (mm/hour). The amount of rainfall during the later stages of the event that infiltrates into the soil and is not converted to surface runoff in the hydrologic model

CRC-CH: Cooperative Research Centre – Catchment Hydrology. In this report, CRCH-CH usually refers to a Monte Carlo sampling method that was developed by the CRC-CH

CSS: Complete Storm Simulation. This is one of the proposed Monte Carlo sampling methods

Cumulative probability: The probability of an event occurring over a period of time, any time in that period. This probability increases over time

DEA: Design Event Approach. A semi-probabilistic approach to establish flood levels, which only accounts for the variability of the rainfall intensity

Design flood event: Hypothetical flood events based on a design rainfall event of a given probability of occurrence (ie AEP). The probability of occurrence for a design flood event is assumed to be the same as the probability of rainfall event upon which it is based (EA, 2003)

DMT: Disaster Management Tool. Work completed by BCC in 2014 for Queensland Government as part of the development of an interim disaster management tool until the completion of the BRCFS

DTM: Digital Terrain Model

EL (m AHD): Elevation (in metres) above the Australian Height Datum

FFA: Flood Frequency Analysis – a direct statistical assessment of flood characteristics

Flood mitigation manual (Flood Manual): A flood mitigation manual approved under section 371E(1)(a) or 372(3) of the Water Supply (Safety and Reliability) Act 2008 (QLD)

FOSM: Flood Operations Simulation Model (refer Seqwater 2014)

Floodplain: Area of land adjacent to a creek, river, estuary, lake, dam or artificial channel, which is subject to inundation by the PMF (CSIRO, 2000)

FSL: Full Supply Level – maximum normal water supply storage level of a reservoir behind a dam

FSV: Full Supply Volume – volume of the reservoir at FSL

GEV: Generalised Extreme Value statistical distribution

GIS: Geographic Information System

GL: Gigalitres This is a unit of volume used in reservoir studies. A Gigalitre = 1,000,000,000 litres or equivalently 1,000,000 m³

GSDM: Generalised Short Duration Method of extreme precipitation estimation for storms of less than 6 hour duration and catchments of less than 1,000 km². Refer BoM, 2003

GTSMR: Revised Generalised Tropical Storm Method of extreme precipitation estimation for storms of tropical origin. Applicable to storm durations of up to 168 hours and catchments up to 150,000km². Refer BoM, 2003

IFD-curves: Intensity-Frequency-Duration curves, describing the point- or area-rainfall statistics. In the current report rainfall depth is generally used as an alternative to rainfall intensity. Rainfall depth is the product of duration and intensity. It was decided to maintain the term “IFD” as this is the terminology that the reader is most likely to be familiar with

IL: Initial Loss (mm). The amount of rainfall that is intercepted by vegetation or absorbed by the ground and is therefore not converted to runoff during the initial stages of the rainfall event

LOC: Loss of Communications dam operating procedure, refer Flood Manual (Seqwater 2013)

LPIII: Log-Pearson Type III statistical distribution

IQQM: Integrated Quantity and Quality Model for water resources planning

JPA: Joint Probability Approach. A general term for probabilistic methods to establish design flood levels

MCS: Monte Carlo Simulation

MHWS: Mean High Water Spring Tide level

ML: Megalitre. This is a unit of volume used in reservoir studies. A megalitre is equal to 1,000,000 litres or, equivalently, 1,000 m³

m³/s: Cubic metre per second – unit of measurement for instantaneous flow or discharge


PMF: Probable Maximum Flood – the largest flood that could conceivably occur at a particular location, resulting from the PMP (CSIRO, 2000) and Australia Rainfall and Runoff, 2003 (EA, 2003)

PMP: Probable Maximum Precipitation – the greatest depth of precipitation for a given duration meteorologically possible over a given size storm area at a particular location at a particular time of year, with no allowance made for long-term climatic trends (CSIRO, 2000; EA 2003)

PMP DF: Probable Maximum Precipitation Design Flood – the flood event that results from the PMP event

Quantiles: Values taken at regular intervals from the inverse of the cumulative distribution function (CDF) of a random variable.

Stochastic flood event: Statistically generated synthetic flood event. Stochastic flood events include variability in flood input parameters (eg temporal and spatial rainfall patterns) compared to design



flood events. Stochastic flood events by their method of generation exhibit a greater degree of variability and randomness compared to design flood events (See also Design flood event)

Synthetic flood event: See Stochastic flood event

TPT: Total Probability Theorem. This is one of the fundamental theorems in statistics. In this report, TPT refers to a Monte Carlo sampling method that is based on stratified sampling and, hence, makes use of the total probability theorem

URBS: Unified River Basin Simulator. A rainfall runoff routing hydrologic model (Carroll, 2012)

12.2 Study related terms

BCC: Brisbane City Council

BoM: Australian Bureau of Meteorology

BRCFS: Brisbane River Catchment Flood Study

BRCFM: Brisbane River Catchment Floodplain Management Study

BRCFMP: Brisbane River Catchment Floodplain Management Plan

Delft-FEWS: Flood Early Warning Systems, a software package developed by Deltares, initially for the purpose of real-time flood forecasting. Delft-FEWS is used all over the world, including by the Environment Agency (UK) and the National Weather Service (US). Currently, it is also being implemented by Deltares and BoM for flood forecasting in Australia. The Monte Carlo framework for the BRCFS-Hydrology Phase will be implemented in Delft-FEWS

DEWS: Department of Energy and Water Supply

DIG: Dams Implementation Group

DNRM: Department of Natural Resources and Mines

DSITIA: Department of Science Information Technology, Innovation and the Arts

DSDIP: Department of State Development and Infrastructure Planning

EA: Engineers Australia formally known as The Institute of Engineers, Australia

GA: General Adapter, an interface between the Delft-FEWS environment and an external module

IC: Implementation Committee of the BRCFS

ICC: Ipswich City Council

IPE: Independent panel of experts to the BRCFS

LVRC: Lockyer Valley Regional Council

ND: No-dams condition. This scenario represents the catchment condition without the influence of the dams and reservoirs. The reservoir reaches have effectively been returned to their natural condition

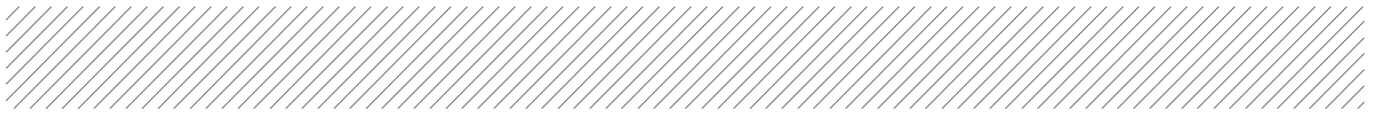
NPDOS: North Pine Dam Optimisation Study conducted in response to the QFCOI Final Report

PIG: Planning Implementation Group

QFCOI: Queensland Floods Commission of Inquiry

RTC: Real-Time Control. A software package for simulations of reservoir operation. RTC tools is used for the simulation of Wivenhoe and Somerset reservoirs

SC: Steering Committee of the BRCFS



SRC: Somerset Regional Council

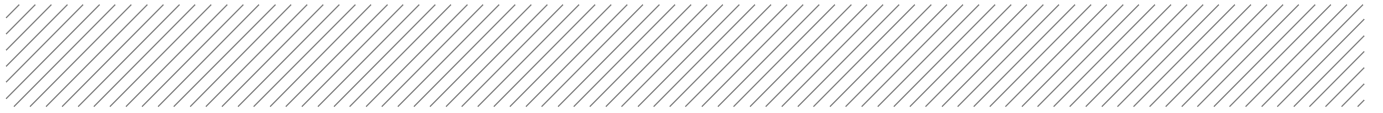
TWG: Technical Working Group

WD: With-dams condition. This scenario represents the catchment condition with the influence of the dams and reservoirs represented in their current (2013) configuration

WSDOS: Wivenhoe and Somerset Dam Optimisation Study conducted in response to the QFCOI Final report

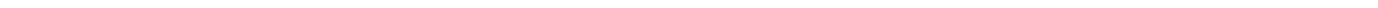
Appendices





Appendix A

'No-dams' design peak discharges



A.1 Table

This appendix contains a table with peak discharges for a range of AEP values for all locations. Note: the 1 in 100,000 AEP peak discharge is only provided for locations for which the AEP of the PMP is below 1 in 100,000.

Table A1 Peak discharges (m³/s) versus AEP; MCS results

Location	AEP (1 in N)												
	2	5	10	20	50	100	200	500	1,000	2,000	10,000	100,000	AEP of PMP
Linville	160	670	1300	1900	2900	3700	4200	4800	5400	6000	7900	13,700	21,400
Gregors Creek	270	1200	2300	3500	5300	6500	7400	8800	9700	10,800	14,500	26,300	36,300
Fulham Vale	280	1200	2300	3400	5100	6400	7400	8800	9700	11,100	14,700	26,600	34,500
Peachester	97	200	280	370	480	610	690	800	900	1000	1300	1800	2400
Woodford	230	470	700	920	1200	1500	1700	2000	2200	2500	3200	4300	6000
Somerset Dam	730	1,500	2200	2800	3900	4600	5200	6100	6700	7400	9500	13,400	18,300
Tinton	37	210	390	590	840	1100	1200	1400	1600	1800	2400	3400	6000
Middle Creek	1100	2700	4200	6200	9000	11,500	12,900	15,000	16,900	18,900	24,400	47,400	57,100
Wivenhoe	980	2700	4300	6300	8900	11,200	12,800	15,100	16,800	19,000	25,000	49,200	54,800
Helidon	28	160	320	500	740	960	1100	1300	1500	1700	2200	3400	6700
Gatton	110	550	1000	1600	2300	3100	3700	4400	5000	5600	7900	13,600	24,000
Glenore Grove	160	750	1400	2000	3200	4000	4900	5800	6500	7400	10,400	18,300	27,700
Savages Crossing	1200	3100	5300	7900	11,200	14,300	16,600	19,100	21,500	23,900	32,600		63,800
Mount Crosby	1200	3000	5200	7900	10,800	13,800	16,100	18,800	21,300	23,400	32,400		62,600
Walloon	170	420	670	890	1300	1600	1900	2200	2500	2800	3700	5200	8400
Kalbar Weir	160	370	540	770	1100	1300	1500	1800	1900	2200	2800	4100	6800
Amberley	230	450	630	970	1400	1800	2100	2500	2700	3100	4200	6100	9700
Loamside	60	140	220	310	430	520	610	720	810	920	1100	1600	2800



Location	AEP (1 in N)												
	2	5	10	20	50	100	200	500	1,000	2,000	10,000	100,000	AEP of PMP
Ipswich	510	1000	1500	2100	2900	3700	4300	5000	5600	6400	8400	12,600	18,100
Moggill	1700	3800	5900	8500	11,700	14,600	17,000	19,900	23,000	25,900	35,800		64,400
Centenary Bridge	1700	3700	5800	8200	11,100	13,900	16,000	18,800	22,000	24,700	34,100		63,900
Brisbane	1700	3800	5700	8200	11,100	13,600	15,500	18,600	21,300	24,200	32,600		61,100





A.2 Figures of frequency curves

This section contains figures with frequency curves for the 22 locations of interest. Each Figure contains the following graphs:

- Empirical frequency estimates from rated flows (if available)
- MCS results

For each location, 2 figures are provided:

1. Results for the AEP range 1 in 2 – AEP of PMP
2. Results for the AEP range 1 in 2 – 1 in 100

This means the first plot displays results for all AEP-values of interest, whereas the second plot zooms in on the results for the higher range of AEP-values.



Figure A.2.1a | Location Linville; no dams conditions

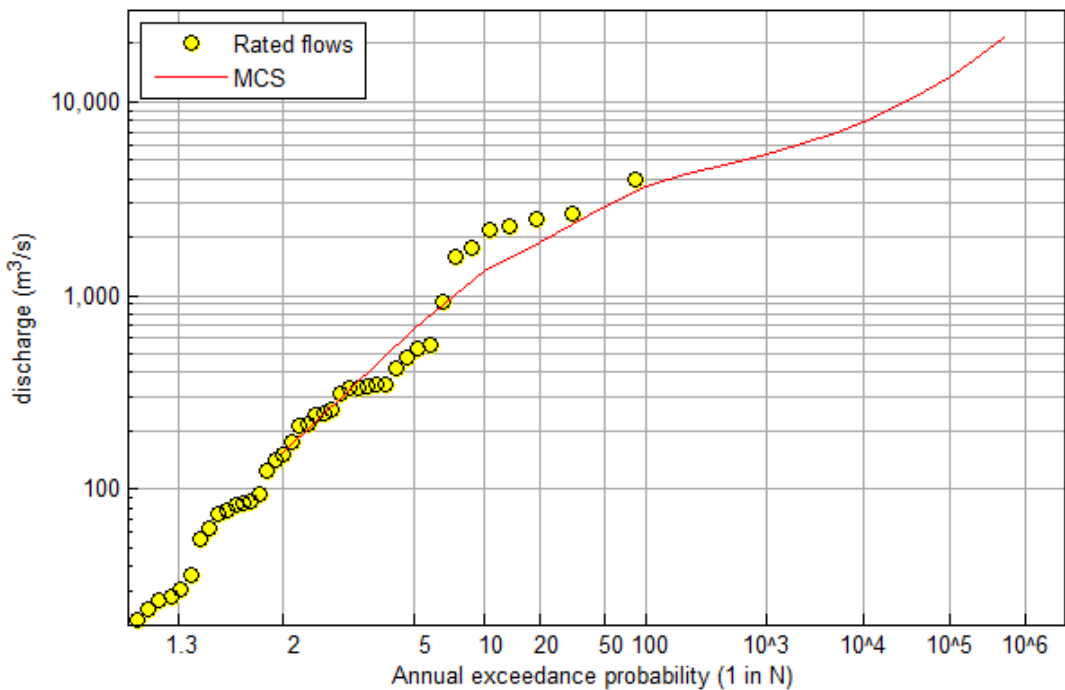


Figure A.2.1b | Location Linville; no dams conditions

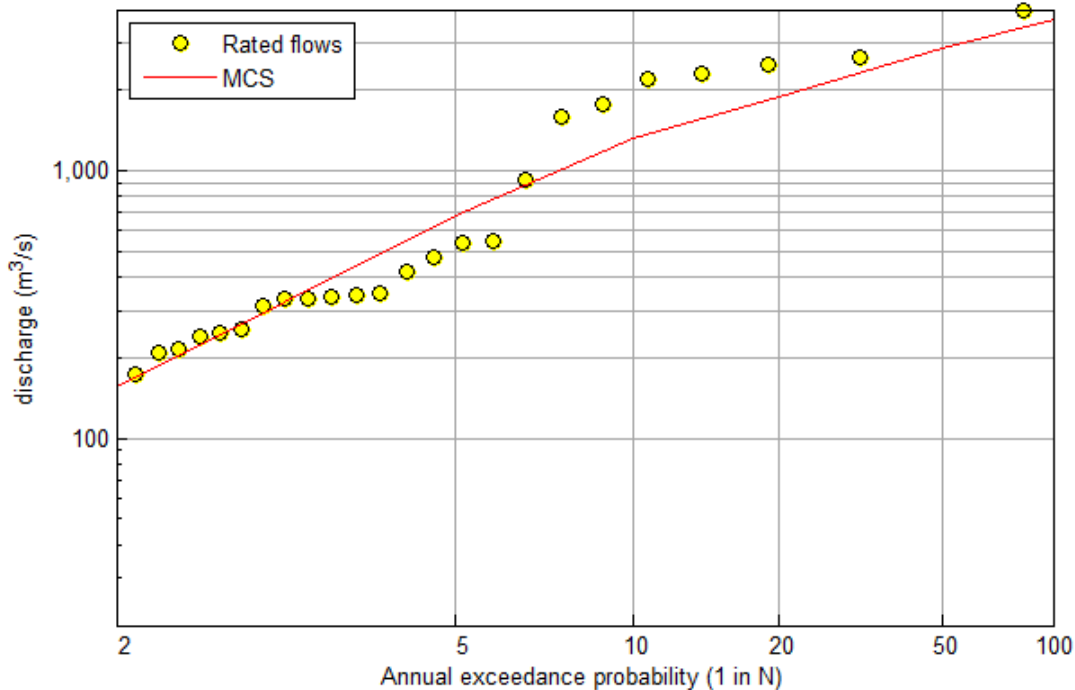




Figure A.2.2a | Location Gregors Creek; no dams conditions

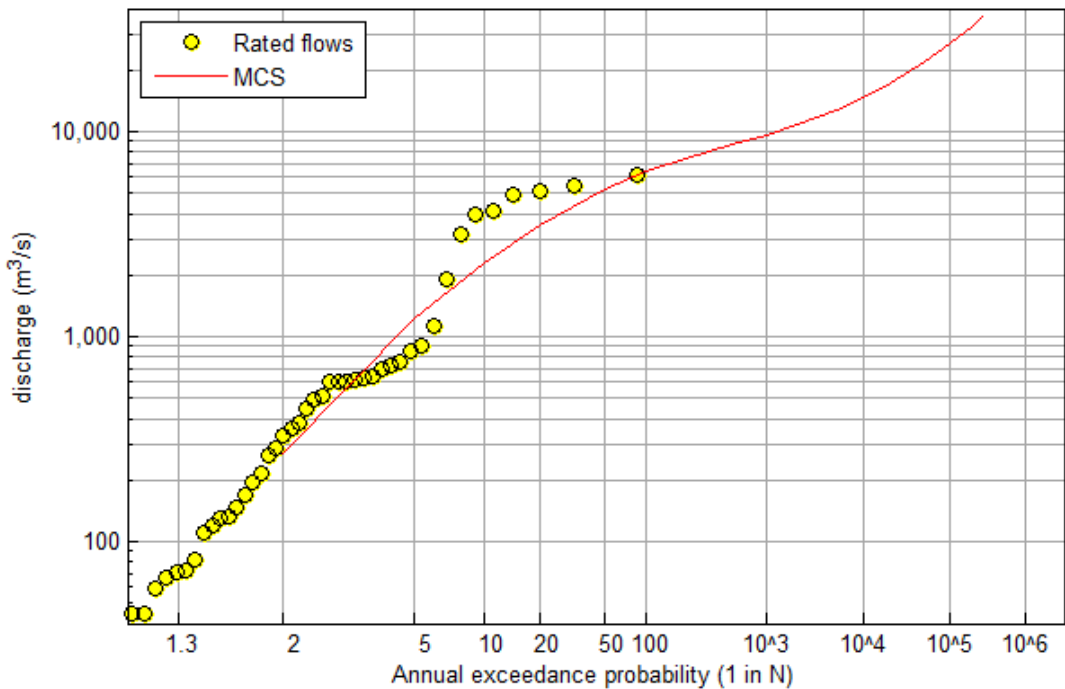


Figure A.2.2b | Location Gregors Creek; no dams conditions

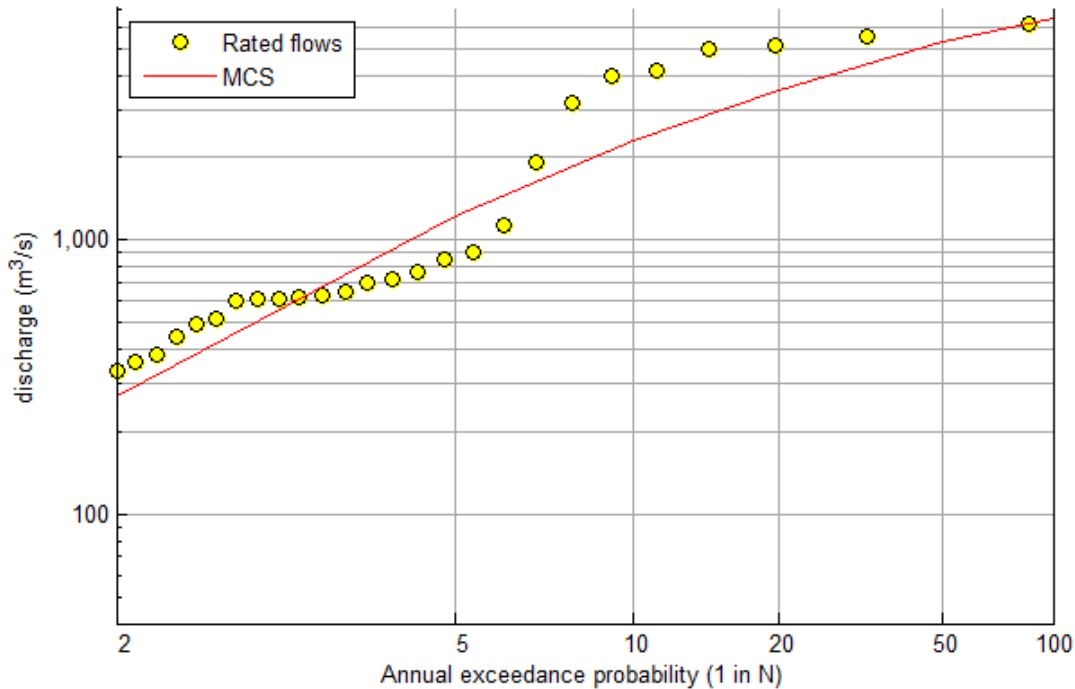




Figure A.2.3a | Location Fulham Vale; no dams conditions

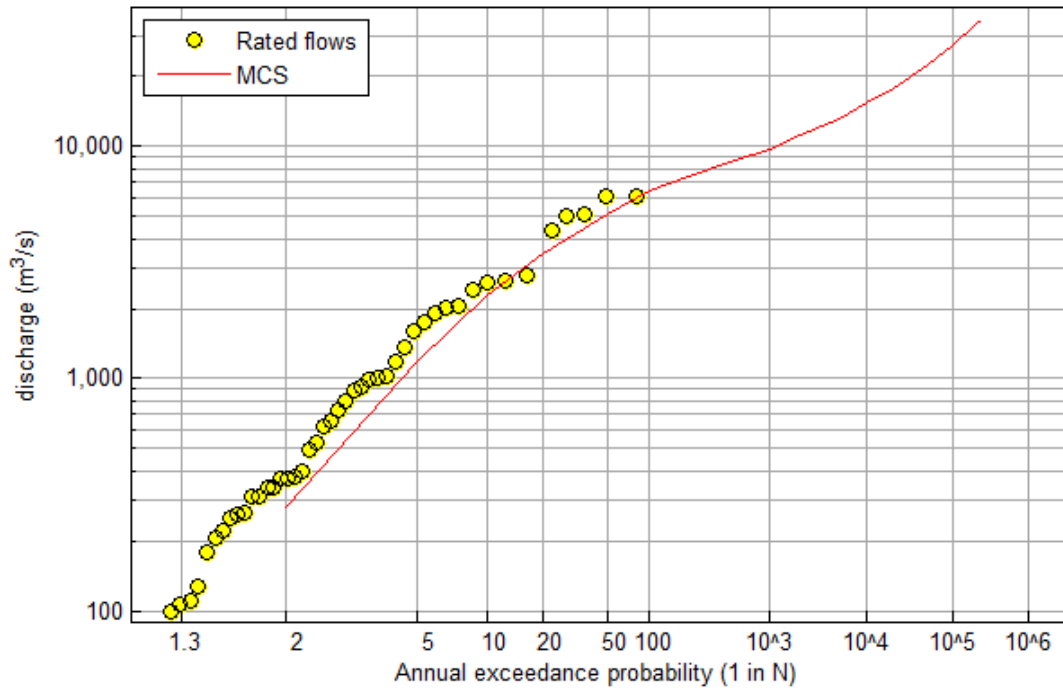


Figure A.2.3b | Location Fulham Vale; no dams conditions

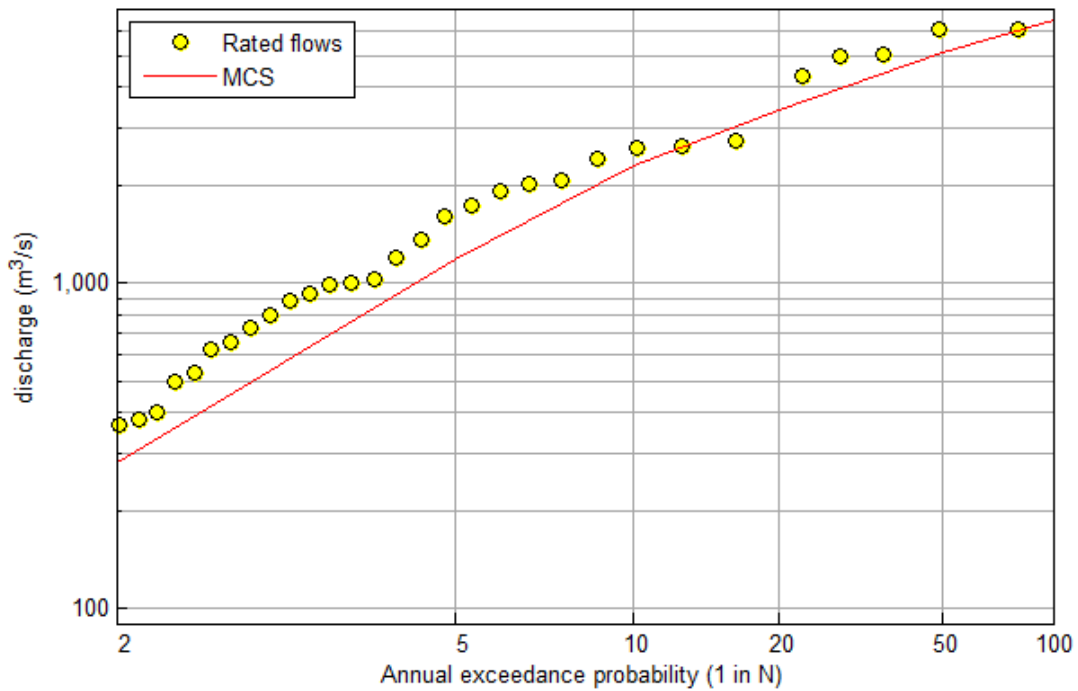




Figure A.2.4a | Location Peachester; no dams conditions

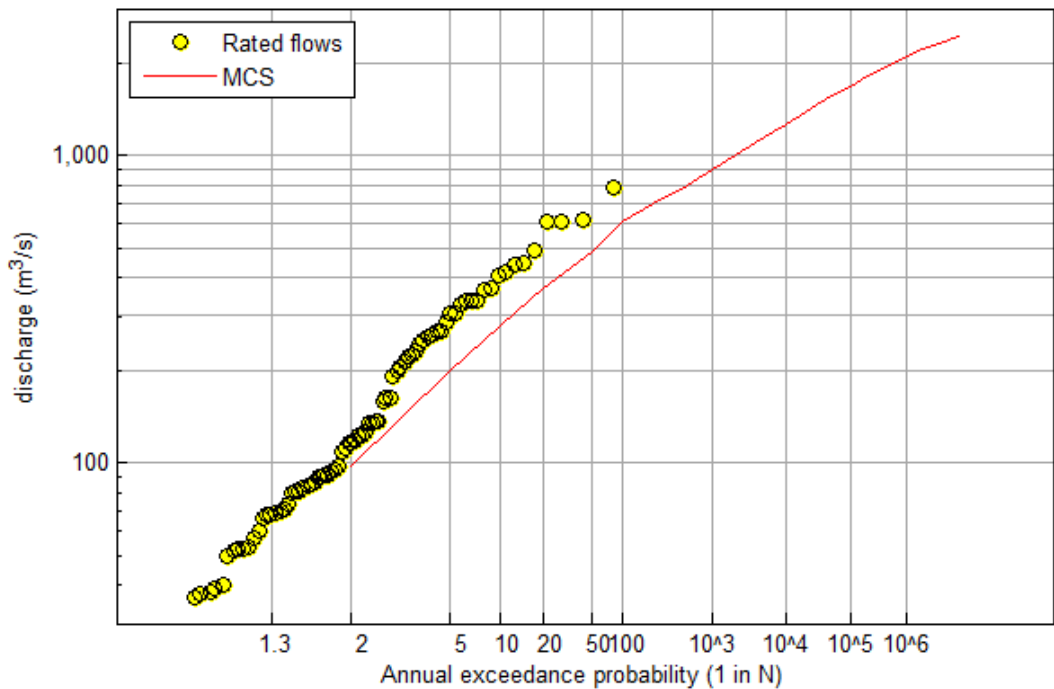


Figure A.2.4b | Location Peachester; no dams conditions

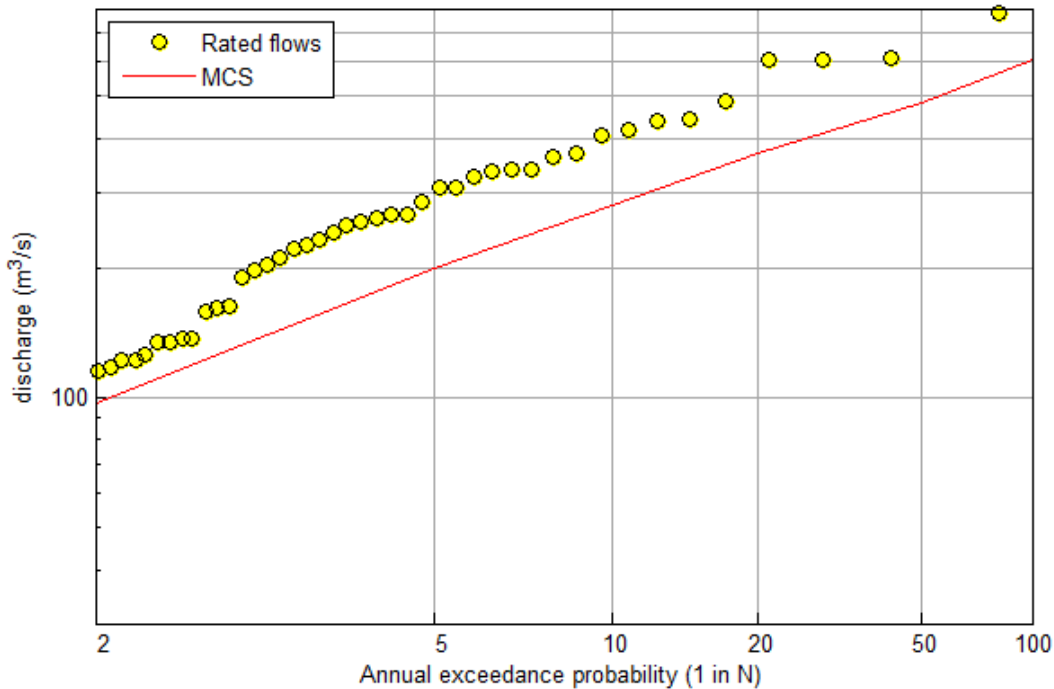




Figure A.2.5a | Location Woodford; no dams conditions

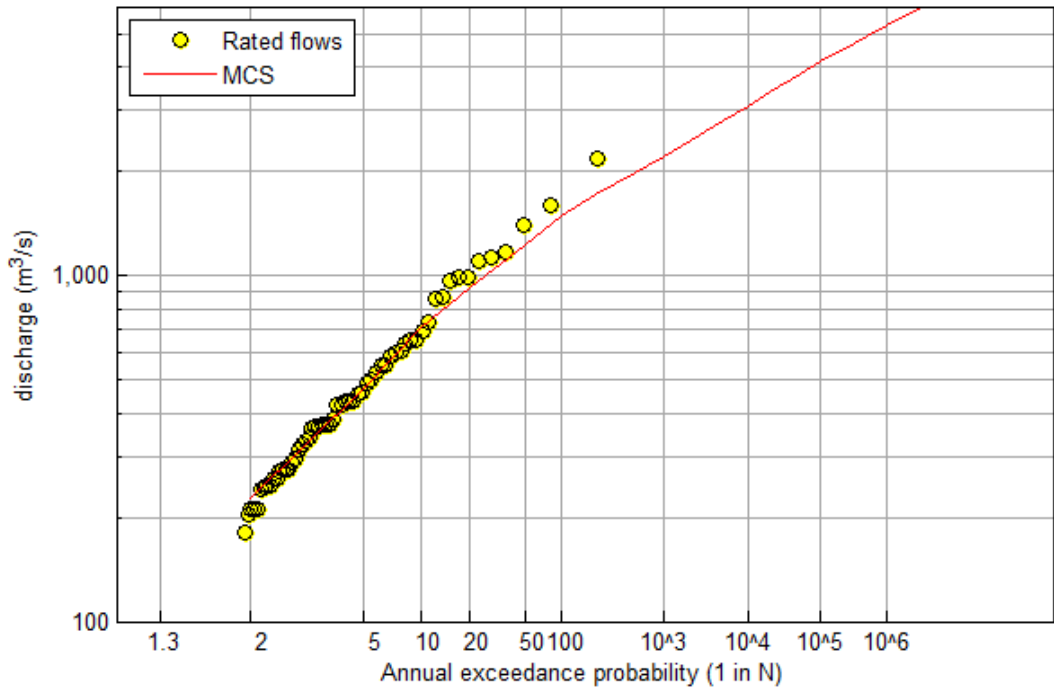


Figure A.2.5b | Location Woodford; no dams conditions

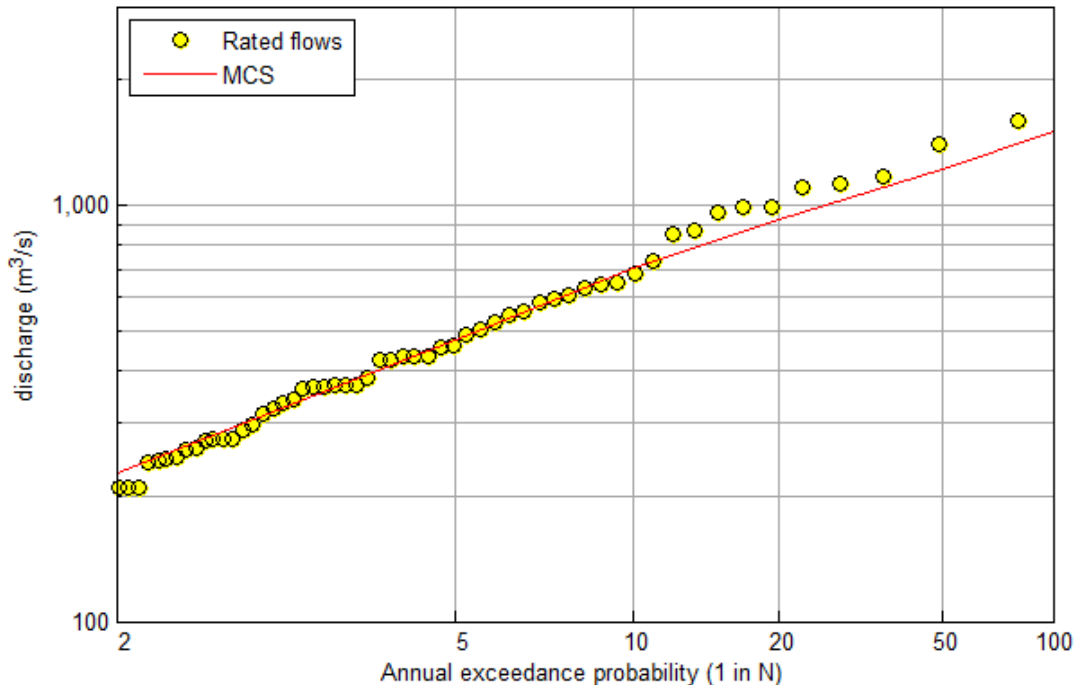




Figure A.2.6a | Location Somerset Dam; no dams conditions

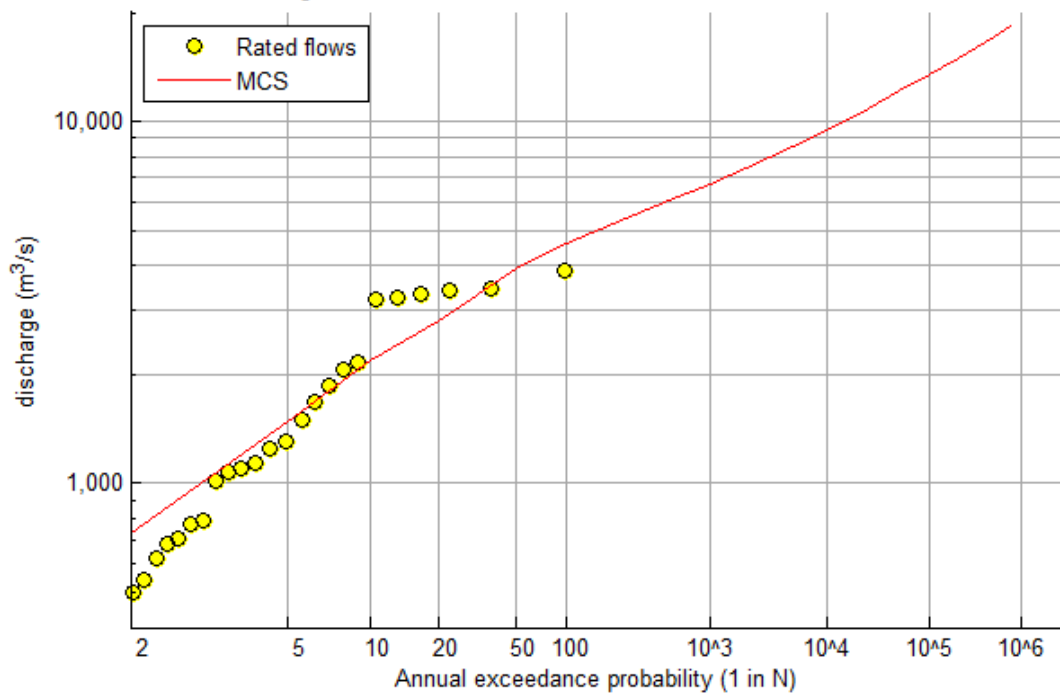


Figure A.2.6b | Location Somerset Dam; no dams conditions

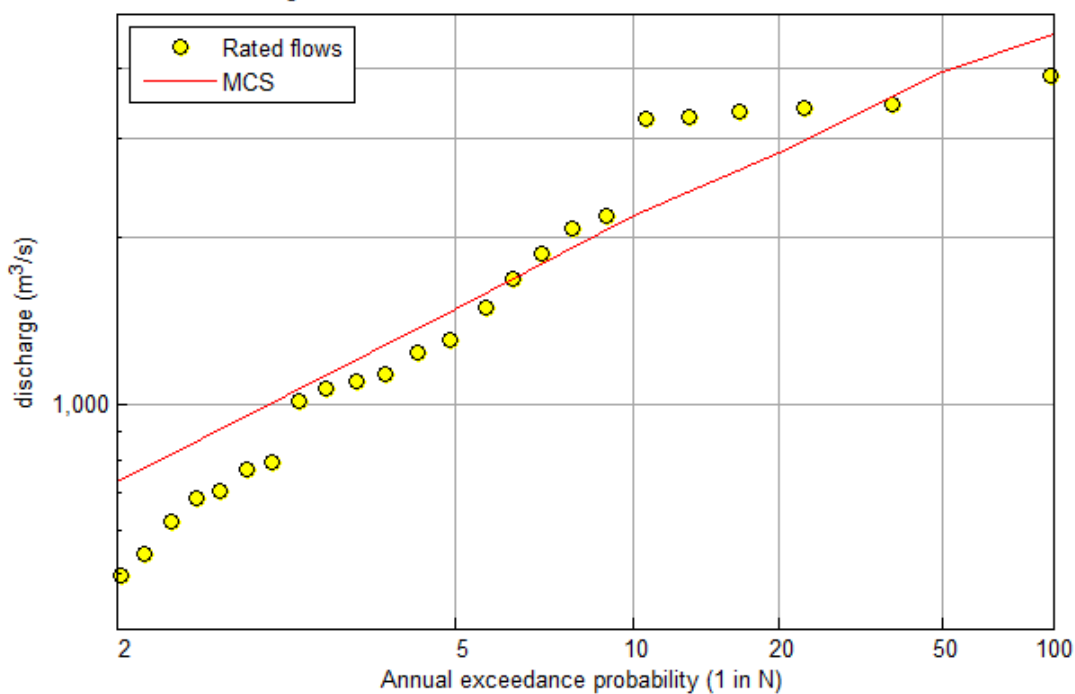




Figure A.2.7a | Location Tinton; no dams conditions

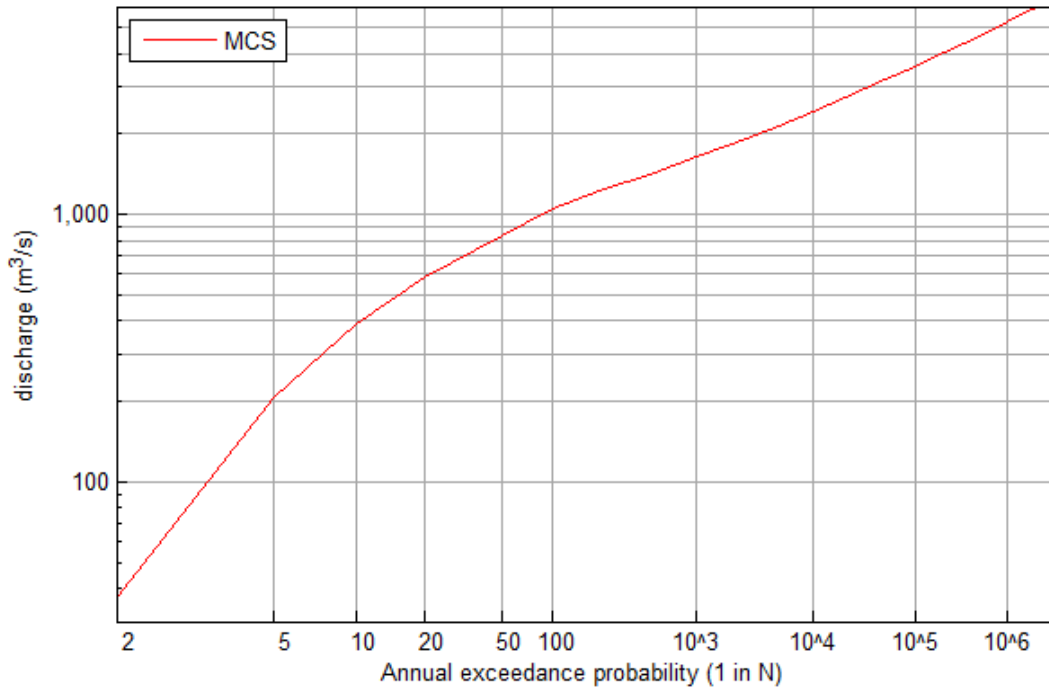


Figure A.2.7b | Location Tinton; no dams conditions

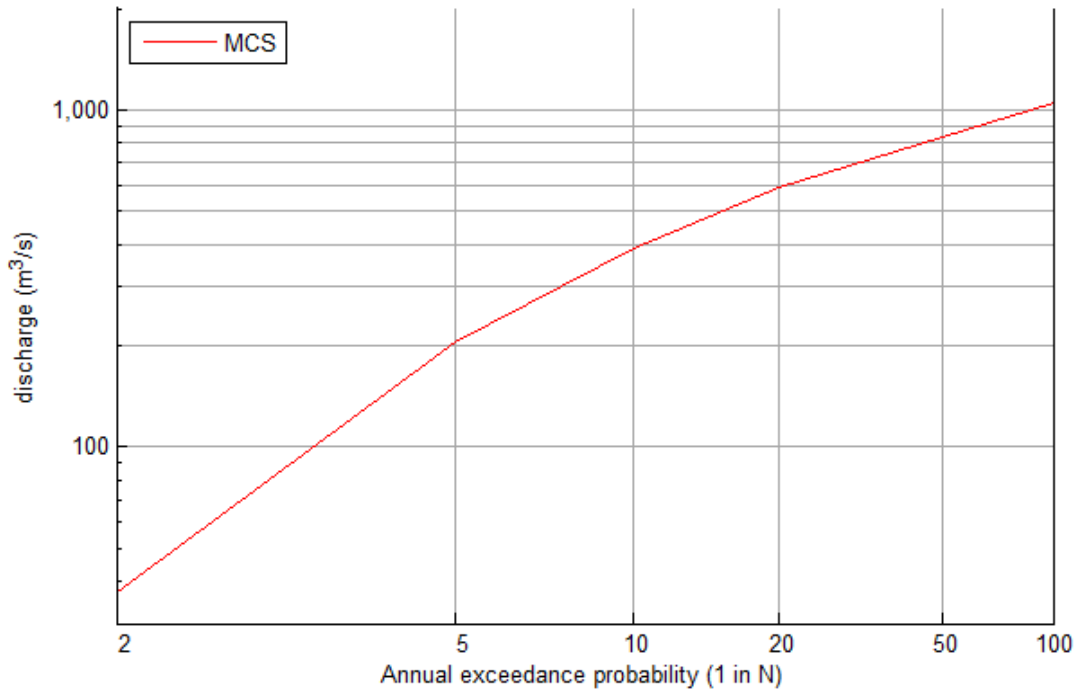




Figure A.2.8a | Location Middle Ck; no dams conditions

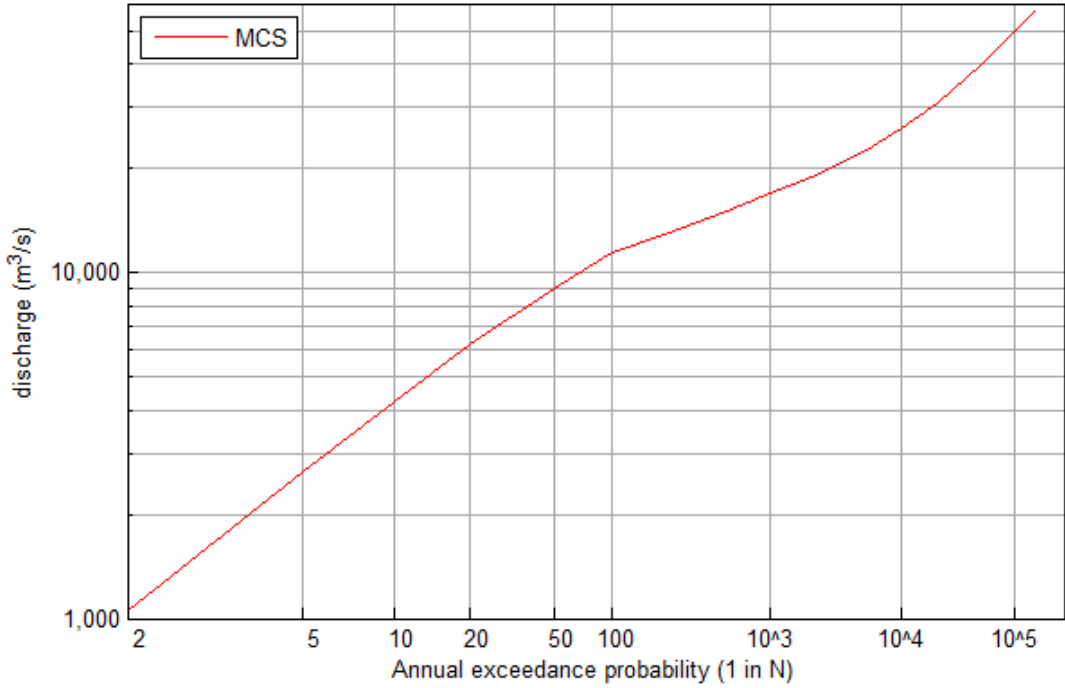


Figure A.2.8b | Location Middle Ck; no dams conditions

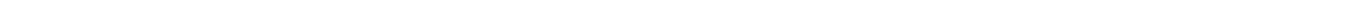
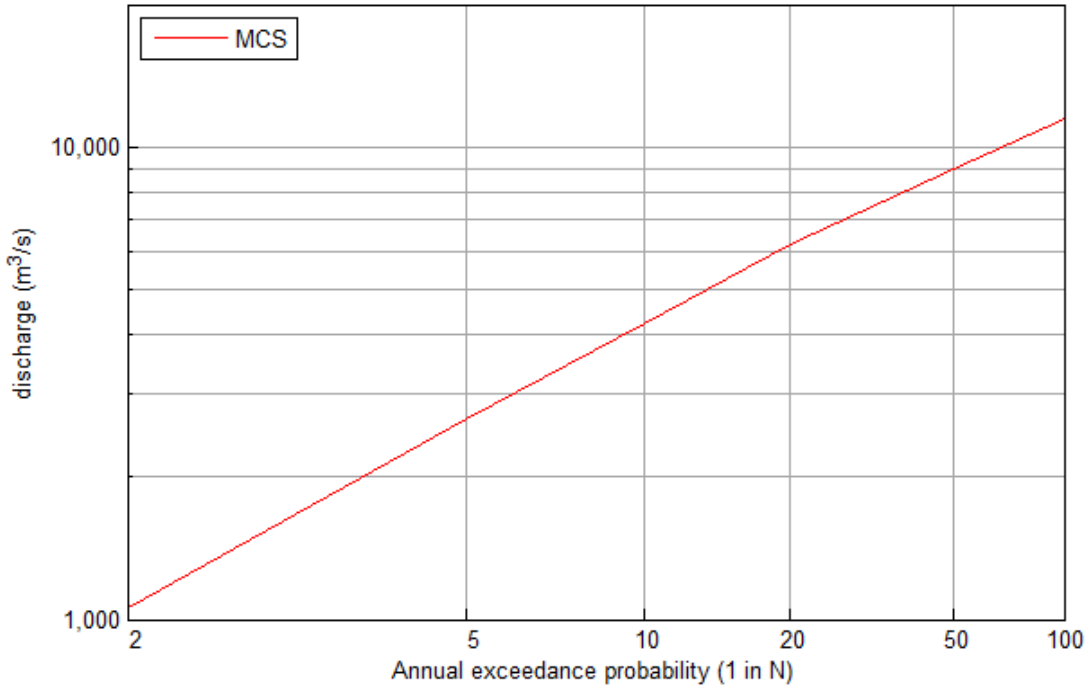




Figure A.2.9a | Location Wivenhoe; no dams conditions

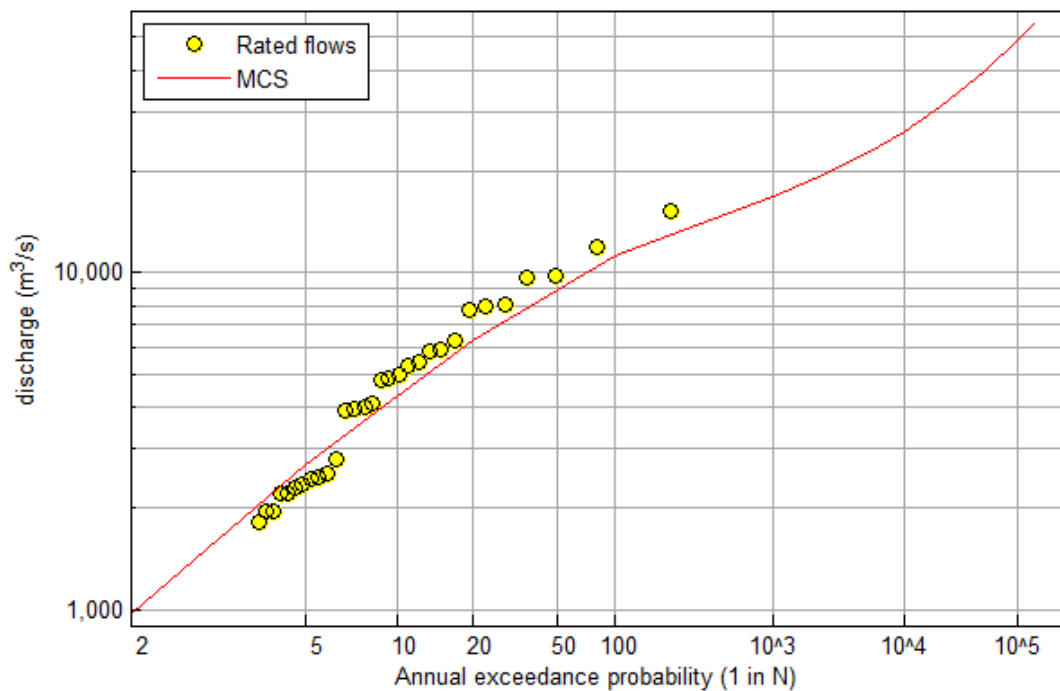


Figure A.2.9b | Location Wivenhoe; no dams conditions

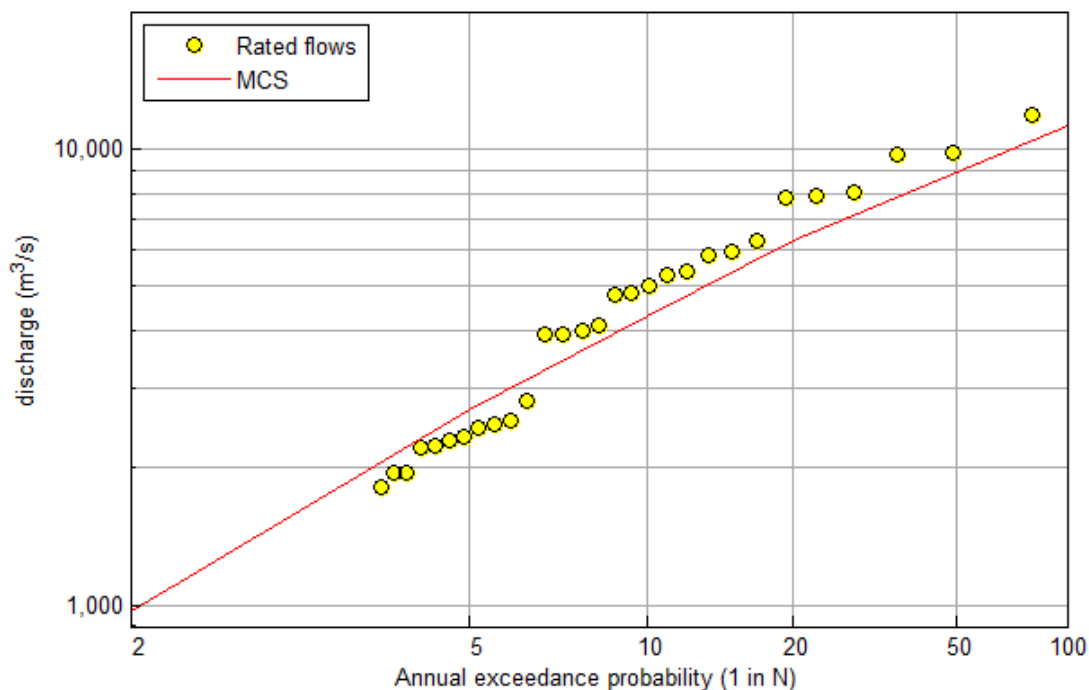




Figure A.2.10a | Location Helidon; no dams conditions

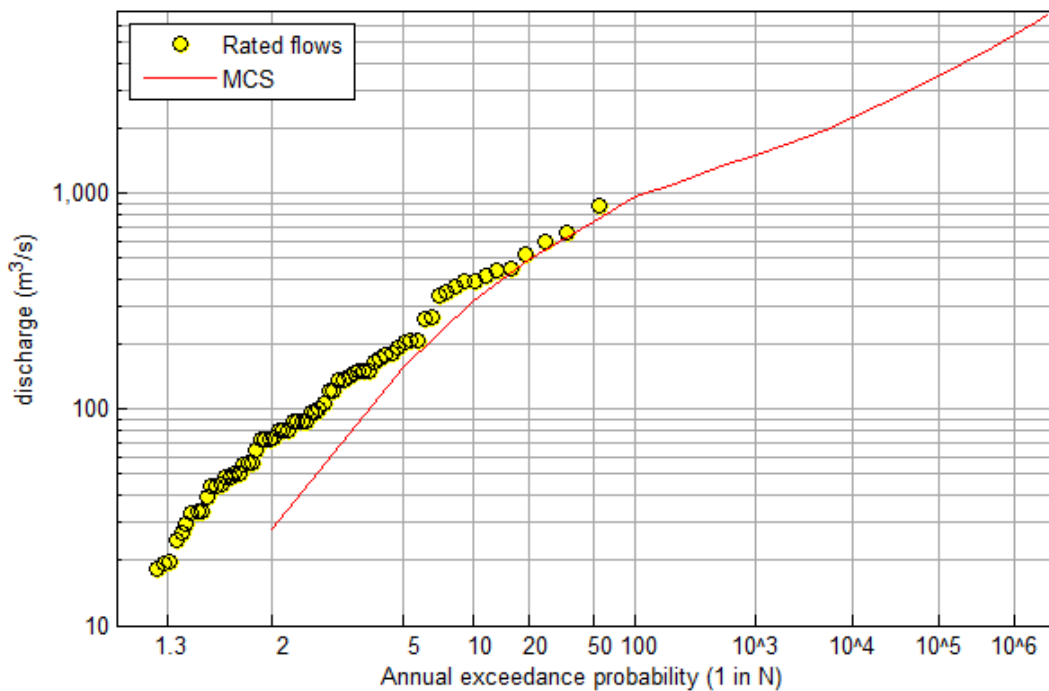


Figure A.2.10b | Location Helidon; no dams conditions

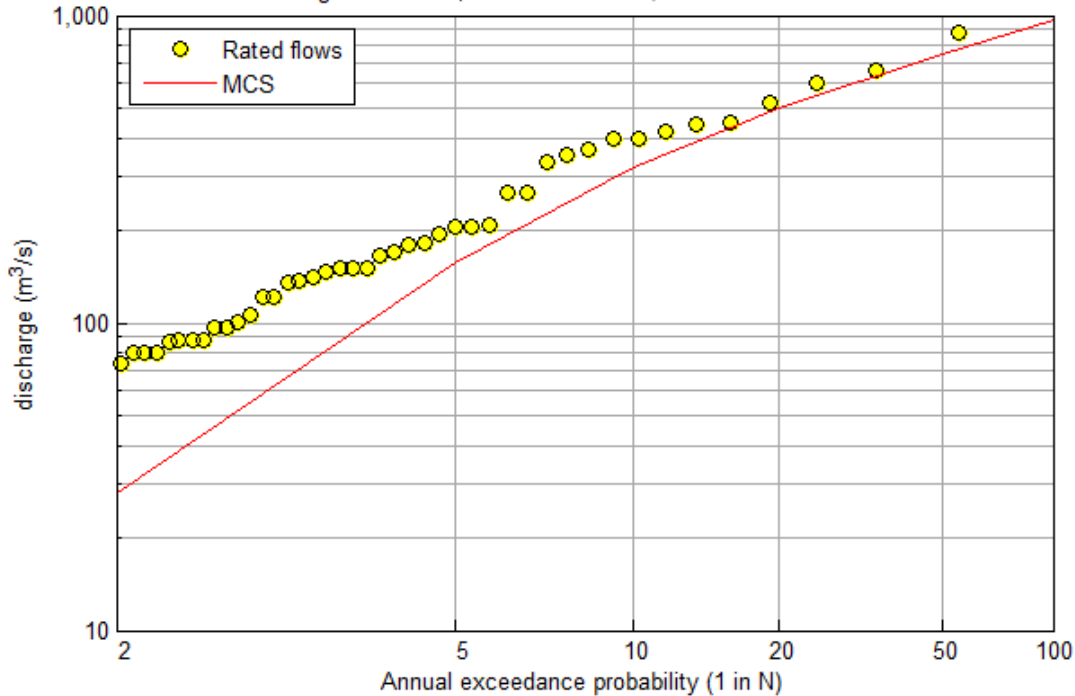




Figure A.2.11a | Location Gatton; no dams conditions

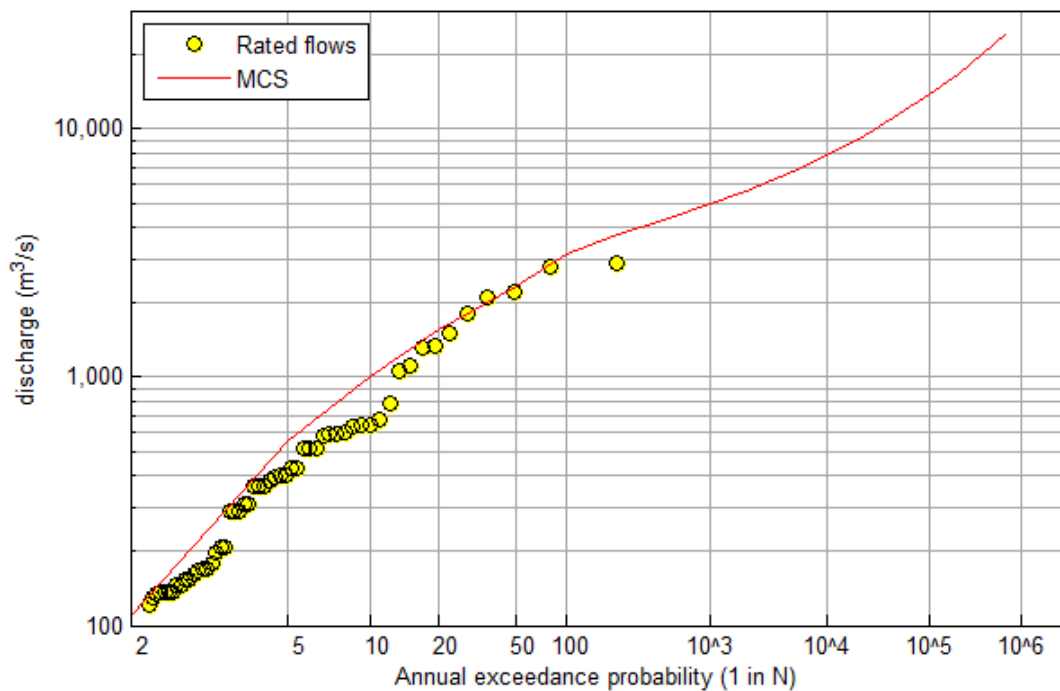


Figure A.2.11b | Location Gatton; no dams conditions

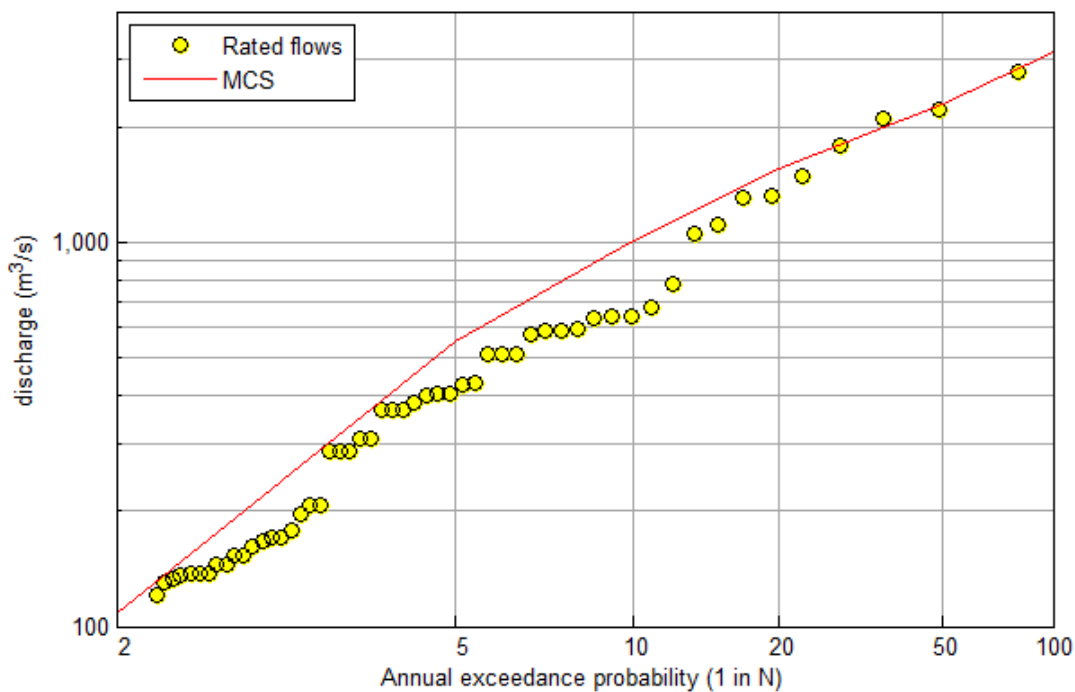




Figure A.2.12a | Location Glenore Grove; no dams conditions

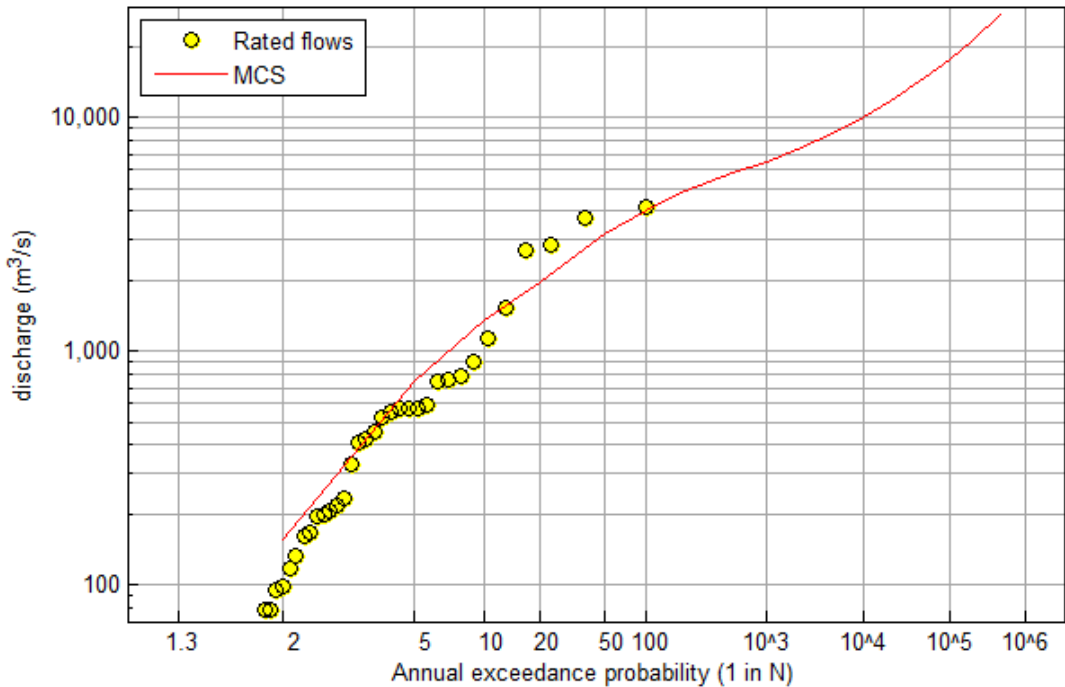


Figure A.2.12b | Location Glenore Grove; no dams conditions

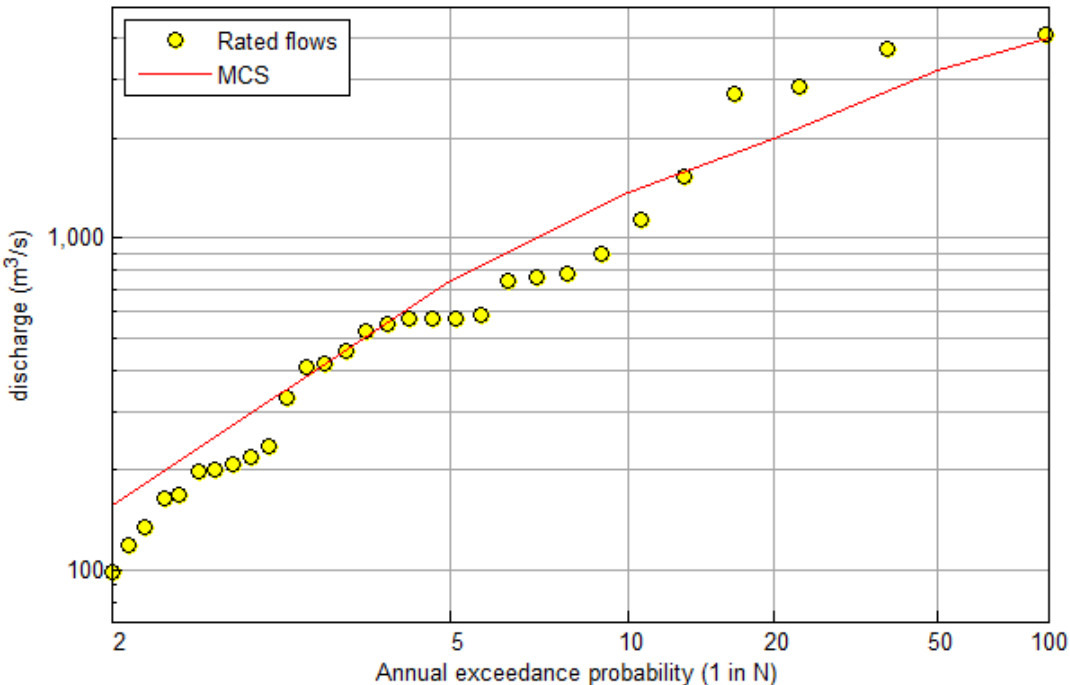




Figure A.2.13a | Location Savages Crossing; no dams conditions

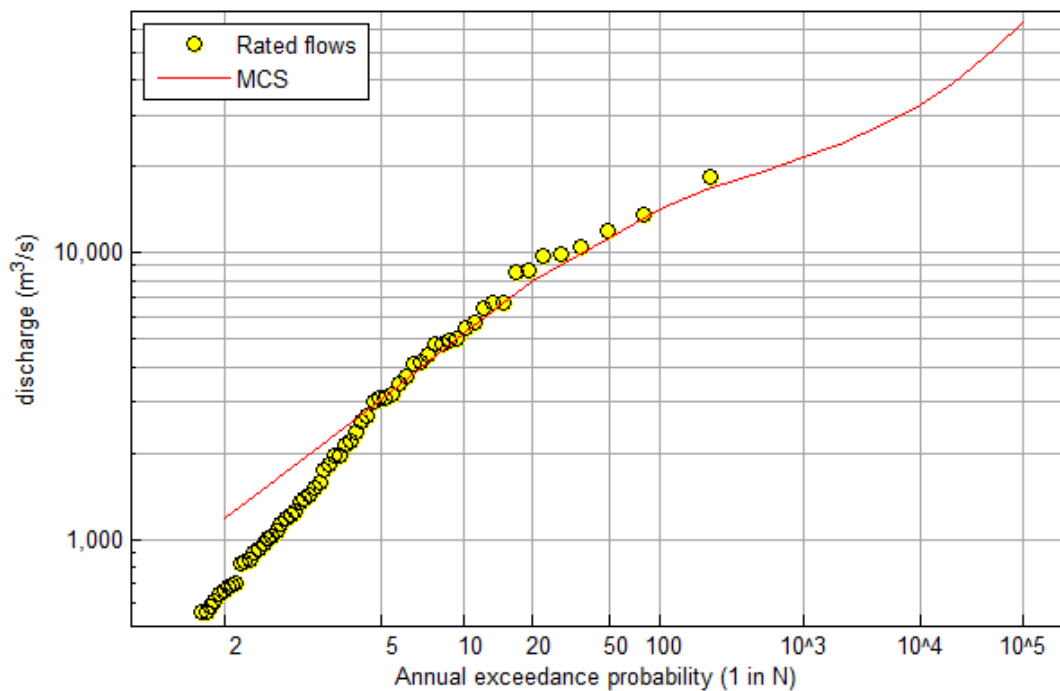


Figure A.2.13b | Location Savages Crossing; no dams conditions

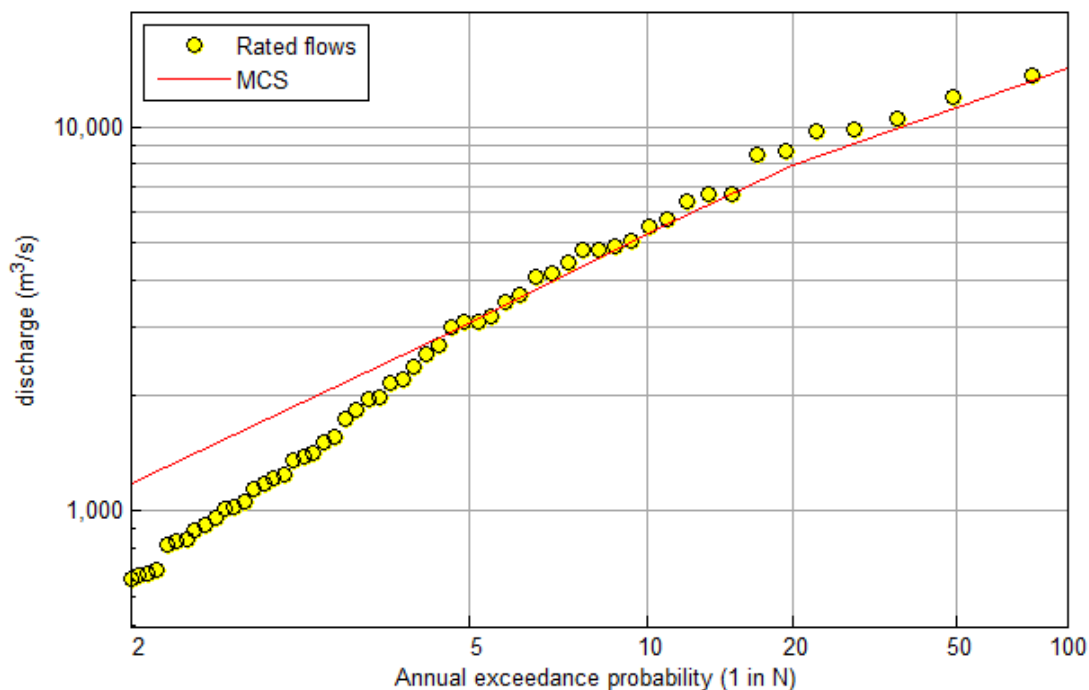




Figure A.2.14a | Location Mount Crosby; no dams conditions

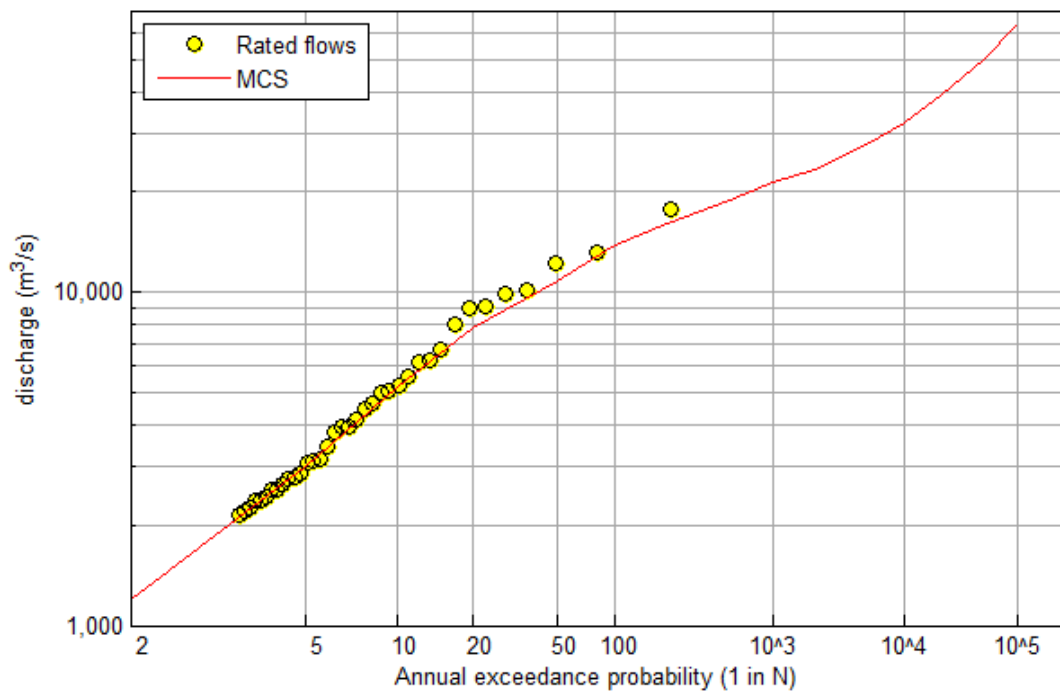


Figure A.2.14b | Location Mount Crosby; no dams conditions

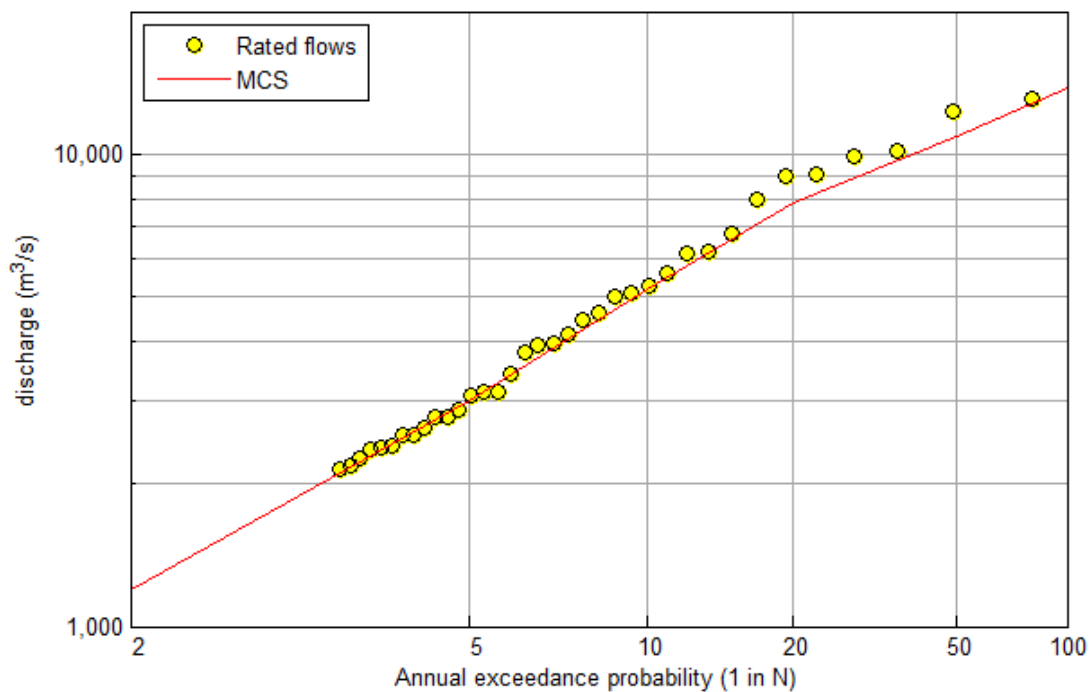




Figure A.2.15a | Location Walloon; no dams conditions

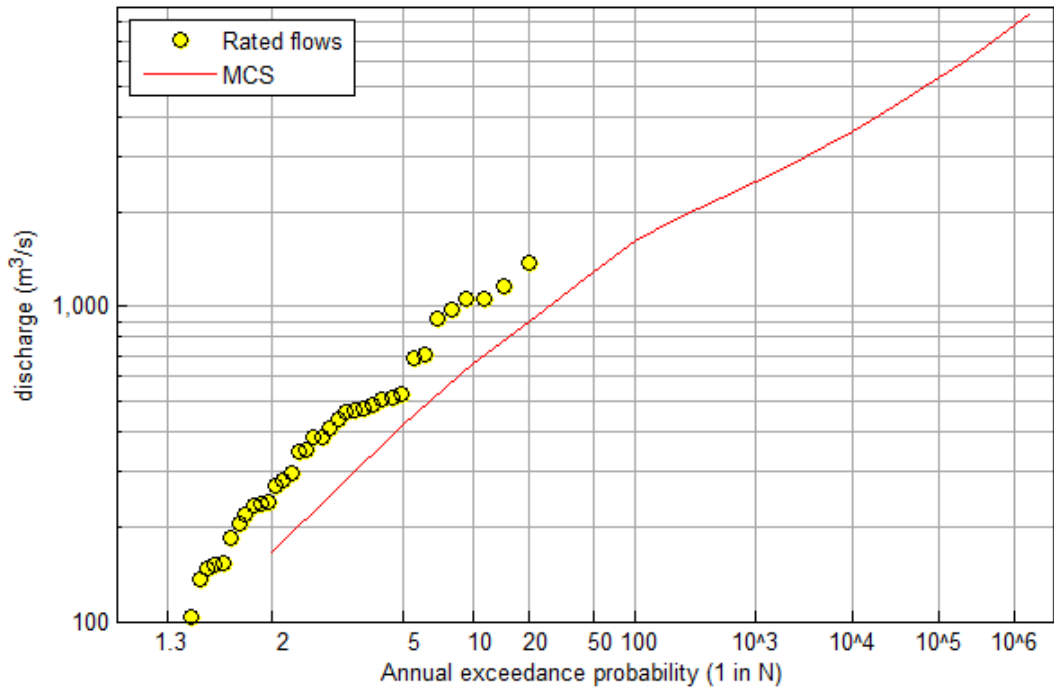


Figure A.2.15b | Location Walloon; no dams conditions

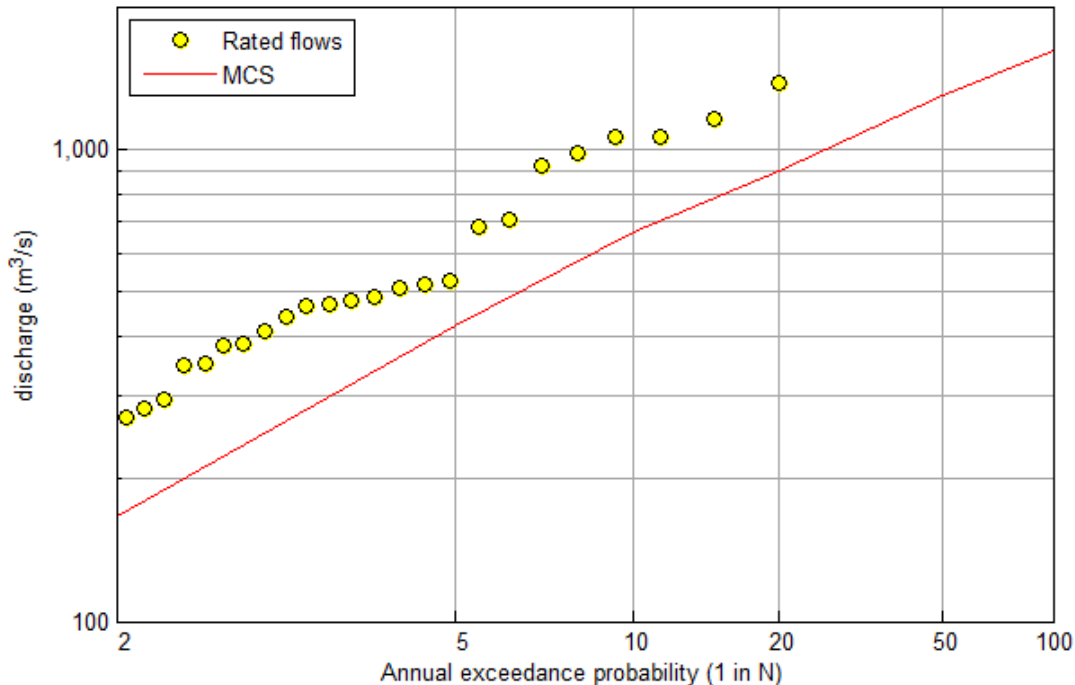




Figure A.2.16a | Location Kalbar Weir; no dams conditions

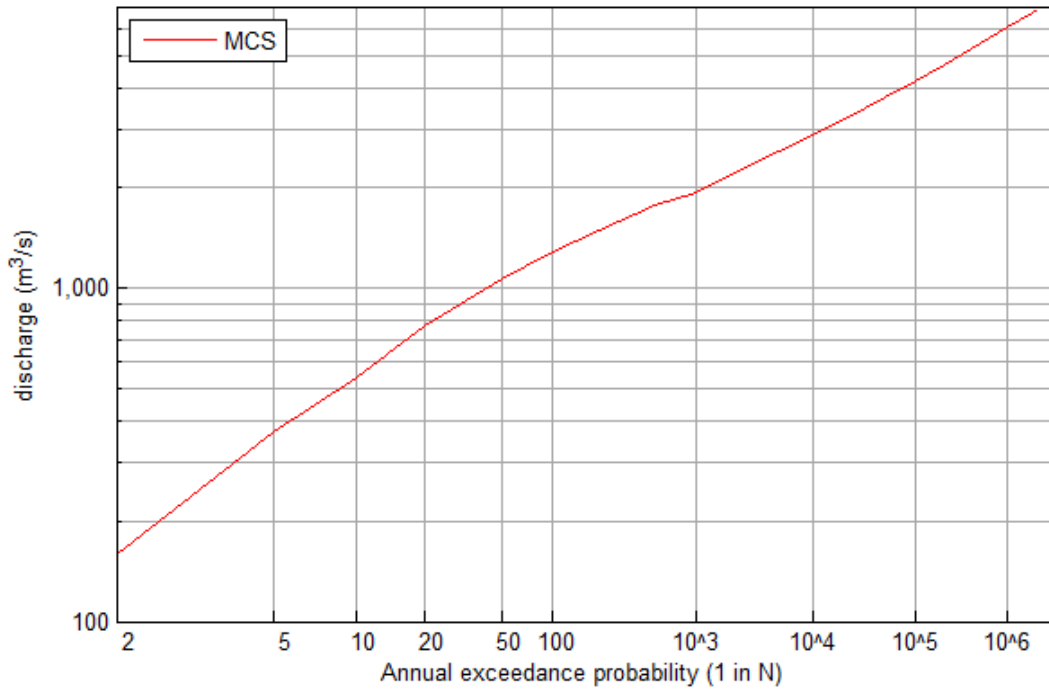


Figure A.2.16b | Location Kalbar Weir; no dams conditions

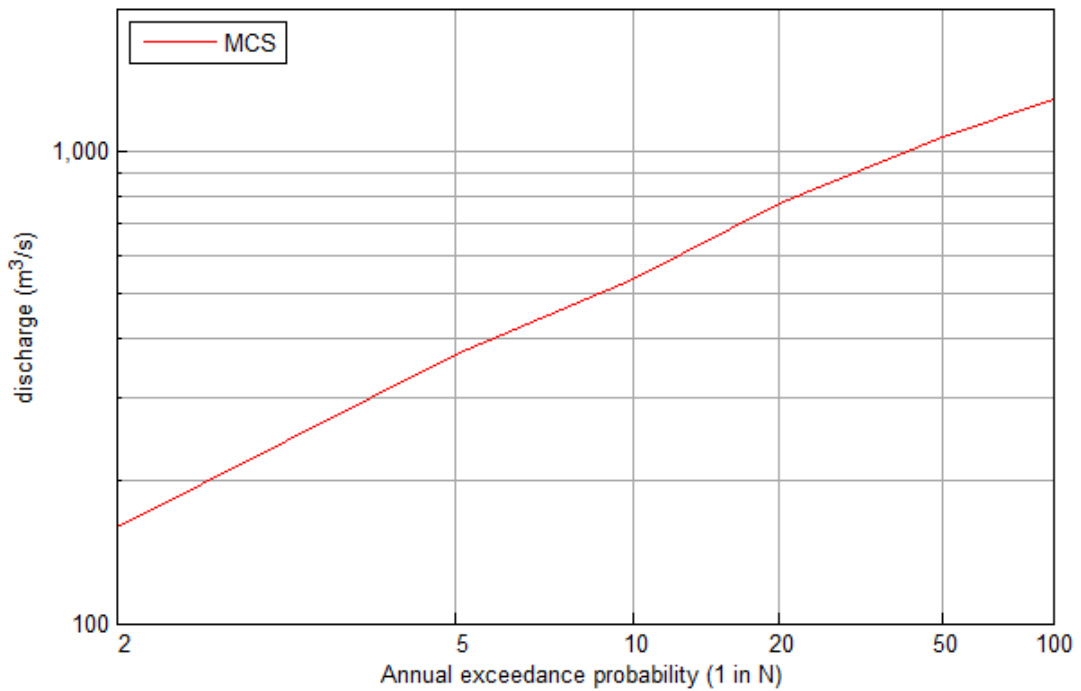




Figure A.2.17a | Location Amberley; no dams conditions

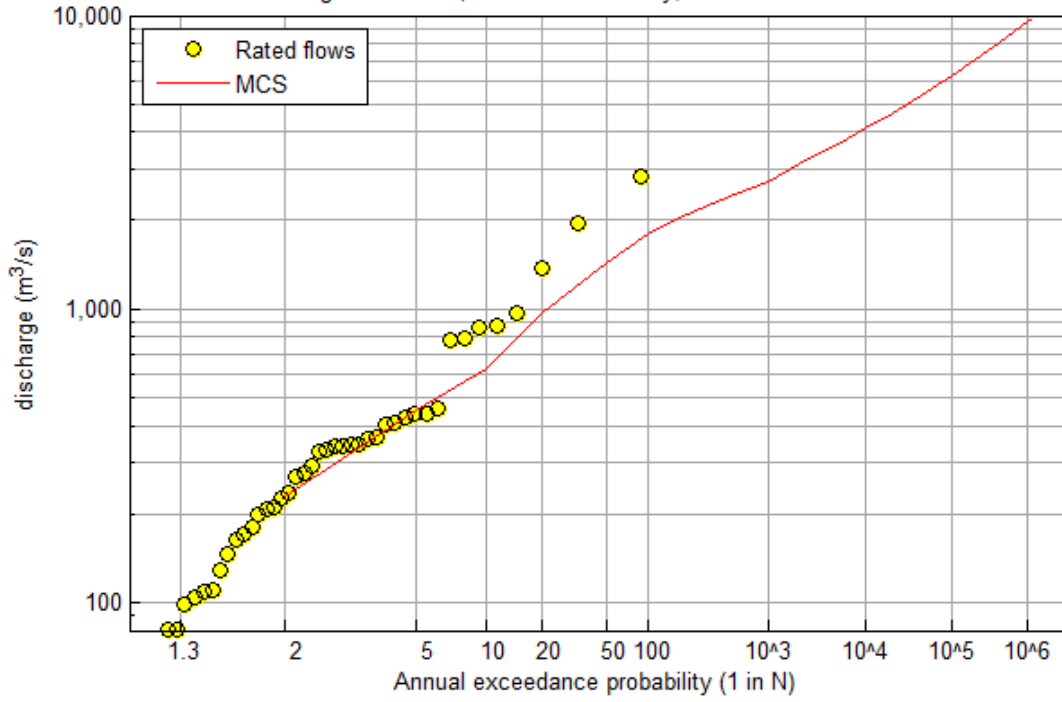


Figure A.2.17b | Location Amberley; no dams conditions

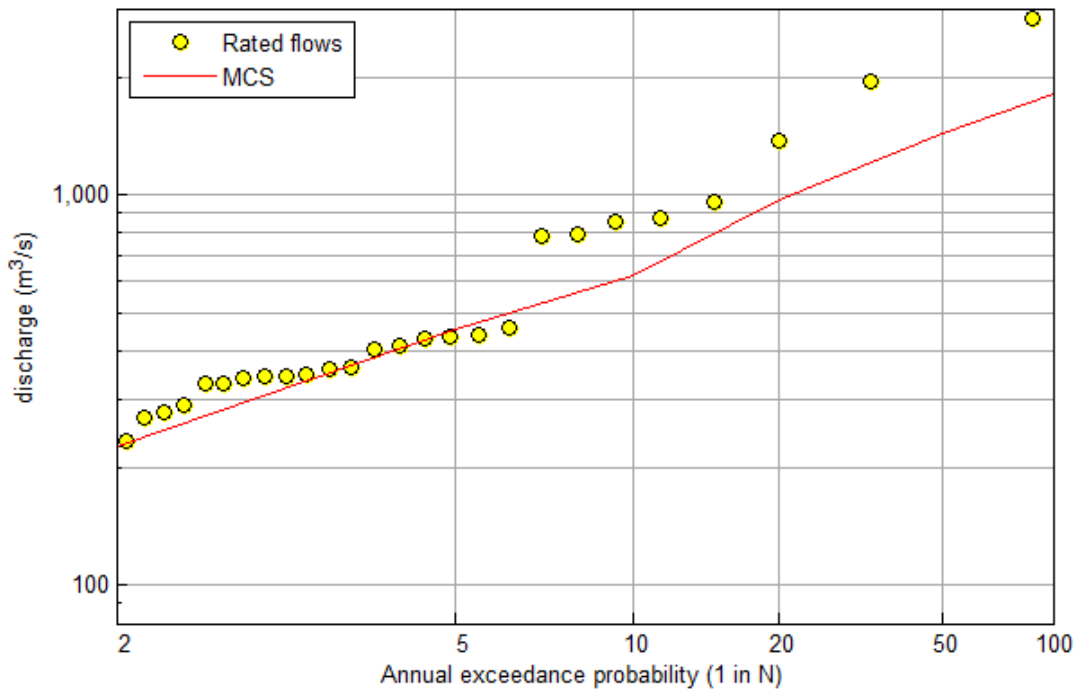




Figure A.2.18a | Location Loamside; no dams conditions

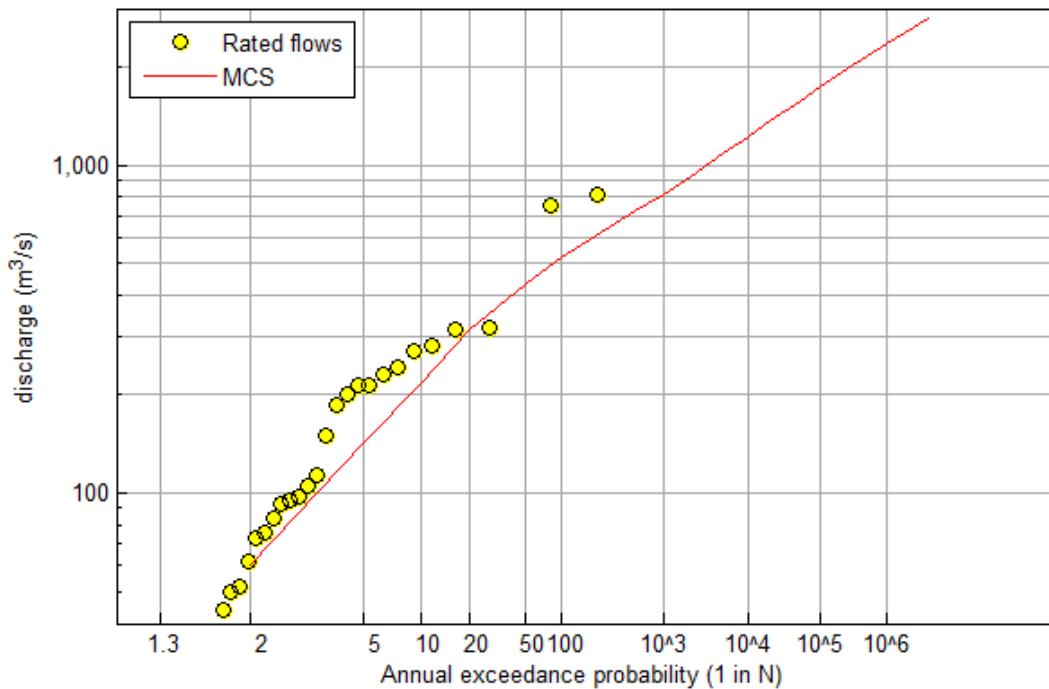


Figure A.2.18b | Location Loamside; no dams conditions

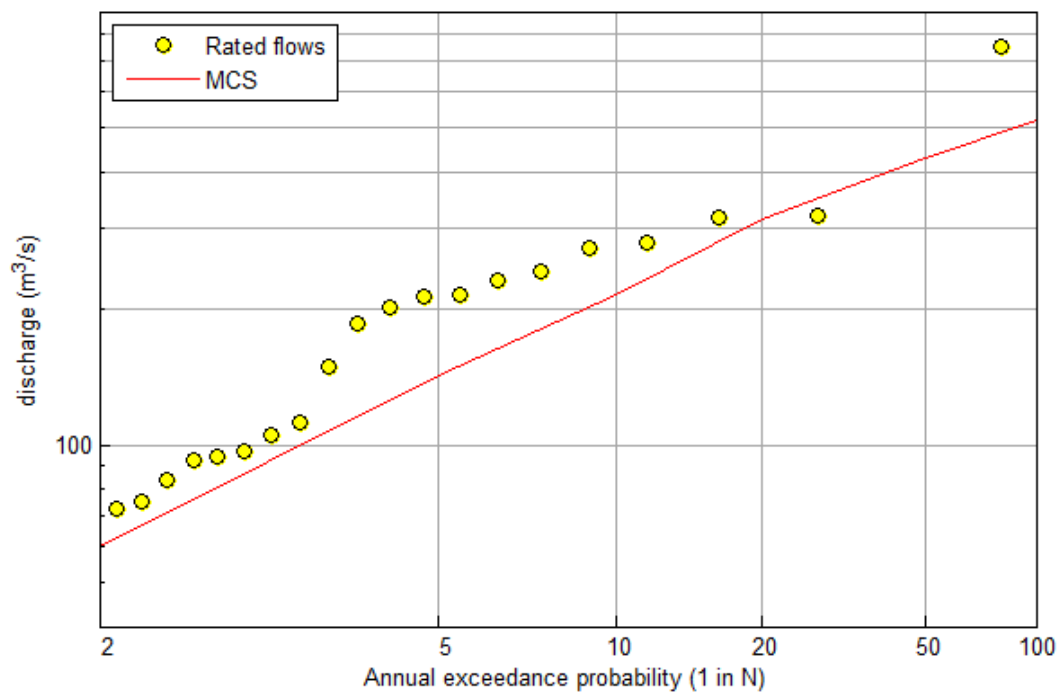




Figure A.2.19a | Location Ipswich; no dams conditions

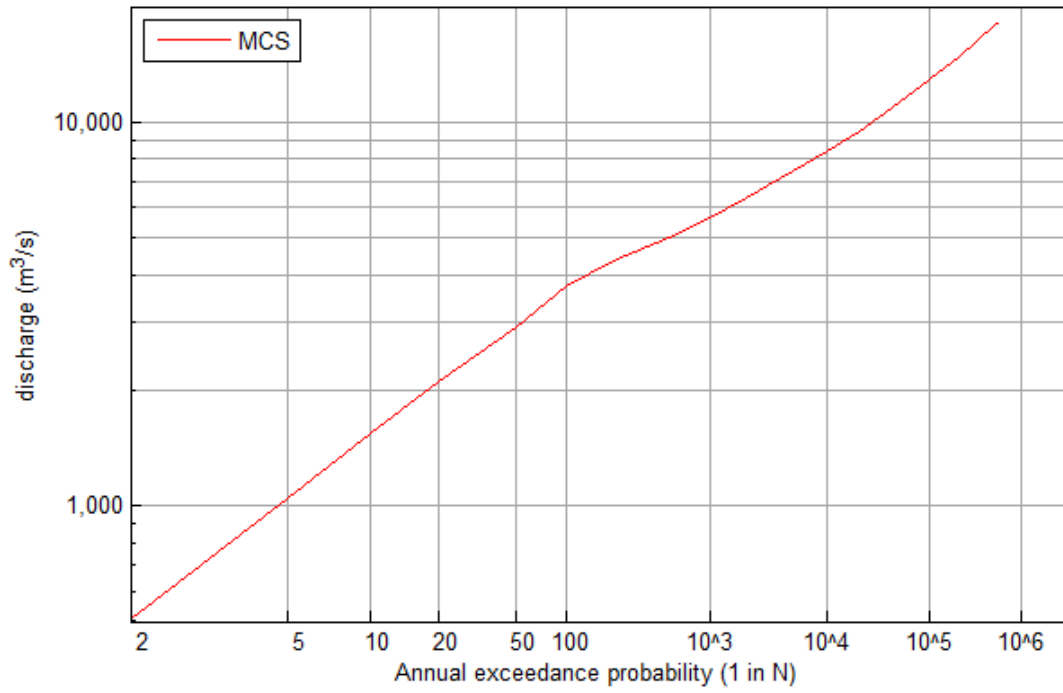


Figure A.2.19b | Location Ipswich; no dams conditions

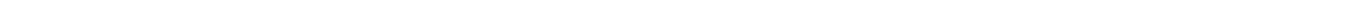
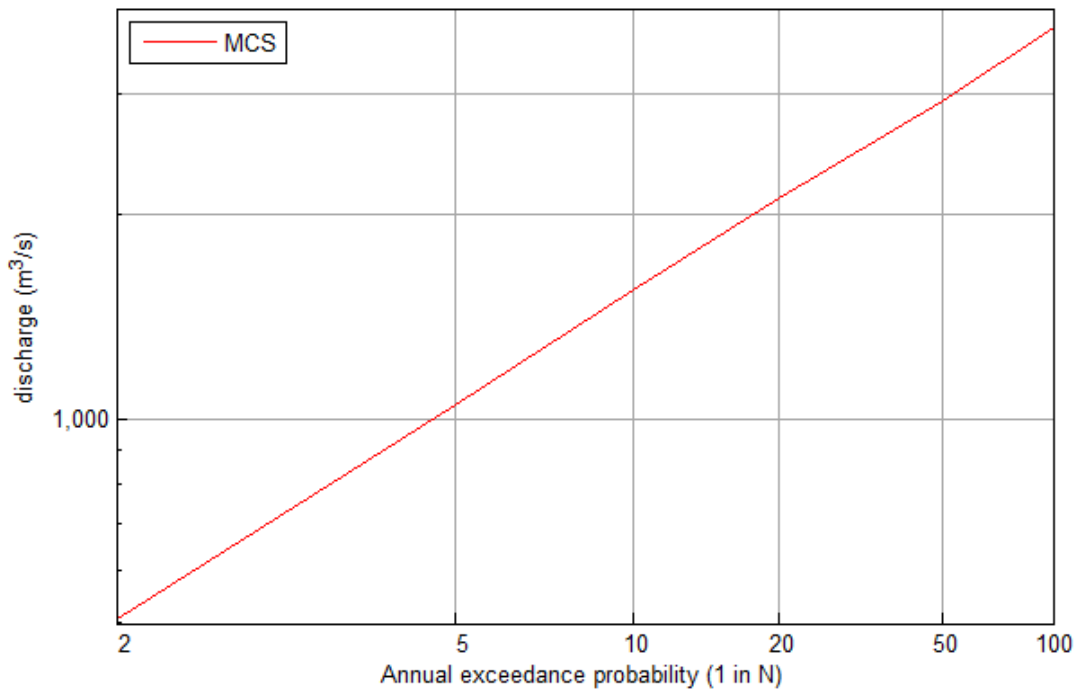




Figure A.2.20a | Location Moggill; no dams conditions

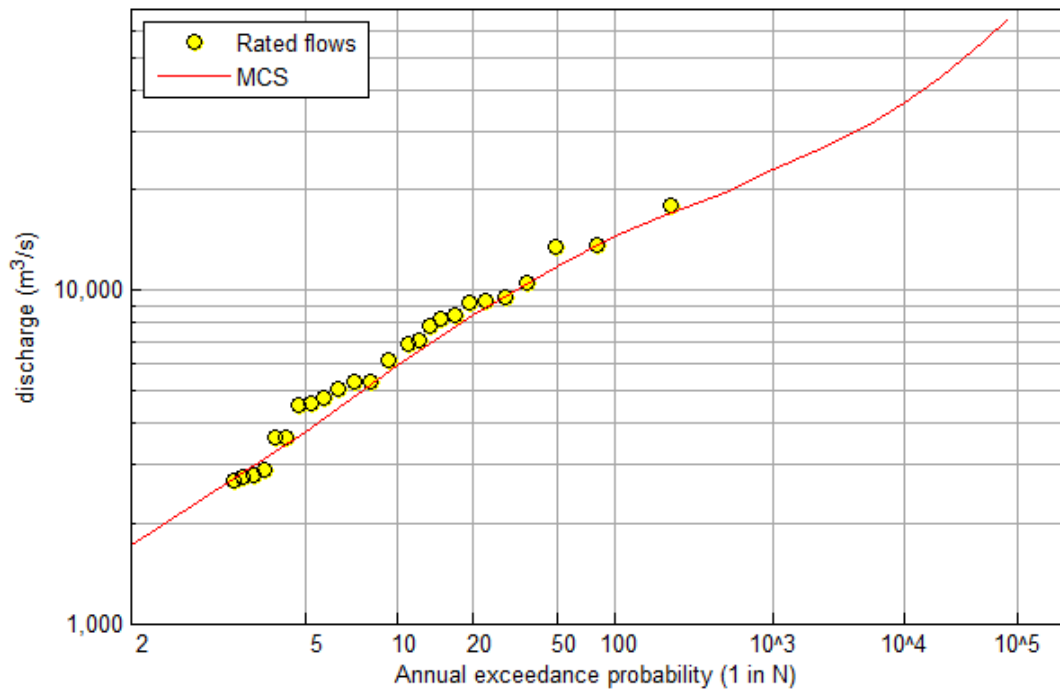


Figure A.2.20b | Location Moggill; no dams conditions

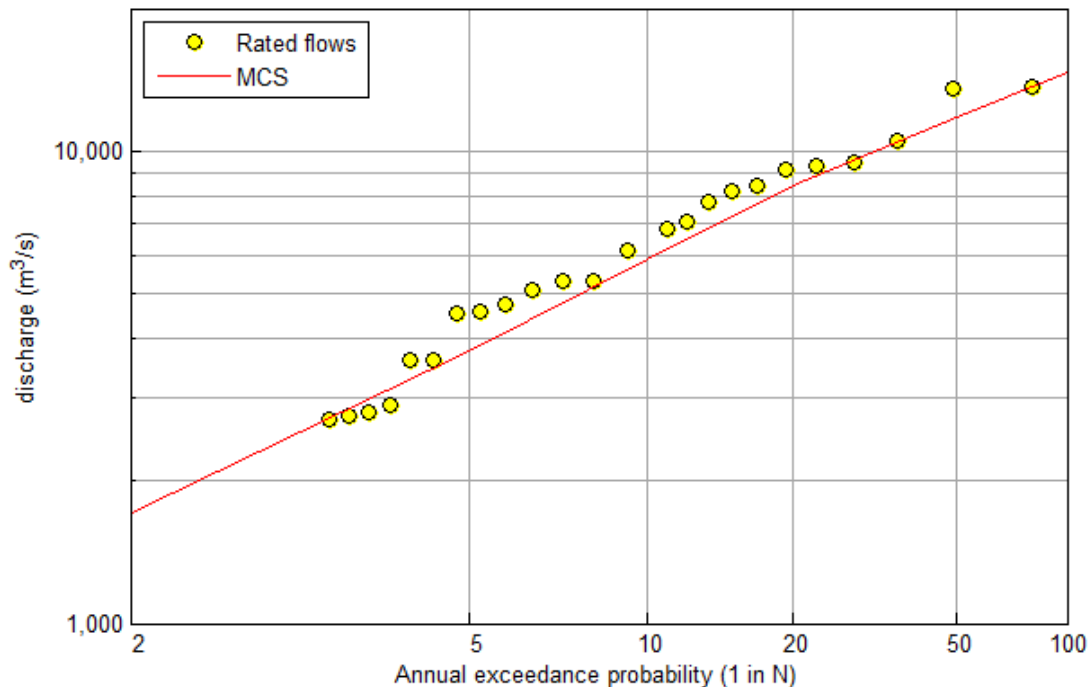




Figure A.2.21a | Location Centenary Bridge; no dams conditions

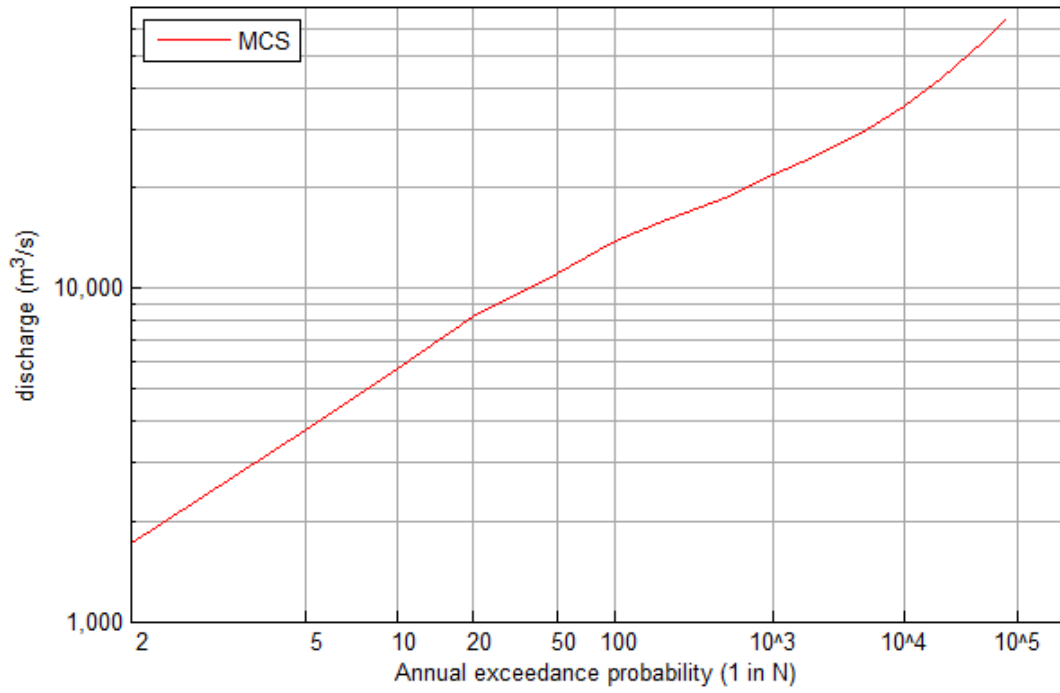


Figure A.2.21b | Location Centenary Bridge; no dams conditions

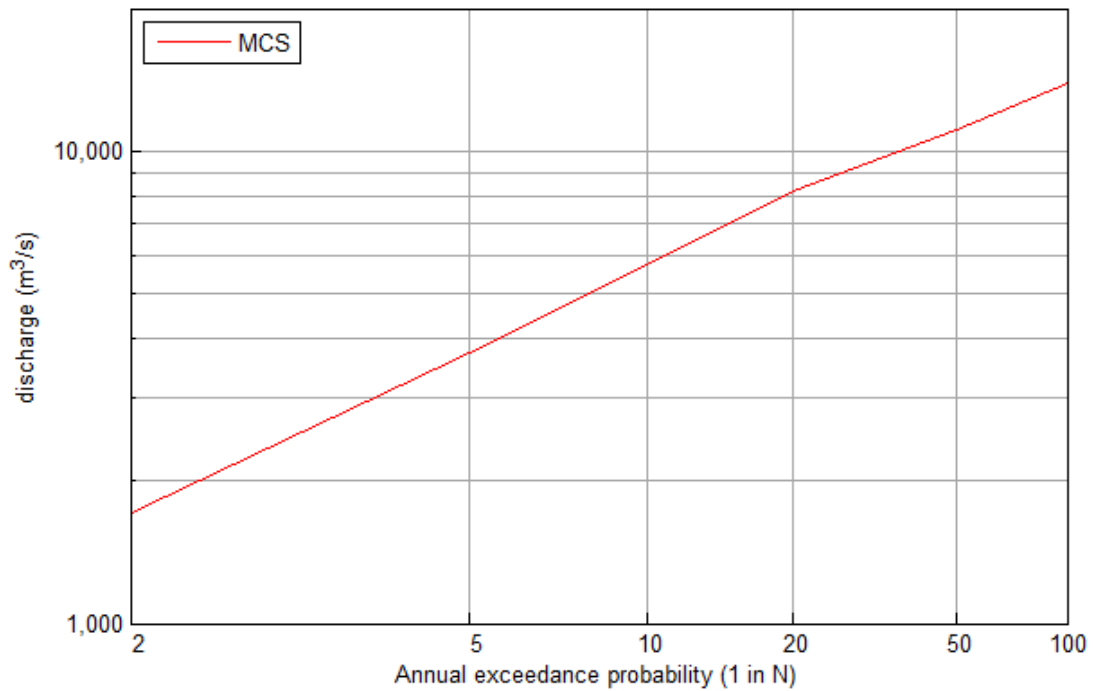




Figure A.2.22a | Location Brisbane; no dams conditions

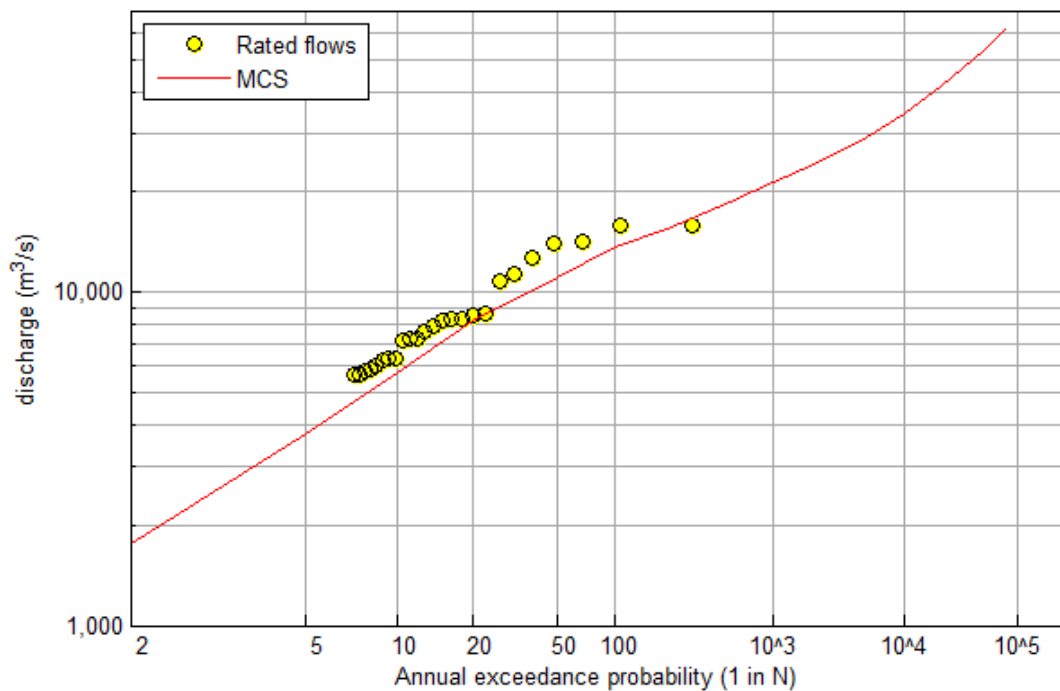
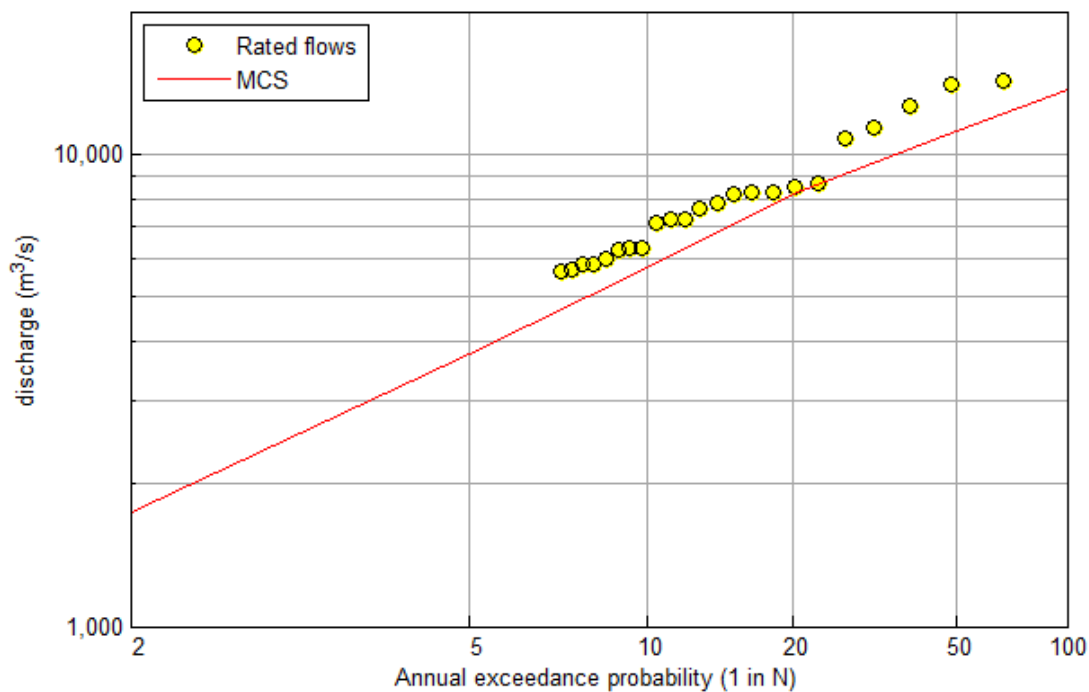


Figure A.2.22b | Location Brisbane; no dams conditions





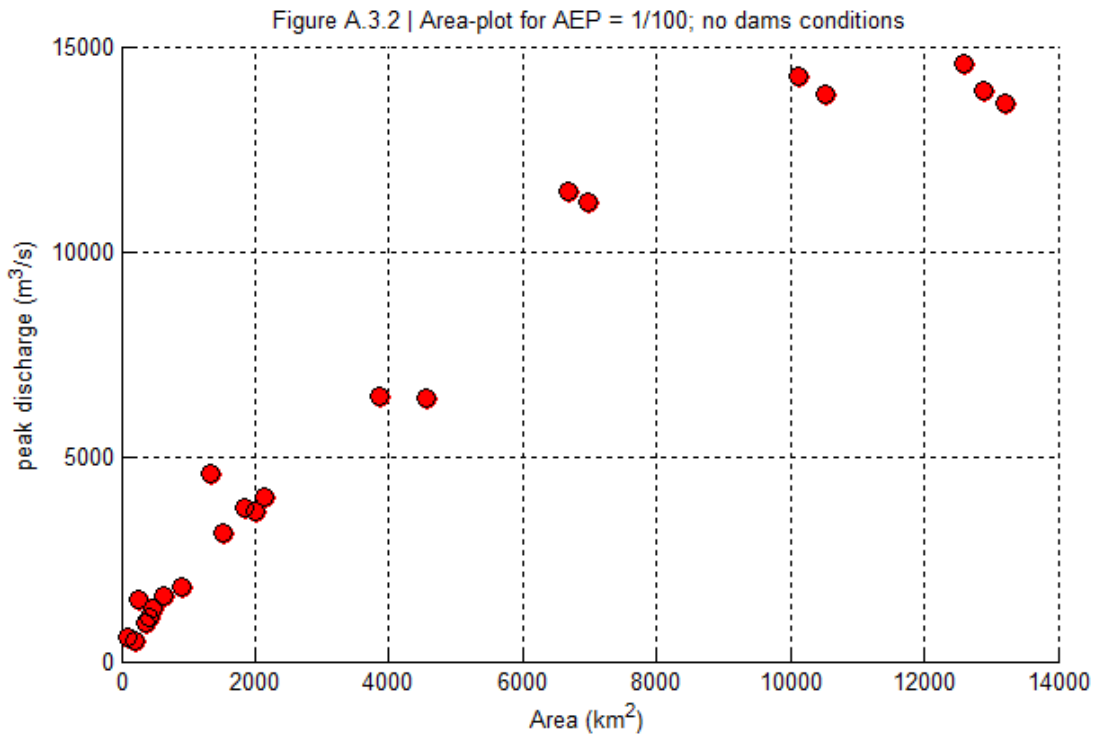
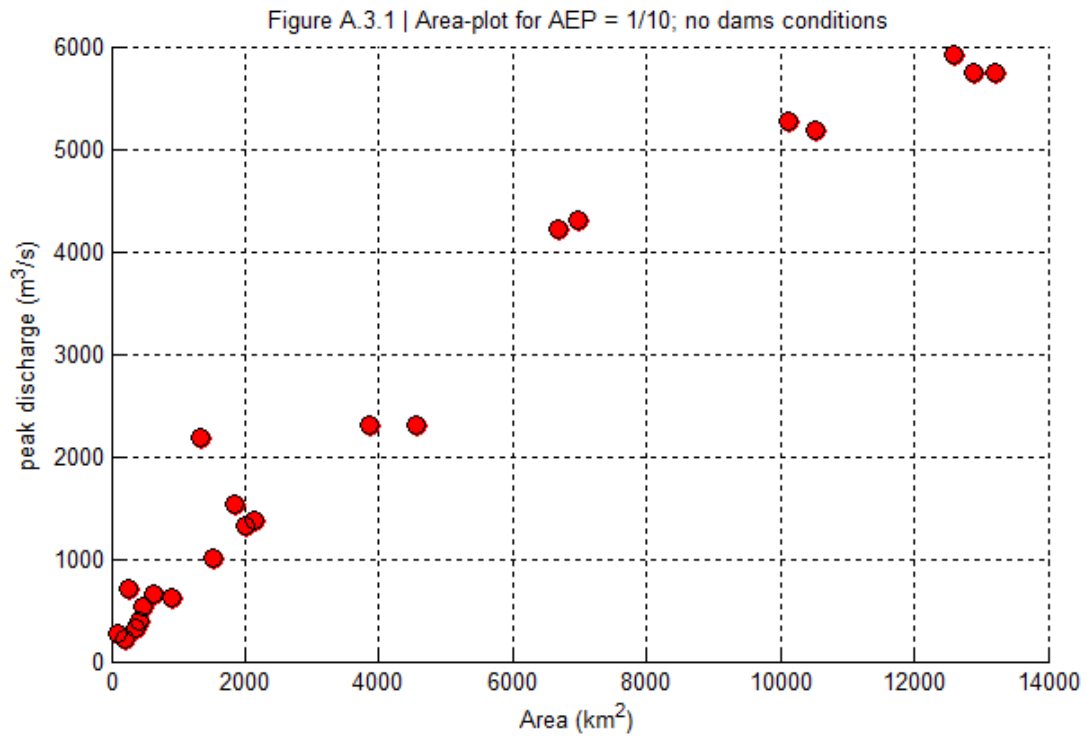
A.3 Plots of catchment area versus peak discharge

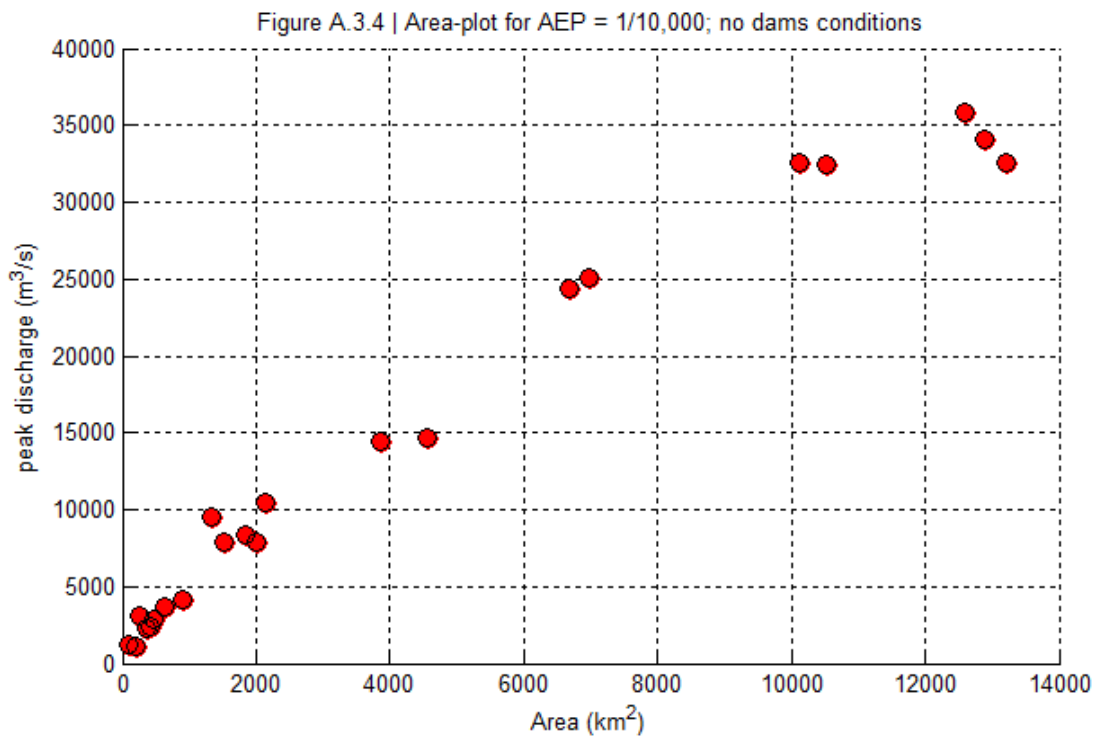
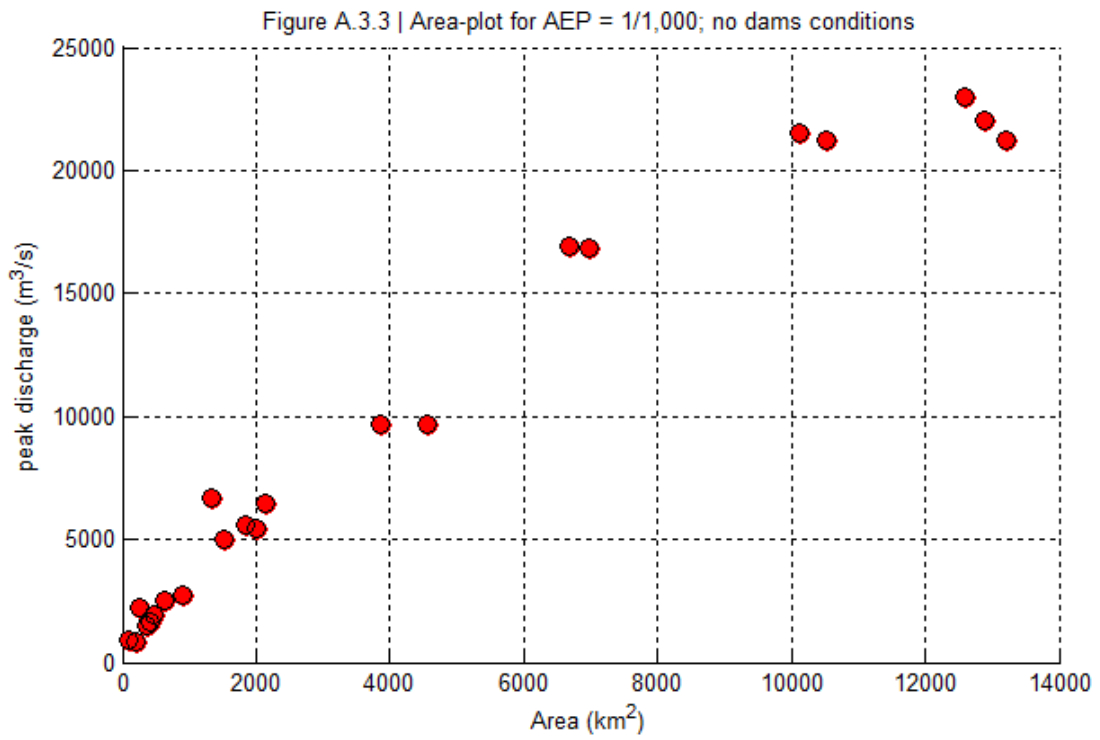
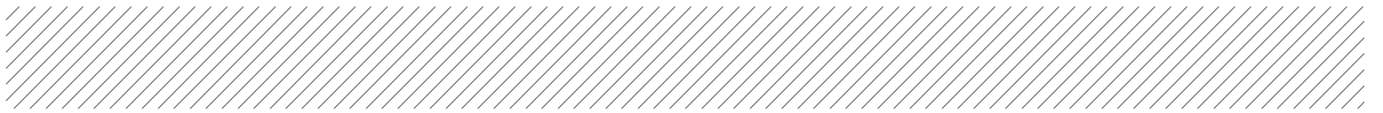
This section provides Figures in which catchment area is compared with peak discharge. For a range of AEP's, the following four Figures are provided:

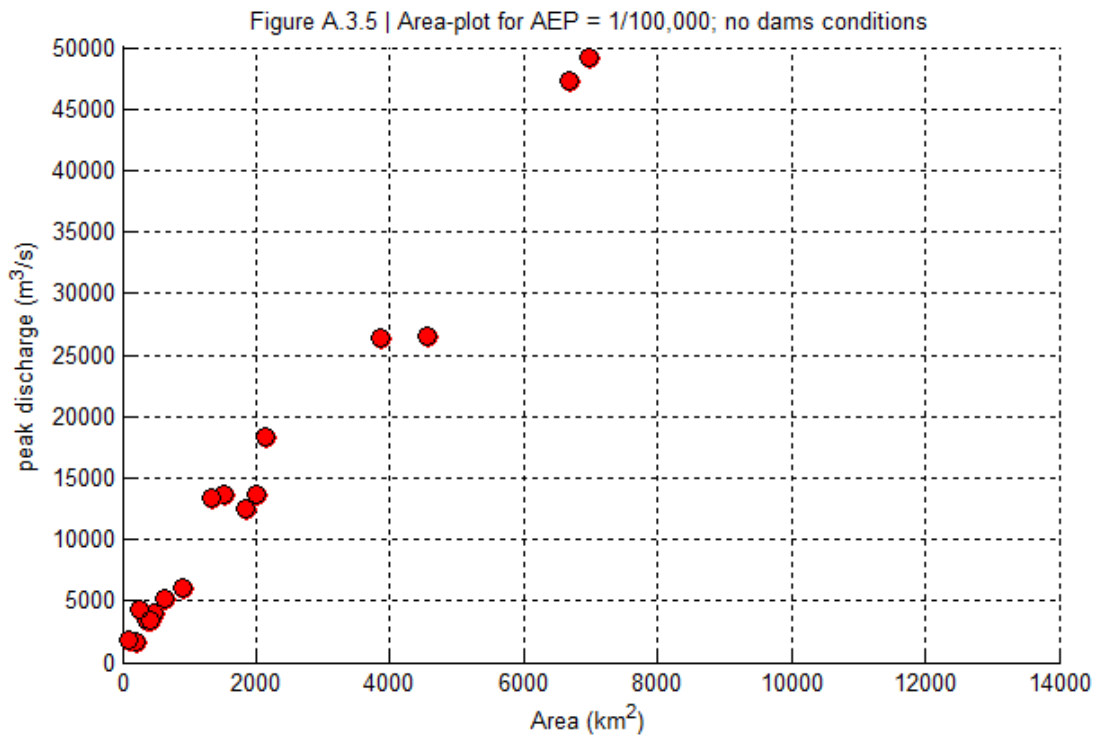
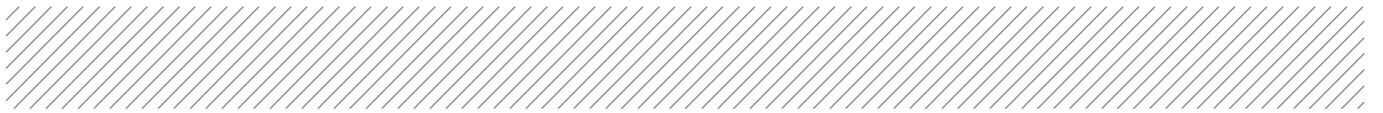
[1] Design peak flow (Q) versus catchment area (A)

[2] Q/A versus A

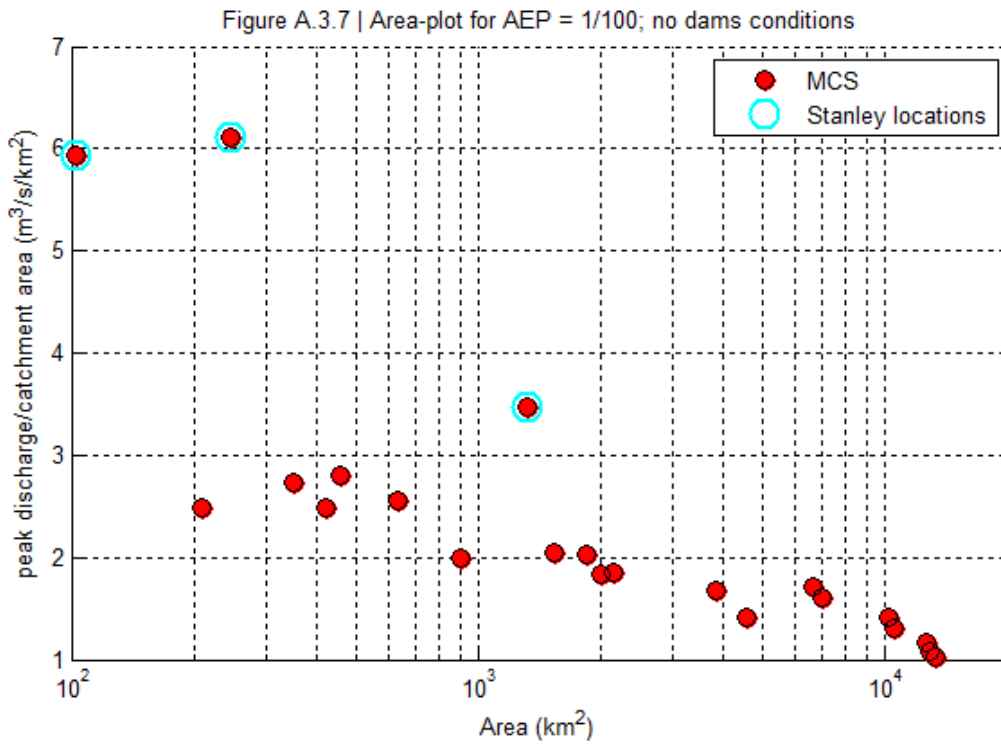
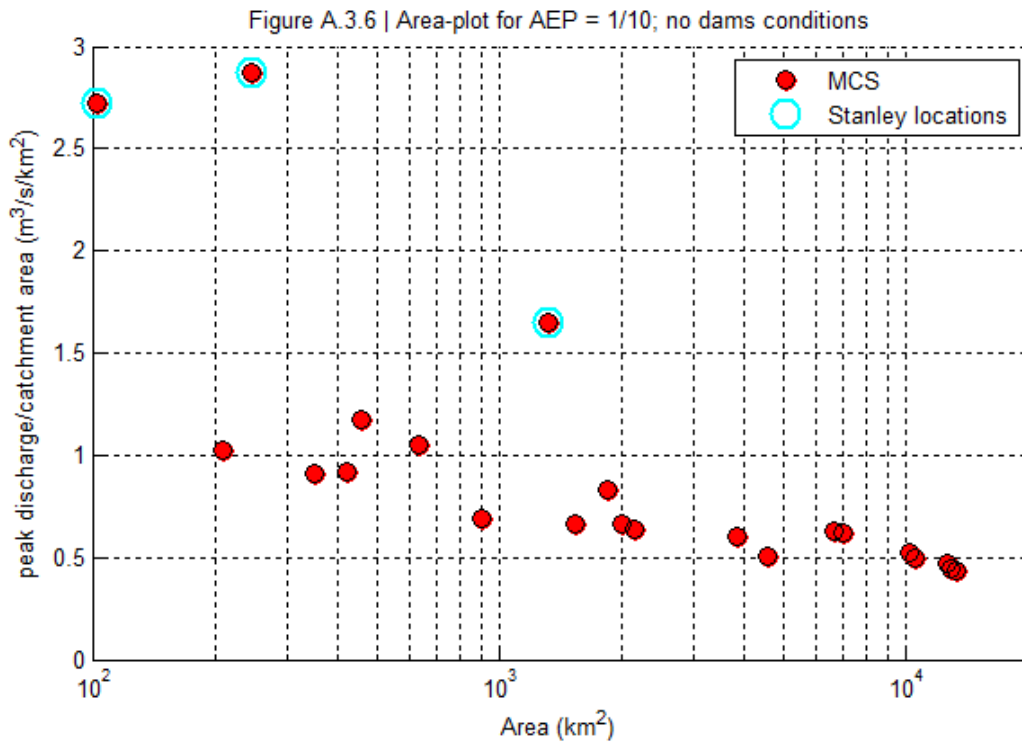
Peak flow (Q) versus catchment area (A)







Q/A versus catchment area



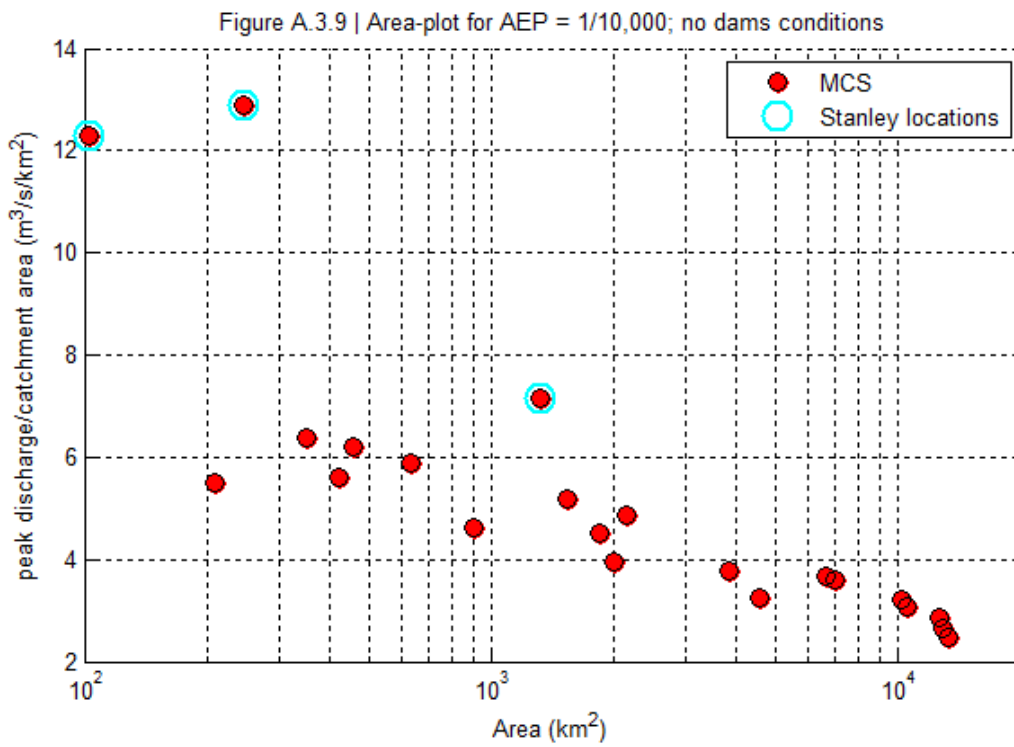
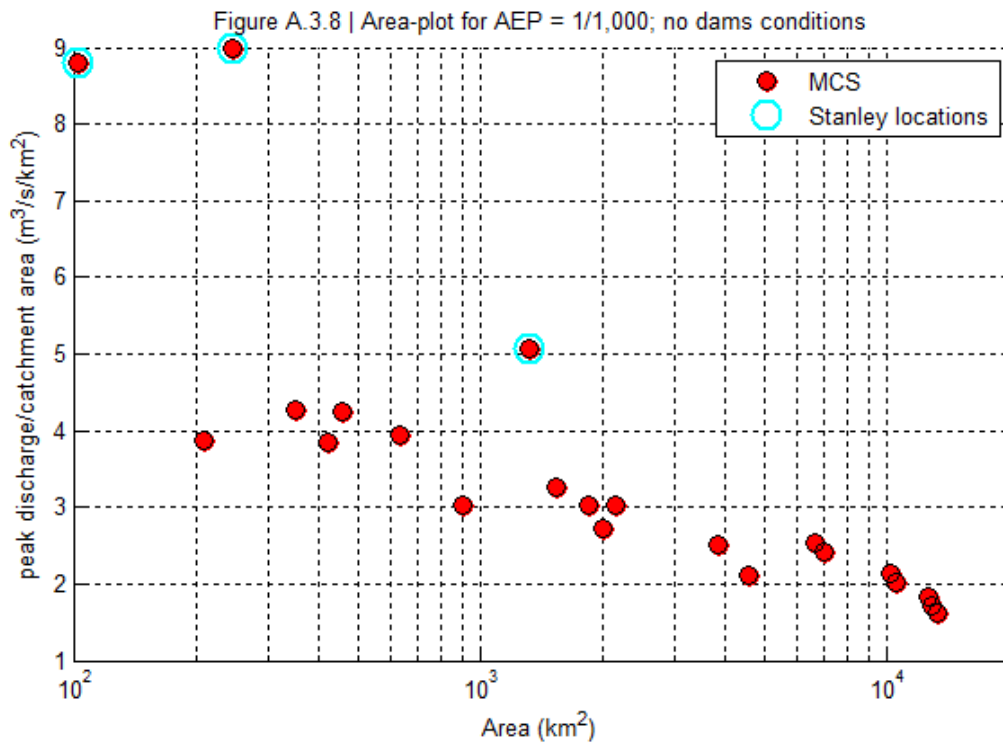
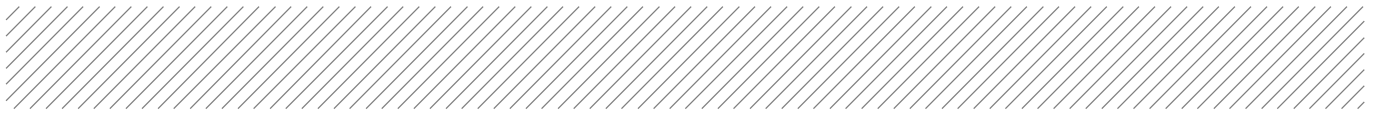
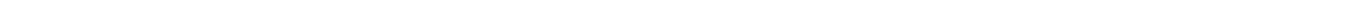
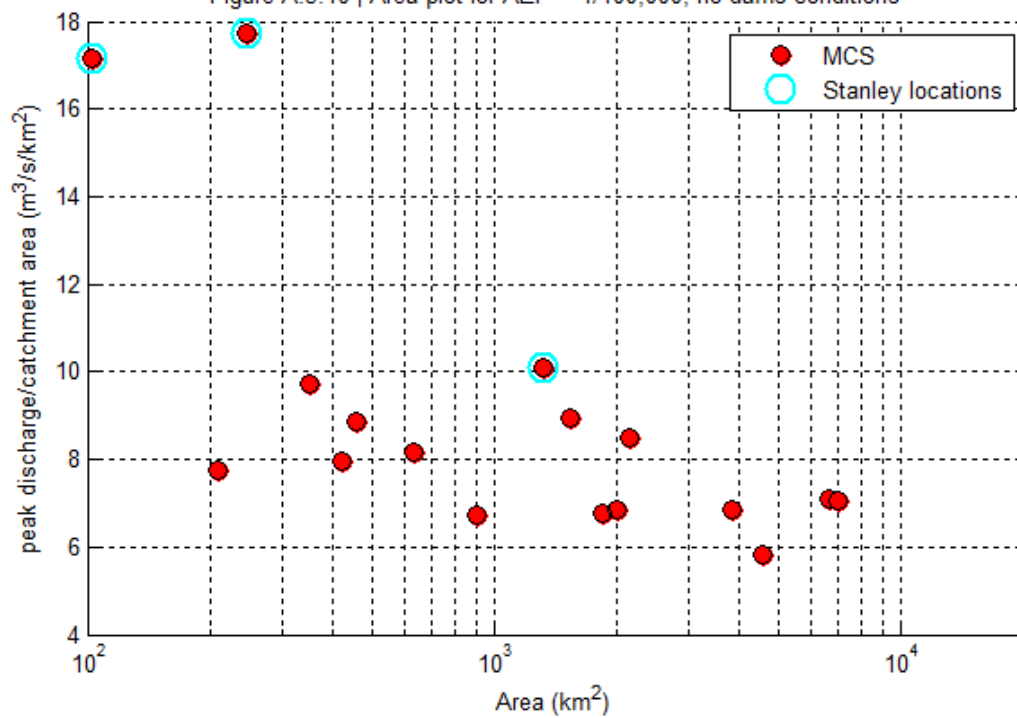
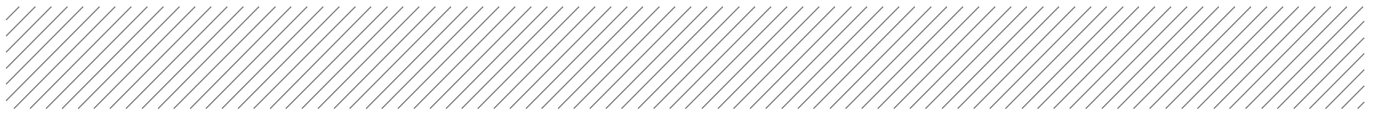




Figure A.3.10 | Area-plot for AEP = 1/100,000; no dams conditions





Appendix B

'With-dams' frequency tables and figures for peak discharges



B.1 Table

Wivenhoe peak outflows above 28,000 m³/s are displayed in red, because the maximum outflow capacity of Wivenhoe dam is equal to 28,000 m³/s. Estimates in excess of the maximum outlet capacity should be treated with caution, as the dam is likely to fail under such circumstances. Note: the 1 in 100,000 AEP peak discharge is only provided for locations for which the AEP of the PMP is below 1 in 100,000.

Table B1 Peak flows (m³/s) versus AEP; MCS results

Location	AEP (1 in N)												
	2	5	10	20	50	100	200	500	1,000	2,000	10,000	100,000	AEP of PMP
Somerset Dam	0	1700	1700	1800	2200	2500	3000	3300	3600	4000	5400	10,700	20,900
Wivenhoe	0	470	930	1700	3300	6300	8800	10,300	12,500	12,900	21,200	35,800	43,700
Savages Crossing	300	1200	2200	3500	6100	9000	12,000	15,500	17,500	20,400	28,000		57,200
Mount Crosby	360	1200	2200	3600	6000	8600	11,700	14,800	17,100	19,700	27,200		55,500
Ipswich	450	960	1400	1900	2700	3400	3900	4800	5400	5900	7900	11,500	16,400
Moggill	850	2100	3300	4800	7300	10,200	12,400	15,700	18,000	20,400	29,300		57,600
Centenary Bridge	880	2200	3300	4800	7200	9700	11,900	14,600	16,800	19,500	28,100		56,700
Brisbane	930	2300	3500	4900	7600	9700	11,700	14,400	16,300	19,100	26,900		54,800

B.2 Frequency plots

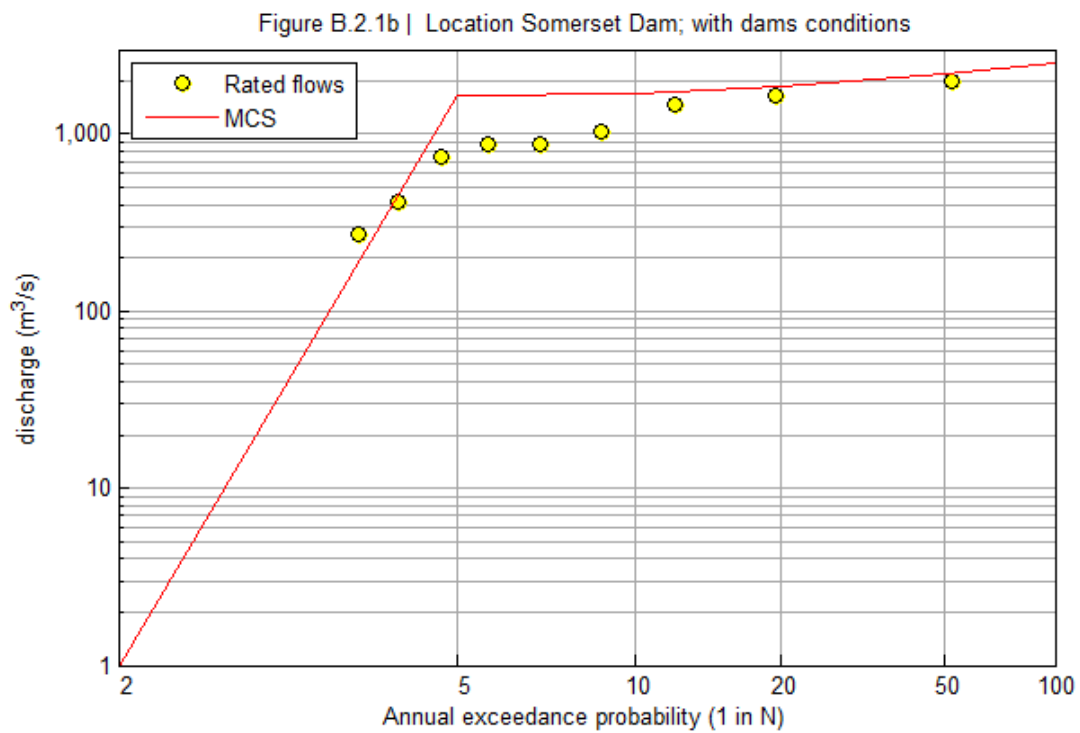
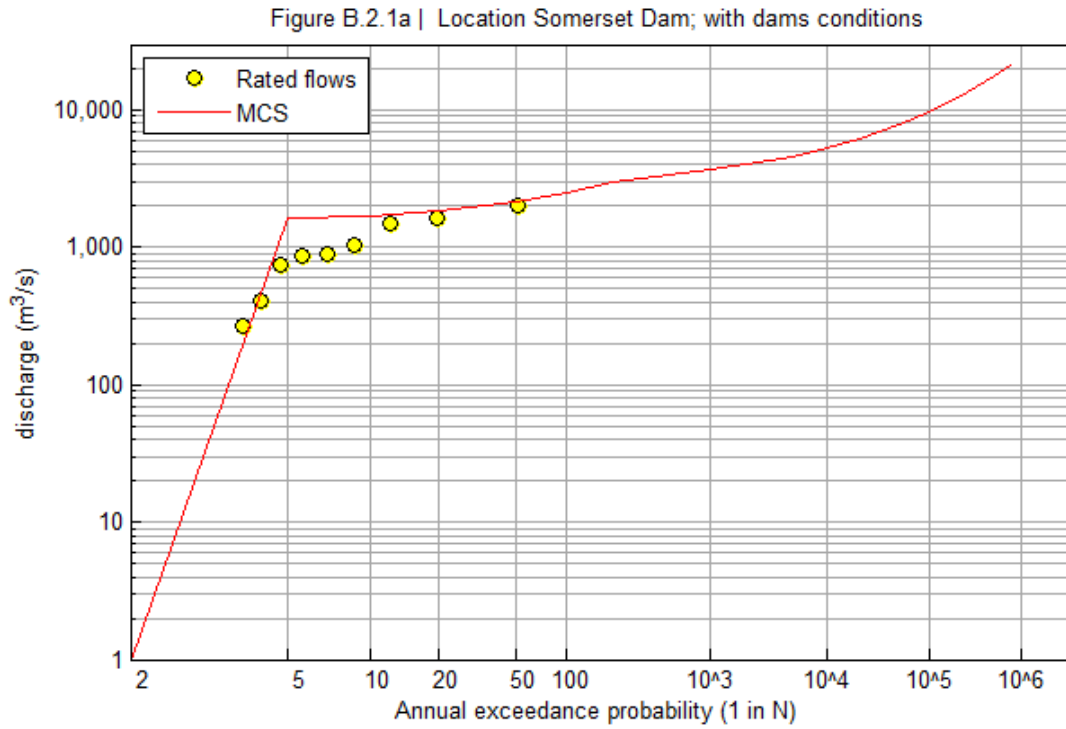




Figure B.2.2a | Location Wivenhoe, with dams conditions

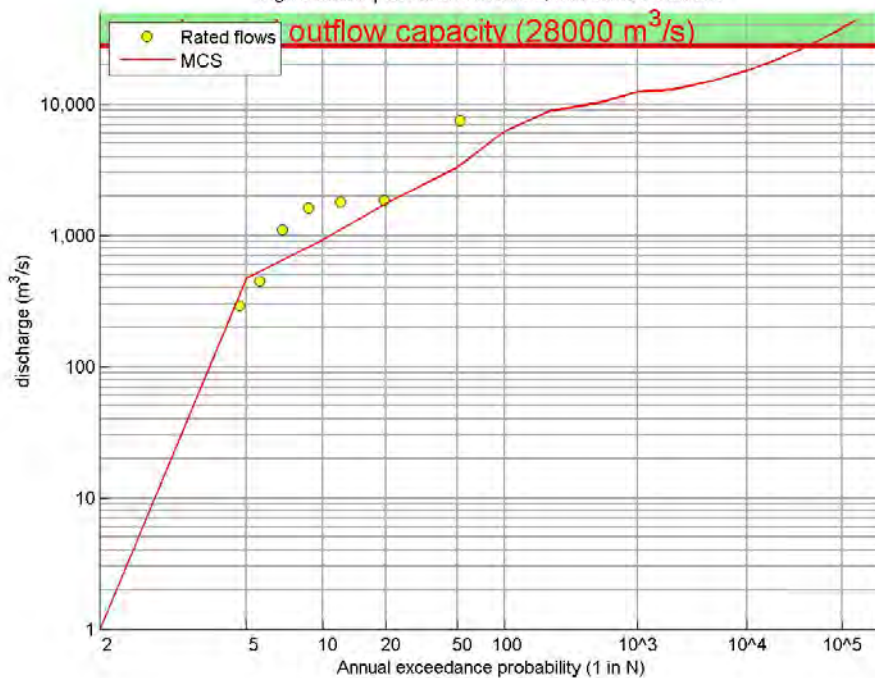


Figure B.2.2b | Location Wivenhoe; with dams conditions

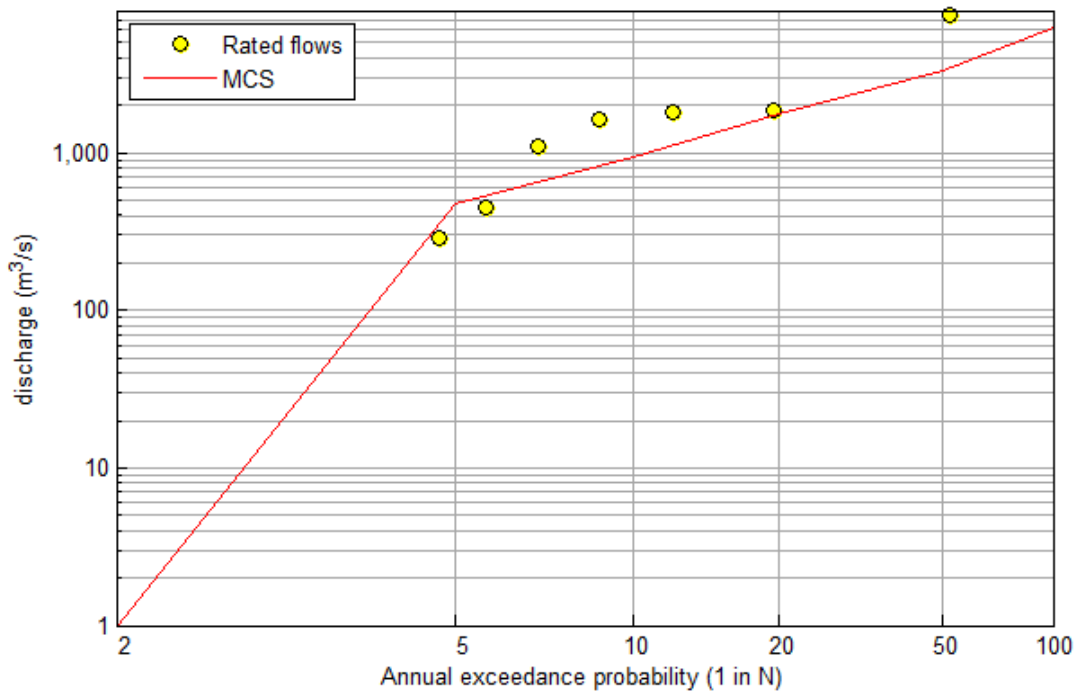




Figure B.2.3a | Location Savages Crossing; with dams conditions

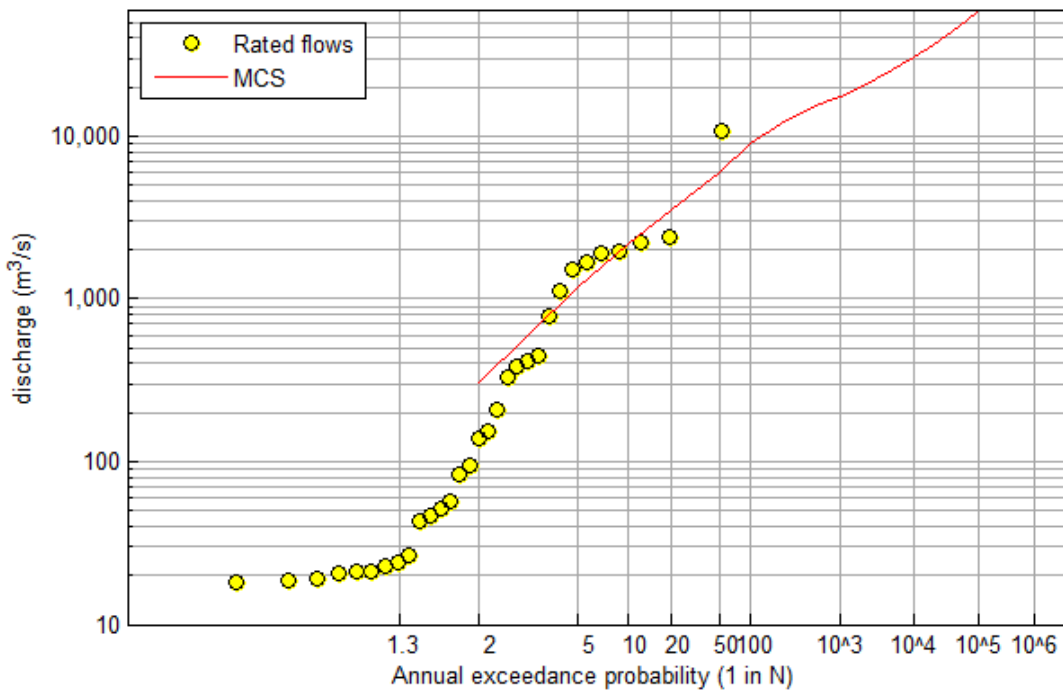


Figure B.2.3b | Location Savages Crossing; with dams conditions

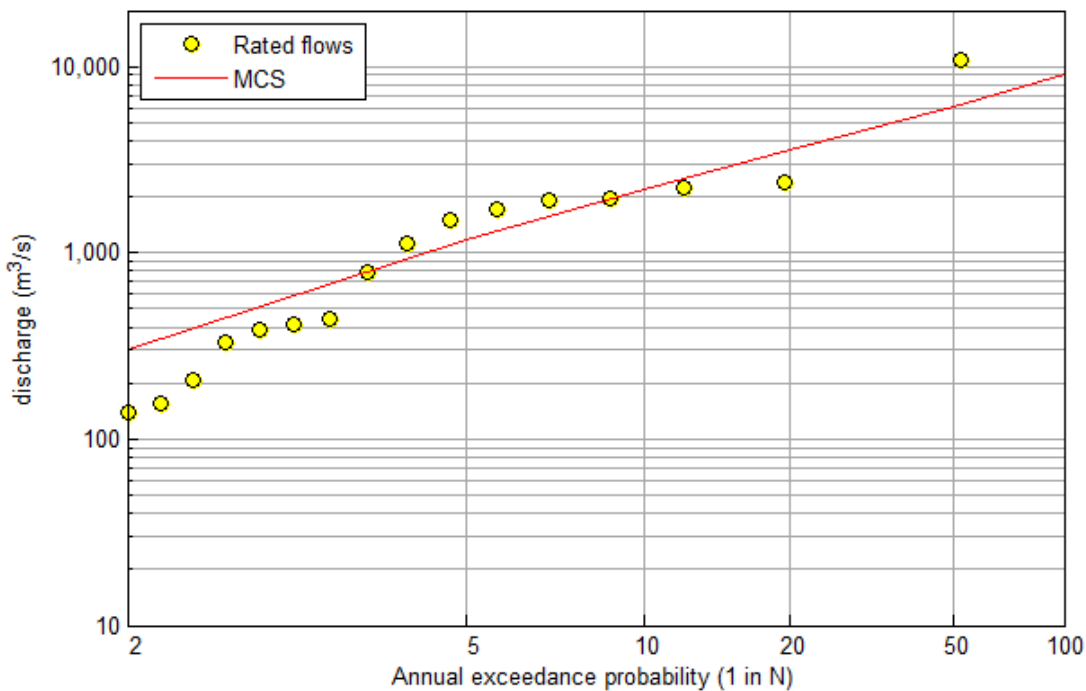




Figure B.2.4a | Location Mount Crosby; with dams conditions

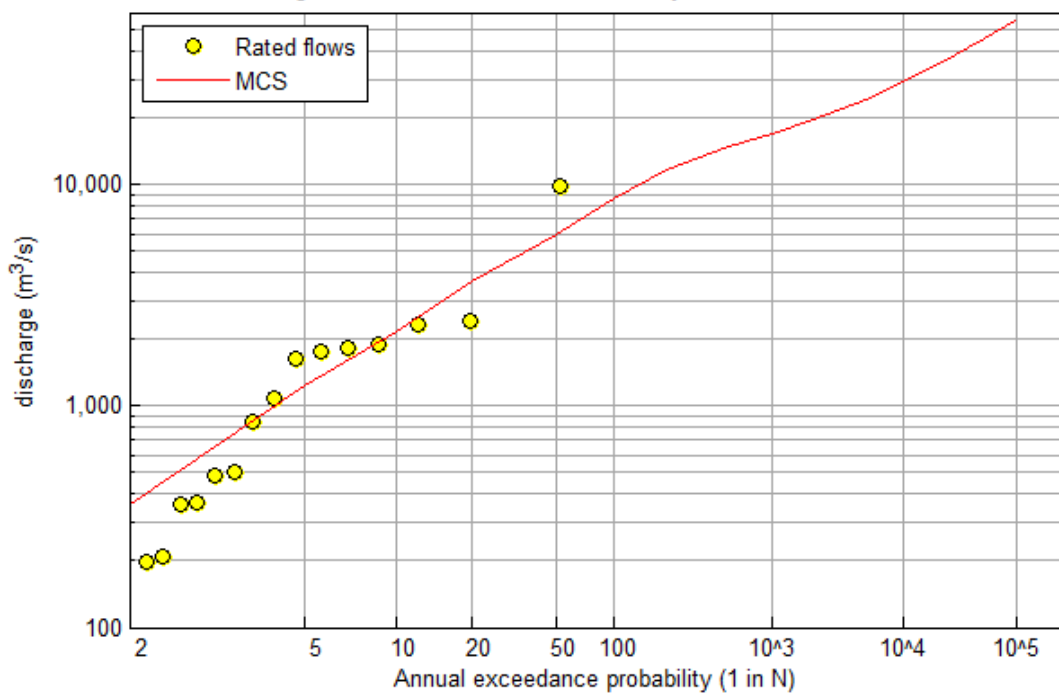
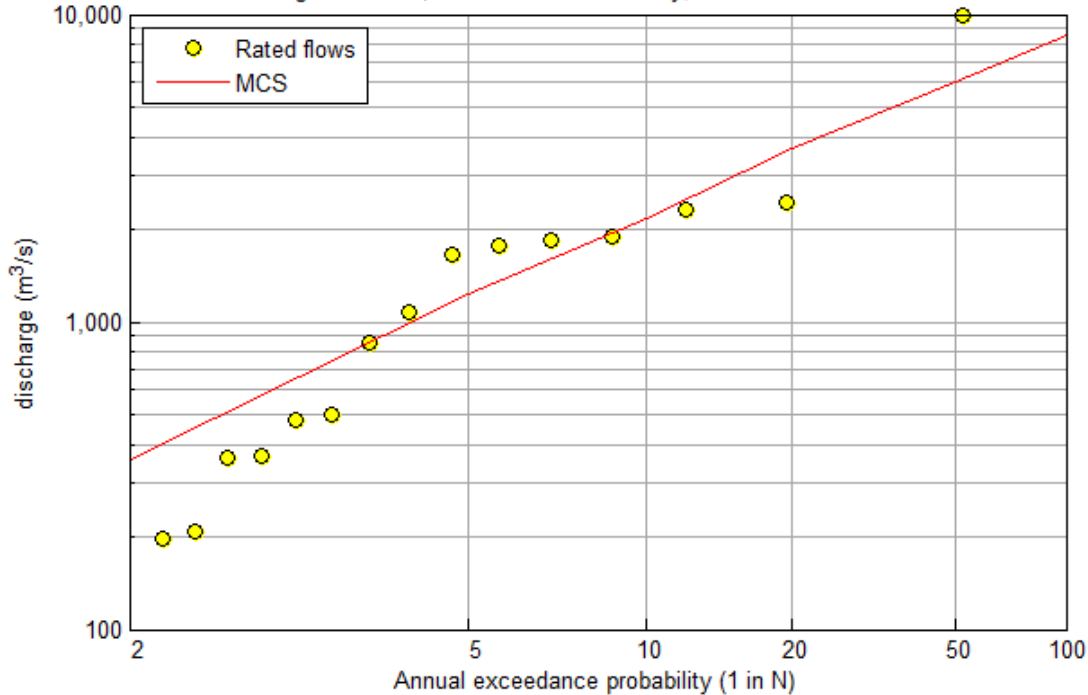


Figure B.2.4b | Location Mount Crosby; with dams conditions



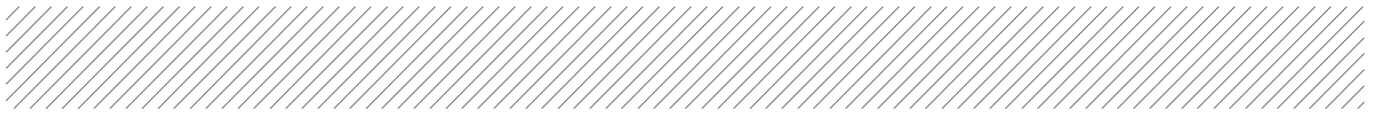


Figure B.2.5a | Location Ipswich; with dams conditions

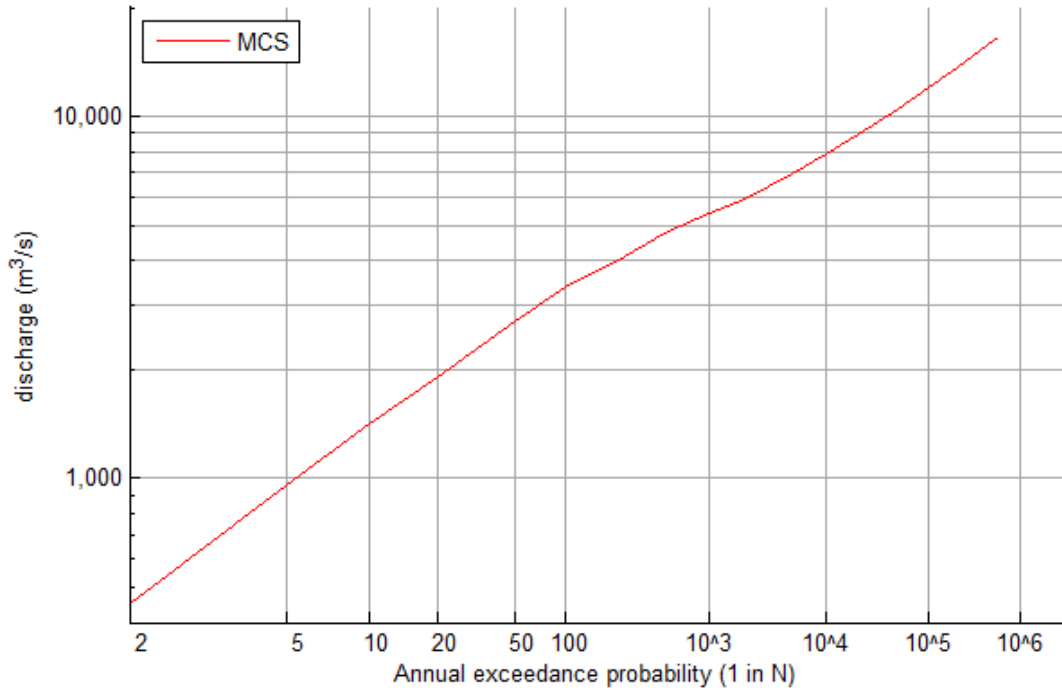


Figure B.2.5b | Location Ipswich; with dams conditions

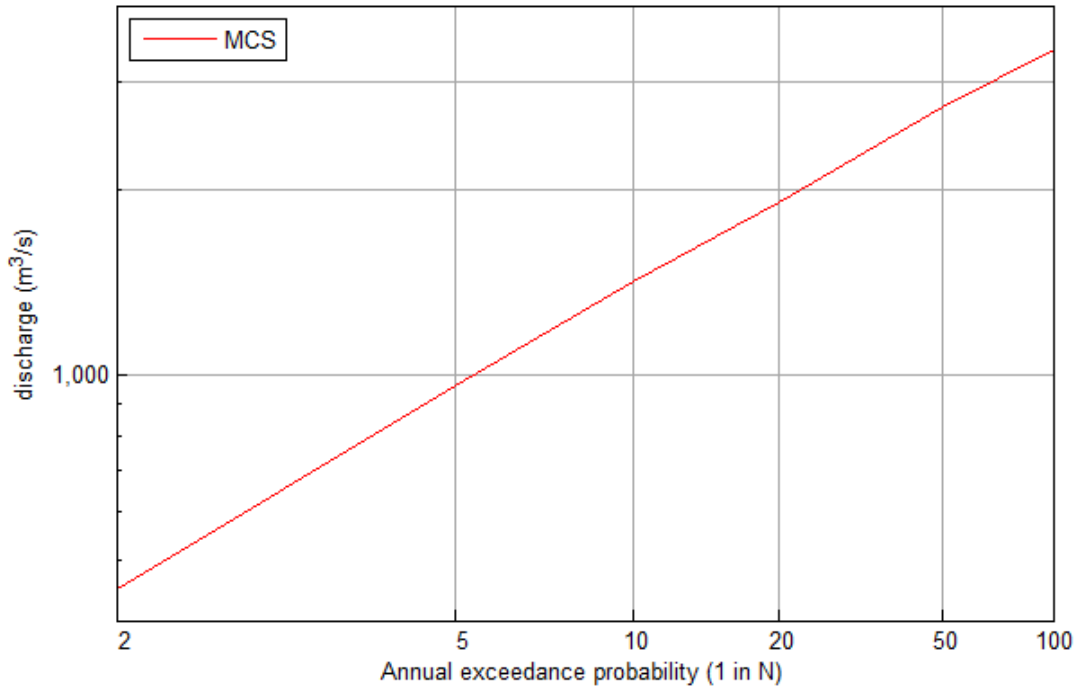




Figure B.2.6a | Location Moggill; with dams conditions

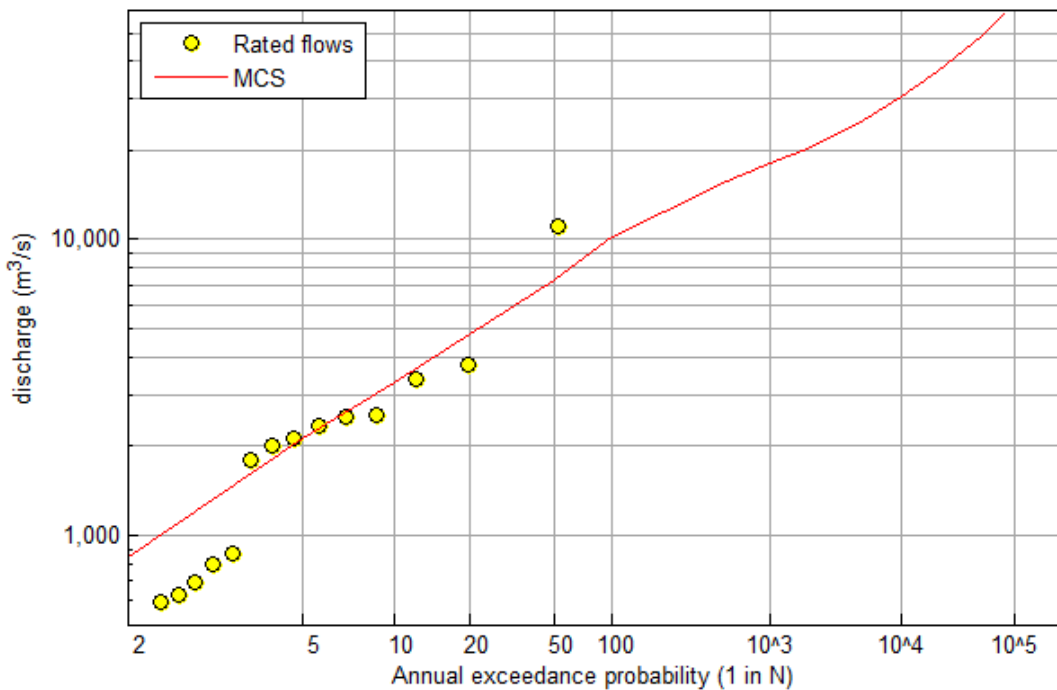


Figure B.2.6b | Location Moggill; with dams conditions

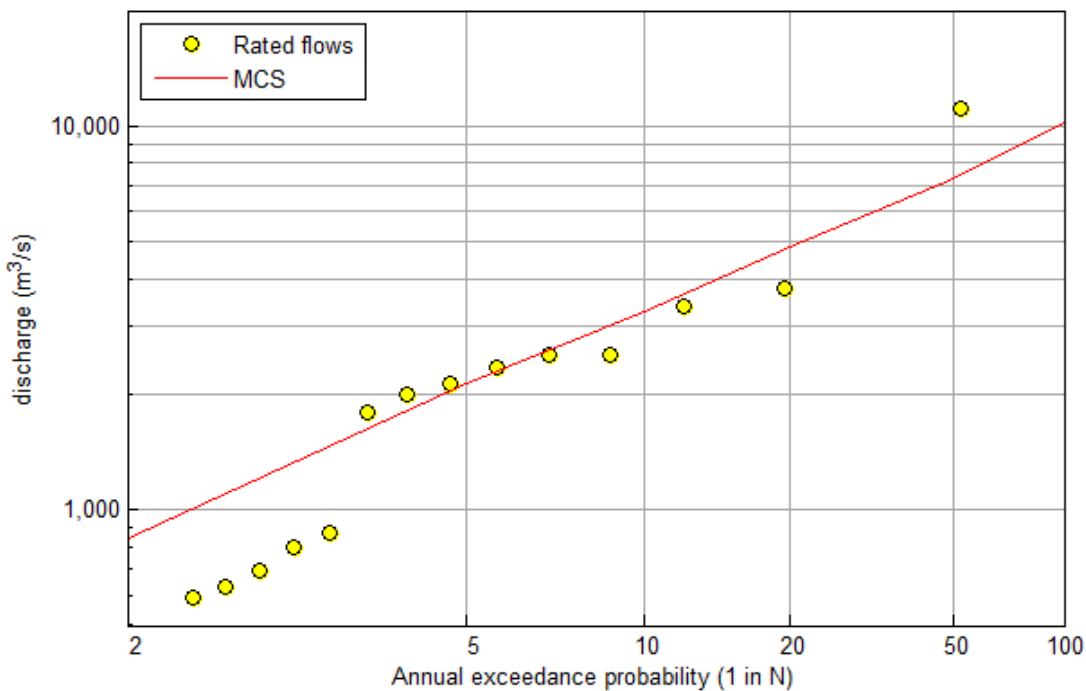




Figure B.2.7a | Location Centenary Bridge; with dams conditions

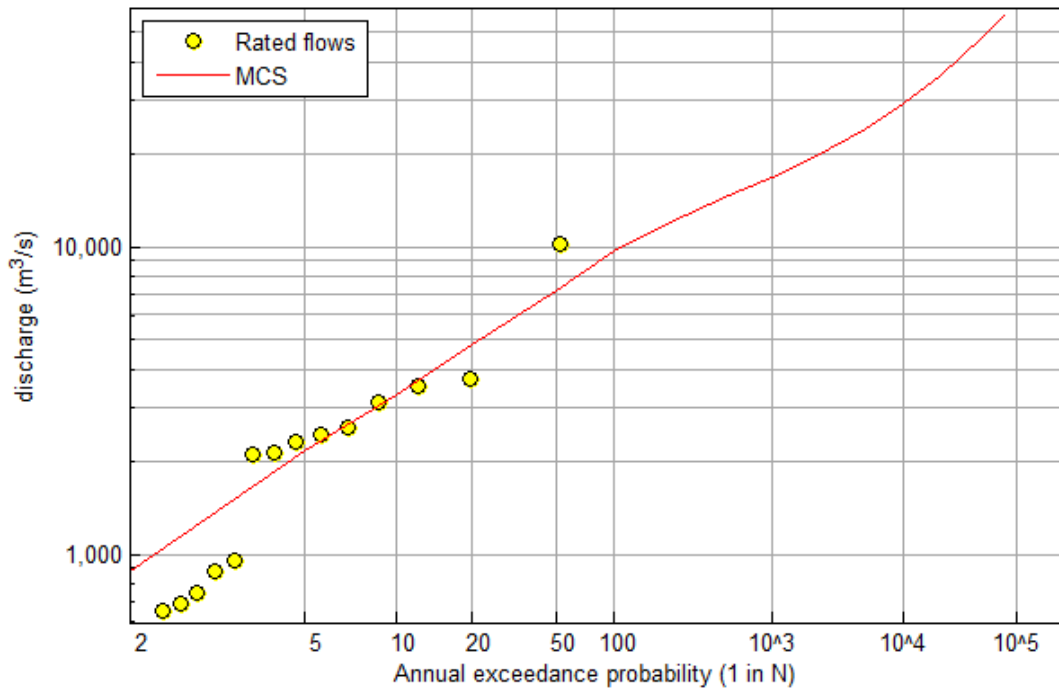


Figure B.2.7b | Location Centenary Bridge; with dams conditions

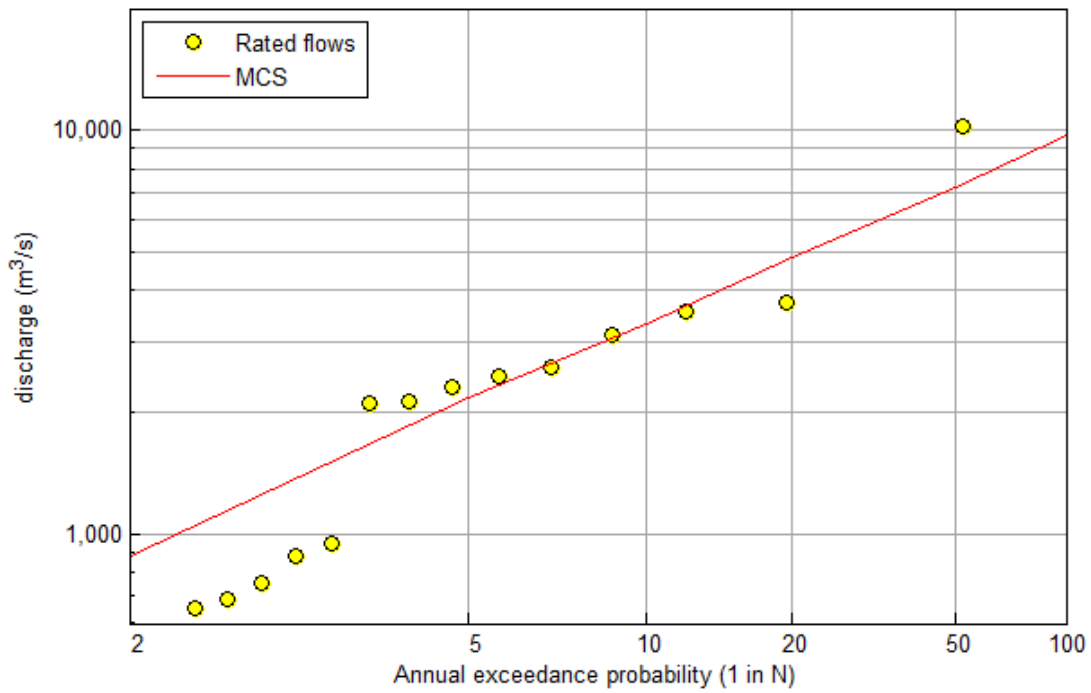




Figure B.2.8a | Location Brisbane; with dams conditions

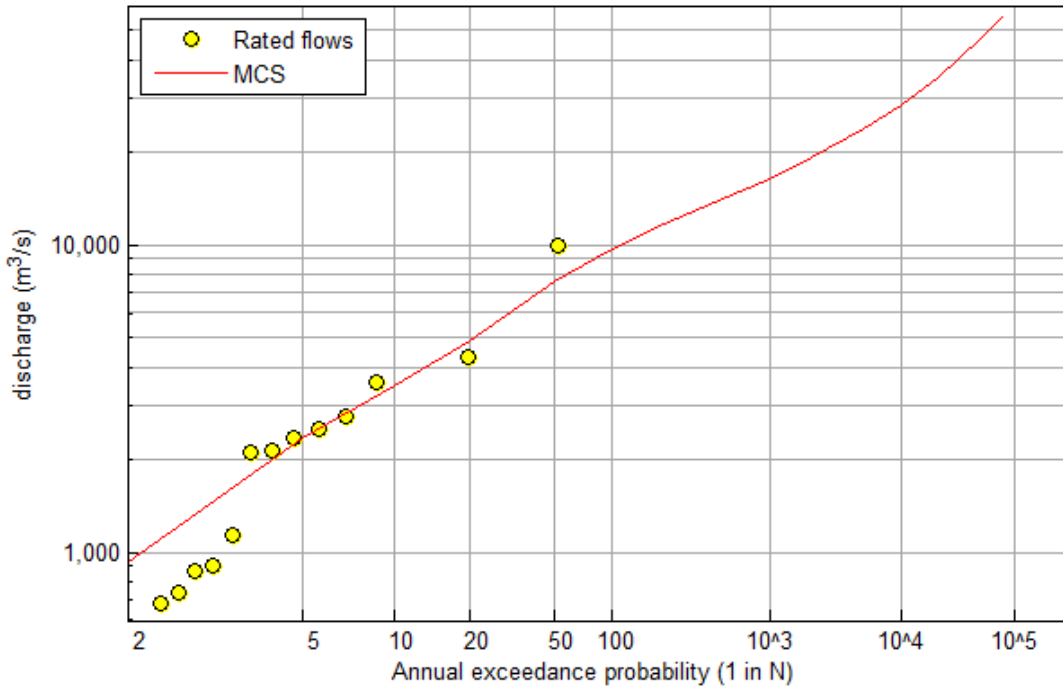
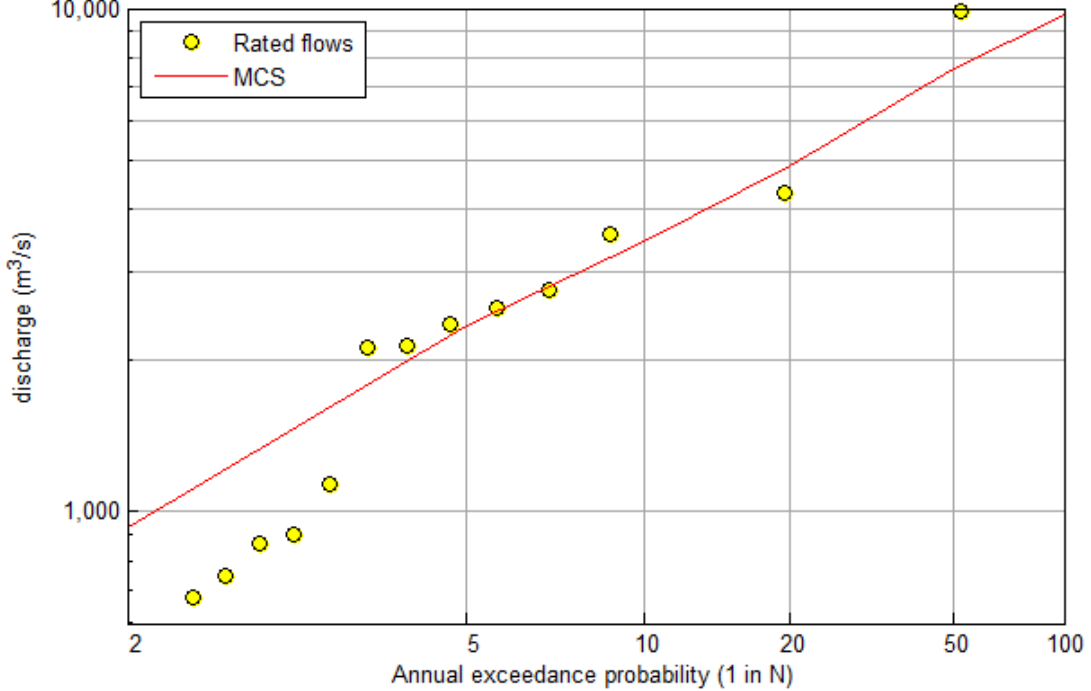
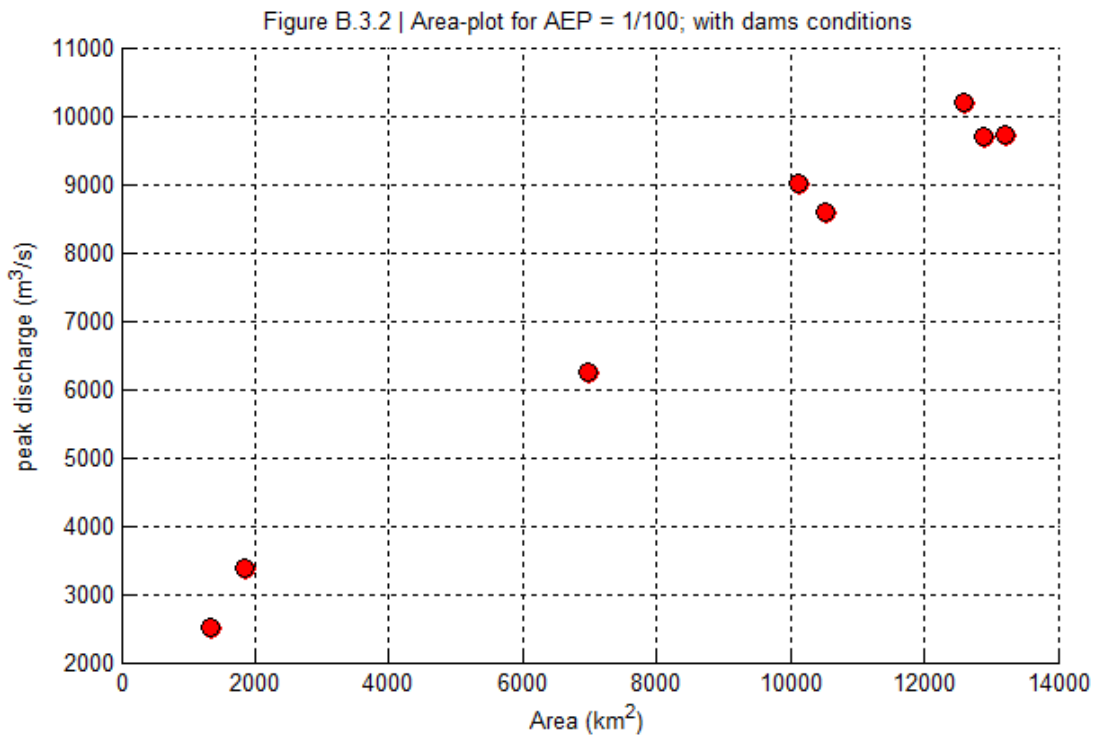
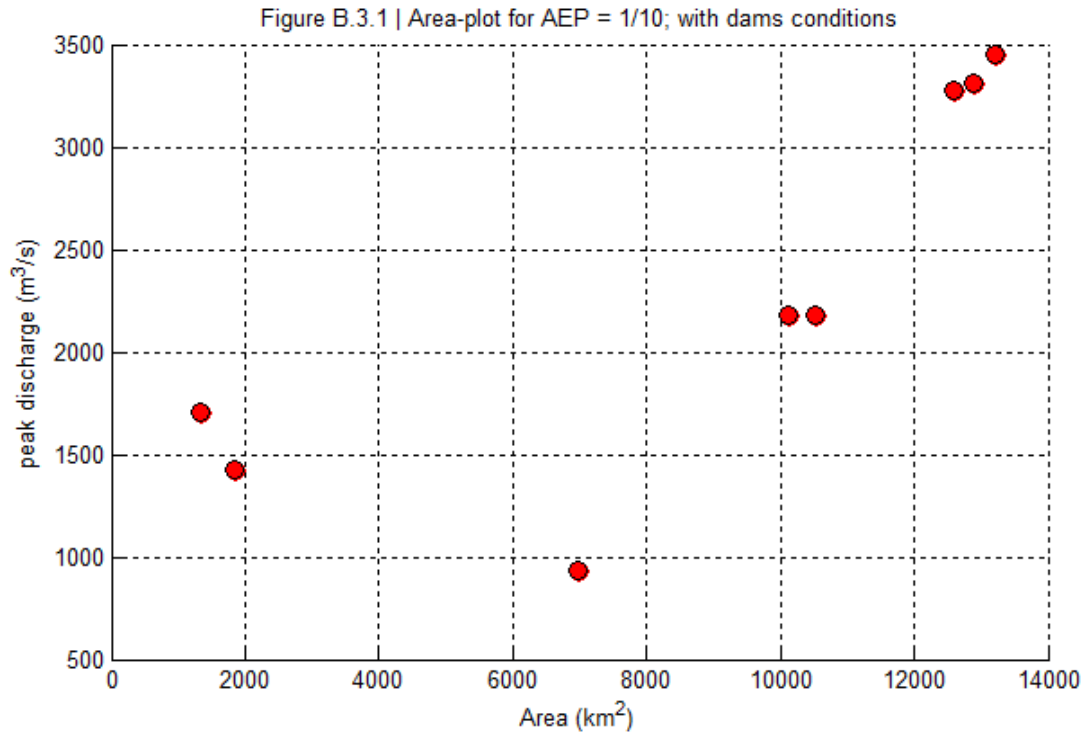


Figure B.2.8b | Location Brisbane; with dams conditions



B.3 Plots of catchment area versus peak discharge

This section contains figures in which catchment area is compared with peak discharge. For a range of AEP's, the design peak flows are plotted against catchment area.



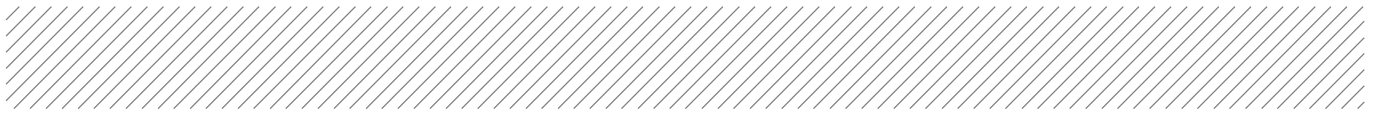


Figure B.3.3 | Area-plot for AEP = 1/1,000; with dams conditions

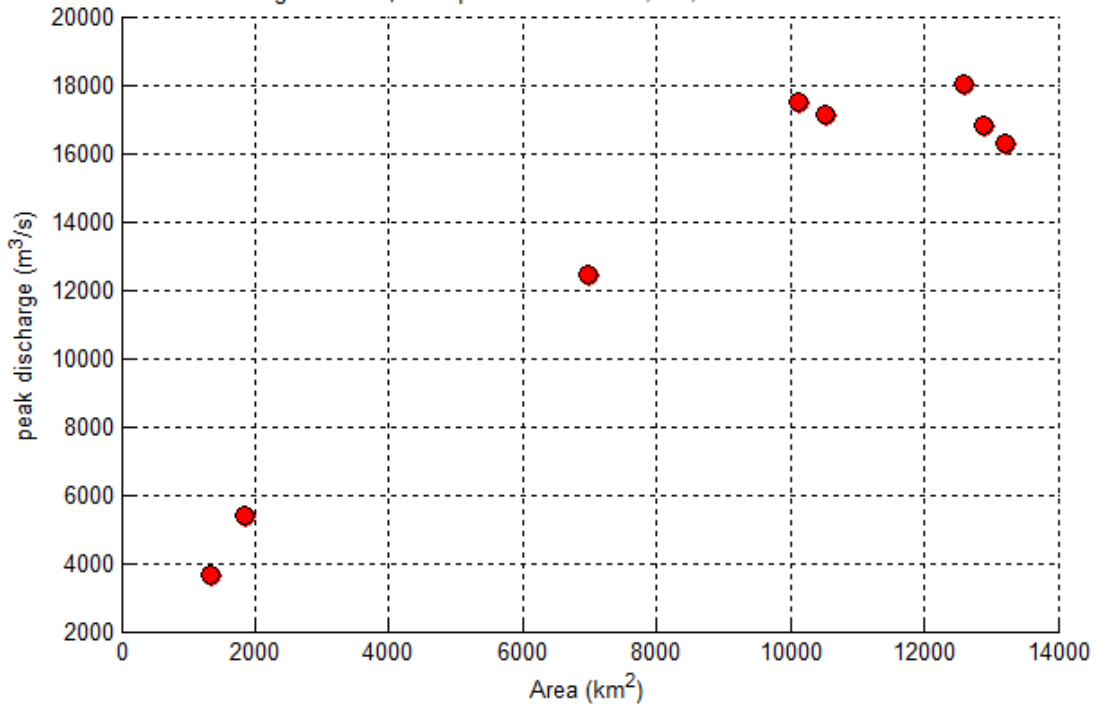
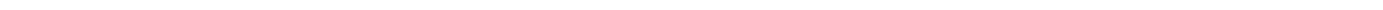
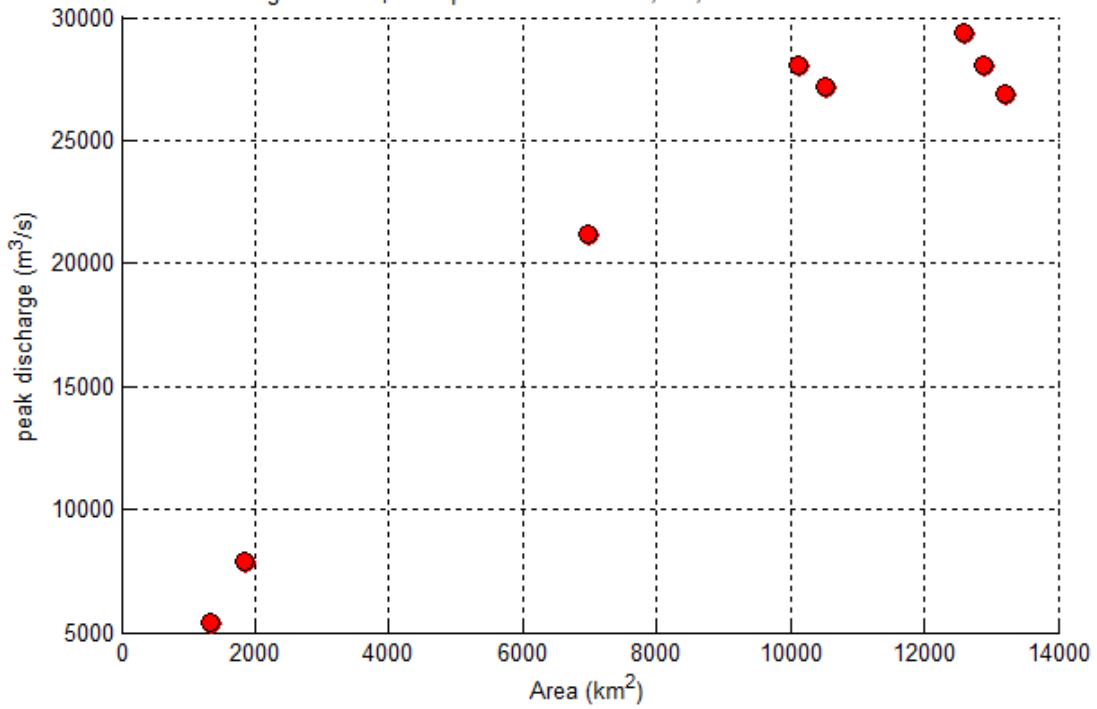
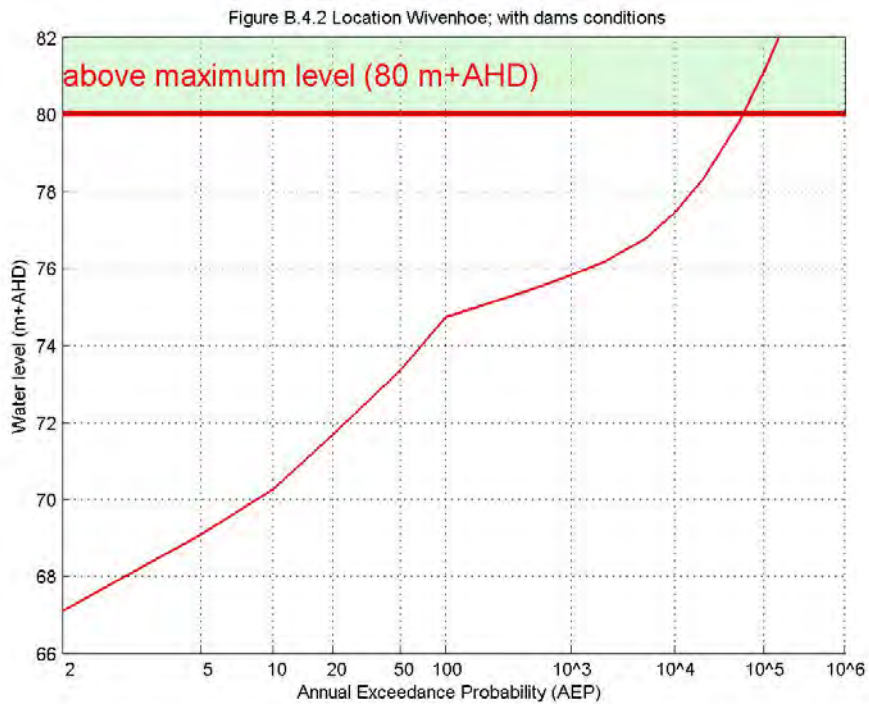
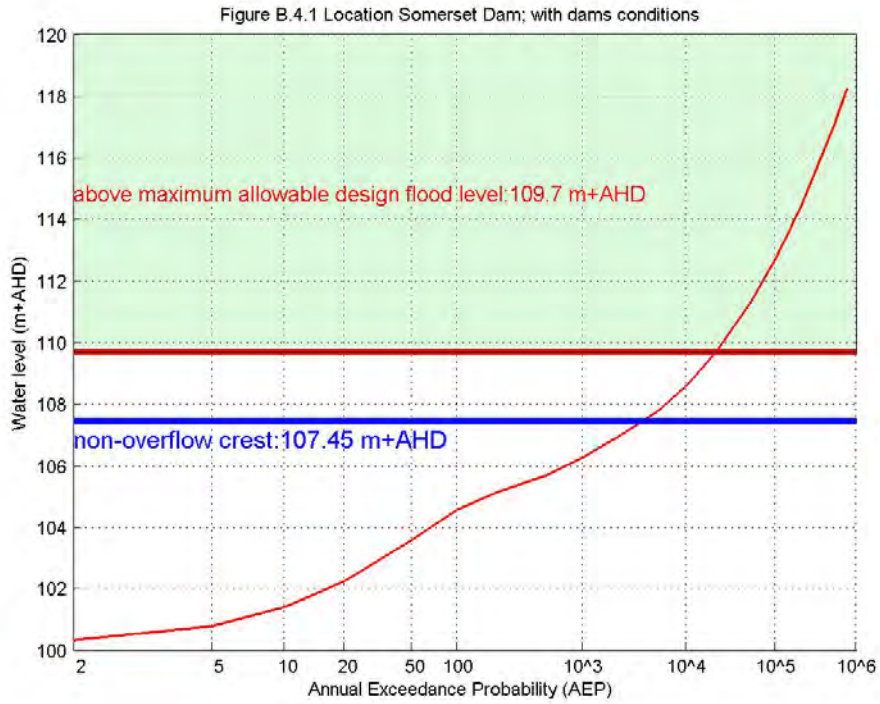


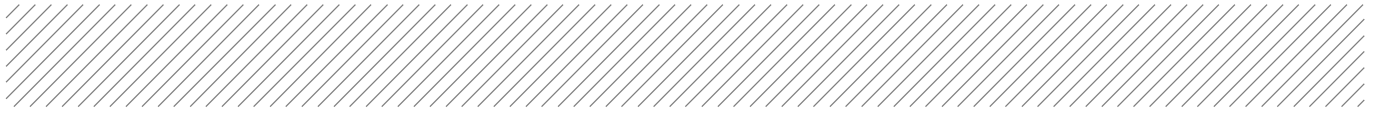
Figure B.3.4 | Area-plot for AEP = 1/10,000; with dams conditions



B.4 Frequency plots of reservoir water levels

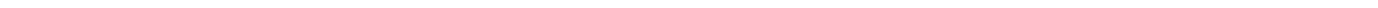
The Figures below show MCS frequency curves for water levels at Somerset Dam and Wivenhoe Dam.





Appendix C

'No-dams' design flow volumes



C.1 Tables

Note: the 1 in 100,000 AEP flow volume is only provided for locations for which the AEP of the PMP is below 1 in 100,000.

Table C1 Maximum 24-hour flow volumes (1000 ML) versus AEP; MCS results

Location	AEP (1 in N)												AEP of PMP
	2	5	10	20	50	100	200	500	1,000	2,000	10,000	100,000	
Linville	11	40	81	120	180	240	270	320	360	390	520	890	1400
Gregors Creek	24	75	140	230	340	450	520	600	670	730	980	1800	2400
Fulham Vale	19	72	140	230	350	440	510	600	670	740	1000	1800	2400
Peachester	7	12	18	24	31	38	45	53	60	65	90	120	150
Woodford	17	33	47	62	84	100	120	140	160	180	230	310	390
Somerset Dam	45	88	130	180	250	310	350	410	450	500	650	930	1200
Tinton	4	13	22	32	46	61	71	82	93	100	140	200	330
Middle Ck	76	190	310	480	670	880	1000	1200	1300	1400	2000	3600	4100
Wivenhoe	73	190	320	480	690	880	990	1200	1300	1500	1900	3600	4100
Helidon	2	8	16	24	35	46	53	62	69	78	110	160	310
Gatton	8	29	51	82	110	160	190	230	260	290	420	720	1200
Glenore Grove	11	43	75	110	160	220	270	330	360	410	590	1000	1600
Savages Crossing	88	230	390	600	860	1100	1300	1500	1700	1900	2600		5000
Mount Crosby	90	230	390	600	860	1100	1300	1500	1700	1800	2600		5000
Walloon	14	26	39	55	78	95	110	130	140	160	220	310	480
Kalbar Weir	13	24	34	47	65	79	91	110	120	130	170	250	390
Amberley	20	38	53	74	100	130	150	180	200	220	280	420	650
Loamside	4	10	14	20	27	33	38	46	52	56	75	100	150

Location	AEP (1 in N)												AEP of PMP
	2	5	10	20	50	100	200	500	1,000	2,000	10,000	100,000	
Ipswich	35	75	110	150	200	250	290	340	380	430	580	900	1200
Moggill	130	290	470	690	960	1200	1400	1600	1900	2100	2900		5300
Centenary Bridge	130	290	460	680	930	1200	1300	1600	1800	2100	2800		5200
Brisbane	130	290	460	700	940	1100	1300	1600	1800	2000	2700		5100

Table C2 Maximum 48-hour flow volumes (1000 ML) versus AEP; MCS results

Location	AEP (1 in N)												AEP of PMP
	2	5	10	20	50	100	200	500	1,000	2,000	10,000	100,000	
Linville	15	53	120	190	270	380	420	480	530	590	760	1300	2000
Gregors Creek	32	110	220	350	520	710	810	930	1000	1100	1500	2700	3600
Fulham Vale	27	98	220	350	520	710	810	920	1000	1100	1500	2700	3500
Peachester	10	19	28	40	51	62	75	89	99	110	140	190	220
Woodford	26	51	73	100	140	170	200	240	280	310	380	500	610
Somerset Dam	69	140	210	300	410	510	590	690	770	860	1100	1500	1800
Tinton	5	17	33	52	71	98	110	130	140	160	200	300	510
Middle Ck	120	290	510	810	1100	1400	1700	1900	2100	2400	3100	5700	6600
Wivenhoe	120	300	520	790	1200	1500	1700	2000	2100	2400	3200	6000	6900
Helidon	3	11	22	38	52	72	83	96	110	120	150	240	460
Gatton	10	37	72	120	180	250	300	360	390	450	610	1000	1700
Glenore Grove	15	56	100	170	250	370	440	510	570	660	880	1500	2200
Savages Crossing	150	370	630	980	1400	1900	2200	2600	2800	3200	4400		8600
Mount Crosby	150	380	650	1000	1500	1900	2200	2600	2900	3300	4400		8900

Location	AEP (1 in N)												AEP of PMP
	2	5	10	20	50	100	200	500	1,000	2,000	10,000	100,000	
Walloon	20	39	61	88	120	160	180	210	230	250	330	470	720
Kalbar Weir	18	34	52	75	100	130	150	170	190	2410	260	380	590
Amberley	30	60	88	130	170	220	250	280	320	350	450	670	1000
Loamside	6	14	21	32	42	54	53	75	82	93.	110	160	230
Ipswich	52	110	170	250	330	420	490	560	630	710	920	1400	1800
Moggill	210	490	790	1200	1700	2200	2500	3000	3300	3800	5000		9800
Centenary Bridge	210	500	790	1200	1700	2200	2500	2900	3300	3700	4900		9800
Brisbane	220	510	810	1200	1700	2200	2500	2900	3200	3700	4900		9700

Table C3 Maximum 72-hour flow volumes (1000 ML) versus AEP; MCS results

Location	AEP (1 in N)												AEP of PMP
	2	5	10	20	50	100	200	500	1,000	2,000	10,000	100,000	
Linville	17	65	140	220	340	470	520	610	660	730	920	1600	2600
Gregors Creek	38	120	260	440	660	920	1000	1200	1300	1400	1800	3300	4500
Fulham Vale	32	120	260	420	650	8890	1000	1200	1300	1400	1800	3300	4400
Peachester	13	25	35	47	64	77	91	110	130	150	190	250	290
Woodford	32	63	92	130	170	210	250	310	360	400	510	660	790
Somerset Dam	87	170	260	380	490	630	750	860	980	1100	1400	1900	2300
Tinton	6	20	40	62	92	120	140	160	180	200	250	360	650
Middle Ck	150	370	630	1000	1400	1900	2200	2500	2800	3100	3900	7400	8600
Wivenhoe	150	390	660	1000	1500	2000	2300	2600	2900	3200	4100	7700	8900
Helidon	3	13	28	45	66	92	100	120	130	150	180	290	590

Location	AEP (1 in N)												
	2	5	10	20	50	100	200	500	1,000	2,000	10,000	100,000	AEP of PMP
Gatton	11	44	90	150	210	310	380	450	490	560	730	1200	2100
Glenore Grove	19	66	130	210	320	460	550	650	730	800	1000	1800	2700
Savages Crossing	190	460	820	1200	1900	2600	3000	3500	3800	4400	5700		11,000
Mount Crosby	190	480	850	1300	2000	2600	3000	3600	3900	4400	5800		12,000
Walloon	23	49	77	110	150	200	220	260	290	320	400	580	910
Kalbar Weir	22	44	66	95	130	170	190	220	240	270	330	470	790
Amberley	38	75	110	170	240	290	330	380	420	460	570	850	1300
Loamside	8	17	26	39	53	68	79	93	100	120	140	200	290
Ipswich	63	140	210	320	440	570	640	740	830	900	1100	1700	2400
Moggill	270	630	1100	1600	2200	3000	3500	4000	4600	5100	6700		13,000
Centenary Bridge	270	650	110	1600	2200	3000	3400	4000	4500	5100	6700		13,000
Brisbane	280	660	1100	1700	2300	3000	3400	4000	4500	5000	6800		13,000

C.2 Frequency plots

Figure C.2.1 | Location Linville; no dams conditions

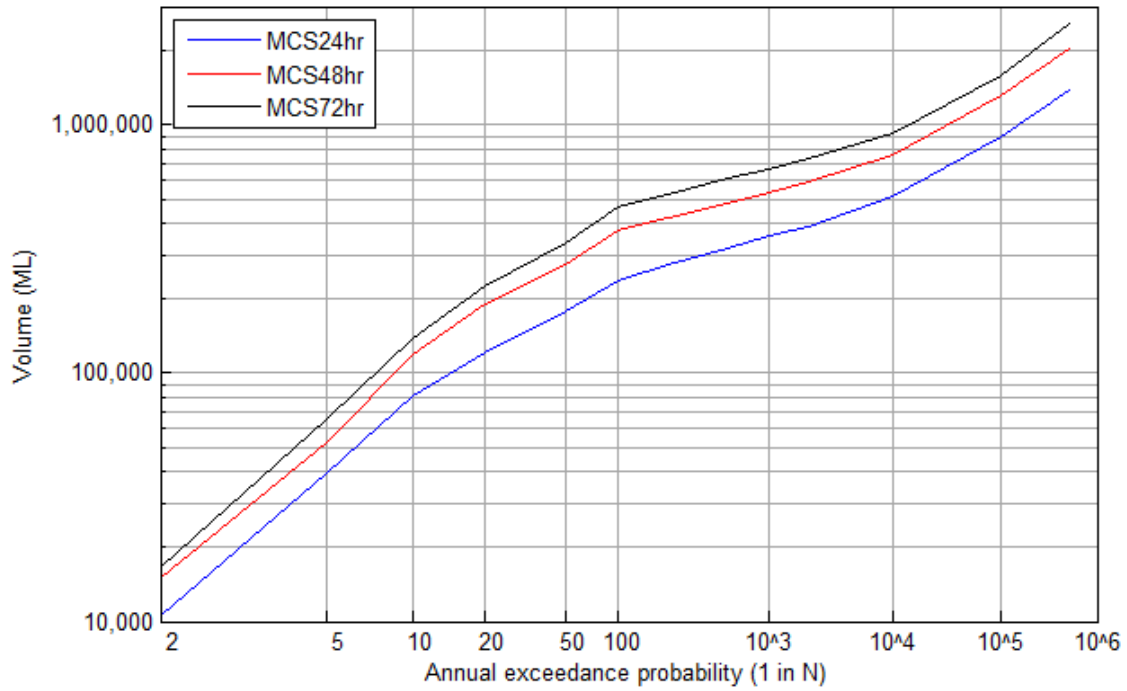


Figure C.2.2 | Location Gregors Creek; no dams conditions

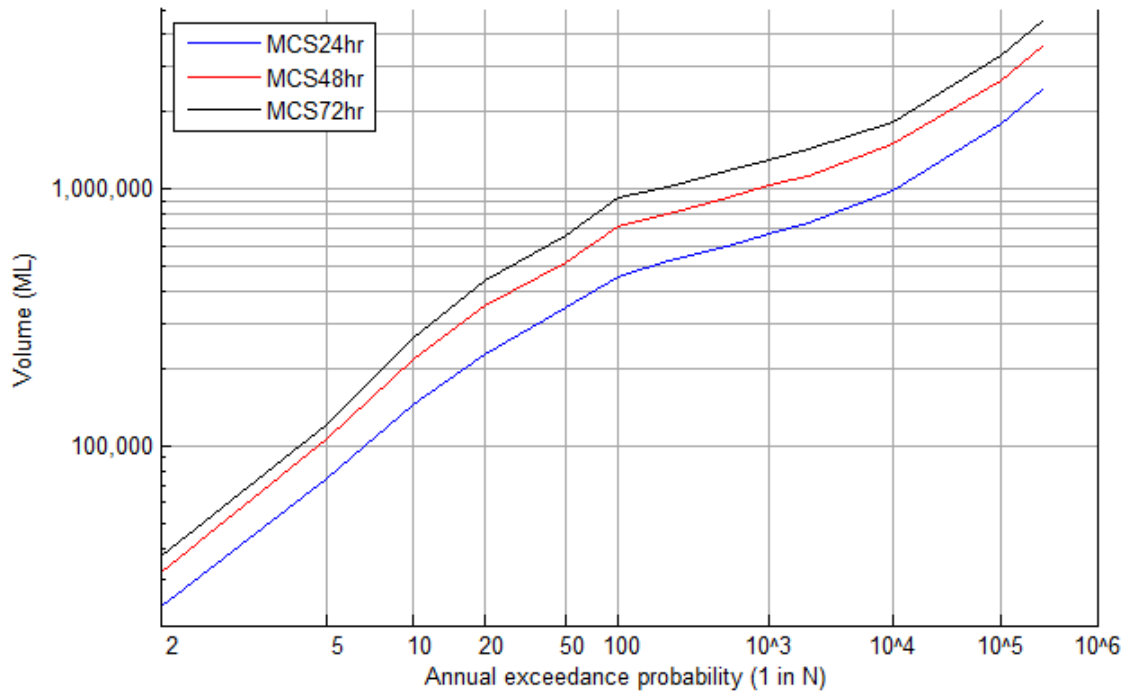




Figure C.2.3 | Location Fulham Vale; no dams conditions

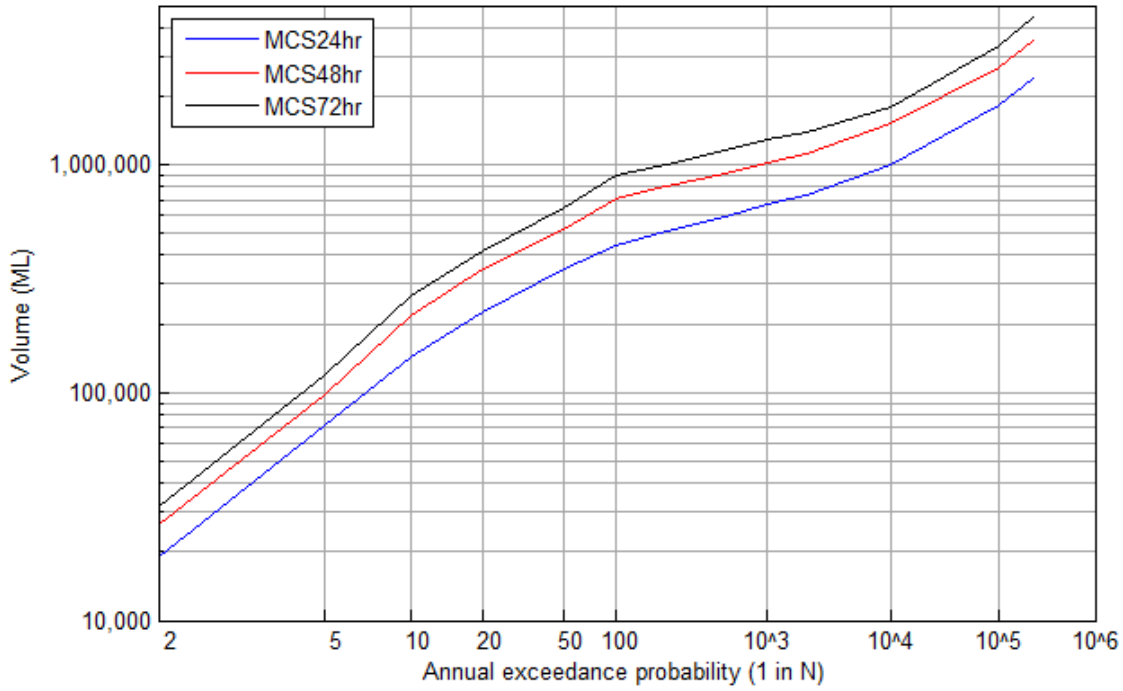


Figure C.2.4 | Location Peacheater; no dams conditions

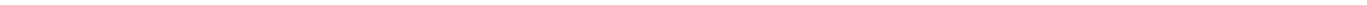
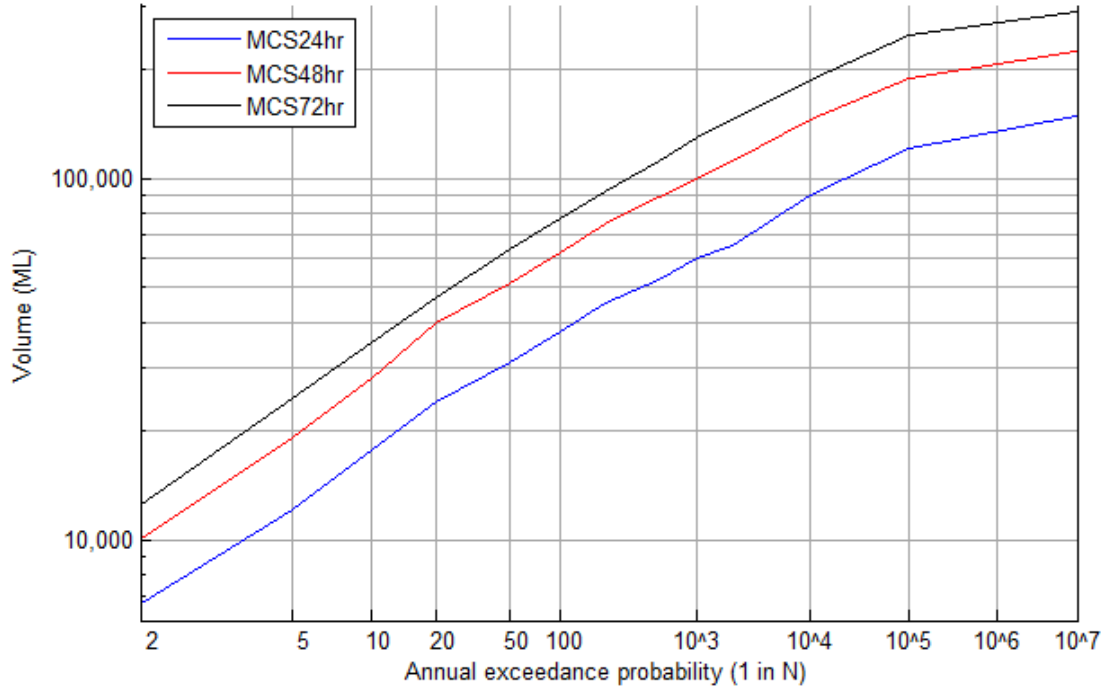




Figure C.2.5 | Location Woodford; no dams conditions

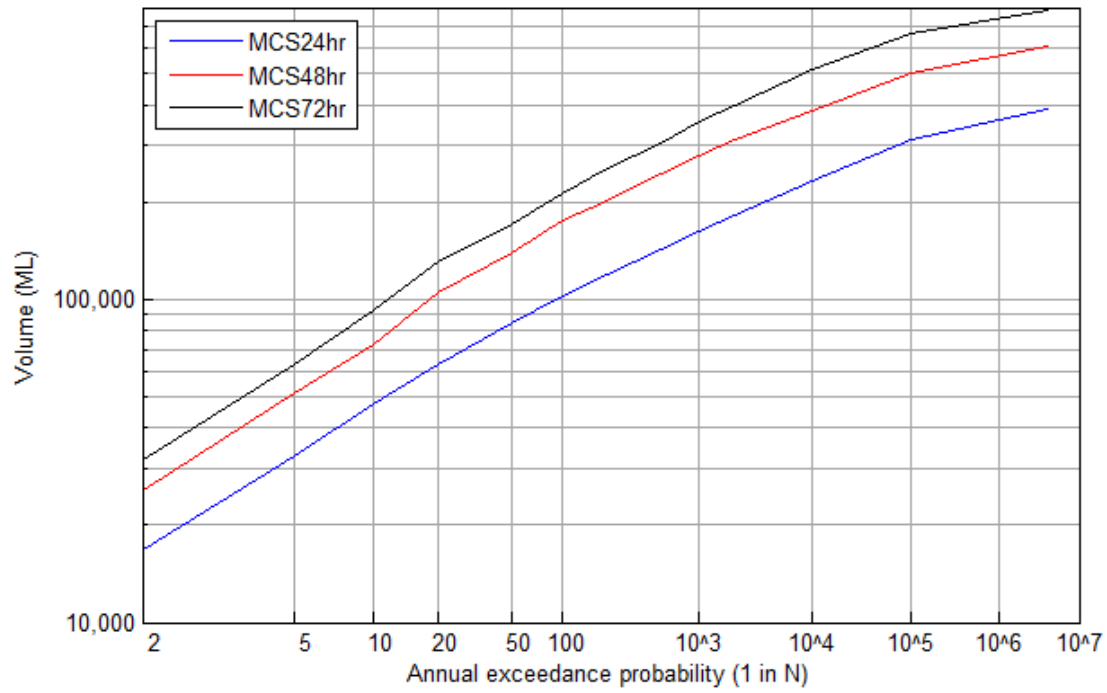


Figure C.2.6 | Location Somerset Dam; no dams conditions

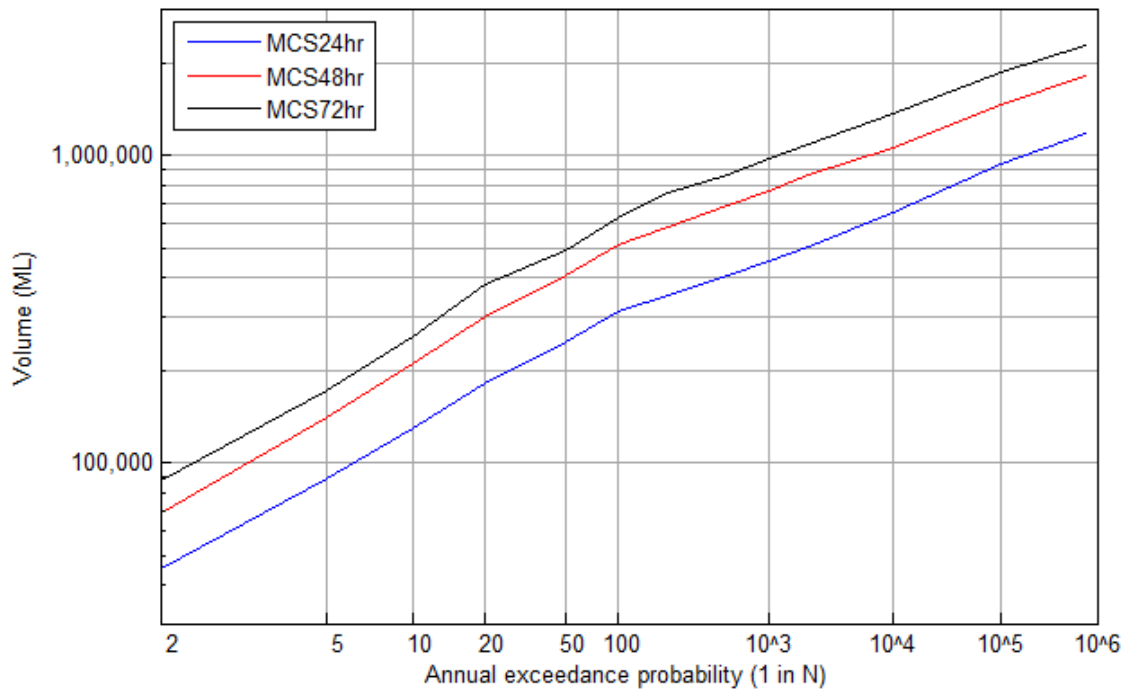




Figure C.2.7 | Location Tinton; no dams conditions

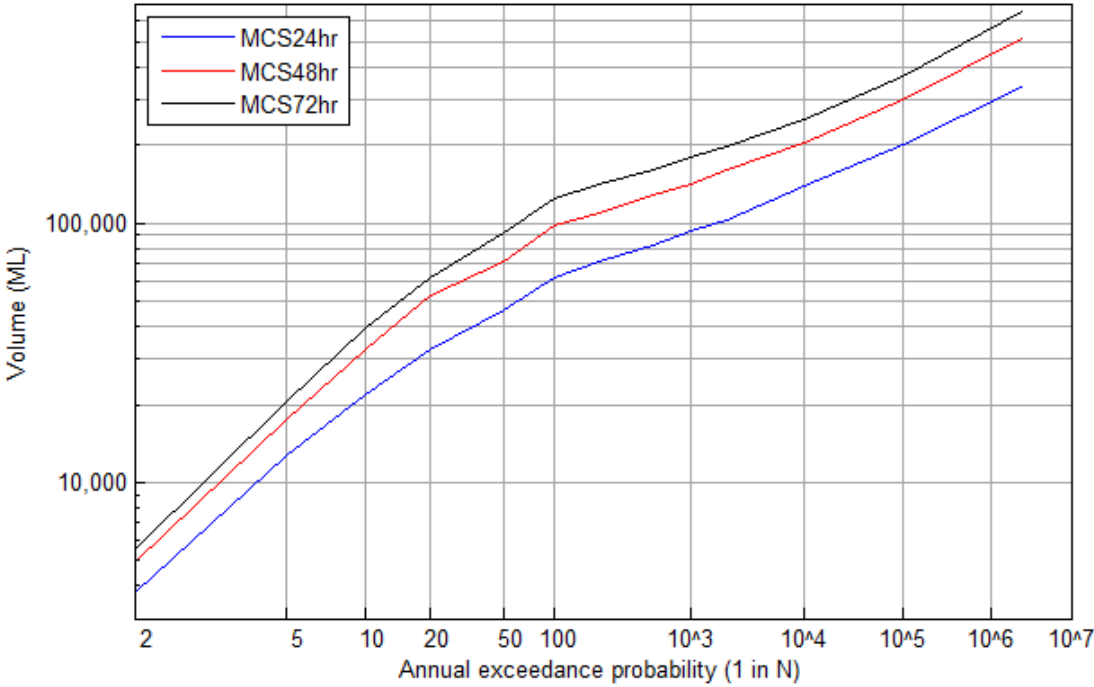


Figure C.2.8 | Location Middle Ck; no dams conditions

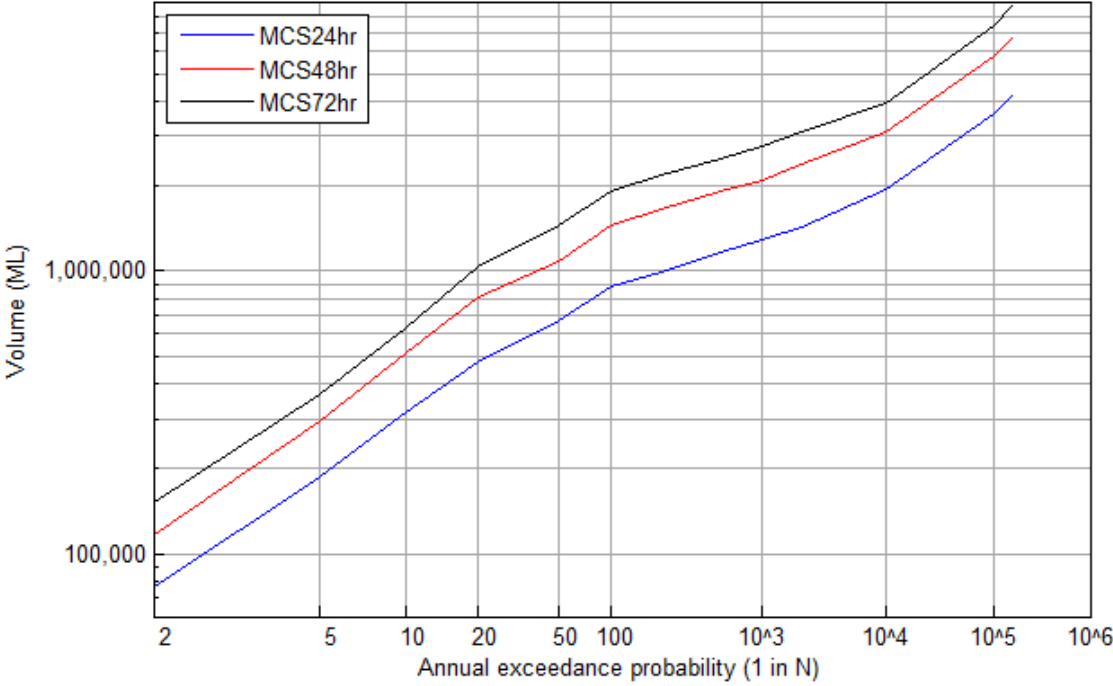




Figure C.2.9 | Location Wivenhoe; no dams conditions

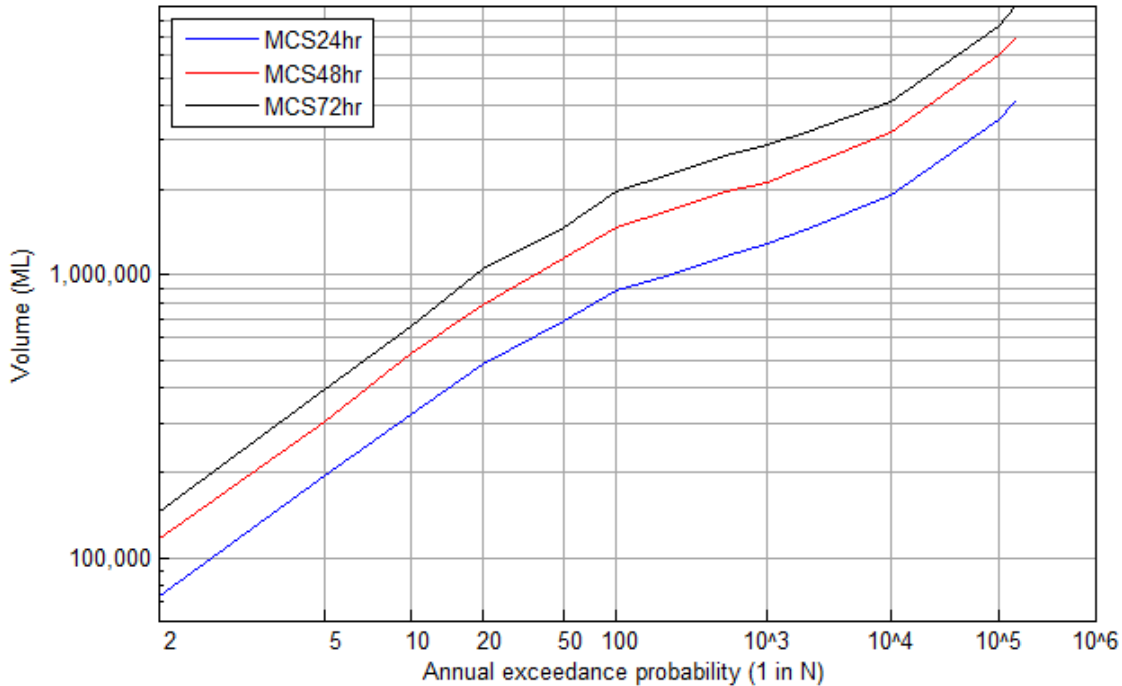


Figure C.2.10 | Location Helidon; no dams conditions

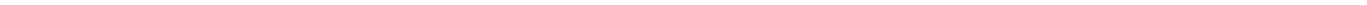
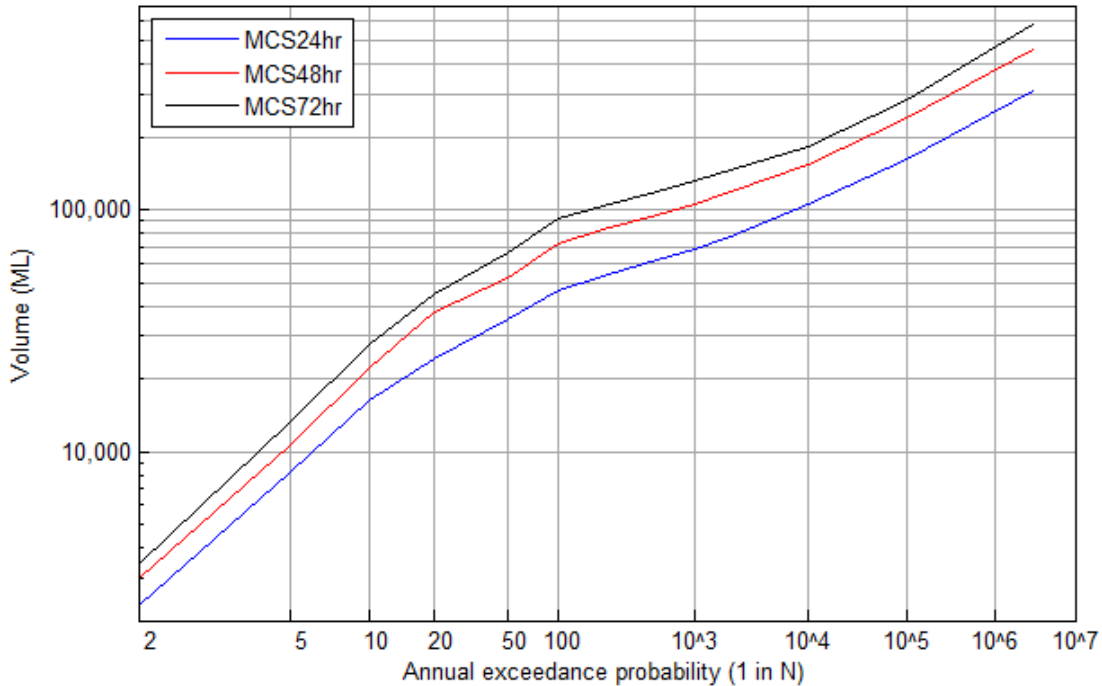




Figure C.2.11 | Location Gatton; no dams conditions

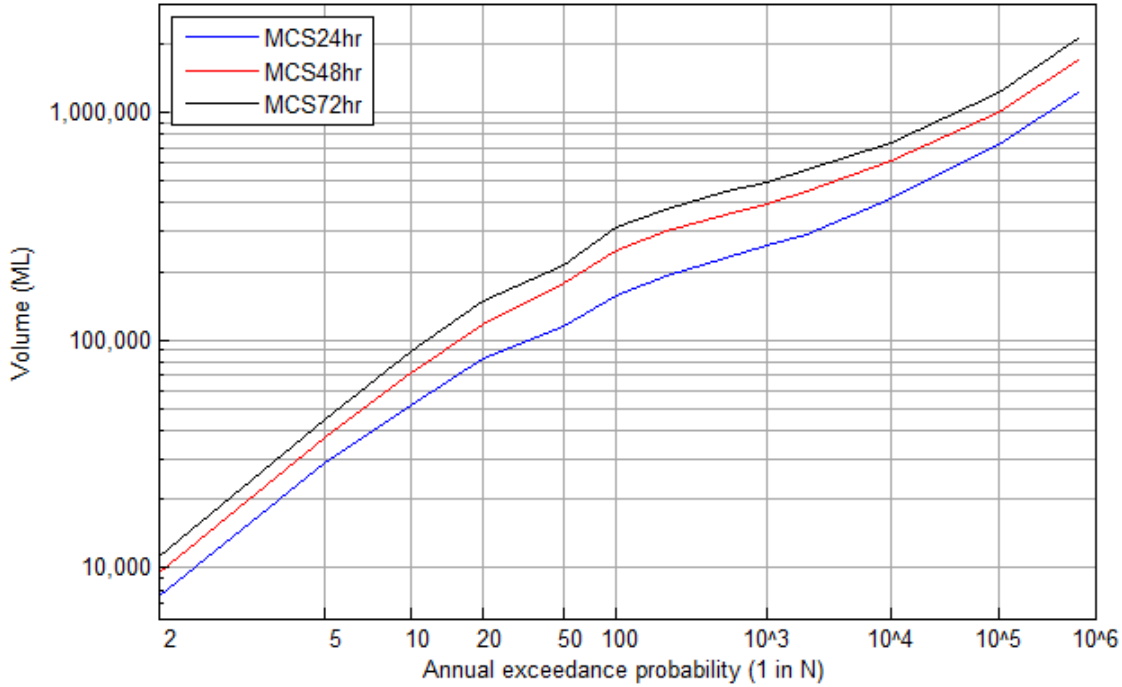


Figure C.2.12 | Location Glenore Grove; no dams conditions

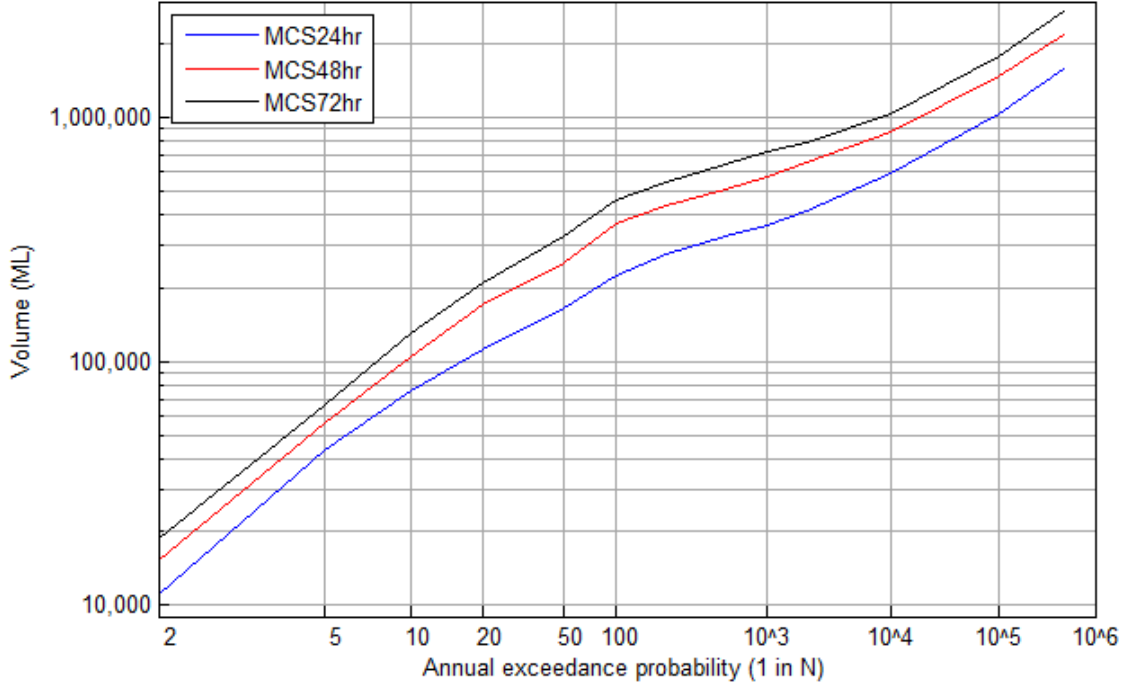




Figure C.2.13 | Location Savages Crossing; no dams conditions

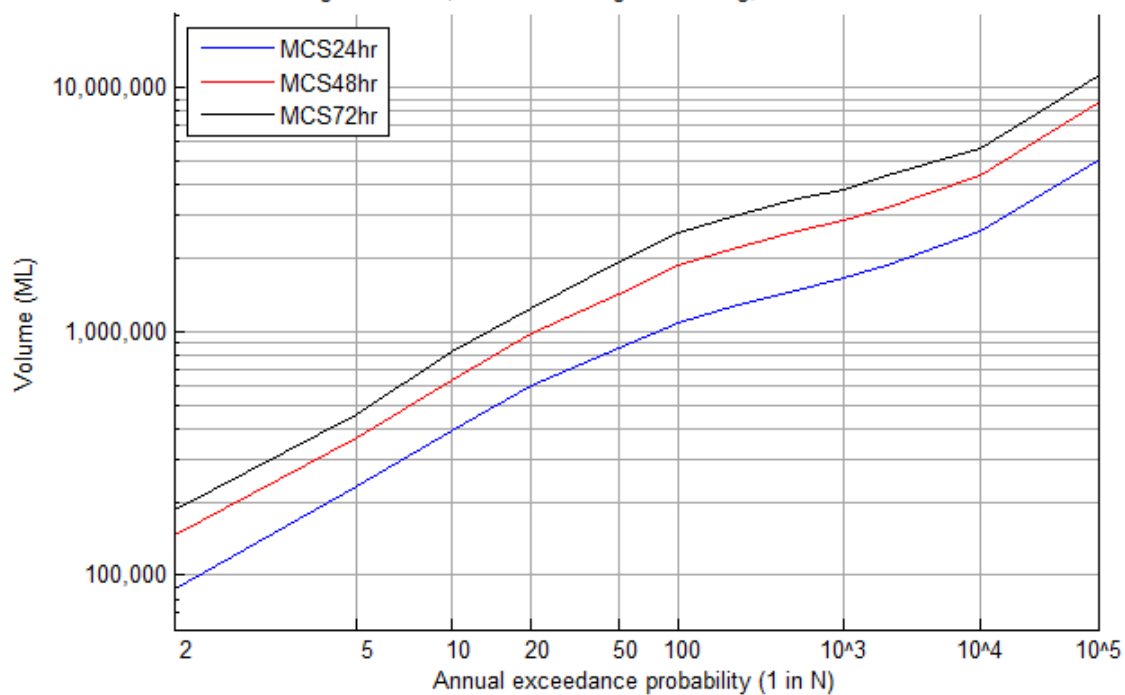


Figure C.2.14 | Location Mount Crosby; no dams conditions

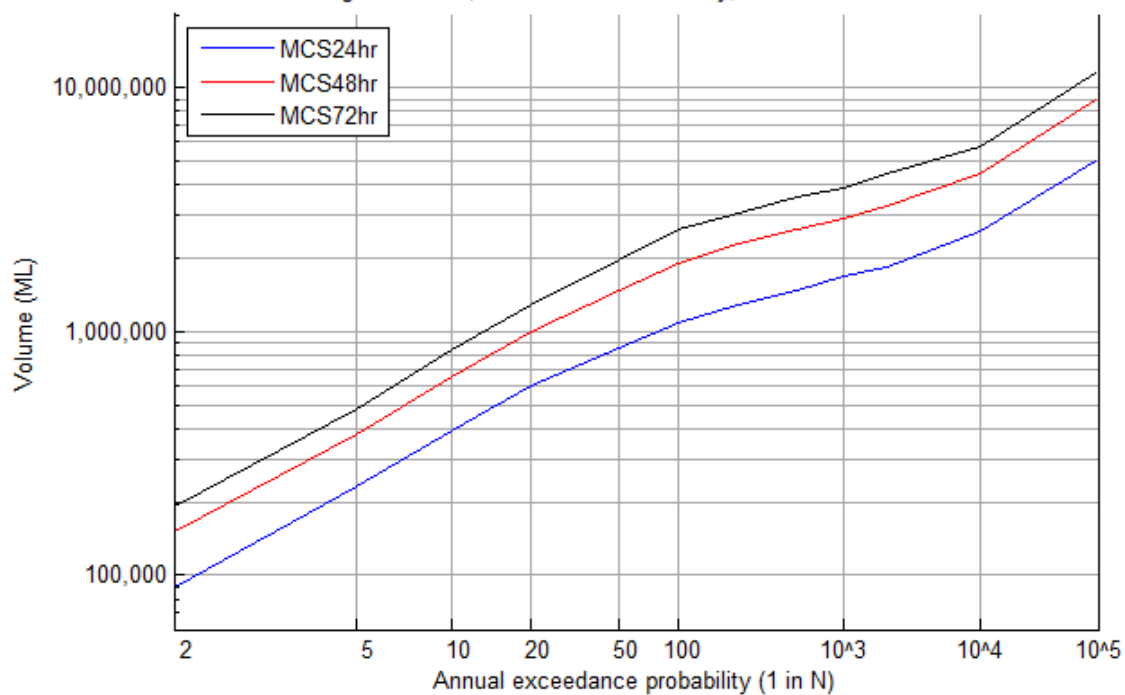




Figure C.2.15 | Location Walloon; no dams conditions

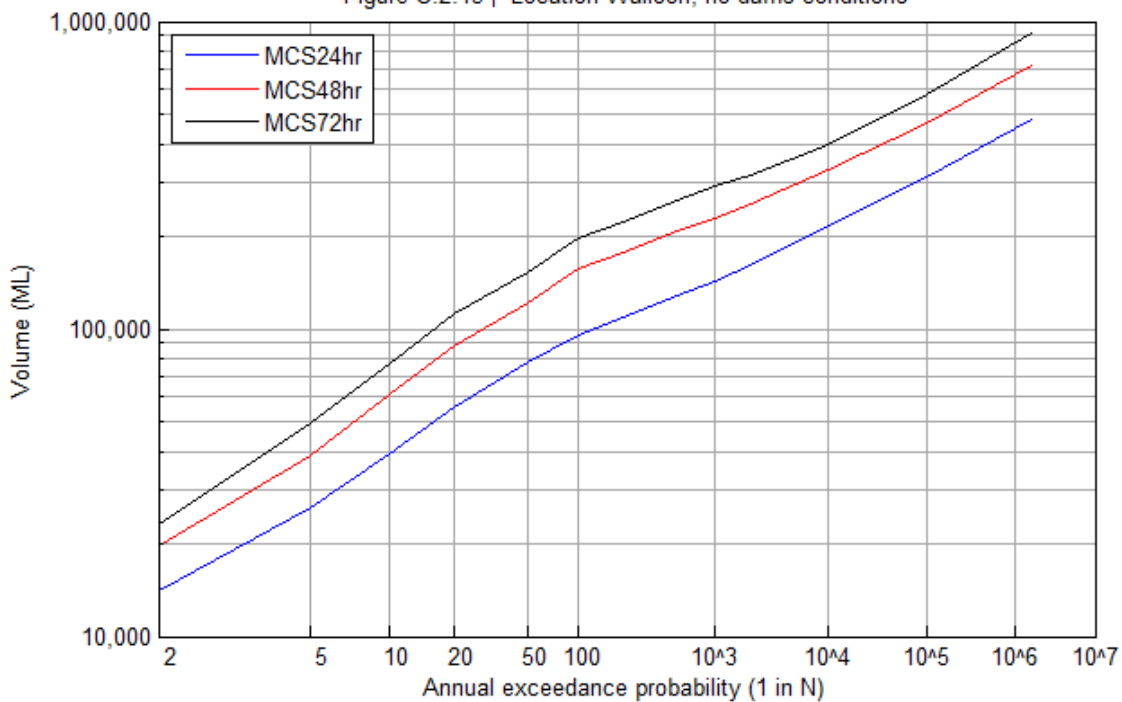
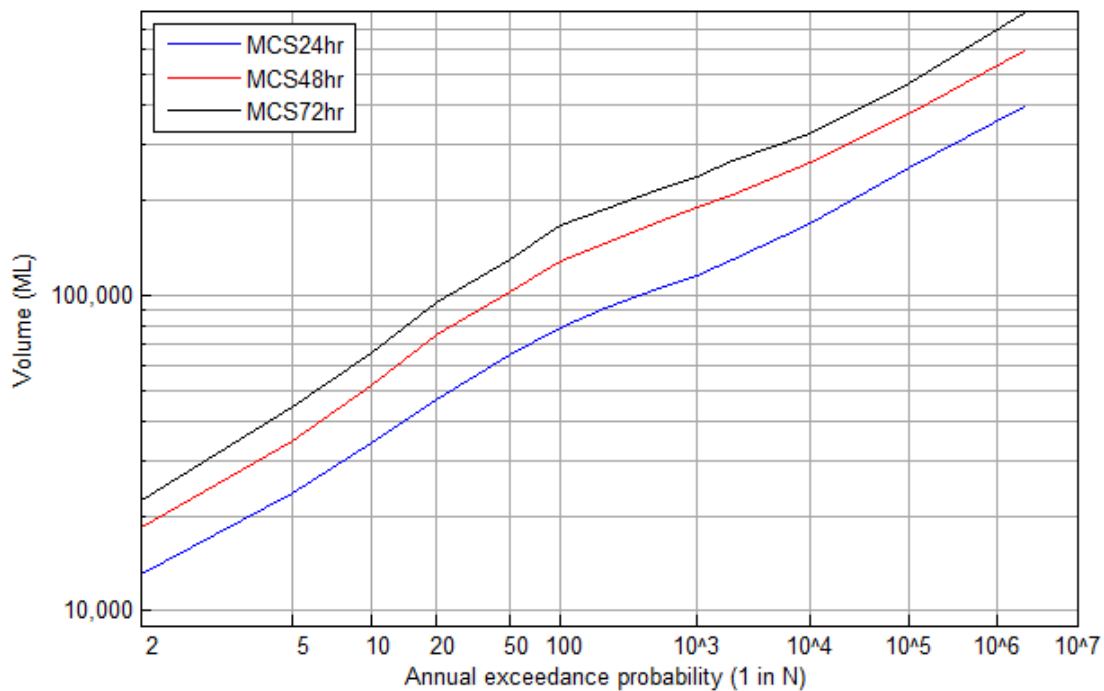


Figure C.2.16 | Location Kalbar Weir; no dams conditions



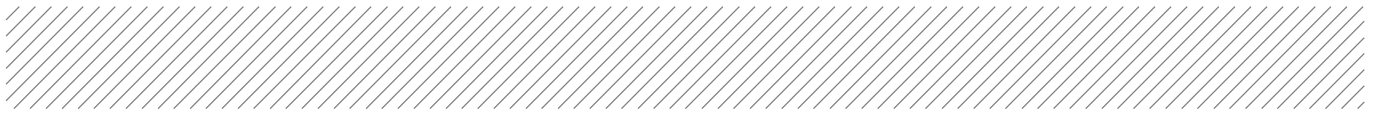


Figure C.2.17 | Location Amberley; no dams conditions

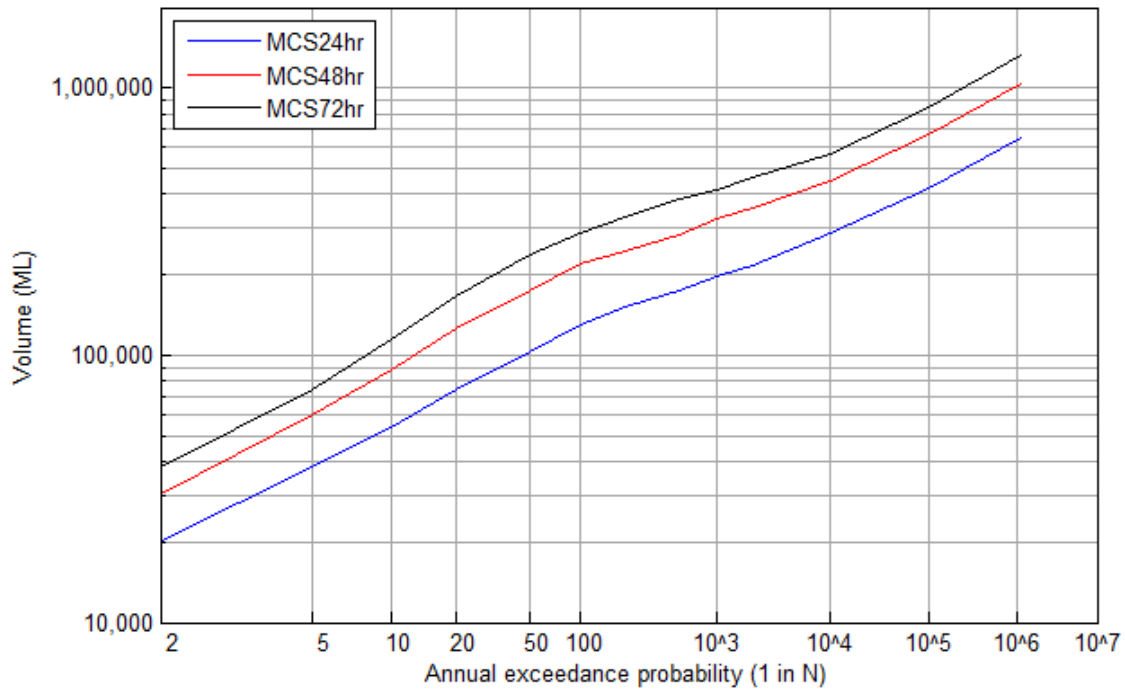


Figure C.2.18 | Location Loamside; no dams conditions

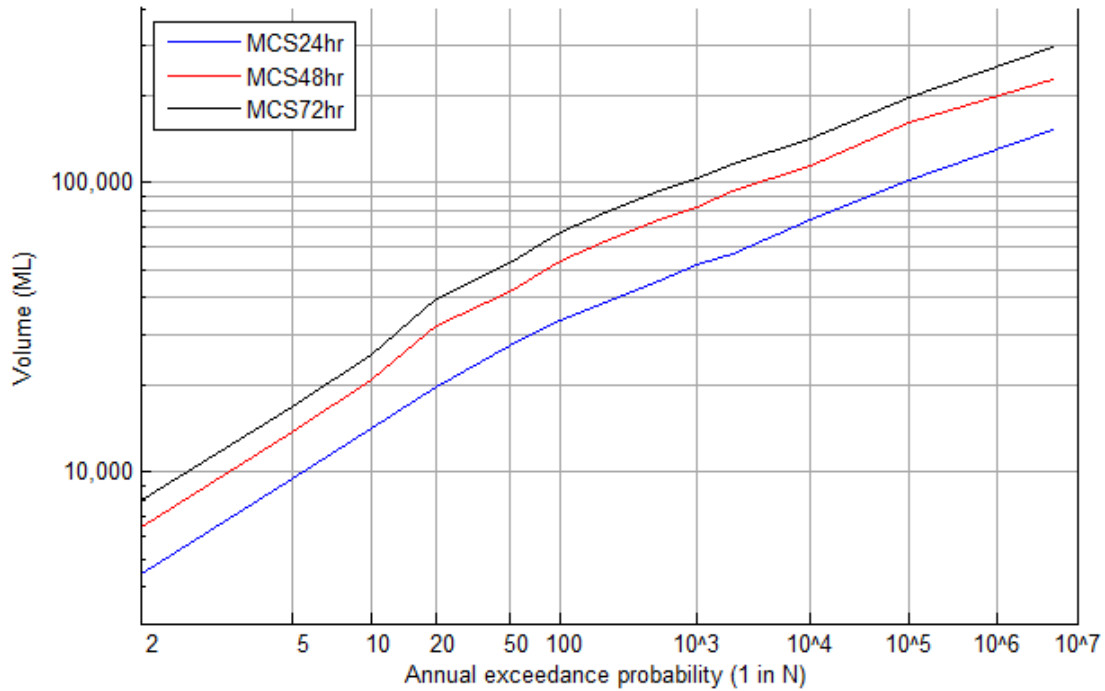




Figure C.2.19 | Location Ipswich; no dams conditions

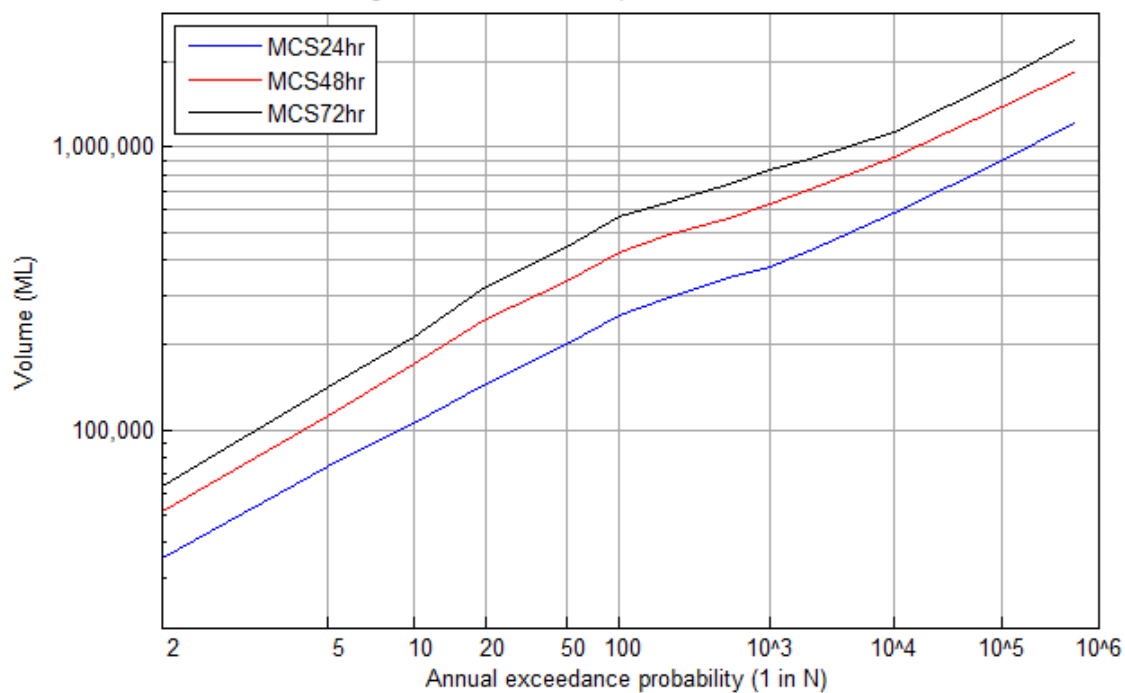


Figure C.2.20 | Location Moggill; no dams conditions

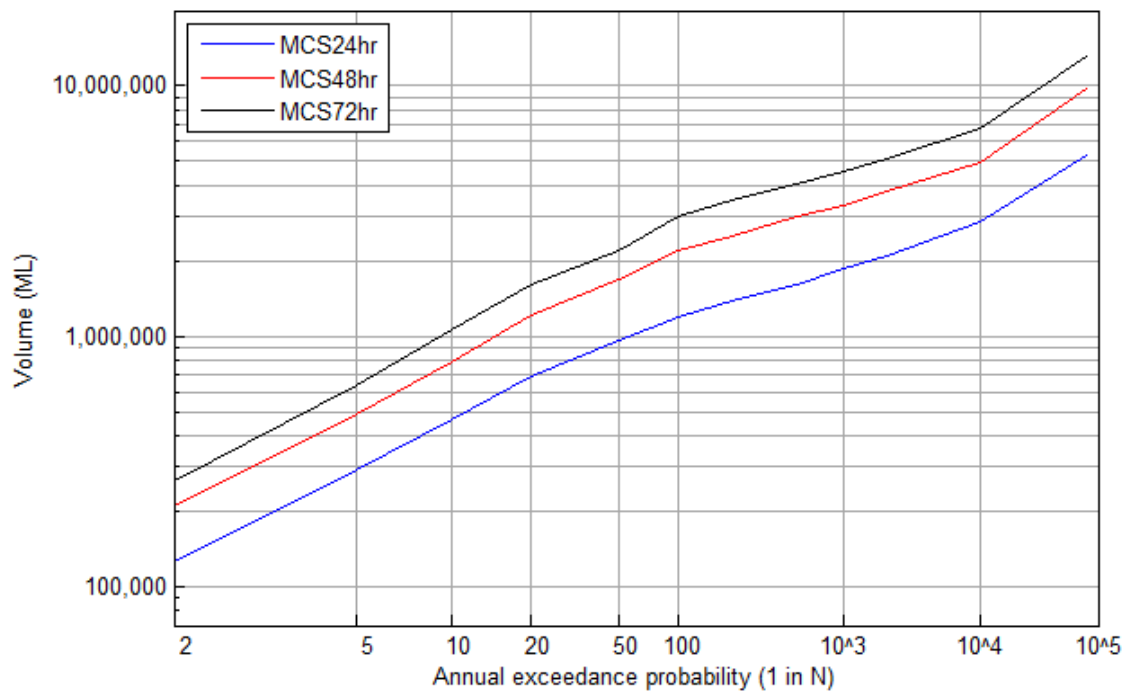




Figure C.2.21 | Location Centenary Bridge; no dams conditions

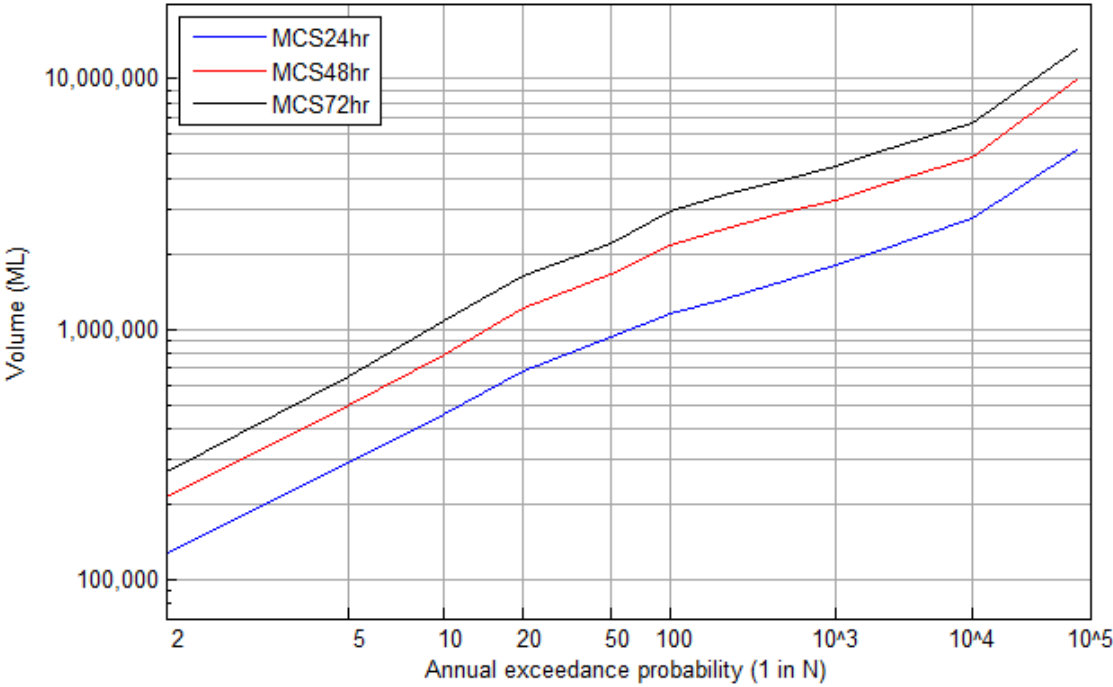
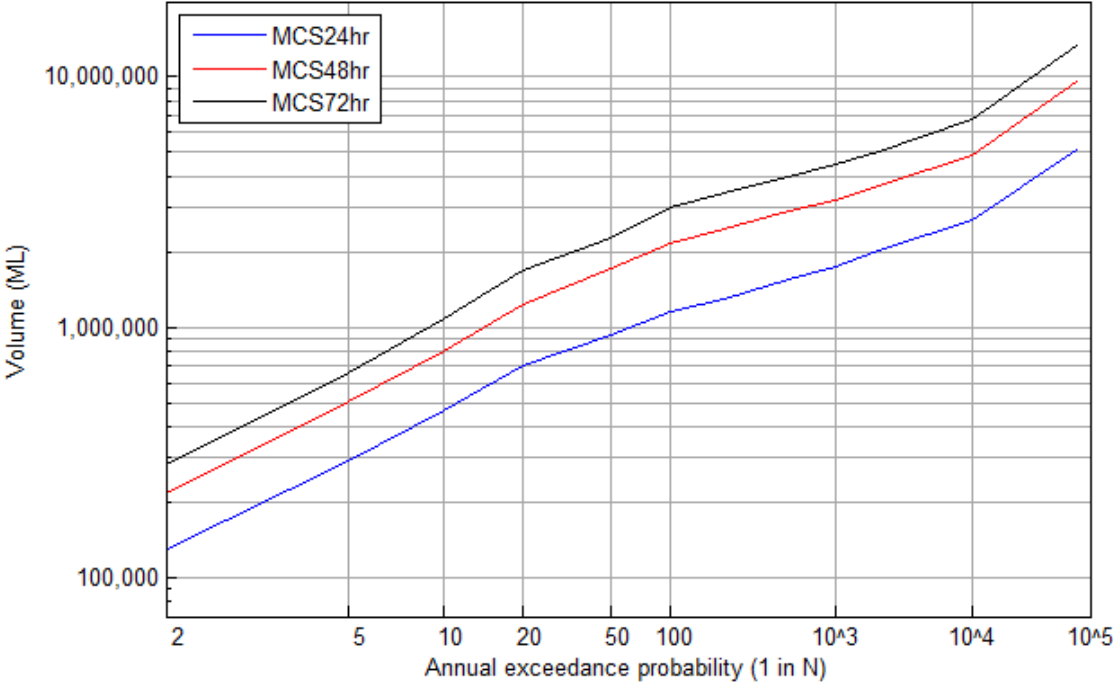
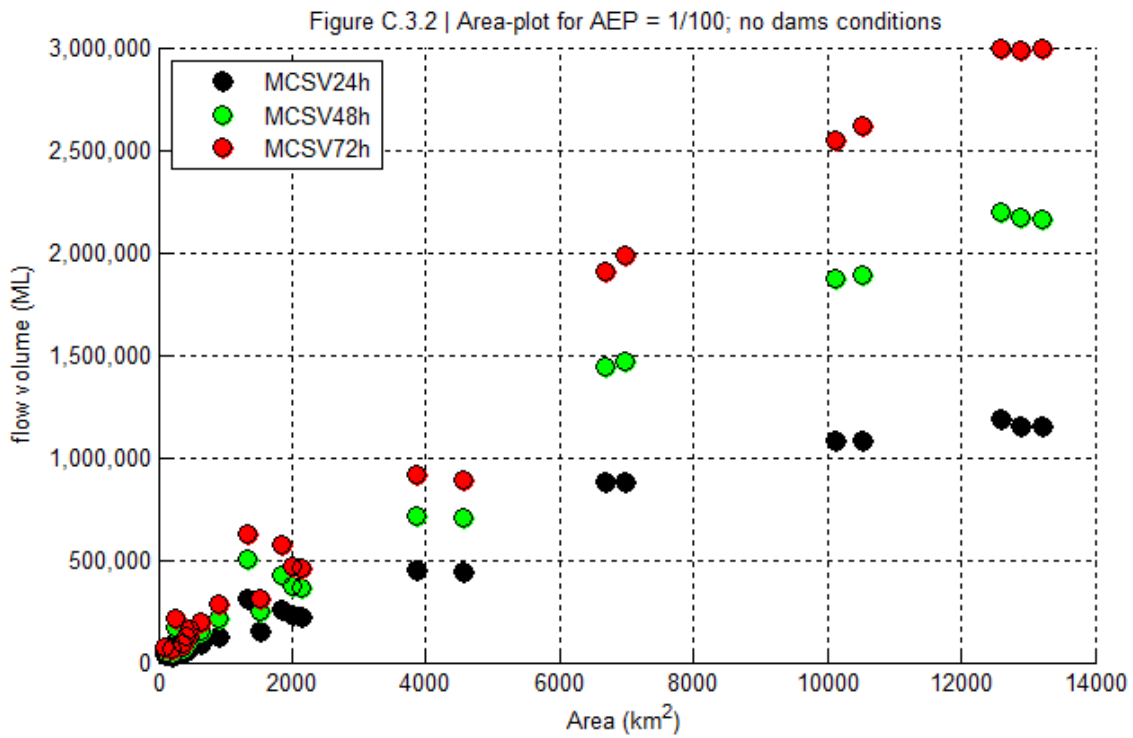
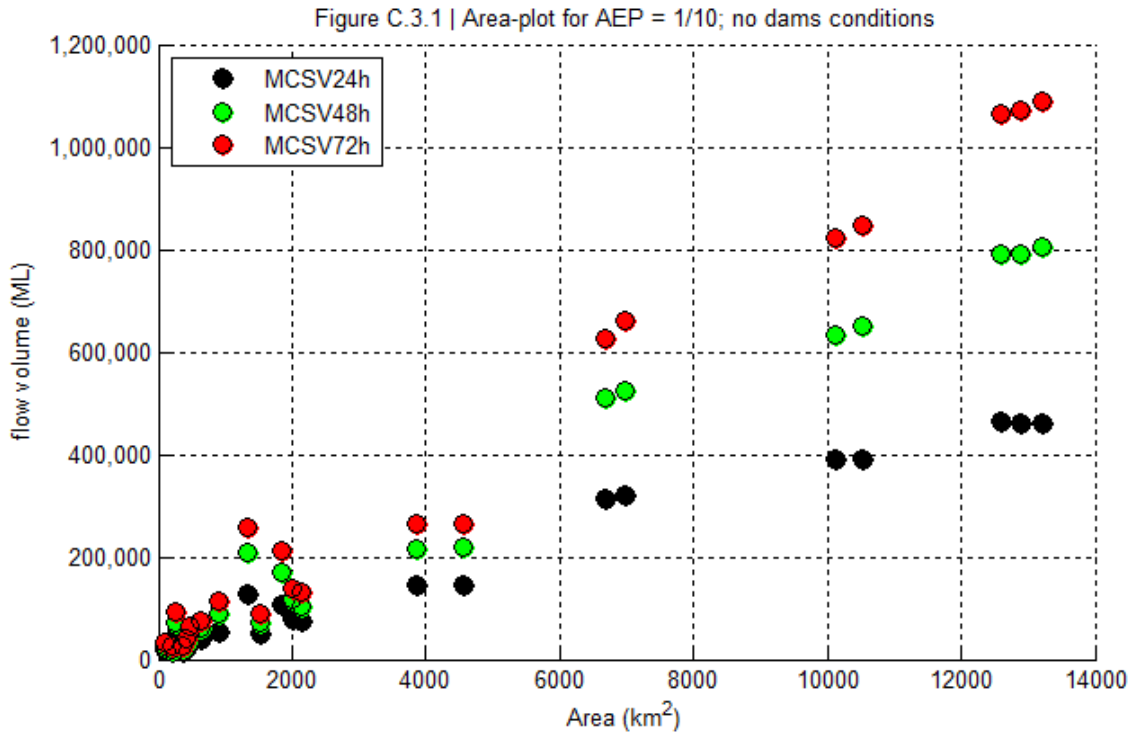


Figure C.2.22 | Location Brisbane; no dams conditions



C.3 Plots of catchment area versus flow volumes

This section contains ten figures in which flows 24-, 48- and 72 hour flow volumes are plotted against catchment area: five for DEA results (one figure per AEP) and five for MCS results.



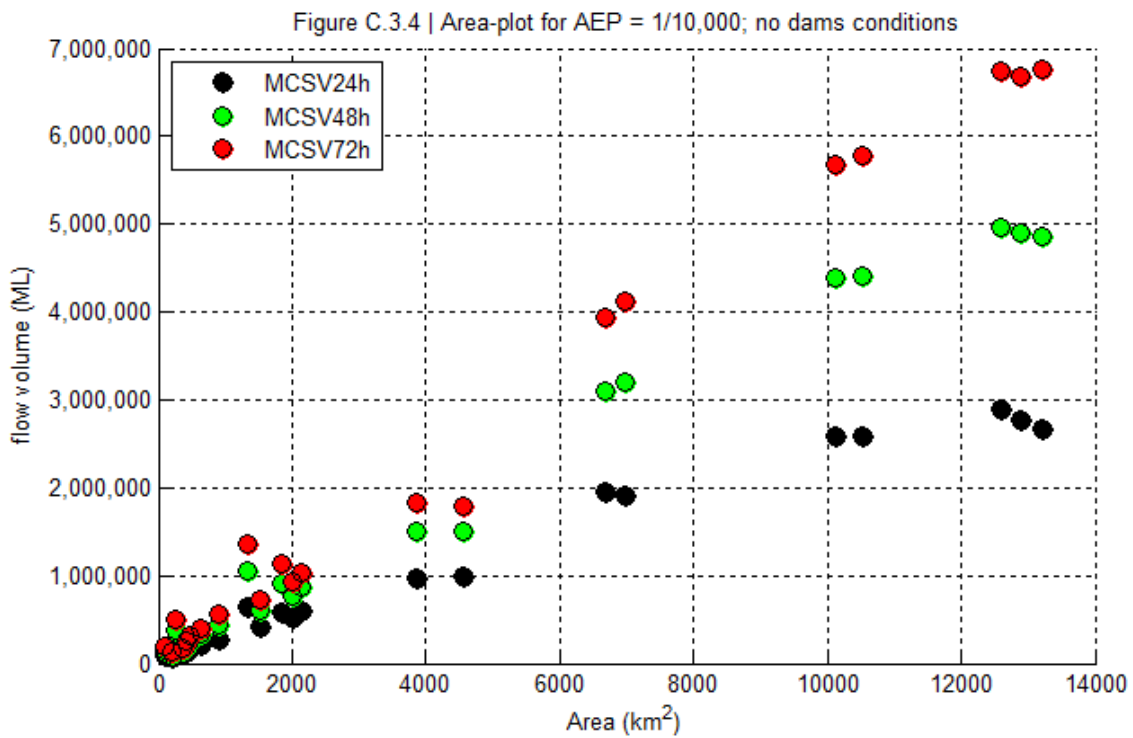
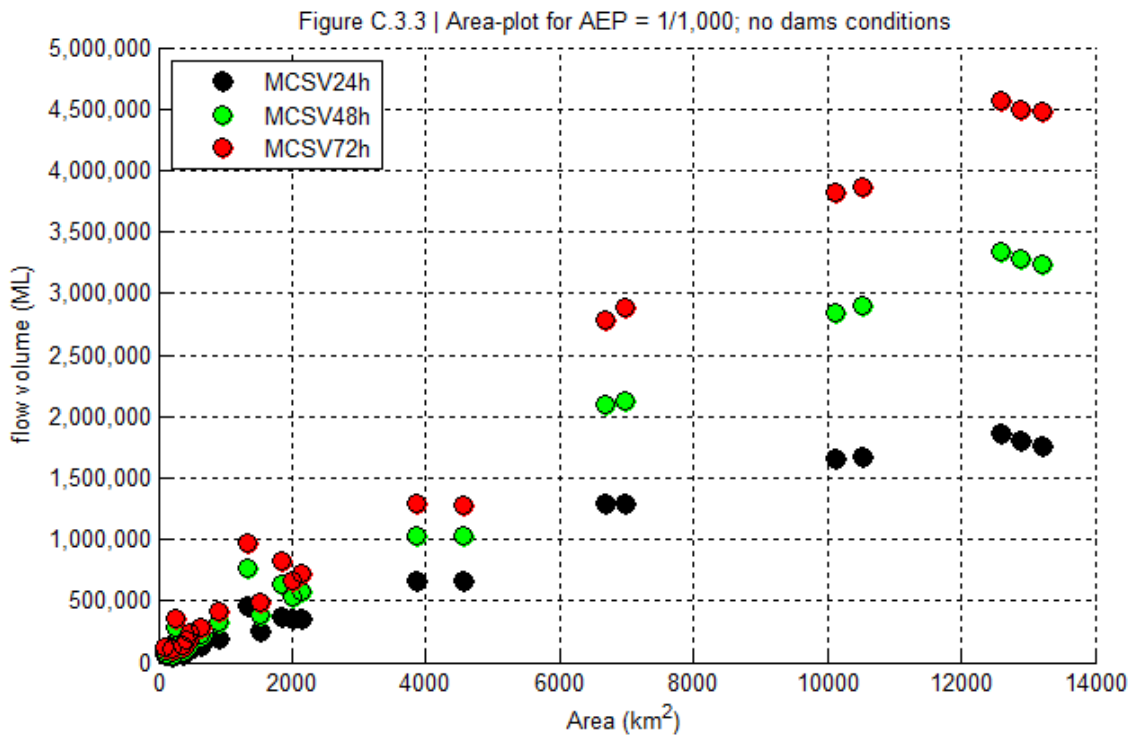
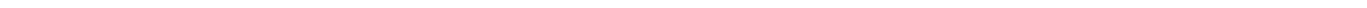
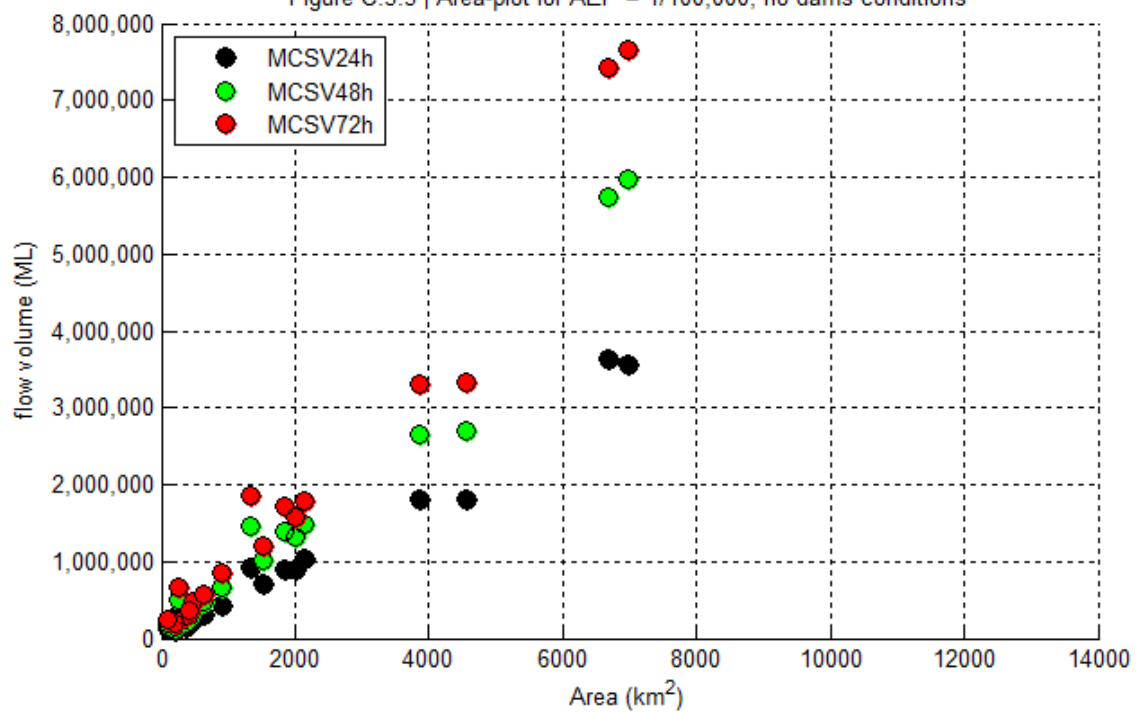




Figure C.3.5 | Area-plot for AEP = 1/100,000; no dams conditions



C.4 Comparison with observed volumes for selected locations

Figure C.4.1 | Location Gregors Creek; no dams conditions; 24-hour flow volume

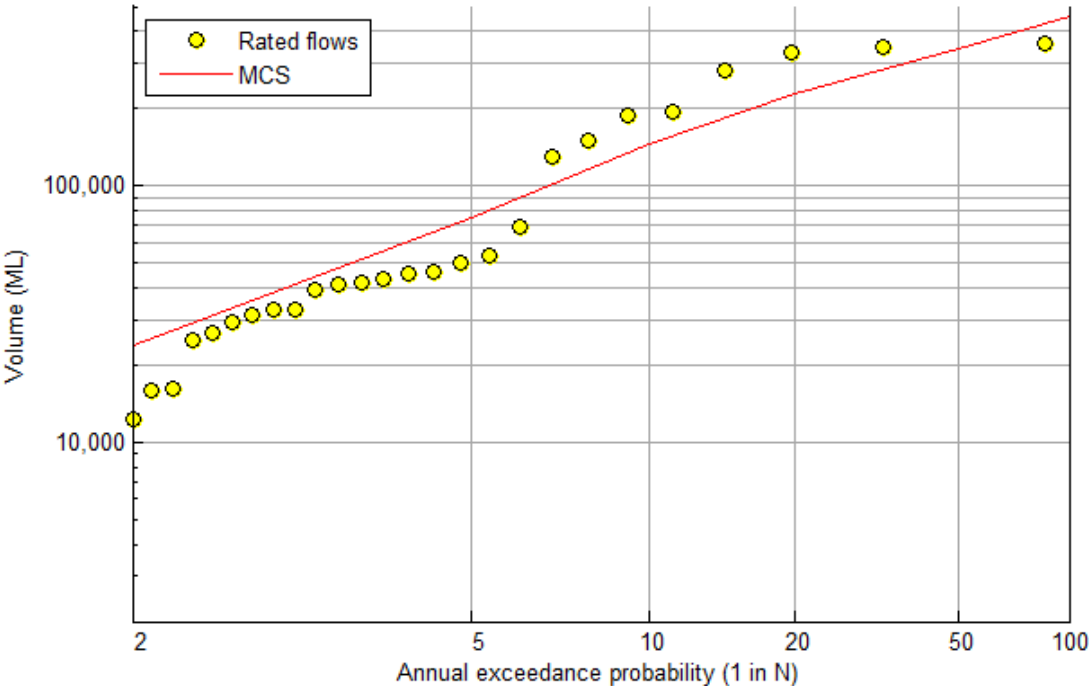
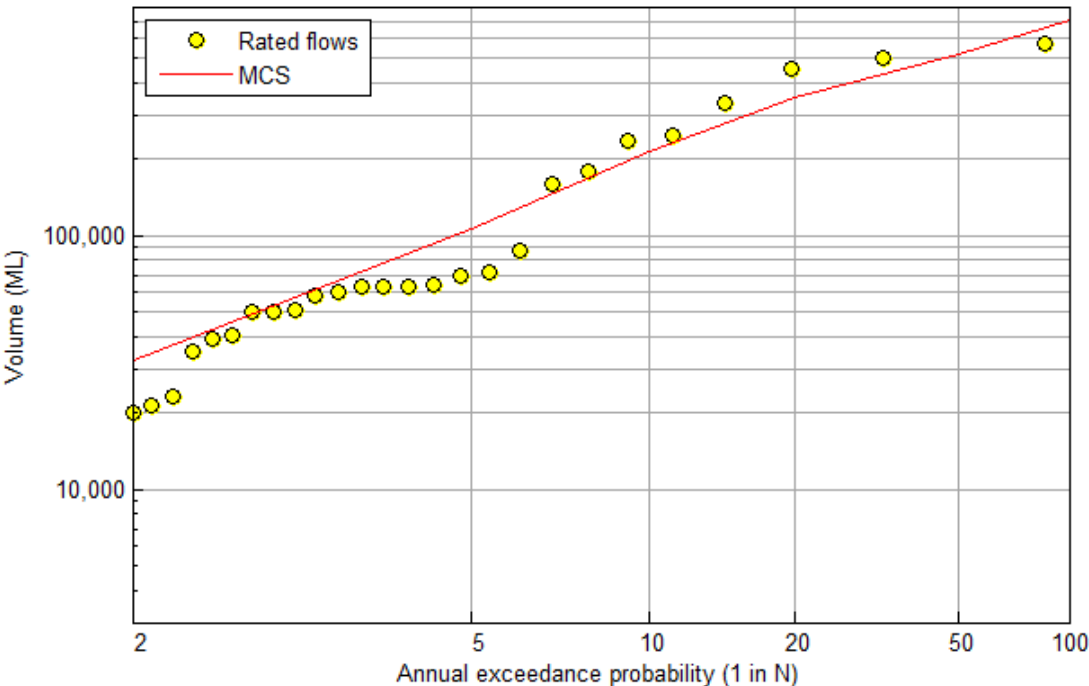


Figure C.4.2 | Location Gregors Creek; no dams conditions; 48-hour flow volume



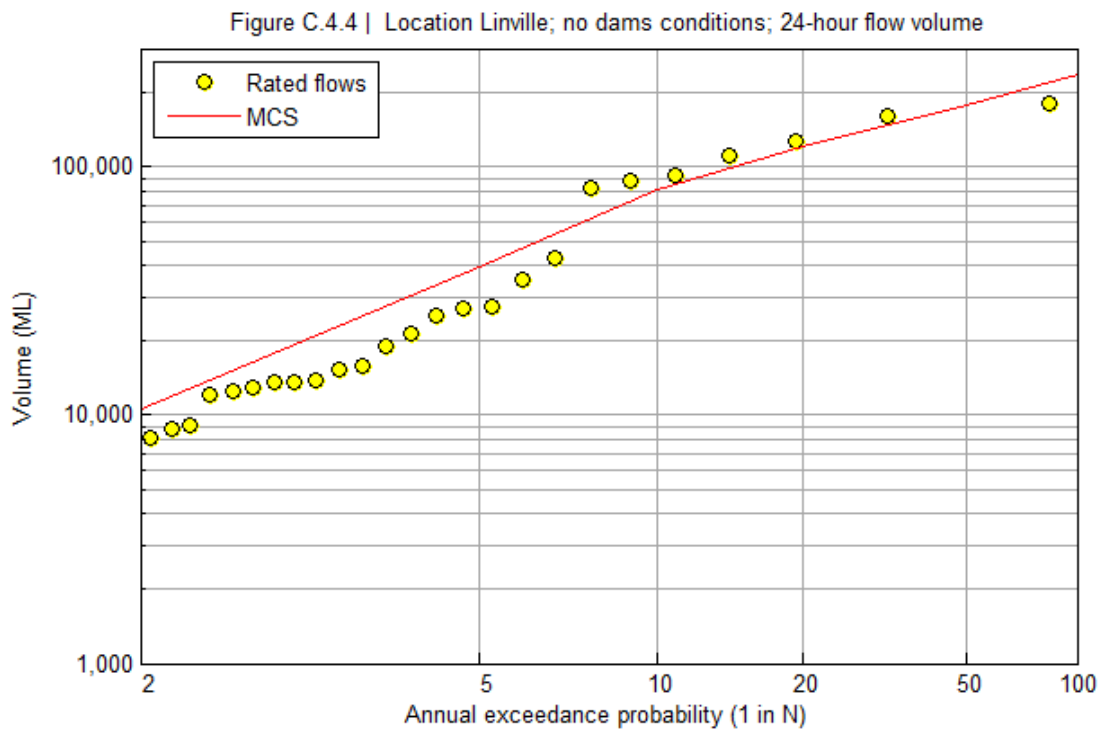
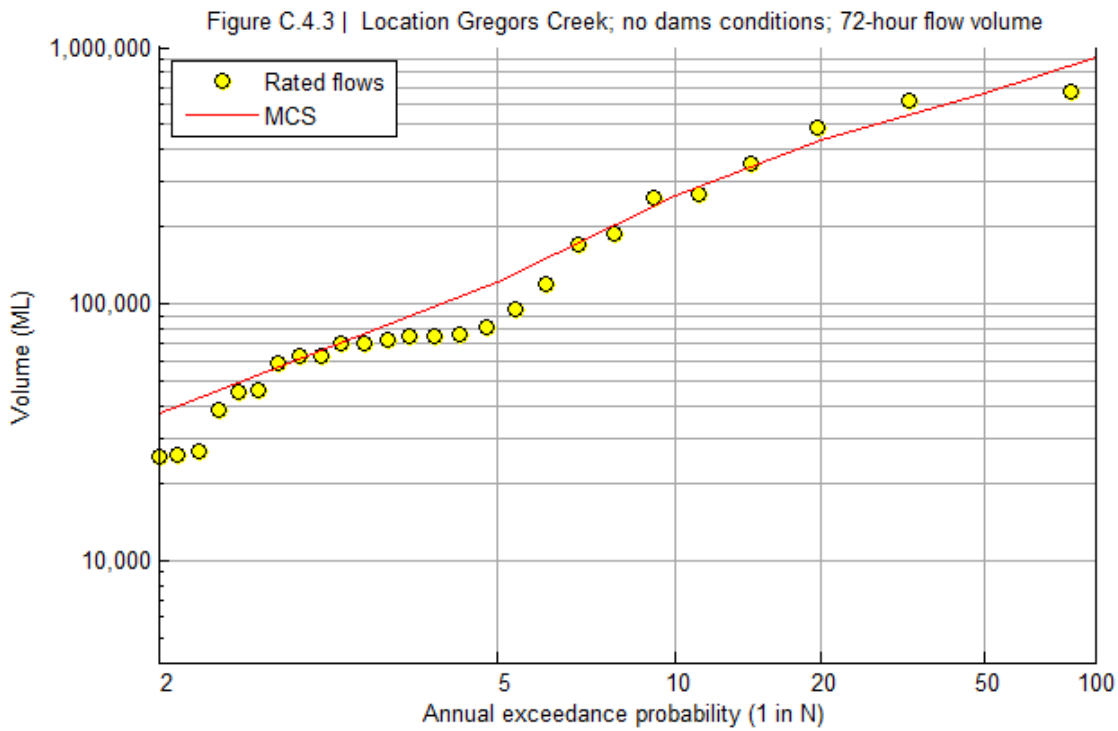




Figure C.4.5 | Location Linville; no dams conditions; 48-hour flow volume

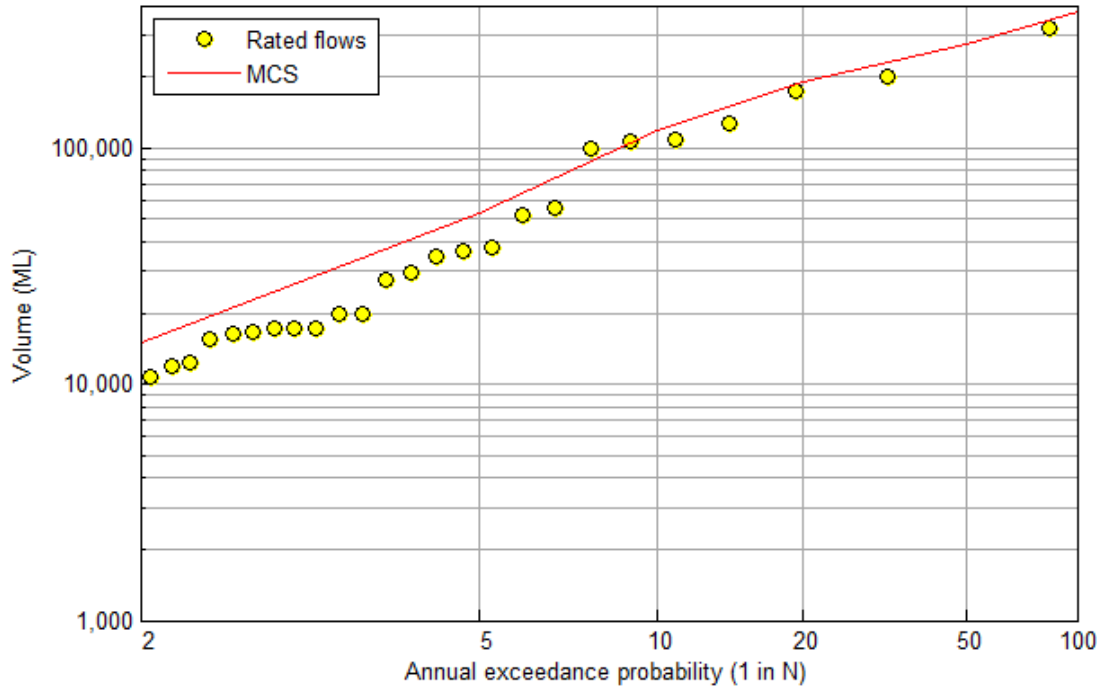


Figure C.4.6 | Location Linville; no dams conditions; 72-hour flow volume

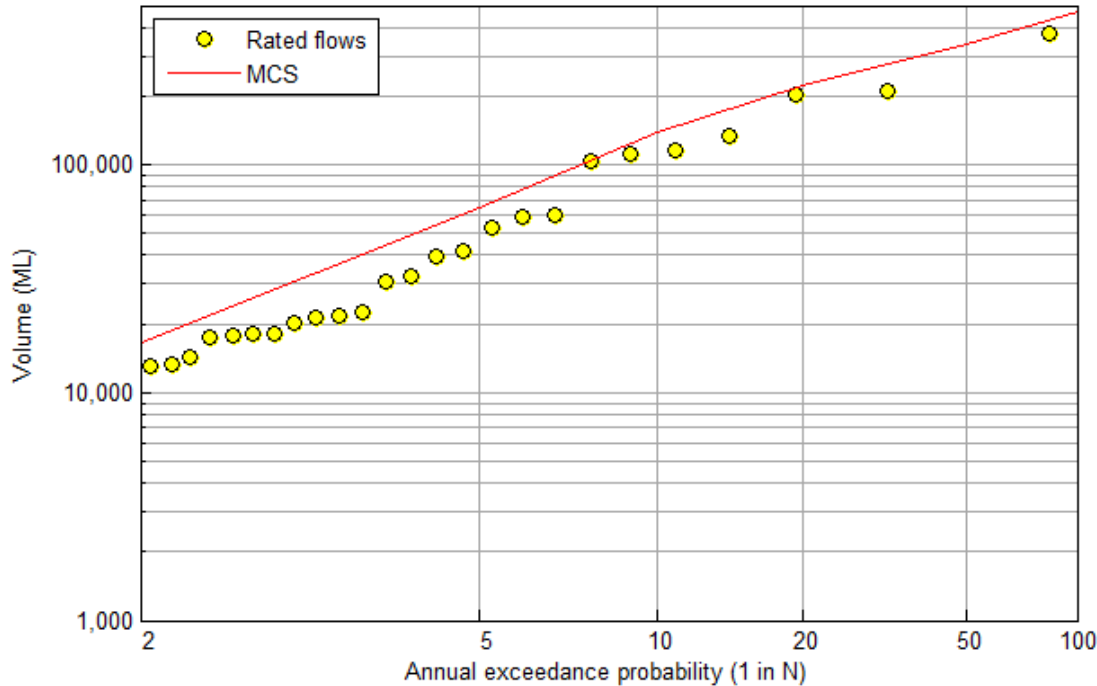




Figure C.4.7 | Location Walloon; no dams conditions; 24-hour flow volume

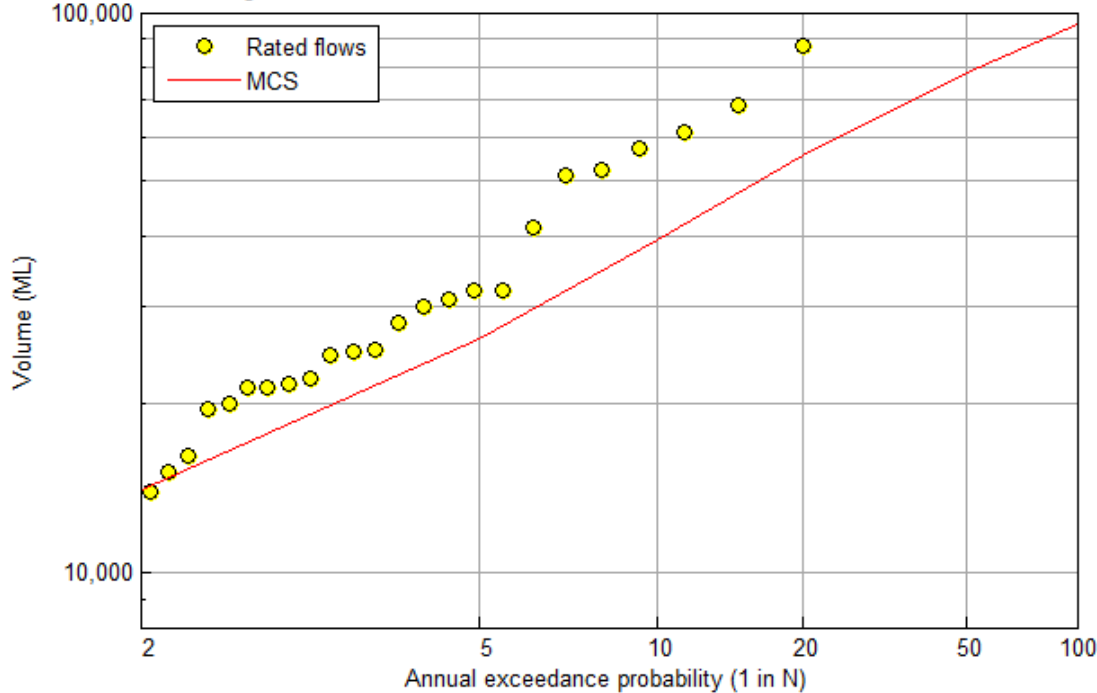


Figure C.4.8 | Location Walloon; no dams conditions; 48-hour flow volume

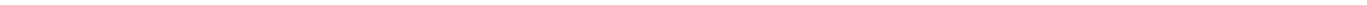
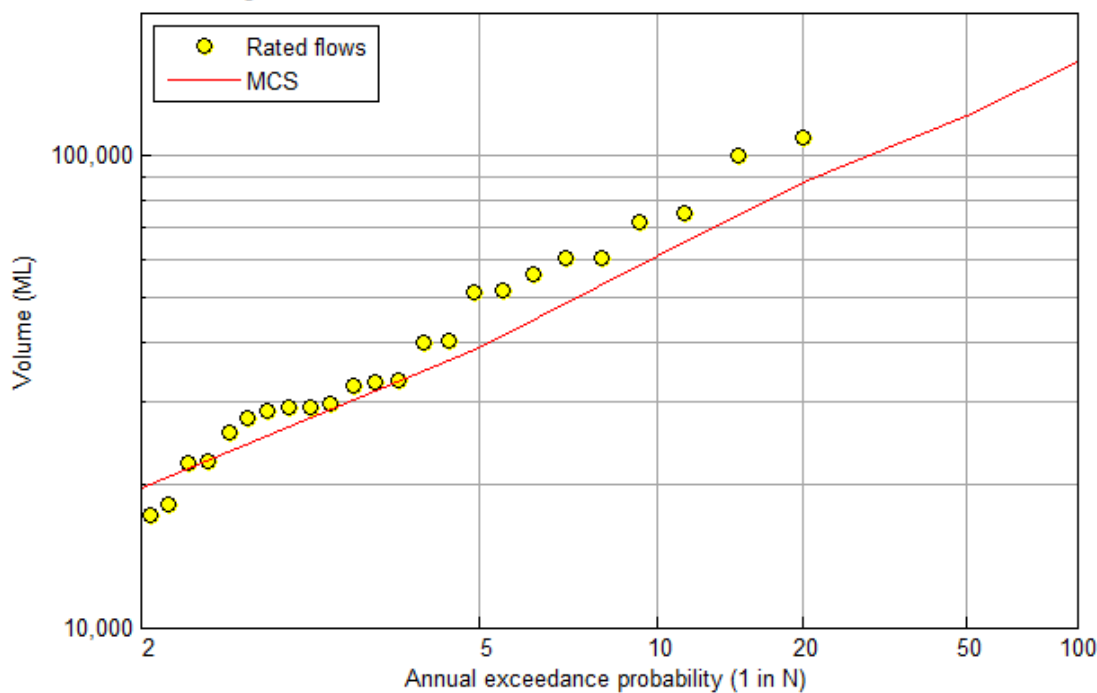
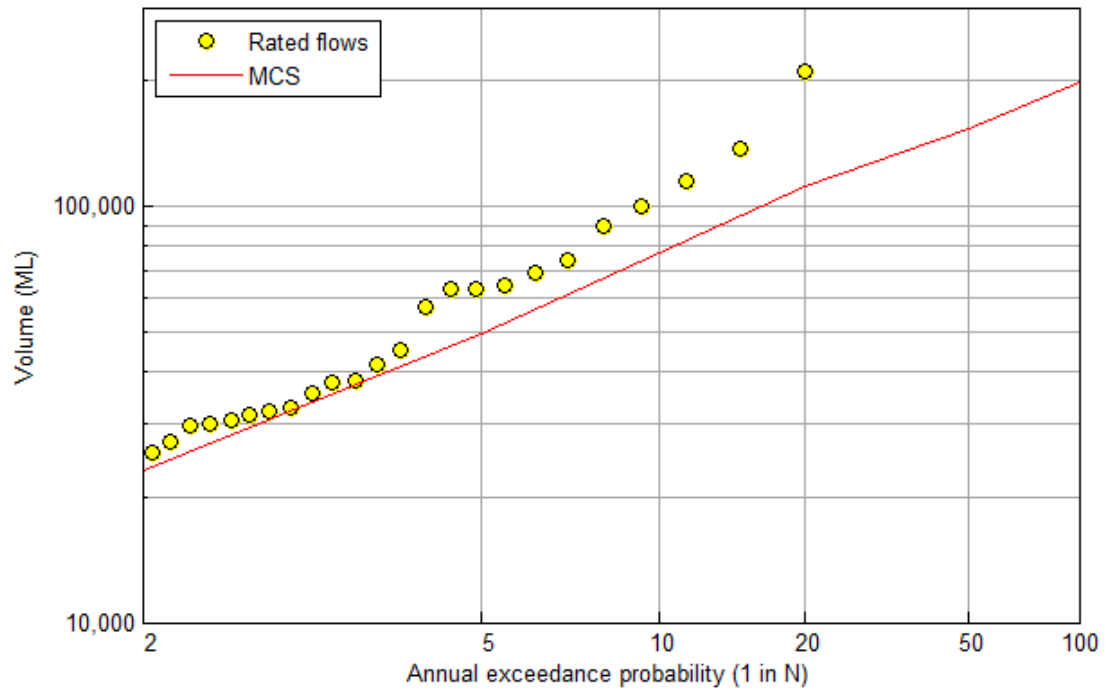
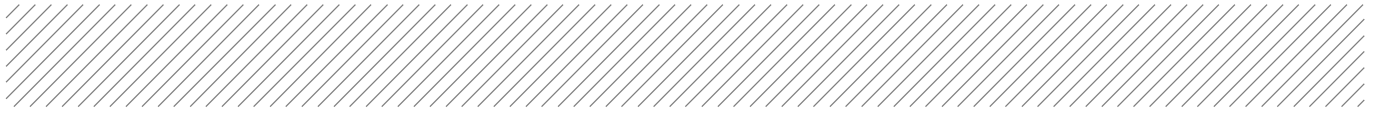


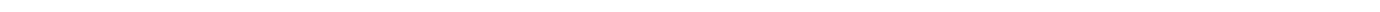
Figure C.4.9 | Location Walloon; no dams conditions; 72-hour flow volume





Appendix D

'With-dams' design flow volumes



D.1 Tables

Note: the 1 in 100,000 AEP flow volume is only provided for locations for which the AEP of the PMP is below 1 in 100,000.

Table D1 Maximum 24-hour flow volumes (1000ML) versus AEP; MCS results

Location	AEP (1 in N)												AEP of PMP
	2	5	10	20	50	100	200	500	1,000	2,000	10,000	100,000	
Somerset Dam	0	94	120	150	170	180	220	270	300	330	430	830	1600
Wivenhoe	0	40	78	150	270	480	640	830	950	1100	1500	2800	3200
Savages Crossing	22	91	170	260	450	670	920	1200	1300	1500	2100		4300
Mount Crosby	26	94	170	280	460	670	910	1200	1300	1500	2100		4300
Ipswich	30	67	95	130	180	220	260	300	330	380	520	800	1100
Moggill	61	150	250	370	580	840	1000	1300	1500	1700	2400		4800
Centenary Bridge	64	160	260	380	590	820	990	1200	1400	1600	2300		4700
Brisbane	67	170	260	390	620	820	980	1200	1400	1600	2200		4600

Table D2 Maximum 48-hour flow volumes (1000ML) versus AEP; MCS results

Location	AEP (1 in N)												AEP of PMP
	2	5	10	20	50	100	200	500	1,000	2,000	10,000	100,000	
Somerset Dam	0	130	180	210	270	300	350	450	490	550	730	1400	2700
Wivenhoe	0	75	150	280	500	830	1100	1300	1600	1800	2500	5000	5700
Savages Crossing	39	150	290	450	770	1100	1500	1900	2200	2600	3600		7600
Mount Crosby	44	160	290	460	800	1200	1500	2000	2200	2600	3600		7600
Ipswich	44	98	150	210	300	390	440	510	580	640	810	1200	1700
Moggill	96	250	430	670	1000	1500	1900	2300	2600	3000	4200		8800

Location	AEP (1 in N)												AEP of PMP
	2	5	10	20	50	100	200	500	1,000	2,000	10,000	100,000	
Centenary Bridge	100	260	450	690	1100	1500	1800	2300	2600	3000	4200		8700
Brisbane	110	270	470	710	1100	1500	1800	2300	2500	3000	4200		8700

Table D3 Maximum 72-hour flow volumes (1000ML) versus AEP; MCS results

Location	AEP (1 in N)												AEP of PMP
	2	5	10	20	50	100	200	500	1,000	2,000	10,000	100,000	
Somerset Dam	0	150	200	260	320	380	460	590	600	680	980	1900	3600
Wivenhoe	0	110	210	390	670	1100	1400	1700	2000	2300	3300	6800	7700
Savages Crossing	52	200	360	610	1100	1500	2000	2500	2800	3300	4600		10,000
Mount Crosby	59	200	390	640	1100	1600	2000	2600	3000	3400	4700		10,000
Ipswich	53	120	190	280	400	490	560	650	740	820	1000	1600	2200
Moggill	120	330	570	900	1400	2100	2500	3100	3500	4100	5700		12,000
Centenary Bridge	130	340	590	950	1400	2100	2500	3100	3500	4100	5700		12,000
Brisbane	140	360	610	670	1500	2100	2600	3100	3500	4100	5700		12,000

D.2 Frequency plots

Figure D.2.1 | Location Somerset Dam; with dams conditions

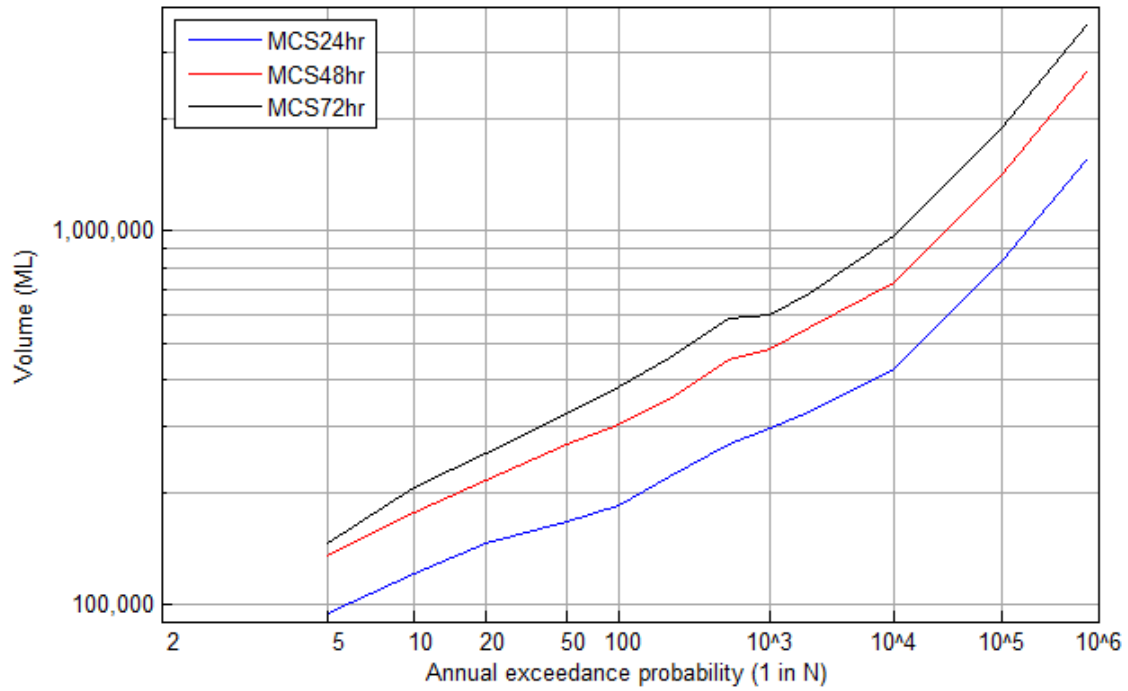


Figure D.2.2 | Location Wivenhoe; with dams conditions

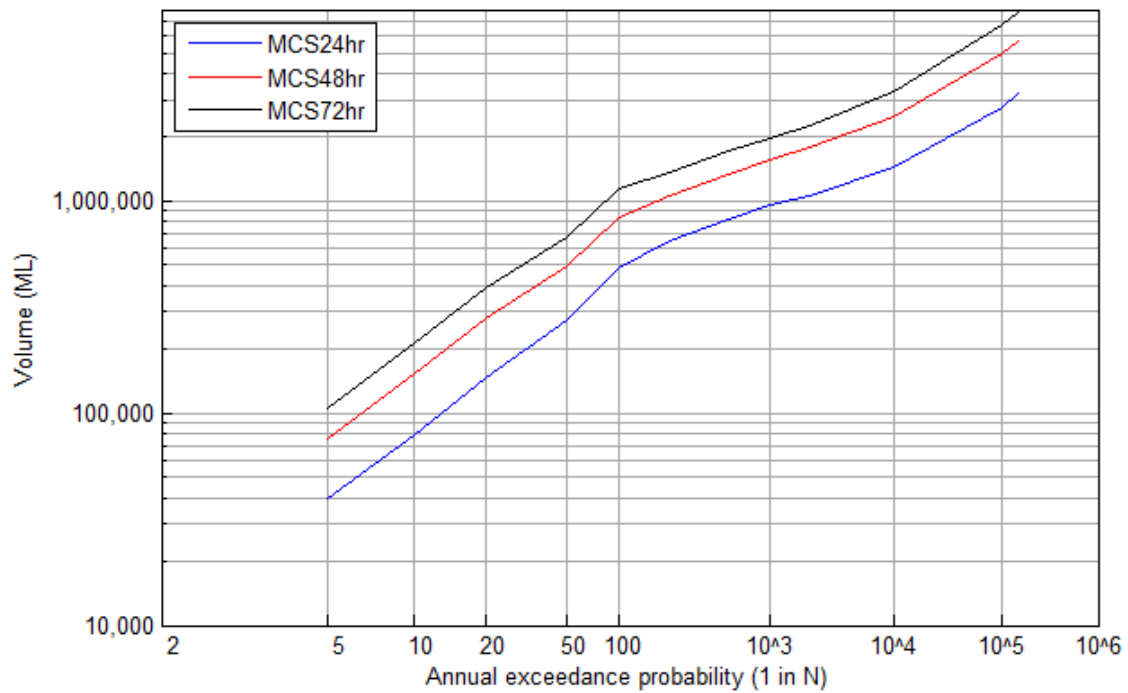




Figure D.2.3 | Location Savages Crossing; with dams conditions

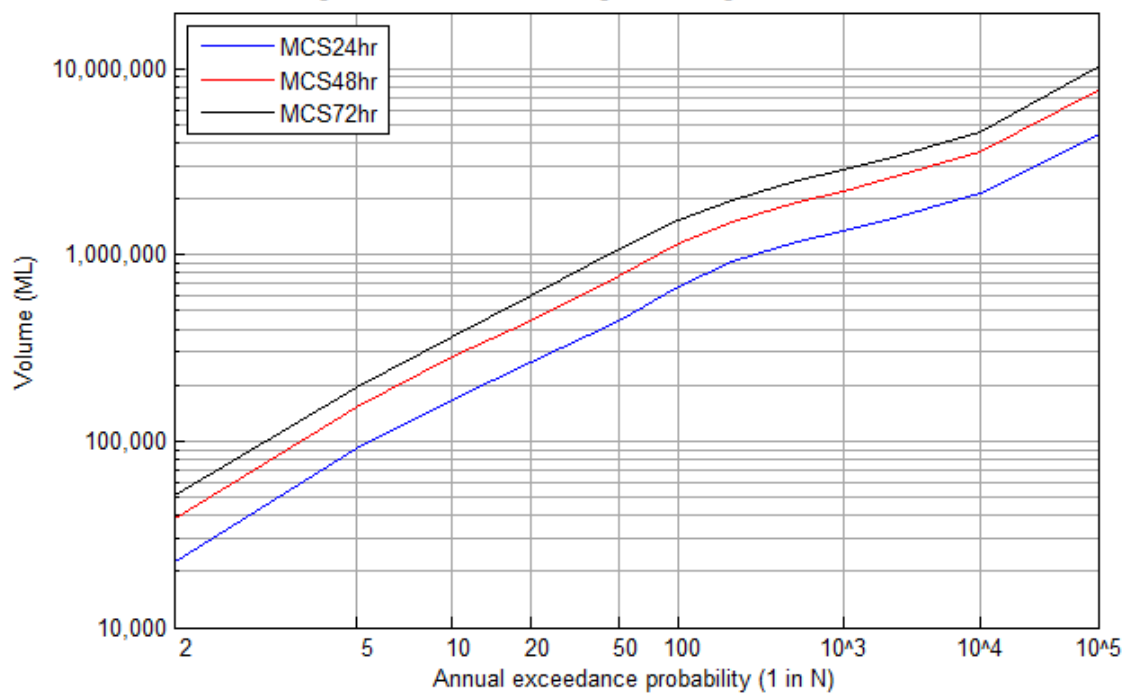


Figure D.2.4 | Location Mount Crosby; with dams conditions

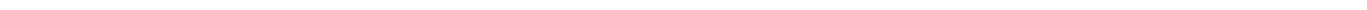
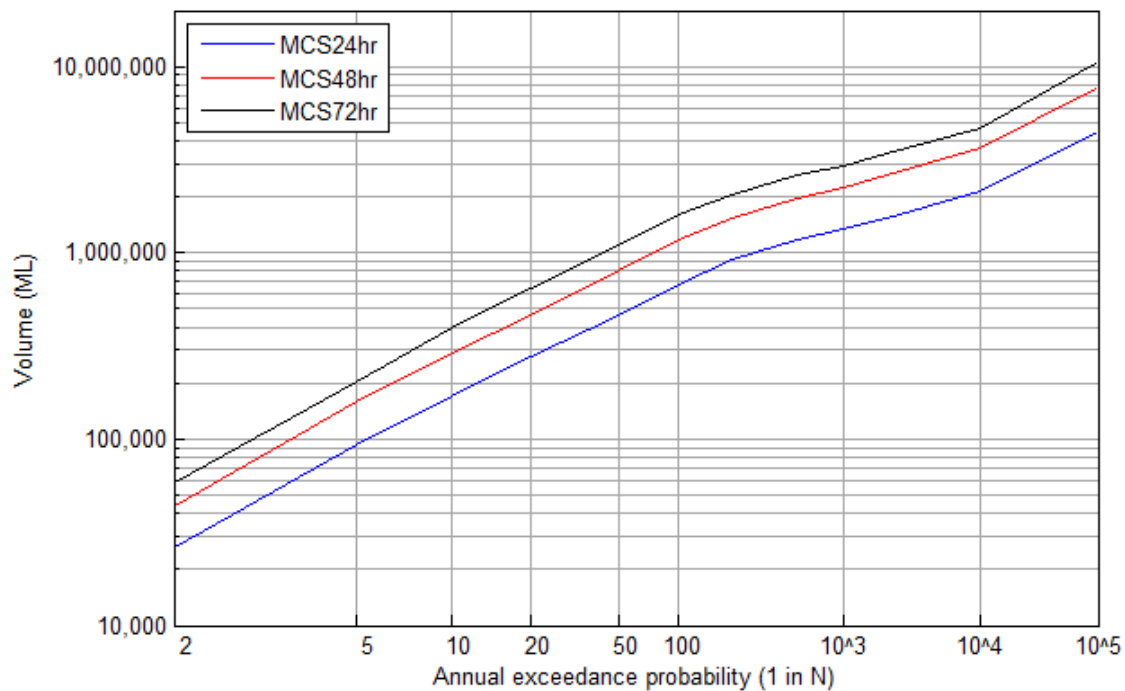




Figure D.2.5 | Location Ipswich; with dams conditions

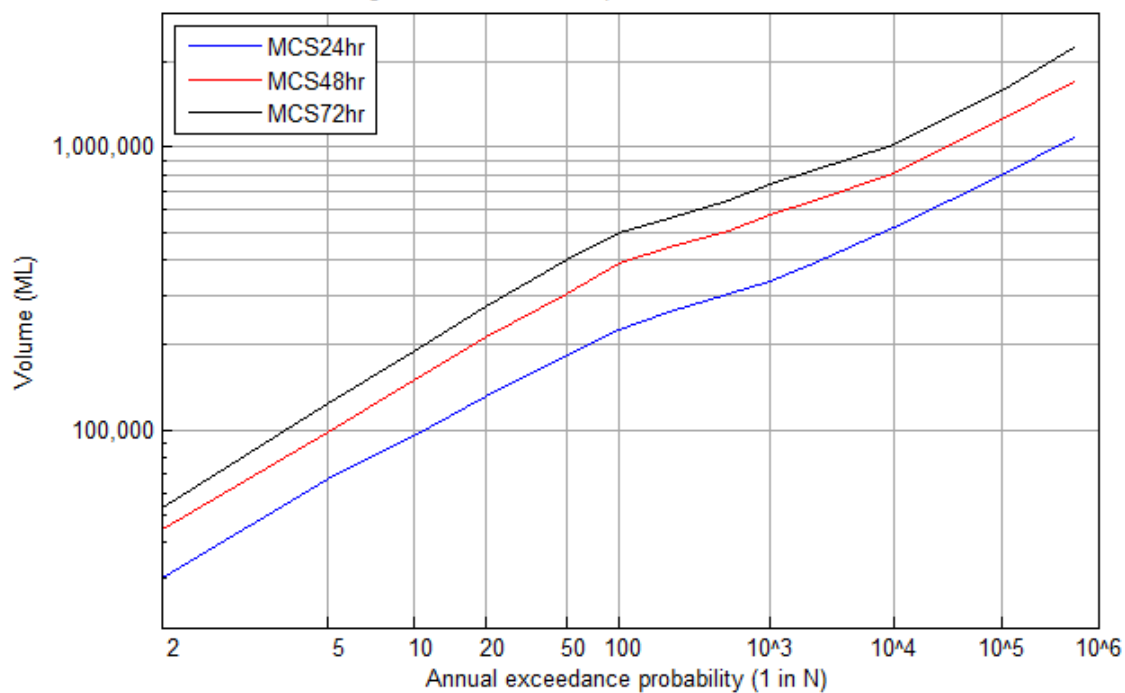


Figure D.2.6 | Location Moggill; with dams conditions

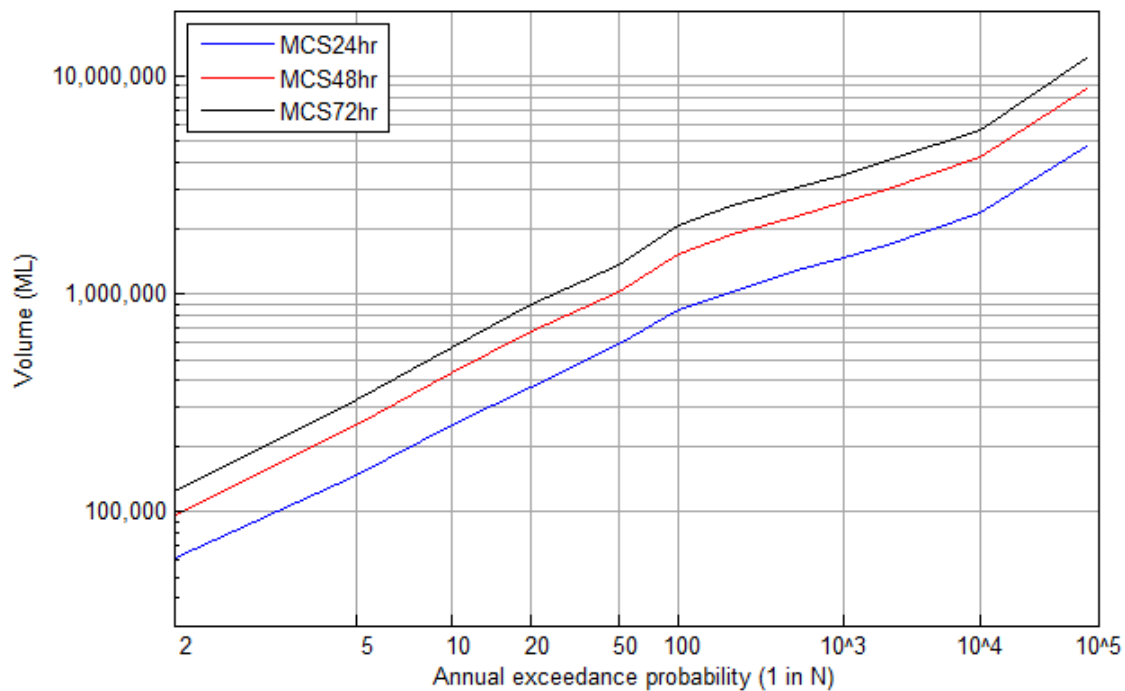




Figure D.2.7 | Location Centenary Bridge; with dams conditions

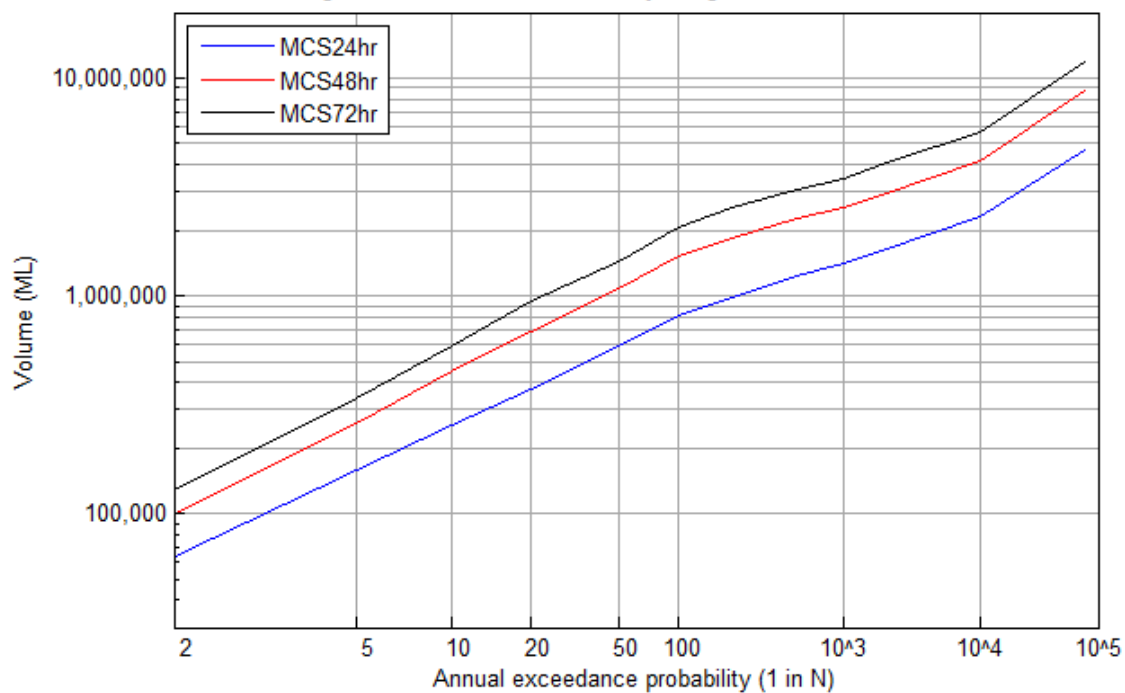
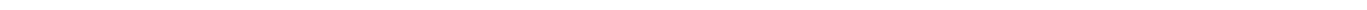
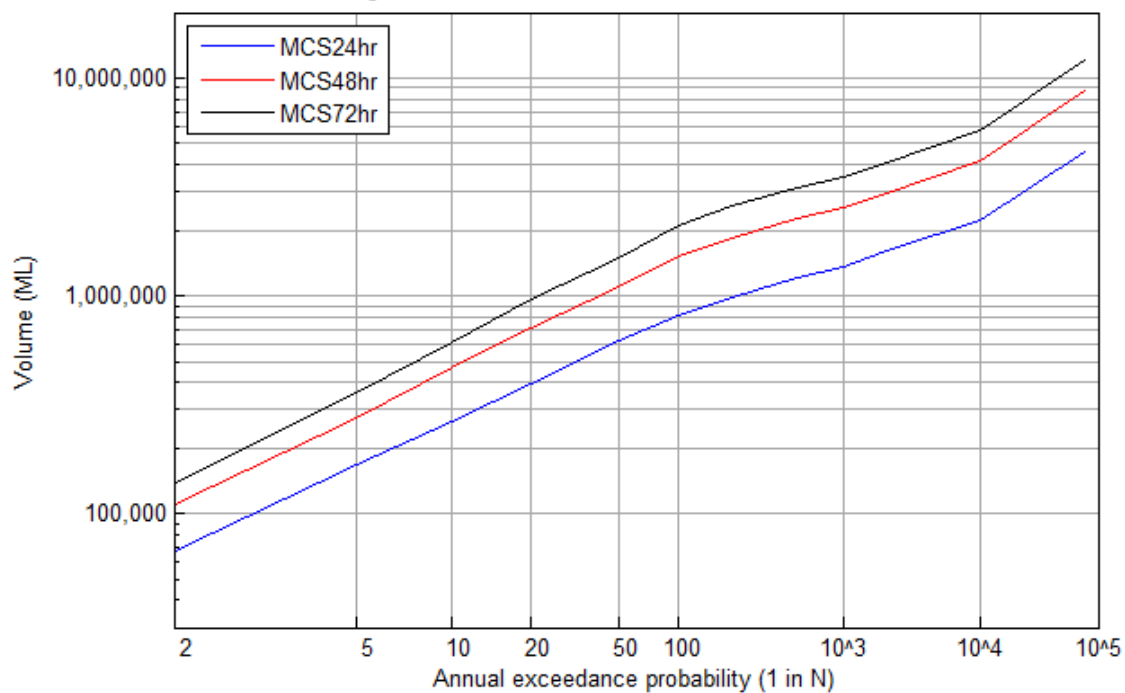
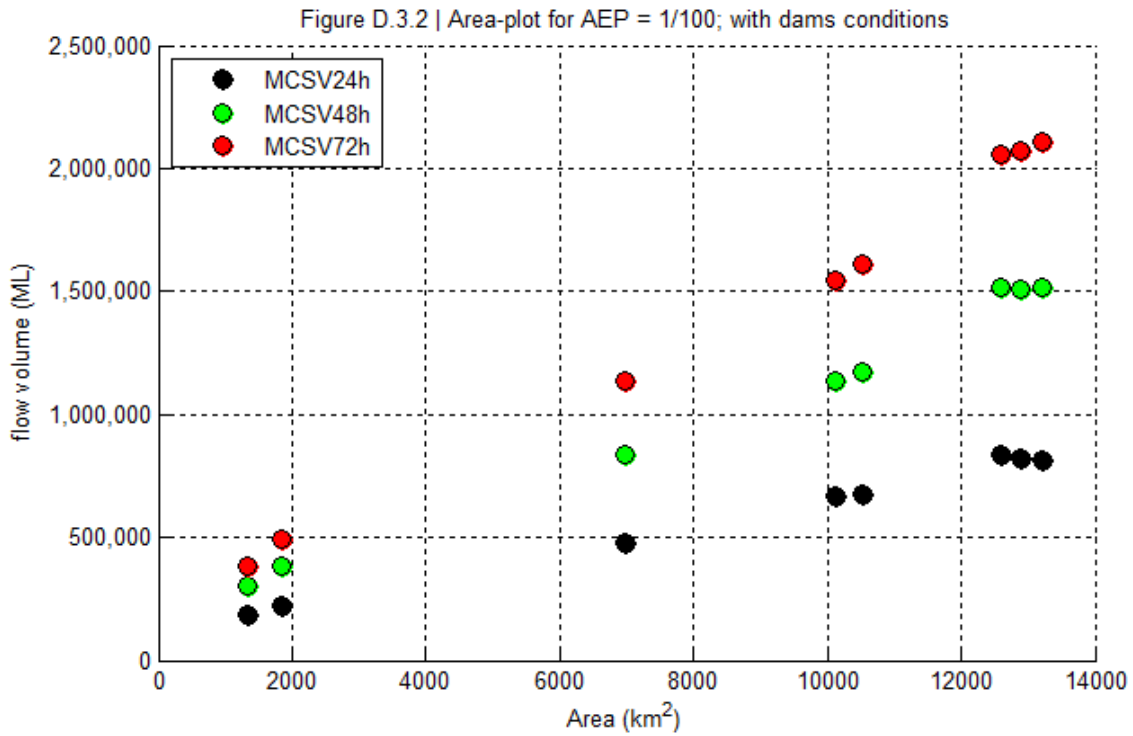
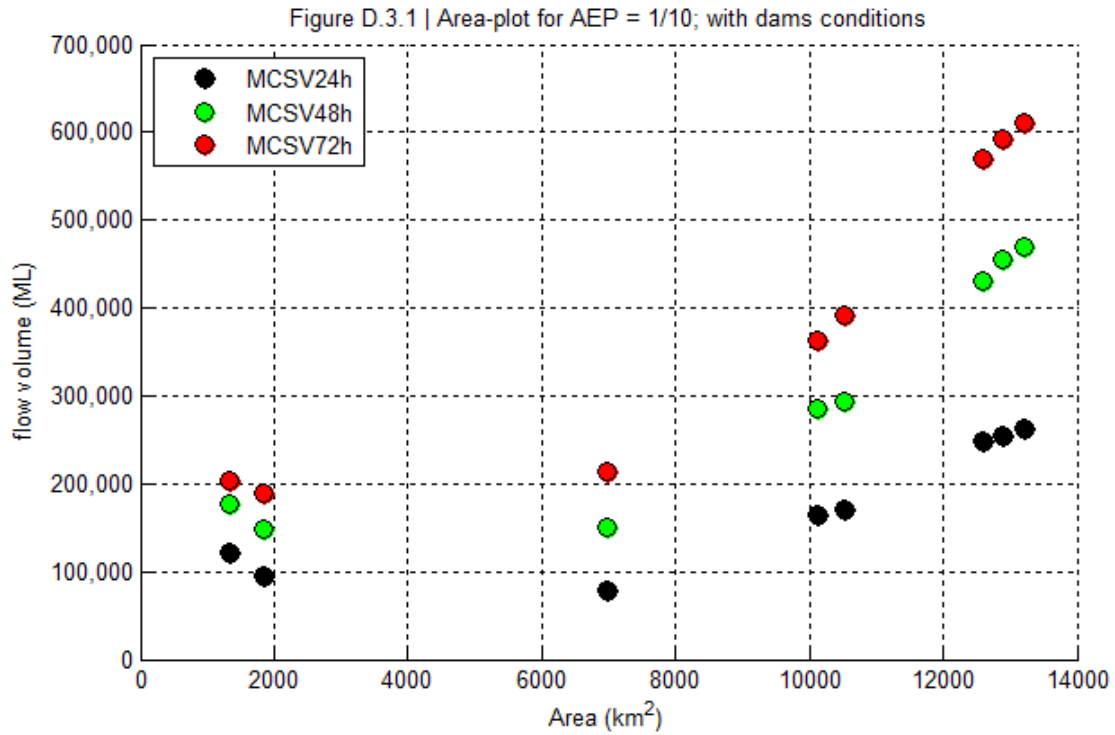


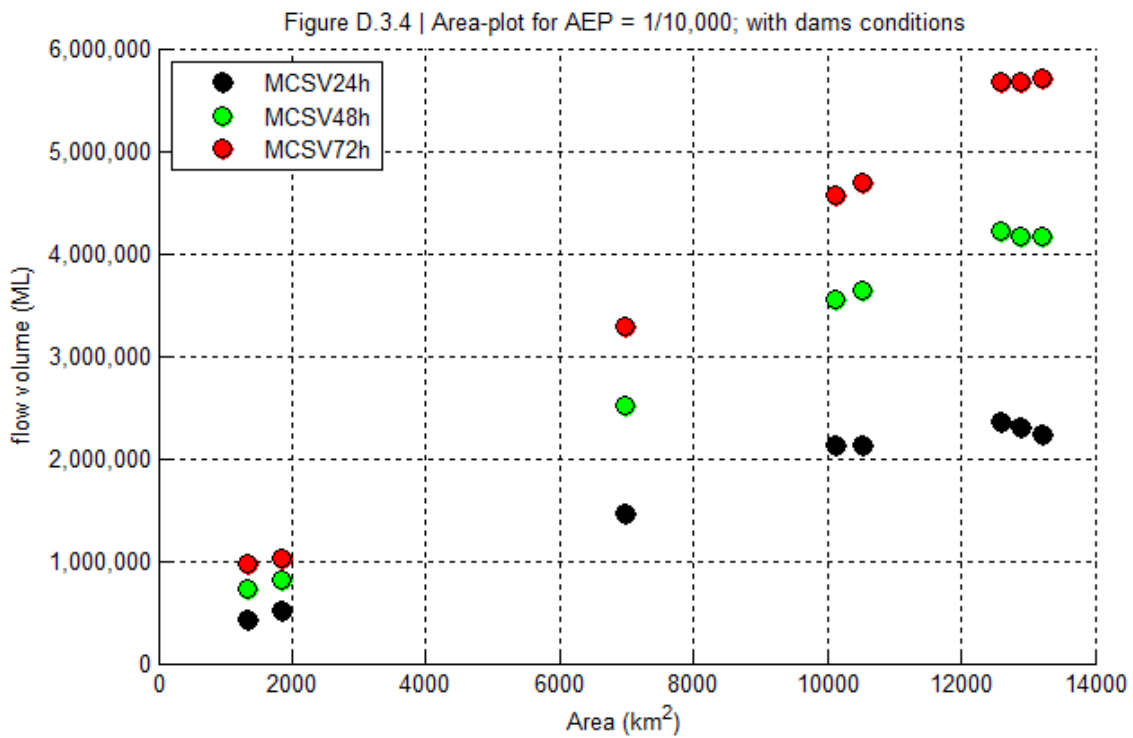
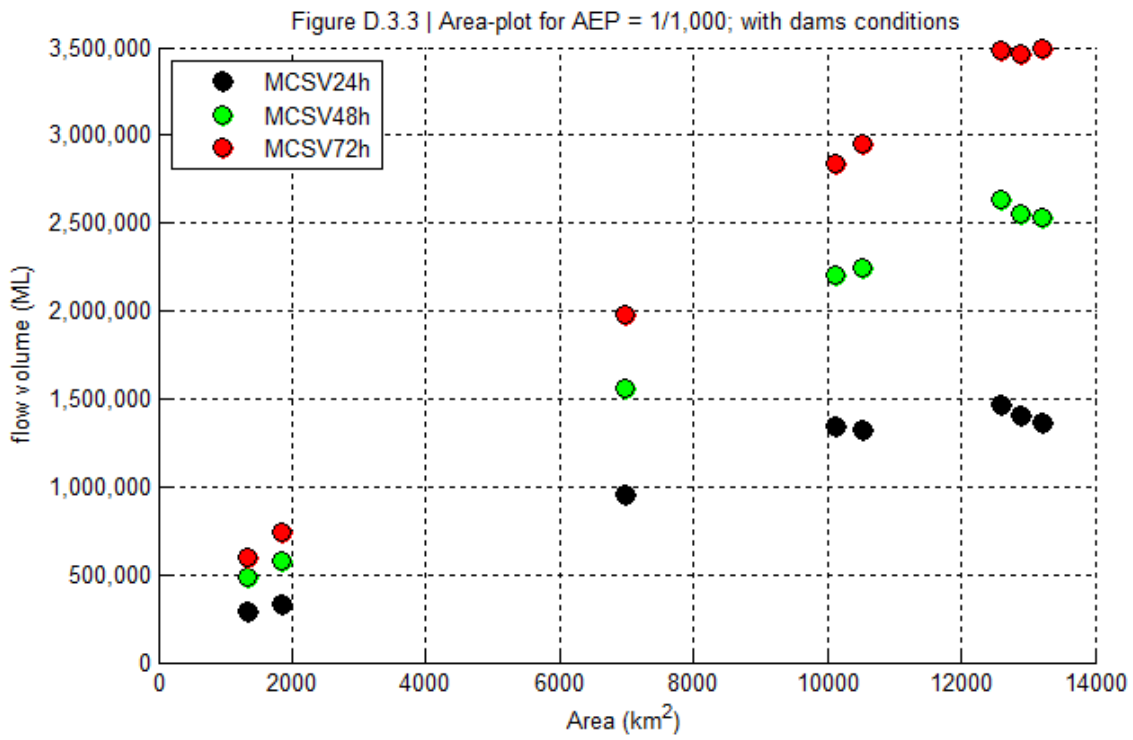
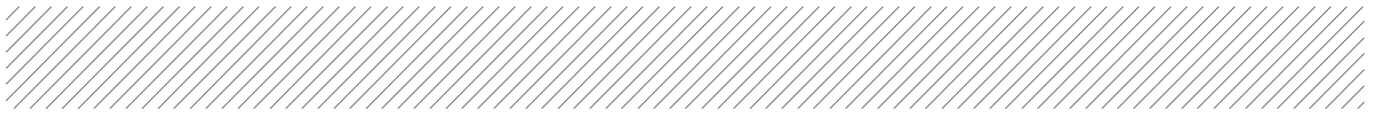
Figure D.2.8 | Location Brisbane; with dams conditions

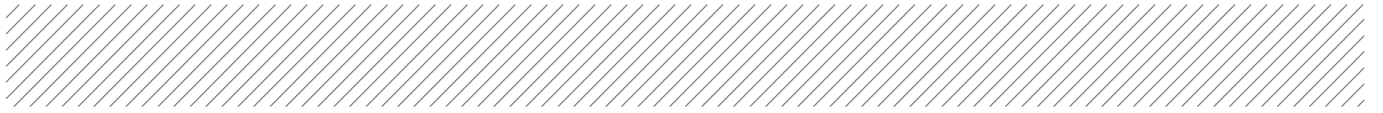


D.3 Plots of catchment area versus flow volumes

This section contains nine figures in which flows 24-, 48- and 72 hour flow volumes are plotted against catchment area.








Appendix E

Comparison of 'with-dams' and 'no-dams' results



This appendix contains Figures in which 'with-dams' results are compared to 'no-dams' results. These Figures are provided for locations Ipswich, Somerset Dam and Wivenhoe Dam and the five Lower Brisbane locations. The following Figures are provided for each location:

1. Frequency plots for 'no dam' peak flows and 'with dam' peak flows
2. Scatter plots of simulated 'no dam' peak flows versus 'with dam' flows
3. Frequency plots for 'no dam' flow volumes and 'with dam' flow volumes

No scatter plot is provided for location Somerset Dam because the simulated synthetic events for 'no dams' and 'with dams' conditions are different for this location. MCS results for Somerset Dam were abstracted from the Wivenhoe Dam simulation run. The reason to use these results instead of carrying out an individual run for the Somerset Dam catchment is that the operation of the Somerset Dam heavily depends on Wivenhoe Dam levels, which means an individual run for the Somerset Dam catchment is not meaningful for 'with dams' conditions. This is a difference with the 'no dams' conditions, for which frequency curves for Somerset Dam were based on an individual run for the Somerset Dam catchment. This means the simulated synthetic events for 'no dams' and 'with dams' conditions are different for location Somerset. For the other seven locations, the simulated synthetic events for 'no dams' and 'with dams' conditions are the same.

This appendix contains the following sections:

- E1. Frequency plots of peak discharges
 - E2. Scatter plots for peak discharges
 - E3. Frequency plots of flow volumes
-

E.1 Frequency plots of peak discharges

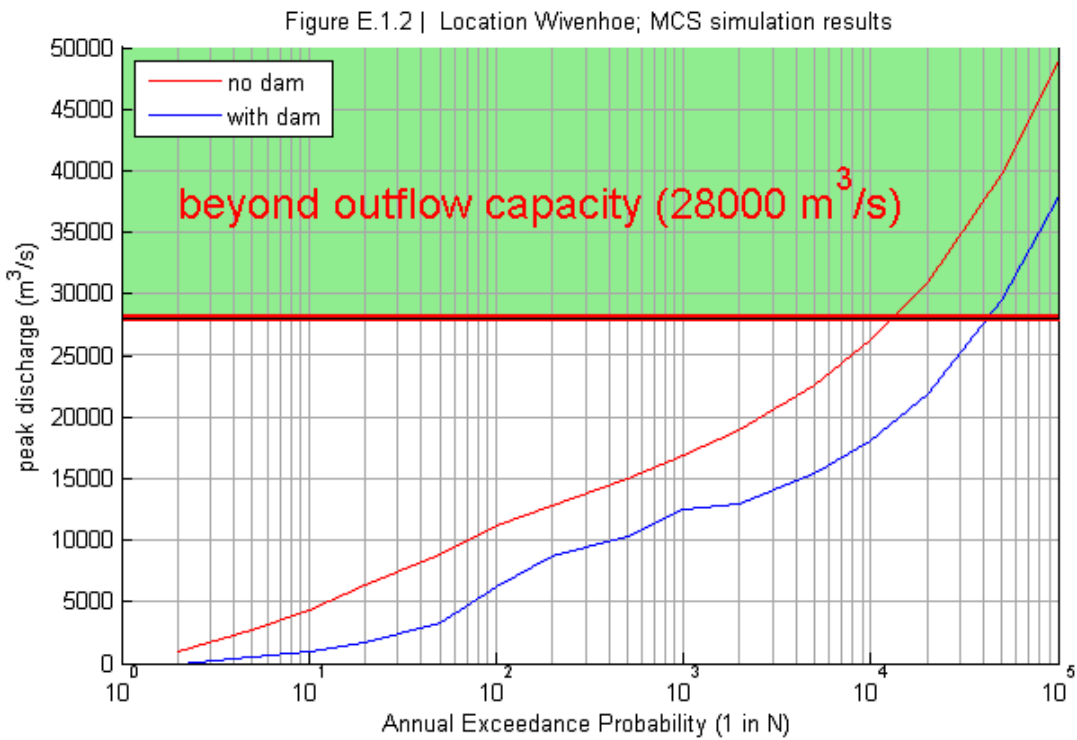
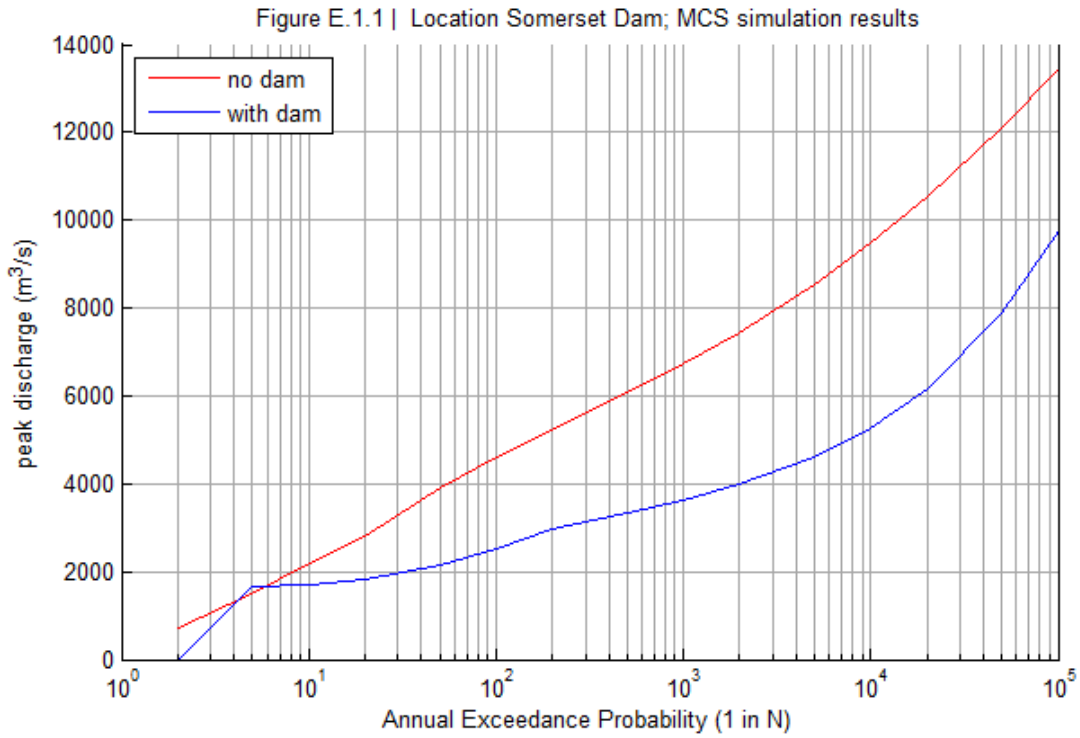




Figure E.1.3 | Location Savages Crossing; MCS simulation results

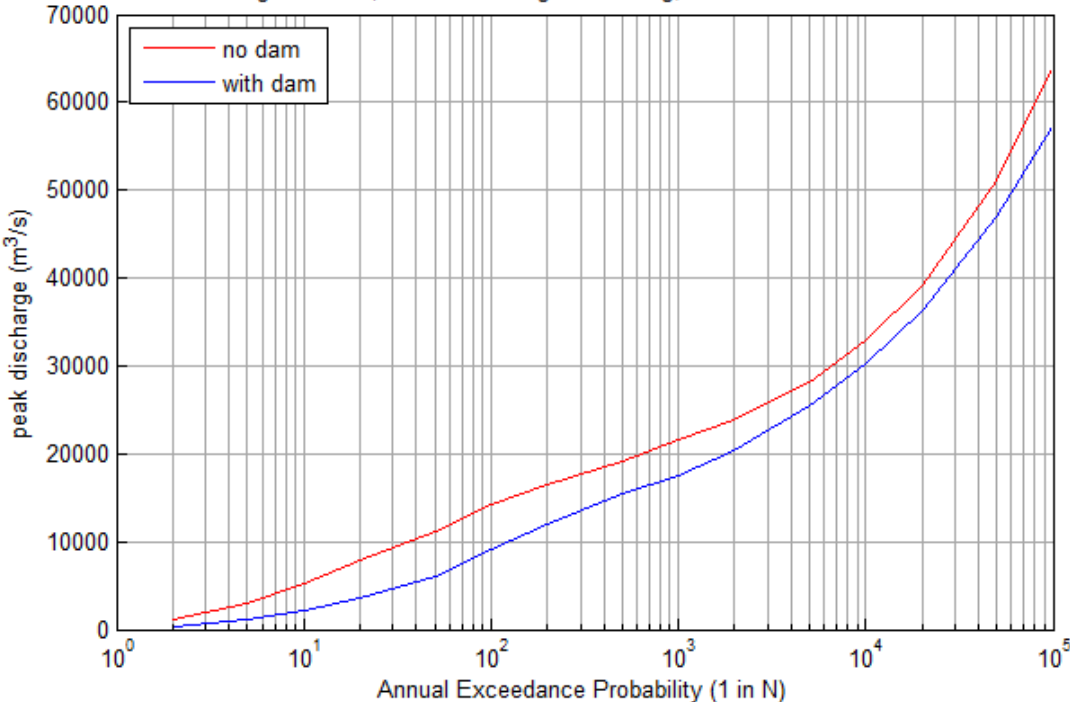


Figure E.1.4 | Location Mount Crosby; MCS simulation results

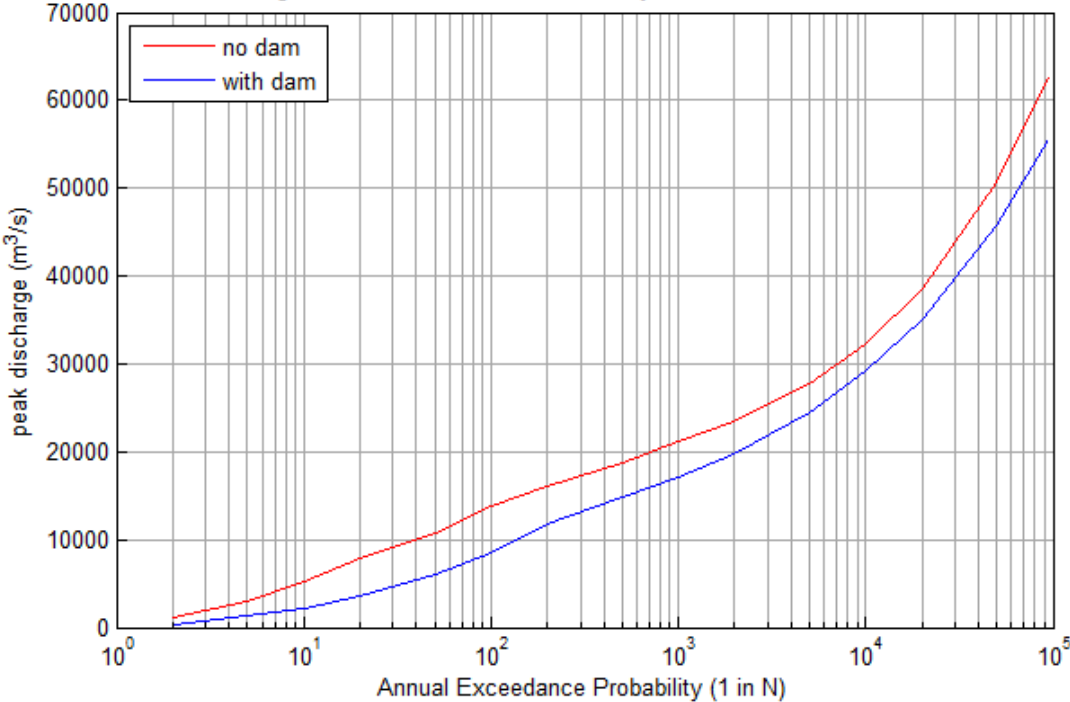




Figure E.1.5 | Location Ipswich; MCS simulation results

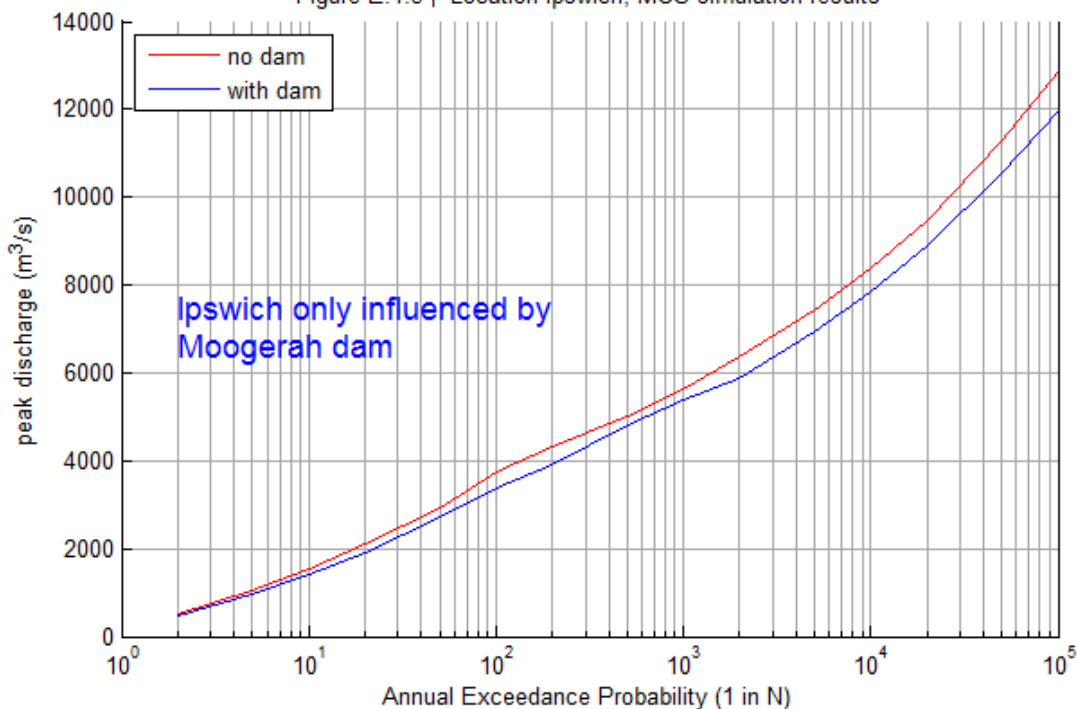


Figure E.1.6 | Location Moggill; MCS simulation results

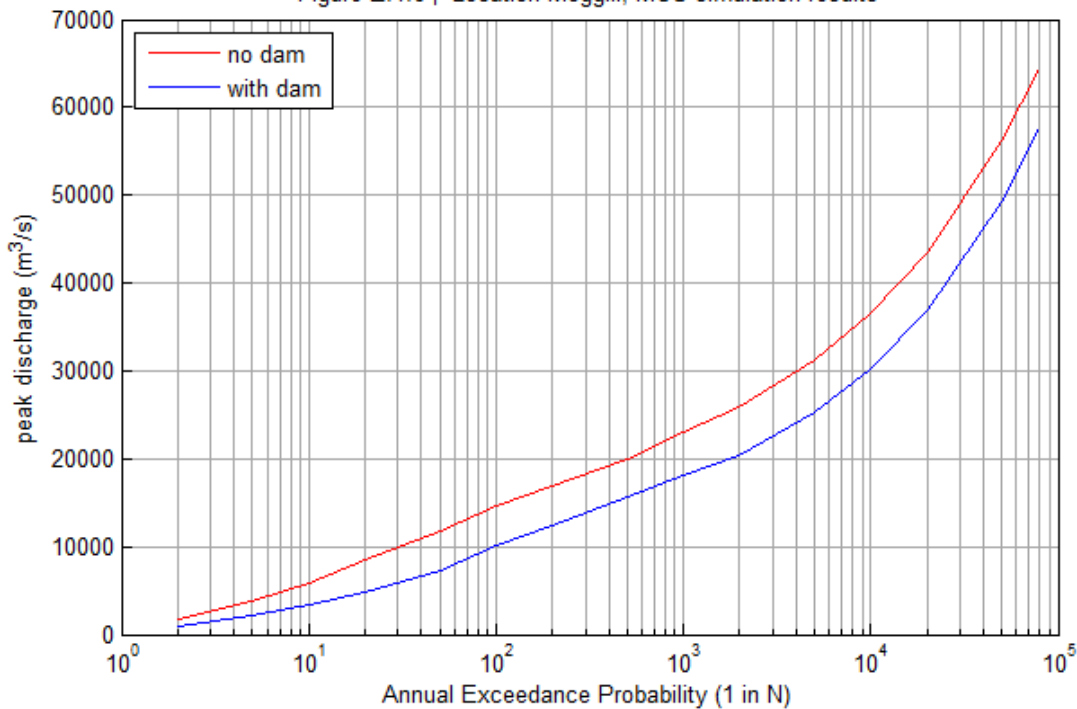




Figure E.1.7 | Location Centenary Bridge; MCS simulation results

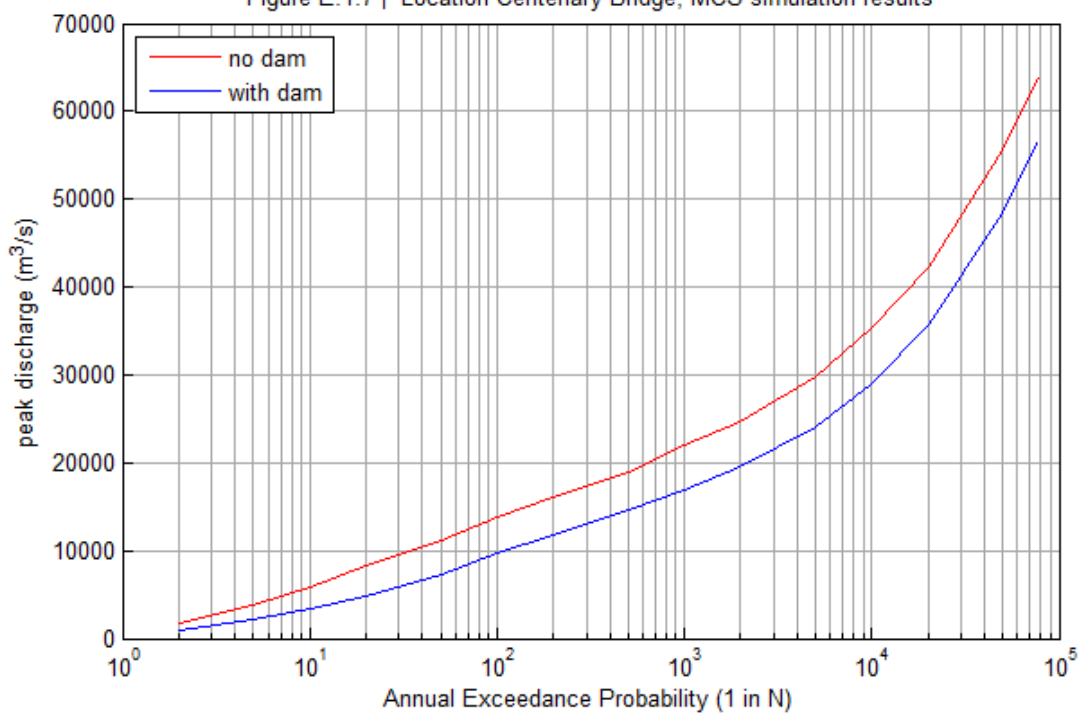
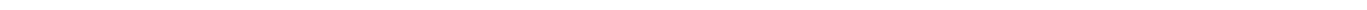
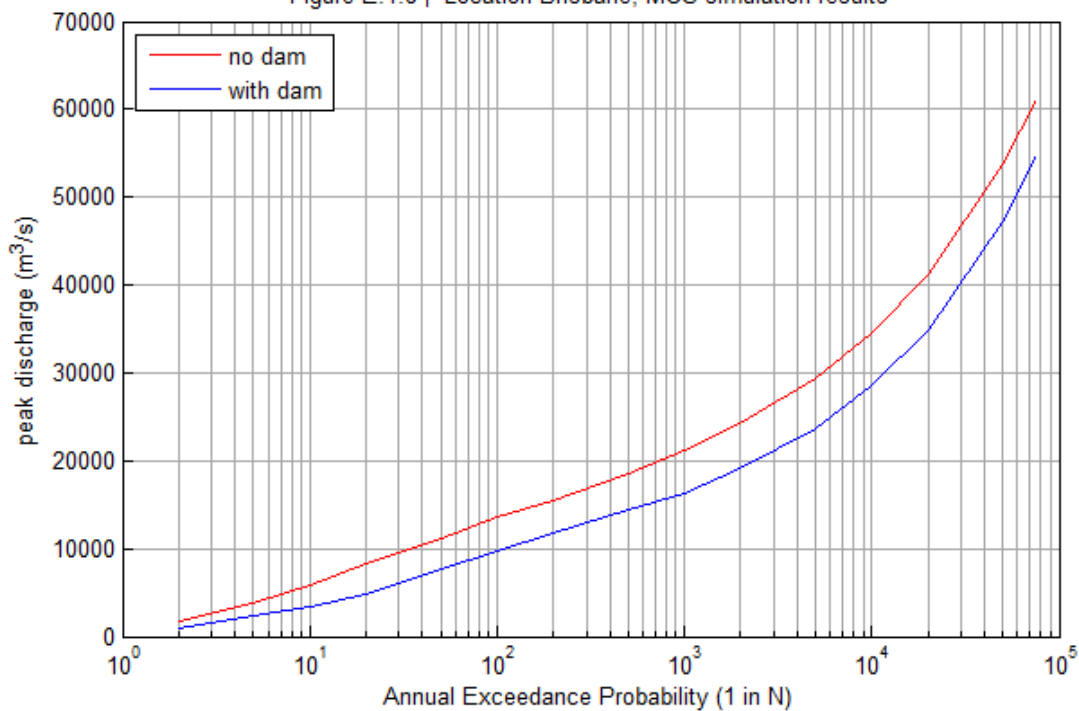
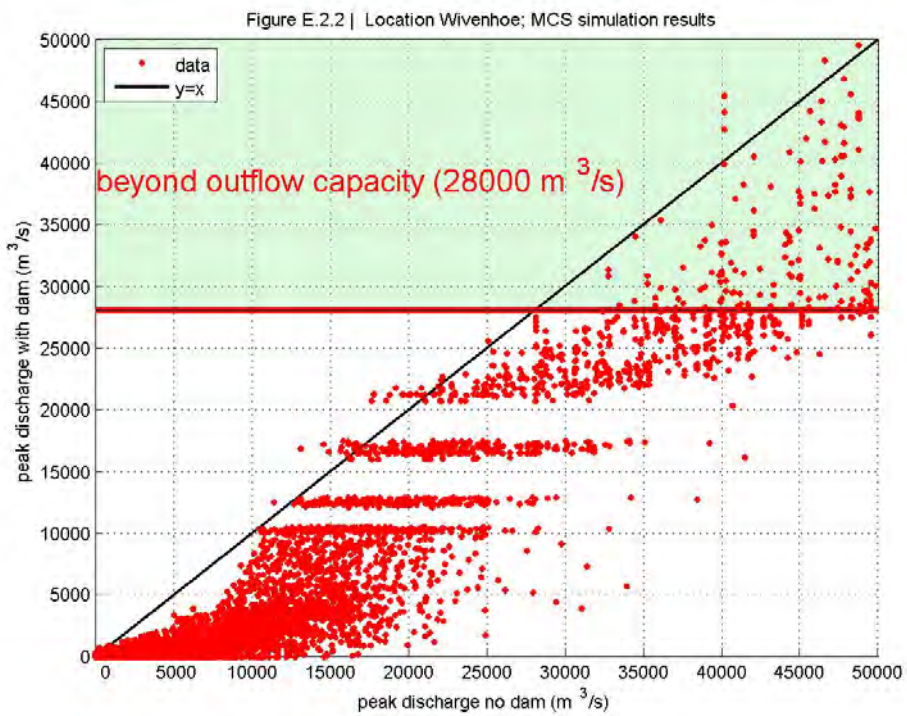
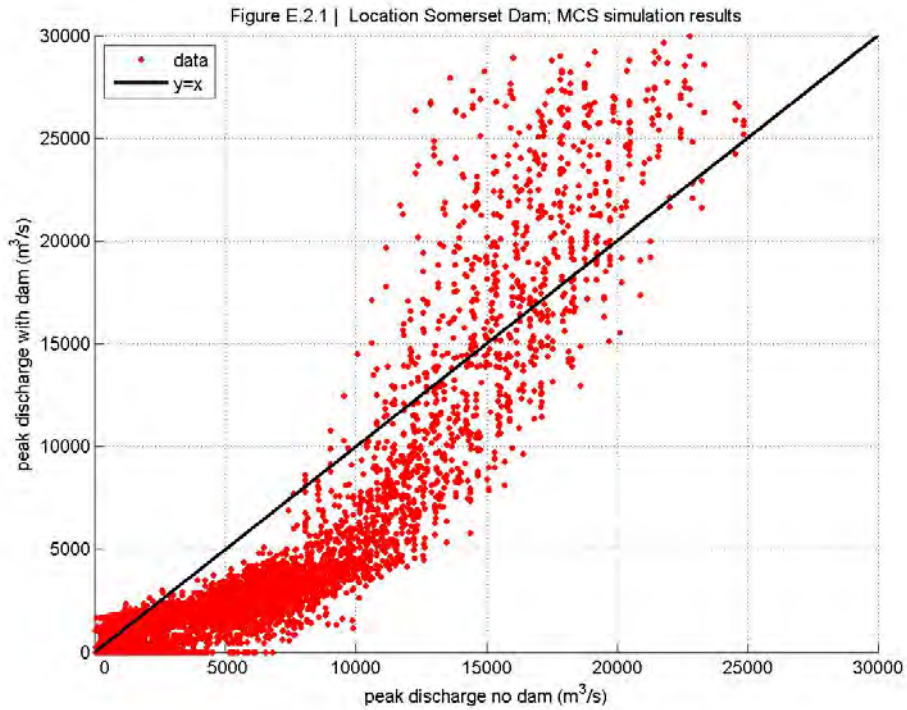
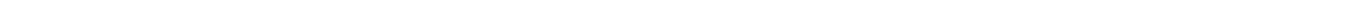
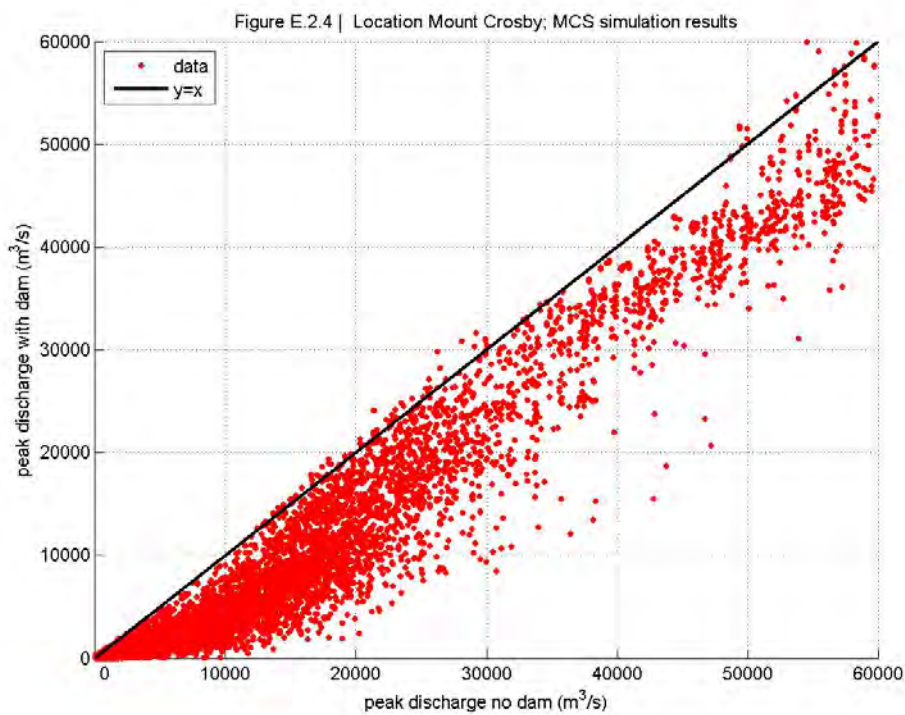
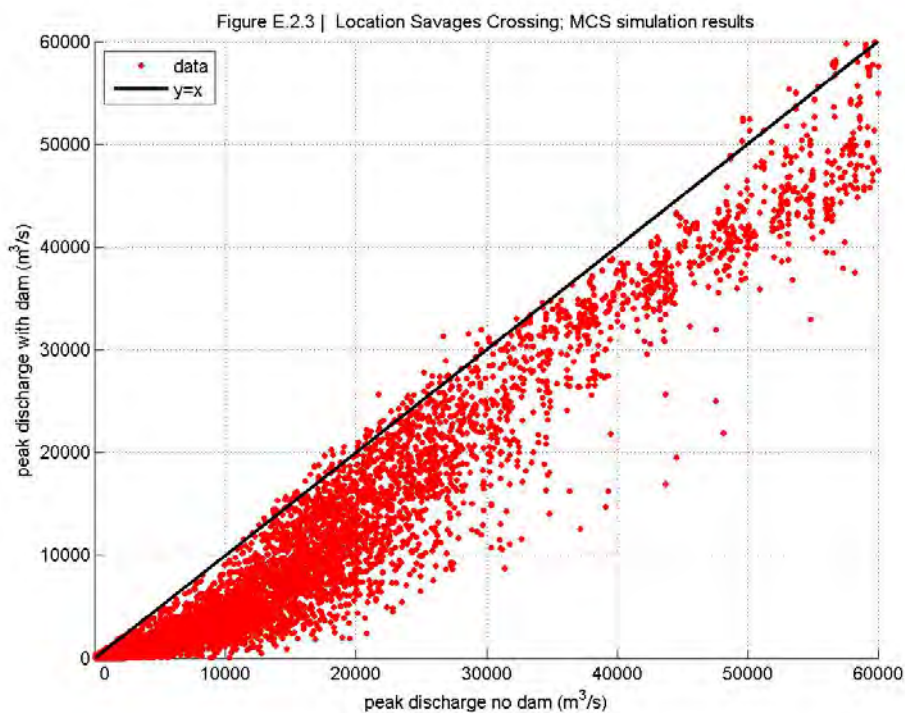


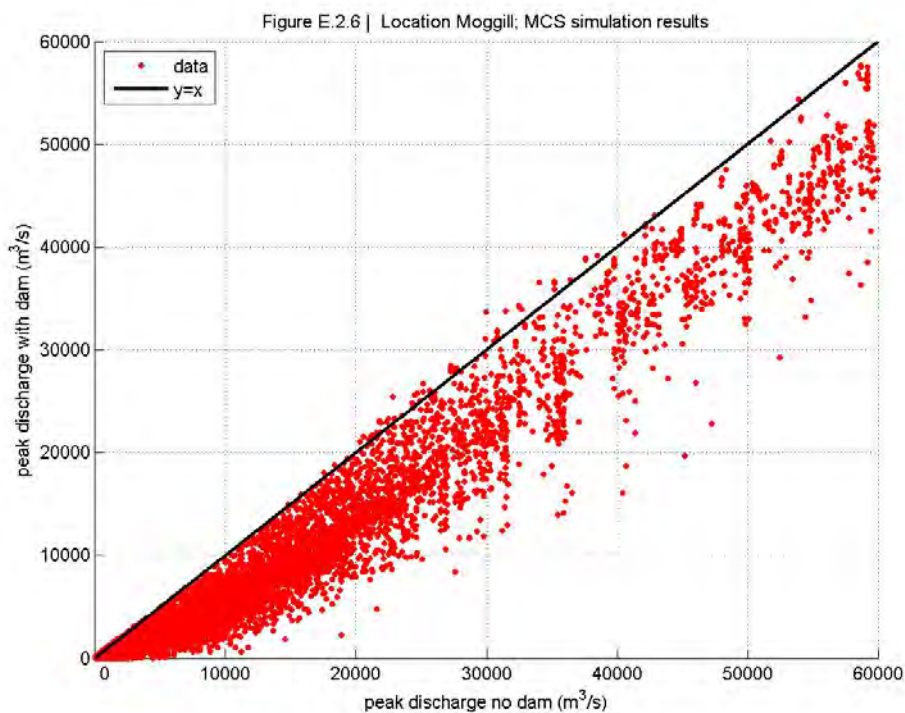
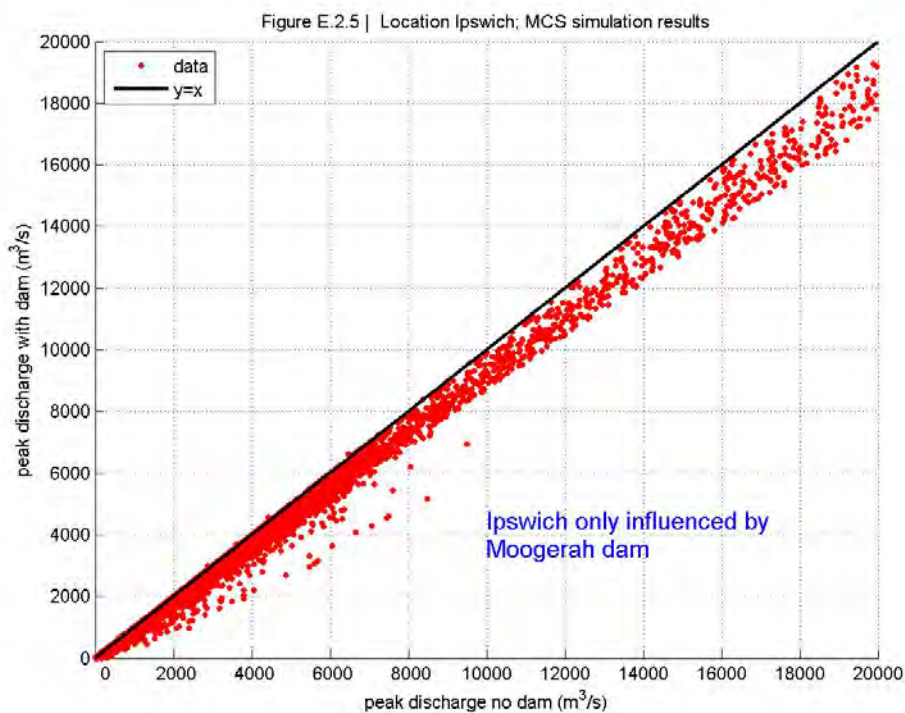
Figure E.1.8 | Location Brisbane; MCS simulation results

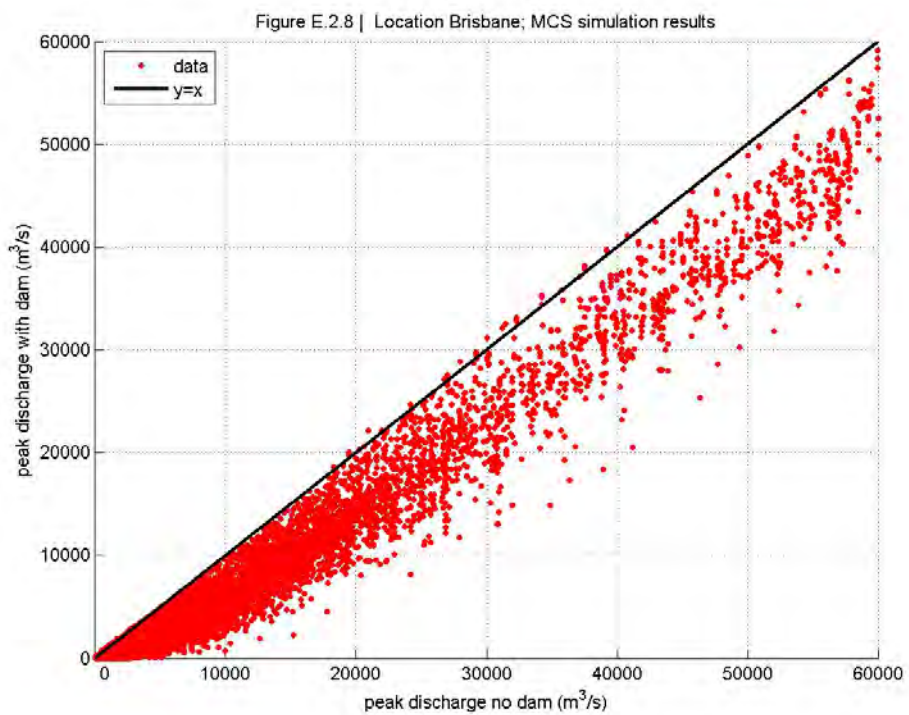
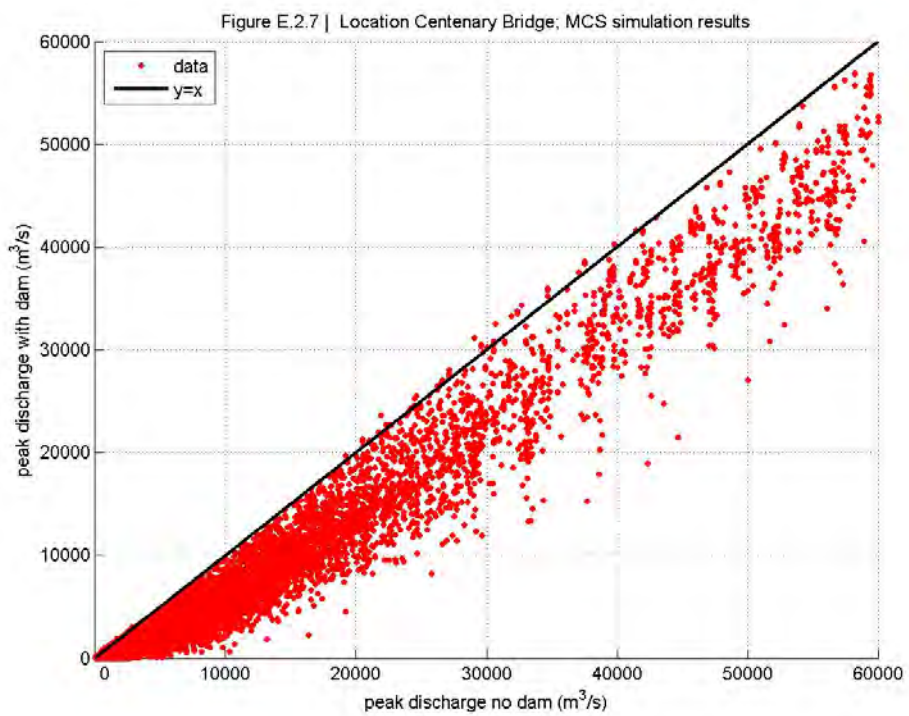


E.2 Scatter plots for peak discharges









E3. Frequency plots of flow volumes

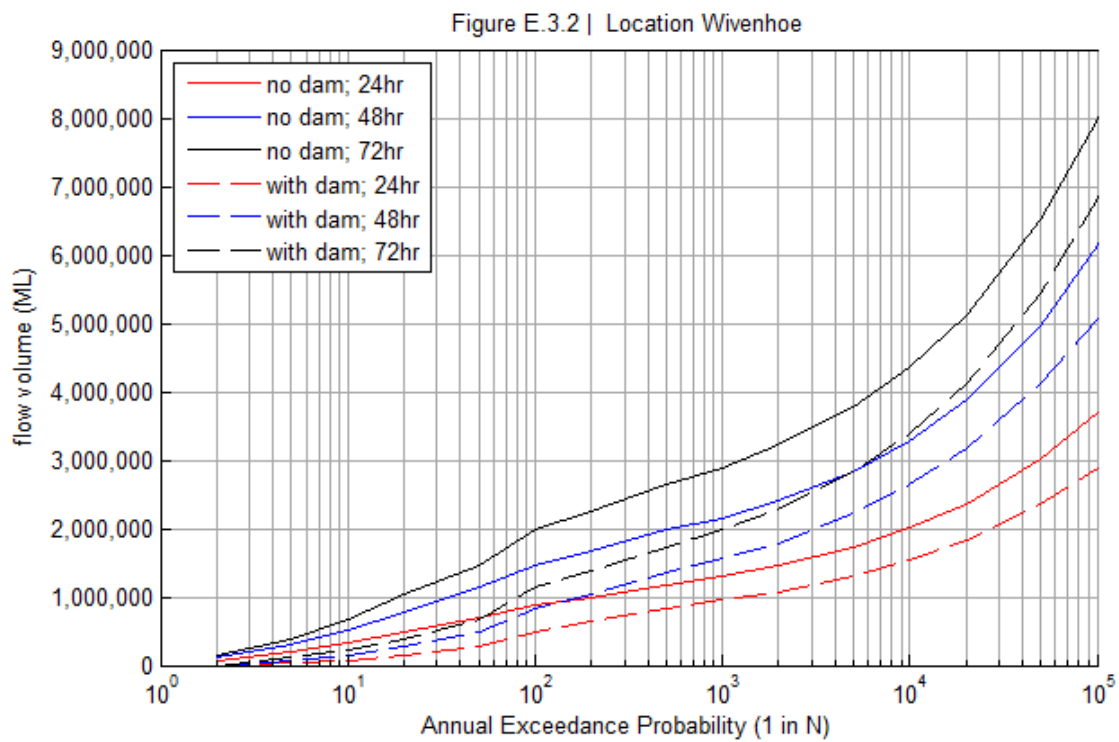
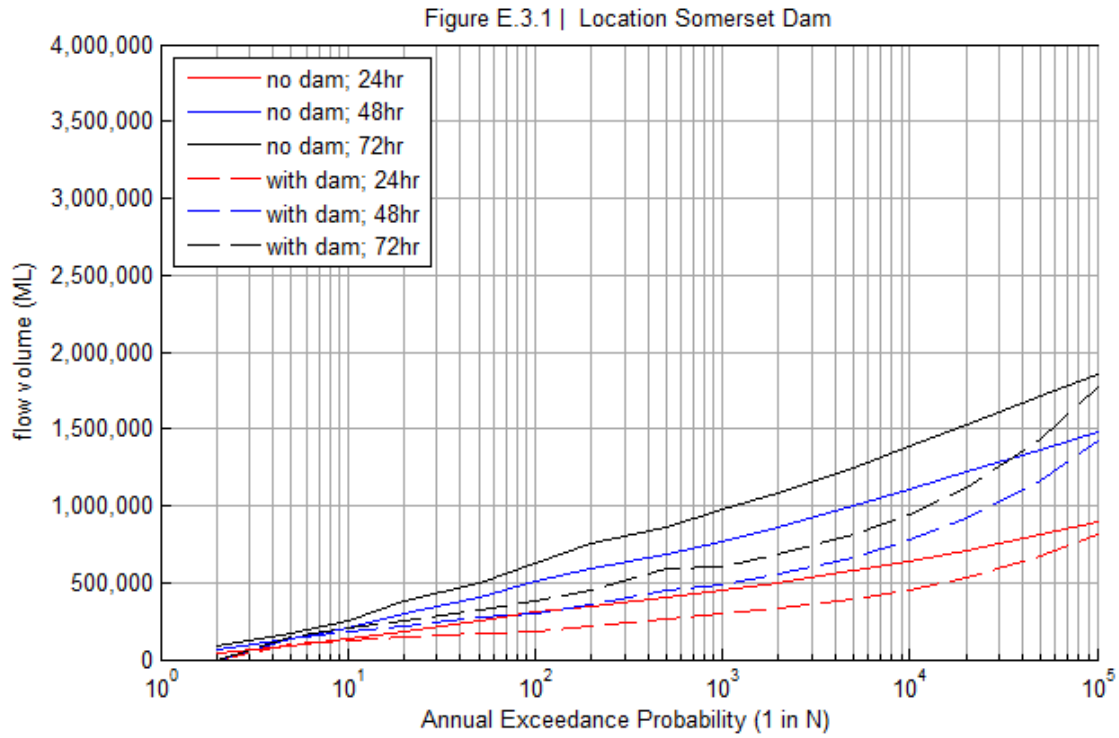




Figure E.3.3 | Location Savages Crossing

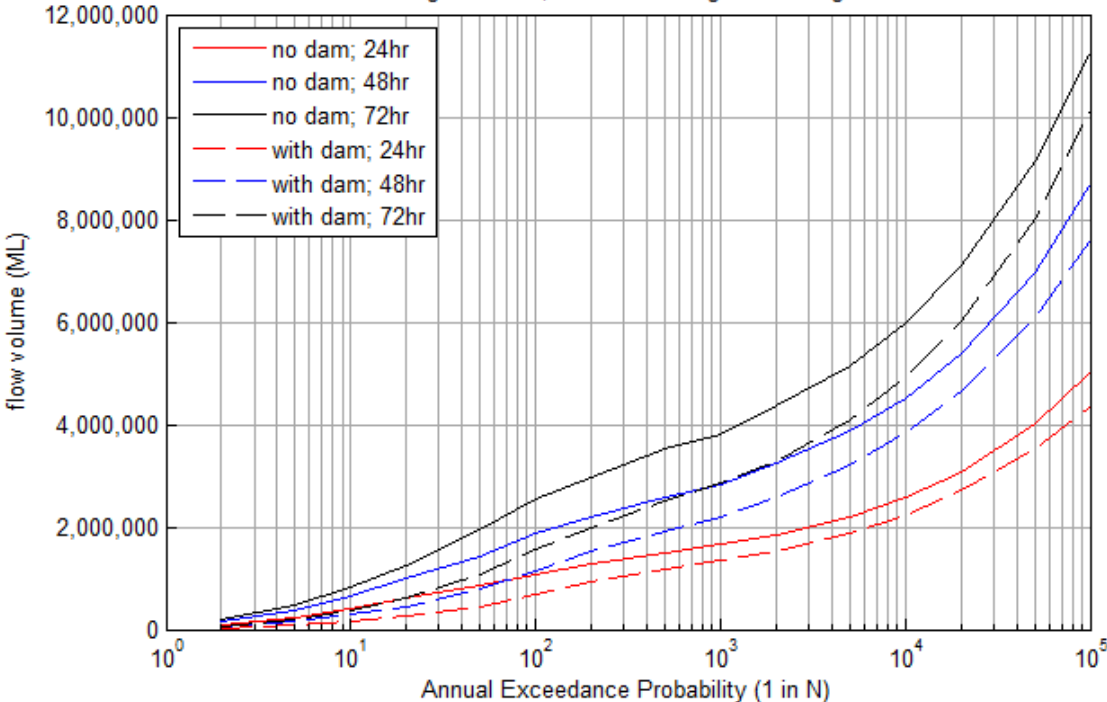


Figure E.3.4 | Location Mount Crosby

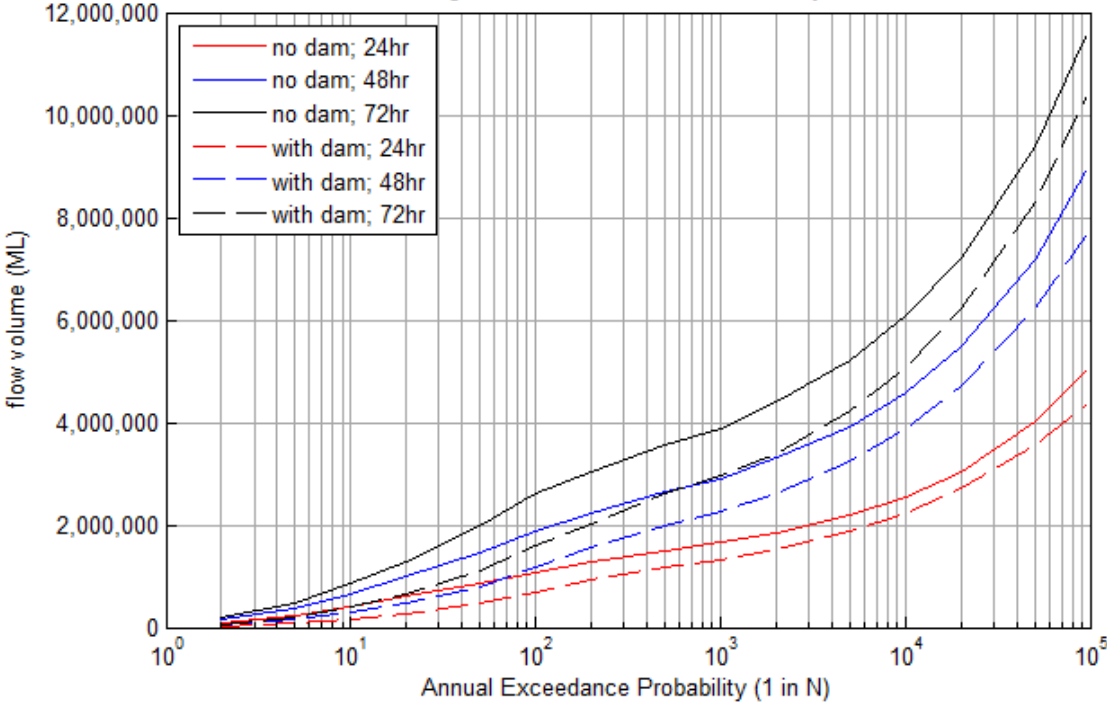




Figure E.3.5 | Location Ipswich

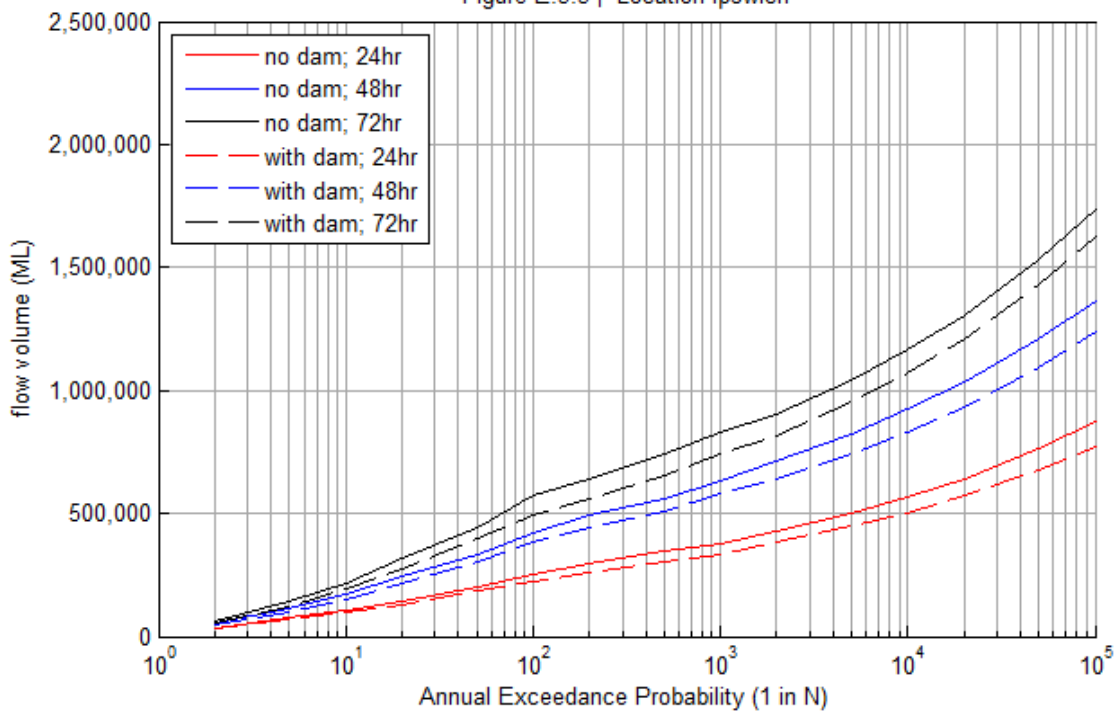


Figure E.3.6 | Location Moggill

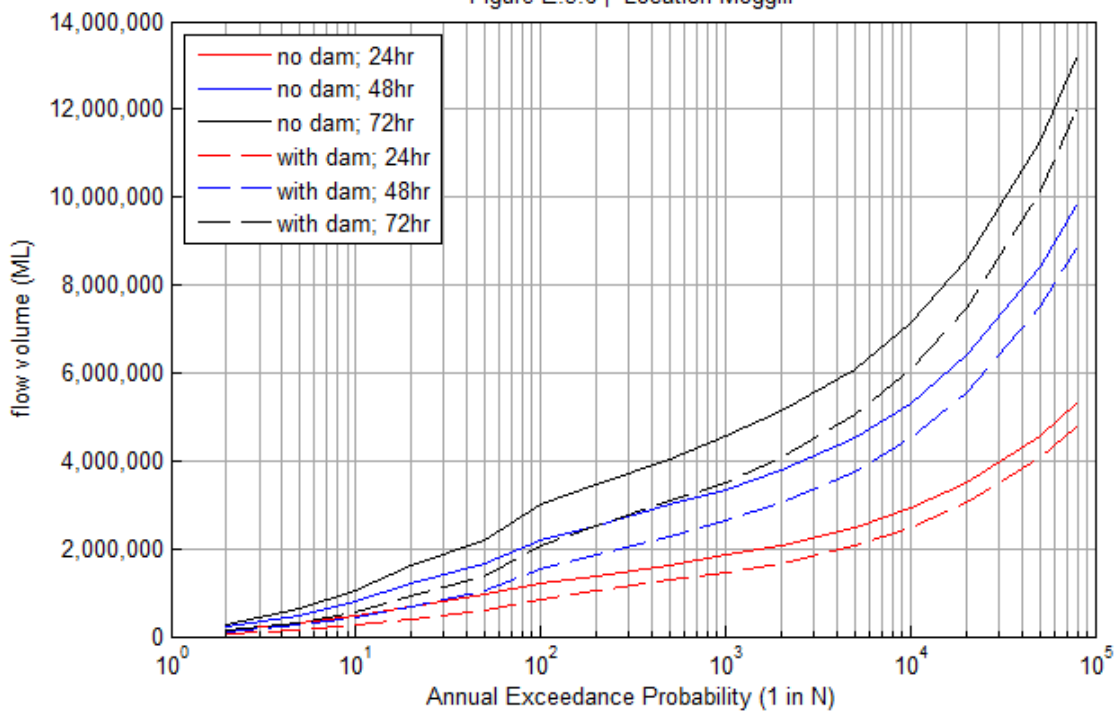




Figure E.3.7 | Location Centenary Bridge

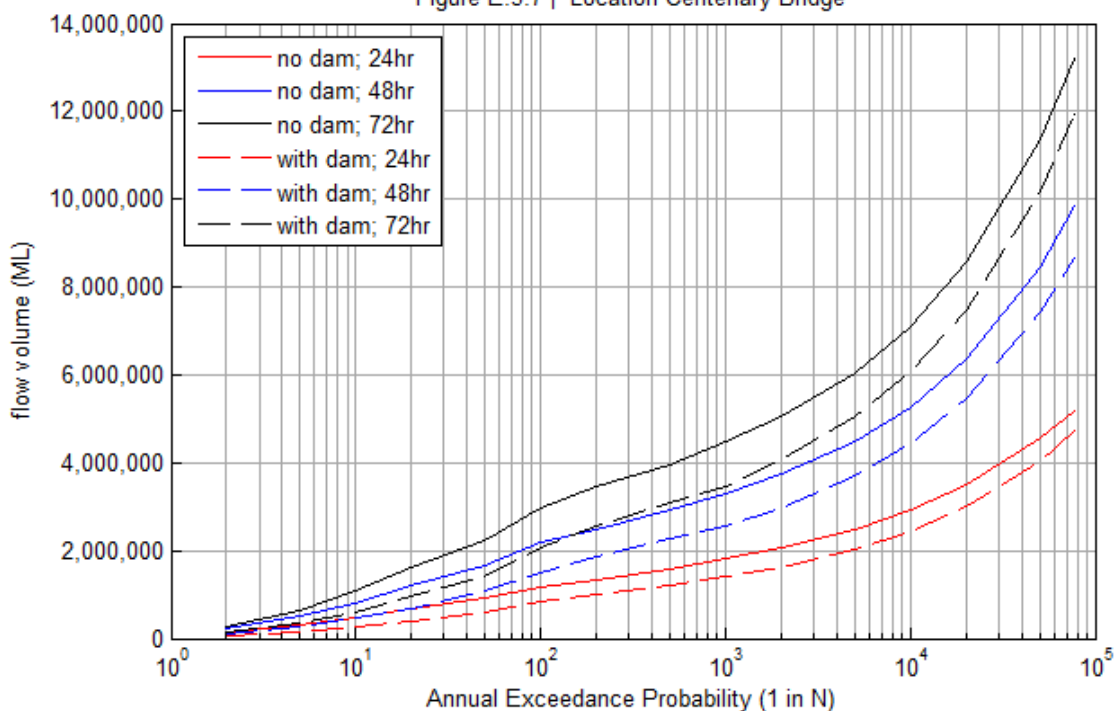
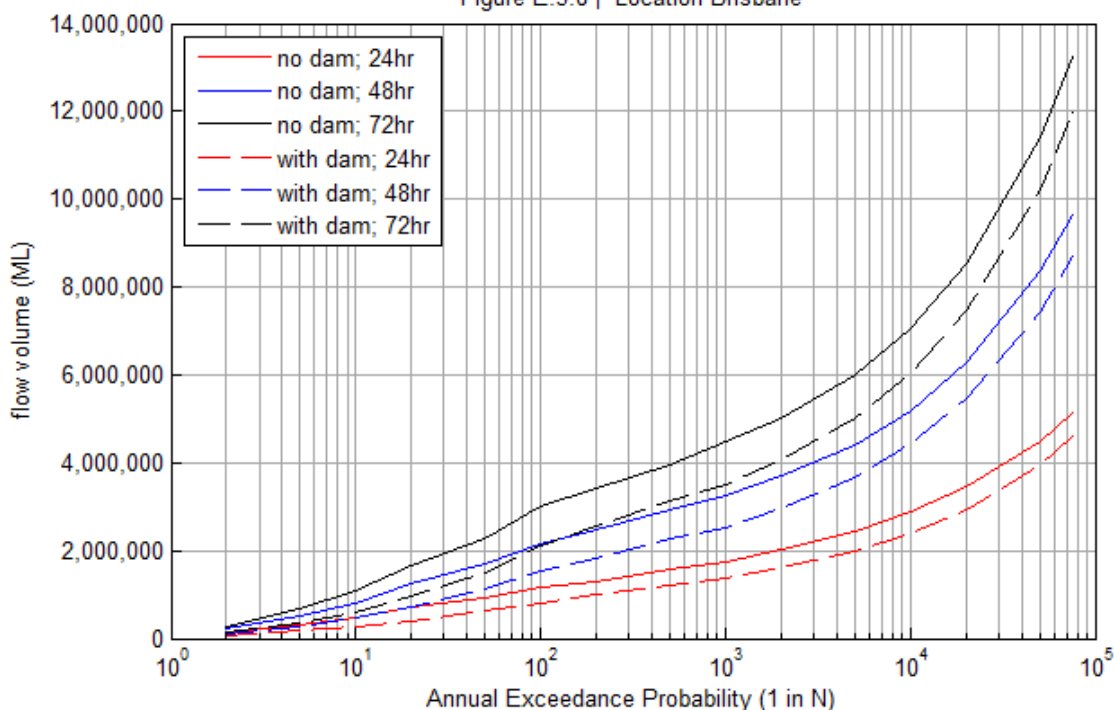
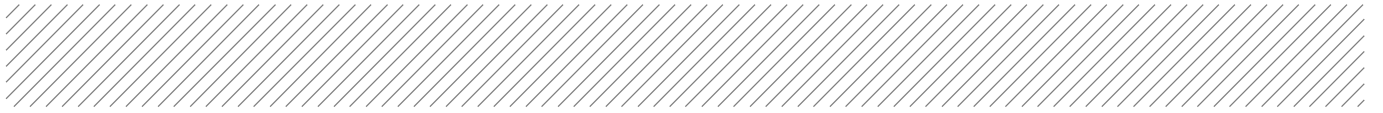


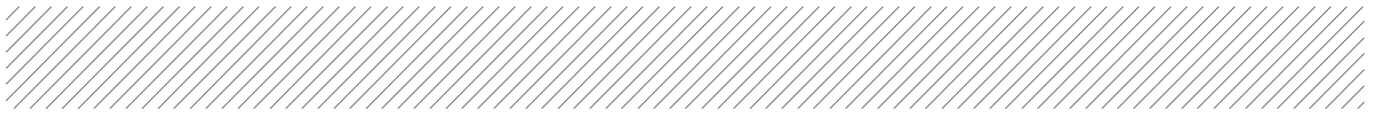
Figure E.3.8 | Location Brisbane





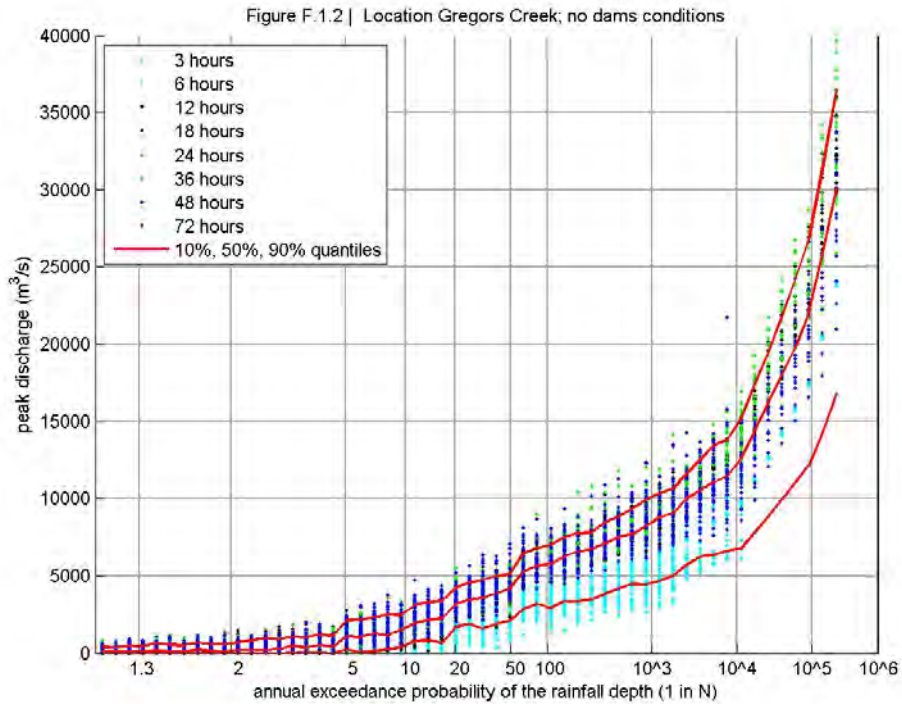
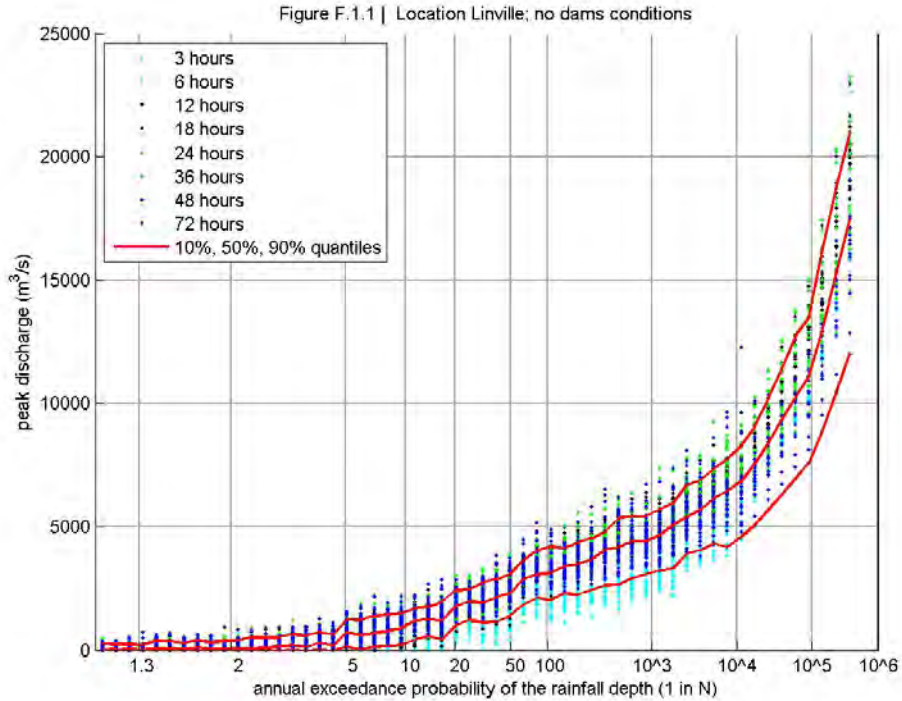
Appendix F

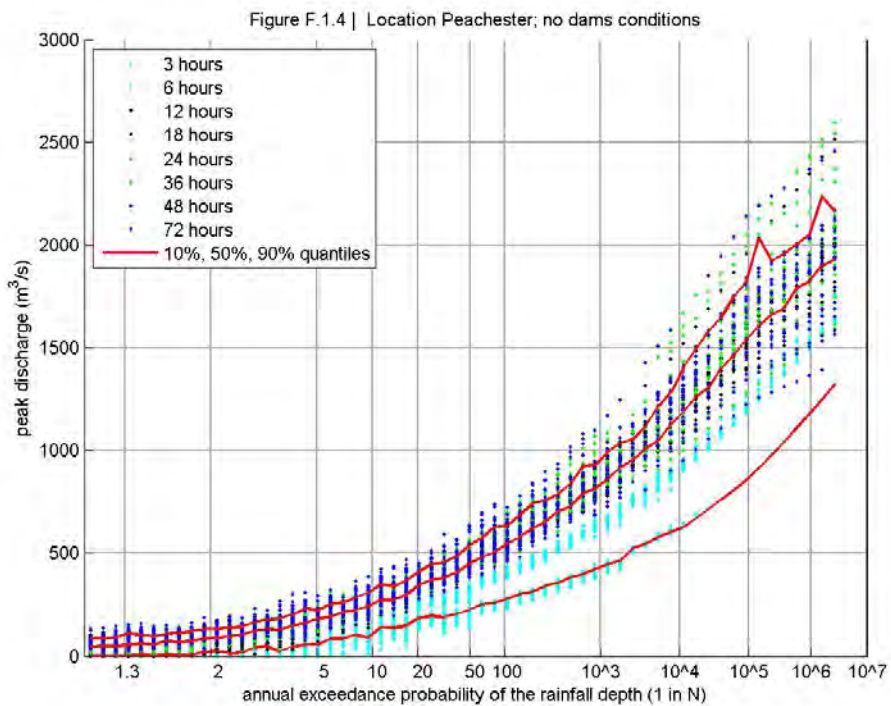
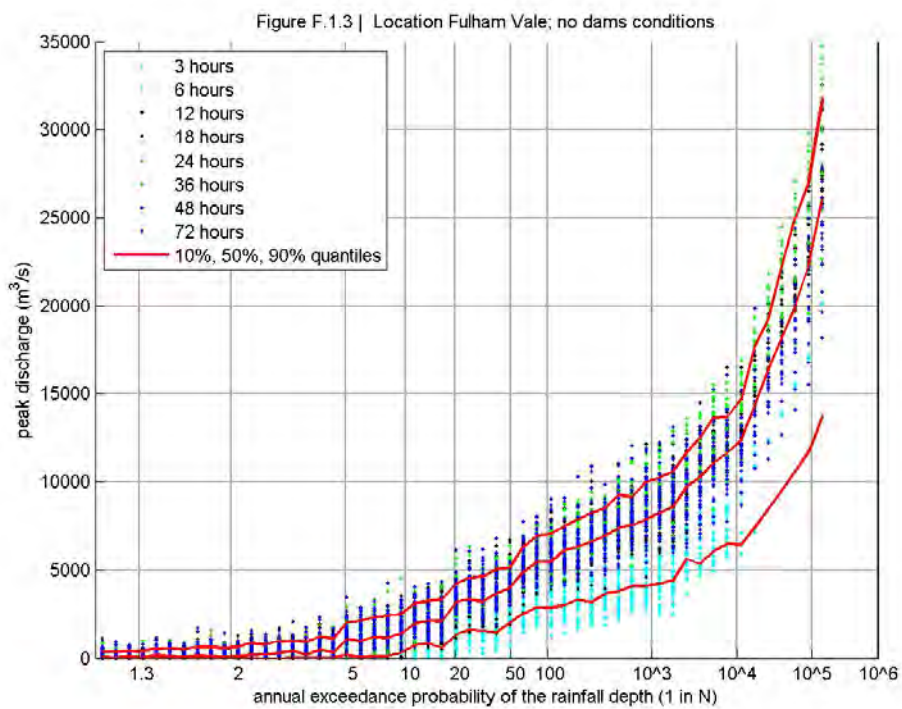
Peak discharge versus AEP of the rainfall depth

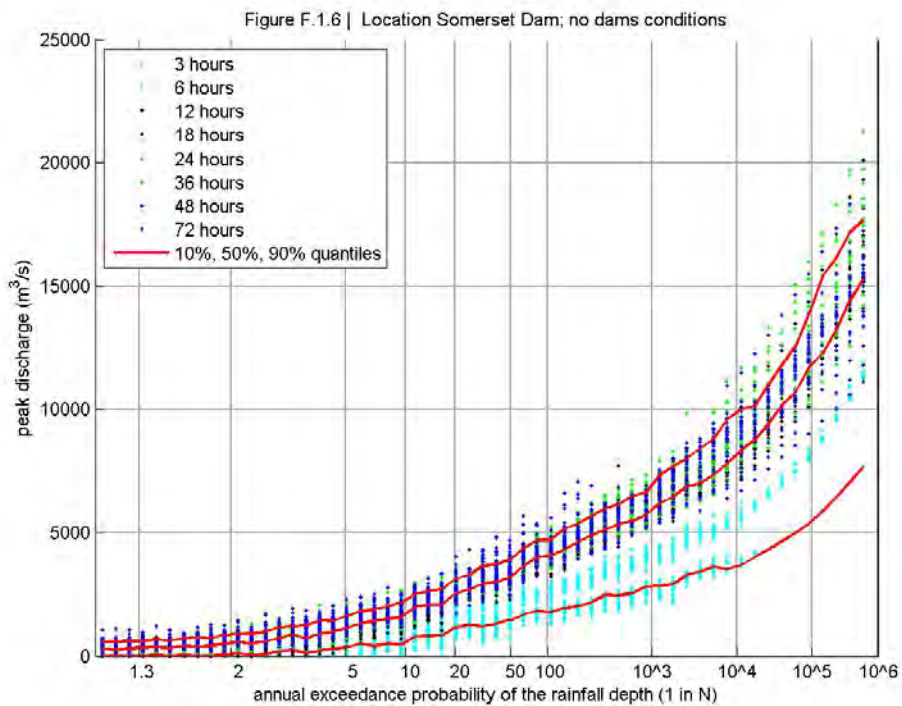
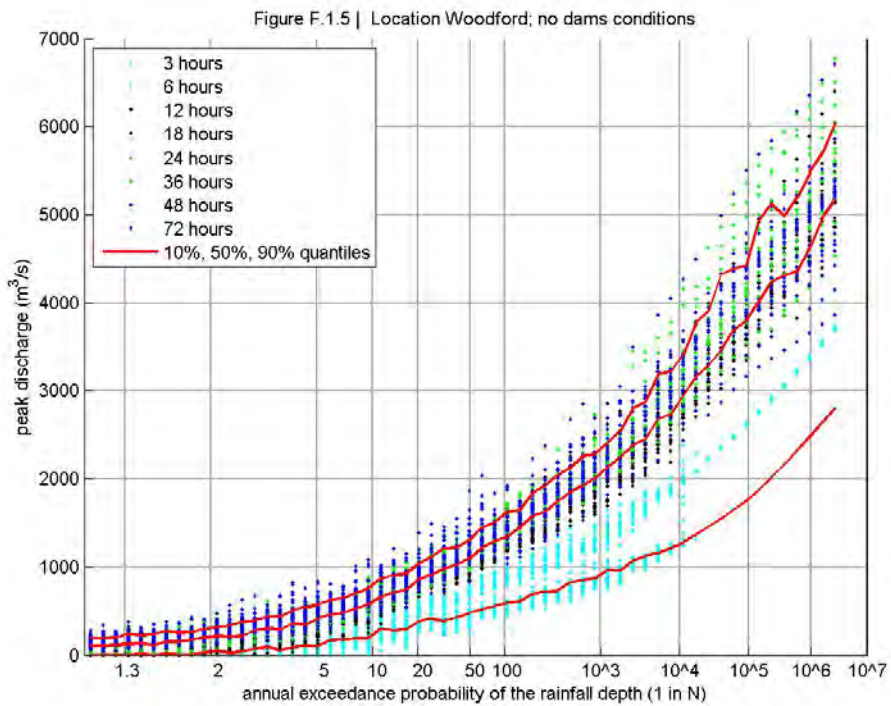


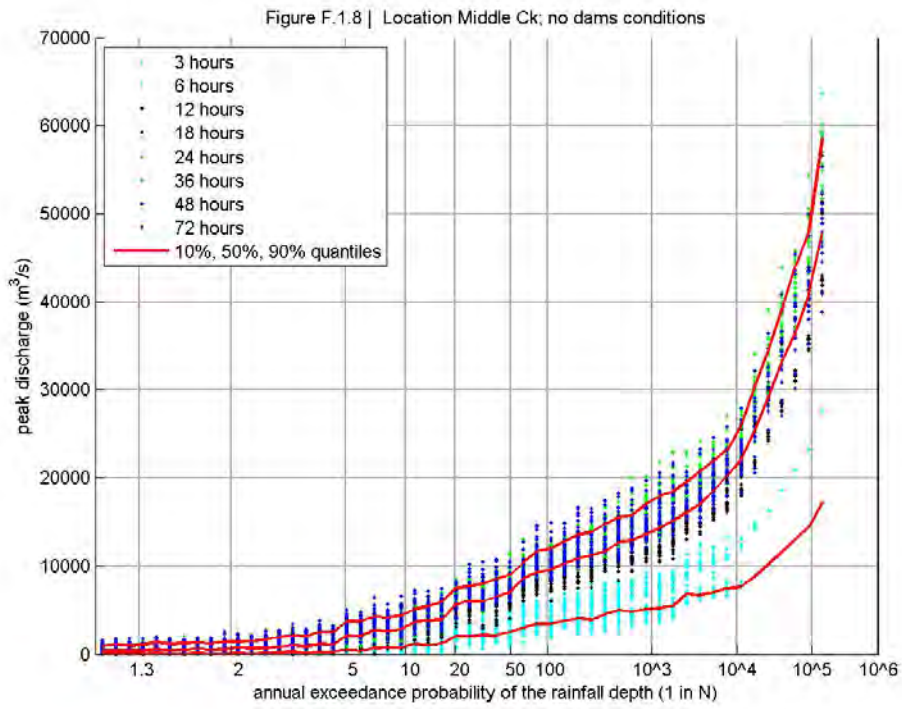
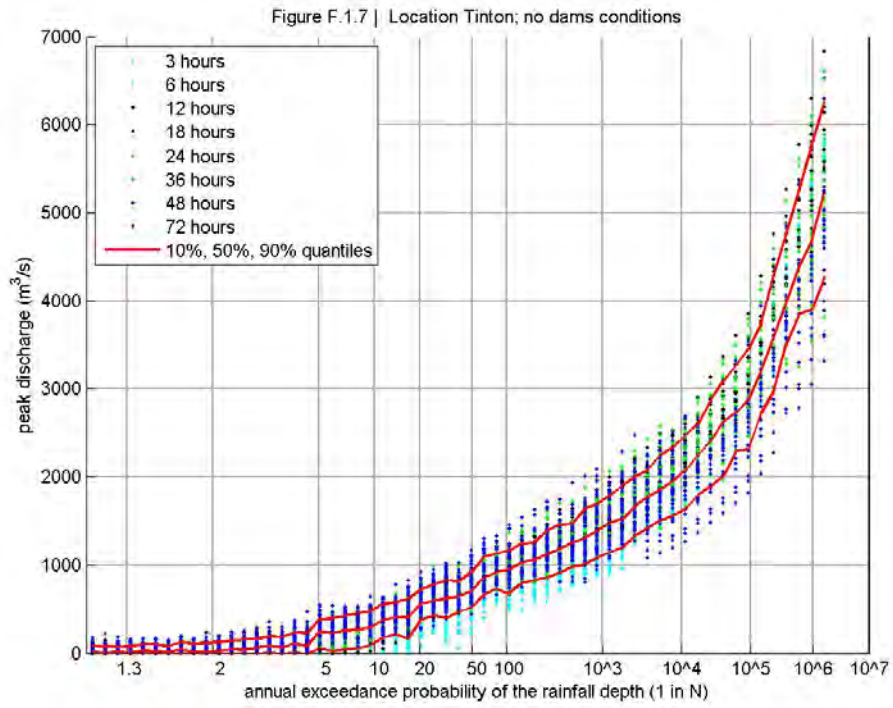
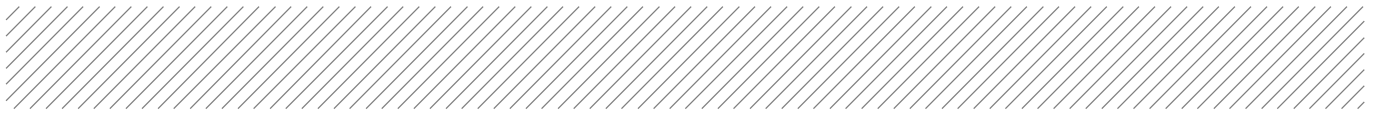
This appendix contains figures in which the peak discharge of each simulated event is plotted against the annual exceedance probability of the rainfall depth. Different colours are used to distinguish for different burst durations. Furthermore, three lines are added that represent the 10%, 50% and 90% quantiles. These lines can be interpreted as follows: for a given rainfall AEP, the p-percentile is the peak discharge which has a p% probability of being exceeded, given the occurrence of a rainfall event with a rainfall depth that corresponds to the AEP shown on the horizontal axis. For a given combination of rainfall burst duration and AEP, the variability of peak discharges in the Figures are caused by the combined influence of the variability of initial losses, spatio-temporal rainfall patterns and, for the 'with dams' case, initial reservoir volumes.

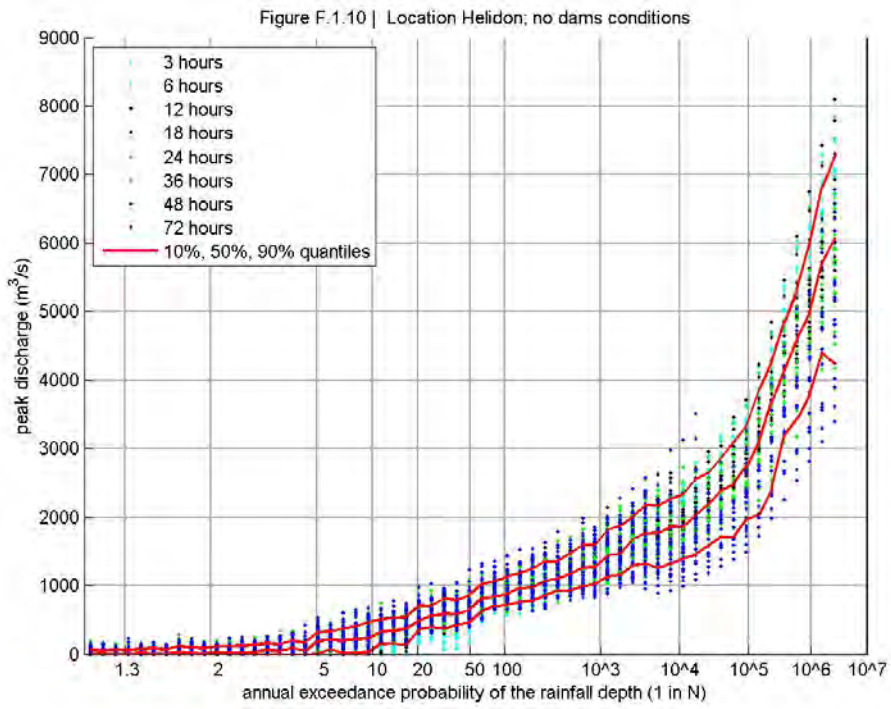
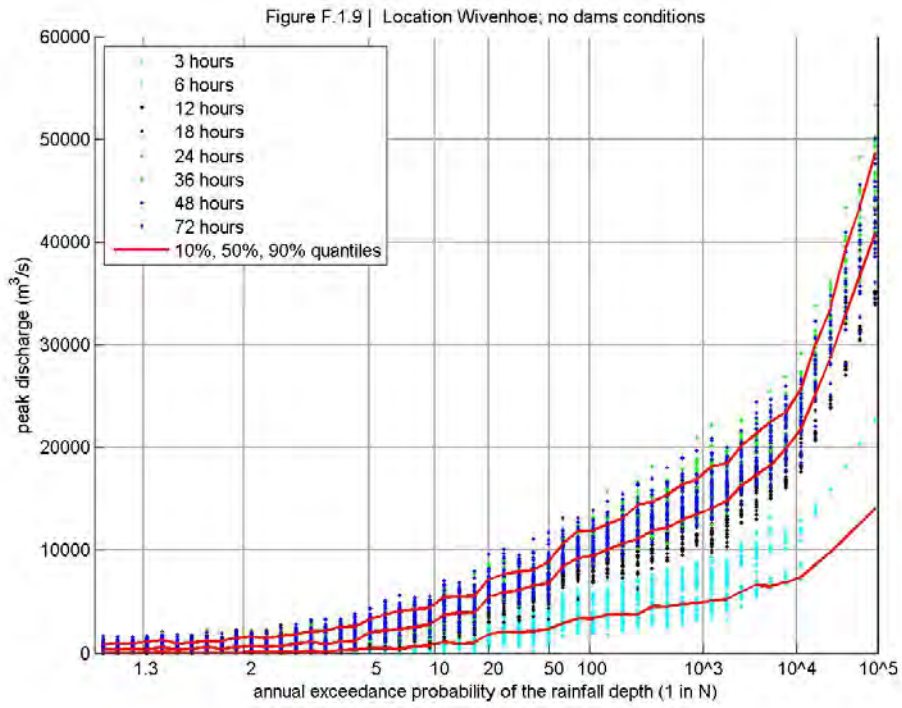
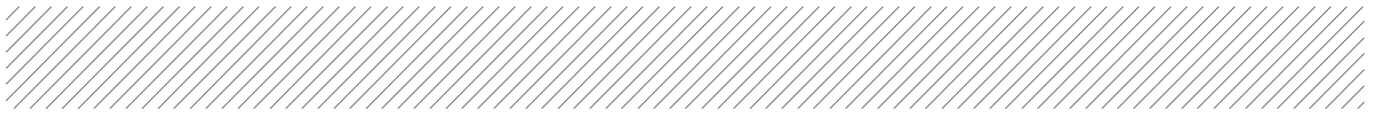
F.1 No-dams conditions

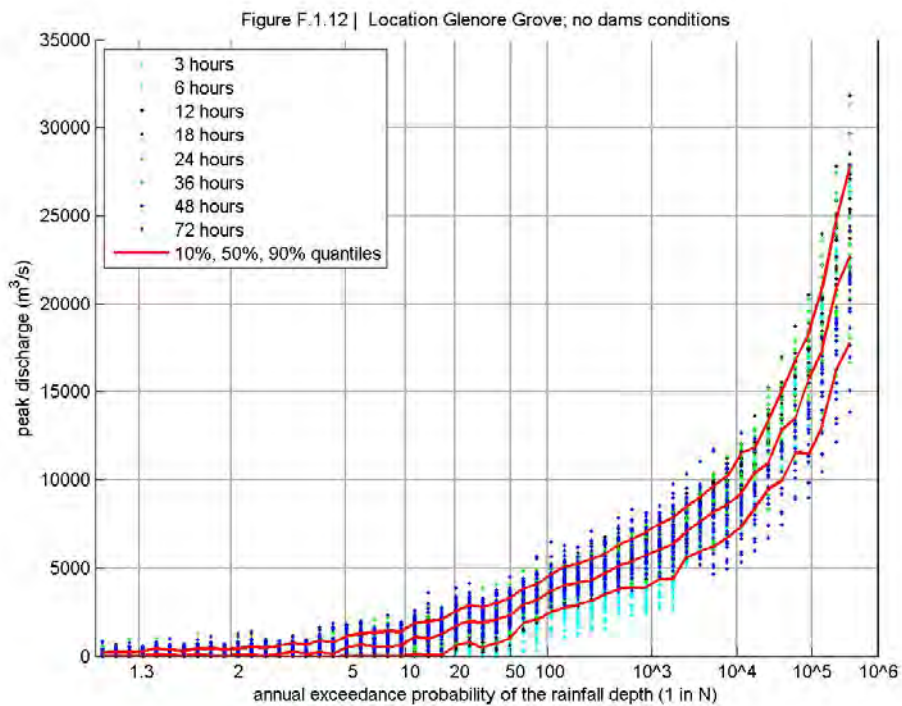
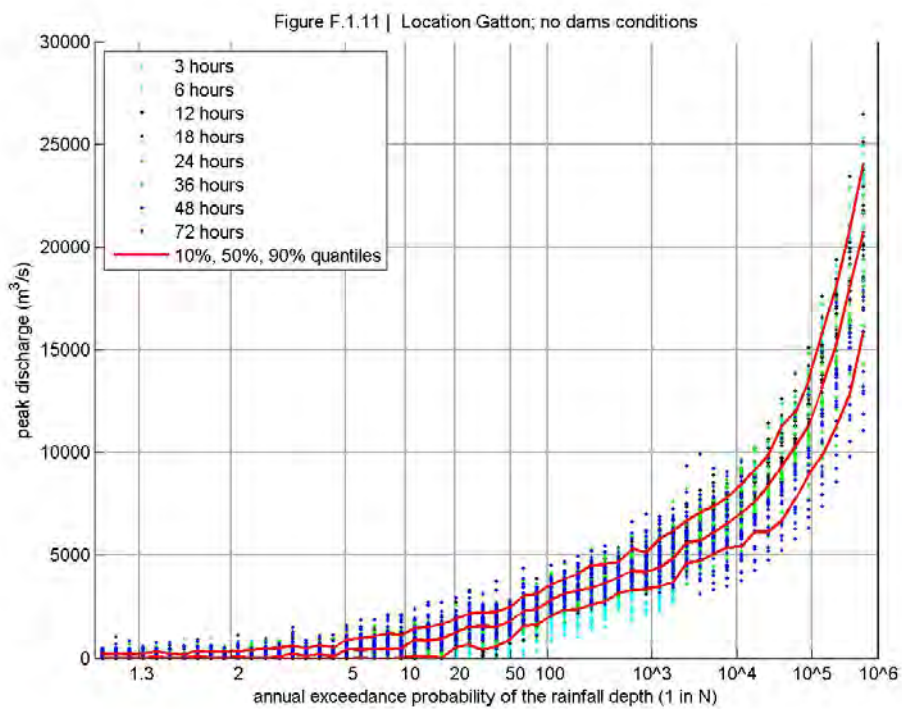


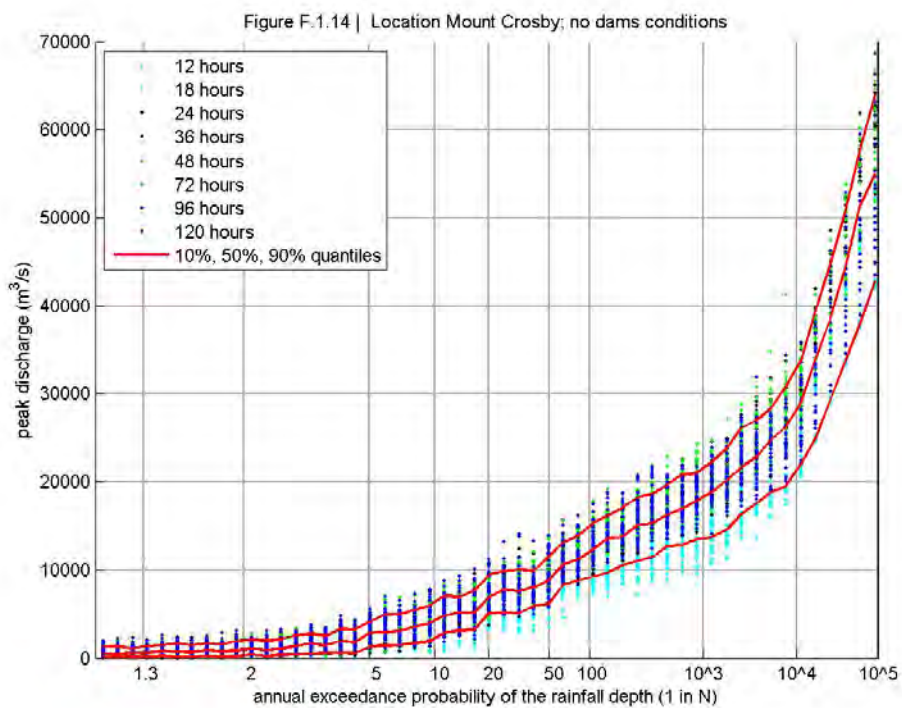
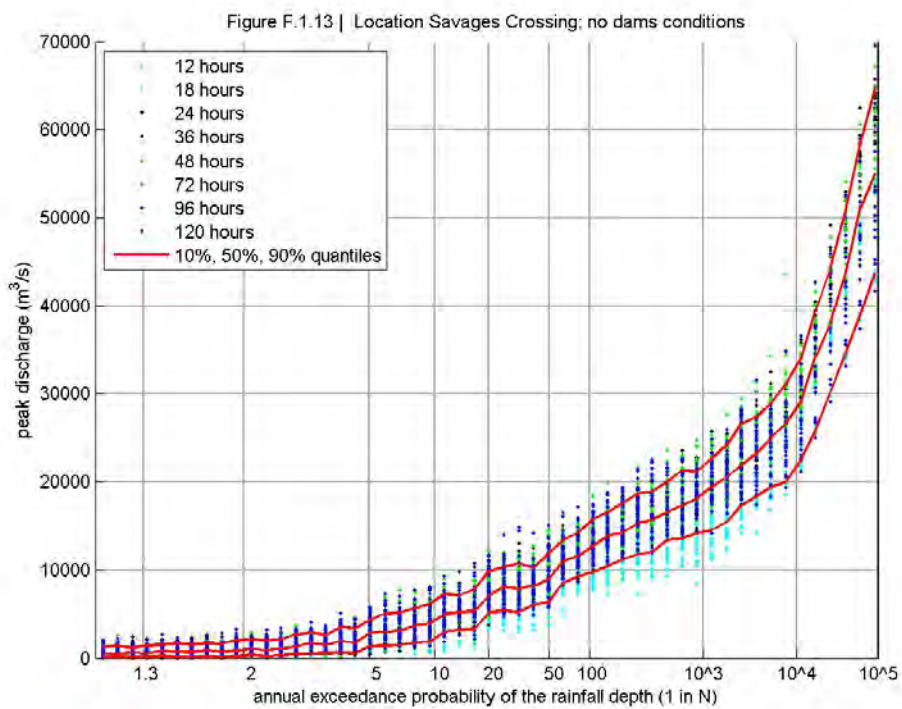


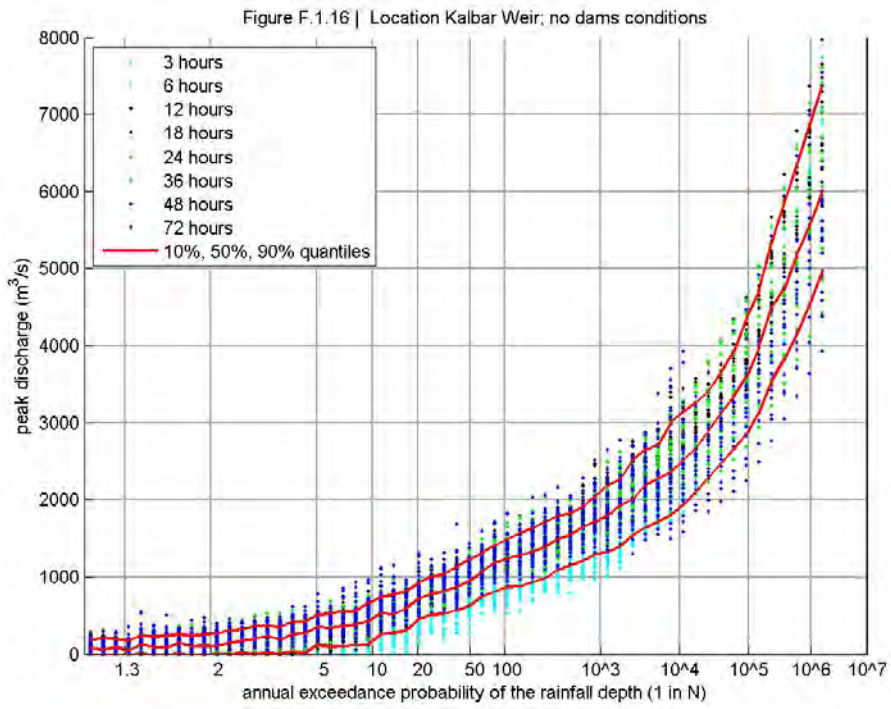
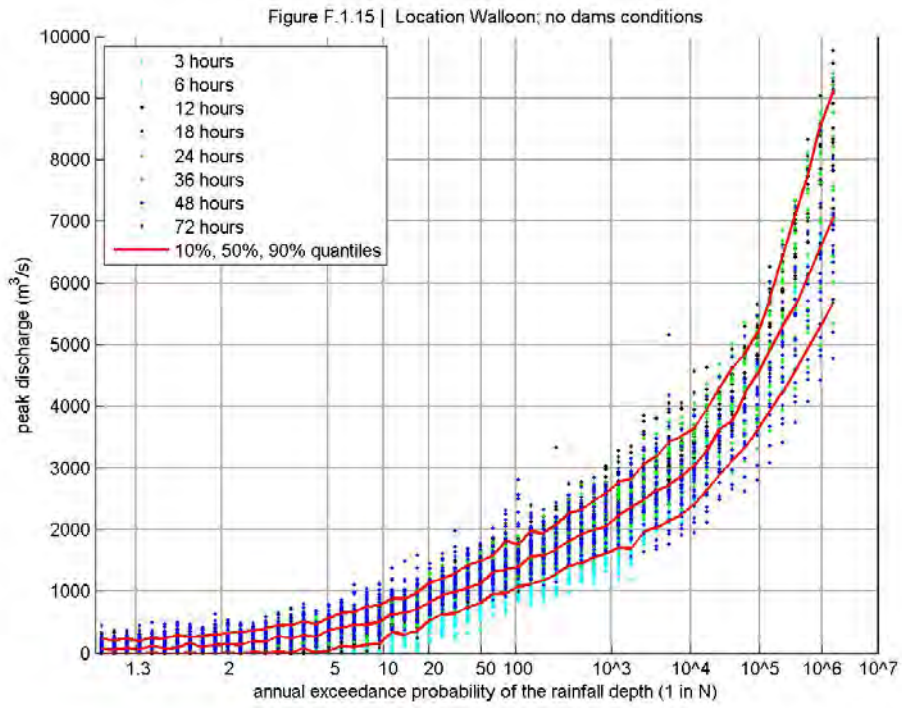
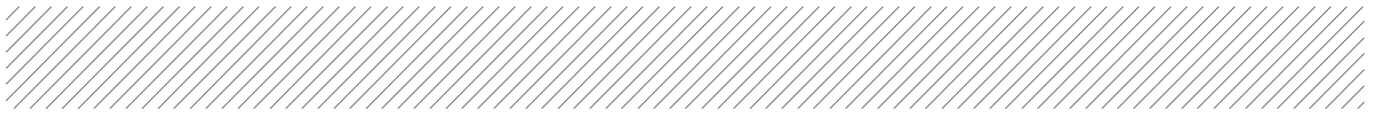


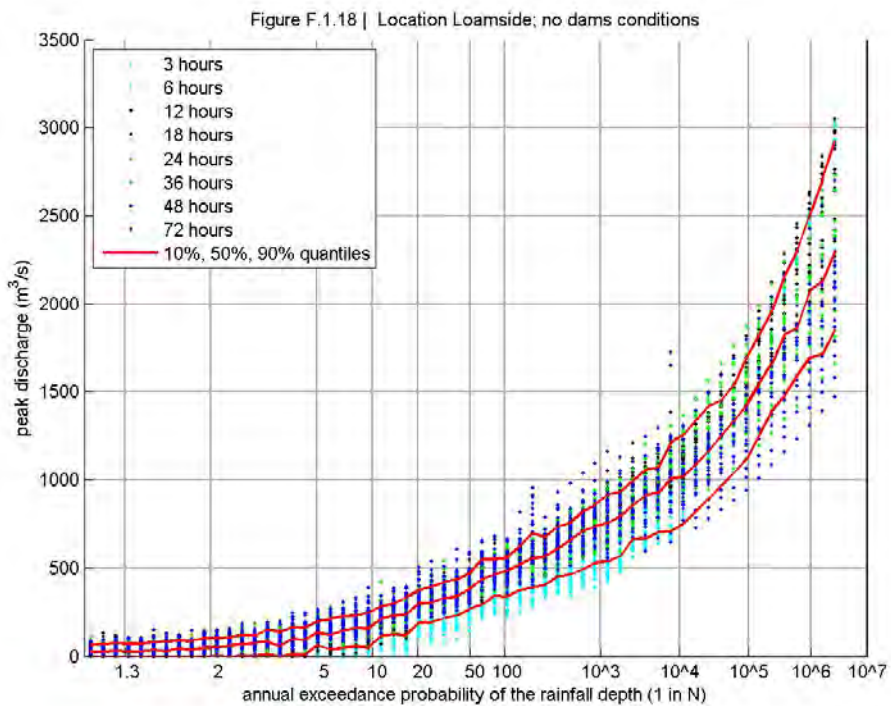
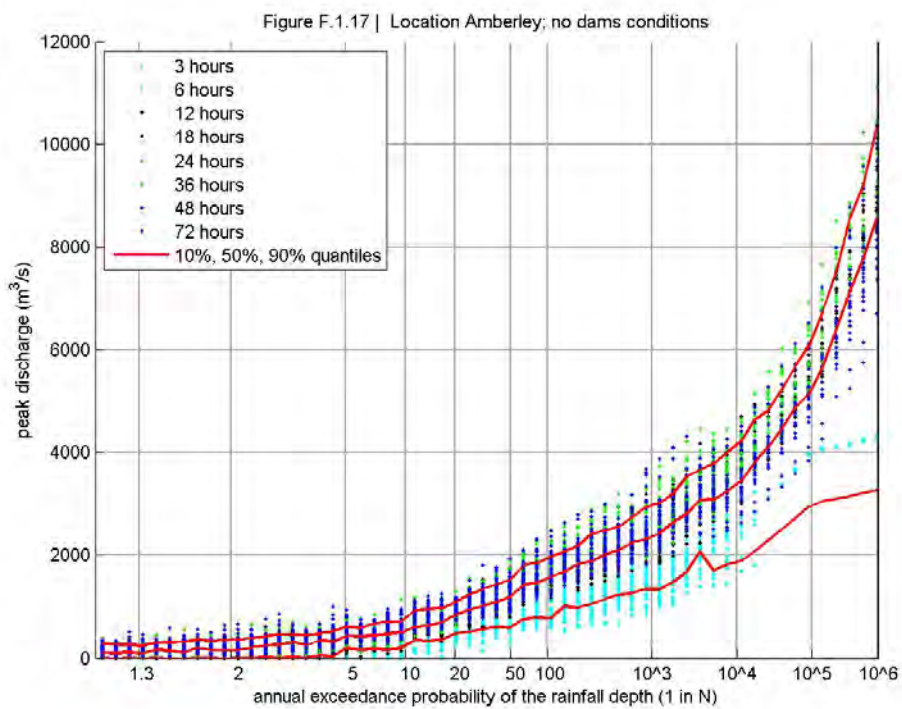


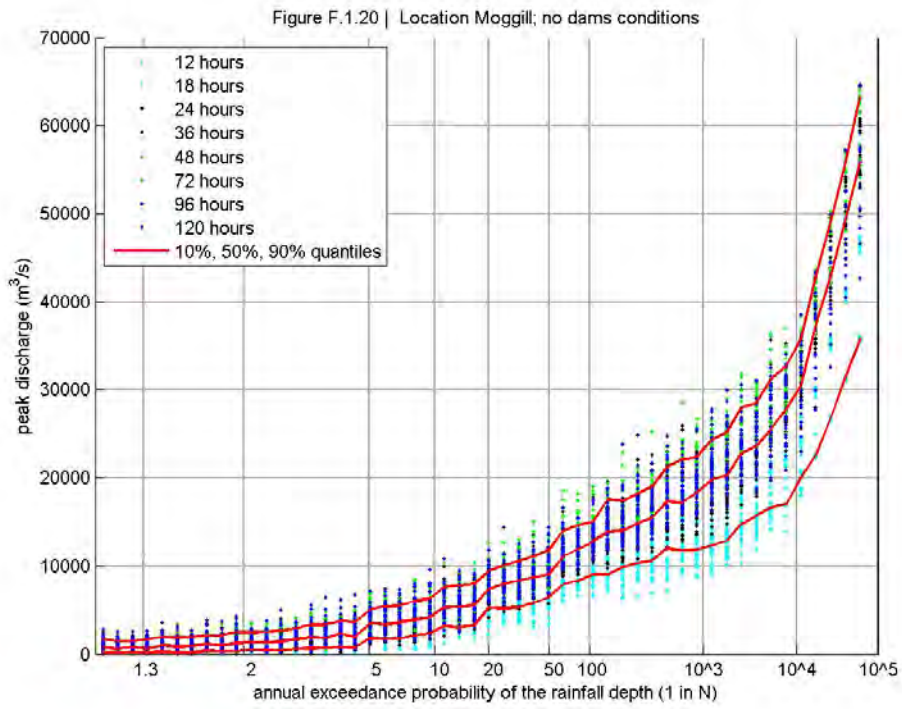
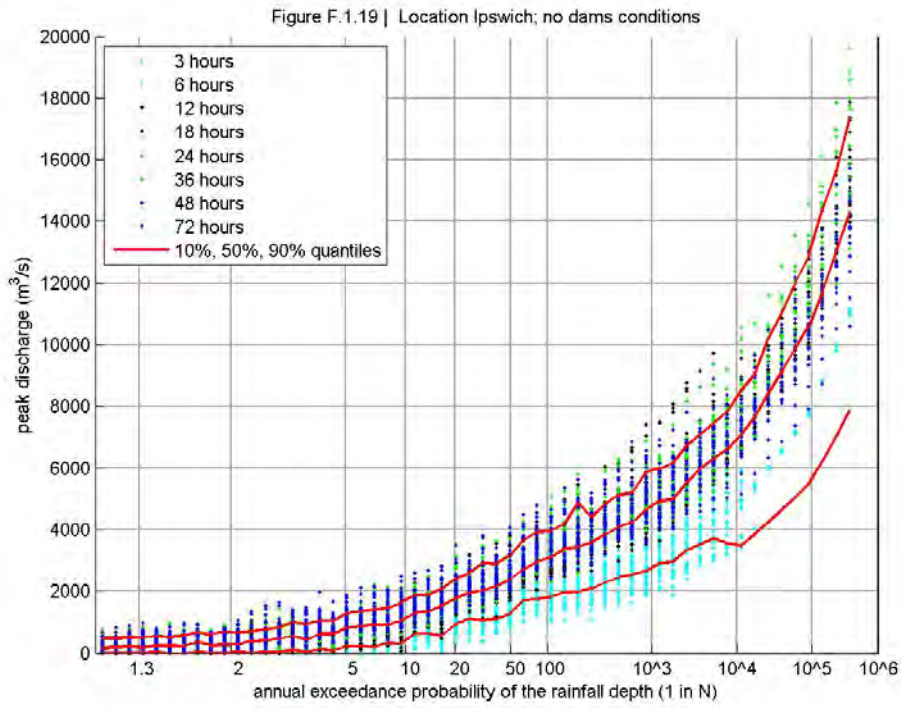
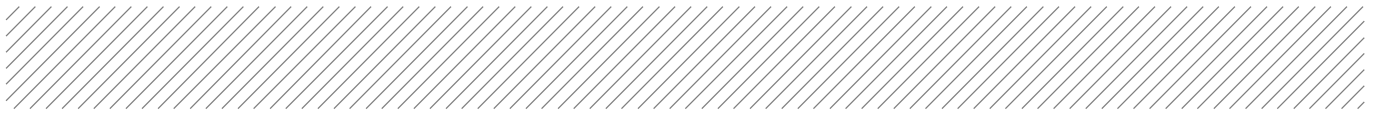


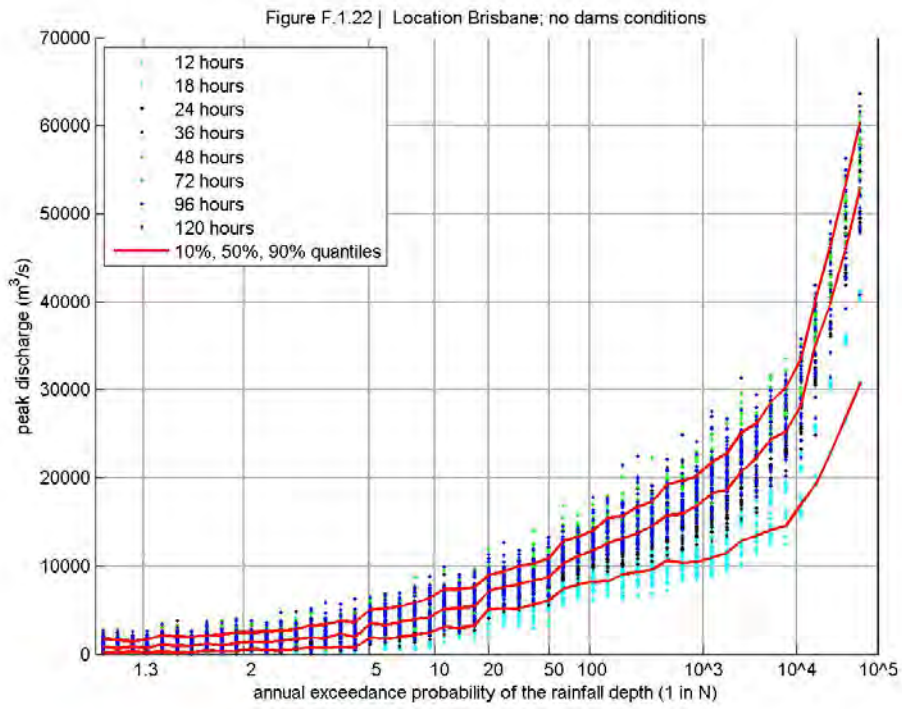
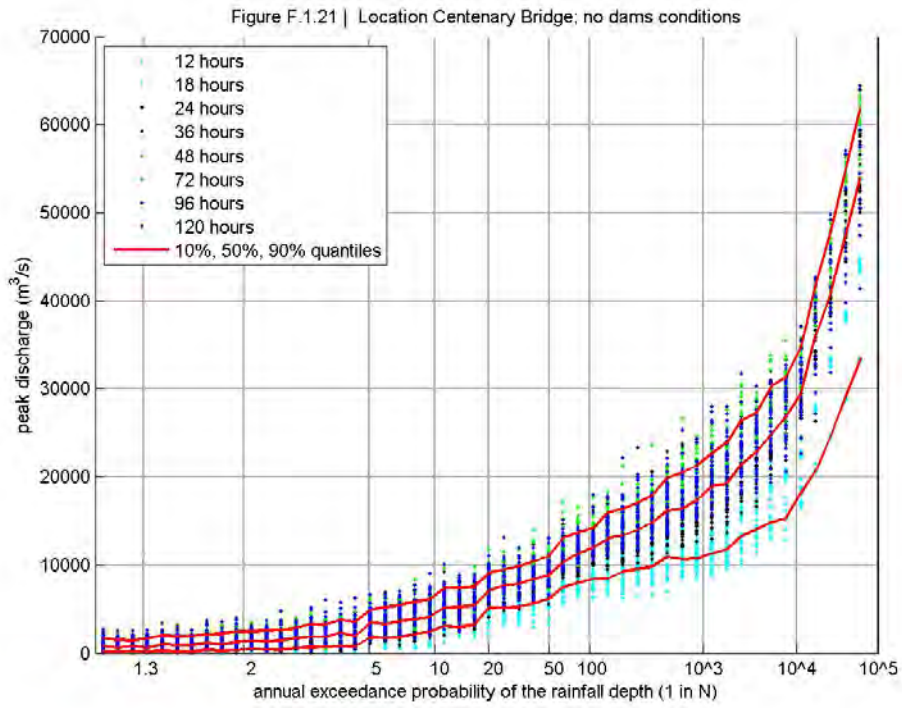
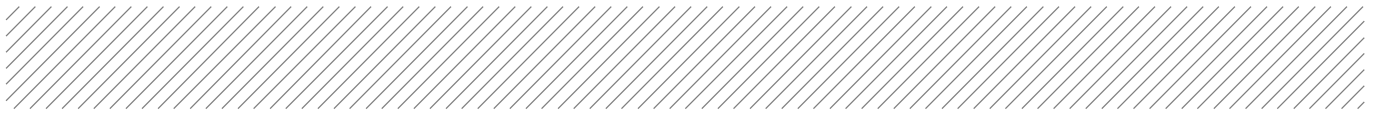




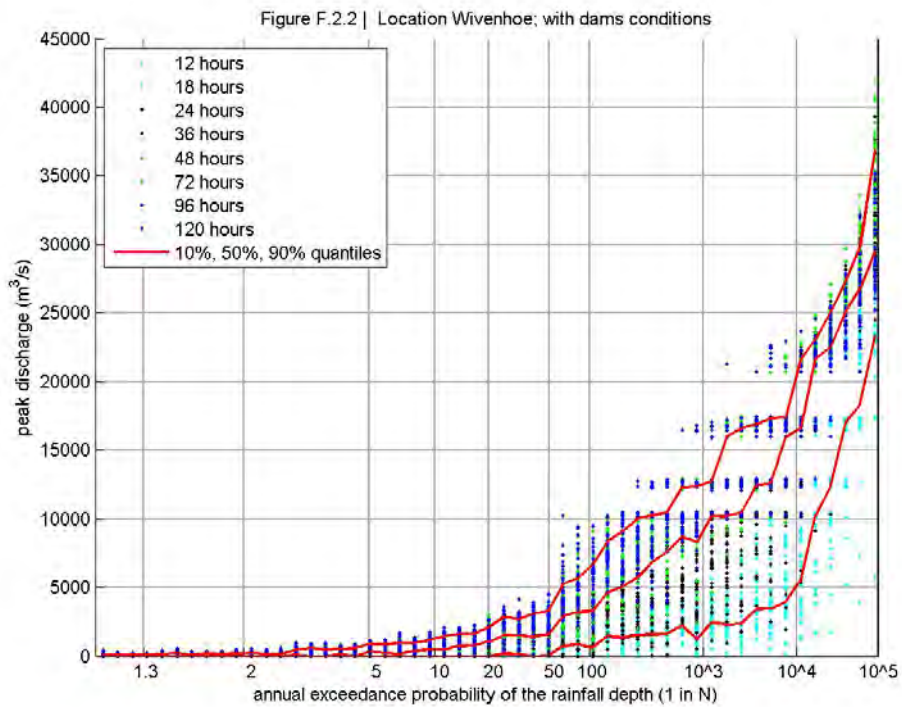
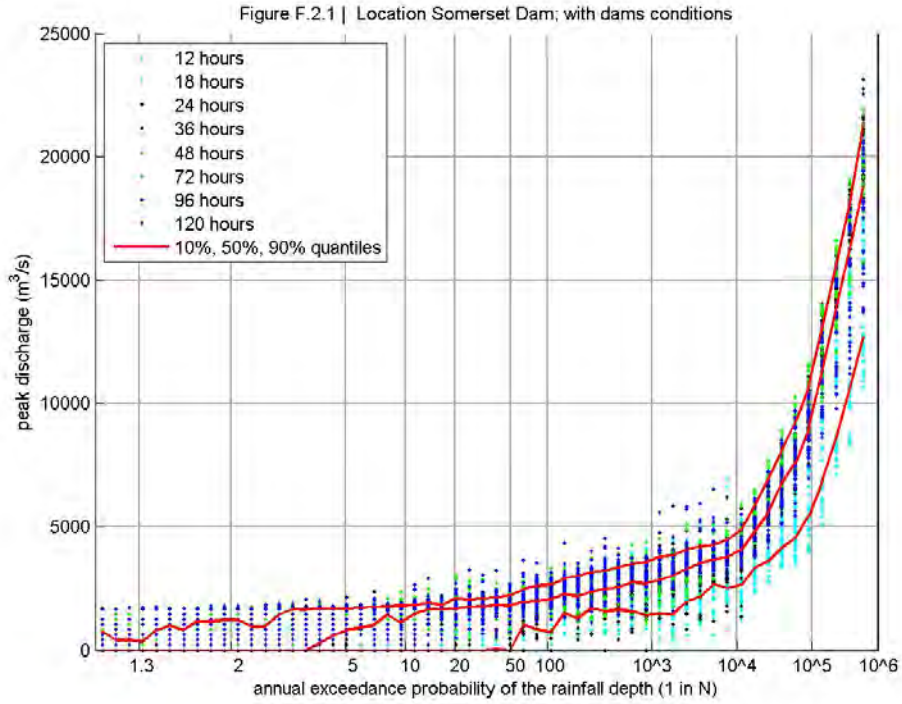


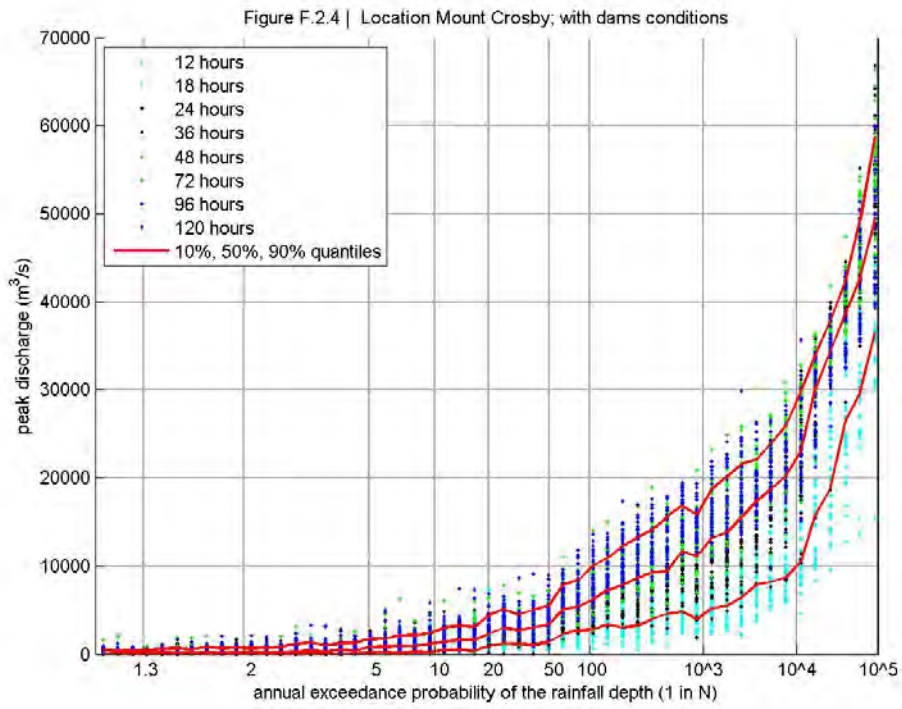
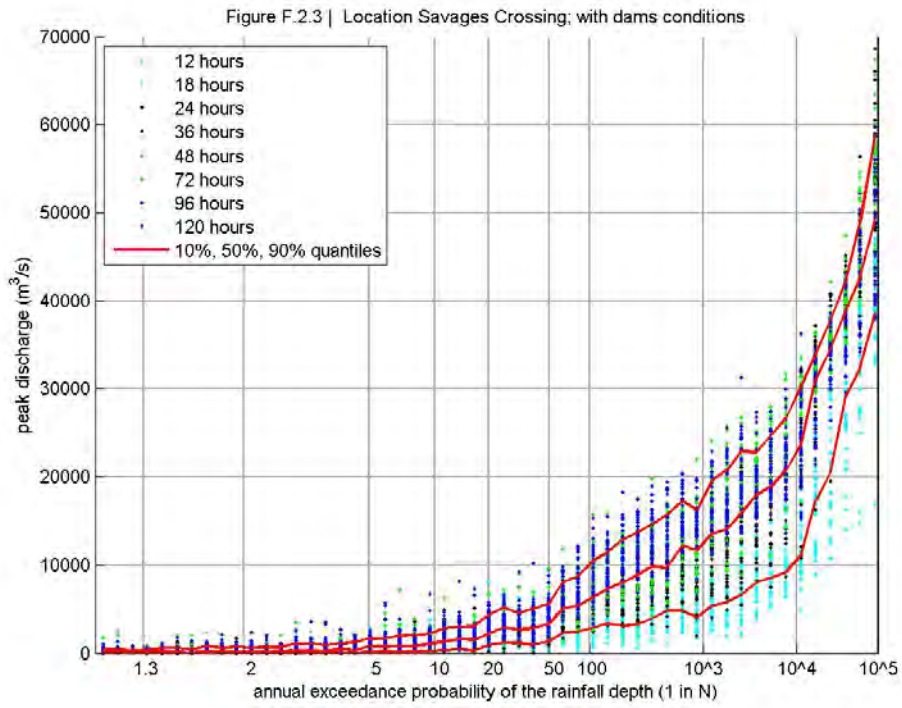
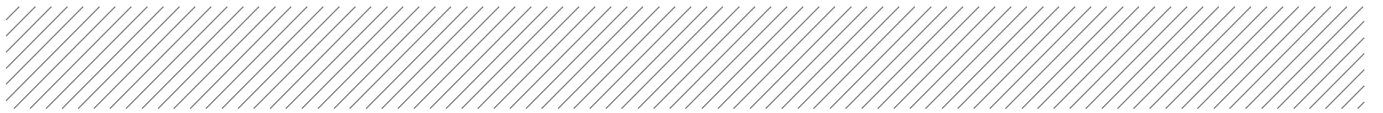


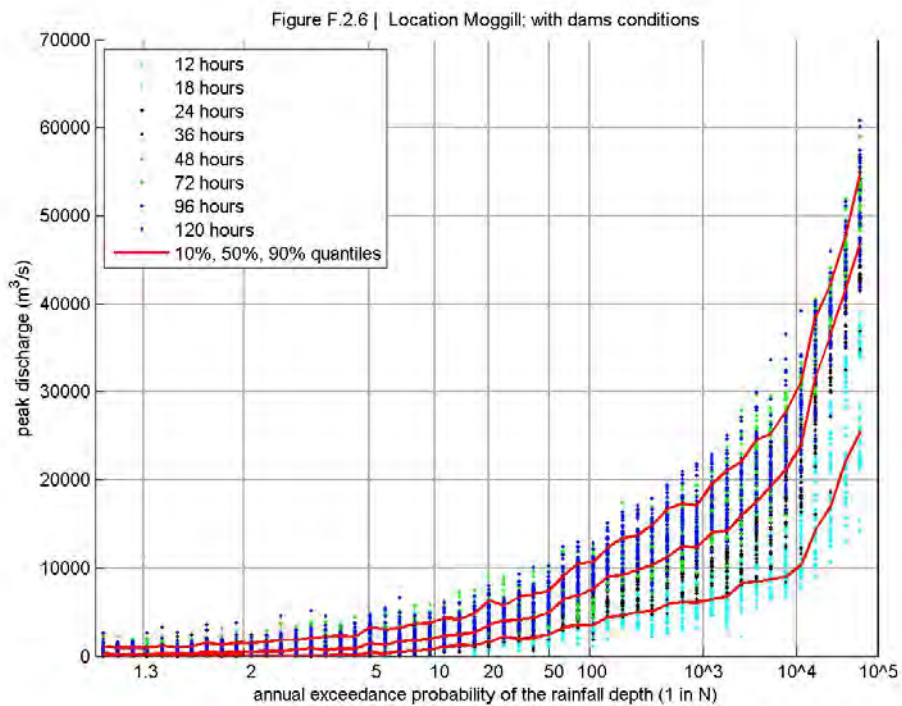
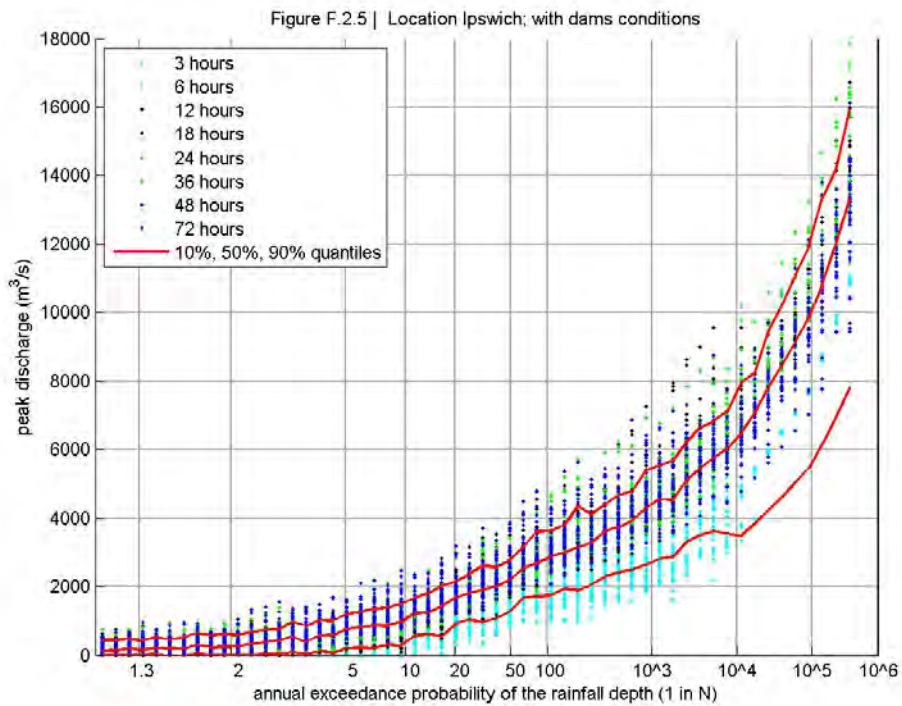


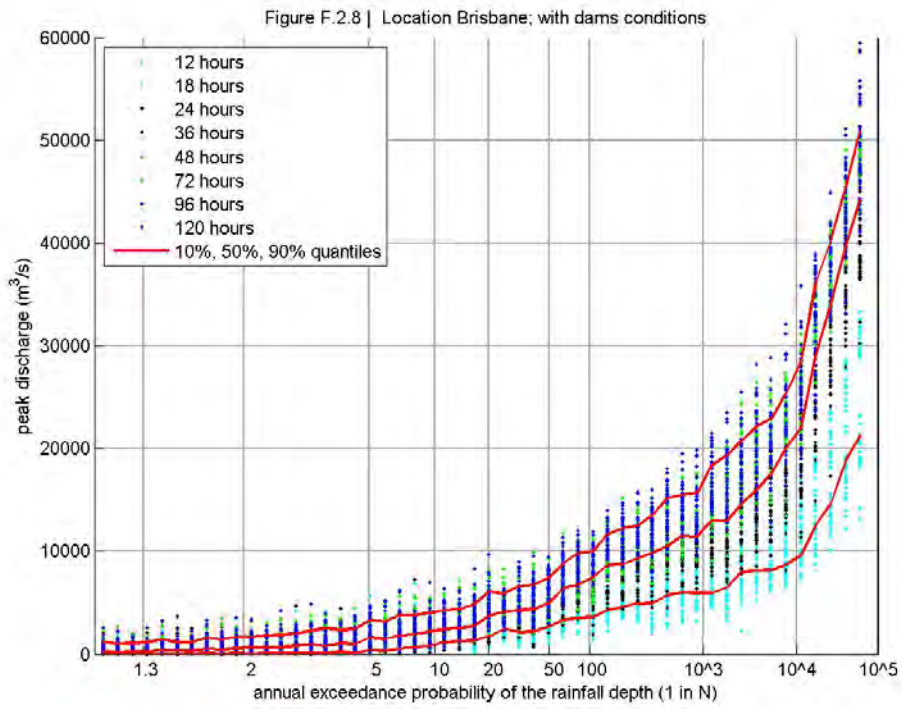
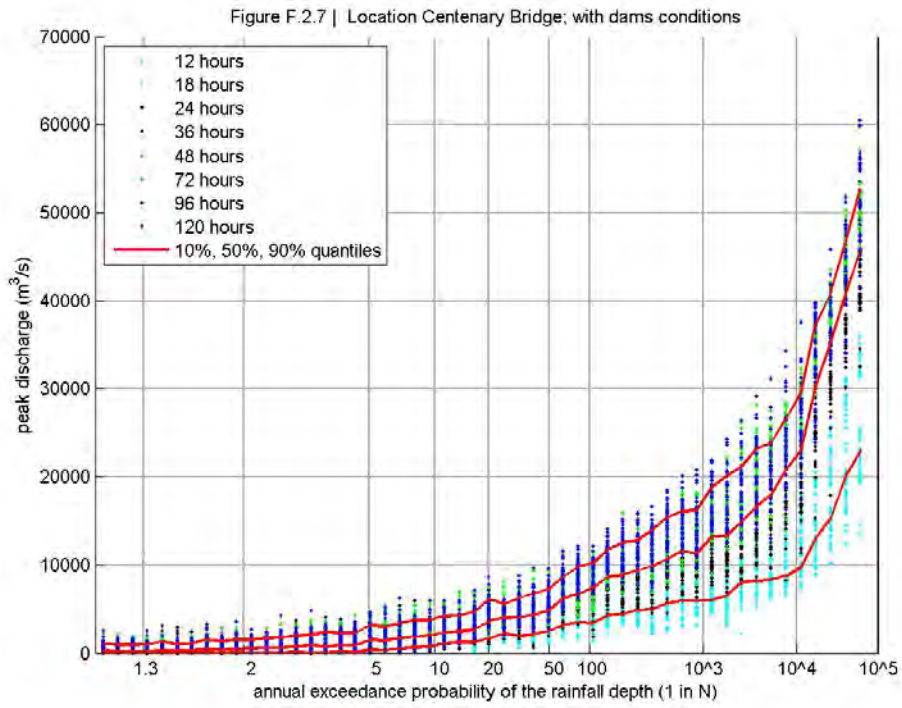
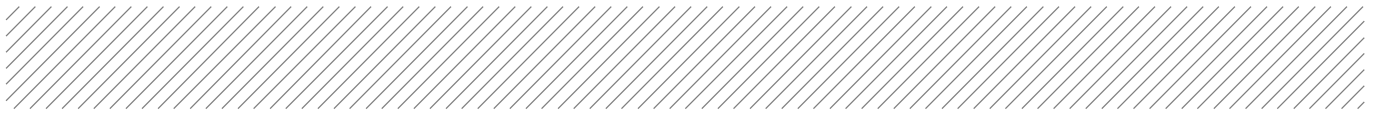


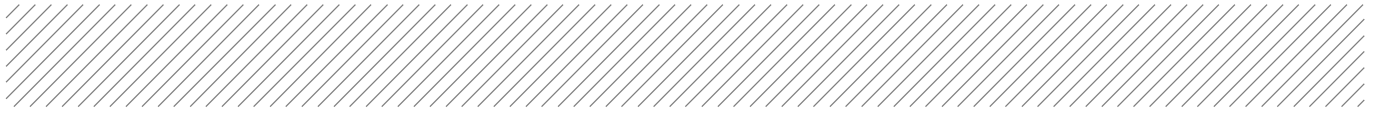
F.2 With-dams conditions









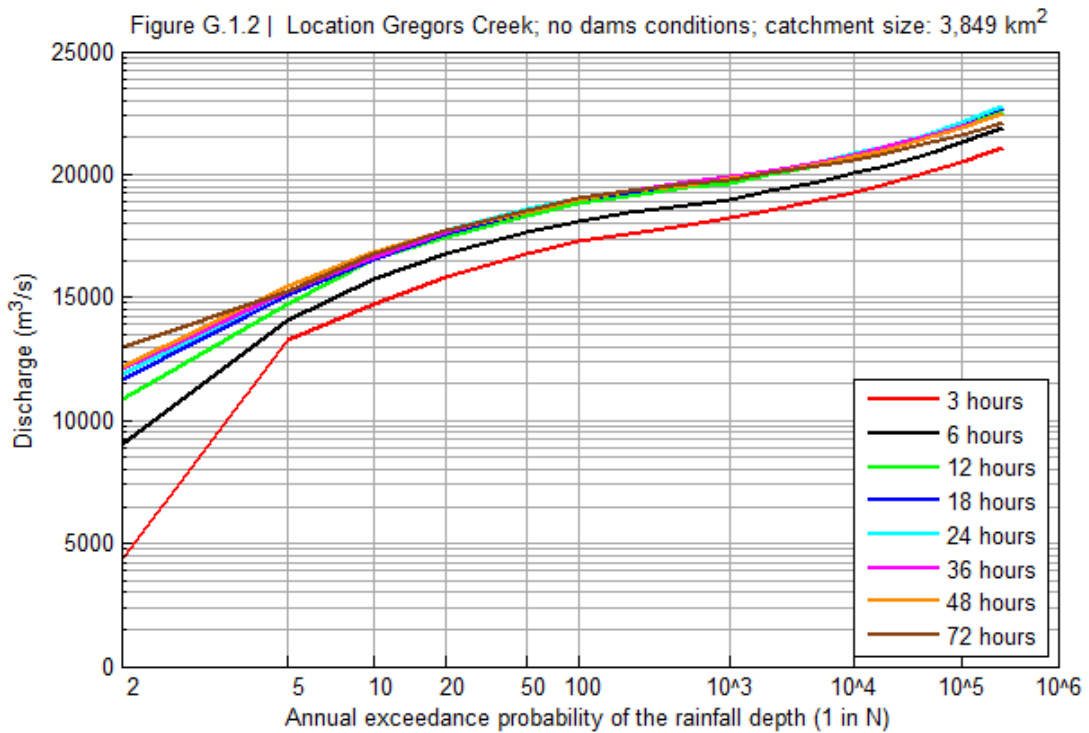
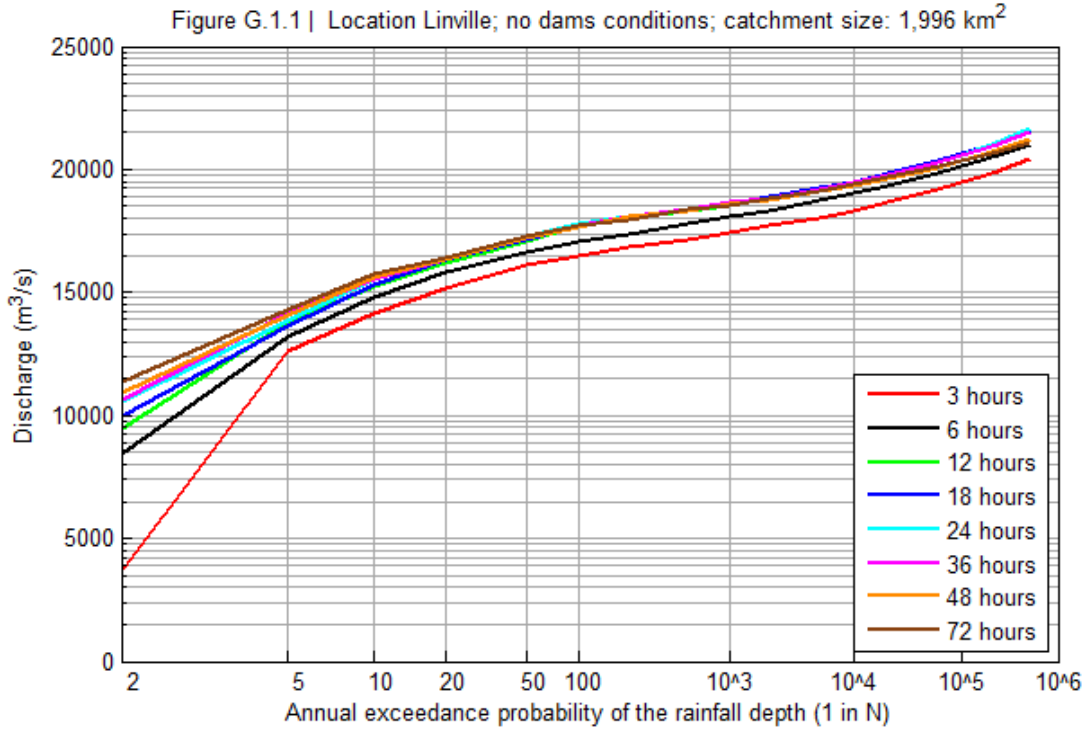


Appendix G

Frequency curves per burst duration

This appendix contains Figures that show frequency curves for various burst durations.

G.1 No-dams conditions



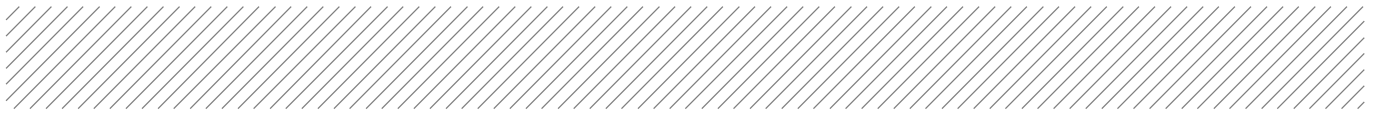


Figure G.1.3 | Location Fulham Vale; no dams conditions; catchment size: 4,553 km²

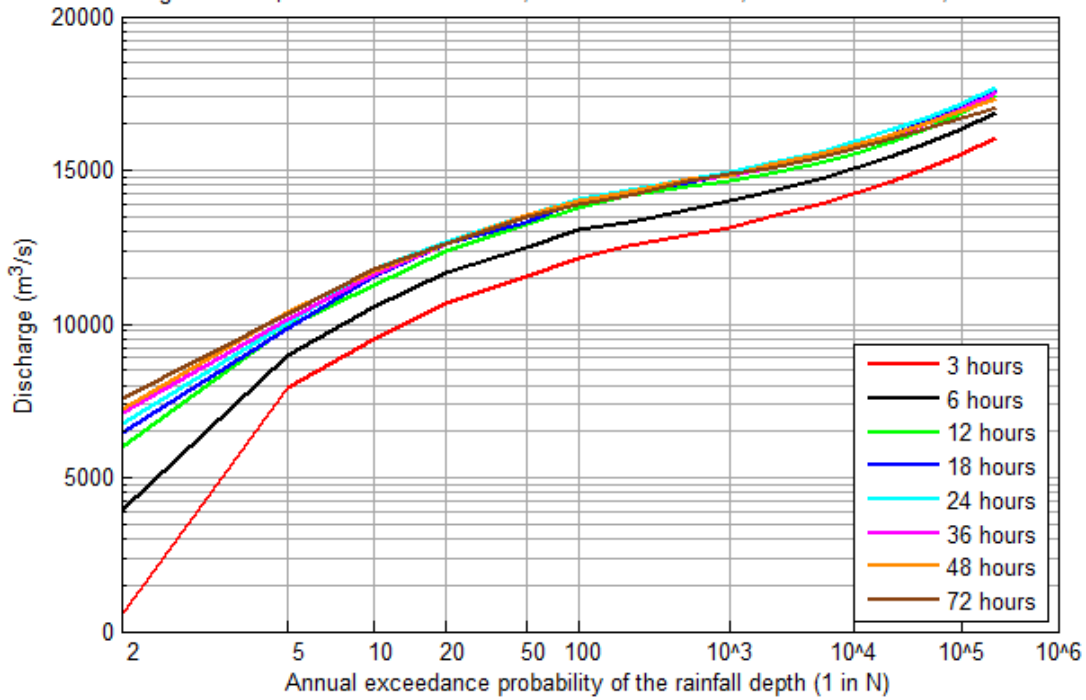
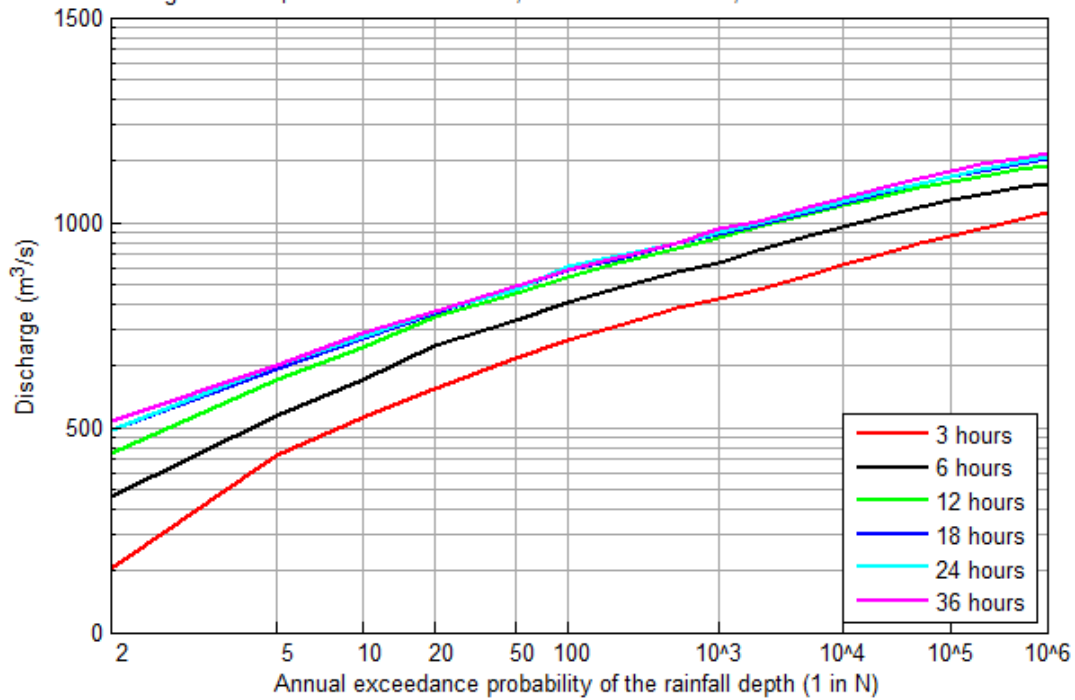


Figure G.1.4 | Location Peacheater; no dams conditions; catchment size: 103 km²



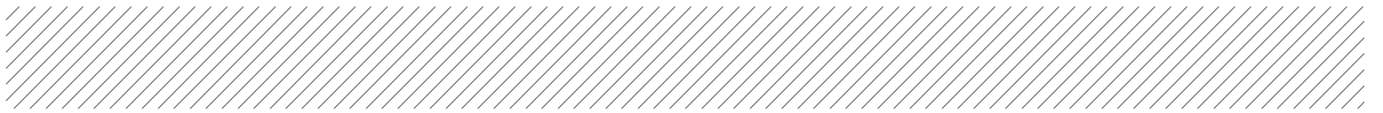


Figure G.1.5 | Location Woodford; no dams conditions; catchment size: 245 km²

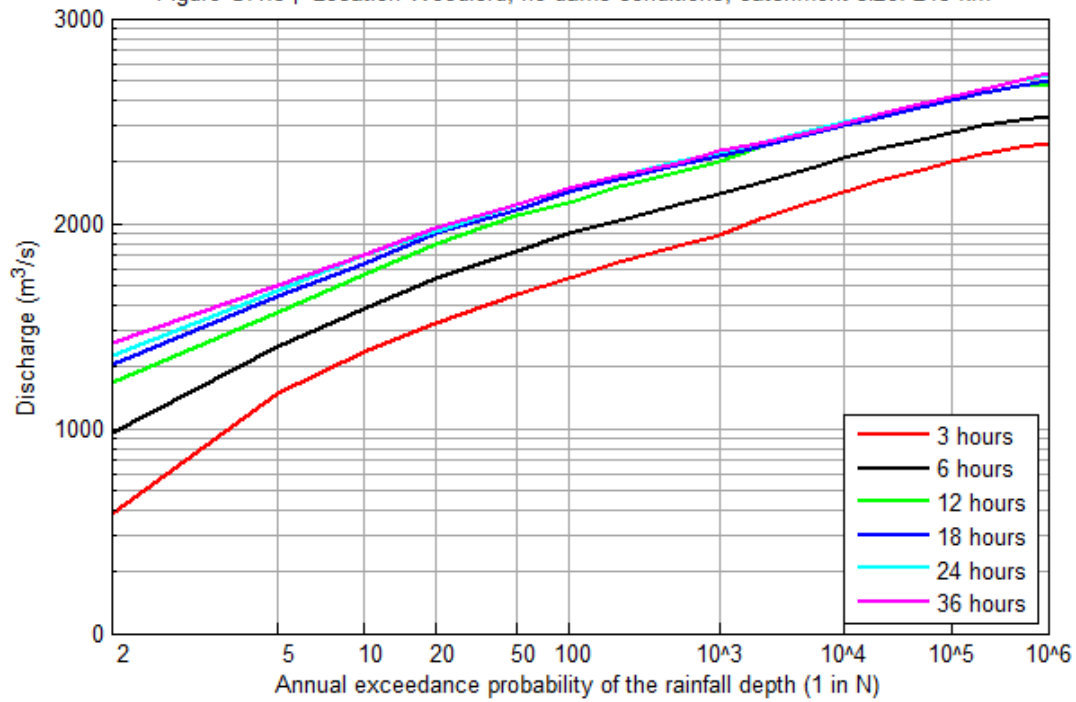
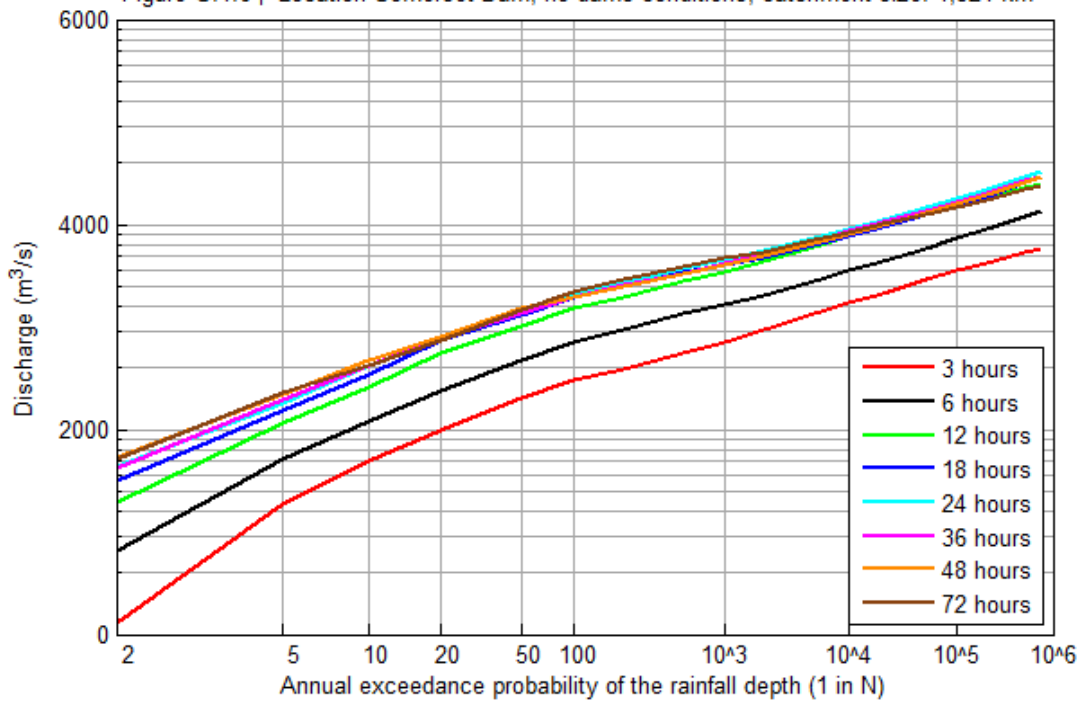
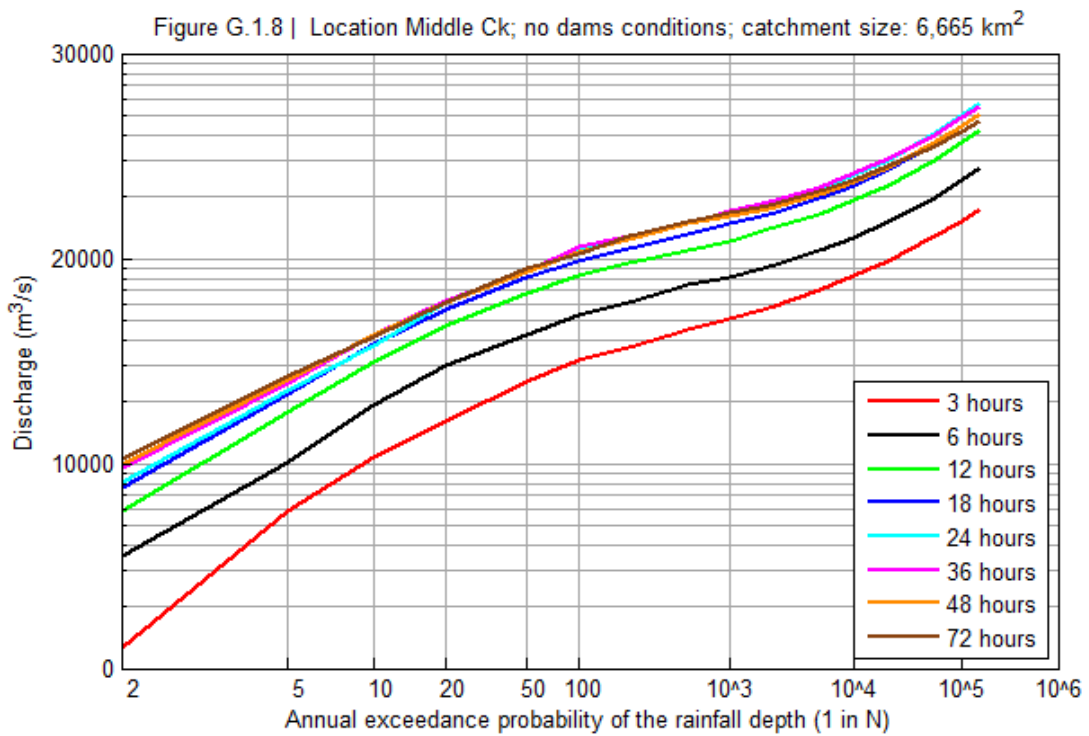
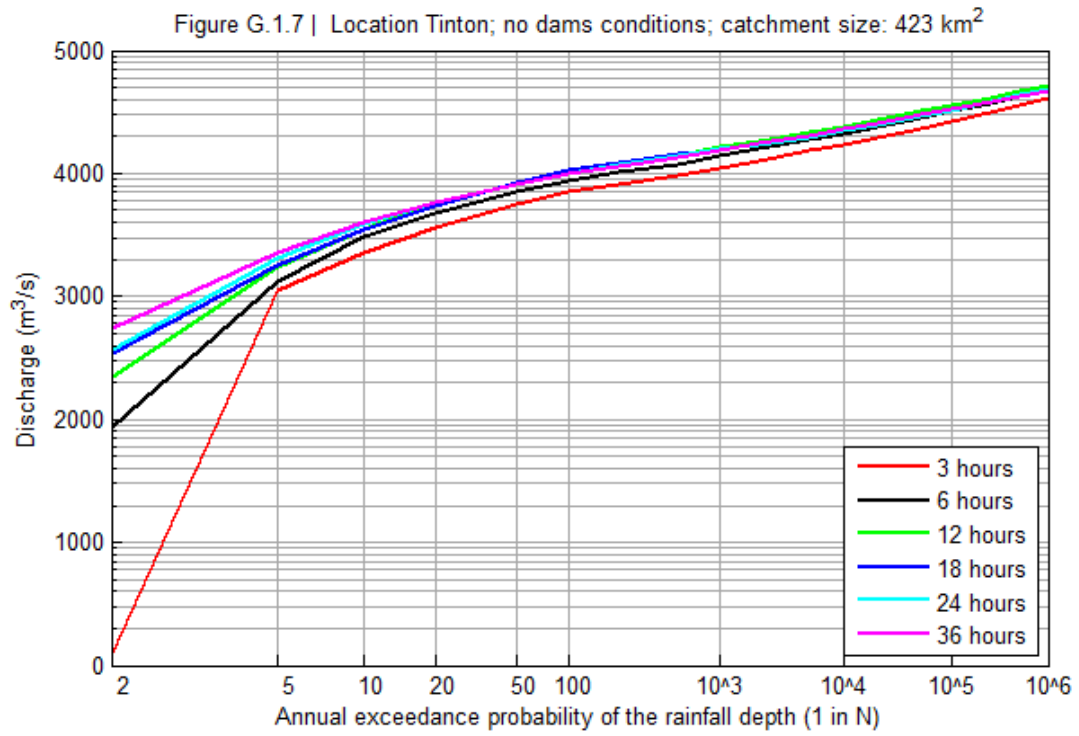
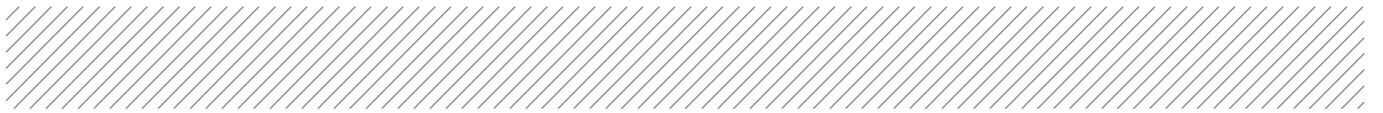


Figure G.1.6 | Location Somerset Dam; no dams conditions; catchment size: 1,324 km²





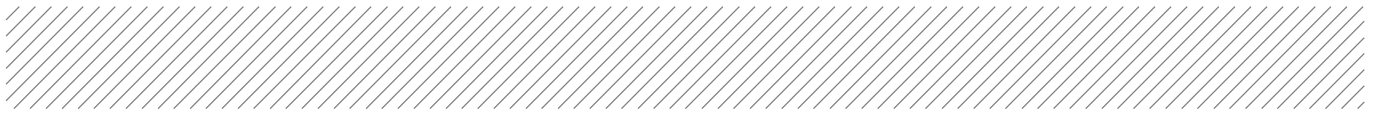


Figure G.1.9 | Location Wivenhoe; no dams conditions; catchment size: 6,980 km²

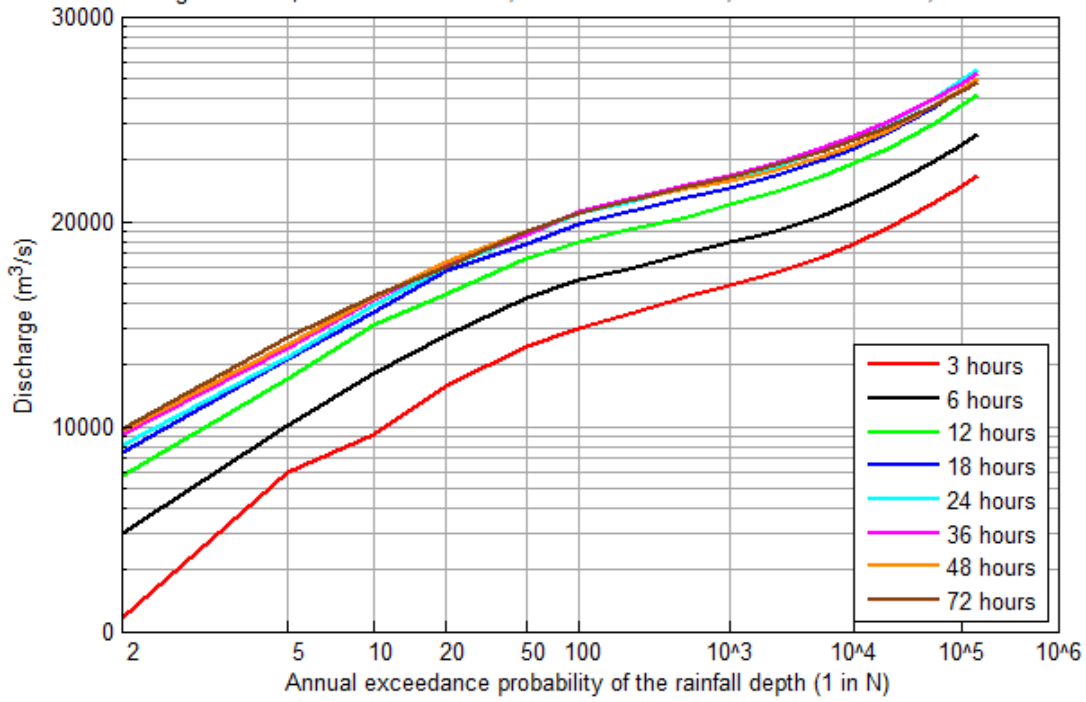
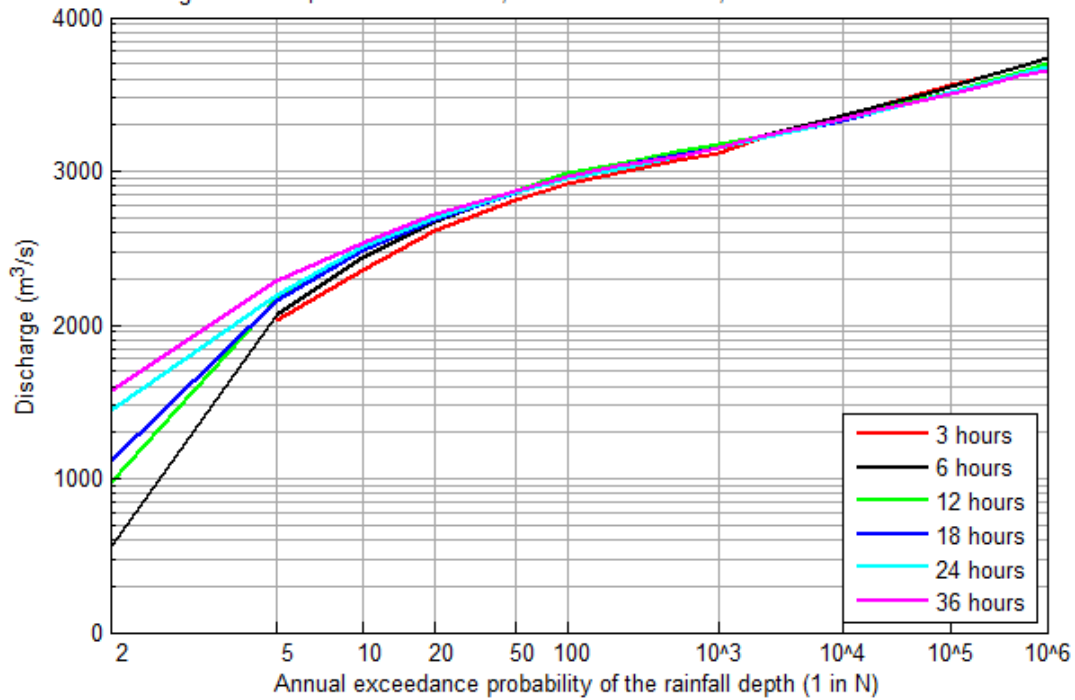


Figure G.1.10 | Location Helidon; no dams conditions; catchment size: 351 km²



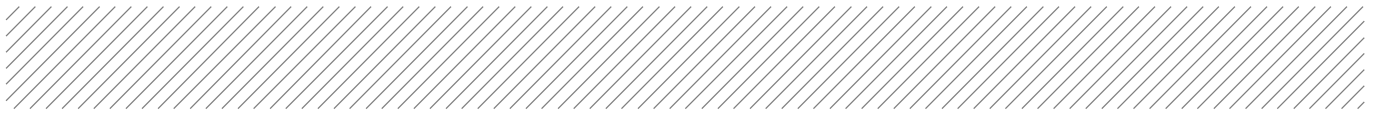


Figure G.1.11 | Location Gatton; no dams conditions; catchment size: 1,527 km²

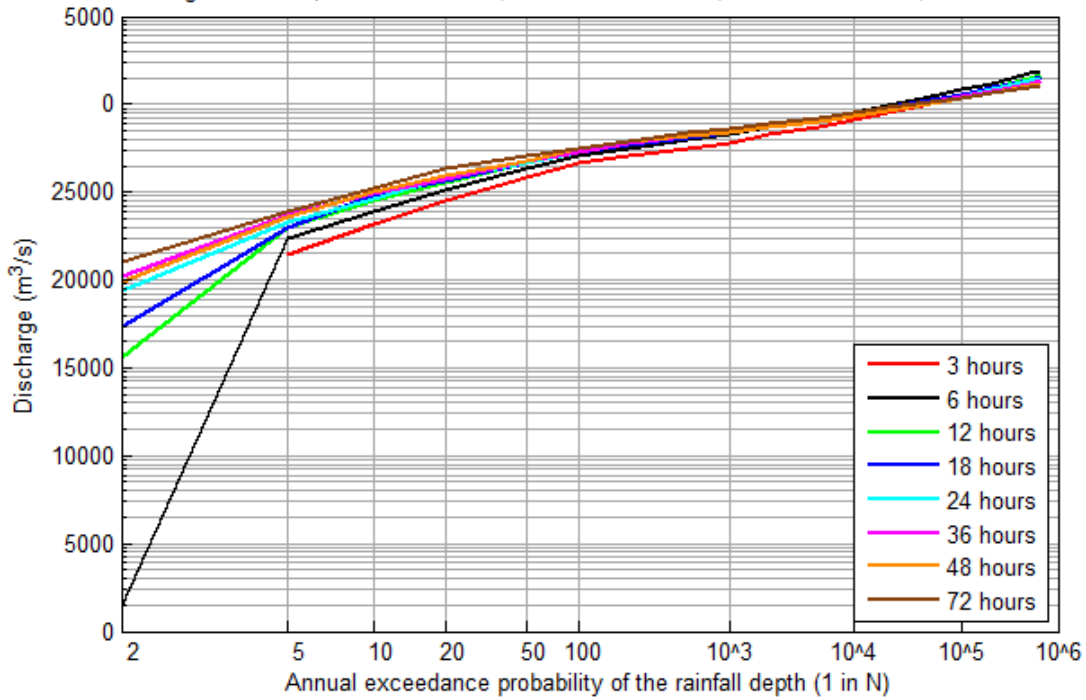
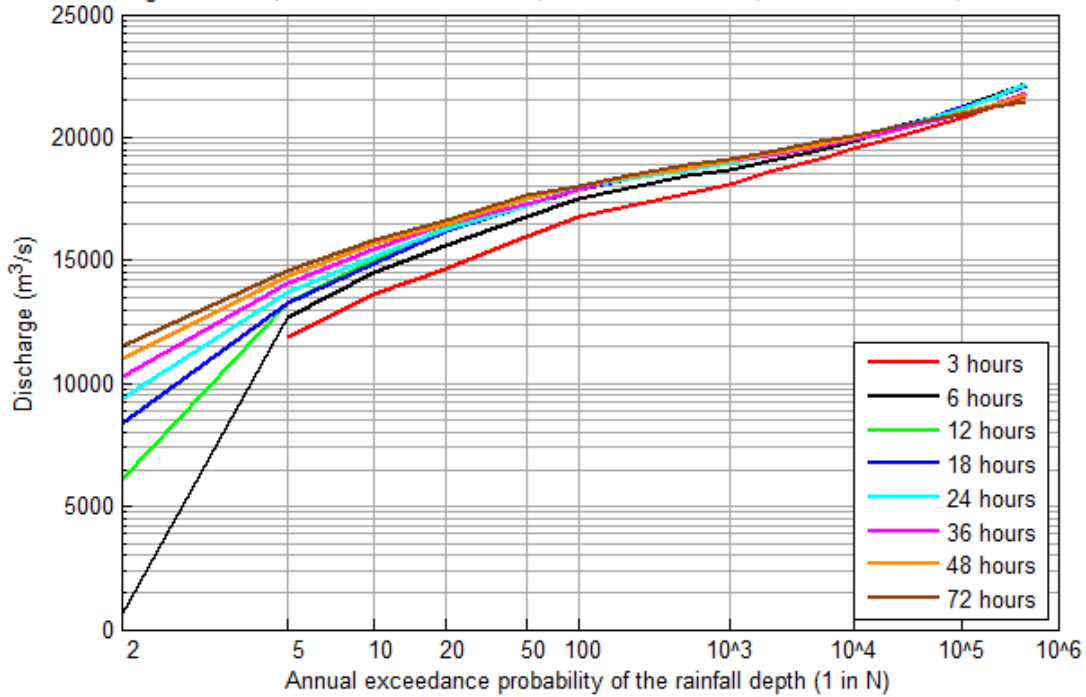
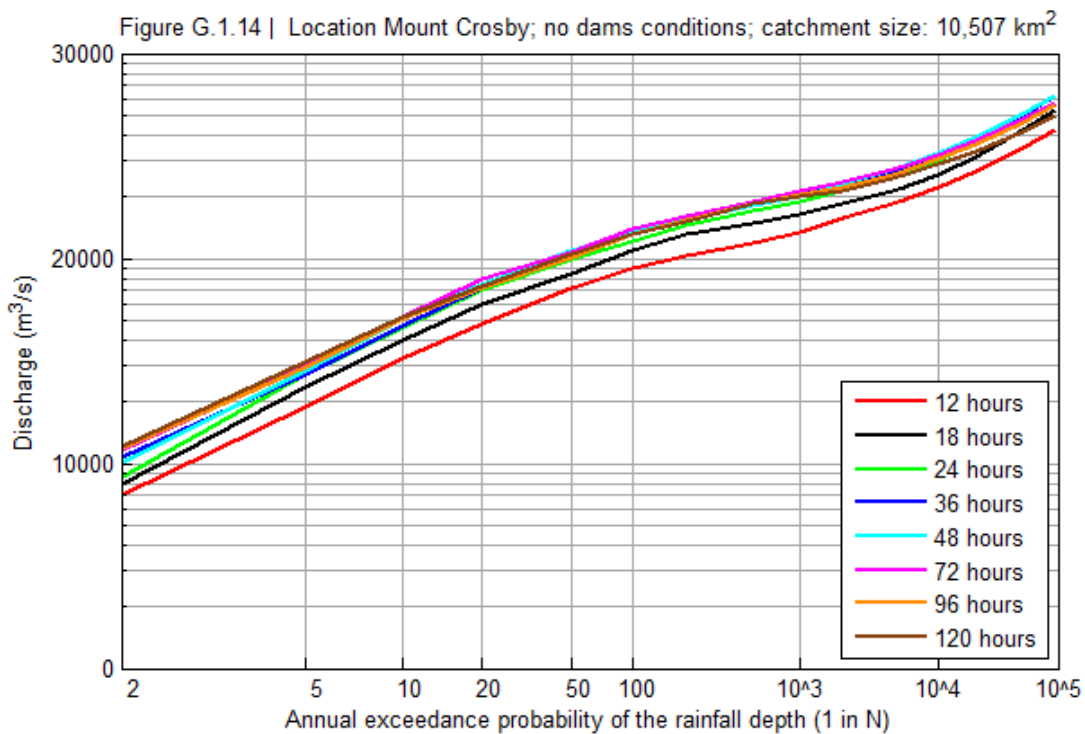
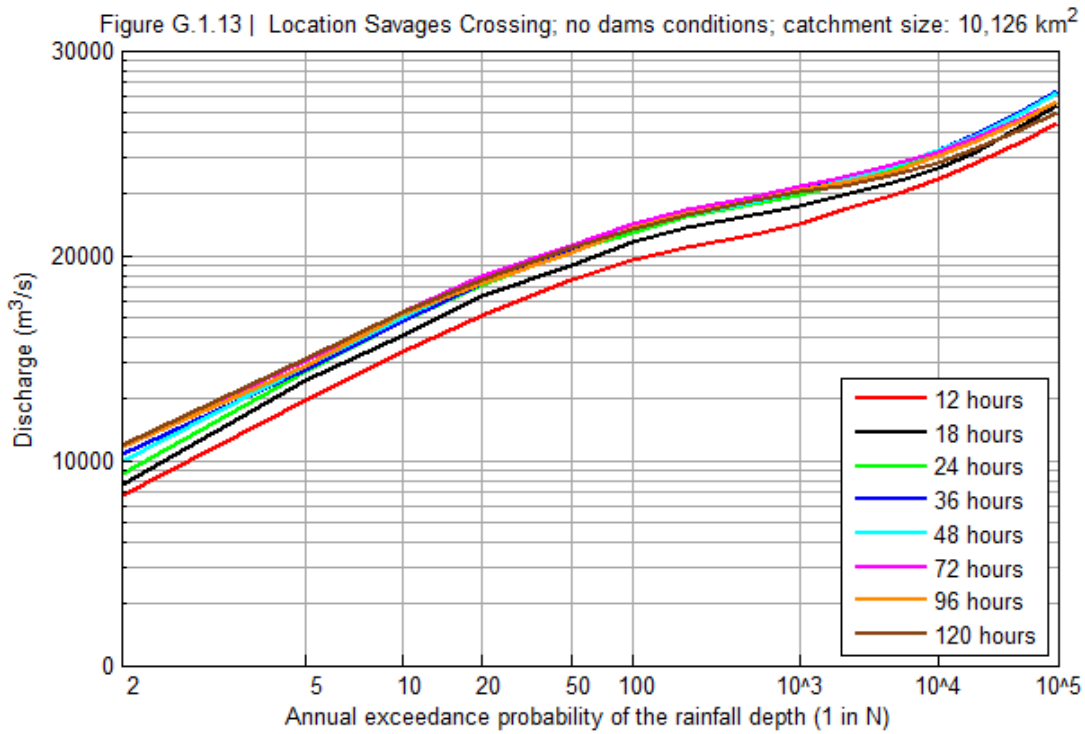
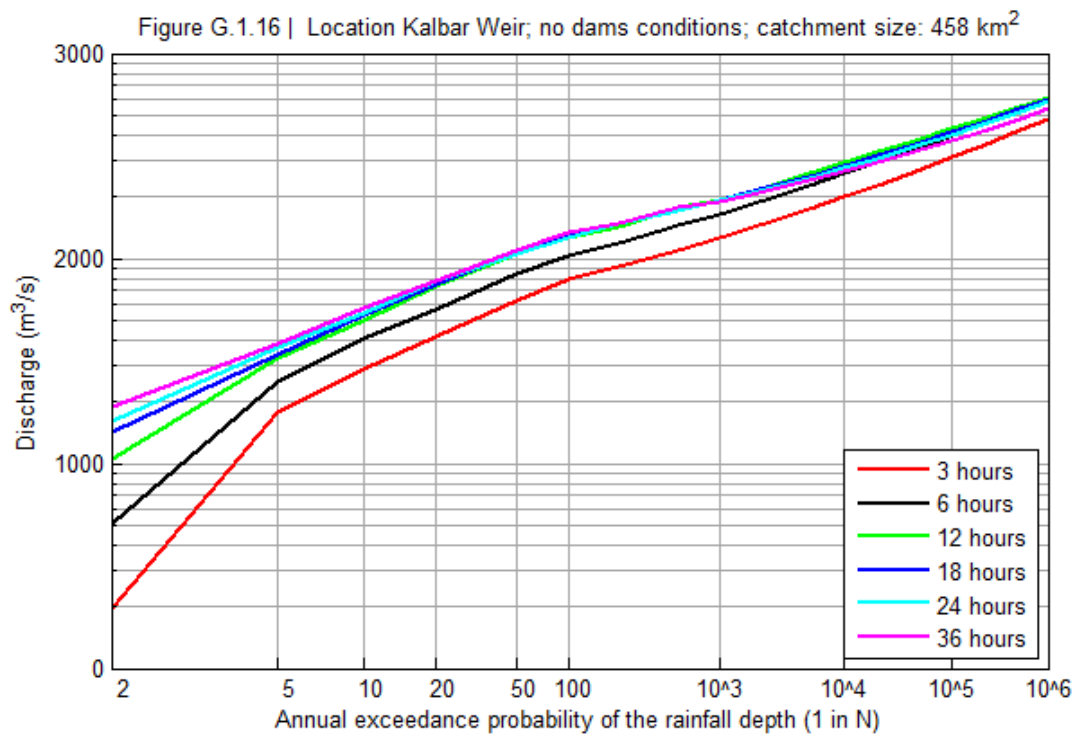
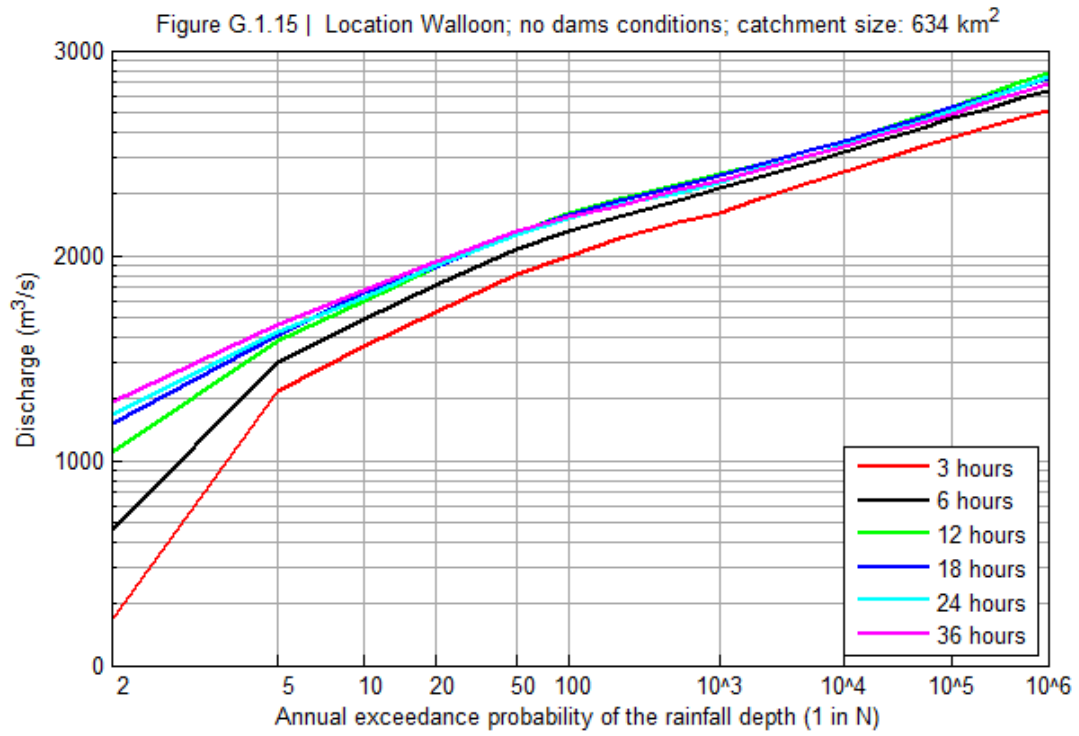
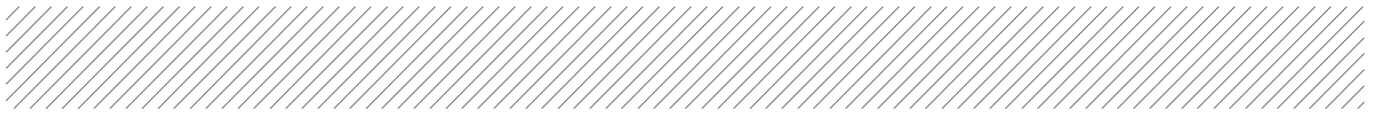
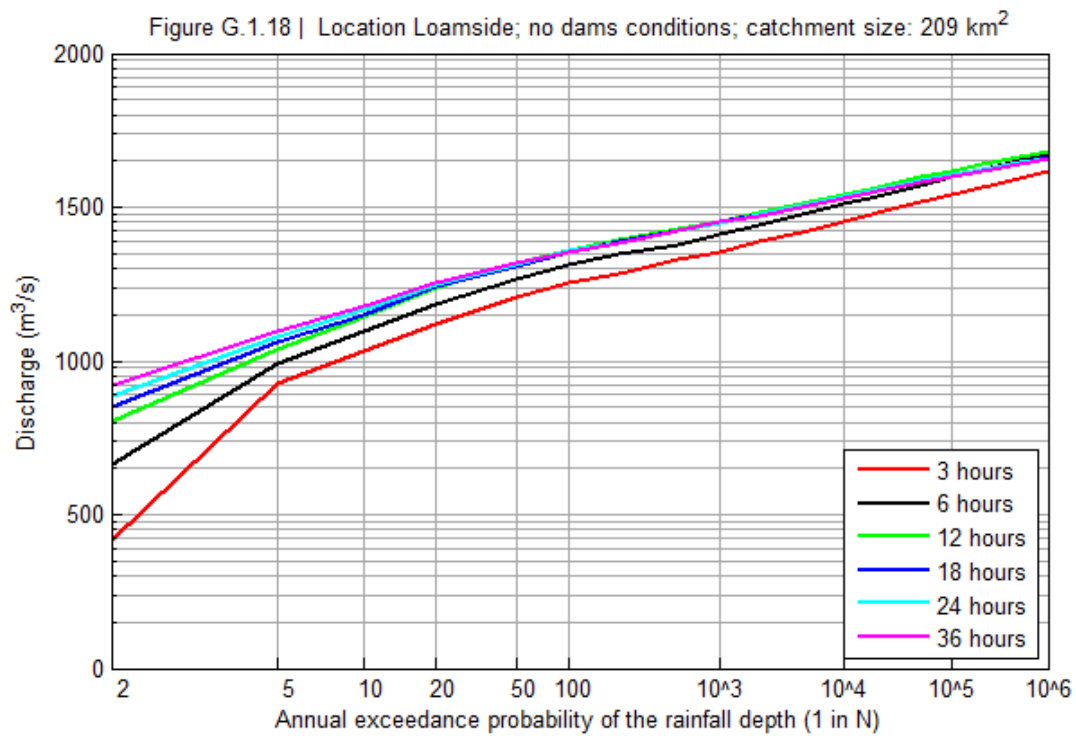
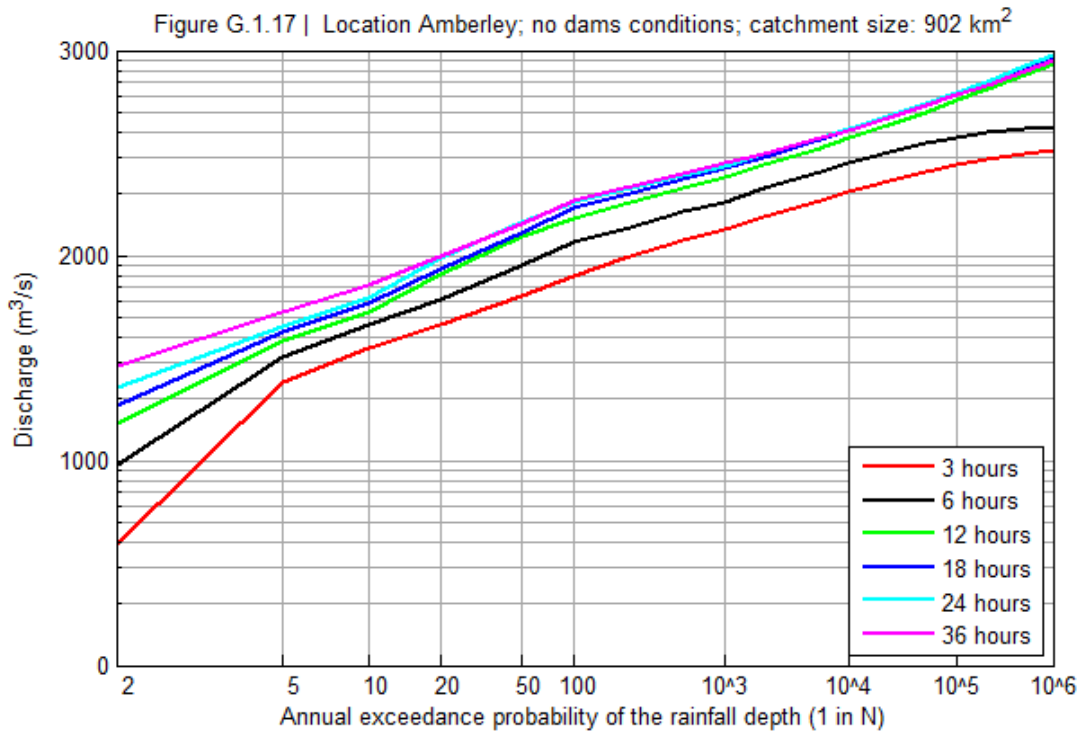
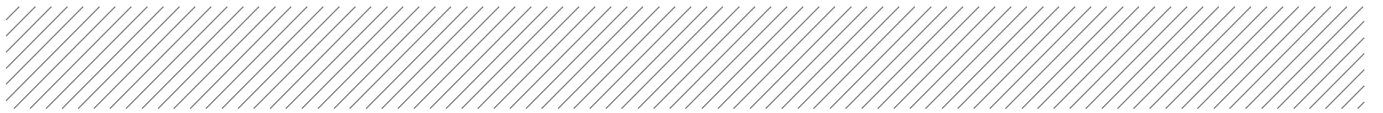


Figure G.1.12 | Location Glenore Grove; no dams conditions; catchment size: 2,149 km²









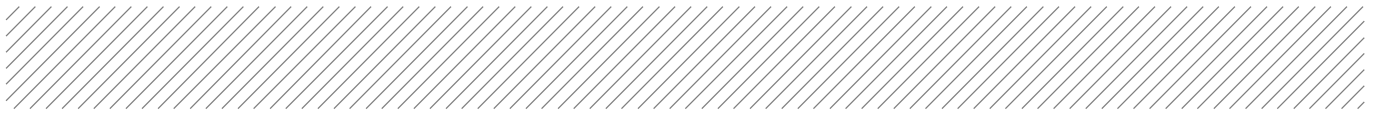


Figure G.1.19 | Location Ipswich; no dams conditions; catchment size: 1,850 km²

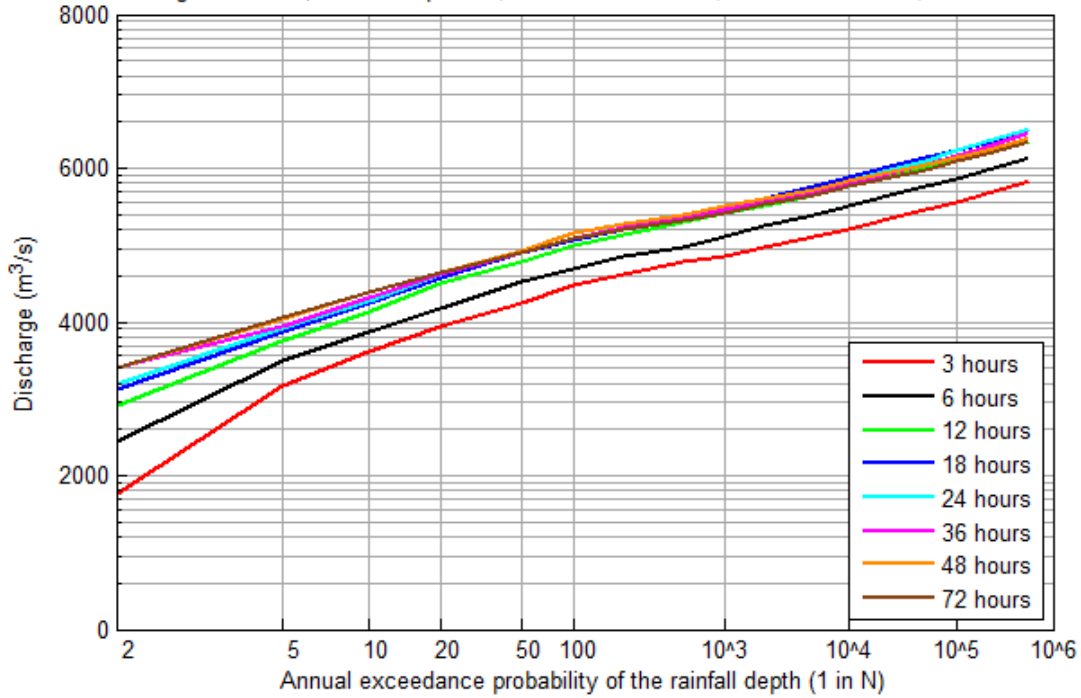
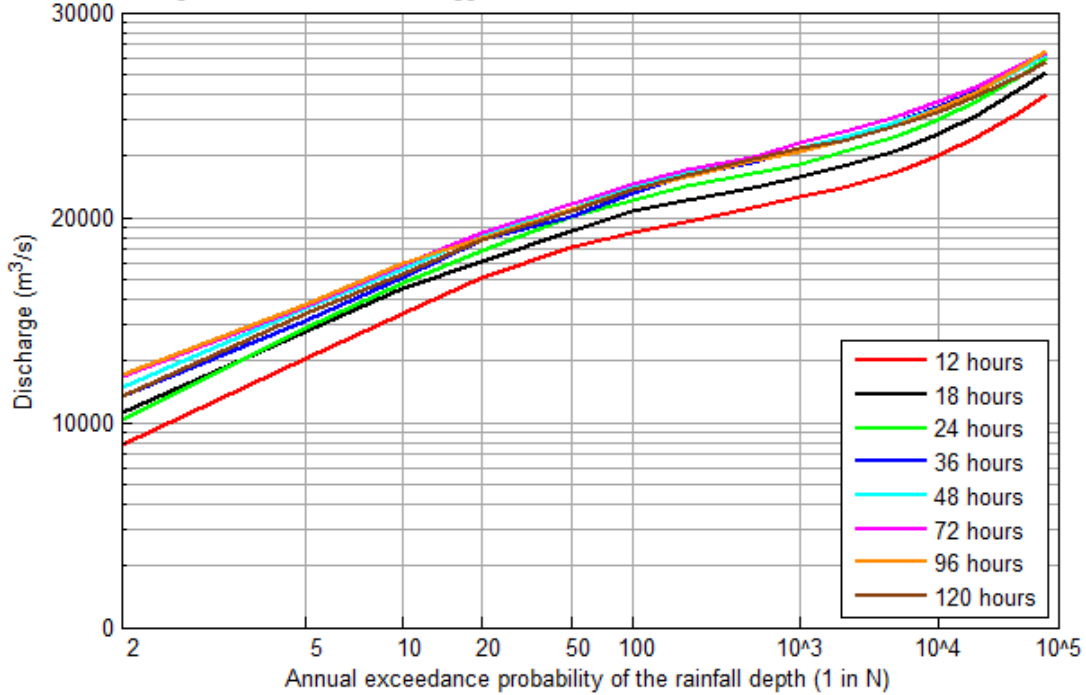
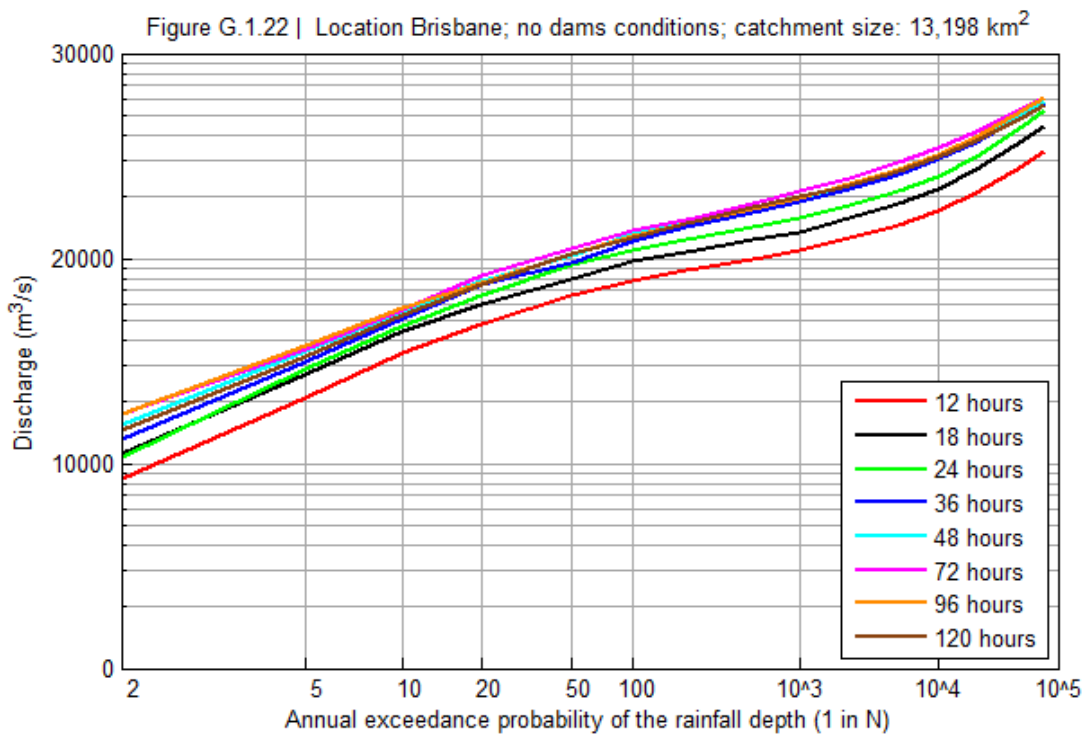
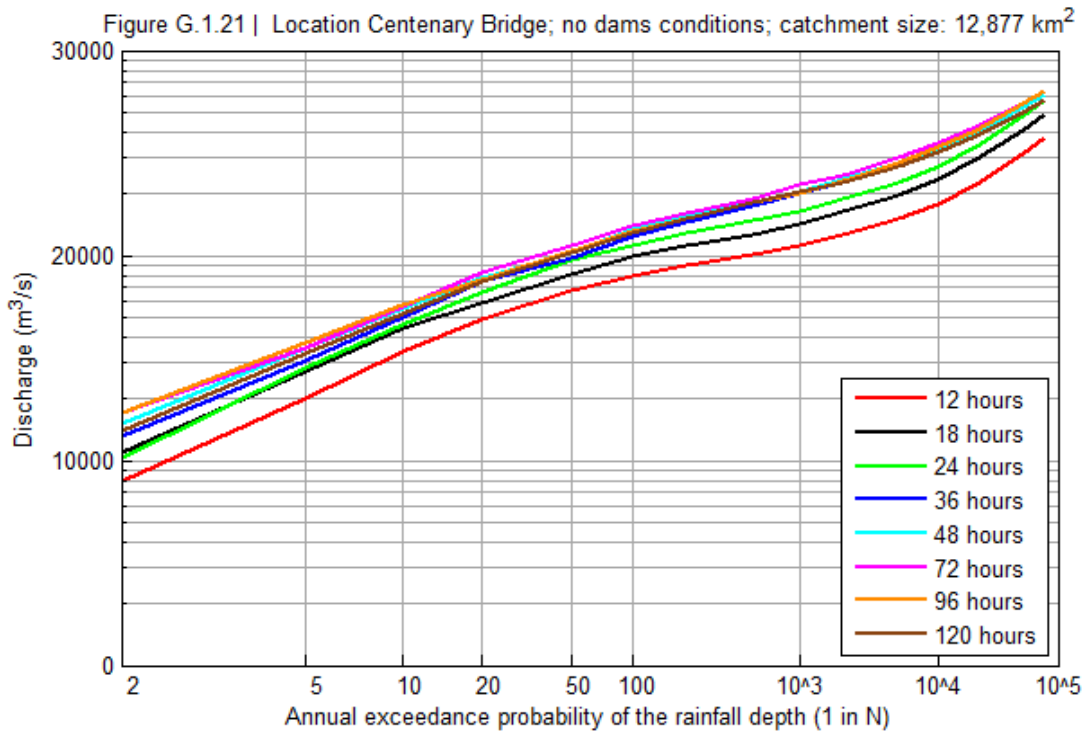
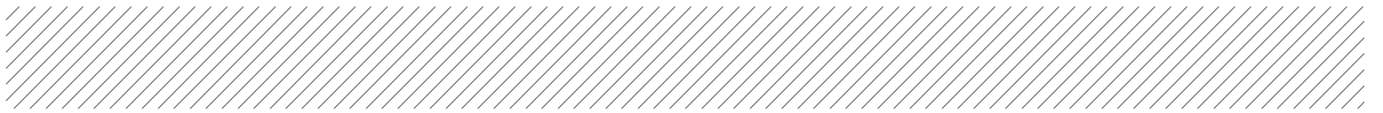
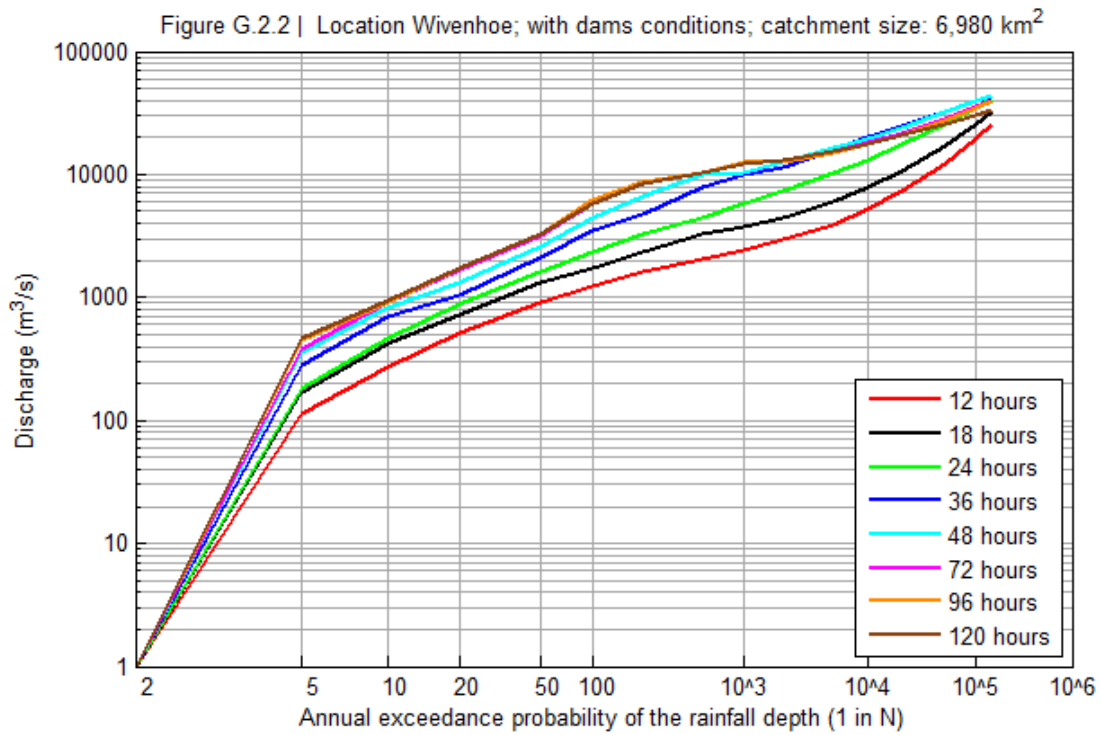
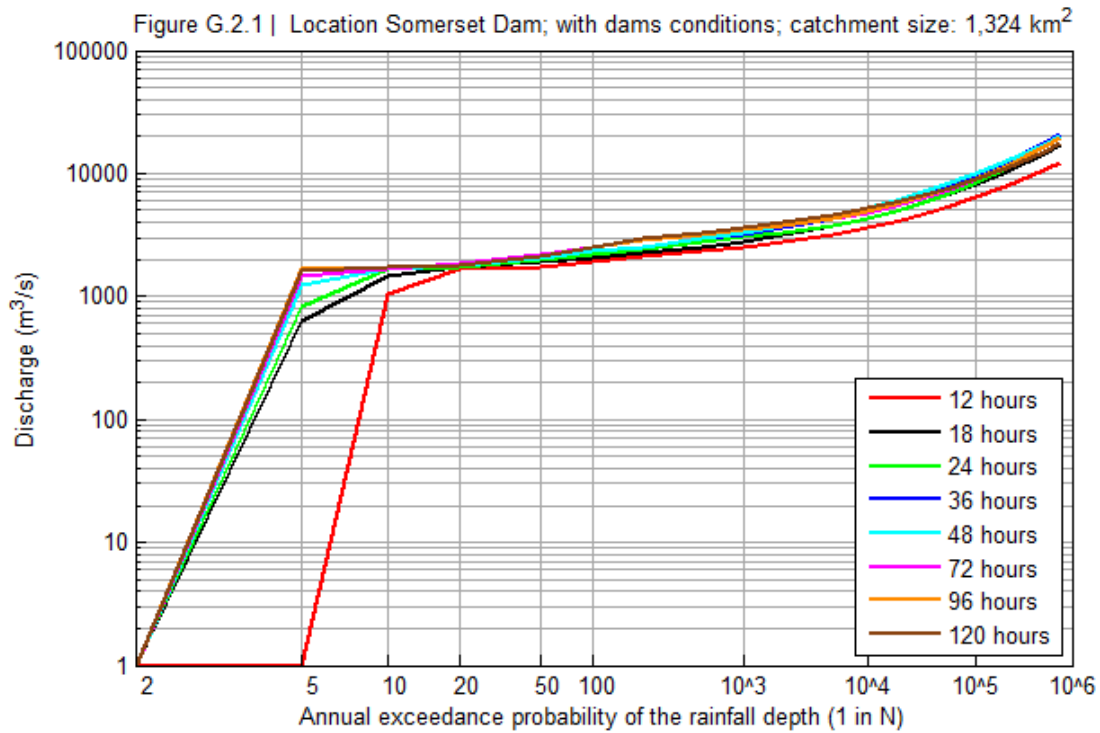


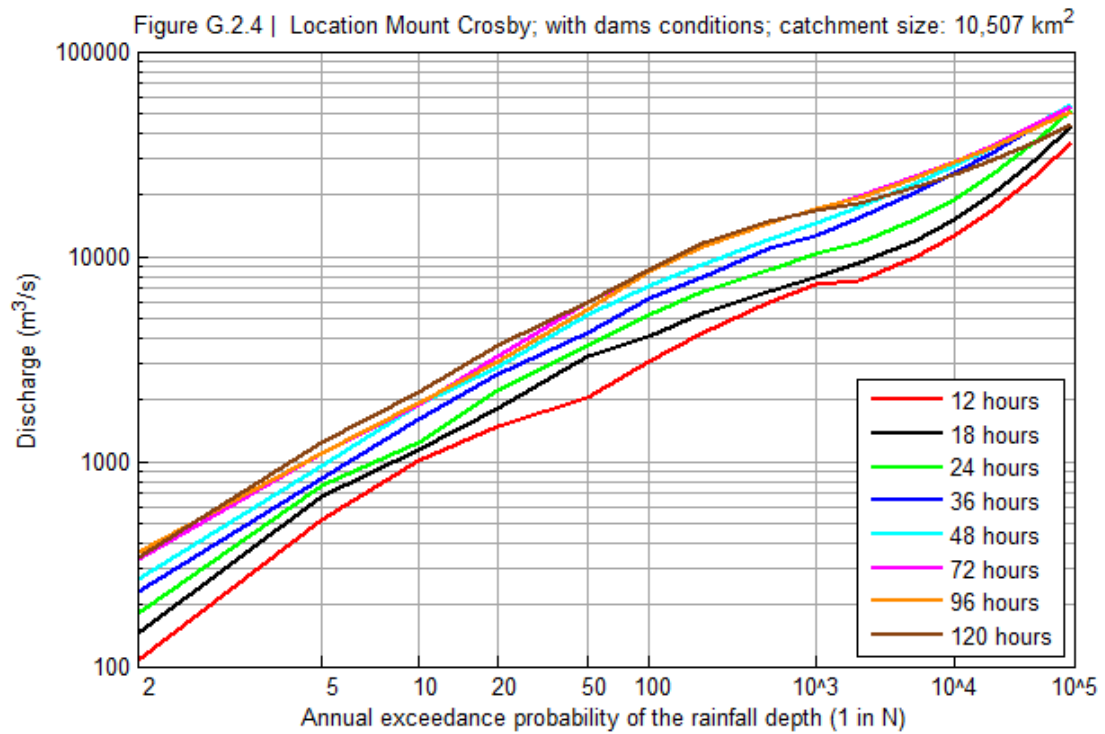
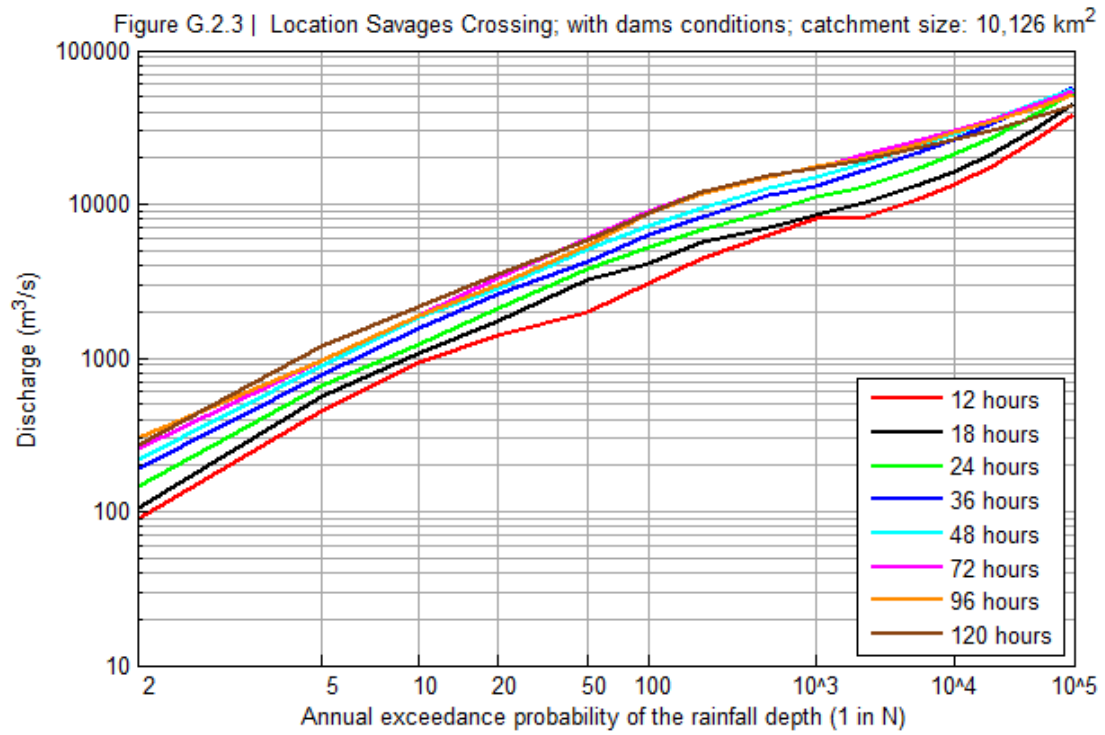
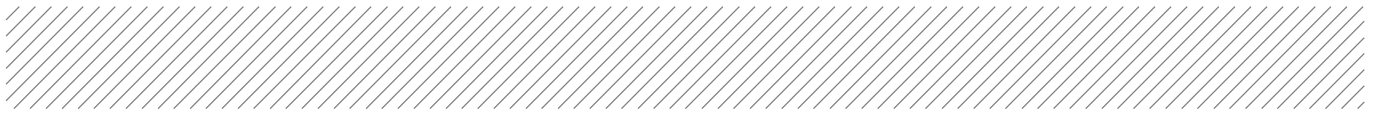
Figure G.1.20 | Location Moggill; no dams conditions; catchment size: 12,578 km²

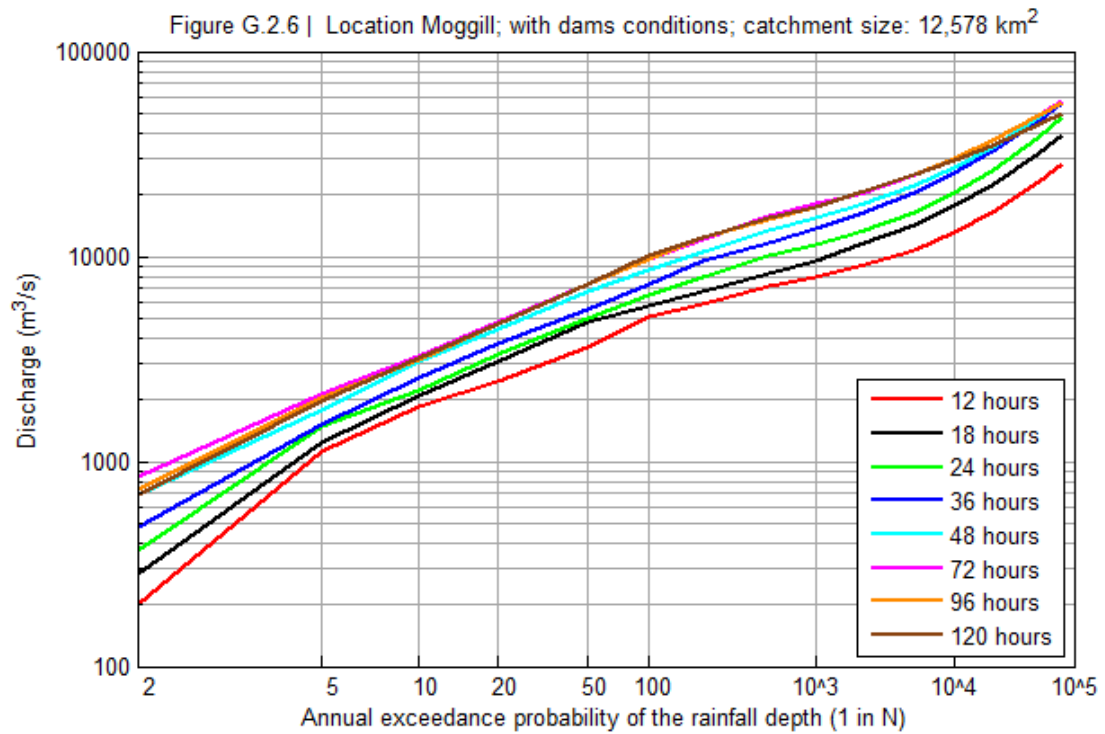
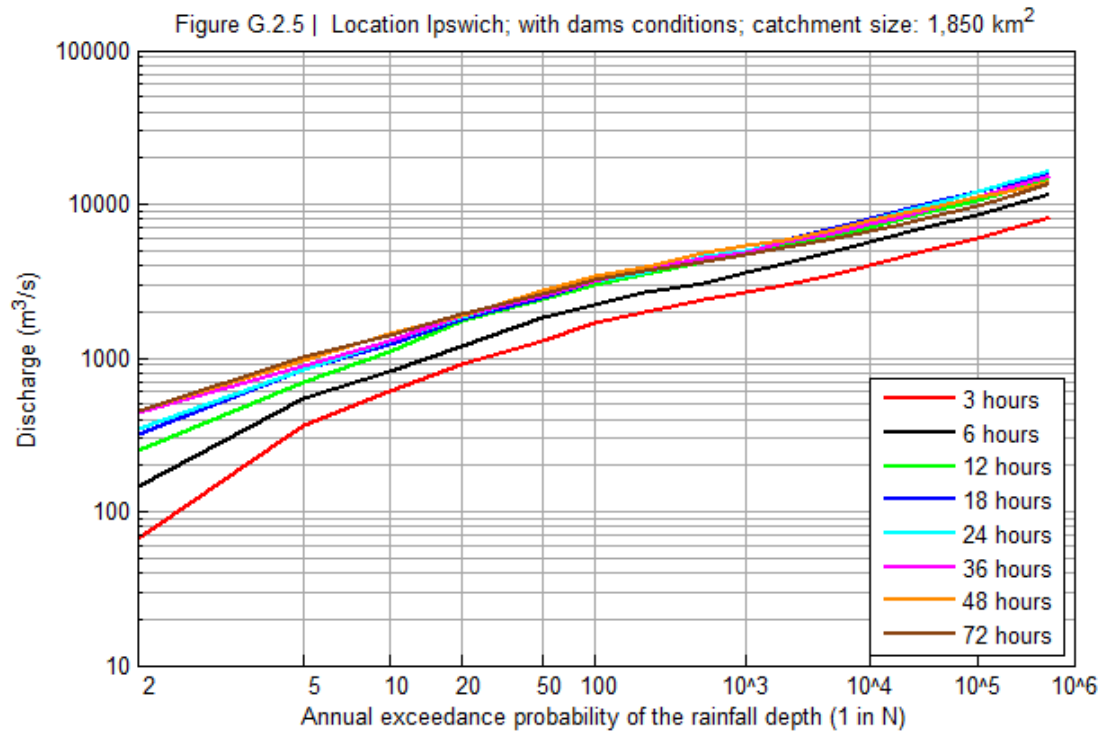
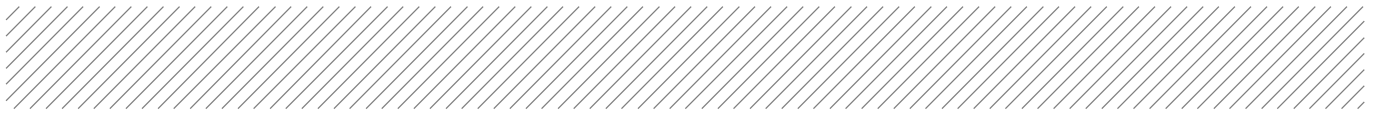


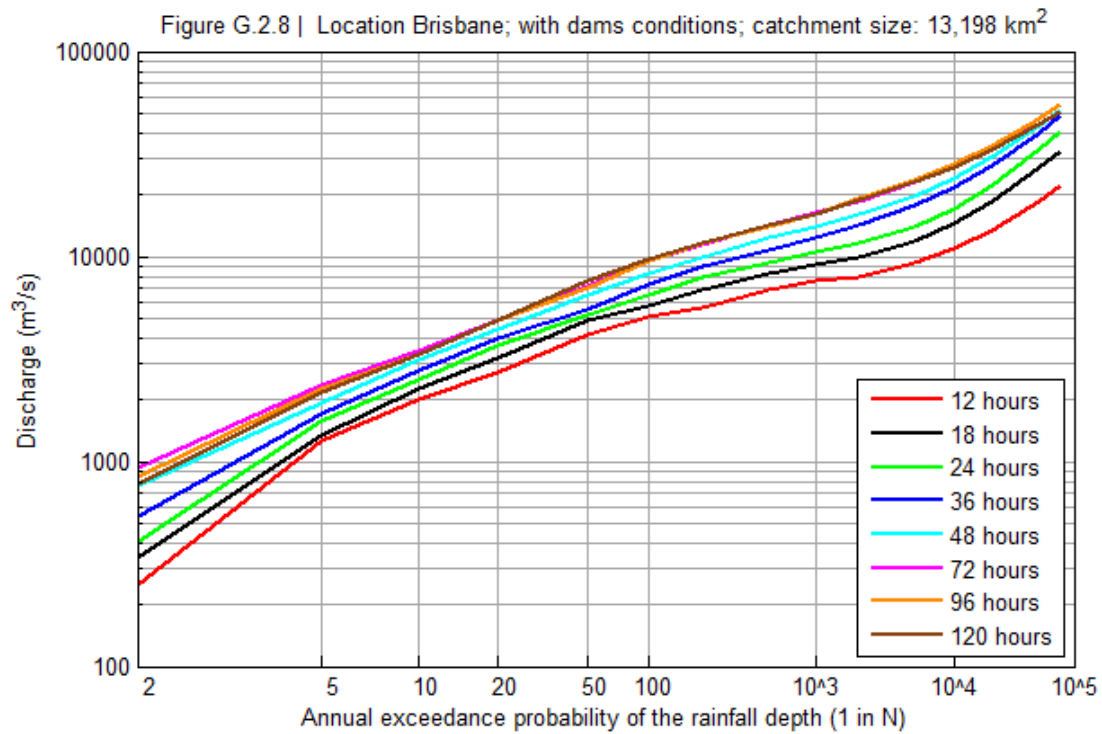
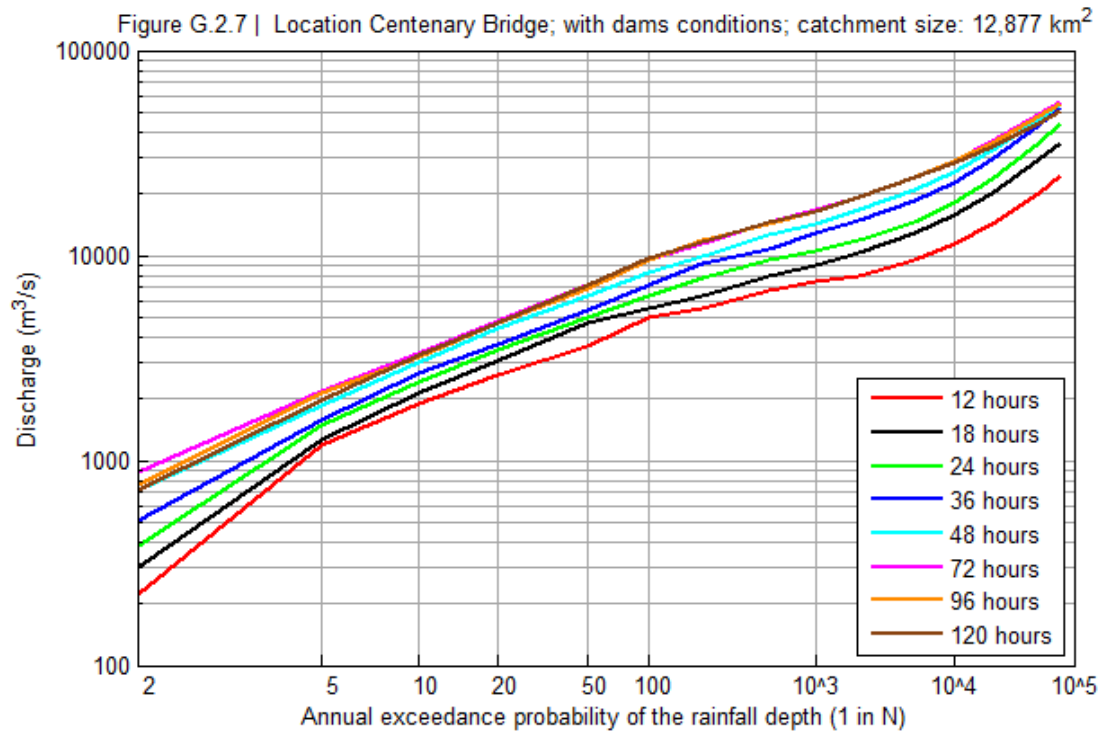
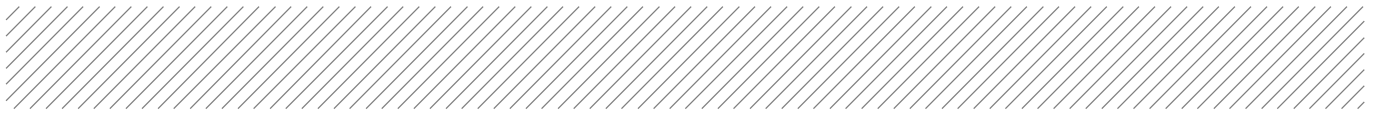


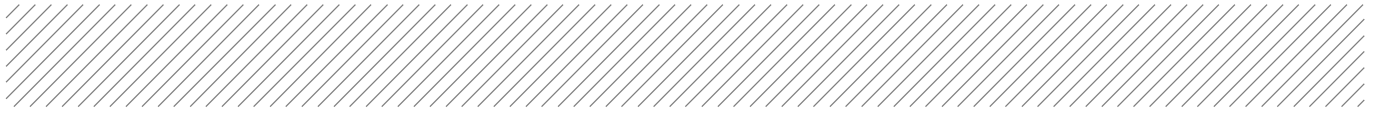
G.2 With dams conditions












Appendix H

Case study for the TPT and CRC –CH methods



An academic case study was carried out for comparison of the TPT and CRC-CH joint probability techniques. Specific objectives of the case study were:

- Gain insight in the details of both methods
- Mutual comparison of resulting design flows
- Influence of numerical settings on the model results
- Investigation of potential benefits from applying importance sampling

A test study for a hypothetical catchment in Australia was set-up. Relatively minor effort was put in the derivation and analysis of input statistics of forcing factors like rainfall depth, rainfall duration, initial losses and temporal and spatial rainfall patterns, as the focus of the case study was not to derive design discharges of a real world catchment. Instead, input statistics were copied from or modelled after related case studies in Australia. There were several reason for carrying out this academic test case:

- It allows for a detailed analysis of the pros and cons of the TPT and CRC-CH methods in a phase of the project in which the actual MCS modelling framework is not available
- The relatively straightforward model set-up allows for millions of hydrological model runs within a matter of minutes, as such providing excellent opportunities for analysis of the accuracy and variability of the MCS design flow estimates
- Differences in results of the TPT and CRC-CH methods can be explained relatively easy in such a “controlled” modelling environment

H1 Catchment and rainfall runoff model

The area of the catchment is chosen to be equal to 100 km². Runoff percentages during a storm event are influenced by the following forcing factors:

1. Rainfall depth
2. Temporal patterns of the rainfall
3. Spatial distribution of the rainfall
4. Initial losses
5. Continuing losses

[1], [2] and [4] are modelled as random variables in the Monte Carlo set-up. For the spatial pattern ([3]) a uniform distribution is assumed and the continuing losses ([5]) are assumed to be 2.5 mm/hr (independent of the storm event). The net rainfall, ie the proportion of the rainfall that becomes available for runoff, is derived by first subtracting the initial loss from the rainfall and subsequently subtracting continuing losses from the “remaining” rainfall. Figure H1 shows an example of a temporal pattern of the rainfall during an synthetic extreme event of 72 hours and the subdivision of the rainfall into initial losses, continuing losses and net rainfall.

The net rainfall in the catchment is modelled with a storage-discharge relation:

$$S = kQ^m \quad (37)$$

In which S is a storage component of the net rainfall (mm), Q is the discharge at the catchment outlet (mm/hr) and k and m are model parameters. Higher values of k and m generally result in an increase in the peak discharge and earlier timing of the peak. In the current studies, k=0.2 and m=1.

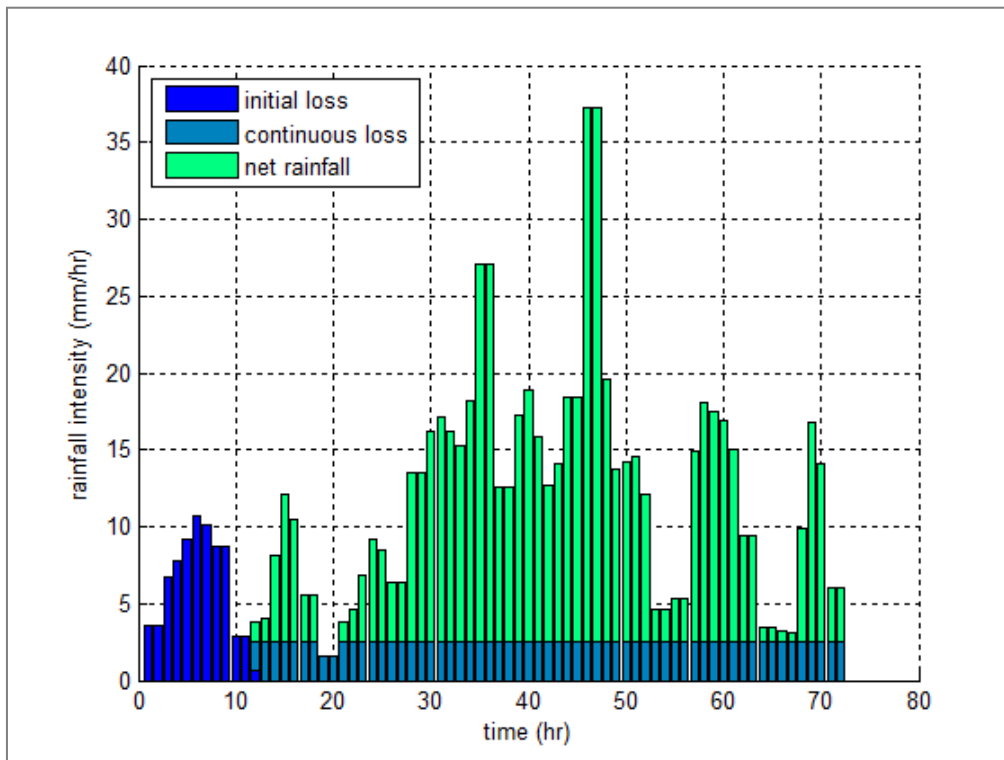


Figure H1 Example of the temporal pattern of the rainfall depth, initial losses, continuing losses and net rainfall

Input statistics

In the Monte Carlo approach, the following factors are treated as random variables:

1. Event duration, D (only in the CRC-CH approach)
2. Rainfall depth, R
3. Temporal pattern of the rainfall
4. Initial losses, IL

H1.1 Duration, D

The duration of storm events is assumed to be exponentially distributed, following the assumption of the pioneering papers of the CRC-CH method by Rahman et al[2001] and Rahman et al[2002]. A mean duration of 20 hours was adopted.

H1.2 Rainfall depth, R

Table H1 shows the assumed IFD relations for the catchment that are used to sample rainfall intensities. Values for 1-100 years ARI and 5 mins – 72 hours were obtained from the BoM website for location Brisbane (ARR, 1987). Values for ARI's >100 years were estimated through extrapolation, assuming a linear relation between $\log(\text{ARI}(I_r))$ and I_r . Values for durations >72 hours were obtained using a linear relationship between $\log(D)$ and $\log(I_r)$.

Table H1 Assumed IFD curve for the catchment (rainfall depth in mm)

D	ARI (years)										
	1	2	5	10	20	50	100	1000	104	105	106
5Mins	9.8	12.6	16.0	18.0	20.7	24.3	27.1	36.2	45.3	54.3	63.4
6Mins	11.0	14.1	17.9	20.2	23.2	27.3	30.4	40.6	50.8	61.0	71.2
10Mins	15.0	19.3	24.7	27.8	32.2	37.8	42.3	56.8	71.3	85.8	100.3
20Mins	22.0	28.5	36.7	41.7	48.3	57.3	64.3	87.0	109.7	132.3	155.0
30Mins	26.9	34.9	45.3	51.5	60.0	71.0	80.0	108.5	137.0	165.5	194.0
1 hr	36.0	46.7	61.2	70.0	81.7	97.5	110.0	150.0	190.0	230.0	270.0
2hrs	45.2	58.8	77.6	89.2	104.4	125.2	141.4	194.0	246.0	298.0	350.2
3 hrs	50.4	66.0	87.3	100.8	118.2	141.9	160.5	219.0	279.0	339.0	399.3
6 hrs	60.6	79.8	106.2	122.4	144.0	174.0	197.4	270.0	348.0	420.0	497.4
12 hrs	75.6	98.4	132.0	152.4	180.0	217.2	246.0	336.0	432.0	528.0	620.4
24 hrs	98.4	127.2	170.4	196.8	232.8	278.4	316.8	432.0	552.0	672.0	796.8
48 hrs	129.6	168.0	220.8	254.4	297.6	360.0	408.0	576.0	720.0	864.0	1012.8
72 hrs	144.0	187.2	244.8	280.8	331.2	396.0	453.6	648.0	792.0	936.0	1116.0
96 hrs	153.6	201.6	268.8	307.2	355.2	432.0	480.0	662.4	835.2	1017.6	1200.0
120 hrs	168.0	216.0	288.0	324.0	384.0	456.0	516.0	696.0	888.0	1068.0	1260.0
168 hrs	184.8	235.2	302.4	352.8	420.0	487.2	554.4	756.0	957.6	1159.2	1360.8

Given the duration of an event, the rainfall depth in the CRC-CH method is sampled as follows (Rahman et al., 2002). First sample the Annual Exceedance Probability (AEP) of the rainfall depth, from a standard uniform distribution. Subsequently, compute the Average Return Interval (ARI):

$$ARI(I_r) = -\frac{1}{\ln(1 - AEP(I_r))} \quad (38)$$

The resulting ARI is then used in combination with the given duration to derive the rainfall depth from Table H1.

Note: The ARI's in Table H1 are expressed in the unit (year). For an event based method like CRC-CH, which allows for the simulation of multiple events per year, it makes more sense to use an IFD table that is expressed in terms of exceedance probability per event instead of per year. The main reason for using IFD-tables with ARI's in years, is that these are readily available for all of Australia (from the Bureau of meteorology) and therefore easy to obtain and implement in design studies.

In order to take into account the fact that there are multiple events per year, while IFD's are defined per year is to use the following approach:

Sample a probability $P(I_r)$ from the standard uniform distribution function. P is the probability of exceedance of the rainfall depth for an individual event. Since we now consider multiple events per year, $P(I_r)$ should not be confused with the AEP. Subsequently, we derive the value of the ARI from $P(I_r)$ as follows:

$$ARI(I_r) = -\frac{1}{\lambda \ln(1 - P(R))} \quad (39)$$

Where λ is the average number of events per year. The AEP of this event can subsequently be derived from the following equation (which is the inverse of equation (38):

$$AEP(I_r) = 1 - \exp\left(-\frac{1}{ARI(R)}\right) \quad (40)$$

The use of equation (39) results in the following distribution function for $ARI(R)$:

$$P[ARI(R) < x] = \exp\left(-\frac{1}{\lambda x}\right) \quad (41)$$

This means that the reciprocal of $ARI(I_r)$, ie the Annual Exceedance Frequency (AEF), is exponentially distributed. This information is relevant later on when importance sampling is applied.

Temporal patterns

Sampling of temporal rainfall patterns is carried out with a 3-layer multiplicative cascade model (Hoang). The multiplicative cascade model sequentially divides each half by assigning weights to each side. For example, the 3-level model yields 8 intervals and requires specification of 7 weights ie 1 for the first split, 2 for the second split and 4 for the third split. The concept is shown in Figure H2. The third layer consists of 8 intervals, each representing $1/8^{\text{th}}$ of the time interval considered. This means each event is subdivided into $2^3 = 8$ intervals of equal size in which the rainfall depth remains constant. The fraction of the total rainfall that falls in the first interval is equal to $W1 \cdot W2 \cdot W4$. The fraction of the total rainfall that falls in the second interval is equal to $W1 \cdot W2 \cdot (1 - W4)$ etc. Each value of $W1 \dots W7$ is sampled from the same distribution function. In the current application, a uniform distribution is used over the interval (0.2-0.8). Figure H3 shows resulting patterns from the cascade model for 10 synthetic rainfall patterns.

1st layer	W1				1-W1			
2nd layer	W2		1-W2		W3		1-W3	
3rd layer	W4	1-W4	W5	1-W5	W6	1-W6	W7	1-W7

Figure H2 Three layer multiplicative cascade model

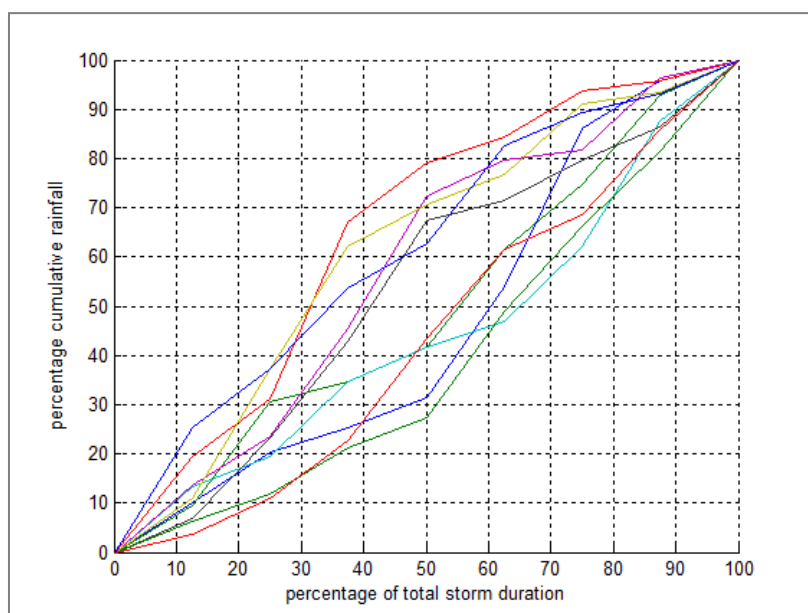


Figure H3 Sampled temporal patterns for 10 synthetic events

Initial losses

Initial losses (variable IL) are assumed to have a four-parameter beta-distribution, after Ilahee et al, [2001]. The first two parameters of this distribution are the minimum, D_{mean} , and maximum, D_{max} , values and these are taken equal to 0 mm and 100 mm respectively. Shape parameters α and β are taken equal to 2 and 5 respectively. In Figure H4 shows the resulting probability density function for variable IL.

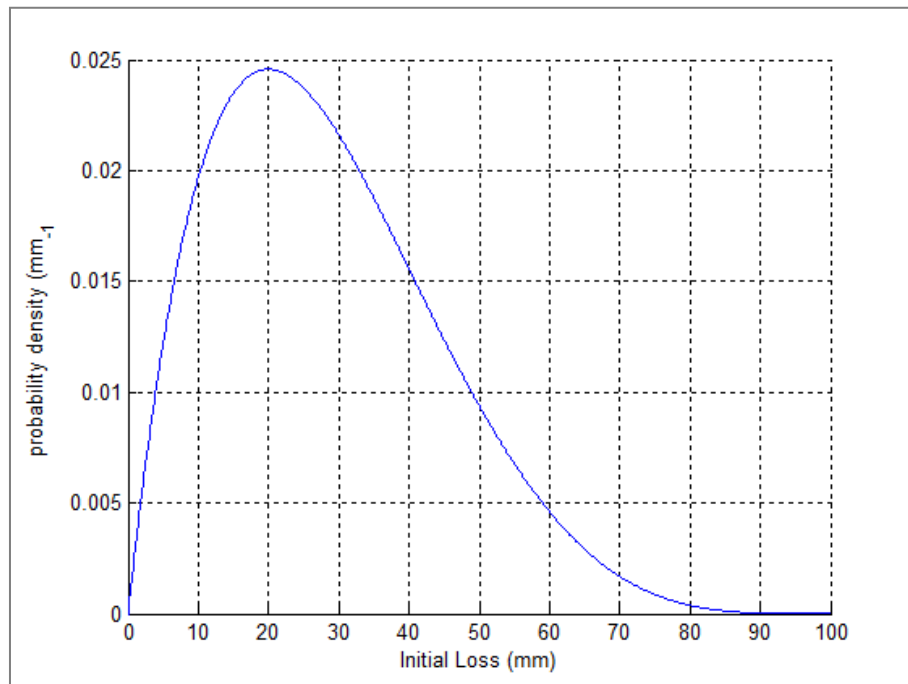


Figure H4 Density function of the initial losses (IL)

H2. Application of the CRC-CH method

H2.1 Procedure

The steps taken in the CRC-CH methodology (Rahman et al, 2001; 2002) can be summarized as follows:

1. Sample the storm event duration from the exponential distribution function
2. Sample the average rainfall depth, conditional on the duration
3. Sample the rainfall temporal pattern from the multiplicative cascade model
4. Sample the initial loss from the beta-distribution
5. Run the rainfall runoff-model to derive the peak discharge at the catchment outlet

Note: The IFD curves of Table H2 have been derived by BoM for bursts. In the current application these will be used to sample average intensities for events. In real-world application this should not be done, as event statistics are different from burst statistics. For the current academic case this is no problem, we just needed “academic” input statistics. The procedure is repeated N times, in order to simulate N storm events. The probability that a selected threshold discharge level q is exceeded in a storm event is subsequently estimated from:

$$\hat{P}_e(q) = \frac{1}{N} \sum_{i=1}^N I_{[q_i > q^*]} \quad (42)$$

Where \hat{P}_e is the estimated probability of exceedance of q per event, q_i is the computed discharge in simulation i and $I_{[A]}$ is the indicator function ($I=1$ if $q_i > q$, $I=0$ otherwise) and N is the number of simulated storm events. In order to estimate the ARI of q , the average number of storm events per year, λ , needs to be taken into account:

$$ARI(q) = \frac{1}{\lambda \hat{P}_e(q)} \quad (43)$$

The value of λ is taken equal to 5, similar to Rahman et al [2002]. Instead of computing the probability of exceedance for a single threshold discharge q , the MC procedure can provide exceedance probabilities for a range of discharges with negligible additional computation time. This can be done with the following procedure:

1. Place the N computed peak discharge q_1, \dots, q_N in descending order
2. Assign exceedance probability per event of $1/N$ to the highest observed value, exceedance probability $2/N$ to the second highest observed value etc

This is a very straightforward procedure, which is one of the reasons of the popularity of the MC procedure. Note that a more formal approach to step 2 is to determine the ARI as follows:

$$ARI(q_r) = \frac{1}{\lambda} \frac{N+1-2c}{r-c} \quad (44)$$

In which r is the ranking number of discharge q_r in the series of N computed discharges ($r=1$ for the highest discharge, $r=2$ for the second highest discharge etc) and c is the plotting constant. Plotting constant c can be chosen between 0 and 0.5. The choice of constant c is somewhat arbitrarily, unless the underlying statistical distribution function of the discharge is known. In the remainder of this section, c is taken equal to 0.

H2.2 Results

The method was applied with $N=20,000$ simulated storm events, representing a series of $20,000/\lambda = 4,000$ years. The number 20,000 was adopted from Rahman et al. [2001]. The procedure was repeated 10 times to assess the variability in the Monte Carlo estimates. Results are shown in Figure 10.5. Two main disadvantages of this method (or any crude Monte Carlo sampling method) are clearly demonstrated in this figure:

1. The variation in estimated design discharges increases with increasing value of ARI
2. For ARI's that are larger than the number of simulated years (4,000 in this case) there is no estimate available

For this reason, the CRC-CH method has been cited on numerous occasions as “not the preferred method” for estimating design discharges for high (extreme) ARI's (ARR, 2013, Mirfenderesk et al., 2013, Aurecon, 2013a). The TPT method is preferred for higher ARI's, because it applies stratified sampling on the rainfall depth, which enables the estimation of discharges with extreme ARI's (up to the PMP) without requiring millions of model simulations. In the CRC-CH method, the stratified sampling approach could also have been adopted. In that case, however, stratified sampling would have to be applied on rainfall depth *and* event duration, whereas in the TPT method the stratified

sampling is only applied on rainfall depth. The reason for this difference is that the rainfall depth is conditionally distributed on the storm event duration, and the event duration is a random variable in the CRC-CH method, as opposed to the TPT method. Stratified sampling on two random variables is significantly more time-consuming than stratified sampling for one variable, which is why this technique is more efficient in the TPT approach. Therefore, it is proposed to apply an alternative efficient sampling technique in the CRC-CH method: “importance sampling”.

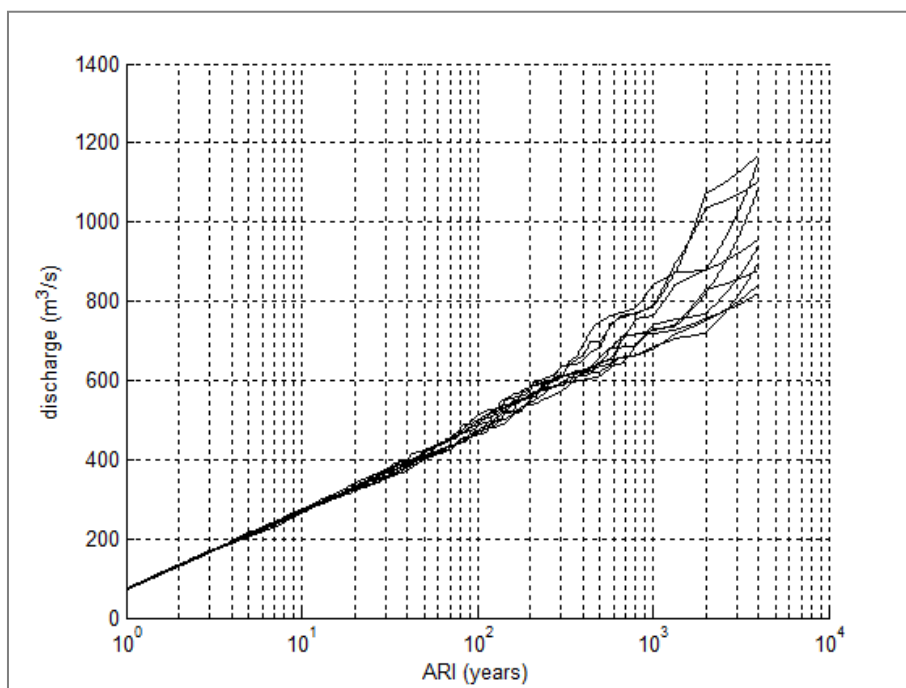


Figure H5 ARI's and corresponding discharges as estimated from 10 different MC runs, using the CRC-CH method

H2.3 Application of importance sampling in the CRC-CH method

The cause of the high uncertainties in estimates of extreme discharges in the CRC-CH procedure (or any crude Monte Carlo procedure) is the fact that the percentage of simulated events resulting in extreme discharges is low. Consequently, the method provides little or no information on exceedance probabilities of the higher range of discharges. This is no problem if one is interested in design discharge in the lower ARI-ranges, eg up to 100 years. However, especially in PMP/PMF studies for dam design, discharges with ARI's of 100,000 – 1,000,000 years are required. In that case, the required number of model simulations in the CRC-CH method is a multitude of these high numbers, which is very impractical with regard to simulation time and data storage.

In the current case study it was therefore decided to investigate the potential benefits of applying importance sampling in the CRC-CH method. Importance sampling (see eg Engelund and Rackwitz, 1993) is a method to increase the efficiency of the crude Monte Carlo method, that is, to decrease the number of samples required to produce a reliable estimate of ARI's and corresponding design discharges. This is done by replacing the actual probability density function, f , of one or more random variables by a more efficient one, h . Efficient refers in this case to the proportion of the samples which will result in exceedance of extreme discharges.

Because the sampling procedure does not use the actual distribution function, the estimator of the failure probability as applied in crude Monte Carlo (see equation above) needs to be adapted. This is done via the following formula:

$$\hat{P}_e(q) = \frac{1}{N} \sum_{i=1}^N \mathbf{I}_{[q_i > q]} \frac{f_X(\mathbf{x}_i)}{h_X(\mathbf{x}_i)} \quad (45)$$

In which \mathbf{x}_i is the vector of samples of the random variables in the i^{th} synthetic event. In equation (45), a factor f/h has been added in comparison with the crude Monte Carlo estimate of equation (42). The reciprocal of this factor, h/f , is the factor by which the sampling probability of \mathbf{x} has been increased through introduction of the importance sampling function h . The correction factor in equation (30) compensates for this increase. Put more simply: if the probability of an event is increased by a factor 10, the contribution of this event to the estimated exceedance probability of discharge level q needs to be divided by a factor 10 there afterwards.

The choice of importance sampling function h determines the efficiency of the importance sampling method and this function can be taken equal to virtually any probability density function. Efficient choices for h depend on the problem under consideration. Ideally, a sampling strategy is chosen that results in a uniform sampling distribution of the simulated peak river discharges, over the range of discharges of interest. In that case, the MC estimates can be expected to be equally accurate for all discharges.

For the current study it was decided to first try out a sampling strategy in which importance sampling was only applied on the rainfall depth. Figure H6 shows the relation between the rainfall depth and the peak river discharge, based on 20,000 simulated events. It shows, not surprisingly, that there is a positive correlation between these two variables. However, it also shows that the correlation is not strong, which is mainly due to the fact that the plotted events can have a variety of durations. For example, an average intensity of 5 mm/hr for a 72 hour storm event can be expected to lead to extreme discharges, but the same intensity will cause little or no runoff for a 1 hour storm event. This makes the relation between rainfall depth and discharge rather disperse, which is further enhanced by the variability in other variables like temporal rainfall patterns or initial losses. This complicates the importance strategy for rainfall depth, as high rainfall intensities will not necessarily result in high river discharges.

A much stronger relation is established when the peak discharge is plotted against the ARI of the sampled rainfall depth (Figure H7). Clearly, extremely high samples of $ARI(I_r)$ will automatically result in (extremely) high peak river discharges. For this reason it was decided to apply importance sampling on the $ARI(I_r)$ of the rainfall. Figure H7 also reveals that there is a near linear relation between the logarithm of $ARI(I_r)$ and the expected peak river discharge. So, in order to have a produce that results in (near) uniform samples of the simulated peak river discharge, it seems a sampling strategy should be chosen in which the logarithm of $ARI(I_r)$ is uniformly distributed:

$$\ln\{ARI(I_r)\} \square U(a, b) \quad (46)$$

The boundaries, a and b , of this distribution are taken equal to the limits of the ARI's for which rainfall intensities are given in the IFD relations of Table H1. This means $a = \ln(1)$ and $b = \ln(1,000,000)$. This will provide samples of intensities over the entire range for which input statistics are available. Equation (31) translates into the following importance sampling distribution function for $ARI(I_r)$:

$$H(x) = P[ARI(I_r) < x] = \frac{\ln(x) - a}{b - a} \quad ; a \leq \ln(x) \leq b \quad (47)$$

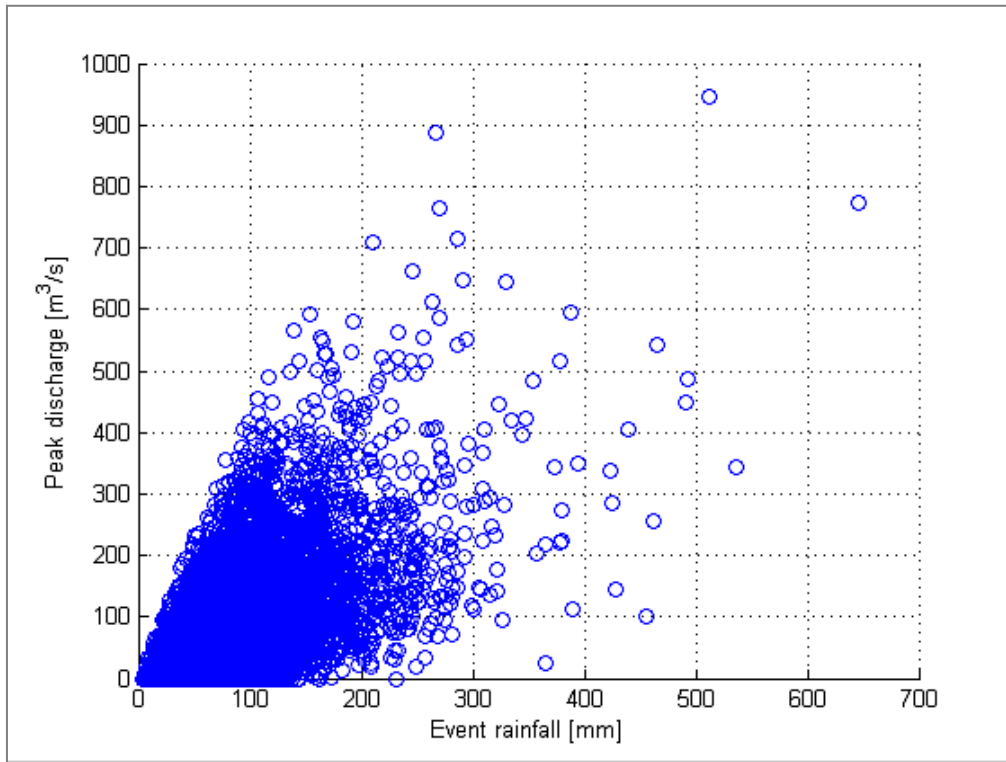
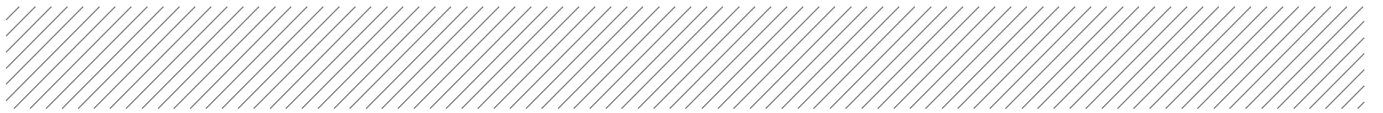


Figure H6 Relation between the event rainfall depth and peak discharge for 20,000 events

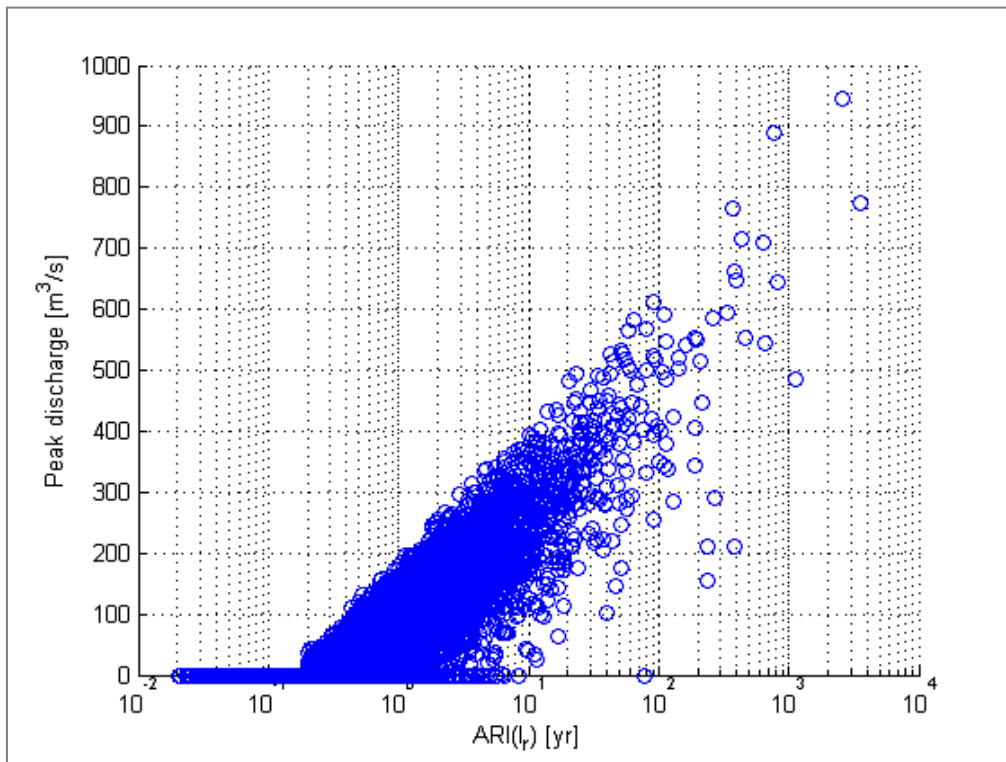


Figure H7 Relation between ARI (I_r) and peak discharge for 20,000 events

The corresponding density function is equal to:

$$h(x) = \frac{1}{x(b-a)} ; a \leq x \leq b \quad (48)$$

The original distribution function of $ARI(I_r)$ is equal to (see equation (26)):

$$F(x) = P[ARI(I_r) < x] = \exp\left(-\frac{1}{\lambda x}\right) \quad (49)$$

The corresponding density function is equal to:

$$f(x) = \frac{\exp\left(-\frac{1}{\lambda x}\right)}{\lambda x^2} \quad (50)$$

This means the importance sampling correction factor (see equation (30)) is equal to:

$$\frac{f(x)}{h(x)} = \frac{\exp\left(-\frac{1}{\lambda x}\right)(b-a)}{\lambda x} ; a \leq \ln(x) \leq b \quad (51)$$

This correction factor needs to be quantified for each simulated event in the Monte Carlo procedure, by replacing the value of x in equation (36) by the sampled value of $ARI(I_r)$. Figure H8 compares the actual density function of $ARI(I_r)$, $f(x)$, and the importance sampling density function of $ARI(I_r)$, $h(x)$ for the case that $\lambda=5$. Figure H9 shows the corresponding importance sampling correction factor $f(x)/h(x)$. It shows that the correction factor is roughly equal to $2.76/ARI(I_r)$, where $2.76 = (b-a)/\lambda$ in this example. This means the probability of sampling a given value of $ARI(I_r)$ has been approximately increased by a factor $ARI(I_r)/2.76$ by the importance sampling procedure. Especially for larger values of $ARI(I_r)$ this means a major increase in the probability of being sampled, which is exactly the purpose of introducing the importance sampling procedure.

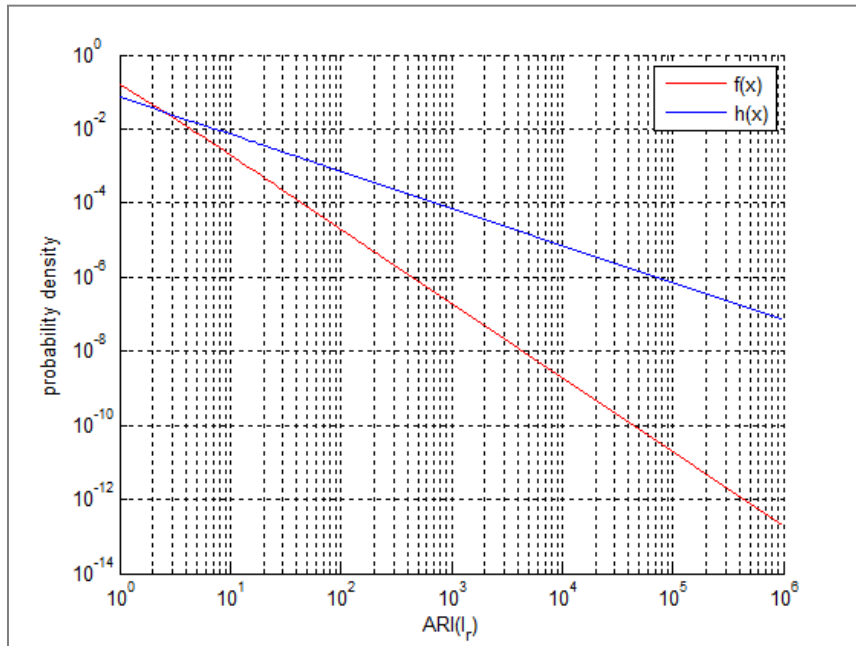


Figure H8 Comparison of the actual density function of $ARI(I_r)$, $f(x)$ and the importance sampling density function of $ARI(I_r)$, $h(x)$

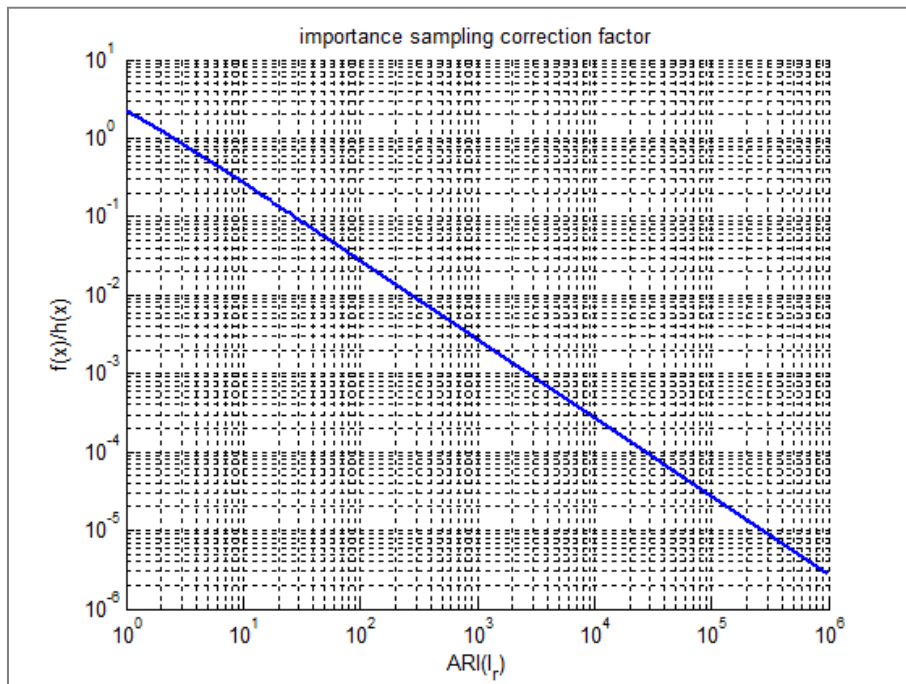


Figure H9 Importance sampling correction factor $f(x)/h(x)$ for a range of values of $ARI(l_r)$

Figure H10 shows the results of the above described importance sampling procedure. The lines represent 10 different Monte Carlo simulations, using 20,000 samples each time. As can be seen, the results for the higher ranges of the ARI have significantly improved in comparison with the original crude Monte Carlo procedure (Figure H5). The variance in the MC estimators have decreased dramatically and estimates are available for a much wider range of ARI's. This clearly demonstrates that importance sampling provides the required counterarguments for the fact that the existing CRC-CH method is not capable of providing reliable estimates for high ARI's without requiring millions of model simulations.

If importance sampling is properly applied, no bias is introduced. Potentially, a bias can be introduced if $h(x)=0$ for values of x that are contributing to exceedance probabilities of relevant discharge levels. So, $h(x)$ needs to be properly chosen that this does not occur. In the current application this seems to be the case as $h(x)>0$ for all values of $ARI(l_r)$ for which IFD relations are available. To verify this, the results of the importance sampling procedure are compared with results from the crude Monte Carlo procedure. The importance sampling procedure is carried out with $N=20,000$ samples while the crude Monte Carlo procedure is carried out with 1 million samples. Each sampling procedure is repeated 5 times to quantify the variability in the results.

Figure H11 shows the results (black line: crude Monte Carlo with 1 million samples, red lines: importance sampling with 20,000 variables). It can be seen that the two methods provide consistent results up to approximately 1000 year ARI. This consistency confirms that no bias is introduced by the adopted importance sampling procedure. For higher ARI's, the variability in the crude MC procedure starts to cause noticeable differences between the two methods. So even though 1 million samples have been used, the crude MC method is still less reliable for high ARI's than the importance sampling procedure with "only" 20,000 samples. The variability of the importance sampling procedure is negligible up to an ARI of at least 1,000,000 years.

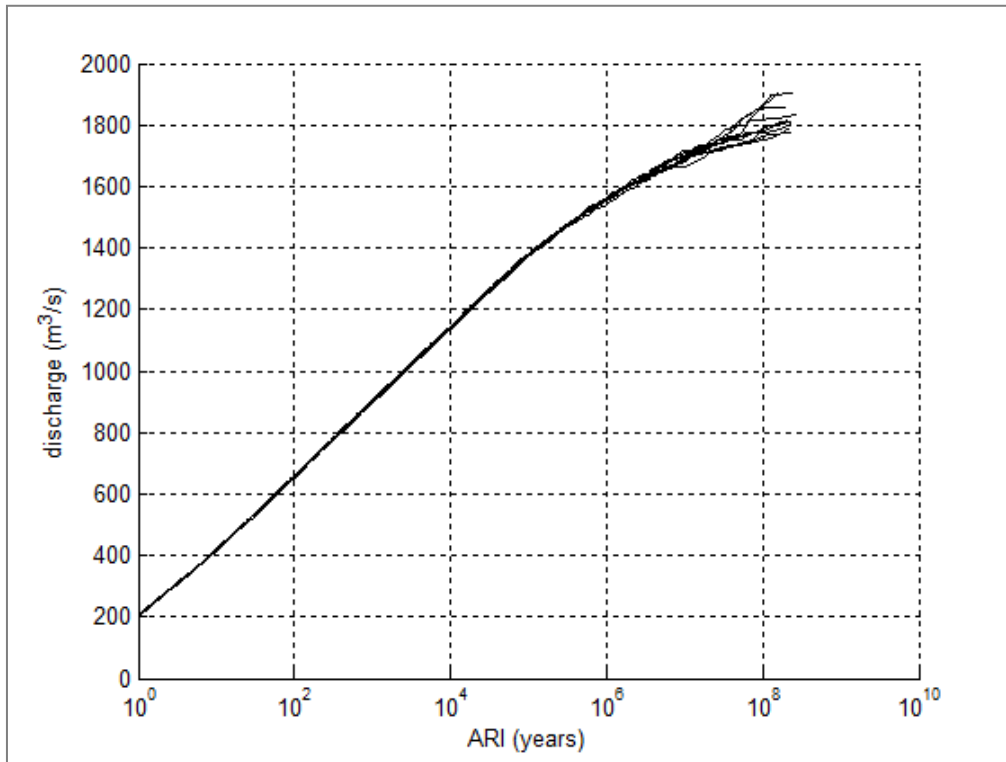


Figure H10 ARI's and corresponding discharges as estimated from 10 different MC runs, using the CRC-CH method with importance sampling

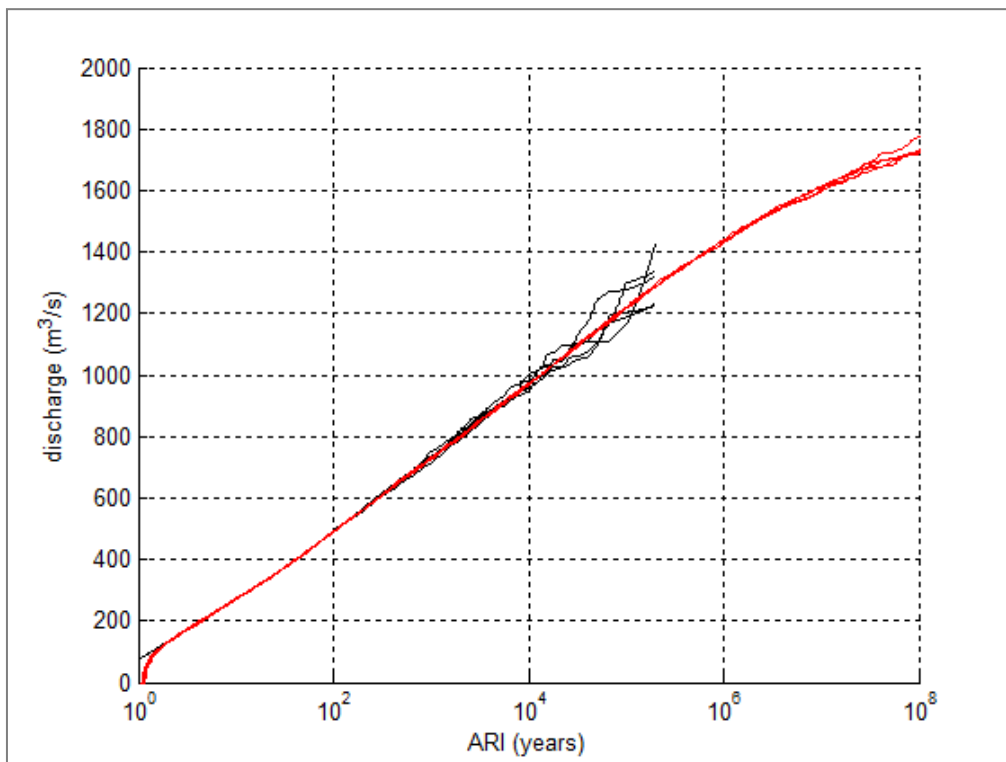


Figure H11 ARI's and corresponding discharges as estimated from 5 different MC runs with crude Monte Carlo, 1 million samples each (black lines) and 5 different MC runs with Monte Carlo with importance sampling, 20,000 samples each (red lines)

Sensitivity analysis

A sensitivity analysis was conducted to verify which parameters may influence the results of the CRC-CH methods. First, the sensitivity analysis was carried out for the CRC-CH method, to verify which parameters can cause significant shifts in the derived design discharges. The Table H2 provides an overview of the variables and the perturbations that were applied in the sensitivity analysis.

Table H2 Estimated design flows (m^3/s) for different ARI's with TPT and CRC-CH

parameter	meaning	Base case	Perturbation
D_{mean}	Mean duration of a storm event	20 hrs	10 hrs
λ	Number of events per year	5	3
# cascades	Number of cascades in the model for temporal variation of rainfall	3	4
ILmax	Maximum initial loss	100 mm	50 mm

Figure H12 shows the results of the sensitivity analysis. It turns out that the model results are fairly insensitive to all of these variables.

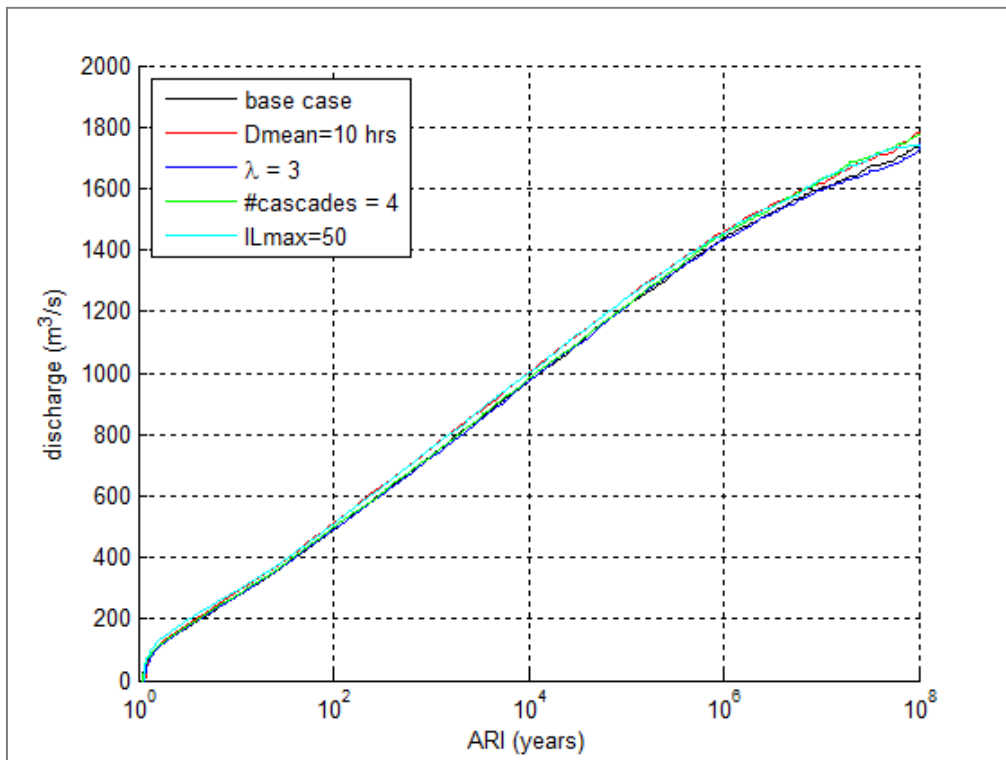


Figure H12 Peak discharges and corresponding ARI's; sensitivity analysis for the CRC-CH method

H2.5 Conclusions

It has been demonstrated that importance sampling solves the problem of excessive number of samples required when applying the CRC-CH method based on crude Monte Carlo sampling. Reliable estimates for (extremely) high ARI's are obtained without requiring millions of model simulations. The uncertainty in the estimated design flows of (extremely) high ARI's can be significantly reduced, potentially in combination with a reduction in the number of model simulations. We are confident that this will apply to other cases than the one described in this report, but this needs to be demonstrated. The importance sampling strategy may need to be tailored to the case under consideration, but it is likely that the currently adopted strategy will provide useful results for the majority of Australian catchments.

H3. Application of the TPT method

H3.1 Procedure

The TPT method (see eg ARR, 2013a) derives frequency curves of discharge levels separately for a set of potentially critical rainfall durations. For each duration, a stratified sampling approach is applied to estimate Average Return Intervals (ARI) or, equivalently, Annual Exceedance Probabilities, AEP. The stratified sampling is applied on the rainfall depth. Stratified sampling is essentially numerical integration, where the Total Probability Theorem (TPT) is used to compute the combined exceedance probability of discharge levels for all potential rainfall intensities. The formulation of the total probability theory in this case is:

$$P[Q > q | D] = \int_0^{\infty} P[Q > q | R, D] f_{I_r, D}(R_i; D) dI_r \quad (52)$$

In which R is the rainfall depth and $f_{I_r, D}$ is the density function of R , conditional on duration D . In practical applications, the discretised version of equation (52) is used:

$$P[Q > q | D] = \sum_i^{N_b} P[Q > q | R \in R_i, D] P[R \in R_i | D] \quad (53)$$

Where N_b is the number of intervals (bins) in which the range of relevant intensities is divided and R_i is the i^{th} interval. The conditional probability of occurrence of interval R_i can be obtained directly from IFD curves. The conditional exceedance probability of q , given R_i and D is determined by the realisations of the "remaining" random variables IL (initial losses) and temporal rainfall patterns:

$$P[Q > q | R \in R_i, D] = \int_{\theta} P[Q > q | R \in R_i, D, \theta] f_{\theta}(\theta) d\theta \quad (54)$$

Where θ is the vector of remaining random variables and f_{θ} is the multivariate probability density function of these random variables. In the TPT approach, equation (54) is evaluated with Monte Carlo simulations that are carried out for each interval (bin) of the rainfall depth (see section 8.3.3). This means random samples are taken of θ and model runs are carried out to compute the resulting river discharge. For any discharge level q , the proportion of samples that results in discharges $> q$ is used as the required estimate of the conditional exceedance probability of equation (54).

The steps in the TPT approach can be summarized as follows (ARR, 2013):

1. Choose a range of durations around the critical storm duration (from Design Event Analysis). For each duration carry out steps 2-4
2. Divide the range of relevant values of $ARI(R)^6$ into N_b bins of equal size in terms of their standardized normal variate
3. For each bin, take N_s samples of the remaining random variables (initial losses and rainfall patterns) and simulate the hydrological model to evaluate the conditional exceedance probability of equation (53)
4. Evaluate equation (54) to derive the exceedance probabilities of a range of discharge levels and translate these into ARI's

The result of this procedure is a set of frequency curves of the peak discharge, one for each individual duration. The overall curve is then taken to be the “envelope” of all frequency curves combined:

$$ARI(q) = \min_D ARI(q | D) \quad (55)$$

In which $ARI(q)$ is the ARI of discharge q and D is the duration of a storm burst.

H3.2 Adaptation of input statistics

For a fair comparison with the CRC-CH method, input statistics are taken the same as much as possible. However, some statistics have to be adapted, because the CRC-CH method requires statistics of complete rainfall events, whereas the TPT method is based on storm bursts. For the CRC-CH method in the current studies, the burst statistics of Table H1 were translated to event statistics by taking into account the factor λ , which represents the number of events per year. This translation then accounts for the fact that IFD tables are expressed in ARI's per year, whereas event samples require ARI's *per event*. Later on in this document further discussion is provided on additional requirements to translate burst statistics to event statistics, however, in the absence of event based IFD tables, adopting the burst tables is not an unreasonable approach. For the TPT approach, the burst statistics of Table H1 can and will be used directly as input. The value of λ , ie the number of simulated storm events per year, therefore has no role in the TPT method.

Storm bursts also require statistics for initial losses that are different from statistics of initial losses for events. Storm events by definition start after a period of at least a couple of hours of no rain, whereas storm bursts can occur in the middle of a storm event. Storm bursts therefore generally occur on wetter initial conditions than storm events. In Rahman et al [2002] a relation was established between the two:

$$IL_c = IL_s \left(0.5 + 0.25 \log_{10} (D_c) \right) \quad (56)$$

Where IL_c and IL_s are initial losses for storm bursts (cores) and storm events respectively and D_c is the considered duration of the storm burst.

⁶ ARR, 2013 actually uses AEP instead of ARI, but essentially that doesn't change the method

Simulation results

The numerical settings for the stratified sampling were initially chosen the same as described in ARR [2013]:

- Sampling of the standard normalised variate was over the interval [0,5], corresponding to AEP's of 0.5 and $2.86 \cdot 10^{-7}$ respectively
- The interval was subdivided in 50 bins of equal size
- For each bin, 200 MC simulation were executed to derive exceedance probabilities conditioned on the rainfall depth that is associated with the bin under consideration

In a second attempt, the sampling interval was extended to [-1,5] and the number of bins increased to 60. This was done to obtain a more reliable estimate for the lowest ARI's (1 – 10 years). The procedure was carried out 10 times to evaluate the variation in output and results are shown in Figure H13. As can be seen, the variation in results is small over the entire range of ARI's.

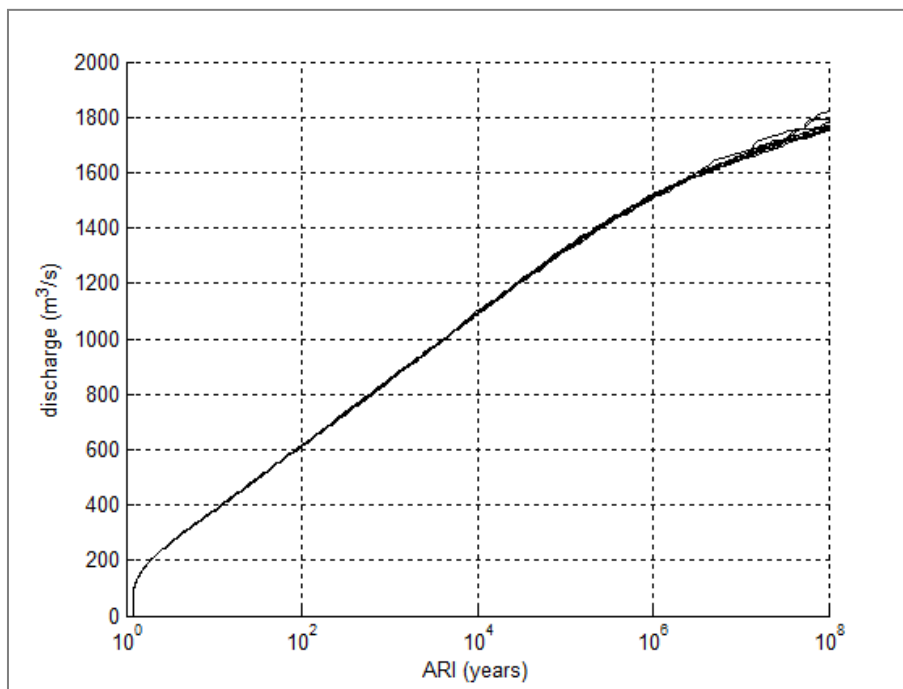


Figure H13 ARI's and corresponding discharges as estimated from 10 different MC runs, using the TPT- method

Application of importance sampling in the TPT method

As described in Section H3, importance sampling provided major improvements in estimated design flows for the higher range of ARI's in the CRC-CH method. A similar improvement cannot be expected in the TPT method, as the application of the stratified sampling makes the existing TPT method already highly efficient. Figure H13 showed that there is negligible variation in results between successive runs, indicating that the accuracy of the MC simulation scheme can hardly be improved. The only reason to introduce importance sampling in the TPT method is if a similar accuracy can be obtained with a lower number of model simulations. This would save valuable computation time, which would be beneficial in the BRCFS project (and other projects) as the Monte Carlo analysis needs to be repeated numerous times.

First of all, it needs to be demonstrated that importance sampling can be used in combination with the TPT method (Note that the use of importance sampling in the TPT method is actually a “contradiction in terms” because the Total Probability Theorem is not required to compute design flows if importance sampling is used instead of stratified sampling). For this purpose, a uniform sampling strategy was applied over the same interval in the standard normal space, [-1,5], that was evaluated with the stratified sampling approach. Note that the actual density function of the standard normal variate is the standard normal density function:

$$f(x) = \frac{1}{\sqrt{2\pi}} \exp\left(-\frac{x^2}{2}\right) \quad (57)$$

By using a uniform sampling approach for the standard uniform variate, the importance sampling density function, h , is:

$$h(x) = \frac{1}{6} \quad ; -1 \leq x \leq 5 \quad (58)$$

This means the importance sampling correction factor (see equation (30)) in this procedure is equal to:

$$\frac{f(x)}{h(x)} = \frac{6}{\sqrt{2\pi}} \exp\left(-\frac{x^2}{2}\right) \quad ; -1 \leq x \leq 5 \quad (59)$$

The steps in the TPT-importance sampling approach can be summarized as follows:

1. Choose a range of durations around the critical storm duration (from Design Event Analysis). For each duration carry out steps 2-4
2. Take N samples from the range [-1,5] and translate the resulting standard normal variates into rainfall intensities
3. Take N corresponding samples of the remaining random variables (initial losses and rainfall patterns) and simulate the hydrological model to derive samples of peak discharges
4. Evaluate equation (30) to derive the exceedance probabilities of a range of discharge levels and translate these into ARI's

At first, N=12,000 samples and corresponding model simulations were carried out, similar to the number of model simulations in the stratified sampling approach (60 bins * 200 samples per bin). Results are shown in A4.4. It shows the two methods (stratified sampling and importance sampling) provide consistent results.

Figure H15 shows the results of the TPT-importance sampling approach if the procedure is repeated 10 times. It shows the method can compete with the stratified sampling approach in term of the small band width (compare Figure H15 with Figure H13). This also makes it hard to distinguish between the two in terms of computational accuracy. The next step was therefore to evaluate the performance of both methods with a 10 times lower number of samples: 20 samples per bin in the stratified sampling method and 1200 samples in total for the importance sampling method. The simulations were repeated 100 times to obtain a good insight in the variation in the resulting frequency curves. Results are shown in Figure H16 (stratified sampling) and Figure H17 (importance sampling). Again, there is no clear distinction between the two, indicating that no major improvements can be expected from introducing importance sampling to the TPT method. It was therefore decided not to further pursue this issue and to leave the original TPT approach unchanged (ie stratified sampling).

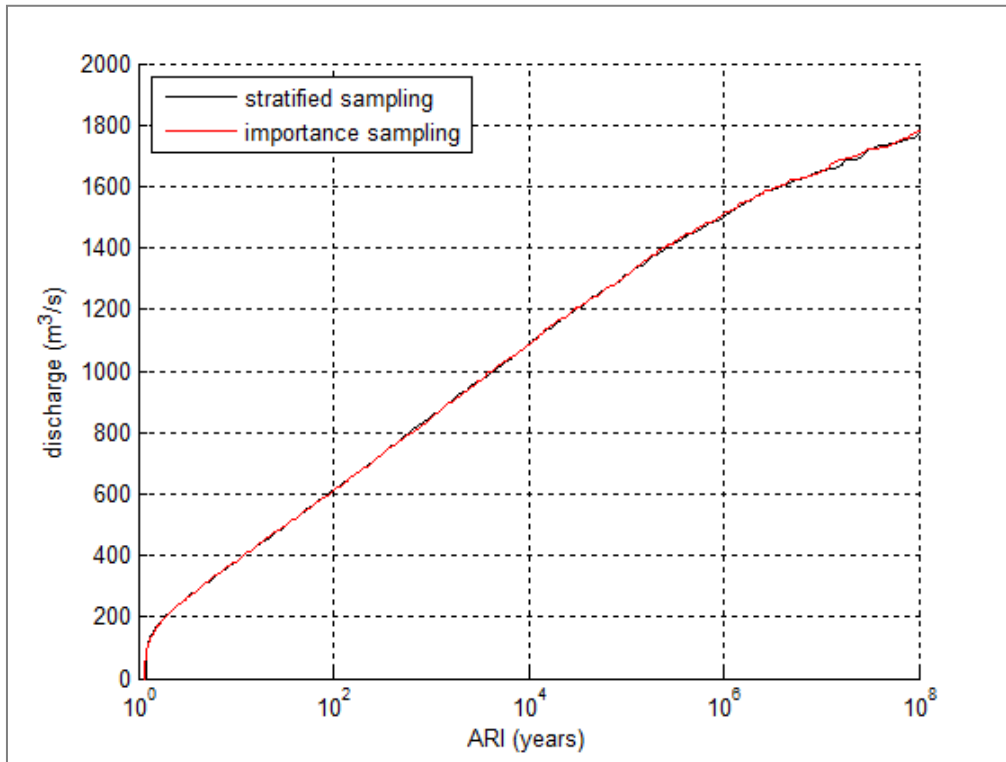
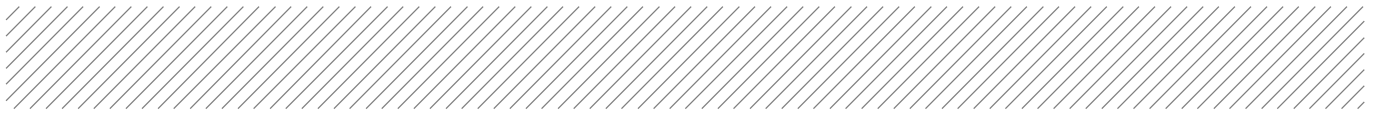


Figure H14 Comparison of results with importance sampling and stratified sampling

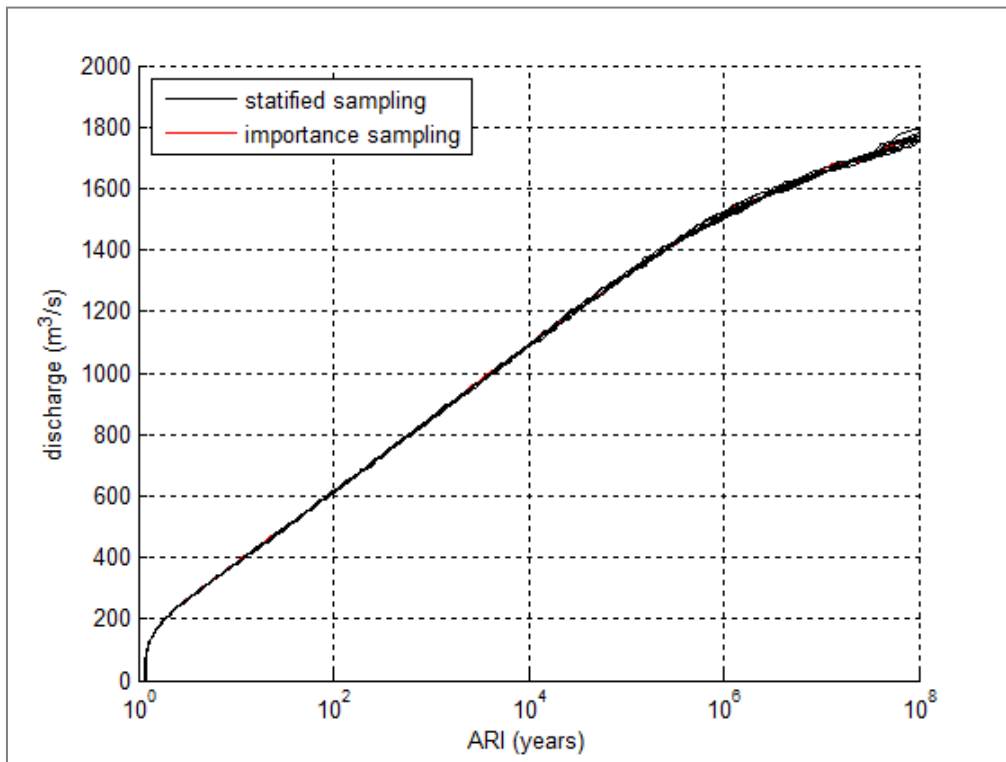


Figure H15 ARI's and corresponding discharges as estimated from 10 different MC runs, using the TPT-importance sampling method

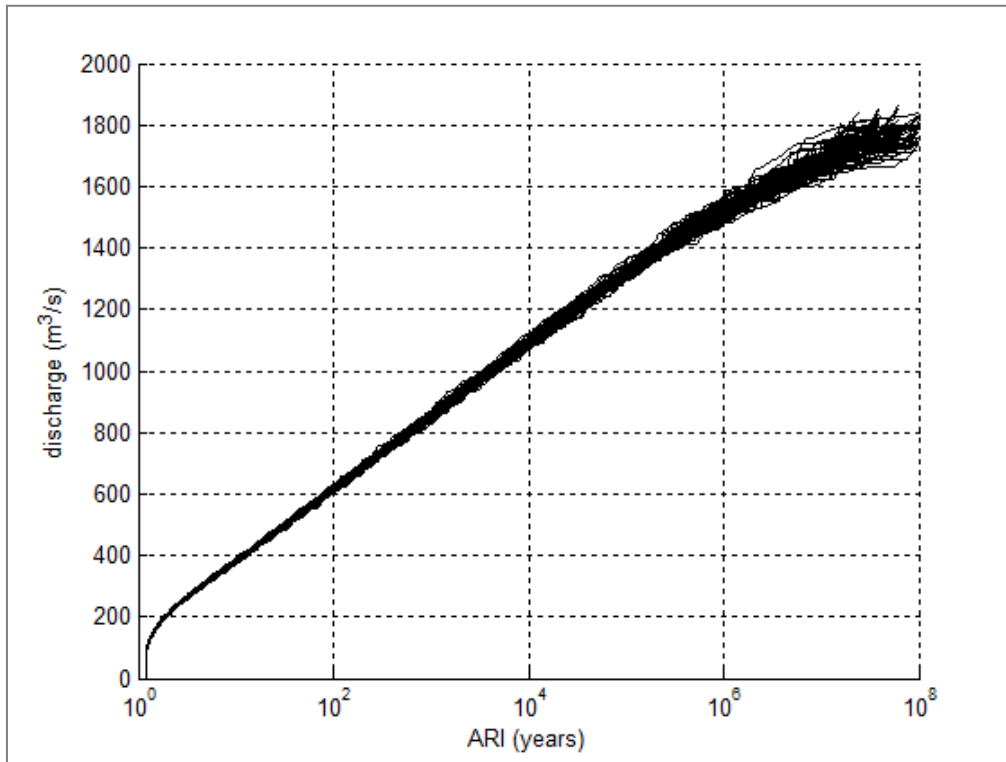
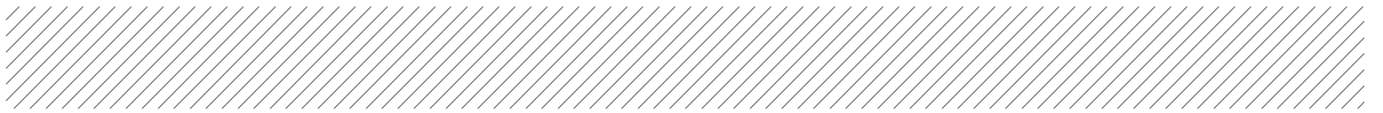


Figure H16 ARI's and corresponding discharges as estimated from 100 different MC runs, using the TPT-stratified sampling method with only 20 samples per bin

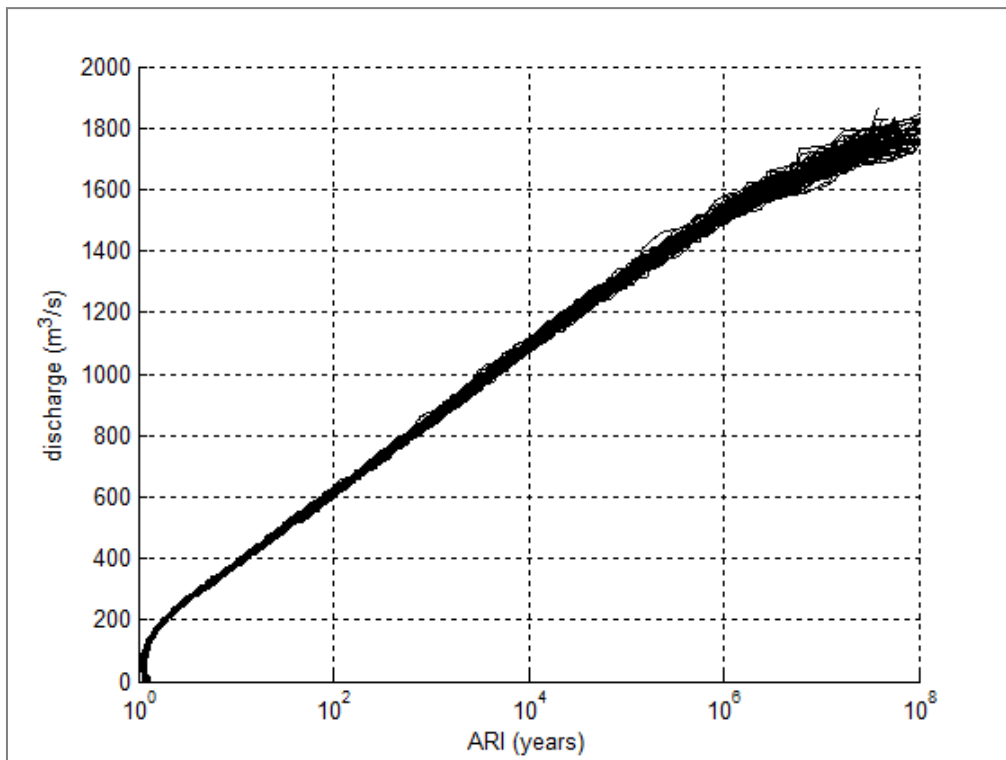


Figure H17 ARI's and corresponding discharges as estimated from 100 different MC runs, using the TPT-importance sampling method





H4. Comparison of results from CRC-CH and TPT

Figure H18 compares the resulting frequency curves of the CRC-CH method and the TPT method. It shows that the TPT provides higher design flows than the CRC-CH method. Differences increase for increasing ARI up to 200 m³/s. So, even though the two methods were applied as much as possible in a mutually consistent manner, they do not provide exactly the same results. One of the main reasons is that, in spite of the attempt to apply consistent input statistics, there are still inconsistencies left. This is best demonstrated by an analysis of 'burst statistics' that follow from the simulated CRC-CH events.

Figure H19 compares the burst statistics for a two hour duration that were derived from 100,000 simulated events. The events were simulated in exactly the same manner as described in Section H3. In this case, no importance sampling was applied. The Figure shows that the burst intensities that follow from the CRC-CH simulations are significantly lower than the original input statistics, which also explains why CRC-CH design discharges are lower than TPT design discharges. This shows that the simulated events do not fully capture the burst extremes for the entire range of durations. This is to a large extent due to the assumed temporal pattern from the cascade model, which determines the intensities of bursts that occur within an event. Once real rainfall patterns are used instead of the temporal patterns from the cascade model, this effect should be reduced, but perfect consistency is not guaranteed. This will be one of the critical items in the set-up and validation of the Monte Carlo framework for the BRCFS.

In order to further test the influence of the assumed temporal distribution on the estimated design flows of the two methods, an alternative distribution for the multiplicative cascade model was used. The 2-parameter beta-distribution was applied for sampling the W-parameters of the multiplicative cascade model. The mean of the distribution is assumed to be equal to 0.5, the standard deviation is equal to 0.25 (events; CRC-CH method) and 0.15 (bursts, TPT method), following the recommendations of Carroll D.G. [2012] and Carroll, D and Rahman [2004]. The differences in standard deviations account for the fact that the temporal variability during events is generally higher than the temporal variation during bursts. Figure H20 shows that with these alternative temporal rainfall patterns, the results of the TPT and CRC-CH are much more in accordance, at least for ARI's <104 year. This shows the relevance of the temporal patterns for the estimated design flows and confirms that correct modelling of temporal patterns will be one of the crucial items in the set-up of the Monte Carlo framework for the BRCFS.

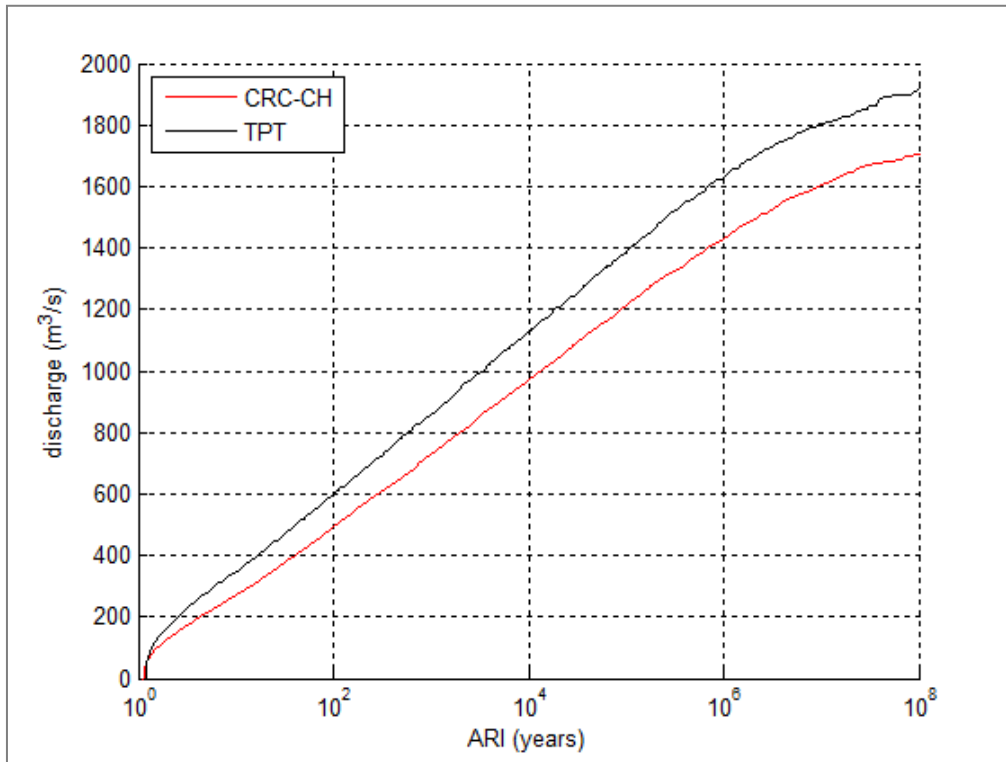
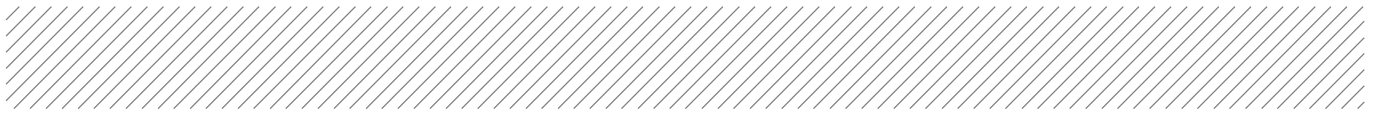


Figure H18 Peak discharges and corresponding ARI's: comparison between the TPT and CRC-CH method

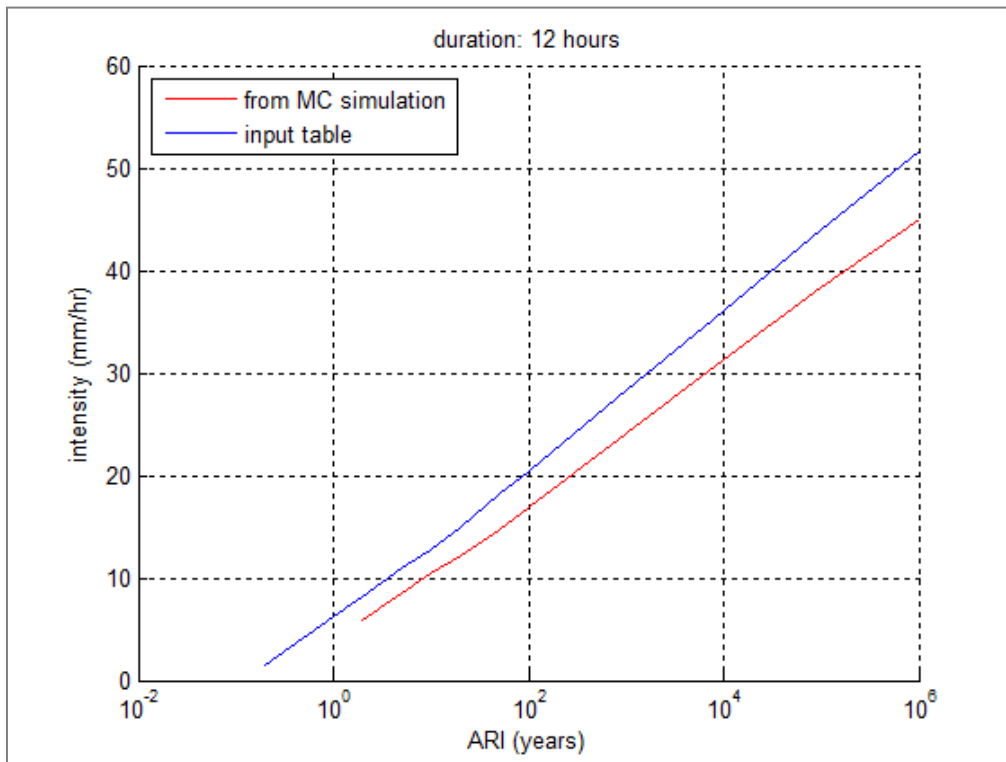


Figure H19 Comparison of input burst statistics and derived burst statistics from MC simulation, for a duration of 12 hours



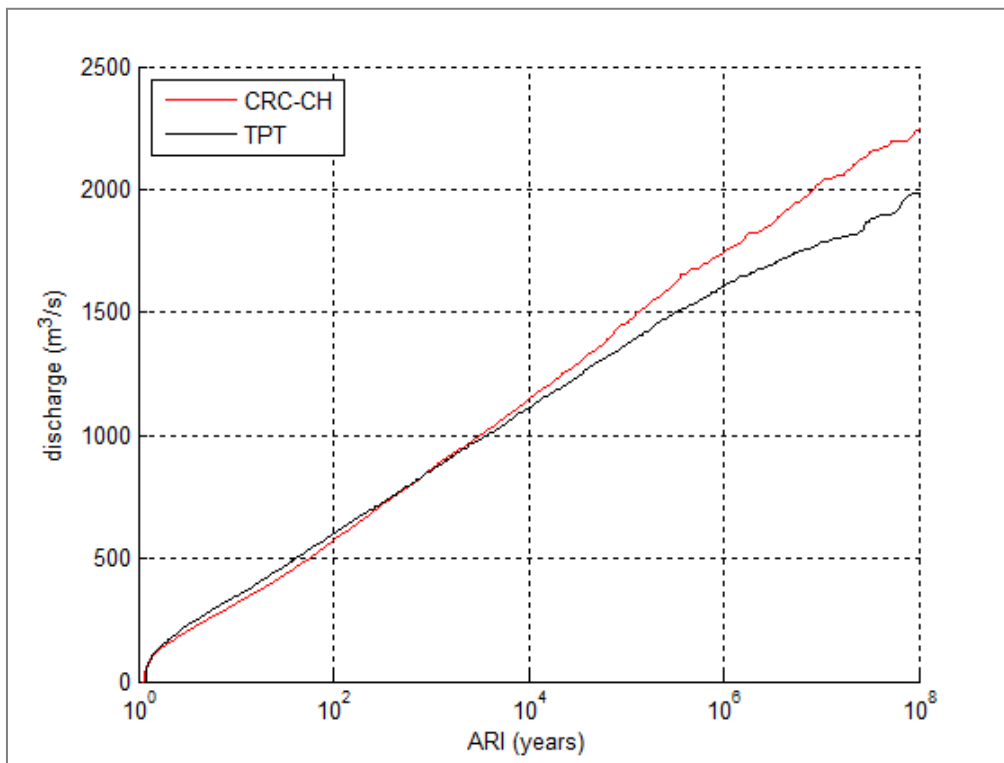


Figure H20 Peak discharges and corresponding ARI's: comparison between the TPT and CRC-CH method, using alternative temporal rainfall patterns

H5. Conclusions

The main conclusions of the pilot study are:

- The CRC-CH can provide accurate results also for high ARI's, without having to carry out millions of model simulations through the use of importance sampling
- The TPT method can also be applied with importance sampling (instead of stratified sampling), but this is not expected to lead to a major improvement in model accuracy and/or reduction in computation times
- Differences in computed design discharges between TPT and CRC-CH were mainly due to differences in IFD table definition (bursts vs events), "losses" and temporal patterns. Consistent modelling of these factors is a high priority in the MCS framework



Aurecon Australasia Pty Ltd

ABN 54 005 139 873

Level 14, 32 Turbot Street
Brisbane QLD 4000

Locked Bag 331
Brisbane QLD 4001
Australia

T +61 7 3173 8000

F +61 7 3173 8001

E brisbane@aurecongroup.com

W aurecongroup.com

Aurecon offices are located in:

Angola, Australia, Botswana, China,
Ethiopia, Ghana, Hong Kong, Indonesia,
Lesotho, Libya, Malawi, Mozambique,
Namibia, New Zealand, Nigeria,
Philippines, Qatar, Singapore, South Africa,
Swaziland, Tanzania, Thailand, Uganda,
United Arab Emirates, Vietnam.